INDIAN JOURNAL OF ECOLOGY

ISSN 0304-5250

Volume 48 Issue-6 Dccember 2021

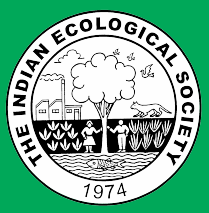

THE INDIAN ECOLOGICAL SOCIETY

THE INDIAN ECOLOGICAL SOCIETY

(www.indianecologicalsociety.com)
Past President: A.S. Atwal and G.S.Dhaliwal
(Founded 1974, Registration No.: 30588-74)

Registered Office
College of Agriculture, Punjab Agricultural University, Ludhiana – 141 004, Punjab, India
(e-mail : indianecologicalsociety@gmail.com)

Advisory Board
Kamal Vatta Chanda Siddo Atwal K.S. Verma Asha Dhawan

Executive Council
President
A.K. Dhawan

Vice-Presidents
R. Peshin S.K. Bal G.S. Bhullar

General Secretary
S.K. Chauhan

Joint Secretary-cum-Treasurer
Vaneet Inder Kaur

Councillors
A.K. Sharma R.S. Chandel R. Banyal N.K. Thakur

Editorial Board

Managing-Editor
A.K. Dhawan

Chief-Editor
Anil Sood

Associate Editor
S.S. Walia K. Selvaraj

Editors
Neeraj Gupta Sumedha Bhandari Maninder K. Walia Rajinder Kumar
Subhra Mishra A.M. Tripathi Harsimran Gill Hasan S.A. Jawad

See detailed regarding editorial board at web site

The Indian Journal of Ecology is an official organ of the Indian Ecological Society and is published bimonthly in February, April, June, August, October and December. Research papers in all fields of ecology are accepted for publication from the members. The annual and life membership fee is Rs (INR) 800 and Rs 8000, respectively within India and US $ 100 and 350 for overseas. The annual subscription for institutions is Rs 6000 and US $ 300 within India and overseas, respectively. All payments should be in favour of the Indian Ecological Society payable at Ludhiana. See details at web site. The manuscript registration is Rs 500.

KEY LINKS WEB
website:http://indianecologicalsociety.com
Membership:http://indianecologicalsociety.com/society/memebership/
Manuscript submission:http://indianecologicalsociety.com/society/submit-manuscript/
Status of research paper:http://indianecologicalsociety.com/society/paper-status-in-journal-2/
Abstracts of research papers:http://indianecologicalsociety.com/society/indian-ecology-journals/
Full journal: http://indianecologicalsociety.com/society/full-journals/

Indian Journal of Ecology (2021) 48(6): 1595-1610

Manuscript Number: 3421
NAAS Rating: 5.79

Using Spectral Indices in Detecting the Degradation of Soil Physiographic Units in Al-Wahda Project South of Baghdad

Jinan Abdul Ameer Abbas

College of Education for Women, University of Baghdad, Iraq
E-mail:Jianaaa11@gmail.com

Abstract: Al-Wahda project at the southern part of Baghdad governorate was selected to detect the degradation of the soil physiographic units during 1990-2005-2020. The images of the location of the project were determined of the three years, where 30 soil sites were chosen, which were distributed to cover most of the lands of these units. Particular physical and chemical properties of soils were measured, their textures varied between moderate and fine. Some have high salinity 23.7 dsm^{-1}, while all samples are low to very low in organic matter with a decrease in the cation exchange capacity values. Land covers were classified into four types, and their extent varied as Non-Vegetation (NV)> Barren (Ba)> Vegetation (V)>, Urban (U) in 1990, and their arrangement changed in (2005) to NV> V> Ba> U. During 2020 were arranged as NV> V> U> Ba. Accordingly, the values of the Normalized Difference Vegetation Index (NDVI) and the Land Degradation Index (LDI) were obtained. The status of lands was evaluated in relation to the ranges of NDVI which were divided into five classes or categorizes. The dominance of the weak class 88.39, 74.01, 53.25 % for the years 1990> 2005> 2020 in the study area, and its dominance varied with the moderate class in the physiographic units. The degrees of lands degradation were specified depending on LDI values. The largest area was for moderate degradation of land at rates of 100.0, 99.04, 97.65 % for the whole study area and for the years 1990> 2005> 2020, and this degree of degradation also has a dominance overall the physiographic unit with the presence of a strong degree of degradation with a greater percentage of light degradation in the year 2005-2020. There are only two types of the relative extent of the degrees of degradation (infrequent> dominant) at a rate of 57.14 and 42.85 % respectively for all the physiographic units and the three years. The significant positive correlation (r) was for NDVI and LDI with organic matter value (0.797, 0.882), respectively, and a significant negative correlation for NDVI values with Bd> $CaCO_3$> EC, -.856, -0.727, -0.679 respectively, and LDI values have a negative correlation with Bd> EC> $CaCO_3$, -0.853, -0.772, -0.708, respectively.

Keywords*:* NDVI, LDI, Land cover, Degradation degree, Al-Wahda project

Land degradation is regarded as one of the environmental problems and it occurs mostly in dry and steep lands. It takes many forms as well as it affects soils, biomass, water, biodiversity, and economy. Cultivated lands were more exposed to degradation than non- cultivated lands, and their degradation was determined by their usage, the change of their usage and associated management with it. Besides, the direct causes of the deterioration may appear due natural causes, yet behind their appearance entirely, partly or indirect human causes resulting from human activity, which lead to a difficulty in determining the general relationship for that. This phenomenon can be easily found in the alluvial Mesopotamian plain due to the increase in salinity and the lack of natural vegetation, which is a form of desertification. The causes, extent, and severity of degradation are in a position of dispute, where land degradation can be defined as a long-term degradation in the functioning and productivity of the ecosystem, which can be assessed with long-term and remote-sensed Normalized Difference Vegetation Index (NDVI) data. Land degradation reduces and destroys the productive capacity of the soil and undermines the future of the earth, especially in developing nations due to the pressure resulted from the increasing population, once soil degradation reaches a certain level of severity, it affects the normalized vegetation and crop yields, while the type of use of the land also affects the reflectivity of the surface soil. Some indicators were used in the clarification of satellite images to identify and monitor patterns of degradation. As well as, the reflectivity of the soil is followed according to what was affected by a physical deterioration such as desquamation and compression, or a chemical deterioration such as salinization and it is easy to interpret while it is generally difficult to discover visually in the field. Upon detection of the spatial change of land cover in northwestern Egypt, it was observed that there is a significant decrease in normalized vegetation and an increase in the area of urban settlements (Shalaby and Tateishi 2007). There is an increasing interest in characterizing plants by using remote sensing techniques because of the information about a single spectral band is usually insufficient to describe vegetation. Therefore, it must develop the combining of two or more spectral bands. The NDVI index was considered one of the most important and common vegetation indicators and includes the reflections of the red rays R and infrared rays

NIR. Desmond et al (2013) observed that remote sensing techniques are useful in monitoring land degradation and that the NDVI index gives good information that matches the density of vegetation on the land, and that the results accuracy of this index can be evaluated with other geographical data of the study site to give better results. Abdullatiff (2019) used the NDVI index to find out the influence of the industrial use at the Nahrawan district within the center of Iraqi alluvial plain for two different years and observed a severe lack of vegetation. Soil salinization is one of the most common land degradation processes, especially in arid and semi-arid regions, where evaporation exceeds rainfall and it is a well-known phenomenon in irrigated agriculture, yet its severity and effects vary from one region to another (Asfaw et al 2018). Moreover,12 types of degradation have been diagnosed, which represent the severity of operations that were described by the degree of degradation and their relative extent. Each of them was given a symbol, including the physical deterioration of soil such as compression, water logging, reduction of organic matter and chemical degradation. The most important of which are nutrient deficiency and salinization. Zhao and Meng (2010) used the Land Degradation Index (LDI) to detect the land degradation of Kenli County for three periods of time through three visual images and found that half of the land area had a heavy and moderate degradation in the first period to improve in the second period. Nevertheless, it re-appeared in the third period because of the man's excessive use of land resources and their conversion from agricultural lands to saline lands. Fadhil (2009) studied the degradation of some lands above the Iraqi alluvial plain for 10 years, and used some spectral indices, including NDVI and Land Degradation Risk and concluded that shortage of vegetation areas, water areas, and sand dunes assembly, soil moisture and vegetation are the much more influential in land degradation in the area. Due to the importance of studying soil degradation, the global assessment of human-induced soil degradation (GLASOD) project in 1990 funded by the United Nations Environment Program, and coordinated by International Soil Reference and Information Centre (ISRIC), produced the first global map of human-induced soil degradation, the map aimed to increase awareness of soil degradation problems. The data were collected in cooperation with a large number of soil scientists around the world; the status of soil degradation was mapped within loosely defined physiographic units (polygons). The type, extent, degree, rate, and main causes of degradation were presented on a global map and documented in a downloadable database. To detect and monitor the degradation of vegetation and soil and by making use of what is provided by satellite images, this study aims at finding and following up the soil degradation of the physiographic units at Al-Wahda project in center of the Iraqi alluvial plain by using some spectral indices used in remote sensing and geographic information systems applications. The change of these indices was estimated.

MATERIAL AND METHODS

Location and climate of the study area: Al-Wahda project is located between (33°.30´.0 - 33 ° .10´.0) N, (44 ° .45´.0 - 44° . 40´.0) E, within the borders of Baghdad governorate particularly 40 km at the south of central Baghdad at the central region of the Iraqi alluvial plain. Its sedimentary soil was formed as a result of the sediments of Tigris River, which passes near the borders of the western and southwestern regions, and its minimum distance separating from it is within 4 km, with a weak spread of natural vegetation as a result of prevailing climatic conditions. Some of its lands were used to cultivate some winter crops, such as wheat, barley, alfalfa, and summer crops such as cotton and vegetables; they were generally irrigated by pumping with a set of pumps on the Tigris River. Besides, particular modern irrigation methods such as (sprinkling and dripping) were used in planting in it. Five sub physiographic units have been identified within the lands of the region depending on the climate data of the Baghdad metrology station in (1985-2019) (Fig. 1). The annual average temperature was 23.28 C ° and the total annual rainfall was 110.3 mm (Table 1). Through the data, it can be concluded that the rain factor according to Lang coefficient is 4.73, which means that the area is under the influence of a very dry climate. Furthermore, the thermal system of the soil is of the hyperthermic regime and the soil moisture regime is of the type Ardic (torric).

Three satellite images were obtained for the study area, the first one is the American satellite Landsat 5 TM was taken on January 8, 1990, the second one is for the American satellite Landsat 5 TM also was taken on February 10, 2005 and the third one is for the American satellite Landsat 8 OLI was taken on Februarys 4,2020, a resolution 30 m was for all of them and the cloud cover is 0% of all the images. The project boundaries were projected on the satellite images and the satellite images were clipped, while the area of the study was then calculated, it reached 31.0284 km^2, where 30 sites of surface soil (0 - 5) cm were identified by the Grid method, and distributed to the physiographic units consistent with the area of each unit, so there were 12, 6, 5, 4, 3 soil samples for the physiographic units Basin, Lower Basin, Depression, Crevasses, Irrigation Levee respectively. A preliminary exploratory survey of the area of study was conducted to determine the possibility of accessing the

samples sites and to detect the difficulties that may be encountered during the process of survey, then by using the GPS of WGS 1984, the 30 sites were identified and soil samples were taken from them. Soil samples were sifted through a 2 mm sieve to be prepared for analysis, where their locations were shown in (Fig. 2). Supervised classification of the three images was made by using Arc GIS 10.8 to determine the types of land cover and identify the change occurring in it during the mentioned periods. The values of the proposed indices NDVI, LDI were determined, each according to its equation, to obtain the maps for each index or indicator, and to compare the differences among them for the specific years.

Physical and Chemical Properties of the Soil

Soil physical properties: Estimate the relative distribution of soil separates by hydrometer and bulk density by using the clod method.

Soil chemical properties: The pH in a soil and the electrical conductivity EC was estimated by soil paste extractor .Organic matter, **C**alcium carbonate an Cation-Exchange Capacity (CEC) were estimated according to Walkely and Black method, CO2 weight loss method and by titration with methyl blue dye .The exchangeable sodium in an ammonium acetate extract was determined by using a flame measuring .The proportion of exchangeable sodium was calculated by dividing the exchangeable. Sodium estimated in the above paragraph by the cation exchange capacity multiplied by 100.

Calculation of Indices

Normalized difference vegetation index NDVI: Calculated from dividing the subtraction between the spectral reflectance of the infrared wavelengths and the red wavelengths to their sum. Besides, it varies between the minimum for light-colored arid soils to the maximum in fully developed dark-colored soils and forms a value is less than 1.

$$NDVI = \left(\frac{R_{IR} - R_R}{R_{IR} + R_R} \right)$$

Depending on NDVI ranges the status of lands were evaluated, as the degrees of vegetation degradation were divided into five classes or categories (Shallal et al 2007) (Table 2).

Land Degradation Index LDI: calculated according to the following equation:

$$LDI = \left(\frac{[255 - (B2 + B3)]}{[255 + (B2 - B3)]} \right)$$

This index was calibrated by using the range method for its values and according to the equation of (Zhao and Meng 2010)

$$LDI_0 = \left(\frac{a - Min\ a}{Max\ a - Min\ a} \right) \times 100$$

LDI_O: Calibrated Land Degradation Index value

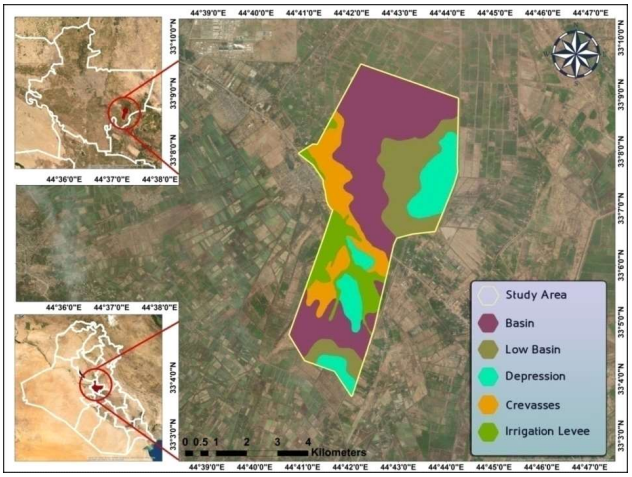

Fig. 1. Location of the study area and its physiographic units

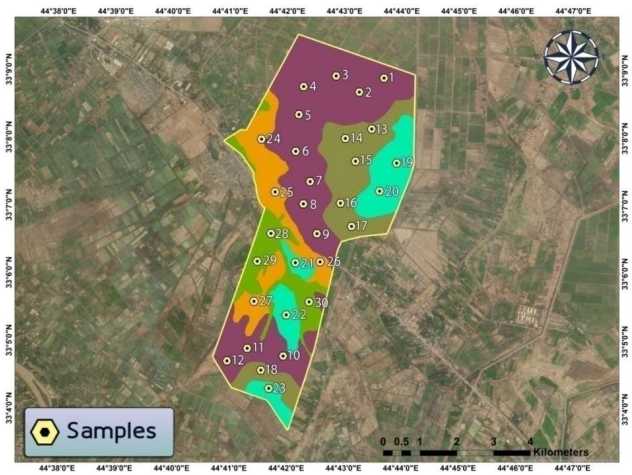

Fig. 2. Soil sample sites in the study area in 2020

a: The value of the land degradation index to be calibrated

Mina and Max a: The lowest highest value of LDI

The degree of degradation was calculated according to Zhao and Meng (2010) (Table 3) and then the relative extent and severity of degradation were calculated.

Relative extent of the degradation degree: This is ratio represented by the degree of degradation of the unit area of the map (here is the area of the physiographic unit) and is divided into five types (Table 4).

Severity of soil degradation: The severity of soil degradation is indicated by a combination of the degree of degradation and the relative extent, and was divided into four classes as in (Table 4).

RESULTS AND DISCUSSION

Land cover in the study area: The total area of land cover types were estimated in 1990-2005-2020 in (Table 5). Despite of the overlapping between the two concepts of Land

Cover/LC used for environmental models and Land Use/LU for policymaking, this study refers to the types of land cover which are less changeable during short periods (Comber 2008). Thus, a period from 1990 to 2020 was chosen. Therefore, 30 years were specified to detect the change in the land cover in the area of the current study, which was related directly and indirectly to the usage of land in it, and these, in turn, might be related to one type of cover. There are four types of land cover in the study area, which are (V) vegetation, Non-vegetation (NV), Barren (Ba), and Urban (U). The one of largest extent is (V)for the three years, with an area that is 18.8757 km^2 in 1990, decreased in 2005 by 6.7959 km^2, at an average decrease 0.45306 km^2 $year^{-1}$, then the area of NV) increased by 1.3491 km^2in 2020, at an average of 0.08994 km^2 $year^{-1}$.The vegetation cover (V) area in 2005 was 11.4813 km^2 with an increase of 6.9183 km^2 and an average increase of 0.46122 km^2 $year^{-1}$, due to the state's policy to encourage planting within the agricultural sector rehabilitation program that began in 1998.With providing support to farmers within the policy of nation to encourage the agricultural sector, especially the private sector, and to provide requirements for the production process area decrease in in 2020 by 2,322 km^2, and at an average decrease 0.1548 km^2 $year^{-1}$. This is due to the instability of the situation in general because of the conditions that all the country went through, including the area of study, which negatively affected various aspects of life, including the agricultural sector, and led many individuals to abandon the agricultural profession and abandon their agricultural fields as well, which led to a deterioration in the area of agricultural lands and a decrease in their areas.

Barren lands (Ba), its area decreases in 2005 by 1.1592 km^2 than it was in 1990, with an average decrease of 0.07728 km^2 $year^{-1}$, to become the total area 4.5387 km^2, and to decrease further in 2020 to become 1.539 km^2. However the area of urban lands (U) increase significantly in 1990 that reaches 1.8918 km^2 to become 2.9286 , 6.9012 km^2 in 2005 ,2020 respectively, and the largest increase was 5.0094 km^2in 2020 at a rate of 0.16698 km^2 $year^{-1}$. This may be due to the increase in the population of Baghdad Governorate in

Table 2. Land classes according to NDVI ranges

NDVI ranges	Vegetation coverage	Vegetation density	Land classes
Negative value	0-20	Very low	Very deteriorated
0.0- 0.19	21-40	Low	Weak
0.2- 0.49	41-60	Medium	Moderate
0.50-0.79	61-80	Good density	Well
0.8-1.0	81-100	High density	Excellent

Table 1. Monthly and annual mean of some climate elements in Baghdad , Baghdad metrology station (1985-2019)

Climate elements	Months												
	Jan	Feb	Mar	Apr	May	Jun	Jul	Agu	Sept	Oct	Nov	Dec	Annual mean
Max of Tem (°c)	17.2	22.0	25.0	31.1	28.2	42.9	47.3	46.5	42.1	34.5	25.6	19.2	31.80
Min of Tem (°c)	4.1	6.2	10.2	18.0	24.0	25.0	28.1	29.0	22.2	17.0	10.2	6.4	16.70
Mean (°c)	10.4	12.4	17.1	23.4	28.4	32.4	35.2	35.4	31.1	24.6	16.1	12.9	23.28
Wind speed m/sec	3.1	3.2	3.5	3.0	4.1	4.2	4.4	3.8	3.0	3.1	2.7	2.5	3.38
Rainfall (mm)	17.8	16.4	20.6	15.5	11.4	0.0	0.0	0.0	0.4	3.8	10.5	13.9	110.30

Table 3. Grade of land degradation

Degradation degree	Extreme	Strong	Moderate	Light
Land Degradation Index (A)	$A \leq 30$	$30 < A \leq 60$	$60 < A \leq 90$	$A > 90$

Table 4. Severity of degradation classes according to the relationship between the degree of degradation and relative extent

Degree of degradation	Relative extent (%)				
	< 5 Infrequent	6 – 10 Common	11 – 25 Frequent	26 – 50 V. frequent	50 Dominant
light	1-1	1-2	1-3	1-4	1-5
Moderate	2-1	2-2	2-3	2-4	2-5
Strong	3-1	3-2	3-3	3-4	3-5
V. strong	4-1	4-2	4-3	4-4	4-5
Low		Moderate	High		Very High

general, as their population increased from 6.726432 million in 2005 to 8.558625 million in 2020. This was considered one of the primary reasons that lead to land degradation, changing its land cover and its uses (Gobin et al 2020). The area of these land covers can be arranged according to the years, and it was in 1990 (UN> Ba> V> U), and in 2005 was(UN> V> Ba> U), to be in 2020 (UN> V> U> Ba). The risk of urban sprawl and changing the gender of the agricultural land is one of the problems that the area of study suffers from, which leads to the deterioration of the vegetation (Table 6).

The area of the physiographic units in the study area was arranged as Basin (B)> Lower Basin (LB)> Depression (D)>

Table 5. Types of land cover and their areas in the study area 1990-2005-2020 (km^2)

Year	Land cover				Total area
	Vegetation (V)	Non – vegetation (NV)	Barren (Ba)	Urban (U)	
1990	4.5630	18.8757	5.6979	1.8918	31.0284
2005	11.4813	12.0798	4.5387	2.9286	31.0284
2020	9.1593	13.4289	1.5390	6.9012	31.0284
			Per cent		
	Vegetation	Non - vegetation	Barren	Urban	Total
1990	14.71	60.83	18.36	6.10	100.0
2005	37.02	38.93	14.62	9.43	100.0
2020	29.60	43.20	4.96	22.24	100.0

Table 6. Types of land cover and their areas for the physiographic units 1990-2005-2020

Physiographic units	Land cover	Area (Km^2)	Per cent	Area (Km^2)	Per cent	Area (Km^2)	Per cent
		1990		2005		2020	
Basin (B)	Vegetation	2.403	17.56	7.5465	55.14	6.3252	46.22
	Non- Vegetation	8.6103	62.92	3.8205	27.91	3.9267	28.69
	Barren	1.9566	14.29	1.1268	8.23	0.162	1.18
	Urban	0.7155	5.23	1.1916	8.72	3.2715	23.91
	Total	13.6854				13.6854	
Lower Basin (LB)	Vegetation	0.7659	13.72	2.0988	37.61	1.2204	21.87
	Non- Vegetation	3.6999	66.32	2.2392	40.14	2.9475	52.82
	Barren	0.8559	15.34	0.9135	16.37	0.4887	8.76
	Urban	0.2583	4.62	0.3285	5.88	0.9234	16.55
	Total	5.58				5.58	
Depression (D)	Vegetation	0.4122	9.07	0.5256	11.57	0.2349	5.17
	Non- Vegetation	2.6523	58.41	2.4075	53.03	3.2274	71.06
	Barren	1.2537	27.61	1.2429	27.36	0.6903	15.21
	Urban	0.2232	4.91	0.3645	8.04	0.3888	8.56
	Total	4.5414				4.5414	
Crevasses (Cr)	Vegetation	0.4086	9.81	0.7551	18.13	0.6687	16.06
	Non- Vegetation	2.0223	48.56	1.9791	47.53	1.6776	40.28
	Barren	1.2717	30.54	0.5742	13.79	0.0846	2.04
	Urban	0.4617	11.09	0.8559	20.55	1.7334	41.62
	Total	4.1643				4.1643	
Irrigation Levee (IL)	Vegetation	0.5733	18.75	0.5724	18.72	0.7101	23.23
	Non- Vegetation	1.8909	61.85	1.6398	53.63	1.6497	53.95
	Barren	0.36	11.78	0.684	22.38	0.1134	3.71
	Urban	0.2331	7.62	0.1611	5.27	0.5841	19.11
	Total	3.0573				3.0573	

Crevasses (Cr)> Irrigation Levee (IL), with an area of 13.6854, 5.58, 4.5414, 4.1643, 3.0573 km^2. Moreover, the areas of the land cover types varied from one unit to another, between the increases and decrease. Generally, the area of vegetation cover increased in 2005 for all physiographic units. Then, it was decreased in 2020 due to the quite little interest of the government and its policies in supporting farmers and the agriculture requirements, as well as the scarcity of water, not providing the necessary water rations, salinization of the soil and the cost of reclamation. This forces many to leave the farming profession and go to other activities such as poultry farming, which was noted to have a field to raise in the area, or fish farming in small ponds, and some abandoned the farming profession because of the poor productivity of the land and its insufficient economic returns.

Despite this decrease, this cover represents the largest area in Unit B, with an area of 6.3252 km^2, the areas were arranged in 2020 as (B> IL> LB> Cr> D), with ratios of 46.22, 23.23, 21.87, 16.06, 5.17% respectively. The basins soil and lands were considered suitable for cultivation in the study area in particular and in the Iraqi alluvial plain in general because of its good soil characteristics with low groundwater table, moderate textures, and less salinity. Additionally, the least area for it was in D, which has high groundwater table, fine and moderately fine textures, and relatively low topography which have increased its salinity values. However, the area of land cover NV, was the higher from the other units area (B> D> Cr> IL)respectively, with a decrease in its areas in 2005 and 2020, due to the use of these lands, either for agricultural or urban.

The barren lands area (Ba) decreased in 2005 and 2020, while the urban lands area increased significantly for all units in general and for the three consecutive years .The percentage of urban land (U) in 2020 is (Cr> B> IL> LB> D) by 41.62, 23.91, 19.11, 16.55, 8.56 %, and was due to increased urban sprawl and the population, as well as the encroachment of agricultural lands which witness not only a decrease in their extents, in period between 2005-2020, but also a transformation of their usages by turning them to urban lands by exploiting the case of not initiating laws as well as activating the rules that forbidden and put an end to the use of those lands. The types of land cover and their distribution in the study area in 1990, 2005, and 2020 are given in Figure 3, 4 and 5.

Soil physical and chemical properties: Some physical and chemical properties of the 30 surface soil samples were measured (Table 7). The results show that there is a variation in the values of the separate of sample texture because of the processes of sedimentation that create a difference within them due to the intensity of water momentum of the Tigris River floods. Besides, their bulk densities varied, which decrease in the cultivated soils to 1.22 Mg m^{-3}as in the soils of the river basins (B), as for the PH, the soils are between neutral and moderately alkaline. Soil salinity increased in the depression unit reached 23.7 $ds.m^{-1}$.The 56.66% of the samples are non-saline and low salinity due to their cultivation and that 16.66% are moderately saline, while the percentage of the very salinity is 26.66%. The parent material of these soils is calcareous, and this was reflected in high levels of lime in all samples ranged between 13.4 - 32.2 % in addition to its sedimentation on the secondary level by increasing its amount with the solution of soil and its sedimentation, with a significant decrease in the organic matter values, ranged from low to very low, to relatively high in the cultivated samples were 1.9 % (sample No. 1), but they are still low values.

Normalized difference vegetation index (NDV1): The highest value of NDVI in (sample No. 10) in 1990 was 0.45, and was 0.47 in 2005 (sample No.8), while its highest value in 2020 was 0.33 (sample No.1), for the same unit of river basins for the three years. The presence of nutrients in the soil was reflected in the plant growth, so a healthy plant has a high NDVI (Daoud 2015). Therefore, the results of the analysis show that the high values of NDVI were in soil with an organic matter of 1.9 %, regardless to its low values in it, but it is relatively higher than its values in most of the other soil samples, as it is non-saline soils 3.5 dsm^{-1} and cultivated. The lowest value, was 0.054 in the sample 15 unit (LB) in 1990, and -0.021 in sample 15 also in 2005 and 0.073 in sample 14 in 2020 for the same physiographic unit for the three years, which is very salinity samples 23.5 dsm^{-1} within barren lands. The difference in the values of this index is due to the effect of vegetation and leaf area of the cultivated plant species on the red and infrared wavelengths, and thus the reflectivity is increased with increasing leaf area and vegetation density. The increase in the index in several sites indicates an increase in the intensity of agricultural land use and an improvement in the biomass which were represented by nutrients and every living parts or matter can participate in the production of organic matter for a specific area and is closely related to the NDVI (Mengetal 2013). A high correlation is found between them and NVDI (AbduL-Ameer et al 2019), as well as exploiting the land due to the increasing population density and its need for food, but this did not prevent the deterioration of NDIV in different areas within the area of study. Here, the possibility of a beneficial usage of NDVI and other indices and within different wavelengths to study the state of vegetation degradation associated in some way with soil degradation (Shrestha and Zinck 2001).The values of this index and their degradation

status and land classes according to NDVI ranges were given in Table 8.

However, by using the IDW (Inverse Distance Weighting) for the values of the INDV and according to its ranges that are previously mentioned in Table 2 and were distributed on maps by using Arc GIS 10.8, which was considered one of the most appropriate methods of classifications and evaluation. Besides, it contributes in determining the distribution of the ranges for this index (Table 9), which observed the presence of only three classes or cases of land degradation according to the division of this index ranges , vegetation coverage and density of vegetation, the classes are, very deteriorated, weak, moderate, while the excellent classes has not appeared for the three years.

The changes occurring in the areas and percentages for the degrees of vegetation degradation, as there is a variation between them within each year. The dominance is for the weak class for the three years and at rates of 88.38 - 74.00 - 53.25% in 1990, 2005, 2020, respectively. Moreover, its area decreases in 2005 by 4,461,204 km^2, at a rate of 0.297 km^2 $year^{-1}$, and to decrease further in 2020 by 6.438851 km^2, at an average decrease of 0.429 km^2 $year^{-1}$ and decrease was taken on the expense of the other deteriorated classes and this was related to either with climate factors or with the human's activity, management or even the characteristics of

Table 7. Physical and chemical properties of soil samples in physiographic units (2020)

Physiographic units	Samples	Clay %	Silt %	Sand %	Bd $Mg.m^{-3}$	pH	EC $Ds.m^{-1}$	EC $Ds.m^{-1}$	OM %	$CaCO_3$ %	CEC $Cmole.kg^{-1}$	ESP %
Basin soils (B)	1	30.4	49.6	19.5	1.22	7.7	3.5	3.5	1.9	14.3	18.9	6.5
	2	39.5	40.7	19.6	1.41	7.3	7.1	7.1	0.7	26.7	17.2	7.7
	3	26.5	30.5	42.2	1.32	8.1	2.3	2.3	1.2	18.5	17.9	7.2
	4	24.6	54.3	20.4	1.39	7.5	4.3	4.3	1.4	13.4	15.4	6.9
	5	26.1	40.2	32.9	1.46	7.2	6.5	6.5	0.6	22.0	13.7	8.1
	6	23.9	55.5	20.1	1.30	7.3	4.7	4.7	1.2	17.7	14.6	7.3
	7	38.5	53.7	7.1	1.44	7.1	7.5	7.5	0.7	32.2	19.5	8.4
	8	31.8	42.6	25.2	1.45	7.9	3.2	3.2	1.1	13.7	19.8	9.8
	9	33.7	36.8	29.3	1.37	8.0	3.4	3.4	1.3	13.5	18.6	7.5
	10	32.6	43.5	23.4	1.33	7.8	2.6	2.6	0.9	19.2	17.7	6.9
	11	42.3	25.5	32.0	1.50	7.2	19.6	19.6	0.3	31.8	24.3	10.9
	12	44.6	24.1	30.9	1.52	7.1	24.3	24.3	0.4	28.4	22.9	12.4
Lower basin soils (LB)	13	23.2	53.5	22.9	1.48	7.4	6.2	6.2	0.6	22.2	18.8	11.3
	14	36.3	29.2	33.8	1.52	7.9	23.5	23.5	0.5	26.9	20.3	13.6
	15	43.4	42.3	14.1	1.49	7.1	11.3	11.3	0.3	30.7	25.4	11.8
	16	38.8	46.7	14.3	1.38	7.3	8.2	8.2	0.7	18.8	20.6	13.2
	17	28.5	53.7	16.9	1.29	7.8	3.8	3.8	1.7	19.1	22.5	10.6
	18	39.7	31.6	28.5	1.42	7.4	7.2	7.2	0.6	20.6	18.2	10.1
Depression soils (D)	19	34.1	40.2	25.1	1.36	7.6	4.9	4.9	1.3	14.4	17.5	9.8
	20	43.2	41.3	15.2	1.55	7.2	23.7	23.7	0.3	27.5	21.9	12.4
	21	30.6	32.1	36.8	1.47	7.3	12.7	12.7	0.4	16.8	15.4	11.0
	22	50.1	33.3	15.9	1.54	7.1	23.6	23.6	0.3	29.1	26.3	8.4
	23	35.4	52.3	12.0	1.56	7.4	21.2	21.2	0.5	25.4	21.4	9.9
Crevasses soils (Cr)	24	25.7	59.3	14.8	1.48	7.4	9.2	9.2	0.9	19.3	13.8	6.8
	25	36.3	44.8	18.9	1.53	7.2	16.4	16.4	0.4	24.7	18.2	11.5
	26	34.8	39.2	25.8	1.46	7.6	9.8	9.8	0.9	16.7	17.8	7.9
	27	29.4	40.3	29.7	1.33	7.8	3.1	3.1	1.2	18.3	14.7	9.3
Irrigation levee soils (IL)	28	27.9	50.5	22.6	1.35	7.8	4.7	4.7	1.8	19.3	21.4	8.0
	29	33.2	45.4	21.1	1.49	7.3	16.4	16.4	0.3	27.5	16.5	7.4
	30	27.6	39.9	31.6	1.29	7.5	3.7	3.7	0.9	15.6	14.9	11.2

Table 8. NDVI values and land classes according its ranges 1990-2005-2020

Physiographic unit	No.	X	Y	NDVI 1990	Land classes	NDVI 2005	Land classes	NDVI 2020	Land classes
Basin soils (B)	1	44.72817113	33.14805643	0.0	Weak	0.128713	Weak weak	0.339218	Moderate
	2	44.72080532	33.14444178	0.240506	moderate	0.175258	Weak	0.192992	Weak
	3	44.71422096	33.14854671	0.013333	Weak	0.260870	Moderate	0.261612	Moderate
	4	44.7057653	33.14643637	0.107692	Weak	0.302326	Moderate	0.208484	Moderate
	5	44.70340244	33.13904318	0.046154	Weak	0.045455	Weak	0.096403	Weak
	6	44.70291656	33.13023734	0.055556	Weak	0.288889	Moderate	0.336913	Moderate
	7	44.70672448	33.1225664	0.090909	Weak	0.087379	Weak	0.181827	Weak
	8	44.70477921	33.11708339	0.160494	Weak	0.470588	Moderate	0.263078	Moderate
	9	44.70874426	33.10975039	-0.030303	Very deteriorated	0.396226	Moderate	0.295773	Moderate
	10	44.6990002	33.07962671	0.456790	Moderate	0.100917	Weak	0.295327	Moderate
	11	44.68854251	33.08151495	-0.044776	Very deteriorated	0.039216	Weak	0.094215	Weak
	12	44.68263603	33.07842371	0.0	Weak	0.009174	Weak	0.113321	Weak
Lower basin soils (LB)	13	44.72461461	33.13553259	0.058824	Weak	0.017241	Weak	0.089712	Weak
	14	44.71695405	33.13319747	0.029412	Weak	0.111111	Weak	0.073843	Weak
	15	44.71992896	33.12759531	-0.054054	Very deteriorated	-0.021277	Very deteriorated	0.074622	Weak
	16	44.71557977	33.11727154	0.013699	Weak	0.191489	Weak	0.150238	Weak
	17	44.71881514	33.11157339	0.012658	Weak	0.166667	Weak	0.300033	Moderate
	18	44.69252734	33.07616255	0.243243	Moderate	0.191919	Weak	0.123586	Weak
Depression soils (D)	19	44.73191348	33.12716021	-0.025	Very deteriorated	-0.034483	Very deteriorated	0.306051	Moderate
	20	44.72753609	33.12103091	0.230769	Moderate	0.053763	Weak	0.075582	Weak
	21	44.70248043	33.10259642	0.015873	Weak	0.009709	Weak	0.295773	Moderate
	22	44.69986014	33.08975993	0.0	Weak	-0.011236	Very deteriorated	0.082774	Weak
	23	44.6948347	33.07168326	0.05	Weak	0.008547	Weak	0.086205	Weak
Crevasses soils (Cr)	24	44.69253662	33.13296337	0.240506	Moderate	0.060000	Weak	0.132425	Weak
	25	44.69651564	33.11999671	0.025641	Weak	0.263158	Moderate	0.076923	Weak
	26	44.70967421	33.10282394	0.030303	Weak	0.040816	Weak	0.135416	Weak
	27	44.6904641	33.09308033	0.042254	Weak	0.360000	Moderate	0.222385	Moderate
Irrigation levee soils (IL)	28	44.69536347	33.10979533	0.014085	Weak	0.030928	Weak	0.279007	Moderate
	29	44.69138088	33.1029379	0.085714	Weak	0	Weak	0.106687	Weak
	30	44.70658348	33.09303427	-0.276596	Very deteriorated	0.011236	Weak	0.279007	moderate

Table 9. Areas of land classes km^{2}according to NDVI ranges 1990-2005-2020

Year	Land classes			Total area km^2
	(V. deteriorated Negative value)	(Weak 0.0 – 0.19)	Moderate (0.49-0.2)	
1990	2.128051	27.423811	1.476538	31.0284
2005	3.174158	22.962607	4.891635	31.0284
2020	0.00	16.523756	14.504645	31.0284
		Percent		
	V. deteriorated	Weak	Moderate	
1990	6.85	88.39	4.76	100.0
2005	10.23	74.01	15.76	100.0
2020	0.00	53.25	46.75	100.0

land. The land of v. deteriorated degree was because of the huge decrease or the absence in the density of the land cover of the natural vegetation which was sometimes referred to as "Barren lands" because the spreading of the natural vegetation reaches to 0.0-20.0 which a limited cover. Its area increases from 2.128051 km^2 in 1990 to 3.174158 km^2 in 2005 by 1.046107 km^2, with an average increase of 0.069 km^2 $year^{-1}$ and might be the major reason behind abandoning these areas and leaving them without any attempt to use them in agriculture. The previously mentioned deterioration vanished in 2020 which in turn was seen as an indication for a slight improvement within the percentage of the natural vegetation and its density. However, the moderate class degradation, which records the lowest percentage in1990, area increases in 2005 to become 4.891635 km^2 by 3.415097 km^2 within an average increase of 0.227 km^2 $year^{-1}$, and in 2020 increases by 9.61301 km^2, with an average increase of 0.640 km^2 $year^{-1}$ to become 14.504645 km^2. This class constitutes a vegetation coverage ranged from 41- 60, despite the increase in the area of moderate class, but it remains at a rate less than the weak. The change and difference in the classes area due to the quality of the plants, which have an effect on the reflection of red and infrared rays, and thus affect the values of NDVI and its ranges. As for the classes land according to NDVI ranges and their distribution on the physiographic units of the study, areas, and percentages, were explained in Table 10. The results indicate that the largest area is for the weak class in all the physiographic units in 1990. Its area decreases in 2005 in units B, Cr with an area of 2.518129 -3.180227 km^2, with an average decrease of 0.16787- 0.2120 km^2 $year^{-1}$, respectively, to become 1.28781 - 9.174939 km^2, respectively, to decrease further in unit B in 2020 by 3.693492 km^2 with an average decrease of 0.246 km^2 $year^{-1}$.

The reason belongs to the fact that the units B is the largest area and it is one of the lands suitable for agricultural exploitation in this region and throughout the lands of the central and southern Iraqi alluvial plain because of the characteristics of its soil which is suitable for agriculture. Especially if we note that 83.33% of the soil samples of this physiographic were non-salty to low salinity. On the contrary, the area of weak class increases in the unit Cr in 2020 by an

Table 10. Areas of land class's according to NDVI ranges for physiographic units in the study area 1990-2005-2020 (km^2)

Physiographic units	NDVI range	Land classes	Area km^2		Area km^2		Area km^2	
			1990	Per cent	2005	Per cent	2020	Per cent
Basin soils (B)	Negative Value	Very deteriorated	0.445116	3.25	0.00	0.00	0.00	0.00
	0 – 0.19	Weak	12.355155	90.28	9.174939	67.04	5.481447	40.05
	0.2 – 0.49	Moderate	0.885129	6.47	4.510461	32.96	8.203953	59.95
			13.6854		13.6854		13.6854	
Lower Basin soils (LB)	Negative Value	Very deteriorated	0.258564	4.63	0.057943	1.04	0.00	0.00
	0 – 0.19	Weak	5.146225	92.23	5.288581	94.78	4.344449	77.86
	0.2 – 0.49	Moderate	0.175211	3.14	0.233476	4.18	1.235551	22.14
			5.58		5.58		5.58	
Depression oils (D)	Negative Value	Very deteriorated	0.422435	9.30	0.239725	5.28	0.00	0.00
	0 – 0.19	Weak	3.926743	86.47	4.301675	94.72	2.741658	60.37
	0.2 – 0.49	Moderate	0.192222	4.23	0.00	0.00	1.799743	39.63
			4.5414		4.5414		4.5414	
Crevasses oils (Cr)	Negative Value	Very deteriorated	0.134385	3.29	2.87649	69.07	0.00	0.00
	0 – 0.19	Weak	3.805939	91.34	1.28781	30.93	2.857871	68.63
	0.2 – 0.49	Moderate	0.223976	5.37	0.00	0.00	1.306429	31.37
			4.1643		4.1643		4.1643	
Irrigation Levee soils (IL)	Negative Value	Very deteriorated	0.867551	28.3	0.00	0.00	0.00	0.00
	0 – 0.19	Weak	2.189749	71.62	2.909602	95.17	1.098331	35.92
	0.2 – 0.49	Moderate	0.0	0.00	0.147698	4.83	1.958969	64.08
			3.0573		3.0573		3.0573	

area of 1.570061 km^2 at an average increase of 0.104 km^2 $year^{-1}$ and the deterioration records about 37.7% of the area of this unit. The reason may be due to the increase in the area of urban land for urban use, especially in this unit that led to the deterioration of the vegetation in it. Also, this weak degree of vegetation decreases in most of the physiographic units in 2020, as for the v. deteriorated, its area and percentage decreases in all units except for the Cr unit in 2005 until its presence was disappeared in all units in 2020. This indicates an improvement in the vegetation where the decrease in the area of v. deteriorated classis at the expense of the increase in the areas of the least degradation as moderate and weak classes. The largest increase for all units is in the area of moderate class in 2005 and 2020, and represents the largest percentage in all physiographic units, with percentages of 64.07, 59.94, 39.62, and 31.37, 22.14% for each of the units IL, B, D, Cr, and LB respectively. This is due to the human awareness of the importance of land reclamation for increasing its production. Thus, the usage of modern irrigation methods to avoid the shortage of irrigation water and water scarcity in general and to cope with high temperatures and drought climate, and therefore the area of moderate class increased at the expense of the weak and v. degradation classes. However, the vegetation coverage in all the physiographic units remains a weak prevalent in them, in addition to the presence of areas with moderate vegetation which requires taking a serious reaction for improving and reforming lands particularly the barren lands and lands of high salinity as it was found in many samples and the problem of urban sprawl, which has acquired many arable lands and some of them have been converted to practice other activities. The spatial distribution of land classes according to NDVI ranges in the study area was shown in (Figs. 6-8).

Land degradation index LDI: The values of the land degradation index and the degradation degree of soil samples for the physiographic units in the area of study in 1990-2005-2020 (Table 11) show that the largest values of the land degradation index in 1990 were 89.98 (sample No.10). The highest values for this index in 2005-2020 are 91.02 - 93.57 (No. 8 and 1 respectively) indicating light degradation in it. The chemical analysis of the samples shows sample were within the cultivated lands category with low salinity, which was reflected in light degradation. The lowest values of this index were 62.31 for sample No. 19 indicating a moderate deterioration in 1990, to be the lowest values in the two samples 24 and 25 indicating the presence of a strong deterioration in 2005-2020, respectively. This was indicated by a high salinity of soil sample 16.4 dsm^{-1} and low organic matter 0.4%. The results show the presence of these two (light, strong) deteriorations in these two years. LDI

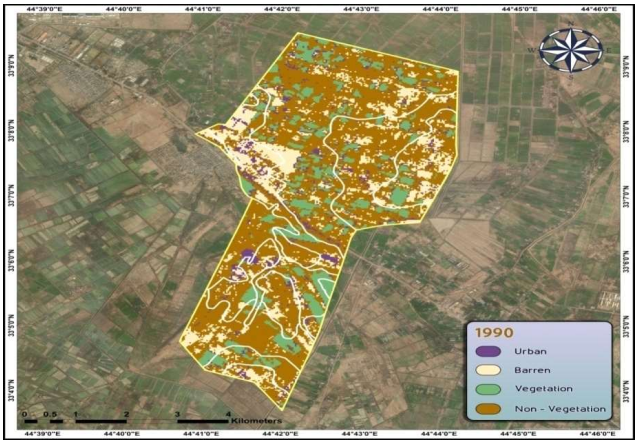

Fig. 3. Types of land cover in the study area in 1990

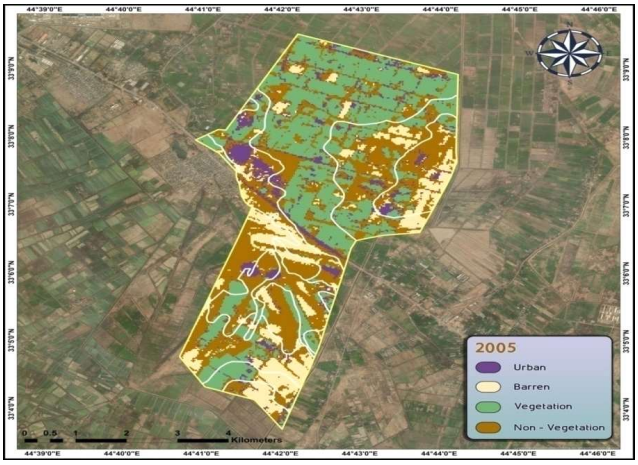

Fig. 4. Types of land cover in the study area in 2005

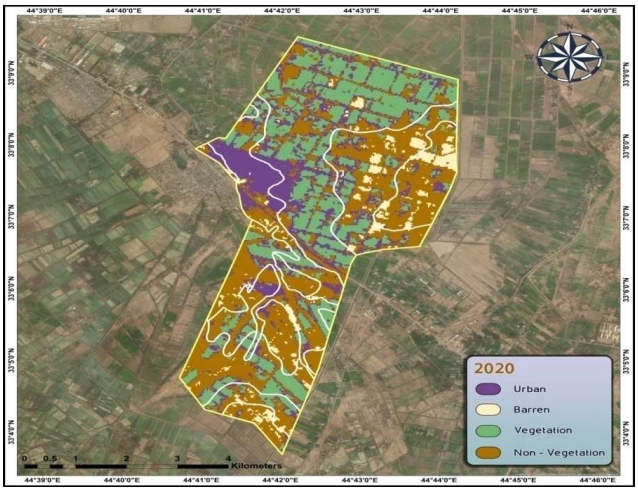

Fig. 5. Types of land cover in the study area in 2020

ranges, degrees, areas, and percentages of degraded lands in the study area were shown in (Table 12) (A: refers to the LDI).

The results show the presence of three degrees of land degradation in the study area, and their areas were arranged as, moderate>strong> light. The dominance deterioration in the study area was the moderate deterioration in general and for the three years by 100% in 1990. As well as, to clarify this degree on a chart, its range was divided into three categories, namely 60 - 70, 70 - 80, and 80 - 90 to clarify the degrees of this deterioration and its spread in the study area for this year. The area of moderate degradation decreases in 2005 by 0.298805 km^2, with an average decrease of 0.0199 km^2 $year^{-1}$, to become 30.729595 km^2 to decrease further in 2020 by 0.428322 km^2 with an average decrease of 0.02855 km^2 $year^{-1}$, so that the area of land with a moderate degree of degradation in 2020 becomes 30.301273 km^2. The strong degree of deterioration can be observed in 2005 with a small area of 0.281763 km^2, to increase by 0.241428 km^2, with an average increase of 0.01609 km^2 $year^{-1}$, and its area is 0.523191 km^2 in 2020. Further, there is a light degree of deterioration, or sometimes called non-degradation, for some lands with an improvement, even if it is very little in 2005, and this improvement will increase its area in 2020 to 0.017042, 0,203936 km^2 respectively. The increase in the area of the degree of strong deterioration amounted to 1.69%

Table 11. Values of land degradation index and the degradation degrees in the study area 1990-2005-2020

Physiographic units	Samples	LDI 1990	Degradation degree	LDI 2005	Degradation degree	LDI 2020	Degradation degree
Basin soils (B)	1	71.646065	Moderate	71.666687	Moderate	93.578056	Light
	2	80.552101	Moderate	76.241165	Moderate	76.298752	Moderate
	3	70.687233	Moderate	84.247673	Moderate	85.026161	Moderate
	4	81.573479	Moderate	88.442169	Moderate	87.492813	Moderate
	5	76.531235	Moderate	75.467201	Moderate	67.798615	Moderate
	6	74.558731	Moderate	85.909599	Moderate	89.051056	Moderate
	7	67.846153	Moderate	68.707001	Moderate	85.630104	Moderate
	8	72.610886	Moderate	91.023605	LIGHT	89.779648	Moderate
	9	74.558731	Moderate	85.076019	Moderate	85.523422	Moderate
	10	89.987221	Moderate	65.816353	Moderate	82.836327	Moderate
	11	70.687233	Moderate	66.532669	Moderate	55.484802	Strong
	12	67.846153	Moderate	60.916687	Moderate	59.295471	Strong
Lower basin soils (LB)	13	65.057037	Moderate	56.209164	Strong	72.885345	Moderate
	14	75.541878	Moderate	75.467201	Moderate	59.231884	Strong
	15	67.846153	Moderate	67.977966	Moderate	57.069653	Strong
	16	70.687233	Moderate	77.019844	Moderate	70.976707	Moderate
	17	66.910744	Moderate	76.241165	Moderate	90.353226	Light
	18	81.573479	Moderate	76.241165	Moderate	69.659248	Moderate
Depression soils (D)	19	62.318485	Moderate	81.793503	Moderate	90.069283	Light
	20	78.528862	Moderate	70.920166	Moderate	60.800385	Moderate
	21	79.537254	Moderate	72.417694	Moderate	73.983795	Moderate
	22	79.537254	Moderate	64.396164	Moderate	56.058865	Strong
	23	67.846153	Moderate	71.666687	Moderate	64.760986	Moderate
Crevasses soils (Cr)	24	75.541878	Moderate	55.551697	Strong	68.691200	Moderate
	25	69.734344	Moderate	68.707001	Moderate	55.458736	Strong
	26	72.610886	Moderate	82.606468	Moderate	67.875618	Moderate
	27	74.558731	Moderate	68.707001	Moderate	88.120903	moderate
Irrigation levee soils (IL)	28	72.610886	Moderate	84.247673	Moderate	92.490250	Light
	29	81.573479	Moderate	69.440361	Moderate	71.674553	Moderate
	30	78.528862	Moderate	70.920166	Moderate	87.039207	Moderate

in 2020, was greater than it was in the light deterioration, at 0.66%, with a decrease in the area of moderate deterioration that gives a negative indication of a deterioration in the lands of the region and that it will increase if it continues for years to come. This is due to the previously mentioned reasons, especially the increase in soil salinity of many samples in some areas, their fine textures, and their location in barren, abandoned, and unexploited areas, as in samples No. 11, 12, 14, 22, 25, and the migration of labor in agriculture, and its conversion from agricultural lands to residential, as well as the lack of state support and the problem of providing irrigation water with a decrease in water resources (Table 13).

The results show that the degree of moderate degradation is dominant in all the physiographic units for the three years, where areas generally decreased in 2005. This varied between the increase and decrease in 2020, but it constitutes the largest percentage of the area for all units, and it was 98.12, 98.07, 97.98, 97.57, 97.31 % for units IL> D> LB> Cr>B. The degree of strong degradation was at the second in terms of area, where it was absent in all physiographic units in 1990, and it appears in 2005 with

Table 12. Degrees of land degradation and its areas km^2 in the study area in 1990-2005-2020

Year	Degradation degree			Total area km^2
	Strong	Moderate	Light	
1990	0.00	31.0284	0.00	31.0284
2005	0.281763	30.729595	0.017042	31.0284
2020	0.523191	30.301273	0.203936	31.0284
		Per cent		
	Strong	Moderate	Light or	
1990	0.00	100.0	0.0	100.0
2005	0.91	99.04	0.05	100.0
2020	1.69	97.65	0.66	100.0

Table 13. Degrees of degradation and its areas km^2 for the physiographic units in the study area in 1990-2005-2020

Physiographic units	Land degradation index (A)	Degradation degree	Area km^2		Area km^2		Area km^2	
			1990	Per cent	2005	Per cent	2020	Per cent
Basin soils (B)	30 < A ≤ 60	Strong	0.00	0.00	0.022155	0.17	0.231204	1.69
	60 < A ≤ 90	Moderate	13.6854	100.0	13.646203	99.71	13.316724	97.31
	A > 90	Light	0.00	0.00	0.017042	0.12	0.137472	1.00
			13.6854		13.6854		13.6854	
Lower Basin soils (LB)	30 < A ≤ 60	Strong	0.00	0.00	0.096572	1.74	0.104525	1.87
	60 < A ≤ 90	Moderate	5.58	100.0	5.483428	98.26	5.467522	97.98
	A > 90	Light	0.00	0.00	0.00	0.00	0.007953	0.14
			5.58		5.58		5.58	
Depression soils (D)	30 < A ≤ 60	Strong	0.00	0.00	0.00	0.00	0.086346	1.91
	60 < A ≤ 90	Moderate	4.5414	100.0	4.5414	100.0	4.453918	98.07
	A > 90	Light	0.00	0.00	0.00	0.00	0.001136	0.02
			4.5414		4.5414		4.5414	
Crevasses Soils (Cr)	30 < A ≤ 60	Strong	0.00	0.00	0.163036	3.92	0.101116	2.43
	60 < A ≤ 90	Moderate	4.1643	100.0	4.001264	96.08	4.063184	97.57
	A > 90	Light	0.00	0.00	0.00	0.00	0.00	0.00
			4.1643		4.1643		4.1643	
Irrigation Levee soils (IL)	30 < A ≤ 60	Strong	0.00	0.00	0.00	0.0	0.00	0.00
	60 < A ≤ 90	Moderate	3.0573	100.0	3.0573	100.0	2.999925	98.12
	A > 90	Light	0.00	0.00	0.00	0.00	0.057375	1.88
			3.0573		3.0573		3.0573	

varying percentages in units Cr> LB> B 3.92, 1.74, 0.17 %, respectively, and it does not appear in the two units IL, D. The area of this deterioration, increases in 2020 in units D> LB> B and became 1.91, 1.87, 1.69%, respectively. Moreover, it decreases in the Cr unit and it was absent in the IL unit. This difference between the increase and decrease in areas of strong and light degradation degrees was related vegetation coverage degrees and characteristics of some measured soils in terms of salinity and organic matter values.As well as there is no light degradation in the Cr unit in which the urban land-use area increased. This difference is due to the difference in using its lands, and from practices that led to a relative increase in vegetation in some of them or to an increase in the degree of its deterioration in others. However, in general, the degrees of moderate and strong deterioration have a dominance in all the physiographic units in the area of study (Figs . 9-11).

Relative extent and severity classes: There are only two types of relative extent (according to what each degradation degree represents from a percentage of the area of its physiographic unit that it contains), which is infrequent and dominant. For severity of the degradation, only three classes of them were observed namely low (L), medium (M), very high(V.H) and was calculated according to the relationship between the degradation degree and relative extent (Table 14).

The dominance was for the infrequent relative extent at a rate of 57.14% which was represented by strong and light degrees of degradation, and it was distributed between two classes of the severity of the degradation, namely medium (M) 3.1 and low (L) 1.1. As for the dominant relative extent, it was at rate of 42.85% , which was represented by the moderate degree of degradation, and it was referred to by the very high (VH) 2.5 because this degree of degradation is dominant and it stands for the largest area. The relative extent and severity classes were the same despite of the variation in degrees, due to the weak variation that was in each degradation degree over the years for the all physiographic units. Despite of the increase and decrease in areas of degradation degrees in 2005 and 2020 and remain within the same relative extent and take the same class of severity of degradation.

Correlation: The statistical package for the social sciences SPSS application was used to obtain Pearson's Correlation Coefficients between the values of the NDVI, LDI, and the physical and chemical soil characteristics (Table 15). The highest positive significant correlation relationship was for the NDVI index with the organic matter within the measured chemical characteristics of the soil samples (r = 0.797). Due to its influential and positive role in soil characteristics such as improving its permeability and density, as well as being a huge reservoir of many nutrients needed by plants, so the NDVI values were positively reflected with the values of organic matter. The results show a negative significant correlation for the values of this index with $CaCO_3$, Ec(r = - 0. 727, r = - 0.679 respectively,) As for the correlative relationship with the physical characteristics, the highest significant negative correlation is with the Bulk Density Bd (r =

Table 14. Relative extent and severity classes of land degradation of physiographic units in 1990-2005-2020

Physiographic units	Land degradation Index (A)	Degradation degree	Relative extent			Severity classes					
			1990	2005	2020	1990		2005		2020	
Basin (B)	30 < A ≤ 60	Strong	-	Infrequent	Infrequent	-	-	3.1*	M	3.1	M
	60 < A ≤ 90	Moderate	Dominant	Dominant	Dominant	2.5	V.H	2.5	V.H	2.5	V.H
	A > 90	Light	-	Infrequent	Infrequent	-	-	1.1	L	1.1	L
Lower basin (LB)	30 < A ≤60	Strong	-	Infrequent	Infrequent	-		3.1	M	3.1	M
	60 < A ≤ 90	Moderate	Dominant	Dominant	Dominant	2.5	V.H	2.5	V.H	2.5	V.H
	A > 90	Light	-	Infrequent	Infrequent	-	-	1.1	L	1.1	L
Depression (D)	30 < A ≤ 60	Strong	-	Infrequent	Infrequent	-	-	3.1	M	3.1	M
	60 < A ≤ 90	Moderate	Dominant	Dominant	Dominant	2.5	V.H	2.5	V.H	2.5	V.H
	A > 90	Light	-	Infrequent	Infrequent	-	-	1.1	L	1.1	L
Crevasses Cr)	30 < A ≤ 60	Strong	-	Infrequent	Infrequent	-	-	3.1	M	3.1	M
	60 < A ≤ 90	Moderate	Dominant	Dominant	Dominant	2.5	V.H	2.5	V.H	2.5	V.H
	A > 90	Light	-	Infrequent	Infrequent	-	-	1.1	L	1.1	L
Irrigation Levee (IL)	30 < A ≤ 60	Strong	-	Infrequent	Infrequent	-	-	3.1	M	3.1	M
	60 < A ≤ 90	Moderate	Dominant	Dominant	Dominant	2.5	V.H	2.5	V.H	2.5	V.H
	A > 90	Light	-	Infrequent	Infrequent	-	-	1.1	L	1.1	L

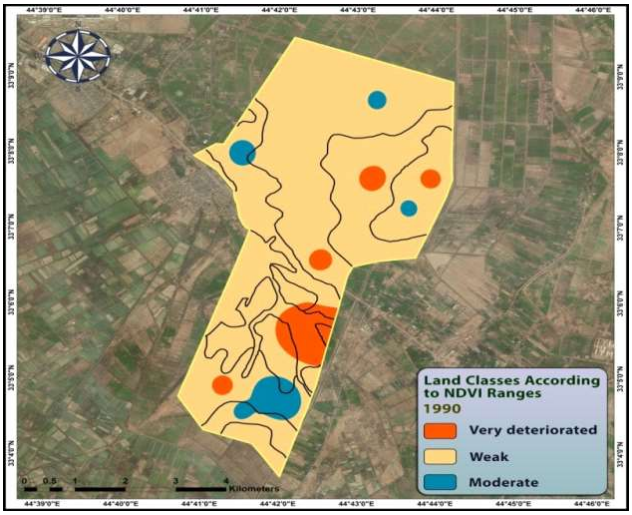

Fig. 6. Land classes according to NDVI ranges in the study area in 1990

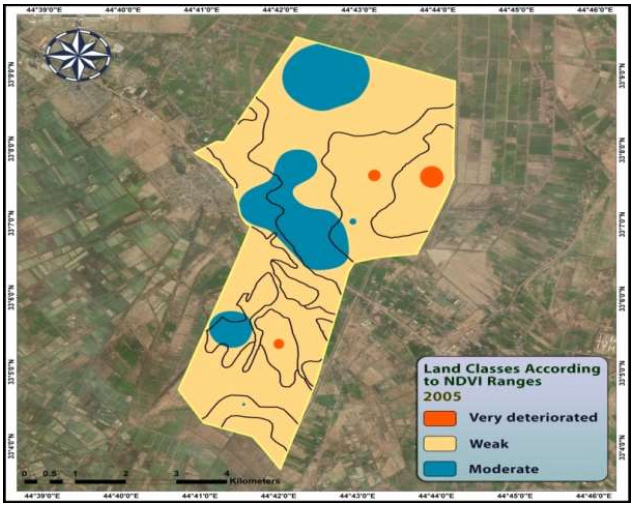

Fig. 7. Land classes according to NDVI ranges in the study area in 2005

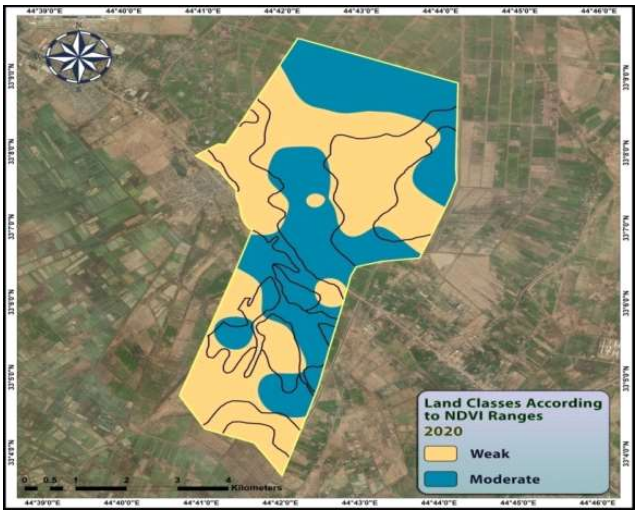

Fig. 8. Land classes according to NDVI ranges in the study area in 2020

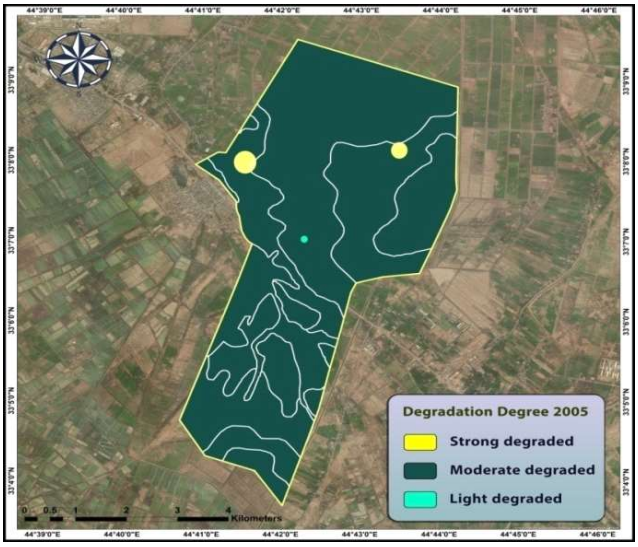

Fig. 10. Degrees of land degradation in the study area in 2005

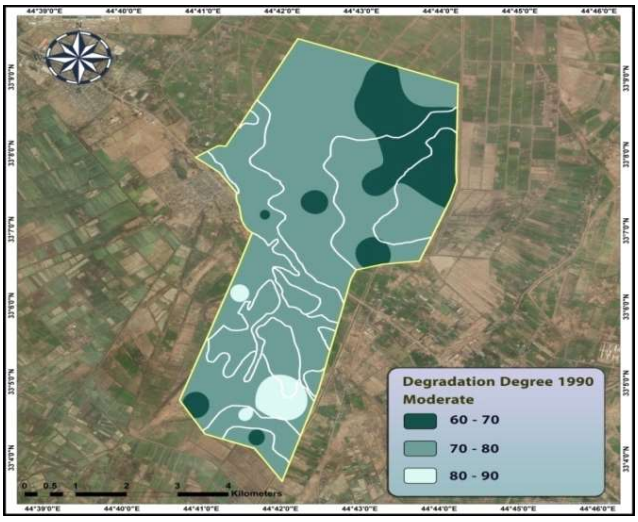

Fig. 9. Degree of moderate land degradation and its gradations in the study area in 1990

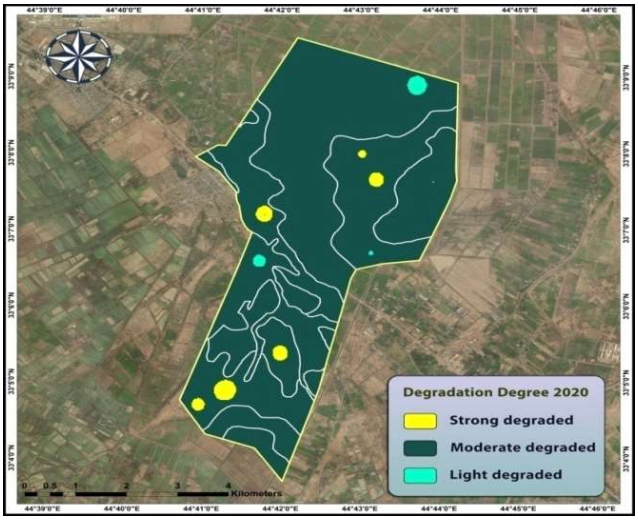

Fig. 11. Degrees of land degradation in the study area in 2020

Table 15. Pearson's correlation coefficients between NDVI, LDI indices values and soil properties

Correlations												
	NDVI	LDI	Clay	Silt	Sand	Bd	pH	EC	OM	CaCo3	CEC	ESP
NDVI	1	.890**	-.514-**	.199	.202	-.856-**	.573**	-.679-**	.797**	-.727-**	-.359	-.436-*
LDI		1	-.642-**	.416*	.062	-.853-**	.606**	-.772-**	.882**	-.708-**	-.437-*	-.505-**
Clay			1	-.524-**	-.242	.537**	-.477-**	.664**	-.640-**	.666**	.724**	.411*
Silt				1	-.699-**	-.253	-.016	-.290	.374*	-.232	-.277	-.357
Sand					1	-.158	.421*	-.226	.110	-.295	-.287	.060
Bd						1	-.552-**	.788**	-.812-**	.660**	.365*	.421*
pH							1	-.579-**	.712**	-.638-**	-.195	-.265
EC								1	-.765-**	.665**	.515**	.441*
OM									1	-.806-**	-.412-*	-.533-**
$CaCO_3$										1	.560**	.345
CEC											1	.434*
ESP												1

**. Correlation is significant at the 0.01 level (2-tailed).
*. Correlation is significant at the 0.05 level (2-tailed).

- 0. 856) due to its role in the permeability of water and air and the movement and extension of plant roots, as whenever their values are higher were reflected in an environment which is unsuitable for the growth of plant .The correlative relationship of the LDI values shows higher value indicates an improvement in the degree of degradation, so it is a positive significant correlative relationship with the values of organic matter within the chemical properties of the soil was observed(r = 0.882). The organic matter appears in supporting and improving the characteristics of soil and reducing its deterioration, even if its percentage is low, and a negative significant correlation with the values of Ec and $CaCO_3$ (r = - 0.772, r = - 0.708, respectively). The role of soil salinization in land degradation appears as one of the environmental problems in irrigated areas, which if left without proper management, will get worse and expand continuously. Finally, the correlation of LDI values with the physical characteristics of the soil, indicate the highest negative significant correlation with the bulk density (r = - 0.853). The managing the land, such as plowing, fertilizing, and creating drainage contributes in limiting the deterioration of soil properties, which were reflected in good plant growth.

CONCLUSION

The largest area for the land cover types in the area of study and in all the physiographic units is still the non-vegetation (NV) and for the three years among the other types which are vegetation (v), Barren (Ba) and (Urban (U) with a clear increase in the area of urban lands for all physiographic units in 2005-2020. Still there are Barren areas which soil suffers from a lack of the organic matter and high salinity especially at LB and D units. The area of land with moderate class according to NDVI ranges increases in 2005 and 2020 for the physiographic units, but despite this, the dominance is for the weak class for all units indicating that the area of study is still suffering from deterioration of vegetation in it. Three degrees of land degradation were found, the dominance is for the degree of moderate degradation for the three years, and a strong degree of degradation which is higher than the light degree of deterioration that appears in 2005-2020, and they were distributed among the physiographic units with weak differences between them, while these two types disappear in 1990. The area of study is still suffering the same types of the severity of deterioration for the three years, which are low, medium and very high. The importance of the organic matter and its effect on the degradation of vegetation and land appeared through a high positive significant correlation of NDVI, LDI and organic matter and a high negative significant correlation appears with the bulk density values with NDVI and LDI.

REFERENCES

Abdul-Ameer HK, Wheib QA and KHudhair DS 2019. Spatial distribution of some nutrients and biomass for the large musayyib project. *Plant Archives* **19**(2):733-739.

Abdullatif RK 2019. Relationship of spectral reflectance and NDVI to some soil properties of bricks factories soil in Nahrawan area, Baghdad Iraq. *Iraqi Journal of Agricultural Sciences* **50**(3): 793-799.

Asfaw E, Suryabhagavana KV and Argaw M 2018. Soil salinity modeling and mapping using remote sensing and GIS: The case of Wonji sugar cane irrigation farm, Ethiopia. *Journal of the Saudi Society of Agricultural Sciences* **17**: 250-258.

Comber A 2008. Editorial: Land use or land cover. *Journal of Land Use Science* **3**(4):199-201.

Daoud JM 2015. *The book of foundations and applications of remote sensing*, Chapter V-applications of remote sensing in agriculture: 115-117.

Desmond OA, Kabo-bah AT, Nkrumah PN, and Murava RT 2013.Evaluation of NDVI Using SPOT-5 Satellite Data for North Ghana. *Environmental Management and Sustainable Development* **2**(1): 167-171.

Fadhil AM 2009. Land Degradation Detection Using Geo-Information Technology for Some Sites in Iraq. *Journal of Al-Nahrain University* **12**(3): 94-108.

Gobin A, Hien LTT, Hai LT, Linh PH, Thang NN and Vinh PQ 2020. Adaptation to Land Degradation in Southeast Vietnam. *Land* **9**(302): 1-25.

Meng J, Du X, and Wu B 2013. Generation of high spatial and temporal resolution NDVI and its application in crop biomass estimation. *International Journal of Digital Earth* **6**(3): 203-218.

Shalaby A and Tateishi R 2007. Remote sensing and GIS for mapping and monitoring land cover and land-use changes in the northwestern coastal zone of Egypt. *Applied Geography* **27**(1): 28-41.

Shallal JK, AI-Hasan AM, and Jassim AM 2007. The use of normalized differences vegetation index in the determination and evaluation of degradation status of vegetation cover in Sinjar Mountain / Ninevah Governorate. *Iraqi Journal of Earth Sciences* **7**(2): 1-14.

Shrestha DP and Zinck JA 2001. Land use classification in mountainous areas: Integration of image processing, digital elevation data and field knowledge (application to Nepal). *International Journal of Applied Earth Observation and Geo information* **3**(1): 78-85.

Zhao G and Meng Y 2010. Remote sensing image based information extraction for land salinized degradation and its evolution: A case study in Kenli county of the Yellow River Delta. *Sixth International Conference on Natural Computation* **8**(1): 4199-4203.

Received 21 March, 2021; Accepted 30 August, 2021

Indian Journal of Ecology (2021) 48(6): 1611-1620

Manuscript Number: 3422
NAAS Rating: 5.79

GIS-Based Projected Land Use: A Case Study of Dhanbad District, Jharkhand, India

S.E. Saranaathan and S. Vaishaly[1]

School of Civil Engineering, SASTRA University, Thanjavur-613 401, India
[1]School of Ecology and Environment, Nalanda University, Rajgir-803 116, India
E-mail: esaranathan@yahoo.co.in

***Abstract*:** Coal mining in the Dhanbad district has resulted in ecological imbalance in land degradation, deforestation, deterioration of soil, air and water pollution etc. There is a need to monitor and plan in the mining district. The present study mainly focuses on the use of remote sensing and GIS for sustainable land use. The multi-spectral and multi-temporal satellite imageries and corresponding to the survey of India toposheets 73I and 72L were interpreted. Thematic maps like land use, geomorphology, soil, contour, slope, wasteland etc., were prepared after field and laboratory studies. Seven aspects of land use planning have been investigated viz. i) assessment of water potential zones, ii) identification of water recharge areas, iii) mapping the land degraded areas due to mining and soil erosion, iv) categorisation of agricultural water quality zones, v) classification of land capability and suitability classes, vi) wasteland development assessment, vii) evaluation of afforested and forest lands. Based on the above inferences, a comprehensive spatial model on the projected best land use of the Dhanbad district has been generated. As per the analysis, 24% of the land is suitable for the double-crop area, and 47% is the best for single and other crops. Among the 9% of Reserved Forest, about half of the land has been demarked suitable for forest plantation. Nearly 2% of the area is apt for rural/urban development, and 3% of the mining area could be reclaimed for grazing and horticultural development. The proposed model has a synchronising disposition with the regional land use outlook if implemented.

Keywords: Remote Sensing, GIS, Land use, Land suitability, Best land use

Overexploitation of available bio-resource is done to meet the growing demands of population growth. Lal and Pierce (1991) estimates, per capita arable land, which was 0.3 ha during 1986, may decline to 0.15 ha by 2050. Land management using the scientific method is important to assess the potentials and constraints of a given land for agricultural needs. The intensive agricultural practice induced a decline in soil fertility and erosion associated with low input forming against a background of overexploitation of natural resources. Dhanbad is one of the vital coal mining districts in the Jharkhand state of India has a long history of coal mining, which is dated back to a century. Due to unplanned mining before nationalization, an appreciable amount of ecological disturbances in and around mining areas in this district has been significantly witnessed. Sustainable development calls for optimal utilization of the land and water resources based on their potential and limitations. Many authors have demonstrated its potential in various facets of mining activities viz. land-use changes, the environmental impact of mining, land degradation etc. (Dwivedi et al 2006, Sarkar et al 2006, Simmons et al 2008, Njoku 2018, Debashri Garai and Narayana 2018, Tuyen et al 2019, Kamga et al 2019). The present study has attempted to identify the best land-use practices in the Dhanbad district using spatial and non-spatial data. Based on geology, geomorphology, soil, drainage density, slope and aspect, lineament density, water quality and water potential (1996), a proposed best land use has been suggested to achieve a maximum return in agricultural production and ecological conservation.

MATERIAL AND METHODS

Study area: Dhanbad district is one of the mineral-rich provenances in India and locates in Jharkhand state. It locates between 86° 06' 11" E to 86° 50' 26" E longitude and 23° 38' 58" N to 24° 03' 30" N latitude (Fig. 1) and spreads over 2057 sq. km area. Damodar and Barakar rivers dominate the drainage network of the region. The study area experiences a sub-tropical climate with dry summer and cold winter. A significant portion of the district is covered by a metamorphic rock of the Achaean age. Sedimentary rocks as Gondwana formation occupy parts of the southern and eastern portion. Gondwana formation houses rich coal seams in various depths. The images of IRS 1B LISS I and LISS II data were acquired from Google images during November, March and October of 1990 and 1993, respectively and 2015. The toposheets of the Survey of India on a 1:50,000 scale (73I / 1, 2, 5, 6, 9, 10, 13, 14 and 72L / 8) were used as a base

reference map. Thematic maps on geology, geomorphology (Anonymous 2008), soil (1995b), land use (Anonymous 2006), contour, slope and aspect, drainage density, lineament density, wasteland map, etc., have been prepared and validated with limited field checks. All thematic maps were digitized and converted into a GIS environment. Multi-criteria overlay was the simple mathematic model for a combined analysis of various thematic maps. Each thematic layer was analyzed, and an individual score to define its suitability towards supporting best land use practice. The higher score was assigned to buried pediments; valley fills, which helps the ideal cropping pattern (Fig. 3). In contrast, hilly areas and rocky ridges were given low scores as these do not support vegetation. Likewise, each thematic layer was scored. Each thematic layer was assigned with suitable weightage value to qualify its importance and influence on the best land use concept. All these rasters formatted thematic layers were then subjected to multi-criteria overlay analysis. The methodology adopted in this study is given in the flow chart (Fig. 2). The derivative results were accumulated into defined classes in a final map to address the best practice land use. Various thematic maps were analysed in the quadtree format. The quadtree method is based on the successive division of the $2^n x 2^n$ array into the quadrant (Finkel and Bentley 1974). A region is titled by sub-dividing the array step by step into quadrants. The lowest division is the simple pixel. More details of the quadtree algorithm have been detailed by many researchers (Zhao et al 2012, Li and Ruichek 2013, Salhi and Irawan, 2015, Zhang et al 2015, Tuyel et al 2016, Ayyanna et al 2019). The quadtree method has many advantages over other methods of raster representations, and specific regions can easily be computed and analysed. Different GIS quad treemaps have been crisscrossed to assess the relationship status of land use patterns in the study area with various themes related to resource parameters, and cross-tabulation analysis was done (Anonymous 1995a).

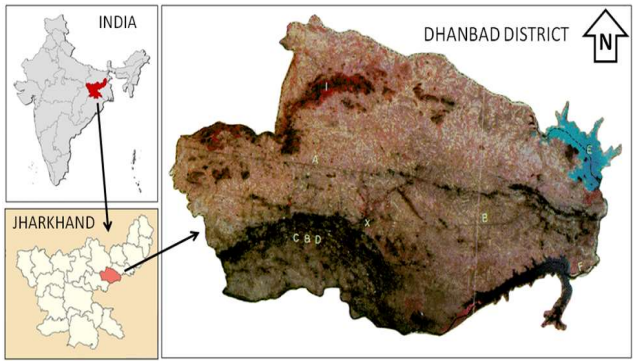

Fig. 1. Location map

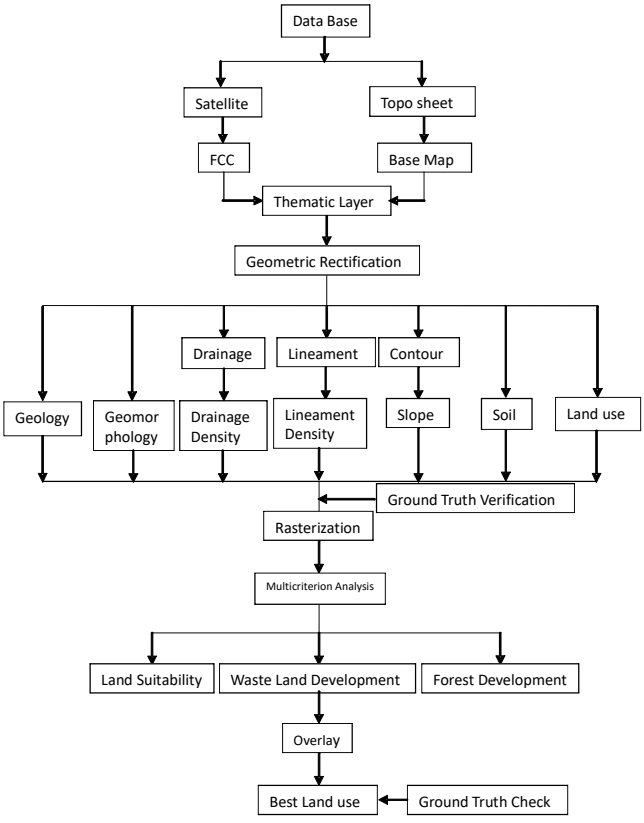

Fig. 2. Generalised flow chart

RESULTS AND DISCUSSION

Basic thematic quadtrees and their inter-relationships: Existing land use classes were delineated per ISRO-NRSC (National Remote Sensing Centre), Hyderabad classification (Anonymous 2006). In addition, thematic quadtrees on

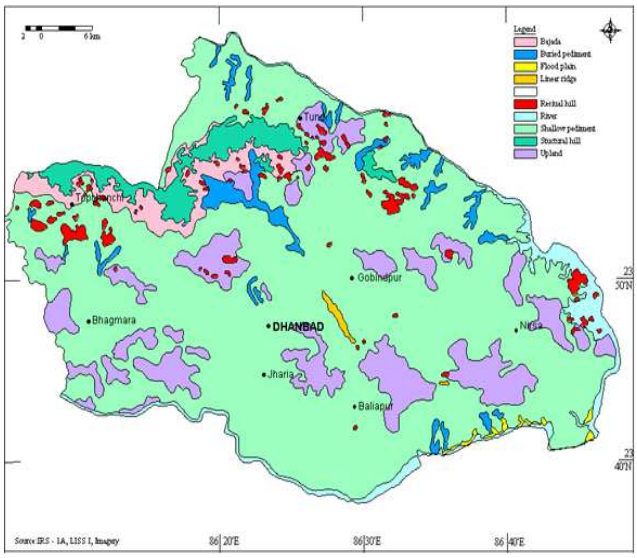

Fig. 3. Geomorphology map

geology, soil and slope were prepared and discussed below:

Existing land use: Agriculture is the dominant land use of the study area. About 72% of the total study area is occupied by cropland representing *Kharif* (July-October) and *Rabi* (October-March) seasons cultivation. The Kharif season crops are dominant and occupy nearly 58% of the study area. In addition, the double-crop area spreads over almost 14%. Under the forest cover, about 9% area represents the degraded forest and forest plantation. Scrubland and grazing lands are significantly less and amount to 2.58 and 0.66 %, respectively. Most of the settlement (semi-urban) is noticed in the southern part and spreads to about 7.92%. Though the mining area occupies only around 2.95% of the total study area, it is a prominent land-use unit in the south-western part, and the impact is felt in the other land-use units (Fig. 4).

Land use association with slope aspects: In accordance with the varied nature of elevation ranges, the slope of the entire study area has varied ranges with typical land use classes (Fig. 5). The degraded forest was found in Tundi and Topchanchi area and to occupy the above 9° slope. Land use classes like double-crop, Kharif and scrublands show significant occupancy in class 6°-9°. Croplands in this slope class depend entirely on groundwater resources (Table 1). Mining and settlement show their secondary dominance in the class of 3°-6° along with croplands and forest areas. The croplands and settlements are the dominating categories in the plain land (below 3°). Barren rocky land occupies more land in plain classes (0o to 3o and 3o to 6o).

Land use classes and geological formations: Lithology significantly influences the land use pattern (Table 2, Fig. 6). Even though the study area is constituted mainly of high metamorphic grade rocks, but an appreciable area is marked with Gondwana sedimentary formations. Mining and settlements are the dominating units in the Barakar formation, along with the *Kharif* cropland. In barren measures and Talchir class, about 59 and 73 sq. km of area is occupied by *Kharif* crop. However, it does not fully support other land use units.

Land use and Soil Thickness classes: Most cropland areas are seen within deep to intense-deep soil class .But

Table 1. Distribution of land use categories in slope classes

Land use category	0-3 (%)	3.1-6 (%)	6.1-9 (%)	9.1-12 (%)	12.1-15 (%)	15.1-18 (%)	>18 (%)	Total (sq.km)
Barren rocky land	5.22 (0.25)	2.74 (0.13)	1.17 (0.06)	0.00 (0.00)	0.00 (0.00)	0.00 (0.00)	0.00 (0.00)	9.13
Degraded forest	38.13 (1.85)	59.17 (2.88)	46.67 (2.27)	18.35 (0.89)	13.53 (0.66)	6.60 (0.32)	0.98 (0.05)	183.43
Double crop	237.98 (11.55)	30.02 (1.46)	11.19 (0.54)	0.00 (0.00)	0.00 (0.00)	0.00 (0.00)	0.00 (0.00)	279.19
Forest plantation	0.79 (0.04)	0.75 (0.04)	1.25 (0.06)	0.00 (0.00)	0.00 (0.00)	0.00 (0.00)	0.00 (0.00)	2.79
Grazing land	9.49 (0.46)	3.32 (0.16)	0.69 (0.03)	0.00 (0.00)	0.00 (0.00)	0.00 (0.00)	0.00 (0.00)	13.50
Industrial area	6.18 (0.30)	0.11 (0.00)	0.32 (0.02)	0.00 (0.00)	0.00 (0.00)	0.00 (0.00)	0.00 (0.00)	6.61
Inundated land	4.70 (0.23)	0.00 (0.00)	0.00 (0.00)	0.00 (0.00)	0.00 (0.00)	0.00 (0.00)	0.00 (0.00)	4.70
Kharif	847.11 (41.20)	235.12 (11.44)	108.89 (5.30)	10.75 (0.52)	0.08 (0.00)	0.00 (0.00)	0.00 (0.00)	1201.95
Mining	37.51 (1.82)	21.11 (1.03)	2.11 (0.10)	0.00 (0.00)	0.00 (0.00)	0.00 (0.00)	0.00 (0.00)	60.73
Plantation	0.37 (0.02)	0.00 (0.00)	0.00 (0.00)	0.00 (0.00)	0.00 (0.00)	0.00 (0.00)	0.00 (0.00)	0.37
River	69.92 (3.40)	3.78 (0.18)	1.06 (0.05)	0.00 (0.00)	0.00 (0.00)	0.00 (0.00)	0.00 (0.00)	74.76
Salt affected land	0.60 (0.03)	0.00 (0.00)	0.00 (0.00)	0.00 (0.00)	0.00 (0.00)	0.00 (0.00)	0.00 (0.00)	0.60
Scrub	38.66 (1.88)	7.27 (0.35)	6.02 (0.29)	1.12 (0.06)	0.00 (0.00)	0.00 (0.00)	0.00 (0.00)	53.07
Settlement	117.42 (5.71)	43.26 (2.10)	2.35 (0.11)	0.00 (0.00)	0.00 (0.00)	0.00 (0.00)	0.00 (0.00)	163.03
Tank	2.34 (0.11)	0.28 (0.01)	0.55 (0.03)	0.23 (0.01)	0.00 (0.00)	0.00 (0.00)	0.00 (0.00)	3.40
Total	1416.42 (68.85)	406.93 (19.78)	182.27 (8.86)	30.45 (1.48)	13.61 (0.66)	6.60 (0.32)	0.98 (0.05)	2057.26

significantly fewer croplands are associated with shallow soil areas (Fig. 7). Most wastelands are occupied with moderate soil thickness class. About 90% of the degraded forest area is coming under shallow soils (Table 3).

Derivative maps: Based on the selected thematic layers, by overlaying them through score based multi-criteria algorithms, desired derivative maps were prepared. Some of them are discussed below:

Groundwater potentiality: This is derived from various thematic maps using overlay analysis in a GIS environment. As far as the groundwater potential is concerned in the district (Fig. 8), classes like very high and high categories occupy a limited area, wherein especially these classes are seen located only in few land-use units such as Kharif, mining area and settlements with lesser area coverage about the 55 and 52% of land use units was identified in the intermediate and low class respectively. Reserve forest categories are absent in the high water potential class, but most of the forest areas are present in low water potential areas. About 23 sq. km. Area of wasteland is identified in high water potential zones, whereas, remaining areas are associated with medium and low potential zones (Table 4).

Agriculture water quality: Agriculture water quality map was derived from overlaying various water quality parameters (Saranaathan and Loveson 2018). In agriculture water quality, about 53% of the land use categories are associated with moderate quality zones (Table 5, Fig. 9). Nearly 27% of the cropland has been coming under good water quality sources, and a minimum area of about 6% is located in the lousy quality class. Most of the forest areas (about 8%) fall in good quality zones. About 2% of the wasteland is associated with good quality areas, and about 4% are coming under moderate zones, whereas the remaining wastelands are falling in bad class.

Land capability: As per ICAR classification, a land capability map was prepared (Anonymous 2012). In this district, about 5% of the land use is presented in cultivable land capability class II. For croplands, 62% of land capability class III and IV

Table 2. Land use categories in different geological classes

Land use category	Al (%)	Ba (%)	Bm (%)	Fe-sh (%)	Meta (%)	Rani (%)	Tal (%)	Total (Sq.km)
Barren rocky	0.00 (0.00)	0.00 (0.00)	0.78 (0.04)	0.00 (0.00)	7.08 (0.34)	0.69 (0.03)	0.58 (0.03)	9.13
Degraded forest	0.00 (0.00)	0.30 (0.01)	0.00 (0.00)	0.00 (0.00)	176.84 (8.60)	0.00 (0.00)	6.29 (0.31)	183.43
Double crop	2.49 (0.12)	12.01 (0.58)	0.00 (0.00)	1.82 (0.10)	249.78 (12.14)	0.00 (0.00)	13.09 (0.63)	279.19
Forest plantation	0.00 (0.00)	0.00 (0.00)	0.00 (0.00)	0.00 (0.00)	2.79 (0.14)	0.00 (0.00)	0.00 (0.00)	2.79
Grazing land	0.00 (0.00)	0.40 (0.02)	0.00 (0.00)	0.00 (0.00)	12.57 (0.61)	0.00 (0.00)	0.53 (0.03)	13.50
Industrial area	0.00 (0.00)	2.09 (0.10)	0.00 (0.00)	0.00 (0.00)	4.52 (0.22)	0.00 (0.00)	0.00 (0.00)	6.61
Inundated land	0.00 (0.00)	0.00 (0.00)	0.00 (0.00)	0.00 (0.00)	4.70 (0.23)	0.00 (0.00)	0.00 (0.00)	4.70
Kharif	2.95 (0.14)	104.74 (5.10)	58.83 (2.86)	0.23 (0.01)	939.90 (45.68)	32.26 (1.58)	63.04 (3.07)	1201.95
Mining	0.00 (0.00)	56.66 (2.75)	0.97 (0.05)	0.00 (0.00)	1.64 (0.08)	0.00 (0.00)	1.46 (0.07)	60.73
Plantation	0.00 (0.00)	0.00 (0.00)	0.00 (0.00)	0.00 (0.00)	0.37 (0.02)	0.00 (0.00)	0.00 (0.00)	0.37
River	6.86 (0.34)	4.91 (0.24)	4.62 (0.22)	0.14 (0.00)	54.35 (2.64)	2.40 (0.12)	1.48 (0.07)	74.76
Salt affected land	0.00 (0.00)	0.00 (0.00)	0.00 (0.00)	0.00 (0.00)	0.60 (0.03)	0.00 (0.00)	0.00 (0.00)	0.60
Scrub	0.01 (0.00)	1.93 (0.09)	0.27 (0.01)	0.00 (0.00)	47.01 (2.29)	3.40 (0.16)	0.45 (0.02)	53.07
Settlement	2.24 (0.11)	85.67 (4.17)	7.66 (0.37)	0.00 (0.00)	55.85 (2.71)	5.37 (0.26)	6.24 (0.30)	163.03
Tank	0.08 (0.00)	0.00 (0.00)	0.00 (0.00)	0.00 (0.00)	2.71 (0.13)	0.00 (0.00)	0.61 (0.03)	3.40
Total	14.63 (0.71)	268.71 (13.06)	73.13 (3.55)	2.19 (0.11)	1560.71 (75.86)	44.12 (2.15)	93.77 (4.56)	2057.26

Al – Alluvium, Ba – Barakar, Bm – Barren measures, Fe-sh – Ironstone shale, Meta – Metamorphic, Rani – Raniganj, Tal – Talchir

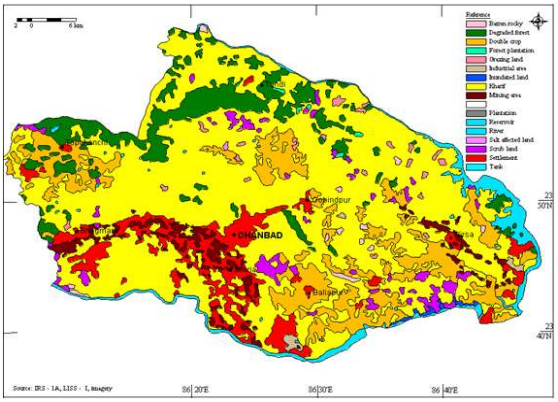

Fig. 4. Land use map

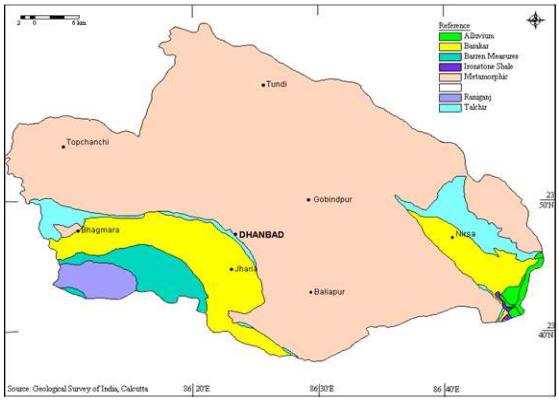

Fig. 6. Geology map

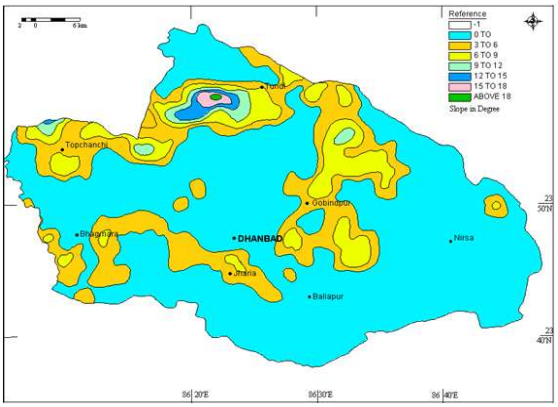

Fig. 5. Slope map

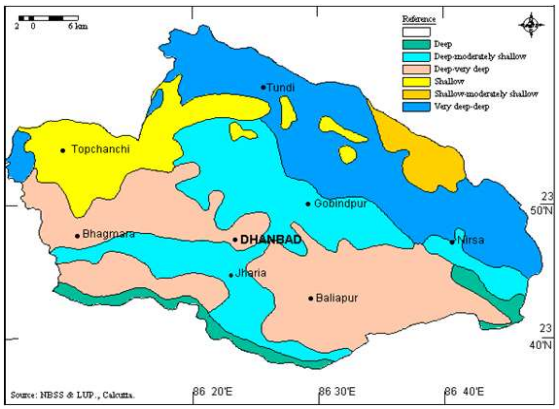

Fig. 7. Soil thickness map

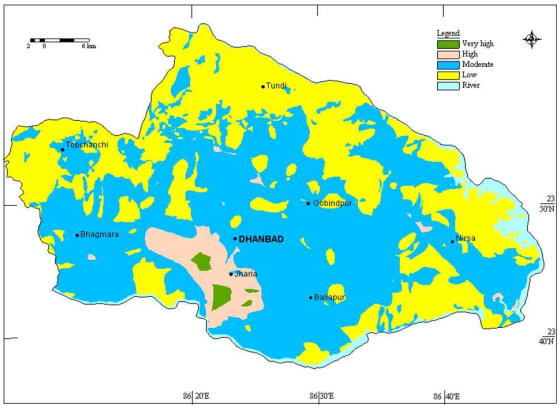

Fig. 8. Water potential map

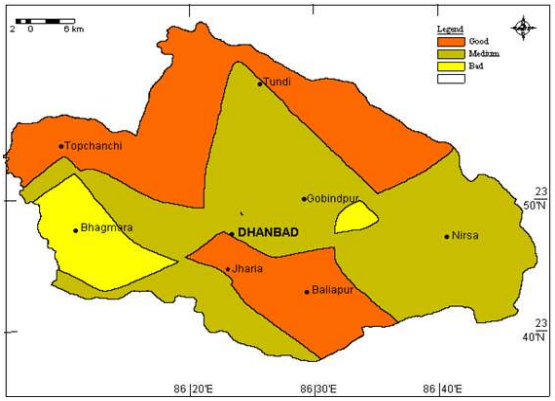

Fig. 9. Agriculture water quality map

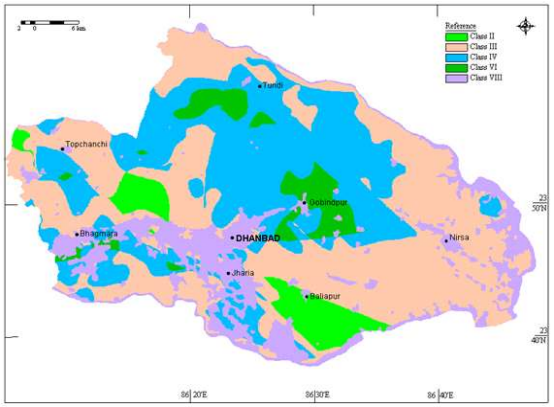

Fig. 10. Land capability map

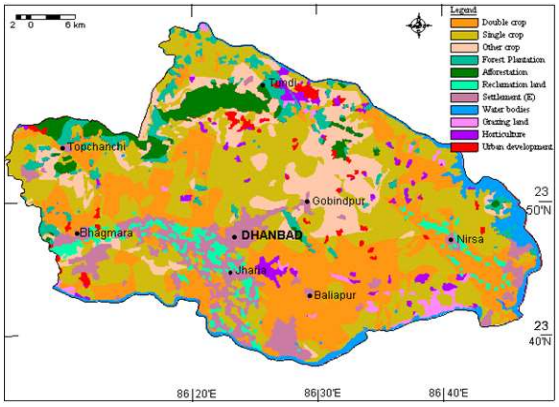

Fig. 11. Best land use map

(Table 6). Nearly 3% of the wasteland categories are associated with cultivable land capability class. Most of the mining and barren rocky areas were in non-cultivable class VIII. Reserve forest areas are occupied in an excellent cultivable class (Fig. 10).

Best practice land use: Identifying the best land use practice always depends on the availability of the natural resources and the land function dynamics (Verburg et al 2009, Aditya et al 2018). From the present study, the evaluation of various derived thematic maps like land suitability, wasteland development, forest development, agricultural water quality etc., clearly shows the availability of natural resources and their association. This encourages the thinking positively of the development strategies based on technological and scientific approaches. An integrated best land use has been derived using a multi-criteria decision by GIS analysis. In the total available agricultural land, about 25% has been identified as double crop area in Baliapur, Nirsa and Bhagmara blocks. The remaining 47% is considered the single and other crop areas. In this district, about 9% of reserved forests, half of the land has been demarked as forest plantation in foothill, and remaining areas are of afforestation in the upper zones. The analysis indicated that about 2% of the area had been considered for urban/rural development. About 3% of the mining area has become suitable for reclamation, and the remaining area has been allotted for grazing and horticultural development purposes. Figure 11 shows the spatial distribution of various best land use development classes, and their dominance is depicted as a bar diagram in Figure 12. Table 7 furnished the data about the percentages of areas of the best land use classes.

Future implications on land use in mining areas: To reinforce the management of best land-use practices in the mining area, the land resources need to be utilised scientifically and reasonably. In addition, utilisation efficiency requires enhancement through well-defined land-use planning (Sheng and Li-zhong 2009, Tuyen et al 2019). The projected model in the study is the best proper planning in the

Table 3. Land use units and various soil thickness classes

Land use category	Deep (%)	De-mod-sh (%)	De-Vd (%)	Sha (%)	Sh-mod-sh (%)	Vd-D (%)	Total (sq.km)
Barren rocky	1.53 (0.08)	2.25 (0.11)	2.61 (0.13)	0.00 (0.00)	0.00 (0.00)	2.74 (0.13)	9.13
Degraded forest	0.00 (0.00)	4.89 (0.24)	12.64 (0.61)	100.29 (4.88)	1.34 (0.06)	64.27 (3.12)	183.43
Double crop	7.01 (0.34)	47.33 (2.30)	133.61 (6.49)	46.10 (2.24)	0.00 (0.00)	45.14 (2.19)	279.19
Forest plantation	0.00 (0.00)	0.00 (0.00)	0.00 (0.00)	0.45 (0.02)	0.00 (0.00)	2.34 (0.11)	2.79
Grazing land	0.00 (0.00)	2.50 (0.12)	1.12 (0.05)	0.33 (0.02)	4.10 (0.20)	5.45 (0.27)	13.50
Industrial area	0.17 (0.00)	6.37 (0.31)	0.04 v	0.00 (0.00)	0.00 (0.00)	0.03 (0.00)	6.61
Inundated land	0.00 (0.00)	0.00 (0.00)	4.70 (0.23)	0.00 (0.00)	0.00 (0.00)	0.00 (0.00)	4.70
Kharif	32.77 (1.60)	319.16 (15.50)	367.73 (17.88)	96.34 (4.68)	52.50 (2.56)	333.45 (16.22)	1201.95
Mining	5.40 (0.26)	33.26 (1.62)	14.49 (0.70)	0.00 (0.00)	0.00 (0.00)	7.58 (0.37)	60.73
Plantation	0.00 (0.00)	0.00 (0.00)	0.37 (0.02)	0.00 (0.00)	0.00 (0.00)	0.00 (0.00)	0.37
River	15.38 (0.75)	5.27 (0.26)	8.02 (0.39)	0.00 (0.00)	10.55 (0.51)	35.54 (1.73)	74.76
Salt affected land	0.00 (0.00)	0.60 (0.03)	0.00 (0.00)	0.00 (0.00)	0.00 (0.00)	0.00 (0.00)	0.60
Scrub	2.24 (0.11)	5.79 (0.28)	31.75 (1.54)	4.73 (0.23)	0.02 (0.00)	8.54 (0.41)	53.07
Settlement	11.16 (0.54)	66.36 (3.23)	71.34 (3.48)	1.83 (0.09)	0.00 (0.00)	12.34 (0.60)	163.03
Tank	0.05 (0.00)	0.78 (0.04)	0.65 (0.03)	1.53 (0.07)	0.00 (0.00)	0.39 (0.02)	3.40
Total	75.71 (3.68)	494.56 (24.04)	649.07 (31.55)	251.60 (12.23)	68.51 (3.33)	517.81 (25.17)	2057.26

De-mod-sh – Deep-Moderately shallow, De-Vd – Deep-Very deep, Sha – Shallow, Sh-mod-sh – Shallow-Moderately shallow, Vd-D – Very deep-Deep

Table 4. Aerial spread of land use in water potential classes

Class	Very high (%)	High (%)	Moderate (%)	Low (%)	River (%)	Total (sq.km)
Barren rocky	0.00 (0.00)	0.00 (0.00)	7.30 (0.35)	1.83 (0.09)	0.00 (0.00)	9.13
Degraded forest	0.00 (0.00)	0.00 (0.00)	35.71 (1.74)	147.72 (7.18)	0.00 (0.00)	183.43
Double crop	0.00 (0.00)	2.16 (0.10)	177.47 (8.63)	99.56 (4.84)	0.00 (0.00)	279.19
Forest plantation	0.00 (0.00)	0.00 (0.00)	0.45 (0.02)	2.34 (0.11)	0.00 (0.00)	2.79
Grazing land	0.00 (0.00)	0.03 (0.00)	8.91 (0.43)	4.56 (0.22)	0.00 (0.00)	13.50
Industrial area	0.00 (0.00)	0.00 (0.00)	6.39 (0.31)	0.22 (0.01)	0.00 (0.00)	6.61
Inundated land	0.00 (0.00)	0.00 (0.00)	1.74 (0.08)	2.96 (0.15)	0.00 (0.00)	4.70
Kharif	3.96 (0.19)	32.03 (1.57)	711.50 (34.58)	454.46 (22.10)	0.00 (0.00)	1201.95
Mining area	1.63 (0.08)	21.64 (1.05)	34.90 (1.70)	2.56 (0.12)	0.00 (0.00)	60.73
Plantation	0.00 (0.00)	0.00 (0.00)	0.00 (0.00)	0.37 (0.02)	0.00 (0.00)	0.37
River	0.00 (0.00)	0.00 (0.00)	0.00 (0.00)	0.00 (0.00)	74.76 (3.63)	74.76
Salt affected land	0.00 (0.00)	0.02 (0.00)	0.45 (0.02)	0.13 (0.00)	0.00 (0.00)	0.60
Scrub land	0.00 (0.00)	0.00 (0.00)	27.09 (1.32)	25.98 (1.26)	0.00 (0.00)	53.07
Settlement	7.34 (0.36)	40.91 (1.99)	98.25 (4.78)	16.53 (0.80)	0.00	163.03
Tank	0.00 (0.00)	0.00 (0.00)	1.99 (0.10)	1.41 (0.07)	0.00 (0.00)	3.40
Total	12.93 (0.63)	96.79 (4.71)	1112.15 (54.06)	760.63 (36.97)	74.76 (3.63)	2057.26

Area in Percentage (%)

Table 5. Special spread of land use type in agriculture water quality classes

Classes (%)	Good (%)	Moderate (%)	Bad (%)	Total (sq.km)
Barren rocky	3.21	4.69	1.23	9.13
Degraded forest	130.35	45.88	7.20	182.43
Double crop	112.28	157.57	9.34	279.19
Forest plantation	2.54	0.25	0.00	2.79
Grazing land	8.16	4.65	0.69	13.50
Industrial area	0.27	6.00	0.34	6.61
Inundated land	0.33	4.37	0.00	4.70
Kharif	451.43	633.65	116.87	1201.95
Mining area	12.22	38.30	10.21	60.73
Plantation	0.00	0.37	0.00	0.37
River	16.57	58.19	0.00	74.76
Saltaffected land	0.00	0.60	0.00	0.60
Scrub land	18.44	30.35	4.28	53.07
Settlement	37.76	103.14	22.13	163.03
Tank	1.66	1.38	0.36	3.40
Total	795.22	1089.39	172.65	2057.26

light of available natural resources, which supports boosting the productivity of the areas around mining land. The study also indicates that the surrounding areas could be significantly developed if the available water resources are judiciously used. Further, one can visualise that an appreciable amount of wastelands could be rejuvenated as the supportive capacity of the land system is productive. It is observed that the quality of the soil, particularly in and around mining areas, has been fertile enough to support even for double-crop performance from present-day single crop practice. The spatial locations of such potential sites are marked in the proposed best practice model. As far as the mining and dumping sites are concerned, the foremost intend of rehabilitation is to create sufficient and sustainable post-mining land use. One of the standard practices is grazing around the mined out and dumping areas (Maczkowiak et al 2012). In general, removing and storing the topsoil layer before mining and refilling them over dumps would undoubtedly enhance the productivity index.

Table 6. Spread of land use categories in land capability classes

Class	LC II (%)	LC III (%)	LC IV (%)	LC VI (%)	LC VIII (%)	Total (sq.km)
Barren rocky	0.00 (0.00)	0.17 (0.00)	0.09 (0.00)	0.06 (0.00)	8.81 (0.43)	9.13
Degraded forest	0.24 (0.01)	59.64 (2.90)	95.34 (4.64)	27.87 (1.36)	0.34 (0.02)	183.43
Double crop	44.35 (2.16)	154.55 (7.52)	71.00 (3.46)	8.54 (0.42)	0.75 (0.04)	279.19
Forest plantation	0.00 (0.00)	0.80 (0.04)	1.99 (0.10)	0.00 (0.00)	0.00 (0.00)	2.79
Grazing land	0.53 (0.03)	6.84 (0.34)	6.13 (0.30)	0.00 (0.00)	0.00 (0.00)	13.50
Industrial area	0.00 (0.00)	(0.00) 0.00	0.00 (0.00)	0.02 (0.00)	6.59 (0.32)	6.61
Inundated land	0.01 (0.00)	0.10 (0.00)	0.00 (0.00)	0.00 (0.00)	4.59 (0.22)	4.70
Kharif	65.40 (3.18)	610.16 (29.67)	457.12 (22.23)	64.38 (3.13)	4.89 (0.24)	1201.95
Mining area	0.00 (0.00)	0.14 (0.00)	0.00 (0.00)	0.11 (0.00)	60.48 (2.94)	60.73
Plantation	0.00 (0.00)	0.37 0.02)	0.00 (0.00)	0.00 (0.00)	0.00 (0.00)	0.37
River	0.00 (0.00)	0.00 (0.00)	0.00 (0.00)	0.00 (0.00)	74.76 (3.63)	74.76
Saltaffected land	0.00 (0.00)	0.00 (0.00)	0.60 (0.03)	0.00 (0.00)	0.00 (0.00)	0.60
Scrub land	1.54 (0.07)	37.69 (1.83)	9.60 (0.47)	1.81 (0.09)	2.43 (0.12)	53.07
Settlement	0.00 (0.00)	0.00 (0.00)	0.00 (0.00)	0.10 (0.00)	162.93 (7.92)	163.03
Tank	0.00 (0.00)	0.11 (0.00)	0.11 (0.00)	0.00 (0.00)	3.18 (0.15)	3.40
Total	112.07 (5.45)	870.56 (42.32)	641.98 (31.21)	102.89 (5.00)	329.75 (16.03)	2057.26

Area in Percentage (%); LC II – Land Capability class II, LC III – Land Capability class III, LC IV – Land Capability class IV, LC VI – Land Capability class VI, LC VIII – Land Capability class VIII

Table 7. Best practice of land use classes

Classes	Area (sq.km)	Area (%)
Double crop	513.04	24.94
Single crop	697.01	33.88
Other crop	246.67	11.99
Forest plantation	91.80	4.46
Afforestation	84.36	4.10
Reclamation land	60.44	2.94
Settlement (e)	168.78	8.20
Water bodies	81.79	3.98
Grazing land	30.30	1.47
Horticulture	45.70	2.22
Urban/Rural development	37.38	1.82
Total	2057.26	

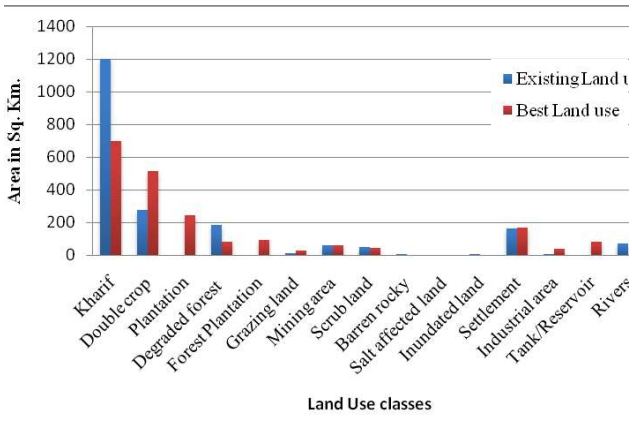

Fig. 12. Distribution of best land use classes

CONCLUSION

Dhanbad is one of India's prime coal mining areas, whereby one can witness the highest degree of land degradation in and around mining areas. The multi-spectral

and multi-temporal satellite images prepared various thematic maps on natural resources and land use. As the present scenario of the study area depicts, about 70% of the total area is occupied by cropland, with 9% of reserved forest cover. The remaining area represents wasteland, settlement and mining and mined out area. Though the mining area is negligible, the impact on cropland is significantly noticeable by air and water pollution and water resource depletion due to mining activities. About 25% of the area could be brought under double-crop performance while leaving 47% as single crop coverage. The lower slope has been demarked as a forest plantation (10,049 ha), and the reaming area remains suitable for afforestation (8,563 ha). About 2% of the total study area has been considered urban development, and 3% of the mined area becomes suitable for reclamation. Wastelands are categorized and analyzed systematically. Out of the total 14, 173, 7,808 ha can be transformed into helpful land and 6,365 ha cannot be developed. The proposed model has the potential to be balanced with the regional land use outlook. Whenever the best land-use planning around mining areas is visualized, there is a need to address the following issues:

- Elucidate the necessity of land use planning in the mined-out area - Understanding the importance of real-time scale would improve the ecological balance and production of the mined-out site.
- Elaborately examine the analogue research, the relations, similarities and difference between regional planning and local land use - The inter-relationship assessment would provide critical clues to maintain the equilibrium and helps to raise the eco-balance with regional land use potential.
- The proposed model justifies the above issues and could support the best practice of land use in the study area.

REFERENCES

Aditya SK, Smitha Asok V, Jenitha Jerome and Rajesh Raghunath 2018. Landscape analysis using GIS and remote sensing for assessing spatial pattern in forest fragmentation in Shendurney Wildlife Sanctuary, Western Ghats, India, *Indian Journal of Ecology* **45**(2): 299-304.

Anonymous 1995a. Manual of SPANS Explorer v.7.1., *PCI Geomatics*, Canada.

Anonymous 1995b. Report on Soil Quality Map and its characteristic of Damodar River Basin, *NBSS & LUP*, Calcutta.

Anonymous 1996. *Identification of Recharge area in 386 Blocks of Tamil Nadu State Using Remote Sensing and GIS*. Recharge Project, Institute of Remote Sensing, Anna University, Chennai.

Anonymous 2006. Manual of National Land use/Land Cover Mapping using Multi-Temporal Satellite Data, National Remote Sensing Agency, Hyderabad.

Anonymous 2008. *Manual of Ground Water Prospects* Mapping for Rajiv Gandhi National Drinking Water Mission, National Remote Sensing Agency, Hyderabad.

Anonymous 2012. *Handbook of Agriculture*, Indian Council of Agricultural Research, New Delhi.

Ayyanna BS, Polisgowdar A, Rama Roa and Harish Babu Bachina 2019. Land use land cover canges detection using remote sensing and geographic information system in canal Commend area, Karnataka. *Indian Journal of Ecology* **46**(4): 683-690.

Debashri Garai and Narayana AC 2018. Land use/land cover changes in the mining area of Godavari coal fields of Southern India. *The Egyptian Journal of Remote Sensing and Space Science* **21**(3): 375-381,

Dwivedi RS, Sreenivas K, Ramana KV, Reddy PR and Ravi Sankar G 2006. Sustainable development of land and water resources using geographic information system and remote sensing. *Journal of Indian Society of Remote Sensing* **34**(4): 351-367.

Finkel RA and Bentley JC 1974. Quadtrees a data structure for retrieval on composite keys, *Acta Informatics* **4**(1): 23-35.

Jeffrey A Simmons, William S Currie, Keith N Eshleman, Karen Kuers, Susan Monteleone, Tim L Negley, Bob R Pohlad and Carolyn L Thomas 2008. Forest reclaimed mine land use change leads to altered ecosystem structure and function. *Ecological Applications* **18**(1): 104-118.

Kim H, Kang S, Lee S and Min JK 2016. The efficient algorithms for constructing enhanced quadtree and using MapRedce, *IEICE Transactions of Information and System E99D* **4**: 918-926.

Lal R and Pierce F 1991. The vanishing resource. In *Soil Management for Sustainability*. Soil and Water Conservation Society U.S.A: 1-5.

Li Y and Ruichek Y 2013. Building variable resolution occupancy grid map from stereoscopic system: A Quadtree based approach, *IEEE Intelligent Vehicle Symposium Proceeding* 744-749.

Maczkowiack RI, Smith CS, Slaughter GJ, Mulligan DR and Cameron DC 2012. Grazing as a post-mining land use: A conceptual model of the risk factors. *Agricultural Systems* **109**: 76-89.

Marc Anselme Kamga, Salomon Cesar Nguemhe Files, Moyosore Oladele Ayodele, Charles Olufisayo Olatubara, Serge Nzali, Adeola Adenikinju and Muhammad Khalifa 2019. Evaluation of land use/land cover changes due to gold mining activities from 1987 to 2017 using Landsat imagery, East Cameroon, *GeoJournal* **85:** 1097-1114

Njoku C 2018 Land use effect on soil properties in Abakaliki Southeastern Nigeria, *Indian Journal of Ecology* **45**(1): 122-125.

Salhi S and Irawan CA 2015. A quadtree based allocation method for a class of large discrete Euclidean location problems. *Computer and Operations Research* **55**: 23-35.

Saranaathan SE and Loveson VJ 2018. Spatial identification of agricultural water quality in Dhanbad district, Jharkhand State, *Journal of Chemical and Pharmaceutical Research* **10**(1): 83-87.

Sarkar D, Gangopadhyay SK and Sahoo AK 2006. Soil resource appraisal towards land use planning using satellite remote sensing and GIS: A case study in patloinala Micro-watershed, District Puraliya, West Bengal. *Journal of Indian Society of Remote Sensing* **34**(3): 245-260.

Sheng J and Li-zhong L 2009. Discussion on theory and methods of land-use planning in mining area. *Procedia Earth and Planetary Science* **1**: 956-962.

Tran Thi Tuyen, Hoang Phan Hai Yen, Hoang Thi Thuy, Nguyen Thi Trang Thanh, Nguyen Kim Quoc, Indra Prakash and Binh Thai Pham 2019. Agricultural land sutability analysis for Yen Khe Hills (AgheAn, Vietnam), using Analytic Hierarchy Process (AHP) combined with Geographic Information System (GIS). *Indian Journal of Ecology* **46**(3): 445-454.

Vaccari F P, Lugato E, Gioli B, D'Acqui L, Genesio L, Toscano P, Matese A and Miglietta F 2012. Land use change and soil organic dynamics in Mediterranean agro-ecosystem: The case study of Pianosa Island. *Geoderm* **175-176**: 29-36.

Verburg PH, Van DE, Steeg J, Veldkamp A and Willemen L 2009. From land cover change to land function dynamics: A major

challenge to improve land characterisation. *Journal of Environmental Management* **90**(3): 1327-1335.

Zhang J, You S and Gruenwald 2015. Quadtree-based lightweight data compression for large-scale geospatial on multi-core CPUs, Proceeding on IEEE international conference o Big Data, *IEEE Big Data* 2015: 478-484.

Zhao X, Fan D, Wang J and Wang L 2012. Seamless expression of the global multi-resolution DEMs based on degenerate quadtree grids, *Cehui Xuebao/Acta Geodaetica et Cartographica Sinica* **41**(6): 918-925.

Received 18 August, 2021; Accepted 12 November, 2021

Indian Journal of Ecology (2021) 48(6): 1621-1626

Manuscript Number: 3423
NAAS Rating: 5.79

Impact of Pre-Monsoonal Rainfall Trend on Vegetation for Ranchi Plateau, Jharkhand, India

Amit Kumar Jha, Ajai Singh and Pratibha Warwade

Department of Water Engineering and Management
Central University of Jharkhand, Ranchi-835 205, India
E-mail: ajai.singh@cuj.ac.in

***Abstract*:** Ranchi has been chosen as the study area to study its changing rainfall pattern, its trend and correlation with vegetation cover during the pre-monsoonal season in the last 20 years. In the year 1998, the western side of the district received a good amount of rainfall but the scenario after that was observed quite alarming.In the next 20 years, the western region received very low rainfall except in the years 2005 and 2014. During 2005, Ranchi received good rainfall in the south-western region of the district. The Eastern region has a good amount of green cover received plenty of rainfall consistently in the last two decades. The central part is the most urbanized zone of the study area having the least green cover. This zone has never received good rainfall in the last two decades. On the contrary despite having good vegetation over the north-western side; the region never received good rainfall. The Non-Parametric trend analysis for the last 20 years shows an overall increase in rainfall with 0.141625 mm/year and the analysis for the last 117 years showed a significant positive trend in the pre-monsoonal month of February, March, and April while May showed a negative trend. The maximum decrease in rainfall was for February (-0.1804803 mm year^{-1}) and the minimum (-0.0007663818 mm year^{-1}) during April. The overall trend of rainfall during the pre-monsoonal season (March-May) was found increasing (0.02156622 mm year^{-1}). The rainfall variability pattern showed the maximum value of CV (105.7%), whereas pre-monsoonal rainfall exhibited the minimum value of CV (60.52%). In general, a high variation of CV was observed which showed that the entire region is very vulnerable to droughts and floods. Disturbance in uniformity of distribution in rainfall pattern and extreme event cases over the district during the pre-monsoonal season in the last two decades was observed.

Keywords: Trend analysis, Temporal series, Non-parametric, CV, Pre-monsoon

Ranchi was famous for its core tropical weather, the city used to experience frequent rainfall almost after every sunny day (convectional rainfall), but the scenario has been changing continuously. Presently it is experiencing rainfall in patches of weeks with huge unevenness and irregularities. There are several factors responsible for this and forests are replaced by pasture or crops, evapotranspiration of moisture from soil and vegetation are often diminished, leading to reduced atmospheric humidity and potentially suppressing precipitation. Spracklen et al (2012) observed that for more than 60% of the tropical land surface (latitudes 30 degrees south to 30 degrees north), air that has passed over extensive vegetation in the preceding few days produces at least twice as much rain as air that has passed over little vegetation. The empirical correlation is consistent with evapotranspiration maintaining atmospheric moisture in the air that passes over extensive vegetation. The severer change in rainfall trend and its variability resulted in the events such as flood and drought (Srivastava et al 2015). Any insignificant changes in the intensity of rainfall or amount impose an intense challenge to the economy of rural people since its main livelihood depends on agriculture which mostly relies on southwest monsoon (Kumar and Jain 2011). Rainfall trend analysis at different spatial and temporal time scales becomes an important concern as it is directly connected to global climate change. Global surface warming is occurring at the rate of 0.74 ± 0.18°C during the period 1906–2005 (IPCC 2007) and future climate variability is likely to affect the agriculture, freshwater availability, livelihood security and rapid melting of the glacier. Rainfall is an important variable that shapes the spatial and temporal pattern of climatic variability over a region and also provides significant information about the management of water resources in the agricultural production system (Khavse et al 2015, Lyra et al 2014, Sobral et al 2018 a,b). The present study is aimed to assess monthly pre-monsoonal rainfall trend variation as well as its yearly changing pattern with change in vegetation cover over Ranchi district of Jharkhand state (India) during the period 1998-2018 using non-parametric methods and remote sensing techniques.

MATERIAL AND METHODS

Study area: Ranchi is situated on the Chotanagpur plateau of eastern India having an area of 5097 $_{km}^{2}$. It lies between 22°52′–23°45′ North latitude and 84°45′–85°50′ East longitude. It is situated at an altitude varying from 500 to

700m above the mean sea level. The district is well known for its natural beauty. The district is bisected by the tropic of cancer and characterized by subtropical climate. The area receives a good amount of annual rainfall. The annual average rainfall is around 1394 mm; 90% of the total annual rainfall occurs because of the southwest monsoon during June to October. District also experiences unique convectional rainfall (equatorial feature) during the summer season (Fig. 1).

Data used:

- The monthly rainfall data for the period 1998–2018 of Ranchi district were obtained from the website http://www.india water porta l.org/met-data/, India metrological Division (IMD), Pune and Department of Agro-Meteorology to evaluate pre-monsoonal rainfall trend in data series.
- Landsat-5TM, Landsat-7ETM and Landsat-8OLI dataset with a spatial resolution of 30 m were used to prepare the NDVI map for the year 1998, 2003, 2008, 2013 and 2018. The details of the data used for the preparation of NDVI (Table 1).
- Landsat-8OLI dataset with a spatial resolution of 30m was used to prepare the LULC map for the year 2018 (Table 2).
- TRMM dataset with a resolution of 25° was used to prepare a pre-monsoonal rainfall map for the years 1998 to 2018. Total 21 rainfall map was prepared (Table 3).

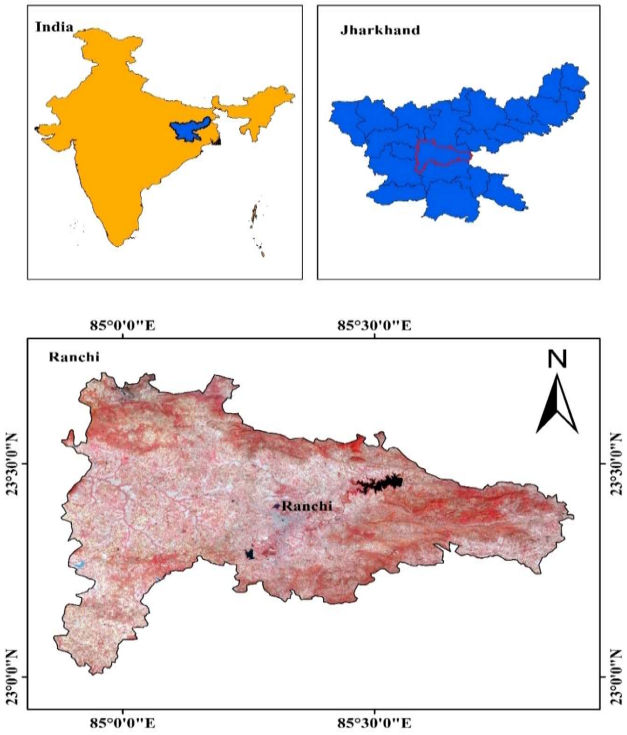

Fig. 1. Location map of the study area

Preparation of NDVI: The forest cover of the Ranchi district was mapped using Arc-GIS. The Normalized Differential Vegetation Index (NDVI) is a standardized vegetation cover index for extracting the vegetation cover areas. The NDVI extracts the vegetation cover by measuring the difference between near-infrared (NIR) and red bands. NIR band reflects the vegetation and Red Band absorb the vegetation cover areas. The value of NDVI is ranging from -1 to +1, the positive value indicates the vegetation cover areas and the negative values indicates the other features such as water bodies, built-up areas, wasteland etc. The NDVI uses the NIR and Red Band images in the equation for extraction of the vegetation and is given by

$$NDVI = \frac{NIR - R}{NIR + R} \qquad (1)$$

NIR is the reflectance in the near-infrared band (760-900 nm), which is strongly reflected by leaf cellular structures; while, R is the reflectance in the red band (630-690 nm) which is characterized by chlorophyll content absorption at the canopy. In the present research, Landsat 8 satellite imagery

Table 1. Data used for NDVI mappreparation

Satellite sensor	Year	No. of bands	Spatial resolution (M)	Projection	Path	Row	Data source
Landsat-5TM	1998	7	30	UTM45	140	044	http://earthexplorer.usgs.gov
					141	044	
Landsat-7ETM^{+}	2003	8	30	UTM45	140	044	
					141	044	
Landsat-5TM	2008	7	30	UTM45	140	044	
					141	044	
Landsat-8 OLI	2013	11	30	UTM45	140	044	
					141	044	
Landsat-8 OLI	2018	11	30	UTM45	140	044	
					141	044	

of 2018 was used for extracting the vegetation cover areas. The Landsat 8 satellite image was downloaded from the USGS earth explorer website (https://earthexplorer.usgs.gov/). The satellite image was processed and atmospheric corrections were carried out with QGIS. All the bands of satellite imagery were layer stack into a single image by using the ERDAS Imagine 2014. Different maps were prepared by using ArcGIS 10.3. The NDVI Map at an interval of 5 years (1998, 2003, 2008, 2013 and 2018) was prepared using Landsat-5TM, Landsat-7ETM and Landsat-8OLI dataset, to analyze the pattern of change in the vegetation cover over the Ranchi district. NDVI map for the respective years is shown in Figure 2. The FCC map for the considered year of NDVI is illustrated in Figure 3.

LULC map preparation: Land Use Land Cover map of the Ranchi district was prepared for the year 2018 using the Landsat-8OLI dataset. Land use refers to man's activities and the various uses which are carried on land. Land cover refers to natural vegetation, water bodies, rocks/soils, artificial cover and others resulting due to land transformations. The steps followed for the preparation of the map is summarized in Figure 4. The final LULC map generated for the study area is depicted in Figure 5. The area statistics of the prepared LULC map is given in Table 4.

Rainfall map preparation: The tropical rainfall measuring mission (TRMM) was started in the year 1997. It is a joint programme of JAXA, (Japanese Space Agency) and NASA (American Space Agency). The Pre-monsoonal rainfall map for the study area was prepared using the TRMM dataset. The map was prepared to analyze the annual variation of pre-monsoonal rainfall over the Ranchi district for the last 2 decades. Total 21 maps were prepared (Fig. 6).

Statistical test for trend analysis: Trend analysis is an important tool helps in the effective planning and management of water resource. Trend analysis of hydrological variables such as rainfall, direct runoff and discharges provides information on the possibility of the change tendency of the variables in the future (Dinpashoh et al 2013). The parametric and non-parametric methods are widely used to analyze the trend in the data set. In this study, Sen's estimator (Sen 1968) was used to determine the magnitude of the trend in the time series while Mann–Kendall (MK) test (Mann 1945, Kendall 1975) was used to analyze the statistical significance of the trend in the rainfall data series. All the statistical analyses of rainfall data were done using an excel spreadsheet and XLSTAT software.

RESULTS AND DISCUSSION

The rainfall maps obtained for the years 1998-2018, clearly depicts that in 1998 the western side of the district received a good amount of rainfall but the scenario after that was observed quite alarming. In the next 20 years, the region received very low rainfall except in the years 2005 and 2014. During 2005, the study area received good rainfall in the south-western region of the district. The rainfall pattern observed in the eastern region is quite consistent throughout the two decades. The Eastern region received plenty of rainfall consistently in the last two decades. This supports the fact of positive correlation between the presence of dense forest cover and a good amount of rainfall. NDVI maps clearly show an ample amount of green cover on the eastern side (Fig. 2). The central part never has received good rainfall in the last two decades. The LULC map of the district clearly shows that this is the most built-up/ Urbanized zone of the district with having least green (Fig. 5). On the contrary, despite having good vegetation over the north-western side, the region never received good rainfall. The computed value of statistics such as mean, standard deviation (σ) and coefficient of variation CV, % of rainfall data series for every month under consideration are presented in Table 7. Results of the Mann–Kendall test (Z-statistics) and Sen's slope estimator for rainfall series for March, April and May during

Table 4. Area statistics of LULC

Pixel count	Resolution in meter	Class	Area in km^2
838751	30 × 30	Dense vegetation	755
2104330	30 × 30	Agricultural land	1894
241368	30 × 30	Built-up land	217
432774	30 × 30	Sparse vegetation	389
608519	30 × 30	Barren land	548
72031	30 × 30	Water body	65

Table 2. Data used for preparation of LULC map

Satellite sensor	Year	No. of bands	Spatial resolution (M)	Projection	Path	Row	Data source
Landsat-8 OLI	2018	11	30	UTM45	140	044	http://earthexplorer.usgs.gov

Table 3. Data used for preparation of rainfall map

Data	Product detail	Resolution	Duration	Data Source
TRMM	3B43 Monthly accumulate precipitation estimates	0.25°	1998-2018	https://giovanni.gsfc.nasa.gov/giovanni/

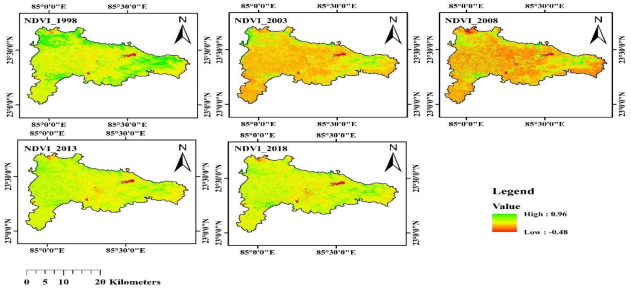

Fig. 2. NDVI map of study area

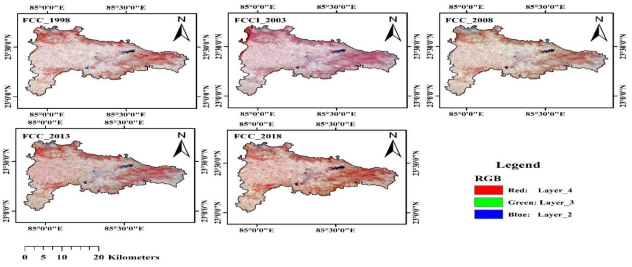

Fig. 3. FCC map of study area

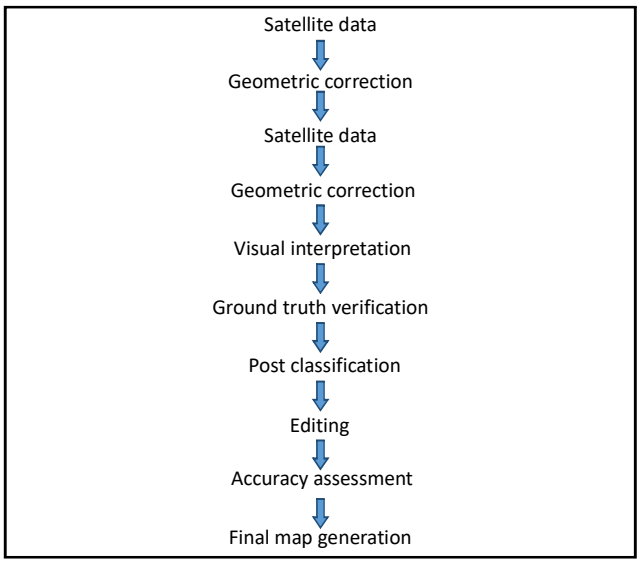

Fig. 4. LULC map generation steps

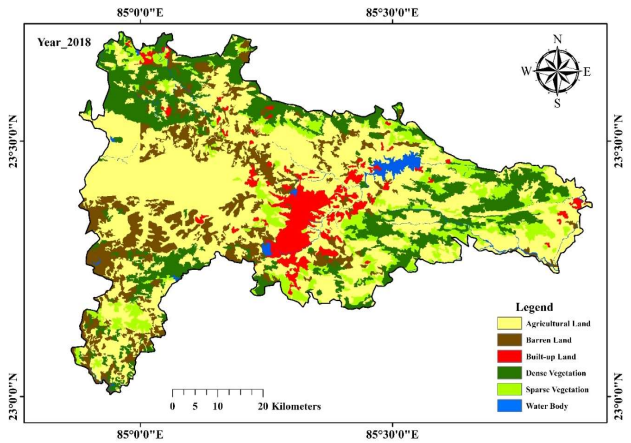

Fig. 5. LULC map of Ranchi district

1998–2018 are presented in Table 5. While the estimation of the Mann–Kendall test (Z-statistics) and Sen's slope for the trend of the last 117 years is presented in Table 6. The positive and negative values of Z-statistics indicated

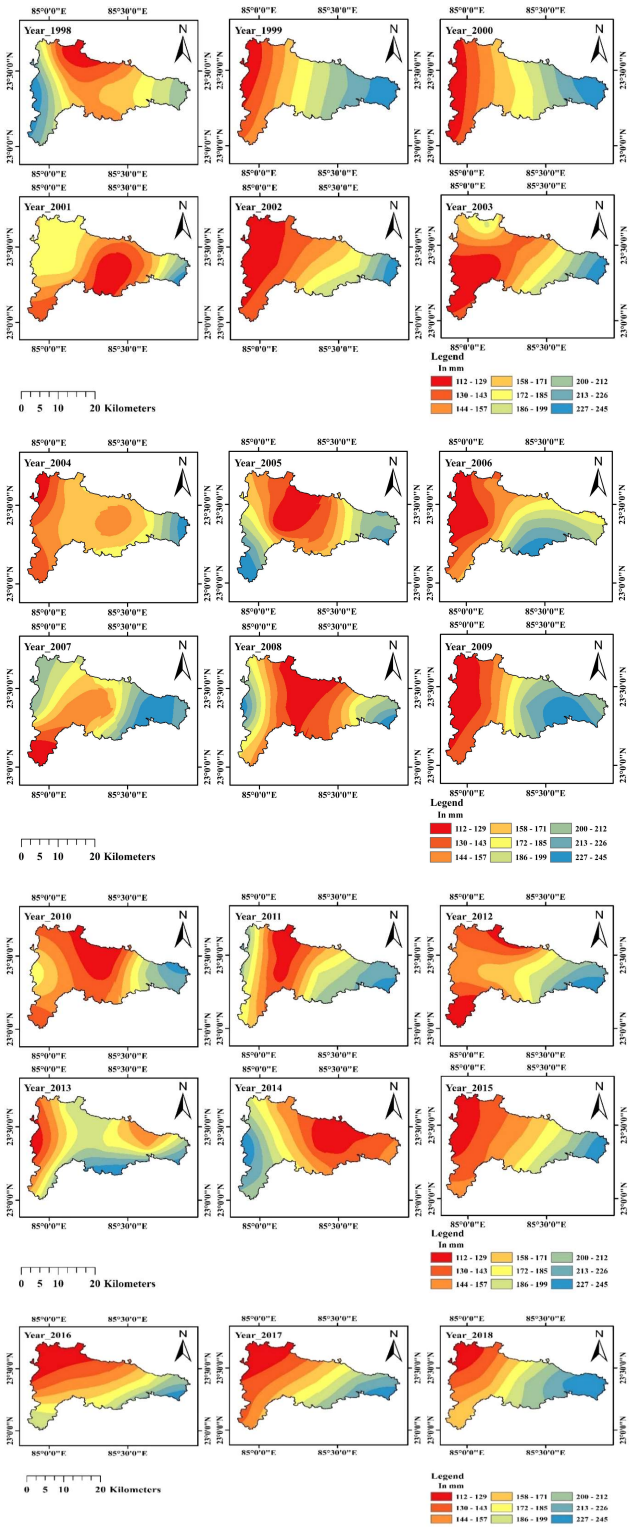

Fig. 6. Rainfall map (1998-2018) of Ranchi District

Table 5. Result of Rainfall trend analysis for pre-monsoonal season and months (at 5% significance level) over Ranchi district (1998–2018)

Parameters	March	April	May	Pre-monsoonal (March-May)
Z statistics value	0	0.57374	0.51335	0.21138
Sen's slope Confidence level -95%	0	0.33188	0.485873	0.141625

Table 6. Result of Rainfall trend analysis for pre-monsoonal season and months including January and February (at 5% significance level) over Ranchi district (1901–2017)

Parameters	January	February	March	April	May	Pre-monsoonal (March-May)
Z	1.204	-3.0154	-0.8057	-0.0282	1.8633	0.67608
Sen's slope Confidence level -95%	0.03589	-0.18048	-0.02546	-0.00076	0.12962	0.02156

Table 7. Mean, Standard Deviation (σ) and Coefficient of variation (CV) for different months and season under consideration for the period 1901-2017

Month/Season	Mean	Standard Deviation (σ)	Coefficient of Variation (CV)
March	23.50	24.86	105.7
April	21.34	21.04	98.62
May	39.99	35.04	87.62
Pre-monsoonal (March-May)	28.27	17.11	60.52

increasing and decreasing trends, respectively. The last 20 year's trend showed an overall increase in the rainfall during the pre-monsoonal season with a Z-statistics value of 0.21138 and Sen's slopes estimated value of 0.141625 mm/year. The results obtained for the analysis of the last 117 years was different. February, March and April showed significant negative trends while May indicated insignificant positive trends. The values of Z-statistics were -3.0154, -0.80579, -0.028268 and 1.8633, for February, March, April and May respectively, while the value of Z-statistics for the overall pre-monsoonal season was found 0.67608. February showed the highest negative value for the Z-statistics whereas April showed the least negative value of Z-statistics. The Sen's slope estimated value for the rainfall trend series was found negative for February (-0.1804803 mm/year), March (-0.02546635 mm/year) and April (-0.0007663818 mm/year) while the positive value was observed for May (0.1296284 mm/year). Chandniha et al (2017) identified positive Z-statistics value for pre-monsoon rainfall time series over the region of Ranchi district between 1901 and 2014. Sharma and Singh (2017) also observed an increasing trend over the state of Jharkhand in pre-monsoon and post-monsoon rainfall while winter, monsoon and annual rainfall series showed decreasing rainfall trends during 102 years.

Rainfall variability patterns: The result of rainfall variability pattern is calculated using CV for the study period for Ranchi district shows high inter-seasonal (pre-monsoonal) variation. Rainfall in March showed the maximum value of CV (105.7%), whereas overall pre-monsoonal (March-May) rainfall exhibited the minimum value of CV (60.52%). The value of CV for rainfall during February, March, April and May were 93.24, 105.7, 98.62 and 87.62% respectively (Table 7). The CV (105.7%) is higher than that of rainfall in April (98.62%), rainfall in February (93.24%) and rainfall in May (87.62%) which shows the more inter-seasonal (pre-monsoonal) variability of rainfall in March than rainfall in other months of pre-monsoon. The degree of rainfall variability was found high during February, March, April and May, whereas overall pre monsoonal (March-May) rainfall showed a low degree of rainfall variability. Overall, the entire months during the pre-monsoonal season reflect high rainfall variation.

CONCLUSIONS

The results showed that the last 20 years received an increasing amount of rainfall in the district during the pre-monsoonal season. But the pattern of rainfall has changed. The western and the central part of the district has the least dense forest cover is receiving less rainfall, on the other hand, the eastern side of the district receives a good amount of rainfall throughout the last two decades. This supports the fact of good precipitation in the more vegetated zone; as this part of the district has a considerable dense forest cover. Therefore, it may be concluded that although rainfall during the season has increased its uniformity of distribution is disturbed. The 117 years of rainfall trend through the Sen's slope test has shown some very interesting results in the pre-monsoonal season. February, March and April have shown a negative trend in their values, out of which the highest negative trend slope line was

observed in February and the only positive trend line was observed in May. There was a significant variation in rainfall trends during the period of the past 117 years. The rainfall variability analysis (CV) indicated high inter-seasonal (pre-monsoonal) variation. Rainfall in March shows the maximum variation in rainfall (105.7%), whereas overall pre-monsoonal (March-May) rainfall exhibited minimum rainfall variation (60.52%). In general, high inter-seasonal variation in rainfall showed that the entire region is vulnerable to droughts and floods. Although the overall increase in seasonal rainfall is there, the cases of extreme events have also increased.

REFERENCES

Chandniha SK, Meshram SG, Adamowski JF and Meshram C 2017. Trend analysis of rainfall in Jharkhand State, India. *Theoretical and Applied Climatology* **130**: 261-274.

Dinpashoh Y, Mirabbasi R, Jhajharia D, Abianeh HZ and Mostafaeipour A 2013. Effect of short-term and long-term persistence on identification of temporal trends. *Journal of Hydrologic Engineering* **19**: 617-625.

Kendall MG 1975. *Rank Correlation Methods*. 4th Edition, Charles Griffin, London.

Khavse R, Deshmukh R, Manikandan N, Chaudhary J L and Khaushik D 2015. Statistical analysis of temperature and rainfall trend in Raipur district of Chhattisgarh. *Current World Environment* **10**: 305-312.

Received 22 May, 2021; Accepted 12 November, 2021

Kumar V and Jain SK 2011. Trends in rainfall amount and number of rainy days in river basins of India (1951-2004). *Hydrology Research* **42**: 290-306.

Lyra GB, Oliveira-Junior JF and Zeri M 2014. Cluster analysis applied to the spatial and temporal variability of monthly rainfall in Alagoas State, Northeast of Brazil. *International Journal of Climatology* **34**(13): 3546-3558.

Mann HB 1945. Nonparametric tests against trend. *Econometrica* **13**: 245-259.

Sen PK 1968. Estimates of the regression coefficient based on Kendall's Tau. *Journal of the American Statistical Association*, **63**: 1379-1389.

Sharma S and Singh PK 2017. Long term spatiotemporal variability in rainfall trends over the state of Jharkhand, India. *Climate* **5**: 18.

Sobral BS, Oliveira-junior JF, Gois G and Pereira-Junior ER 2018a. Spatial variability of SPI and Rdist drought indices applied to intense episodes of drought occurred in Rio De Janeiro State, Brazil. *International Journal of Climatology* **1**(1): 34.

Sobral BS, Oliveira-Junior JF, Gois G, Terassi PMB and Muniz-Junior JGR 2018b. Variabilidade Espaço-temporal e Interanual da Chuva no estado do Rio de Janeiro. *Revista Brasileira de Climatologia* **22**: 281-308.

Spracklen DV, Arnold SR and Taylor CM 2012. Observations of increased tropical rainfall preceded by air passage over forests. *Nature* **489**: 282–285.

Srivastava PK, Islam T, Gupta M, Petropoulos G and Dai Q 2015. WRF dynamical downscaling and bias correction schemes for NCEP estimated hydro-meteorological variables. *Water Resources Management* **29**: 2267-2284.

Indian Journal of Ecology (2021) 48(6): 1627-1634

Manuscript Number: 3424
NAAS Rating: 5.79

Determination of Geomorphological Characteristics of Jakham River Basin using GIS Technique

Vinay Kumar Gautam, Mahesh Kothari, P.K. Singh and K.K. Yadav

Department of Soil and Water Engineering, CTAE, MPUAT, Udaipur-313 001, India
E-mail: vinaykumargautam24@gmail.com

Abstract: This study was conducted for Jakham River Basin to understand the relationship between geomorphological characteristics and to delineate the various parameters depends upon the slope, geology of the basin, and elevation. Remote sensing and GIS observed as a most effective and time saving technique for determination of geomorphometric parameters. This methodology was found very relevant for extraction of morphometric parameters using ASTER DEM. The study involves morphometric linear, areal and relief aspects of Jakham river basin, which is a tributary of Mahi River in southern Rajasthan. The catchment area of river basin is 950km^2 with dendritic drainage pattern. It is divided in to four sub-watersheds. The geological set-up of the basin is represented by various igneous and meta-sedimentary rocks. The parameters which were worked out includes stream order, stream number, stream frequency, basin length, stream length ratio, bifurcation ratio, form factor, relative relief, circulatory ratio, elongation ratio, relief ratio, ruggedness number and drainage density. The stream order of the basin is mainly controlled by the physiographic condition. The mean bifurcation ratio ranges 3.28 to 4.02 indicate the effect of geological formations to the drainage pattern in the basin. Drainage density (D_d=1.82km km^{-2}) of the watersheds shows the course nature of drainage pattern and permeable for infiltration. Shape factor (circulatory and elongation ratio) indicates that sub-watersheds are less to moderate elongated in shape have less susceptibility to peak flood.

Keywords: Geomorphology, Morphometric, GIS, DEM, Linear, Aerial, Relief aspects

In emerging nations, land management sustainability and water resource development are at risk from soil erosion and sediment-related issues. These issues result in water storage capacity loss in watersheds, damage to water reservoirs and dams, and pollution of surface waters (Ninija 2017). The morphometric studies involve area, altitude, shape, size, slope, and profiles of watershed (Rai et al 2017, Singh et al 2018). Morphometric analysis could be used for prioritization of sub-watersheds by analyzing different linear and aerial parameters of the watershed. To evaluate and manage the basin for soil and water conservation, quantitative investigation of morphometric attributes is of tremendous. Remote sensing using satellite images are convenient tools for morphometric analysis. Patle et al (2020) has used remote sensing and GIS technique for morphometric analysis of Nahra watershed of Balaghat district, M.P. Different studies have been completed morphometric analysis of different river basins, watersheds under umbrella of remote sensing and GIS technique. The functions of remote sensing and GIS technologies provide wide applications over water resource management plans, especially on characterization and prioritization of sub watersheds (Kumar and Ramaraj 2021). These geomorphic investigations of drainage network are utilized with the appraisal of groundwater quantification and artificial recharge (Sreedevi et al 2005).

In recent years, the Digital Elevation Model (DEM) and GIS have become effective tools in watershed morphometric analysis (Singh et al 2019). The digital elevation model (DEM) was extracted from the Advanced Space Borne Thermal Emission and Reflection Radiometer (ASTER) has provide a perfect and easy path for analyzing hydrological systems and morphometric parameters viz., drainage basin area, drainage density (D_d), drainage order, and relief are analyzed in GIS atmosphere (Smith and Sandwell 2003). Once the drainage characteristics of a watershed has defined, different topographical and geometrical attributes can be determined (such as area, length, perimeter, slope, circularity ratio, elongation ratio, drainage density and the total stream lengths) and afterwards their empirical inter relationships can be determined using classic statistical method (Karuppannan et al 2015). The grouping of these factors may provide positive clues about the characteristic of the geological structure of a watershed, water movement and the recharge potential. An integrated analysis of various parameters provides better estimate of subsurface characteristics from groundwater perspective (Valliammai and Prabhakaran 2020).

Combination of the satellite imagery data and hydrogeological spatial analysis in geospatial environment is made easy to recognize and differentiate the drainage region (Pirasteh et al 2010). The geomorphologic properties of

drainage basin are important for hydrological analysis relating the estimation of ground water potential etc. The morphometric parameters are recognition tools used to analyze and assess the various aspects of the watershed, such as lithological features, geomorphic landslides and hydrological behavior (Singh 2005; Singh et al 2018). The factors such as topsoil thickness, weathered zone thickness, anisotropy (formation compactness) and geology are considered, to determine the area most suitable for groundwater recharge in a hard rock aquifer in basin by using GIS environment (Kalphana et al 2018). The morphometric study of the drainage basin is aimed to obtain precise and perfect data of assessable stream network features of drainage system. Looking to the importance of geomorphological parameters in the basin the current study was carried out for Jakham river basin through RS and GIS technique, which drains in to Mahi river basin of southern Rajasthan.

Study area: Study area is characterized as semi-arid climate and hard rocks over the basaltic region. The catchment area of Jakham river basin is 950 km^2. The basin area lies between latitude 23°53' and 24°30' N and longitude 74°14' and 74° 47' E (Fig. 1). The average annual rainfall of region is 780 mm.

The soils of the basin fall under the broad categories of red soil, black soil and clayey loam. The geological set-up of the basin is represented by various igneous and meta-sedimentary rocks. Rocks of Bhilwara super group of Archaean age comprising of granites and gneisses are exposed in southwestern part of the basin. Deccan traps are exposed in major part of the basin. The topography level in the basin ranges from 281 to 537 m, highest being in the central part and lower in southern part. The climate is characterized as semi-arid, warm and well distributed rainfall in monsoon. The 90% of rainfall received during monsoon months and 50% is recorded between July to August (Indiawaris 2020).The normal maximum temperature is recorded 44.5^{0}C in the month of May and minimum 6.2 ^{0}C in January. Based on the morphological characteristics, Jakham river basin in divided in to two zones. The first zone, characterized with hilly, rocky, mountain profile, whereas second zone identified as dense forest and vegetation over the center part of basin (Raj et al 1999), which provides a habitat to different sort of ecological units. It is also native place of different tribal groups, since long time.

MATERIAL AND METHODS

Extraction of drainage network from Jakham river basin through ASTER DEM data using remote sensing and GIS environment has been used for analyzing morphometric parameters (linear, areal and relief).This method shows less tedious work over manual extraction and delineation of

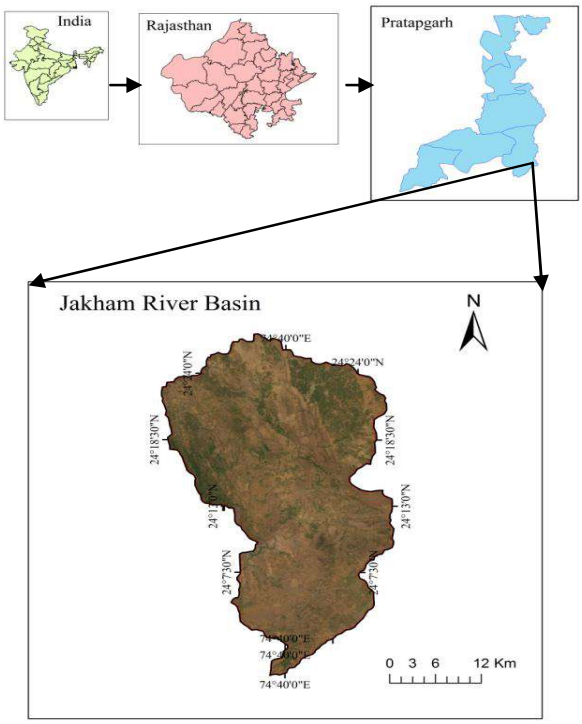

Fig. 1. Geographical map of Jakham River Basin

watersheds from SOI toposheets. The ASTER DEM data was collected from the NASA EARTH DATA (GDEM) having 30 m of ground resolution. The shape file of the study area was clipped and processed from the DEM file. Drainage map of Jakham River Basin is shown in the Figure 2.

Digital elevation model (DEM): DEM are usual source of data that can be used to discern the mechanics behind the geomorphologic process (Fig. 3). These elevation data were developed by different data source like, manual survey, aerial photography, LIDAR and RADAR, which are the common acquirement methods (Arabameri et al 2020). Remote sensing and GIS data and environmental data were utilized to analyze the basin/watershed drainage characteristics and also facilitate competent analysis of huge amount of spatial information. (Kamp et al 2005, Singh et al 2013).

Morphometric analysis of Basin: The basic morphometric parameters like stream order, stream length, basin perimeter, Max. Basin length was analyzed from the DEM layer. These parameters were calculated based as per earlier studies (Table 1).

Extraction of Jakham River Basin: The Jakham river basin is extracted from the ASTER DEM (15m resolution) data base using geo-referenced Survey of India toposheet.

Delineation of sub watershed: Delineation of sub watersheds was done by using toposheet no. 45L/9, 45L/11, 45L/12, 45L/15, 45L/16(scale of 1:50,000).A georeferenced topopsheet was digitized in ArcGIS 10.4 software. The

delineation of watersheds was performed using following steps (Fig. 4.).

Extraction of drainage streams: The DEM data was also used for extracting drainage network and characteristics of watershed. Spatial analysis tool (ArcGIS 10.4) was used for drainage network analysis.DEM data was used for extracting drainage network, because topographic map and DEM map shows 85% of similarity to the drainage network. The process used for extracting drainage network consisted of filling sinks in DEM data to determine the stream order of the watersheds is given below (Fig. 5).

Some of drainage parameters like mean bifurcation ratio, drainage density, stream frequency, farm factor, circulatory ratio, elongation ratio and compactness coefficient are also known as erosion risk assessment parameters and used for prioritizing sub -watersheds in the basin. The developed DEM map was processed to delineate sub-watersheds in the basin (Fig. 6). The basic parameters of different watershed like basin length, no. of stream basin area and perimeters are calculated in the Arc Map 10.5 software (Table 2).

Table 1. Linear and areal morphometric parameter used for Jakham river basin

Morphometric parameter	Formula	References
Linear aspects		
Stream order (u)	Hierarchal rank	Strahler (1964)
Stream length (L_u)	Length of stream	Horton (1945)
Mean stream length (L_{sm})	$L_{sm}= L_u/N_u$ Where L_u is total length of stream of order u, N_u is a total no. of stream segment of u order	Strahler (1964)
Basin length (L_b)	$L_b= 1.312A^{0.568}$ L_b is a length of basin(km)	Nooka et al (2005)
Bifurcation ratio (R_b)	$Rb = \frac{Nu}{Nu + 1}$	Schumn (1956)
Stream length ratio (R_L)	$R_L= L_u/(L_u-1)$	Horton (1945)
Areal aspects		
Drainage density (D_d)	$D_d=L_u/A$ A is area of watershed	Horton (1945)
Form factor (R_f)	$Rf = \frac{A}{Lb_2}$ L_b is a length of basin(km)	Horton (1945)
Stream frequency (F)	$Fs= \frac{Nu}{A}$ Nu is total no. of stream	Horton (1945)
Circulatory ratio (R_c)	$Rc = \frac{4\pi A}{P^2}$ P is perimeter of watershed	Miller (1953)
Elongation ratio (R_e)	$Re = \frac{2\sqrt{\frac{A}{P}}}{Lb}$ L_b is a length of basin(km)	Schumn(1956)
Texture ratio (T)	$T=N_1/P$ N_1 is total no. of 1st order stream	Horton (1945)
Relief aspects		
Watershed relief (H) m	It is the vertical distance between lowest and highest point of watershed	Hadley and Schumm (1961)
Relative relief (R_r)	$Rr = \frac{H}{P} * 100$ H is watershed relief	Melton (1957)
Relief ratio (R_h)	$R_h= H/L_b$	Schumn (1956)
Ruggedness number (R_n)	$R_n=H*D_d$	Strahler (1964)

RESULTS AND DISCUSSION

The results of the morphometric analysis of river basin are calculated and presented in the Table 3 to 6. The total area of the basin is 950 km^2.The morphology of the study area is seems to be easily influenced by the hydrogeological and topographic condition of the surroundings. The other aspects of watershed's morphology are calculated using the equations as defined in the Table 1.

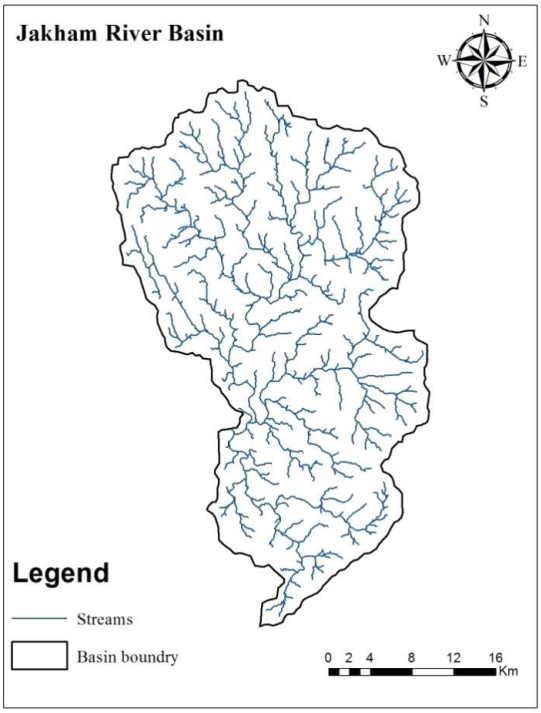

Fig. 2. Drainage map of Jakham River Basin

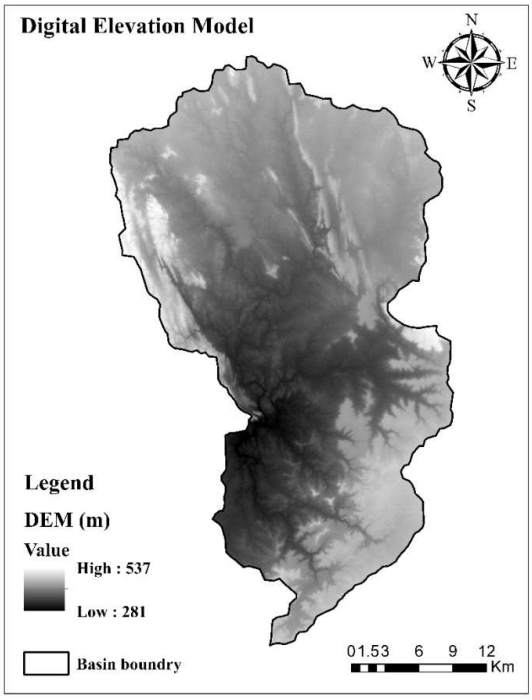

Fig. 3. DEM of Jakham River Basin

Stream order (u): The maximum stream frequency was, 2.19 in Sub-watershed 3(SW3) and minimum, 1.96 in Sub-watershed (SW2). Increase in stream order, related to decrease in stream frequency. In this study only sub-watershed 4 shows deviation from the linear relation, because of regional upliftment. The difference in the order and length of the tributary basins is primarily due to the region's physiographic and structural conditions. Generally, 3rd order streams are labeled as headwater streams, from 4th to 6th order streams are labeled as medium streams (Prabhakarn and Raj 2018). Therefore, In all the sub-watersheds, trunk order (highest order) stream is a medium stream.

Stream number (N_u): Stream number has inverse relationship with stream order. The SW3 has 654 streams, maximum number in the basin. Total 1944 no. of streams has been identified in the basin, including all the sub-watersheds (Table 3). Stream frequency was observed decreasing as stream order has increased in the different watersheds. Horton (1945) has suggested a method for stream number. It is the number of stream segments within the watershed (Prabhakarn and Raj, 2018).

Stream length (L_u): SW2 has longest stream length, whereas SW4 gets minimum length of stream. In the study area, stream length is directly associated with drainage

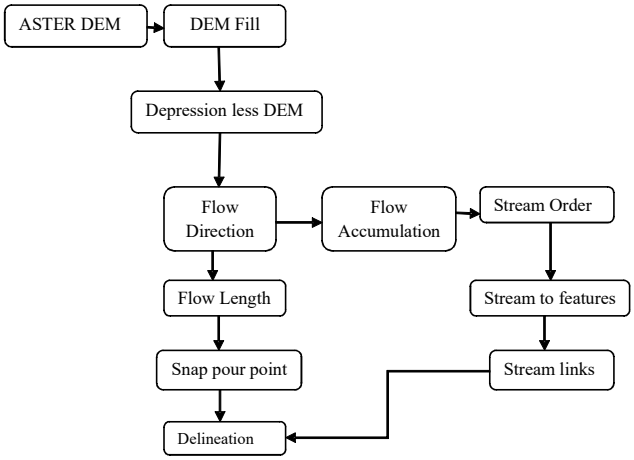

Fig. 4. Flow chart of watershed delineation

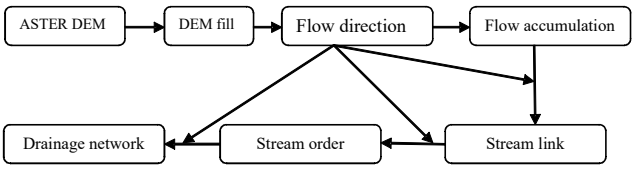

Fig. 5. Process of drainage network generation

network. Each order's stream segments generate an inverse geometric series with order number (Waikar and Nilawar 2014). Almost all small streams are generated through specific intrusive and hilly terrains. It is observed that stream segments up to the third order cross high altitudinal areas with steep slopes, while the fourth and fifth order stream segments occur in marginally flatlands (Table 3). Stream length of watershed is an extent of hydrological and drainage characteristics. Horton's (1945) law proposed that, stream length increases with decrease in the order.

Bifurcation ratio (R_b): The SW4 has less mean Rb value 3.2, whereas SW3 has maximum value of mean R_b value 4.02. The higher R_b value for some sub-watersheds is due to a wide disparity in frequencies between successive orders, indicating mature topography (Sreedevi et al 2005). Horton (1945) stated that, the number of streams of different orders in given drainage basin tend closely to approximate a geometric series in which the ratio is bifurcation ratio, R_b. Lower Rb value has less structurally distributed watershed, without any distortion in drainage pattern (Nag 1998), whereas higher value of R_b shows the strong structural control in drainage pattern. Mean bifurcation ratio can be stated as the average of bifurcation ratios of all the order of stream. The value of mean R_b is given in the Table 3.

Drainage density (D_d): Watershed with high D_d will have low infiltration, promotes considerable runoff and have moderate susceptibility of erosion. Lower drainage density associated with course drainage texture**.** Sub-watershed 1 has highest D_d (1.82 km/km^2), which shows watershed has highly permeable material with proper vegetation and low to mild relief, whereas low D_d is identified for Sub-watershed 4 (Table 6).

Form factor (R_f): For circular shape basin, value of R_f will always greater than 0.78.Less R_f value indicates the elongation of the basin. The sub-watershed 4 has lower value (0.31), where as sub-watershed 1 has higher value (0.60) (Table 6). Hence sub-watershed 4 will have less peak discharge with longer interval, though watershed 1 will have higher peak discharge with short interval.

Elongation ratio (R_e): The R_e values nearer to 1, shows the circular shape of watershed. The Elongation ratio of study area varies from 0.58 to 0.84, which indicate higher to less elongate (Table 6). This parameter also helps in flood routing. High value of R_e indicates the low runoff potential, while lower value shows the higher exposure sedimentation and soil loss.

Circulatory ratio (R_c): It is directly affected by the hydrological (stream length and frequency), geological factors and relief aspects of watershed. This parameter shows the dendritic phase of watershed. The range of R_c is 0.20 to 0.59 in the different watershed (Table 6). The lower and higher value of circulatory ratio represents the young and old phase of watershed.

Length of overland Flow (L_g): Low value shows the short flow length, high relief and high runoff generation, which leads to susceptibility of flood, while high value of L_g indicates mild slope and long flow length, less runoff generation and maximum infiltration (Chandrasekhar et al., 2015).Result shows that SW3 has maximum value of L_g (0.57), whereas SW1 has minimum value of L_g(0.27).

Constant of channel maintenance (C_c): The high constant of channel maintenance indicates more area is required to produce surface runoff, which suggests that a part of water may get lost by percolation, evaporation etc. (Singh, 2002).The range of C_c is 0.54 to 0.58 in the basin. This low value directs less chance of percolation and more runoff may observe in the basin.

Relief ratio (R_h): Total relief (H) can be defined as difference between highest and lowest elevation point in a watershed. Low value of Rh indicates low degree of slope in watershed with resistant basement rocks, meanwhile higher value is characterized as high degree of slope. In this study R_h value

Table 2. Some basic parameters of Jakham River Basin

Sub-watershed	Basin area (sq.km)	Basin length L_b (km)	Perimeter (km)
SW1	205.87	18.49	82.49
SW2	319.95	27.91	101.16
SW3	297.96	27.71	106.77
SW4	108.70	18.77	58.38

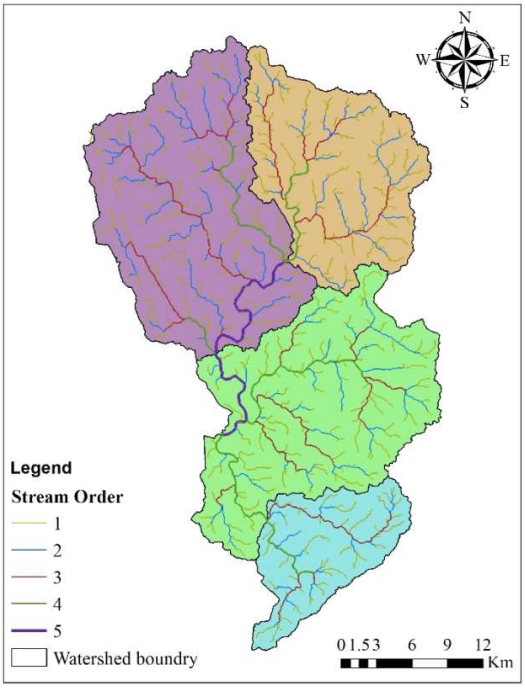

Fig. 6. Sub-watersheds and stream order of the Jakham River Basin

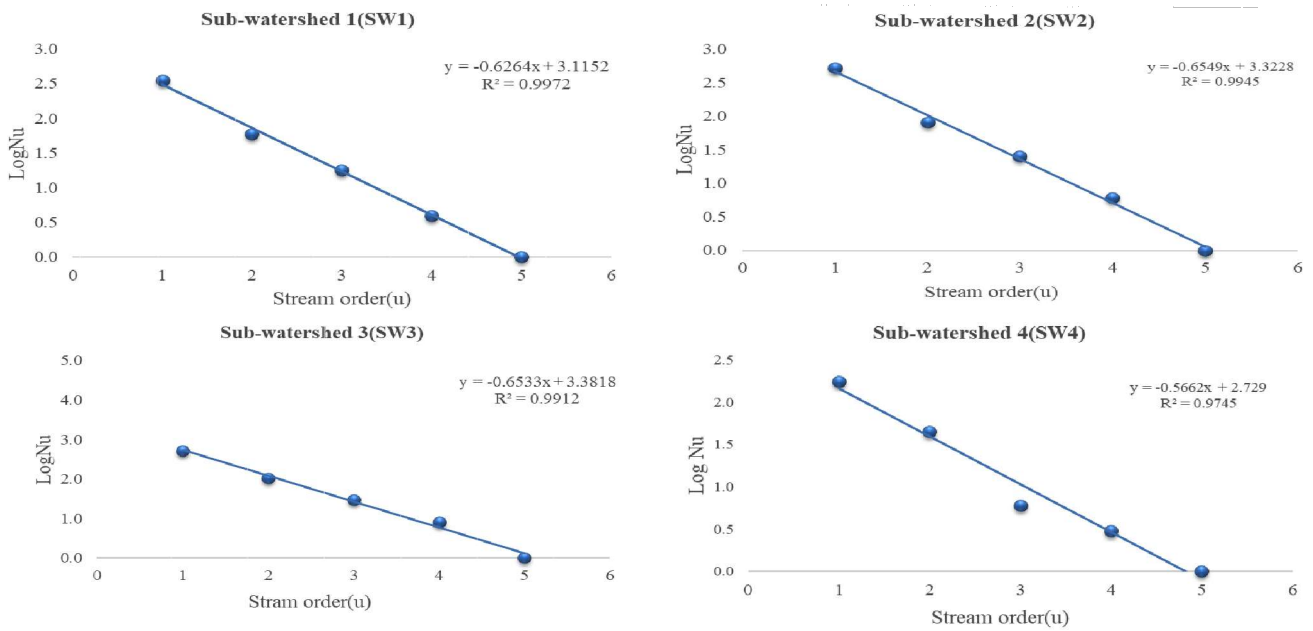

Fig. 7. Regression of stream number with stream order

Table 3. Linear morphometric parameters of Jakham River Basin

Sub-watershed	Steam order (u)					Total stream no. (N_u)	Total length of stream (L_u)	Mean Bifurcation ratio (R_b)
	I	II	III	IV	V			
SW1	350	60	18	4	1	433	374.34	3.53
SW2	515	80	25	6	1	627	572.79	3.96
SW3	510	105	30	8	1	654	522.13	4.02
SW4	175	45	6	3	1	230	187.43	3.28

Table 4. Mean stream length (L_{sm}) of different sub-watersheds

Sub-watershed	Steam order (u)				
	I	II	III	IV	V
SW1 Mean stream length (km)	0.55	1.46	2.94	7.23	12.89
SW2 Mean stream length (km)	0.56	1.76	2.65	7.53	30
SW3 Mean stream length (km)	0.51	1.18	2.26	6.14	19.35
SW4 Mean stream length (km)	0.54	1.16	2.34	6.30	6.88

Table 5. Stream length ratio of different sub-watersheds

Sub-watershed	Steam length ratio (R_L)				Mean steam length ratio (R_L)
	I-II	II-III	III-IV	IV-V	
SW1	2.65	2.02	2.46	1.78	1.78
SW2	3.12	1.51	2.85	3.97	2.29
SW3	2.32	1.10	2.72	3.15	2.02
SW4	2.12	2.02	2.70	1.10	1.59

Table 6. Areal and relief parameters of different watersheds

Sub-watershed	Areal parameters						Relief parameters			
	D_d	R_f	F	R_c	R_e	T	H	R_r	R_h	R_n
SW1	1.82	0.60	2.10	0.38	0.71	5.25	256	0.31	0.01	0.47
SW2	1.80	0.41	1.96	0.59	0.58	6.20	215	0.25	0.01	0.46
SW3	1.75	0.39	2.19	0.55	0.58	6.13	243	0.24	0.01	0.44
SW4	1.72	0.31	2.12	0.20	0.86	3.94	153	0.44	0.01	0.45

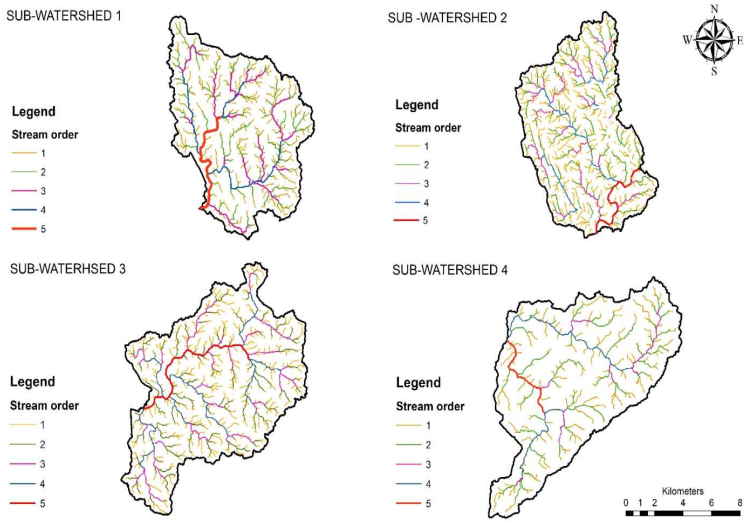

Fig. 8. Sub watersheds of Jakham River Basin

ranges from 0.006 to 0.01.The R_h value for each watershed of Jakham River Basin (Table 6). Low value of relief ratio indicates the characteristics features of less resistant rocks of the study location (Sreedevi, 1999).

Relative relief (R_r): The maximum value of R_r for SW4 is 0.44, while minimum for SW3 is 0.24.R_r is considered to be most reliable potential predictor of denudation rates (Summerfield and Hulton 1994).

Texture ratio (T): Texture ratio (T) is ratio of total number of stream of all order in the basin/watershed to perimeter of the basin/watershed. Higher T value (6.20) is identified in SW2, while low value (3.94) calculated in SW4 (Table 6). Hence SW2 has more runoff generation and high risk of erosion than SW4 in the basin.

Ruggedness number (R_n): It is the product of relief (H) and drainage density (D_d) is an index which shows the length steepness of slope. Is also indicates the susceptibility of erosion to the watershed. SW1 has maximum R_n value, whereas, SW3 has minimum R_n value (Table 6). Hence, it is clearly visible that SW1 has more roughness and structural complexity than other sub-watersheds in the basin.

CONCLUSION

The detailed morphometric study was carried out on four sub-watersheds of Jakham River Basin. All the sub-watersheds has 5th order of stream and controlled by the lower order streams. For determination of different features like linear, areal and relief aspects of morphology GIS technique was used. The comprehensive study shows the dendritic to sub-dendritic pattern of drainage network in the sub-watersheds. Drainage density (D_d) of the watersheds shows the course nature of drainage pattern and permeable for infiltration. Shape factor (circulatory and elongation ratio) shows that sub-watersheds are less to moderate elongated in shape have less susceptible to peak flood. The graph between logarithm of stream number and stream order showing deviance due to regional upliftment in sub-watershed-4. The deviation in the stream-length ratio may be due to topographical condition of basin. The final result shows that all the sub-watershed has less susceptible to soil loss, sedimentation and permeable in nature. The approaches applied in this study have comprehensive analysis and graphical representation, which can be functional in any drainage network in India. The significance of such research is highlighted by the use of its findings to identify the groundwater potential and artificial recharge sites. The following remarks are referred to this study area. Almost all small streams are generated through specific intrusive and hilly terrains. It is observed that stream segments up to the third order crosses high altitudinal areas with steep slopes, while the fourth and fifth order stream segments occur in marginally flatlands, which may be important locations for building check dams and other recharge structures.

REFERENCES

Bali R, Agarwal KK, Ali SN, Rastogi SK and Krishna K 2011. Drainage morphometry of Himalayan Glacio-fluvial basin, India: hydrologic and neotectonic implications. *Environmental Earth Science* **66**(4): 1163-1174.

Chandrashekar H, Lokesh K V, Sameena M, Roopa J and Ranganna G 2015. Proc. *Int. Conf. on Water Resources, Coastal and Ocean Engineering* (Mangalore) **4**: 1345-1353.

Chen NS, Hu GS, Deng W, Khanal N, Zhu YH, Han D 2013. On the water hazards in the trans-boundary Kosi River basin. *Natural Hazards Earth System Science* **13**: 795-808.

Chopra R, Raman DD and Sharma PK 2005. Morphometric analysis of sub-watersheds in Gurdaspur district, Punjab using remote sensing and GIS techniques. *Journal Indian Society Remote Sensing* **33**(4): 531-539.

Dhoke Shailja, Singh M, Singh PK and Yadav K K 2018. Estimation of

soil loss and sediment yield in small watershed under humid condition of Rajasthan. *International Journal of Chemical Studies* **6**: 1209-1214.

DragičevićN, Karleuša B and Ožanić N 2019. Different approaches to estimation of drainage density and their effect on the erosion potential method. *Water* **11**(3): 593.

Franklin S 1987. Morphometric PROCESSING OF DIGITAL ELEVATION MODEL. *Computer Geosciences* **13**: 603-609.

Hart MG 1986. *Geomorphology-pure and applied.* Allen and Unwin Pub. Ltd., London, p 211.

Horton RE 1932. Drainage basin characteristics. *Transfer Geophysics Union* **13**: 350-361.

Horton RE 1945. Erosional development of streams and their drainage basins hydrophysical approach to quantitative morphology. *Bulletin of Geological Society* **56**: 275-370.

Kalphana KR and Velkennedy R 2018. Determination of artificial ground water recharge adequacy in Vaniyar Sub-Basin, Tamil Nadu, India. *Indian Journal of Ecology* **45**(4): 756-762.

Kamp U, Bolch T and Olsenholler J 2005. Geomorphometry of Cerro Sillajhauy (Andes, Chile/Bolivia): Comparison of Digital Elevation Models (DEMs) from ASTER Remote Sensing Data and Contour Maps. *Geocarto International* **20**: 23-33.

Kumar M, Kumar R, Singh PK Singh M, Yadav KK and Mittal HK 2015. Catchment delineation and morphometric analysis using geographical information system. *Water Science Technology* **72:** 1168-1175.

Kumar R and Ramaraj M. 2021. Prioritization of sub-watersheds in the Arasalar-Palavar region using Sediment Production Rate (SPR). *Indian Journal of Ecology* **48**(3): 1005-1010.

Mahala A 2019. The significance of morphometric analysis to understand the hydrological and morphological characteristics in two different morpho-climatic settings. *Applied Water Science* **10**(1), doi:10.1007/s13201-019-1118-2.

Melton MA 1957. *An analysis of the relations among elements of climate, surface, properties and geomorphology.* Project NR 389-042 Technical Report 11. Columbia University, Department of Geology, ONR, Geography Branch, New York.

Melton MA 1959. A derivation of Strahler's channel ordering. *Journal of Geology* **67**: 345-346.

Meshram SG and Sharma SK 2017. Prioritization of watershed through morphometric parameters: A PCA-based approach. *Applied Water Science* **7**: 1505-1519.

Miller VC 1953. *A quantitative geomorphic study on drainage basin characteristics in the Clinch mountain area, Virginia and Tennessee,* Project NR 389-042, Technical report 3. Columbia university, New York.

Nag SK 1998. Morphometric analysis using remote sensing techniques in the Chaka sub-basin Purulia district, West Bengal. *Journal of Indian Society Remote Sensing* **26**: 69-76

NASA 2015. *ASTER Global Digital Elevation Model (GDEM).* NASA EOSDIS Land Processes DAAC, USGS Earth Resources Observation and Science (EROS) Center, Sioux Falls (https://lpdaac.usgs.gov).

Ninija Merina R 2017. Evaluation of sediment using GIS approach in Southern Tamilnadu, India. *Indian Journal of Ecology* **44**: 179-184.

Pirasteh S, Safari HO, Pradhan B and Attarzadeh I 2010. *Litho morphotectonics analysis using Landsat ETM data and GIS techniques:* Zagros Fold Belt (ZFB), SW Iran.

Prabhakaran A and Jawahar Raj N 2018. Drainage morphometric analysis for assessing form and processes of the watersheds of Pachamalai hills and its adjoinings, Central Tamil Nadu, India. *Applied Water Science* **8**: 31. https://doi.org/10.1007/s13201-018-0646-5.

Rai PK, Mohan K and Mishra S 2017. A GIS-based approach in drainage morphometric analysis of Kanhar River Basin, India. *Applied Water Science* **7:** 217-232.

Reddy OGP, Maji AK and Gajbhiye SK 2004. Drainage morphometry and its influence on landform characteristics in a basaltic terrain, Central India: A remote sensing and GIS approach. *International Journal of Applied Earth Observations Geoinformatics* **6**:1-16.

Schumm SA 1956. Evolution of drainage systems and slopes in badlands at Port Amboy, New Jercy. *Bulletin of Geological Society* **67**: 597-646.

Singh D, Singh PK, Patil PR and Singh M 2019. Morphometric analysis of Mewado Ka Math Micro-Watershed using remote sensing and GIS. *Green Farming* **10**: 354-359.

Singh M 2002. *Study on climatic changes of Udaipur Region*. Unpublished thesis, College of Technology and Engineering, MPUAT, Udaipur.

Singh M 2005. *Planning and designing of appropriate soil and water conservation measures in Kadmal watershed*. M.E. Thesis, College of Technology and Engineering, MPUAT, Udaipur

Singh P, Thakur J and Singh U 2013. Morphometric analysis of Morar River Basin, Madhya Pradesh, India, using remote sensing and GIS techniques. *Environmental Earth Science* **68**: 1967-1977.

Singh PK, Dahiphale P, Yadav KK and Singh M 2018. Delineation of groundwater potential zones in Jaisamand basin of Udaipur district. Groundwater, *Water Science and Technology*, *Springer: Singapore*, pp. 3-20. https://doi.org/10.1007/978-981-10-5789-2_1

Sinha R, Bapalu GV, Singh LK and Rath B 2008. Flood risk analysis in the Kosi River Basin, North Bihar using multi-parametric approach of analytical hierarchy process (AHP). *Journal of Indian Society Remote Sensing* **36**: 335-349.

Smith B and Sandwell D 2003. Accuracy and resolution of shuttle radar topography mission data. *Geophysics Research Letter* **30**(9): 20-21.

Sreedevi PD 1999. *Assessment and management of groundwater resources of Pageru River basin, Cuddapah district, Andhra Pradesh, India*. Unpublished Ph.D. Thesis, Sri Venkateswara University, Tirupati.

Sreedevi PD, Subrahmanyam K and Ahmed S 2005. Integrated approach for delineating potential zones to explore for groundwater in the Pageru River basin, Kuddapah District, Andhra Pradesh, India*. Hydrogeology Journal* **13:** 534-545.

Sreedevi PD, Subrahmanyam K and Ahmed S 2005. The significance of morphometric analysis for obtaining groundwater potential zones in a structurally controlled terrain. *Environmental Geology* **47**: 412–420.

Strahler AN 1964. Part II. Quantitative geomorphology of drainage basins and channel networks. *Handbook of Applied Hydrology*. McGraw-Hill, New York, pp 4–39.

Strahler AN 1952. Hypsometric (area – altitude) analysis of erosional topography. *Bulletin of Geological Society* **63**: 1117-1142.

Strahler AN 1958. Dimensional analysis applied to fluvially eroded landforms. *Bulletin of Geological Society* **69**: 279.

Summerfield MA and Hulton NJ 1994. Natural controls of fluvial denudation rates in major world drainage basins. *Journal of Geophysics Research* **99:** 13871-13883.

Valliammai A and Prabhakaran J 2020. Delineation of recharge zones for Panapatti watershed of Coimbatore District. *Indian Journal of Ecology* **47**(1): 36-39.

Verstappen H 1983. The applied geomorphology. *In: International Institute for Aerial Survey and Earth Science (ITC).*

Waikar ML and Nilawar AP 2014. Morphometric analysis of a drainage basin using geographical information system: A case study. *International Journal of Multidisciplinary Current Research* **2**: 179-184.

Received 12 August, 2021; Accepted 15 November, 2021

Indian Journal of Ecology (2021) 48(6): 1635-1640

Manuscript Number: 3425
NAAS Rating: 5.79

Runoff Estimation by Integration of GIS and SCS-CN Method for Kanari River Watershed

Ayushi Trivedi and Manoj Kumar Awasthi

Department of Soil and Water Engineering
Jawaharlal Nehru Krishi Vishwa Vidyalaya, Jabalpur-450 001, India
E-mail: ayushikhandwa@gmail.com

***Abstract*:** Conventional water management is the only alternative to overcome the gap between demand and supply and for this surface water resource management is interpretative issue. Kanari river watershed, located between 23°33′36.73″N and 80°06′57.49″E at an elevation of about 490 m in Jabalpur district of Madhya Pradesh State, India has been used for the study. The major component of the hydrologic cycle is rainfall, directly related to runoff. Integration of GIS and SCS-CN method can be beneficial to overcome this problem of runoff estimation. The runoff varies from 465.59 to 1119.24 mm (1990–2019). The amount of rainfall varies from 1136.7 to 1592.98 mm in the Kanari river watershed. The calculated average annual runoff was 729.87 mm and average runoff volume for the period of 29 years is 218.36. The model finally depicted the runoff in the area kept on increasing as rainfall kept on increasing following a linear trend which predicted that the infiltration opportunity decrease and ultimately resulting in decreased infiltration rate causing decreased base flow. Artificial recharge structures can be recommended in the study area.

***Keywords*:** Soil conservation service, Curve Number, GIS, Runoff, Water resource management

Remote sensing and Geographic Information System is currently in transition from a descriptive to a quantitative technology. Field measurements are laborious and time consuming but the advantages of remote sensing applications in runoff measurement as a source of spatial information becomes more obvious if sensors are air or space-borne platforms used. Geographic Information Systems (GIS) in addition to SCS-CN method and remote sensing have contributed to applied hydrology in government monitoring and forecasting projects. Rivers are suffering from flow degradation because of numerous possible reasons, including the water usage for agriculture and dam installation. But in most of the cases the depleted flow is mainly due to climate change, including increasing evaporation due to high temperature range and altering rainfall patterns. Dimishing run-off is elevating burden on freshwater resources all over the world and in India, because of high demand rate for water due to increasing population. Spatial data have made it practicable to accurately calculate the runoff has led to significant increases in its use in hydrological and meteorological applications. The curve number method (SCS–CN, 1972) is most adaptable widely used for run-off estimation. This method is most relevant property of the watershed, specifically soil permeability, land use and antecedent soil water conditions which take into consideration (Bans ode et al 2014). Stream gauging data and observations in different parts of India shows that there is visible decline in the non-monsoon flow practically in all river systems. The noticeable decline of flow and drying of rivers in non-monsoon period is observed by smaller hydrologic units (sub-catchments and watersheds). Uncontrolled ground water extraction is the basic cause and foremost problem of ceasing effluent discharge into the water stream. Keeping this in view a comprehensive study was proposed to revive Kanari River in Jabalpur district. The aim of this study is to quantify spatial and quantum recharge requirement to revive the river and for this runoff estimation was key factor.

Study area: Kanari River is a river of Madhya Pradesh state in Central India. The river originates at Ghutehi hill, whose, latitude is 23.56441 and longitude is 80.11622, which is situated in Ghutehi village, Tehsil Sihora, District Jabalpur of State Madhya Pradesh (Fig. 1). Geographically, the origin is located at a distance of about 63 km at northeast of Jabalpur and 32 km at South west of Jabalpur and the location of the area falls on Survey of India Toposheet no. F44C2, F44C3 and F44B15. The average MSL of the Kanari River is 399-401 m and climatically it comes under subtropical region. This river joins the Suhar river, whose, latitude is 23.489271 and longitude is 79.98575, which is situated in Budhi Village, Tehsil Majholi, District Jabalpur of State Madhya Pradesh (Fig. 1). The climate here is mild, and generally warm and temperate. Precipitation here is about 1277 mm/50.3 inch per year. Precipitation is the lowest in April, with an average of 6 mm/0.2 inch. Most precipitation falls in July and August, with

an average of 419 mm/16.5 inch. At an average temperature of 33.4 °C/92.1 °F, May is the hottest month of the year. In December and January, the average temperature is 16.5 °C/61.7 °F and is the lowest average temperature of the whole year. According the data collected from 1982-2012, between the driest and wettest months, the difference in precipitation is 413 mm/inch. The wettest is July (244.9 mm a) and windiest is June (5 km/h). The study area consists of a long narrow plain running north-east and south-west, and shut in on all sides by highlands. Topographically, the area has gentle rolling topography with 1-2 metre elevation difference. This plain, which forms an offshoot from the great valley of the Narmada, is covered in its western and southern portions by a rich alluvial deposit of black cotton-soil. At study area, the soil is black cotton soil, and water plentiful near the surface.

MATERIAL AND METHODS

The methodology applied for runoff calculation is depicted in Figure 2. The Soil Conservation Service Curve Number approach is usually utilized empirical methods to determine the direct runoff from a drainage basin (USDA 1972) in the Kanari basin. The surface storage are combined with infiltration losses by the relation of

$$Q = (P-Ia)^2 / P-Ia+S \quad (1)$$

Here, Q – gathered/collected runoff (mm), P – effective rainfall depth (mm), Ia - initial abstraction (mm) (surface storage, interception, and infiltration preceding to runoff in the entire watershed). The empirical relation was obtained in the terms of Ia and is depicted below.

$$Ia = 0.3S \quad (2)$$

The potential maximum retention (S) for Indian conditions is given by,

$$S = \left(\frac{25400}{CN}\right) - 254 \quad (3)$$

where,

CN - Curve Number (Source : SCS handbook of Hydrology (NEH-4), section- 4 (USDA 1972))

Rewriting the equation as,

$$Q = (P - 0.3S)^2 / (P + 0.7S) \quad (4)$$

The runoff from the entire area was calculated in significance of value of CN using Eqs. 3 and 4.

Thematic layers depicted in Figures 3, 4, 5 and 6 were overlayed and the SCS curve number method was used that serves for determination of capability of soils to accommodate infiltrated water in regards of Land use/ Land cover (LU/LC) and antecedent soil moisture condition (AMC) (Amutha and Porchelvan 2009) (Table 1, Fig 3). U.S soil conservation service (SCS) soils distributed the soil into four hydrologic soil groups namely group A, B, C & D in regards of probable rate of runoff and final infiltration. CN, S and P calculated for various years (Table 2).

The different parameters required to compute the runoff were computed and presented. Precipitation data was used

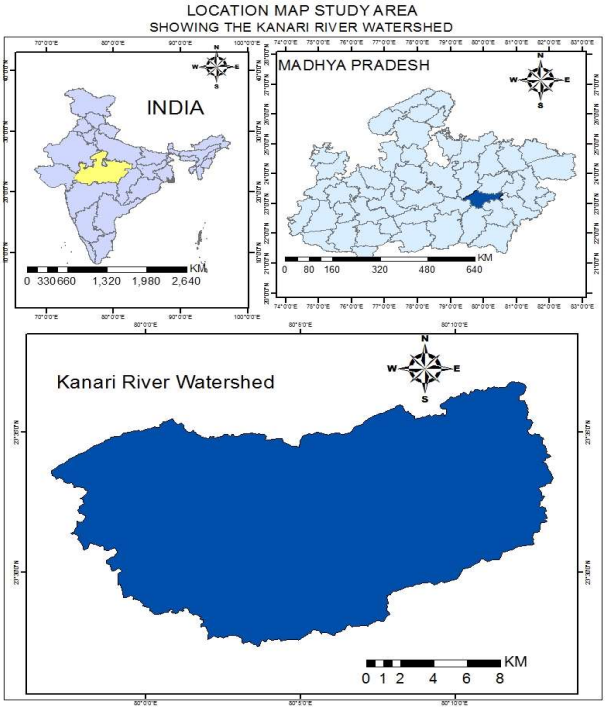

Fig. 1. Location map of the study area

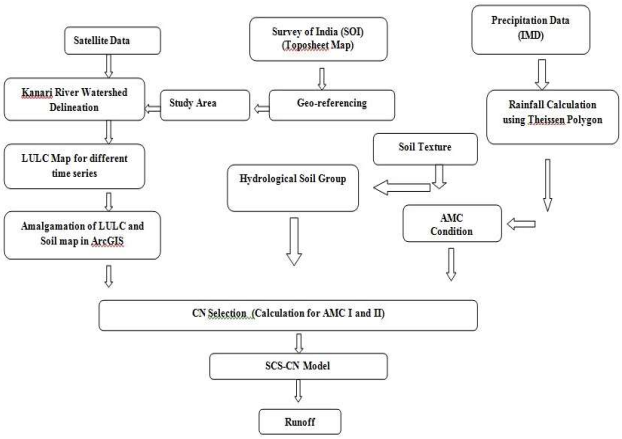

Fig. 2. Methodology for runoff calculation

Table 1. Antecedent soil moisture classes (AMC) group

AMC group	Soil characteristics	Five day antecedent rainfall in mm	
		Dormant season	Growing season
I	Wet condition	Less than 13	Less than 36
I	Average condition	13-28	36-53
III	Heavy rainfalls	Over 28	Over 53

Table 2. Hydrological and quantative calculations in the watershed

AMC	CN				S				P>0.3S			
	1990	2004	2009	2019	1990	2004	2009	2019	1990	2004	2009	2019
I	67.75	71.33	73.48	75.06	120.88	102.06	91.64	84.38	36.26	30.61	27.49	25.3
II	82.76	85.05	86.37	87.32	52.91	44.63	40.06	36.88	15.86	13.38	12.01	11.0
III	92.00	93.02	93.68	94.16	22.07	19.05	17.10	15.74	6.62	5.71	5.13	4.24

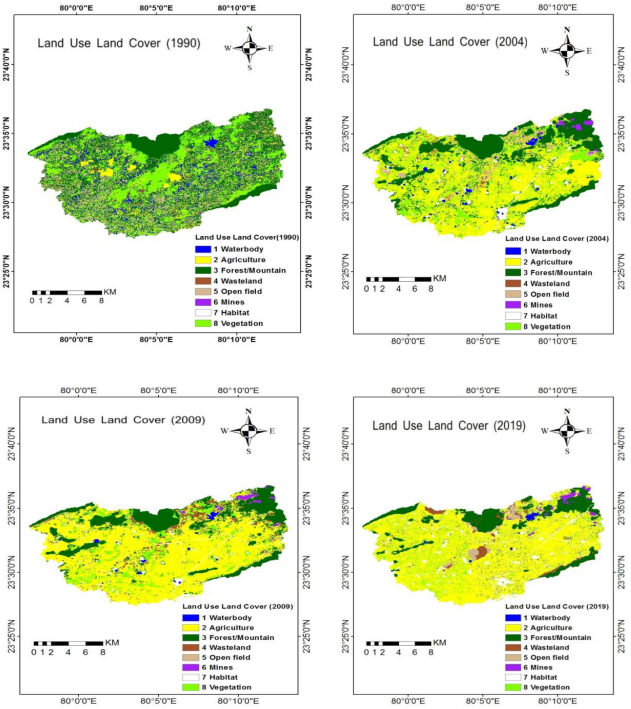

Fig. 3. LULC map for different time series

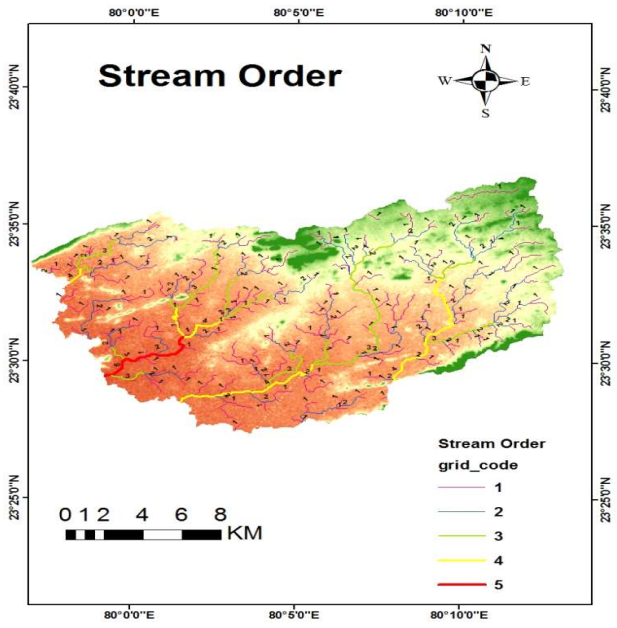

Fig. 4. Stream order map

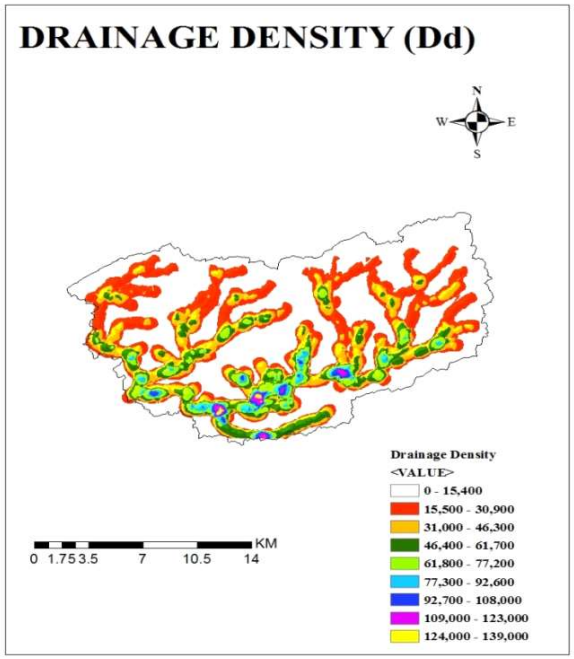

Fig. 5. Drainage density map

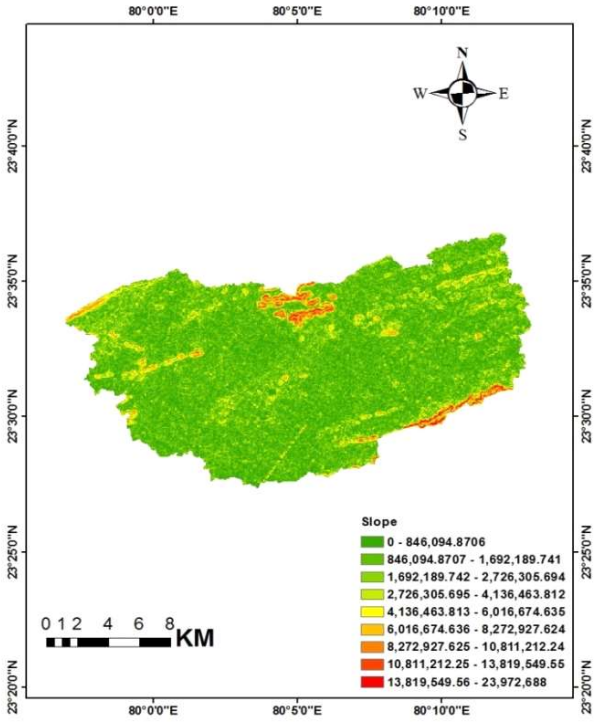

Fig. 6. Slope map

to calculate the antecedent moisture condition for the study period. Soil map was converted into hydrological soil group map and the land use map derived from the satellite data was combined with it to extract the curve number value. The runoff was estimated by knowing the antecedent moisture condition and the curve number. Using the SCS rainfall-runoff relation the daily runoff was computed. The calculation was done on excel spread sheet. The following equation is used in the case of AMC-I and AMC-III:

$$CN\ (I) = \frac{CN\ (II)}{2.281 - 0.128\ CN\ (II)}$$

$$CN\ (III) = \frac{CN\ (II)}{0.427 + 0.00573\ CN\ (II)}$$

RESULTS AND DISCUSSION

The curve number method is used for estimating the direct surface runoff volume using the recorded rainfall data and weighted curve number of the Kanari river watershed. SCS-curve number method takes into account the parameters characterizing a farm such as land use, soil cover, antecedent moisture condition and wetness for estimating yield from the area. These parameters are used to calculate the curve number for Kanari river watershed as shown in Table 2. The curve number indicates the runoff potential of a complex storm during the particular period. The annual surface runoff depth (465.59 mm) for the year 1990 is multiplied by watershed area (A = 299033962 m^2) provides the total average runoff volume as (139228136.1 m^3). The result for the year 1990 (Table 3). Annual surface runoff depth (597.21 mm) for the year 2004 is multiplied by watershed area (A = 299033962 m^2) provides the total average runoff volume as (178807886.9 m^3). Annual surface runoff depth (737.44 mm) for the year 2009 is multiplied by watershed area (A = 299033962 m^2) provides the total average runoff volume as (220599996.4 m^3).

Annual surface runoff depth (1319.24 mm) for the year 2019 is multiplied by watershed area (A = 299033962 m^2) provides the total average runoff volume as (361883866 m^3). The runoff varies 465.59 to 1319.24 mm (1990-2019) (Table 7). The amount of rainfall varies between 1136.7 to 2466.9 mm in the Kanari river watershed. The calculated average

Table 3. Aimed weighted curve number (WCN) at Kanari river watershed (1990)

Land use cover	Soil type (HSG)	Area in ha	Area in m^2	CN	Area	Area * CN	Weighted Curve Number (WCN)
Waterbody	D	2265.4	22654000	100	0.075757	7.575728	AMC I - 67.75
Agriculture	D	2941.15	29411500	90	0.098355	8.851954	AMC II - 82.76
Forest/Mountain	D	12028.5	120285000	77	0.402245	30.97289	AMC III - 92.00
Wasteland	D	119.827	1198270	94	0.004007	0.376671	
Openfield	D	3780.12	37801200	84	0.126411	10.61853	
Mines	D	46.7092	467092	95	0.001562	0.14839	
Habitat	D	149.38	1493800	86	0.004995	0.429606	
Vegetation	D	8572.31	85723100	83	0.286667	23.79334	
Total			299033962			82.76711	

Table 4. Aimed Weighted curve number (WCN) at Kanari river watershed (2004)

Land use cover	Soil type (HSG)	Area in ha	Area in m^2	CN	Area	Area * CN	Weighted Curve Number (WCN)
Waterbody	D	400.68	4006800	100	0.013383	1.33827	AMC I - 71.33
Agriculture	D	12891.8	128918000	90	0.430586	38.75272	AMC II - 85.05
Forest/Mountain	D	7675.83	76758300	77	0.256373	19.74069	AMC III - 93.02
Wasteland	D	347.58	3475800	94	0.011609	1.091261	
Openfield	D	1212.84	12128400	84	0.040509	3.402742	
Mines	D	263.16	2631600	95	0.00879	0.835006	
Habitat	D	770.67	7706700	86	0.02574	2.213671	
Vegetation	D	6377.58	63775800	83	0.213011	17.67992	
Total			299033962			85.05428	

annual runoff is found to be 779.87 mm and average runoff volume for the period of 29 years is 225129971.3 m^3depicting rising linear trend in aspect of both the parameters simultaneously decreasing opportunity time and hence infiltration decreasing base flow of the area.

Runoff and volume was determined by SCS-CN method and was further analyzed on yearly basis for the year 1990,

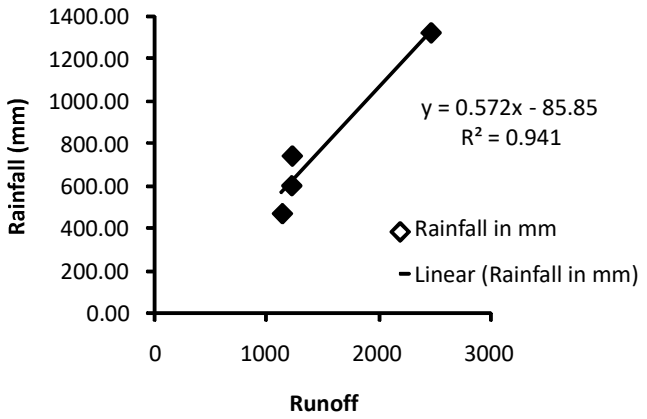

Fig. 7. Scatter plot between the rainfall and calculated runoff

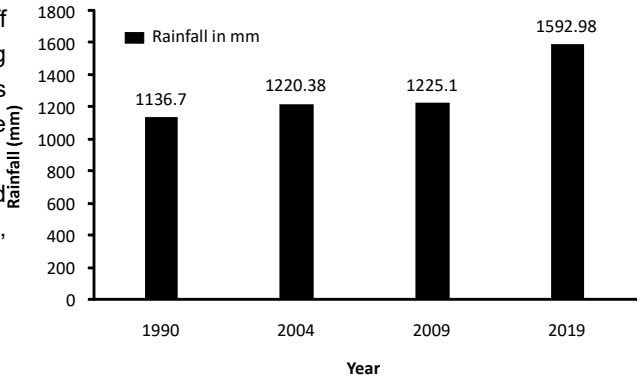

Fig. 8. Rainfall variation in Kanari Watershed

Table 7. Annual average runoff depth and volume

Year	Rainfall in mm	Runoff in mm	Volume (MCM) = (Runoff*area)	Runoff Co.= (RO/RF)
1990	1136.7	465.59	139.22	0.4
2004	1220.38	597.22	178.80	0.48
2009	1225.1	737.44	220.59	0.6
2019	1592.98	1119.25	334.86	0.49
Average	1293.79	729.87	218.36	0.49

Table 5. Aimed Weighted curve number (WCN) at Kanari river watershed (2009)

Land use cover	Soil type (HSG)	Area in ha	Area in m^2	CN	Area	Area * CN	Weighted Curve Number (WCN)
Waterbody	D	268.38	2683800	100	0.008972	0.897168	AMC I - 73.48
Agriculture	D	16981.5	169815000	90	0.567675	51.09072	AMC II - 86.37
Forest/Mountain	D	6535.08	65350800	77	0.218461	16.82152	AMC III - 93.68
Wasteland	D	862.11	8621100	94	0.028819	2.709031	
Openfield	D	1052.01	10520100	84	0.035168	2.954083	
Mines	D	316.44	3164400	95	0.010578	1.004936	
Habitat	D	803.79	8037900	86	0.02687	2.310812	
Vegetation	D	3094.83	30948300	83	0.103457	8.586939	
Total			299033962			86.3752	

Table 6. Aimed weighted curve number (WCN) at Kanari river watershed (2019)

Land use cover	Soil type (HSG)	Area in ha	Area in m^2	CN	Area	Area * CN	Weighted Curve Number (WCN)
Waterbody	D	187.11	1871100	100	0.006254	0.625402	AMC I - 75.06
Agriculture	D	18507.1	185071000	90	0.618587	55.67284	AMC II - 87.32
Forest/Mountain	D	4417.92	44179200	77	0.147666	11.37028	AMC III - 94.16
Wasteland	D	1205.64	12056400	94	0.040298	3.787983	
Openfield	D	591.75	5917500	84	0.019779	1.661422	
Mines	D	360.63	3606300	95	0.012054	1.145112	
Habitat	D	1617.8	16178000	86	0.054074	4.650352	
Vegetation	D	3030.39	30303900	83	0.101289	8.406963	
Total			299033962			87.32035	

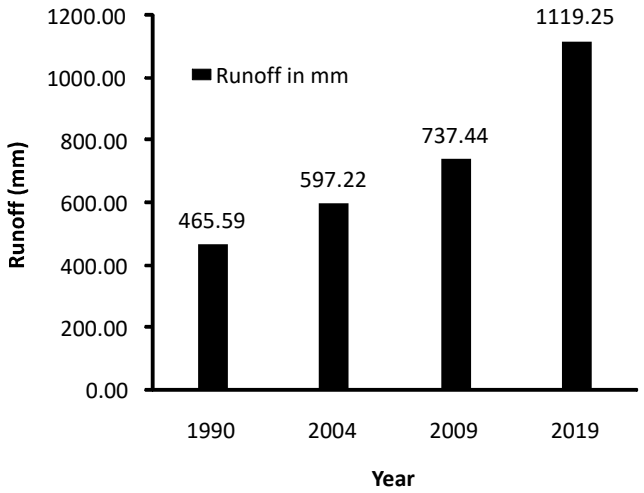

Fig. 9. Runoff variation in Kanari Watershed

2004, 2009 and 2019. The same were inserted in tabular format and histograms were prepared for the purpose of interpretation. Farther the graphs were processed depicting linear rainfall-runoff variation, based on this the correlation coefficients were estimated. The runoff varies 465.59 to 1119.24 mm (1990–2019) (Table 7). The amount of rainfall varies between 1136.7 to 1592.98 mm in Kanari river watershed (Table 7). The calculated average annual runoff is found to be 729.87 mm and the average runoff volume for period of 29 years is 218.36 MCM. The rainfall-runoff relationship is presented (Fig. 7) for the Kanari watershed. Rainfall and Runoff variation in Kanari Watershed (Fig. 8 and Fig. 9) respectively depicts rising linear trend in aspect of both the parameters simultaneously decreasing opportunity time and hence infiltration decreasing base flow of the area.

CONCLUSION

Curve number estimation was performedusing extracted geo-morphological data including thematic layers of such as land use, soil type, drainage order, etc under the environment of RS and GIS. In the study it was found that integration of SCS-CN method with environment RS and GIS can enhance model performance significantly. It was also found that GIS is the most effective and efficient tool for thematic map preparation as an input for SCS-curve number method. GIS was utilized to find out the weighted curve number for antecedent moisture condition-II for year 1990, 2004, 2009 and 2019 was found for the watershed. It was noted that SCS-CN method was formulated for humid type catchments, yet it is found to be a suitable method for sub humid regions of Madhya Pradesh. Finally it was concluded in this study that curve number method in integration with environment of RS and GIS techniques is very effective and efficient method for simulating rainfall-runoff and to determine total surface runoff.

Received 18 August, 2021; Accepted 30 November 2021

REFERENCES

Amutha R and Porchelvan P 2009. Estimation of surface runoff in Malattar sub-watershed using SCS-CN method. *Journal of Social Remote Sensing* **37**(2): 291-304.

Bansode A and Patil KA 2014. Estimation of runoff by using SCS curve number method and arc GIS. *International Journal of Science Engineering Resources* **5**(7): 1283-1287.

Jun LI, Changming LIU, Zhonggen W and Kang L 2015. Two universal runoff yield models: SCS versus LCM. *Journal of Geographical Science* **25**(3): 311-318.

Kadam A 2012. Identifying potential rainwater harvesting sites of a semi-arid, Basaltic Region of Western India, using SCS–CN method. *Water Resource Management* **26**: 2537-2554.

Kudoli AB and Oak RA 2015. Runoff estimation by using GIS based technique and its comparison with different methods: A case study on Sangli Micro Watershed. *International Journal of Emergent Resource Management Technology* **4**(5): 2278-2359.

Mishra SK, Jain MK and Singh VP 2004. Evaluation of the SCS–CN-based model incorporating, antecedent moisture. *Water Resource Management* **18**: 567-589.

Ponce VM and Hawkins RH 1996. Runoff curve number: Has it reached maturity? *Journal of Hydrologic Engineering* **1**(1): 11-19.

Saravanan S and Manjula R 2015. Geomorphology based semi-distributed approach for modeling rainfall-runoff modeling using GIS. *Aquatic Process* **4**: 908-916.

Schulze RE, Schmidt EJ and Smithers JC 1992. SCS-SA User Manual PC based SCS design flood estimates for small catchments in Southern Africa. *Pietermaritzburg: Department of Agricultural Engineering, University of Natal* **14**(2): 13-28

Shrestha MN 2003. *Spatially distributed hydrological modeling considering land-use changes using remote sensing and GIS*. pp 37-56.

Soil Conservation Service-SCS 1985. Hydrology, *National Engineering Handbook*. Washington, D.C: Soil Conservation Service, USDA **1**(4): 45-56

Trivedi A, Pyasi SK and Galkate RV 2019. Impact of Climate Change Using Trend Analysis of Rainfall, RRL AWBM Toolkit, Synthetic and Arbitrary Scenarios. *Current Journal of Applied Science and Technology* : 1-18.

USDA 1972. Soil Conservation Service, *National Engineering Handbook*. Hydrology Section **4**: 4-10 Washington, D.C: USDA.

Vinithra R and Yeshodha L 2016. Rainfall–runoff modelling using SCS–CN method: a case study of Krishnagiri District, Tamilnadu. *International Journal of Scientific Research* **5**(3): 2319-7064.

Yu BF 1998. Theoretical justification of SCS method for runoff estimation. *Journal of Irrigation and Drainage Engineering* **124**(6): 306-310.

Zhan XY and Huang ML 2004. ArcCN-Runoff: An ArcGIS tool for generating curve number and runoff maps. *Environmental Modeling and Software* **19**: 875-879.

Indian Journal of Ecology (2021) 48(6): 1641-1646

Manuscript Number: 3426
NAAS Rating: 5.79

Seasonal Rainfall Prediction for Tamil Nadu Using Climate Predictability Tool

G. Senbagavalli, N.K. Sathyamoorthy, S. Kokilavani, G.A. Dheebakaran and Patil Santosh Ganapati [1]

Agro Climate Research Centre,
[1]Department of Physical Science and Information Technology,
Tamil Nadu Agricultural University, Coimbatore-641 003, India
E-mail: senbagavallibsc@gmail.com

***Abstract*:** Seasonal rainfall prediction is potentially valuable input for agriculture and allied sectors. Climate Predictability Tool (CPT) is a computational statistical software and intended to facilitate the widespread development and dissemination of quality-controlled seasonal climate forecasts. In the present study, CPT was used to predict South West Monsoon (SWM) rainfall by utilizing the Canonical Correlation Analysis (CCA) technique. Results indicate that observed sea surface temperature (SST) from the ERSSTv5 model of March-April-May (MAM) months for the Nino 3.4 region exhibited a strong association with rainfall (the CCA score of 0.71). Thus, MAM SST was used to predict the SWM (2021) rainfall for 32 districts of Tamil Nadu. The prediction accuracy was tested with ROC score, Pearson correlation and 2AFC score. The good predictive skill of cross-validated hindcast in the below and the above-normal category of rainfall (1981-2020) was observed in 17 districts and poor discrimination was observed in 15 districts of Tamil Nadu.

***Keywords*:** SWM, SST, Climate predictability tool, Canonical correlation analysis, Relative operating characteristics

Rainfall is one of the primary meteorological factors that have a direct impact on agriculture. Since Indian agriculture is a gamble of monsoon, more than 50 percent of all cultivated land is reliant on monsoon rainfall, and 80% of total annual rainfall is contributed by South West Monsoon (Vittal et al 2020). Rainfed agriculture is the most significant source of global food production, accounting for more than 80% of the cultivable area and 60% of global crop production (FAO 2020). Extremities in monsoon rainfall *viz.,* drought and flood can adversely affect the rainfed agriculture and leads to the substantial decline in food grain production of country (Prasanna 2014). Climate change is one of the most pressing challenges confronting humanity can have a direct impact on rainfall patterns. Excess rainfall impacts plant regeneration and growth and also inadequate rainfall restricts output during the dry season (Mittal et al 2021). Thus, seasonal rainfall forecasting with acceptable accuracy helps in farm-level decision-making which can head off not only crop failure but also to increase the productivity to sustain the food production under future climate expected with more weather abnormalities. Seasonal rainfall forecasting known as the prediction of rainfall for the succeeding few months has a lot of socio-economic potentials when it is reliable and skillful (Gubler et al 2020). When the seasonal forecast is obtained in advance, it might be possible to adjust or minimize the adverse effects on agriculture. A reliable long-range forecast can help the farmers for crop planning by choosing appropriate crops and varieties, in addition to proper soil and water management practices (Chinchorkar et al 2012). Sympathetic climatic parameters, in particular rainfall, can help in developing optimal strategies of refining the socio-economic well-being of smallholding farmers (Sathyamoorthy et al 2017). Various empirical, statistical, numerical, and deterministic techniques have been used across the world to model and forecast rainfall behaviour (Dumka and Kumar 2021).

According to India Meteorological Department (IMD), the Pacific and the Indian Ocean Sea Surface Temperature (SST) has a strong impact on Indian Monsoon. The NINO 3 and NINO 3.4 SST indices exhibited pockets of stronger correlation over South-Central India (Gupta et al 2020). More specifically SST anomalies over the equatorial Pacific and the northern Indian Ocean provide greater teleconnections between rainfall and the seasonal anomalies of surface temperature over India (Misra and Bhardwaj 2020). Inconsistencies in SST will be utilized as a primary indicator for forecasting rainfall in India (Refonaa and Laksmi 2020) and for most of the monsoon predicting models, the SST is used as a significant oceanographic parameter (Ali et al 2015). The ability to forecast the SWM rainfall is extremely valuable to India's socioeconomic stability (Vittal et al 2020) and accurate predictions at the regional level are critical for reducing the effects of hydro-meteorological catastrophes and achieving sustainability. At

present, district-wise prediction of SWM rainfall for the Tamil Nadu region using SST anomalies is limited. With this background, a study was conducted to predict the SWM seasonal rainfall over Tamil Nadu using NINO 3.4 SST using Climate Predictability Tool developed by International Research Institute for Climate and Society (IRI).

MATERIAL AND METHODS

The observed monthly precipitation data of 32 districts of Tamil Nadu was collected (1981- 2020) from IMD. Four sets of SST (both observed (ERSSTv5) & GCM SSTs (CanCM4i, CanSIPSV2, ECMWF SEAS5)) for the Nino3.4 region (5^0N-5^0S, 170 ^{0}W-120 ^{0}W) used as predictors (Fig. 1). CPT has the facility to select SST data from the IRI data library and that has been used to attain the March-April-May (MAM) months SST at 2° x 2° Km resolution. The data of 40 years (1981-2020) was used to validate the model and rainfall for 2021 SWM season was predicted. The observed rainfall was converted to a text (.txt) format which is compatible with the CPT software version 17.5.1.CPT allows to build a seasonal climate forecast model and has the facility to validate it and generate forecasts using the updated data. For forecasting, Canonical Correlation Analysis (CCA) has been used as a statistical method, which investigates the linear relationships between two multivariate sets of variables. X= ($X_{1....}$ X_n) and Y = ($Y_{1....}$ Y_n). U and V are formed based on the linear combinations of X and Y and canonical correlation calculated as,

$$Cor\ (U,V) = \frac{COV\ (U,V)}{\sqrt{Var\ (U), Var\ (V)}}$$

U(Predictor) = a^TX (Nino3.4 region SST), V(Predictand)=b^TY (Observed rainfall)

Empirical Orthogonal Functions (EOF) or Principal Components (PC) were used to prefilter the predictor and target field and also to reduce the problems associated with multiplicity and collinearity. A correlation matrix was used to calculate the principle components. An optimum number of modes were fixed based on the goodness index. A gamma distribution was used to transform the rainfall data into normal distribution prior to analysis. Zero bound was selected to ensure that not to predict negative values. Cross-validation was used to evaluate the model skill and also to avoid artificial skills in prediction. For computing the skill of the forecast, the model was trained using leave-5-out cross-validation. CCA score demonstrates the strong spatial and temporal relationship between the predictor and predictand. Since the coefficient of CCA lies within positive, the value closer to one reflects better prediction. The skill of cross-validated hindcast was verified using Relative Operating Characteristics curve (ROC curve), Pearson correlation, Two

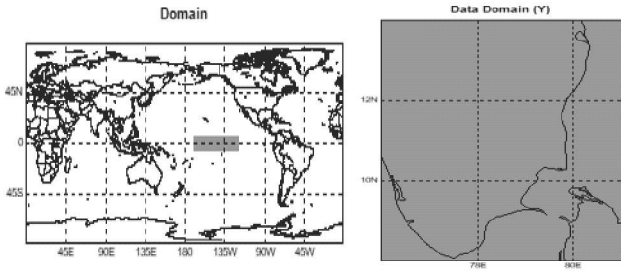

Fig. 1. Location of predictor (Nino3.4 region) and predictand region

Alternative Forced Choice (2AFC score) test. The projected hit rates are plotted against the false alarm rates to generate the ROC curve. Linear straight lines represent non-skill lines on the ROC curve. A positive skill (reliable) has a curve above the non-skill line, whereas a negative skill has a curve beneath the non-skill line (unreliable) (Rustiana et al 2017). The ROC score ranges from 0 to 1. A score of 0.5 represents no skill, 1.0 indicates perfect discrimination, and 0.0 indicates perfectly bad discrimination.

Pearson correlation shows the magnitude of the strength of the association between the observed and the forecast values. Its value ranges from -1 to +1 indicating a perfect positive and negative relationship. It gives the association of the trend of forecast with observation (Manzano and Ines, 2015). The other test namely, Two Alternative Forced-Choice (2AFC test) indicates the probability of correctly discriminating “the above-normal" observation from a "normal" observation. If the proportion of properly chosen observations will exceed 50 percent indicates the predictions are skilful, and the better forecasts are, the closer the proportion of 100% (Sahu et al 2017).

RESULTS AND DISCUSSION

CPT was used to predict the SWM seasonal rainfall of 2021 for 32 districts of Tamil Nadu using SST of Nino3.4 region.

Predictor selection: The analysis was made by utilizing four different SST sources with different monthly lead times and the best predictor was customized based on CCA score to predict the SWM rainfall for the year 2021. The coefficient of CCA reveals a good prediction (Table 1). The low CCA score indicates that less relationship with rainfall for the study area. The highest score of 0.71 was registered in the ERSSTv5 source when March, April, and May were taken and the lowest score of 0.23 was registered SST of March-April. In ECMWF-SEAS5 source, the highest CCA score of 0.67 was observed when March-April months were taken as well as April was taken alone. The lowest score of 0.35 was noticed when MAM was taken together. The sources like CanCM4i

and CanSIPSV2 registered the highest CCA score of 0.5 during March, 0.48 during May and the lowest score of 0.23 was registered during April. ERSSTv5 during March–April–May together exhibited the strongest relationship as shown by its CCA score of 0.71 (Fig. 2). Rustiana et al (2017) observed that CPT was accurate in predicting rainfall with CCA score of above 0.7 and Pearson correlation score of 0.3 to 0.9 for a region. The models' skill disparities may be attributed in part to intrinsic characteristics like their sensitivity to nonlinear dynamics of linking SST to rainfall (Manzano and Ines 2015). Pokhrel et al (2016) concluded that, in general, the best skill of forecast observed in the zeroth lead time of SST but, when it comes to Indian Summer Monsoon Rainfall (ISMR), the three-month lead forecast period has the best ISMR prediction skill. Rajendran et al (2021) reported that a projected year-to-year variance of ISMR shows the highest skill in lead-time of late-April/early-May initial condition. The Nino-3.4 SST anomaly tendency is one of the predictors used for the second stage forecast of SWM by IMD (Rajeevan et al 2007). ERSSTv5-MAM SST exhibited the strongest relationship as shown by its CCA score of 0.71 (Fig.2)

Cross Validated Hindcast Skill Verification

ROC curve: Among 32 districts, Virudhunagar showed the highest ROC score of 0.69 in the below normal category.

Table 1. CCA score of CPT using different sources of SST

Measures	CCA Score of CPT Model (CCA Mode 1)			
Predictor month	ECMWF-Seas5	CanCM4i	CanSIPSV2	ERSSTV5
March	0.11	0.50	0.36	0.36
April	0.67	0.23	0.23	0.36
May	0.65	0.41	0.48	0.36
March- April	0.67	0.43	0.38	0.23
March- April -May	0.35	0.30	0.31	0.71

Cuddalore, Dharmapuri, Dindigul, Kanchipuram, Krishnagiri, Madurai, Pudukkottai, Tiruvannamalai, Villupuram, Virudhunagar, Trichy districts showed good skill in both below and above-normal categories. The districts like Namakkal, Sivaganga, Tanjore showed poor skill in the below normal category and good skill in the above-normal category. The districts like Perambalur, Ramanathapuram, Tiruppur, Tuticorin showed poor skill in the above-normal category and good skill in the below normal category. The districts like Ariyalur, Chennai, Coimbatore, Erode, Karur, Nagapattinam, The Nilgiris, Salem, Kanyakumari, Tirunelveli, Vellore, Theni, Tiruvallur, Tiruvarur, and Salem showed poor discrimination in both categories (Fig. 3). Sibusiso et al (2019) found that both Sep-October-November and June-July-August predictors able to discriminate above normal category efficiently than below normal category of seasonal rainfall (December-Janary-February) over Eswatini, South Africa by using ROC scores. Similarly, based on the ROC curves the model's dependability at five typical places in the Java Island was analysed and, both rainy and dry season had curves that were above the linear line of non-skill (ROC score >0.5) (Rustiana et al 2015).

Two alternative forced choices (2AFC test): 2AFC score normally indicates a probability of correctly discriminating a higher from a lower value. A score of more than 50% was observed in Cuddalore, Dharmapuri, Dindigul, Kanchipuram, Krishnagiri, Nagapattinam, Namakkal, Pudukkottai, Tanjore, Tiruvannamalai, Tuticorin, Villupuram, Virudhunagar, Tiruppur, and Trichy districts. The lowest 2AFC score was observed in Coimbatore (41.6%) and the highest score was observed in Virudhunagar (69.2%) (Fig. 4.)

Similar work undertaken based on 2AFC skill score analysis to predict summer drought over Texas and the southern Great plains region in spring and found that best skill in April initial condition found to have better prediction skill with 2AFC score of 89% (Fernando et al 2015). Monsoon

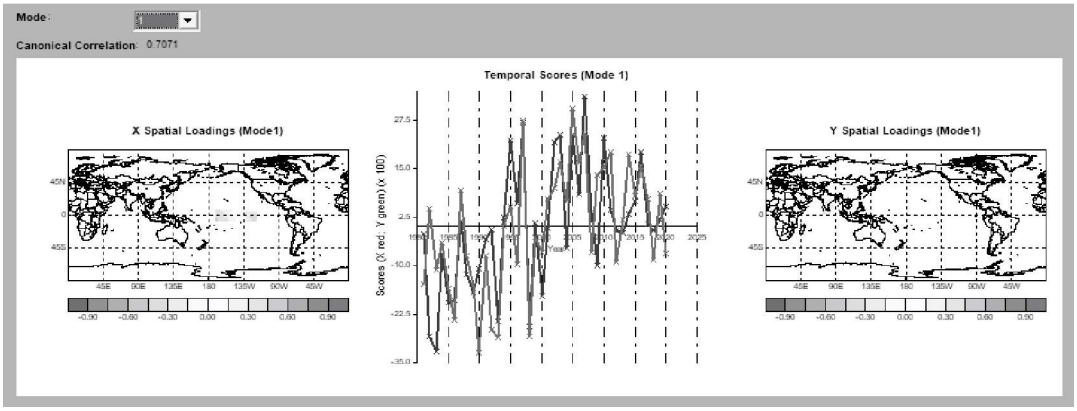

Fig. 2. Mode of CCA, with SST as a predictor and seasonal rainfall as a predict and using ERSSTv5

rainfall over north-eastern part of Bangladesh was predicted using SST over east central Pacific Ocean and magnitude of 2AFC score for that prediction were 55.8 and 55.3 per cent in March, April, May and April-May averaged SST respectively (Mannan et al 2015)

Pearson moment correlation coefficient: Pearson correlation was observed in the range of 0.3 to -0.56 (Fig. 5). Positive Pearson correlation was observed in Cuddalore, Dharmapuri, Dindigul, Kanchipuram, Krishnagiri, Madurai, Namakkal, Pudukkottai, Salem, Tanjore, Villupuram, Virudhunagar, and Trichy districts. The negative correlation was observed in the districts of Ariyalur, Chennai, Coimbatore, Erode, Karur Nagapattinam, The Nilgiris, Perambalur, Ramanathapuram, Sivaganga, Theni, Tiruvallur, Tiruvarur, Tuticorin, Vellore, Kanyakumari, Tirunelveli and Tiruppur.

Manzano and Ines (2015) observed Pearson correlation range was 0.29 to 0.71 with CCA score of 0.65 while predicting May to August seasonal rainfall of Northern Philippines using ERSSTv3 SST. Based on Pearson correlation. Alfaro et al (2016) reported that positive Nino 3.4 SST anomalies along with negative SST anomalies in the Atlantic Multidecadal Oscillation during February and April leads to drier condition in Isthmus, Central America during May-June rainfall season and vice versa. Hossain et al (2019) predicted JJA rainfall over Bangladesh using May and June using SST and they observed Pearson correlation of 0.21 to 0.53 and 0.23 to 0.35 respectively. Das (2015) predicted monsoon rainfall over Bangladesh using SST and observed Pearson correlation of -0.63. Cross-validated hindcast skill was varied among the districts. Since, SWM rainfall was influenced by multidimensional factors such as

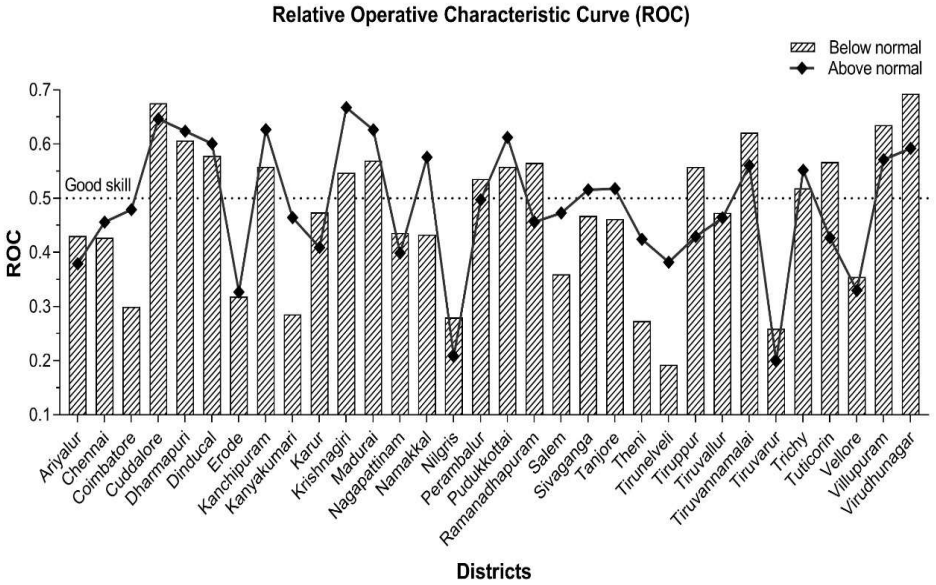

Fig. 3. ROC score for 32 districts of Tamil Nadu for the below and the above-normal rainfall

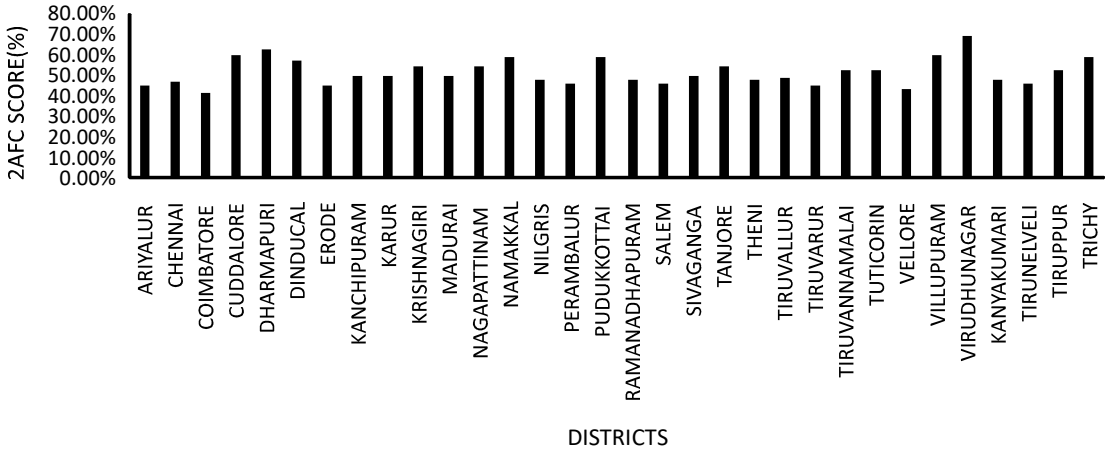

Fig. 4. 2AFC scores for 32 districts of Tamil Nadu

the wind component, temperature and pressure difference over land and ocean, topography (Das 2015). Poor skill or uncertainties in the prediction level of some regions may be due to not inclusion of other predictors.

SWM rainfall prediction: ERSSTv5 - MAM SST was used to predict the SWM rainfall of 2021 for different districts of Tamil Nadu (Fig. 6). The number of modes was fixed based on the goodness index (5 EOF mode for predictor, 8 EOF mode for predict and 2 CCA mode). As per India Meteorological Department categorization for rainfall distribution, normal rainfall is categorized when percentage departure of realized rainfall is within ± 10 % of the long period average and >10% for the above-normal and <10% for the below normal (https://www.imdpune.gov.in/Weather/Reports/glossary.pdf) . The results indicated that the above-normal rainfall was predicted for Coimbatore and Tirunelveli. The below normal rainfall was predicted for Dharmapuri, Dindigul, Erode, Madurai, Nagapattinam, The Nilgiris, Pudukkottai, Ramanathapuram, Sivaganga, Tanjore, Tiruvarur, Tiruvannamalai, Villupuram, Virudhunagar, and Trichy. Other districts like Ariyalur, Chennai, Cuddalore, Kanchipuram, Karur, Krishnagiri, Namakkal, Perambalur, Salem, Theni, Tiruvallur, Tuticorin, Vellore, Kanyakumari, and Tiruppur were predicted with normal rainfall.

CONCLUSIONS

Recognizing and predicting SWM variations is crucial in practice. Due to climate change, the usage of seasonal

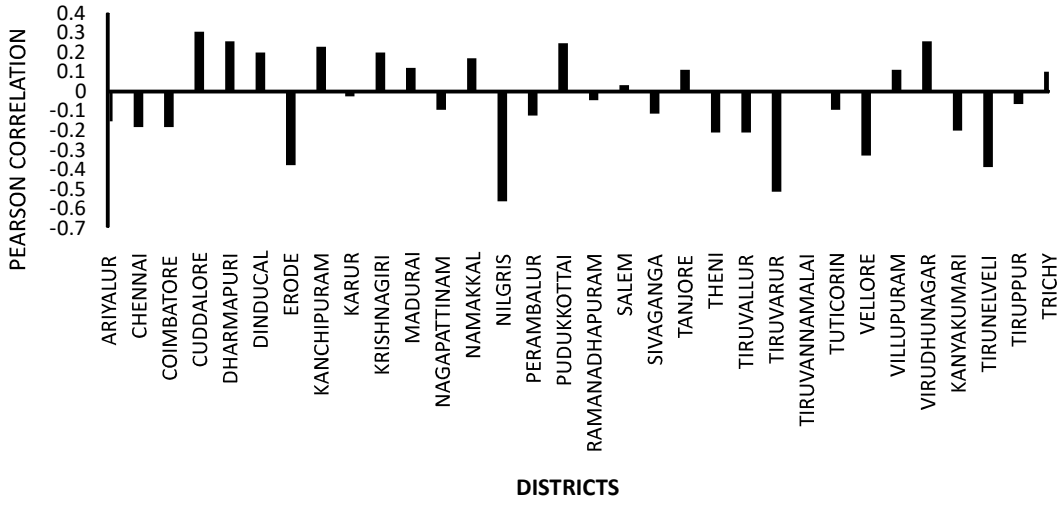

Fig. 5. Pearson correlation scores for 32 districts of Tamil Nadu

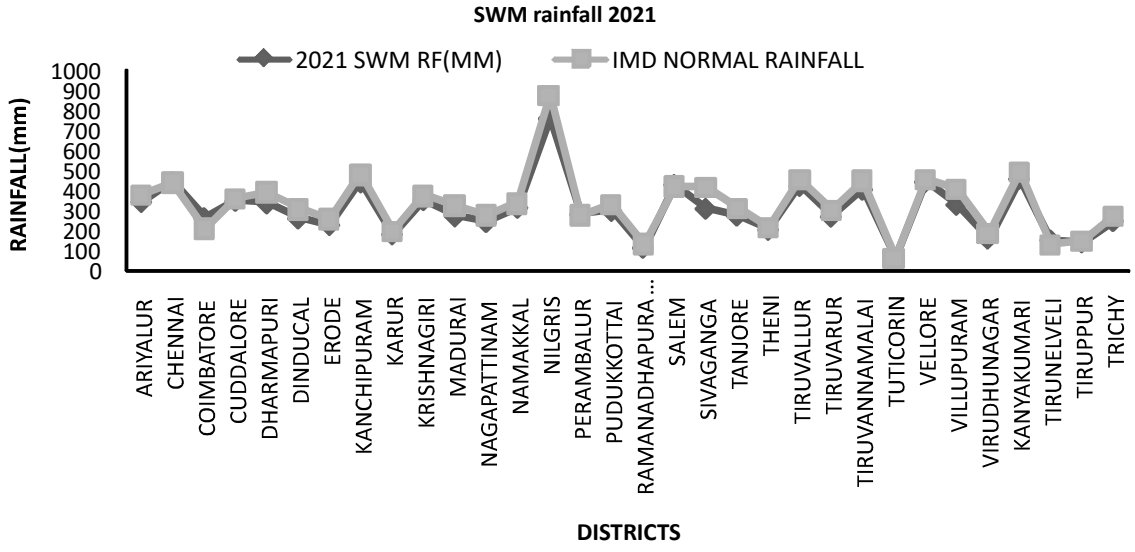

Fig. 6. Predicted SWM rainfall of 2021 and IMD normal rainfall for 32 districts of Tamil Nadu

rainfall prediction has become incredibly valuable. The seasonal rainfall forecast was examined using CPT with different scores and findings revealed that the March-April-May months SST from the ERSSTv5 model of the NINO 3.4 region showed promising results in forecasting SWM rainfall. In the cross-validated hindcast, 17 districts had a good prediction performance and 15 districts had poor discrimination in the below and the above-normal category. The predicted SWM rainfall of 2021 was compared with IMD's normal rainfall and the prediction results exposed that, 15 districts with normal other 15 districts with below normal rainfall, and two districts with the above-normal category. The CPT has the facility of assessing advanced climate information and builds cross-validation and rigorous skill estimation techniques. Hence, CPT can be used to predict location-specific seasonal rainfall.

REFERENCES

Alfaro EJ, Hidalgo H and Mora N 2016. Prediction of MJ rainfall season using CCA models. *Topicos Meteorologicos Oceanograficos* **15**(2): 5-19.

Ali MM, Nagamani PV, Sharma N, Venu Gopal RT, Rajeevan M, Goni GJ and Bourassa MA 2015. Relationship between ocean mean temperatures and Indian summer monsoon rainfall. *Atmospheric Science Letters* **16**(3): 408-413.

Chinchorkar SS, Vaidya VB and Pandey Vyas 2012. Forecasting seasonal rainfall in different locations of Maharashtra. *Journal of Agrometeorology* **14**: 386-389.

Das SR 2015. *Monsoon rainfall forecasting for different hydrological regions of Bangladesh using climate predictability tool (CPT)*. MSc. Dissertation, Institute of Water and Flood Management, Dhaka, Bangladesh.

Dumka BB and Kumar P 2021. Modeling rainfall-runoff using artificial neural network (ANNs) and wavelet based anns (WANNs) for Haripura Dam, Uttarakhand. *Indian Journal of Ecology* **48**(1): 271-274.

FAO 2020. *The State of Food and Agriculture 2020*. Overcoming Water Challenges n Agriculture. Rome.

Hossain MZ, Azad MAK, Karmakar S, Monda, MNI, Das M, Rahman MM and Haque MA 2019. Assessment of better prediction of seasonal rainfall by climate predictability tool using global sea surface temperature in Bangladesh. *Asian Journal of Advanced Research and Reports* 1-13.

Gubler S, Sedlmeier K, Bhend J, ÁvalosG, Coelho C A S, Escajadillo Y and Spirig C 2020. Assessment of ECMWF SEAS5 seasonal forecast performance over South America. *Weather and Forecasting* **35**(2): 561-584.

GuptaV and Jain MK 2020. Impact of ENSO, global warming, and land surface elevation on extreme precipitation in India. *Journal of Hydrologic Engineering* **25**(1): 05019032.

IMD, Meteorological terminologies and glossary; India Meteorological Department.

Mannan MA, Chowdhury MAM, Karmakar S, Ahmed S and Mason SJ 2015. Rainfall prediction over northeastern part of Bangladesh during monsoon season. *DEW-DROP, A Scientific Journal of Meteorology and Geo-Physics, Bangladesh Meteorological Department* **1**: 14-25.

Manzano V and Ines VM 2015. Predictability of May to August (MJJA) seasonal rainfall in northern Philippines. *Journal of Nature Studies* **14**(2): 32-39.

Misra V and Bhardwaj A 2020. The impact of varying seasonal lengths of the rainy seasons of India on its teleconnections with tropical sea surface temperatures. *Atmospheric Science Letters* **21**(3): e959.

Mittal A, Tewari A, Singh N and Shah S 2021. Assessment of soil seed bank on three different vegetation types in Kumaun Central Himalayan Forest. *Indian Journal of Ecology* **48**(2): 381-386.

Nelun Fernando D, Rong Fu, Ruben S Solis, Robert E, Ying Sun, Binyan Yang and Bing Pu 2015. Early warning of summer drought over Texas and the southcentral United States: Spring conditions as a harbinger of summer drought. *Technical note* 15-02.

Pokhrel S, Saha SK, Dhakate A, Rahman H, Chaudhari HS, Salunke K and Sikka D R2016. Seasonal prediction of Indian summer monsoon rainfall in NCEP CFSv2: Forecast and predictability error. *Climate Dynamics* **46**(7-8): 2305-2326.

Prasanna V 2014. Impact of monsoon rainfall on the total foodgrain yield over India. *Journal of Earth System Science* **123**(5): 1129-1145.

Rajeevan M, Pai DS, Kumar RA and Lal B 2007. New statistical models for long-range forecasting of southwest monsoon rainfall over India. *Climate Dynamics* **28**(7-8): 813-828.

Rajendran K, Surendran S, Varghese SJ and Chakraborty A 2021. Do seasonal forecasts of Indian summer monsoon rainfall show better skill with February initial conditions? *Current Science (00113891)*: **120**(12).

Refonaa J and Lakshmi M 2020. Rainfall prediction model with sea surface temperature using soft computing techniques. *Journal of Computational and Theoretical Nanoscience* **17**(8): 3502-3505.

Rustiana S, Hermawan E and Kusumah NA 2015. Rainfall prediction of java island during the dry and rainy season with Climate Predictability Tool (CPT) (Based on CHIRPS Data). In *the 5th International symposium for sustainable hymanosphere, Jakarta*, 29-30.

Rustiana S, Ruchjana BN, Abdullah AS, Hermawan E, Sipayung SB and Jaya IGNM 2017. Rainfall prediction of Cimanuk watershed regions with canonical correlation analysis (CCA). *Journal of Physics*: *Conference Series* **893**(1): 012021

Sahu N, Robertson AW, Boer R, Behera S, DeWitt DG, Takara K and Singh RB 2017. Probabilistic seasonal streamflow forecasts of the Citarum River, Indonesia, based on general circulation models. *Stochastic Environmental Research and Risk Assessment* **31**(7): 1747-1758.

Sathyamoorthy NK, Ramaraj AP, Dheebakaran G, Arthirani B, Senthilraja K and Jagannathan R 2017. Characterization of rainfall and length of growing period over North Western Zone of Tamil Nadu. *Indian Journal of Ecology* **44**(2): 232-238.

Sibusiso MN 2019. Assessing *The Predictability of Rainfall in Southern Africa with focus on Eswatini using Global Ocean and Atmosphere Indicators*, Doctoral dissertation, University of Nairobi, Kenya.

Vittal H, Villarini G and Zhang W 2020. Early prediction of the Indian summer monsoon rainfall by the Atlantic Meridional Mode. *Climate Dynamics* **54**(3): 2337-2346.

Received 29 August, 2021; Accepted 12 November, 2021

Indian Journal of Ecology (2021) 48(6): 1647-1654

Manuscript Number: 3427
NAAS Rating: 5.79

Efficient Internet of Things Smart Agricultural Crops Growth using Machine Learning with Mobile Applications

V. Arulkumar, G. Kalpana[1], Sweta Gupta[2], A. Devipriya[3] and Saroj Kumar[4]

Computer Science and Business Systems, Sri Krishna College of Engineering and Technology, Coimbatore-641 008, India
[1]Computer Science and Engineering, Rajalakshmi Institute of Technology, Chennai600 124, India
[2]Jagran Lakecity University, Bhopal-462 044, India
[3]Computer Science and Engineering, KPR Institute of Engineering and Technology, Coimbatore-641 048, India
[4]Computer Science and Engineering, Chandigarh University, Gharuan-140 413, India
E-mail: arulkumaran.ckpc@gmail.com

***Abstract*:** Agriculture produces the great bulk of the world's food supply. The Internet of Things (IoT) is transforming agriculture, allowing farmers to tackle challenges like precision farming and sustainable agriculture head-on. The Internet of Things (IoT) helps gather data regarding weather, moisture, temperature, and soil fertility. Crop online monitoring allows for agriculture and weed detection. Crop online monitoring allows for pest identification, animal entry into fields, crop development, and agricultural production. Farmers can access their fields remotely via the Internet of Things (IoT) at any time. Wi-Fi sensor networks monitor agricultural conditions, while embedded systems automate and regulate farm operations. Wireless cameras sent photos and video to a central point to monitor the situation. Using IOT, farmers may monitor the status of their agricultural land from anywhere in the world at any time. The Internet of Things (IoT) can reduce costs and enhance yields in conventional farming. How farmers re-imagine computing and analysis helps avoid costly mistakes. Soil moisture, soil PH, soil NPK, temperature, and field moisture sensors are all incredibly powerful and low-cost Wireless Sensor Network – Microcontroller IC Node MCU. Using machine learning, it automatically irrigates, anticipates crop varieties, and detects leaf diseases. Cayenne is our farmer's remote eyes and hands as a localhost PC database and smartphone app.

***Keywords*:** Smart agriculture, Data analysis, Internet of things, Machine learning, Mobile application

As a major contributor of 14.65% to India's GDP, agriculture is the bedrock of the Indian economy. Every year, though input decreases because of low technical activity, it contributes most. In the Indian policy-making, holds a leading role not only because of its contribution to GDP, but also because of the significant proportion of the dependent population. The major Covid-19 pandemic epidemic shutdown businesses and factories in India but farmers continued their noble farming career. Covid-19 remained primarily an urban epidemic and could not revive agricultural occupations. The industry has taken enormous steps to expand its capacity through less use of technology. The Internet of Things, which along with farmers in the region, will hit a whole new edge of traditional farming. Farmers can minimize waste and achieve surplus productivity by improving AI-ML IoT in agriculture (Smart Precision Agriculture). Farmers can cultivate, harvest and regenerate their crops to full yield, with automation and data processing. "Exact technology," the US Farm Bureau says, will cut costs by some 15 per cent and raise crop yield by 13 percent by combination planting, sensors and algorithms intended for optimizing activities. In season after year, there is heterogeneity. Farmers need more understanding of real-time data such as temperature, soil quality, soil needs and planning processes. Farmers monitor processes and have access to consistent predictive control of crop risk on their remote presence using IoT sensors on the ground. In addition to artificial intelligence and machine learning, farmers take hundreds of dynamic, intertwined decisions that have an effect on their risk, sustainability and market returns (Jagadish et al 2005).

This change in decision-making will also save money and lives. In conjunction with stable and efficient processes, its large-scale adaptation is indispensable in the agricultural field. The primary goal of this project is to develop a smart agriculture system that would allow for the monitoring of crop progress. The Raspberry-pi Microcontroller, the Pi Camera, the Humidity Sensor, the Moisture Sensor, the Temperature Sensor, the Water Level Sensor, and the LCD Display are the primary components of the system. Initially, the system would gather all of the crop-related information and show them on the LCD-display. For the same reason, the system will anticipate and analyse for animal incursion using the Pi camera, and the information will be sent to the server. Using ZigBee technology, Liu Dan (Patel et al 2013) conducted experiments on an intelligent agriculture greenhouse

monitoring system. The system is responsible for the collection, processing, transmission, and receipt of digital data. The goal of their investigations was to develop a greenhouse environment system in which the efficiency of the system is used to control the environment area while simultaneously reducing money and farming costs while also saving energy. The B-S structure is utilized in this IOT technology, and the cc2530 is used as a processor chip to function as a wireless sensor node and coordinator, among other things. The gateway runs on the Linux operating system, with the cortex A8 processor serving as the central processing unit. Overall, the design allows for remote intelligent monitoring and management of the greenhouse, as well as the replacement of conventional wired technology with wireless technology, which lowers the cost of personnel.

Control and rescheduling of irrigation systems based on WSN are strong solutions for optimal water management because they use automated communication to know the soil moisture conditions of irrigation design. The method employed in this case is to identify the appropriate frequency and time of watering, which are critical for ensuring effective water usage, high quality of crop detection, and throughput and load on the irrigation system. OPNET is a company that simulates agricultural operations. WSN design is being used for an irrigation system, and it is utilizing the Zig bee protocol, which will have an effect on battery life. The WSN is still in the development stage has its disadvantages, including unpredictable communication times and a weak network that consumes too much power and causes communication to be lost in agricultural fields. (Kumar et al 2018). DHT11, MQ2, soil humidity, sensors of light intensity, transmit readings to the cloud server in real time. Data are seen on a website to the customer. The Machine Learning Algorithm is used to determine the crop that is best cultivated in a given area based on the real-time values obtained. A structured dataset with the minimum criteria is maintained for a given plant and used for crop prediction.

PIC GSM based technology includes temperature sensor, humidity sensor, soil humidity sensor, light sensor, module. GSM technology is a microcontroller. Both sensors are interfaced with a pic microcontroller successfully. The pic microcontroller is attached separately to each sensor. In GSM is used the pic microcontroller. This pi-microcontroller transmits the entire data that each sensor collects to the GSM and sends a mobile alert. So we get a specific name on mobile telephone for this disorder and for medicines (Sushma et al 2019). The breadboard is connected to the Arduino UNO optimized DHT11 humidity and temperature, water level sensor, Soil Humidity Sensor. The language of programming uses instructions to retrieve and represent results. The method stops if the data is not accurate (Anitha et al 2020).

The sensors are linked together such as Soil Moisture, Temperature and Humidity. The Arduino YUN microcontroller interprets the instructions from the PC and turns the sensors on/off. The pump is powered and held in the same status until the water level enters a safe zone if watering of the plant is needed. The data can be track by having user log in and password through the device and mobile site (Ravi Kant Jain et al 2020). Together with Arduino UNO, sensors such as pH, temperature and humidity sensors and macronutrients are used to calculate pH in soil moisture levels. It predicts the crop suitable for this soil based on these factors. In the data base for yield analysis, all data obtained from sensors are processed (Pravallika et al 2020).

On receiving the signal, the Arduino UNO provides the correct output that activates and pumps relays according to soil and atmosphere conditions with sensors such as soil moisture sensors, water level sensors and temperature sensors. The ON and OFF state information for the pump can be sent to the user with the aid of GSM. This GSM module uses the TDMA technique to transmit the message to the recipient.Existing systems communicate different soil parameters sensed mainly by Arduino Uno via cloud sensors. Additional microcontrollers can be viewed as cost reduction and performance optimization. The data are processed by the user for manual processing and gathered in real time. It is user-dependent and is not mainly used to simplify irrigation processes. Although several sensors are related, only a few of them are known as system classification parameters. When these are taken into consideration, the consistency of the algorithm decreases. So a comprehensive scheme is not implemented (Karpagam et al 2020).

MATERIAL AND METHODS

Crops prediction for seeding by machine learning techniques**.** The project is an Internet of Things (IoT) framework utilizing peripheral interface controllers (POIs) in the agricultural sector

Automatic irrigation: Machine-learning technique for leaf disease detection using image processing (Naresh et al 2019)

Details Visualization Soil Parameters Monitoring

Real-time WSN data are saved on the PC Local Host, processed and accessed via myCayenne devices'.

Hardware: Ready, economic, energy-efficient components for industry.

Transmitter: PIC 16F877A IC, soil and humidity, soil humidity, pH Soil & Soil NPK, relay driver module, water pump engine, LCD screen, and power supplier (Premkumar et al 2018).

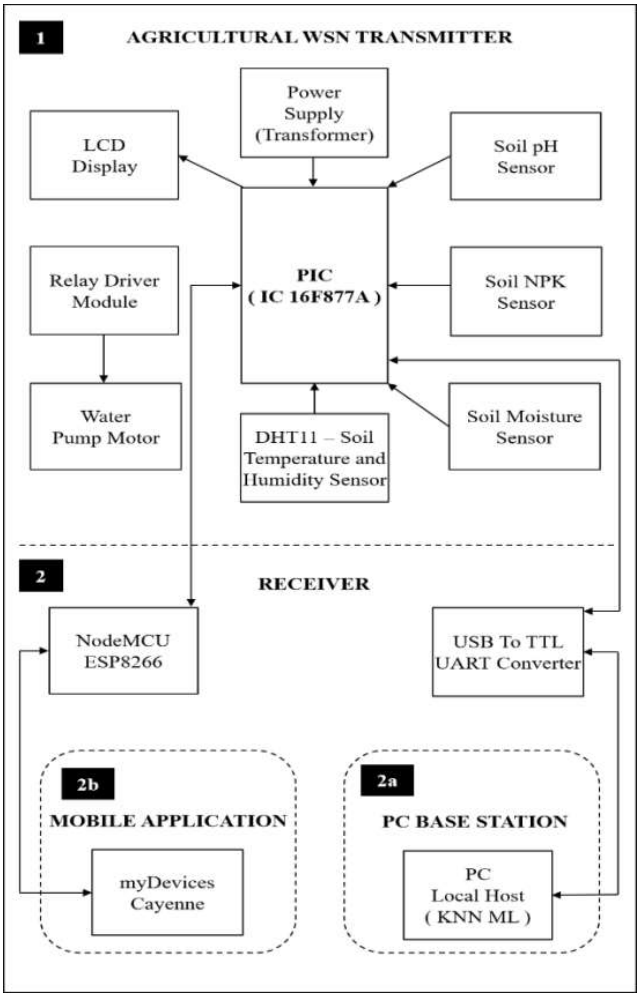

Fig. 1. Diagram of proposed system architecture

Sensor integrated

Gateway: USB to PC Localhost TTL *UART Converter*. Mobile Use ESP8266 Wi-Fi Module.

Receiver: Localhost PC Base Station for data storage and machine-learning.

My Devices Cayenne mobile phone downloads.

Software: Integrated Development Environments (IDEs) Dynamic, simple, comprehensive, smart, official and open source.

Process Steps

Step 1: connections – Sensors (Soil Temperature and Humidity, Soil Moisture, Soil pH and Soil NPK) are embedded to the PIC Microcontroller IC 16F877A for sensing/transmitting the agricultural field soil quality data are in Figure 2 and 3.

Step 1.1: This is converted and transmitted as serial data to the PC Localhost through USB to TTL UART Converter as well as to the myDevices Cayenne Mobile Application every 3 seconds (real-time) through Wi-Fi Module NodeMCU ESP8266 (Ravi Kant Jain et al 2019).

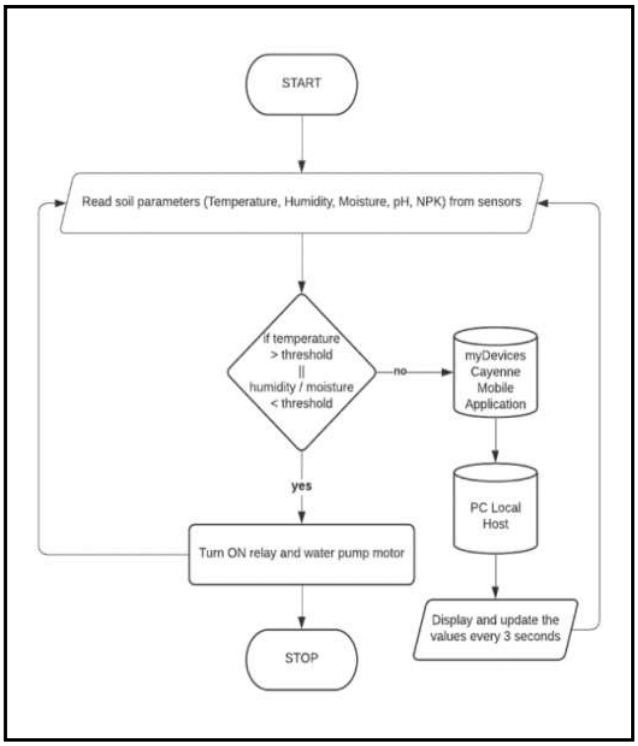

Fig. 2. Dataflow diagram of PIC microcontroller

Fig. 3. Machine learning in my devices Cayenne mobile application

Step 2: *Automatic irrigation* – When the Soil Temperature, Humidity and Moisture content go below the threshold value, the driver and relay are commanded to switch ON / OFF the water pump.

Step 3: Machine learning in Pc localhost – K-Nearest Neighbour (KNN) Classifier Algorithm (Nikesh Gondchawar 2016).

Step 3.1: Crop prediction– A dataset named, crop.csv with 152 entries each of Soil NPK, temperature, humidity, pH and moisture values, totally 760 values corresponding to the crop labels rice, maize, dhal, is trained using KNN Classifier ML Algorithm with accuracy of 98%. When the user requests crop prediction for his field, through USB-UART Converter, PIC and ESP8266, the predicted crop for the current soil parameters is sent from the PC as result to the Cayenne Application.

Step 3.2: Leaf diseases detection –A train dataset named, leaf.csv having 348 parameters each for, 'total areas affected', 'no. of s.p. (number of spots of disease)', totally 696 values derived through image processing of 348 healthy and unhealthy mango leaves images corresponding to the disease severity, 'none', 'low', 'medium', 'high' status labels, is used for training the model using KNN Classifier ML Algorithm with 97% accuracy (Ibrahim Mat et al 2019). A test dataset with images of both healthy and unhealthy leaves is used for testing the model results. When the user requests leaf disease detection, through USB-UART Converter, PIC and ESP8266, the health status messages for the current soil parameters is sent from the PC as result to the myDevices Cayenne Application (Aher et al 2018) (Fig. 4.)

Step 4: Soil quality monitoring through data analysis – All the soil parameters are represented as time-series line plots for easy data visualization and analysis. They are plotted as value / (live, month, hour, day, week, 1, 3, 6months, 1year). The history of data can be downloaded for reference (Gondchawaret al 2016).

Machine Learning Technique

Machine Learning (ML) is an artificial intelligence division focused on the concept that systems should learn from input, detect patterns and decide on a minimum level of human interaction. Learning is supervised if the model is being trained on a labeled dataset. Labeling is one that has parameters of input and output. An algorithm for ML Classifier orders or categorizes information automatically into one or more of the "classes" (AAnusha et al 2019).

KNN Classifier

K-nearest neighbours (KNN) algorithm is a kind of ML algorithm that can be used to prevent both grouping and regression. It is used, however, principally in industry for predictive classification problems. We have chosen the KNN Classifier Supervised ML Algorithm for our system as it

Table 1. Rice sample dataset

NPK	Temperature *C	Humidity g kg^{-1}	pH	Soil Moisture kg water^{-1}
0	20.18	200	2	130
1	20.36	200.4	2.1	130.4
2	20.54	200.8	2.2	130.8
3	20.72	201.2	2.3	131.2
4	20.9	201.6	2.4	131.6
5	21.08	202	2.5	132
6	21.26	202.4	2.6	132.4
7	21.44	202.8	2.7	132.8
8	21.62	203.2	2.8	133.2
9	21.8	203.6	2.9	133.6
10	21.98	204	3	134
11	22.16	204.4	3.1	134.4
12	22.34	204.8	3.2	134.8
13	22.52	205.2	3.3	135.2
14	22.7	205.6	3.4	135.6
15	22.88	206	3.5	136

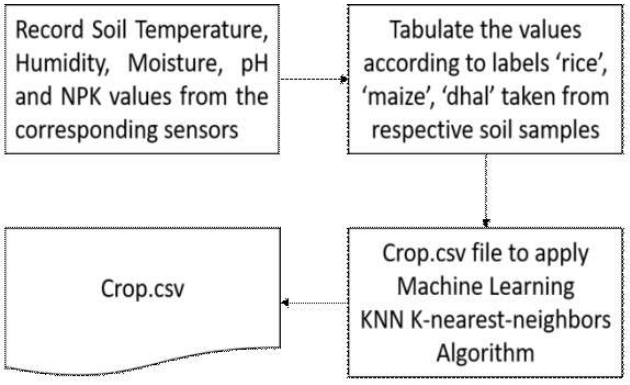

Fig. 4. Working procedure

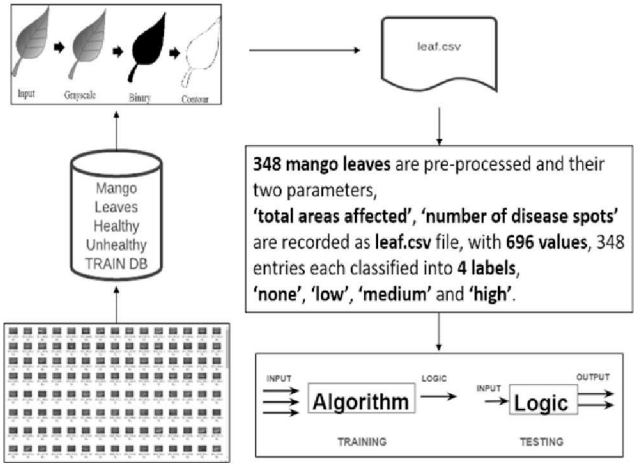

Fig. 5. Flow graph to create crop.csv train dataset

satisfies our necessity. Our KNN algorithm is a Multi-class Classification (Anushaet al 2019)

Working of KNN Algorithm

Step 1 − For implementing any algorithm, we need dataset. So, during the first step of KNN, we must load the training as well as test data. Our datasets here are crop.csv and leaf.csv (Vennila et al 2020).

Step 2 − Next, we need to choose the value of K i.e. the nearest data points. K can be any integer. Here, K = 3.

Step 3 − For each point in the test data do the following

Step 3.1 − Calculate the distance between test data and each row using one of the methods: Euclidean, Manhattan and Hamming. Euclidean is the most general tool for determining distances.

Step 3.2 − Now, sort them in ascending order depending on the distance value.

Step 3.3 − Next, the top K rows of the sorted array will be selected.

Step 3.4 − The test points class depending on the most common class of such rows will be assigned now.

Stage 4 - Finish

Table 2. Leaf health status detection dataset for normal, slightly, medium and highly affected leaf

Total areas affected	No of samples	Status normal/Slightly/ medium
0	0	N
0	0	N
0	0	N
0	0	N
0	0	N
0	0	N
0	0	N
0	0	N
0	0	N
0	0	N
0	0	N
103	1	S
189	5	S
76	5	S
23	5	S
163.5	2	S
228	2	S
411.5	5	S
186.5	1	S
128	4	S
1	1	S
185.5	1	S
177.5	1	S
109.5	1	S
195	2	S
173.5	1	S
103.5	5	S
580	5	M
411.5	5	M
329.5	3	M
543	5	M
561.5	2	M
474	3	M
286	4	M

Datasets

Crop.csv – We have recorded all soil temperature, humidity, moisture, pH and NPK values from the sensors for the rice, maize, and dhal crop soil samples and tabulated them as crop.csv training file in fig 5.

Leaf.csv – 348 mango leaves from Mango Leaves database are pre-processed through image processing in python and their parameters, 'total areas affected' and 'no. of s.p.' are tabulated as leaf.csv train dataset.

RESULTS AND DISCUSSION

Implemented system

'1' in Figure 5.2 Rice shows that Rice is the best crop to be cultivated for the current soil condition and other crops are thus marked '0'. '1' in Figure 5.3 & 5.4 Maize shows that Maize is the best crop to be cultivated for the current soil condition and other crops are thus marked '0'. '1' in Figure 5.6 & 5.7 Dhal shows that Dhal is the best crop to be cultivated for the current soil condition and other crops are thus marked '0'. '0' in Figure 6 leaf shows that the plant leaf is not affected by any disease, i.e., it is 'healthy'. '1' in Figure 7, 7.1, 7.2, 7.3 Leaf shows that the plant leaf is affected by a disease, i.e., it is 'unhealthy'.

With regard to Internet of Things strategies, this article

Fig. 5.1. Rice soil test

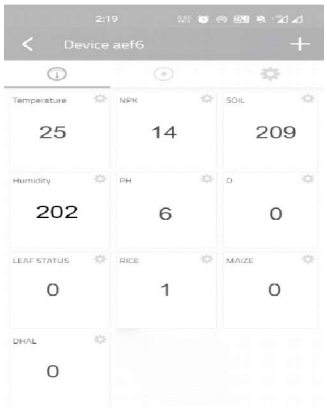

Fig. 5.2. Rice soil sample result

Crop prediction – Maize

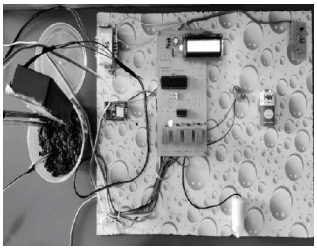

Fig. 5.3. Working model of sensors

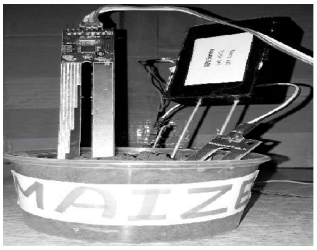

Fig. 5.4. Maize soil test

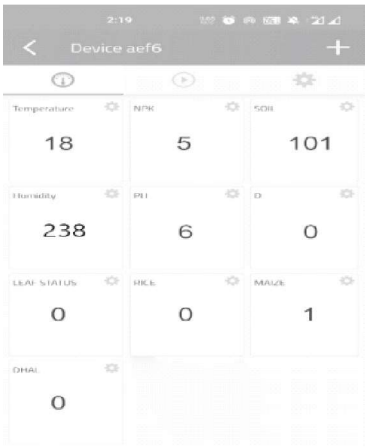

Fig. 5.5. Maize soil sample result

Crop prediction – DHAL

Fig. 5.6. Dhal soil test

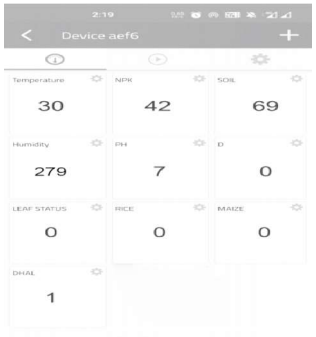

Fig. 5.7. Dhal soil sample result

Leaf health status detection – Healthy leaf

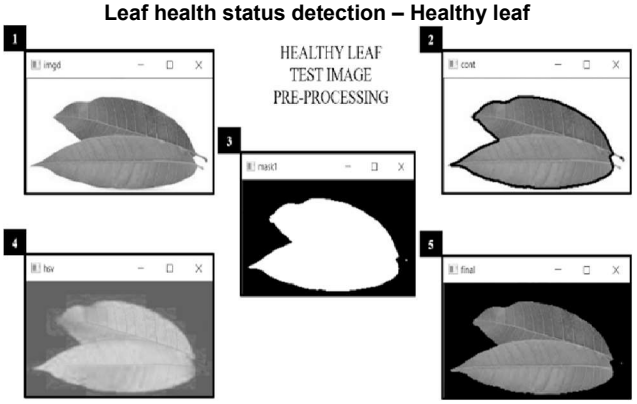

Fig. 6. Healthy leaf status

introduces a novel technique for Intelligent Crop Monitoring Scheme (ICMS) that is based on a remote server management scheme and is compatible with Internet of Things technologies. It is possible to monitor crop details as well as agricultural field details instantly with this Internet of

Fig. 7. Sample data plots of sensor values

Fig. 7.1. Unhealthy leaf output

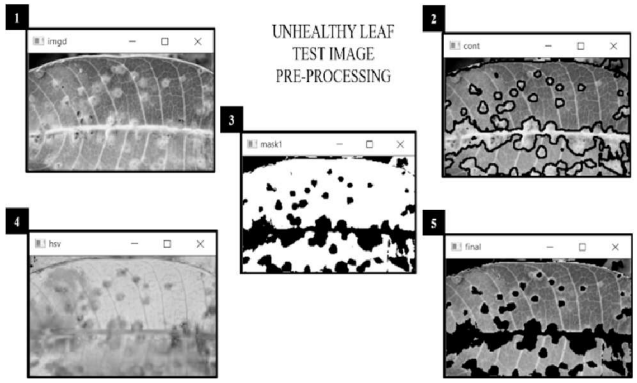

Fig. 7.2. Leaf samples

Leaf health status detection – Unhealthy leaf

Fig. 7.3. Unhealthy leaf status

Model Accuracy

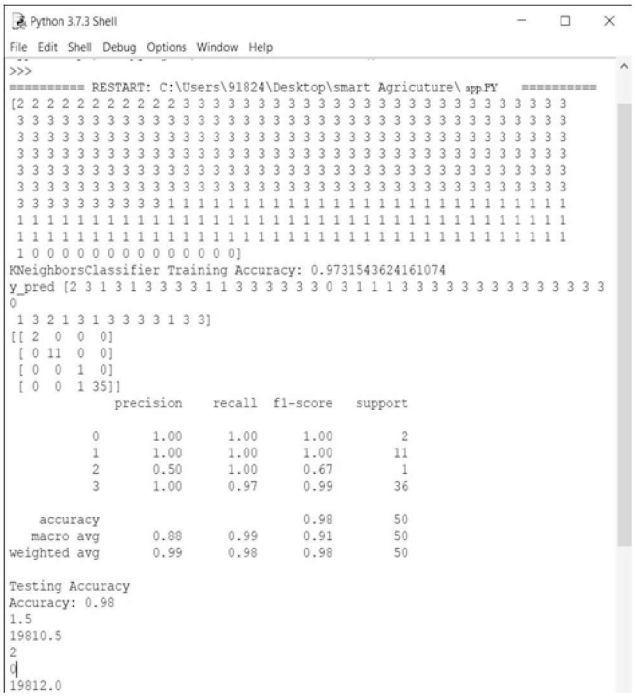
Python 3.7.3 Shell
File Edit Shell Debug Options Window Help
>>>
========== RESTART: C:\Users\91824\Desktop\smart Agricuture\app.PY ==========
KNeighborsClassifier Training Accuracy: 0.9731543624161074
y_pred [2 3 1 3 1 3 3 3 3 1 1 3 3 3 3 3 3 0 3 1 1 1 3 3 3 3 3 3

Jain Ravi Kant, Partha Pratim Ray, Bikash Gupta and Mustaq Ansari 2020. IOT Enabled Smart Drip Irrigation System Using Web/Android Applications in *International Conference on Computing Communication and Networking Technologies (ICCCNT)*. DOI: 10.1109/ICCCNT49239.2020.9225345

Karpagam J, I Infranta Merlin, Bavithra P and Kousalya J 2020. Smart Irrigation System Using IoT in *International Conference of Advance Computing & Communication Systems (ICACCS).* DOI: 10.1109/ICACCS48705.2020.9074201

Kumar T R, Aiswarya B, Suresh A, Jain D, Balaji N and Sankaran V 2018. Smart management of crop cultivation using iot and machine learning. *International Research Journal of Engineering and Technology (IRJET)* **15**(11): 236-245.

Muthunoori Naresh and P Munaswamy 2019. Smart agriculture system using IoT technology. *International Journal of Recent Technology and Engineering (IJRTE)* **7**(5): 98-102.

Nikesh Gondchawar and RS Kawitkar 2016. IoT based smart agriculture. *International Journal of Advanced Research in Computer and Communication Engineering* **5**(6): 838-842.

Patel NR, Lanjewar RB, Mathurkar S and Bhandekar A 2013. Microcontroller based drip irrigation system using smart sensor. *Annual IEEE India Conference (INDICON)* DOI:10.1109/INDCON.2013.6726064.

Premkumar A, Thenmozhi K, Praveenkumar P, Monishaa P and Amirtharajan R 2018. IoT assisted automatic irrigation system using wireless sensor nodes in *International Conference on Computer Communication and Informatics (ICCCI)* IEEE. DOI: 10.1109/ICCCI.2018.8441209

Sai Pravallika G, K Sri Thanvi, Ch Rupa, Kundana L and Sirisha G 2020. Proficient Smart Soil based IoT System for Crop Prediction in *International Conference on Inventive Research in Computing Applications (ICIRCA).* DOI: 10.1109/ICIRCA48905.2020.9183054.

Sushma A Mane, Snehal T Bhosale, Pournima D Nikam and AG Patil 2019. Smart agriculture using pic microcontroller and GSM based technology. *International Research Journal of Engineering and Technology* (IRJET) **26**(2): 365-371.

Vennila G, Arivazhagan D and Jayavadivel R 2020. An investigation of IOT based smart agriculture. *International Journal of Scientific and Technology Research* **9**(1): 2054-2056.

Received 07July, 2021; Accepted 22 November, 2021

Indian Journal of Ecology (2021) 48(6): 1655-1657

Manuscript Number: 3428
NAAS Rating: 5.79

Exploration of SCATSAT-1 Ku Band Data to Develop MPDI and Assessment of Rice Crop Ecosystem using Brightness and Temperature

Mahesh Palakuru and Sirisha Adamala[1]

Malla Reddy University, Hyderabad-500 043, India
[1]Central Island Agricultural Research Institute, Port Blair-744 101, India
E-mail: pmahesh89@gmail.com

***Abstract*:** Microwave remote sensing playing significant role especially where optical remote sensing and climate influence the data acquisition.SCATSAT-1 scatterometer launched by ISRO offers data in Ku band with SH and SV polarizations. Brightness temperature (BT) or radiance temperature is defined as the measurement of radiance released from atmosphere towards satellite sensor and is measured in temperature units similar to blackbody. The present study focuses on development of Multi-polarized difference index (MPDI) for rice crop. SCATSAT-1 derived BT and NDVI has been used to perform this study. The correlation between MPDI and NDVI is 0.84 for rice crop. The results shows that the MPDI influenced by the moisture. Therefore, it is concluded that MPDI will provide significant stats to testify and see the response of rice crop in horizontal, vertical polarization and temperature environment.

Keywords: Rice crop, BT, MPDI, NDVI, SCATSAT-1

Brightness temperature (BT)or radiance temperature is defined as the measurement of radiance released from atmosphere towards satellite sensor and is measured in temperature units similar to blackbody. Microwave passive radiometer sensor measures antenna temperature and the Earth's Brightness temperature.BT is used in various remote sensing platforms to monitor sea surface temperature, vapour, wind, and precipitation (Chaube et al 2019, Palakuru et al 2019a). Microwave radiometer observations with low frequencies have been studied hugely due to their potential to penetrate into the soil and collection of target information. Studies showed that by applying appropriate vegetation, dielectric constant, and surface roughness properties and is possible to retrieve precise information from BT. SCATSAT-1 is launched in 2016 by Indian Space Research Organisation, which offers three products, namely sigma-0, gamma-0, and BT(EUMETSAT OSI SAF 2018, Palakuru et al 2019b). SCATSAT-1 has Ku band real aperture radar and it operates at 13.55 GHz frequency. SCATSAT-1 provides data in microwave region of Electro Magnetic Radiation (EMR) spectrum with no image of target and only with backscatter value of target. This satellite data provides sigma-0, gamma-0, and BT in horizontal and vertical polarizations (Shimada et al 2005, Palakuru et al 2018). *Oryza sativa* is the scientific name of rice crop. Rice crop plays vital to minimise food scarcity in most of the countries in the world. Asia is the most consumed and producing of rice products in the world. China, India and Bangladesh are in top list of rice producing countries in Asia. Therefore, due to significance of rice crop among the food crops, it is important to perform various crop growth studies which improve availability of information or infrastructure for government policy makers and researchers for effective decision making. The present study focus on developing MPDI for rice crop and understanding influence of BT on rice crop.

MATERIAL AND METHODS

In the current study, Ku band radiometry has been used. Ku band sensor receives and calculates surface emitted energy range from 12 to 18GHz. The microwave sensors have potential to receive emitted power from target surface precisely. Emissions from crop will be influenced by angle of incidence, surface properties, and polarization. The backscatter of wave energy from target feature in horizontal polarization is less than vertical polarization (Fore et al 2015, Palakuru et al 2019c). This study was performed to explore SCATSAT-1 Ku band BT product for rice crop growth assessment and relationship of MPDI and NDVI on Indian soils. In Ku band radiometry, soil moisture emits less energy than dry soil due to influence of electrical conductivity and surface properties. Radiance from black body is higher than any other body at similar temperatures (Singh and Dadhwal 2003, Palakuru et al 2020a) and the radiance of any material body is calculated using following equation:

$$B_i(\theta,\phi) = \frac{2(k * [T(\theta,\phi)]}{\lambda^2} \qquad (1)$$

Where T = radiance temperature of material, θ, ϕ= angle of incidence, k =Boltzmann constant and λ = type of polarization.

Emissivity of material is calculated using following equation:

$$\varepsilon_i(\theta,\phi) = \frac{B_i(\theta,\phi;T)}{B_b(T)} \qquad (2)$$

MPDI and NDVI indices are influenced by leaf area index and vegetation fraction of crop. NDVI of rice crop measured using following equation:

$$NDVI = \frac{NIR - RED}{NIR + RED} \qquad (3)$$

Where RED and NIR = bands of EMR spectrum.

The change in response of emissivity can be studied from the results derived from following equation:

$$DPDI_{BT} = 100 * \left(\frac{T_{BV} - T_{BH}}{T_{BV} + T_{BH}} \right) \qquad (4)$$

Where T = brightness temperature from vertical and horizontal polarization. DPDI is duel polarized difference index of BT for rice crop. DPDI is used to perform MPDI, which provides accurate results for rice crop (Palakuru et al 2020b). The multi polarized change in emissivity can be studied using below equation:

$$MPDI = DPDI_0 + \left[\frac{NDVI_{Max} - NDVI}{NDVI_{Max} - NDVI_0} \right]^{2\gamma} * (DPDI_{Max} - DPDI_{BT}) \qquad (5)$$

Where $NDVI_0$, NDVI, and $NDVI_{Max}$ = vegetation index maximum, zero and normal NDVI of rice crop (Palakuru et al 2021).

RESULTS AND DISCUSSION

Rice crop NDVI value at initial stage of season is 0.28 and for forest 0.52. Rice crop and forest NDVI increased from initial stage of season and rice crop decreased to 0.52 at end of season due to decrease in vegetation (Table 1 and 2). The NDVI curve slightly decreased from peak 0.87 to nearly 0.7 due to leaf canopy reduction in summer season. The MPDI values of rice crop and forest stated that the polarized index derived for both rice crop and forest are started decreasing from initial stage of season i.e. at low vegetation index (Suchandra et al 2019, Palakuru et al 2020c). The decreasing trend of MPDI is observed due to sensor properties namely optical sensor and microwave polarized real aperture radar sensor data. In microwave region of EMR, waves are greatly influenced by geometry, electrical conductivity, and leaf area cover.

Crop geometry acts as scattered of radiance in the microwave region of EMR spectrum. The scattering radiance from crop increases with respect to growth compared to barren land. The difference between emission decreases as horizontal and vertical emissivity increases from target surface (Madsen et al 2016, Palakuru et al 2020d). The emission difference between rice crop and forest changed from initial to and of season (Fig. 2). NDVI increases and the MPDI value of rice and forest decreases due to difference in soil moisture (Fig. 3). The correlation between MPDI and

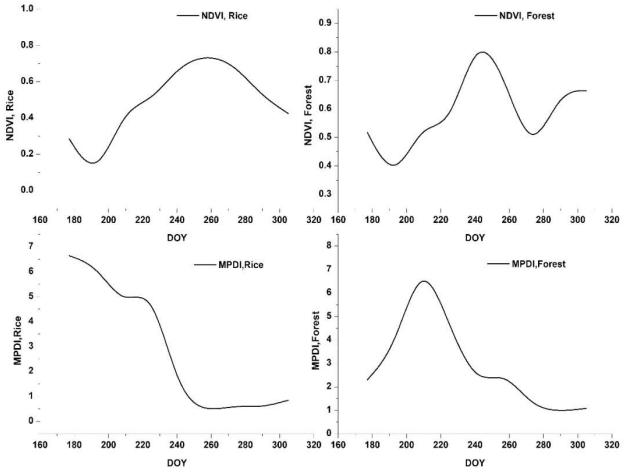

Fig. 1. Response of rice crop and forest in NDVI and MPDI

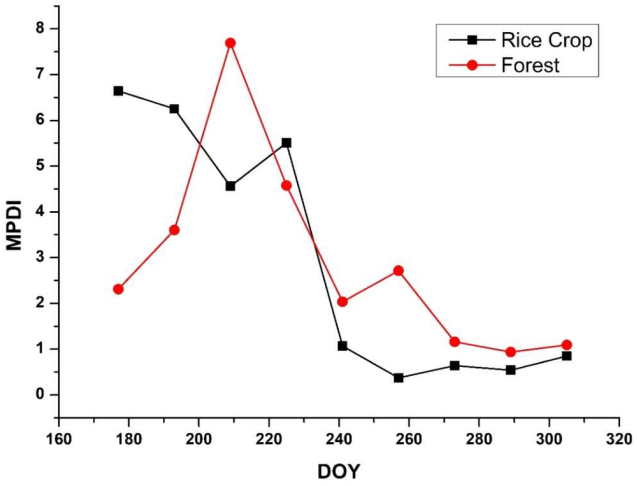

Fig. 2. MPDI of rice crop and forest

Table 1. BT, DPDI, and NDVI values of rice crop

BH_{Max}	588.46 ^{0}k	BV_{Max}	561.89 ^{0}k
BH_{Min}	169.2 ^{0}k	BV_{Min}	223.47 ^{0}k
$NDVI_{Max}$	0.65	$NDVI_{Min}$	0.28
$DPDI_{Max}$	13.00	$DPDI_{Min}$	-9.74

Table 2. NDVI and MPDI statistical values

Class	$DPDI_{Max}$	$DPDI_0$	$NDVI_{Max}$	$NDVI_0$	n	r
Rice	13.00	-9.74	0.65	0.28	120	0.80
Forest	13.75	-10.70	0.87	0.30	120	0.64

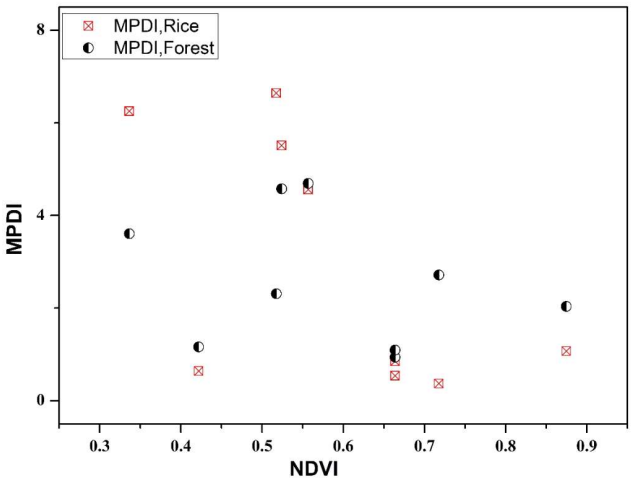

Fig. 3. Response of MPDI for rice and forest at various NDVI levels

NDVI is 0.84 for rice crop (Palakuru et al 2020e). Therefore, MPDI will provide significant stats to testify and see the response of rice crop in horizontal, vertical polarization and temperature environment.

CONCLUSIONS

Potential of SCATSAT-1 Scatterometer Ku band data explored to study rice crop response in the present study. Brightness Temperature (BT) product of Ku band has been used to investigate rice crop and forest. The scattering radiance from crop increases with respect to growth compared to barren land. The NDVI curve slightly decreased from peak 0.87 to nearly 0.7 due to leaf canopy reduction in summer season. The MPDI of rice crop and forest polarized index derived for both rice crop and forest start decreasing from initial stage of season i.e. at low vegetation index. The decreasing trend of MPDI is observed due to sensor properties namely optical sensor and microwave polarized real aperture radar sensor data. From the results it is observed that the MPDI of rice crop is influenced by moisture. In microwave region of EMR, waves are greatly influenced by geometry, electrical conductivity, and leaf area cover. MPDI will provide significant stats to testify and see the response of rice crop in horizontal, vertical polarization and temperature environment.

REFERENCES

Chaube NR, Chaurasia S, Tripathy R, Teheliani P and Ray SS 2019. Crop phenology and soil moisture applications of SCATSAT-1. *Current Science* **117**(6): 1022-1031.

EUMETSAT OSI SAF 2018. SCATSAT-1 wind product user manual, SAF/OSI/CDOP2/KNMI/TEC/MA/287.

Fore AG, Neumann G, Freedman AP, Chaubell MJ, Tang W, Hayashi AK and Yueh SH 2015. Aquarius scatterometer calibration. *IEEE Journal of Selected Topics in Applied Earth Observations and Remote Sensing* **8**(12): 5424-5432.

Madsen NM and Long DG 2016. Calibration and validation of the RapidScat scatterometer using tropical rainforests. *IEEE Transactions onGeoscience and Remote Sensing* **54**(5): 2846-2854.

Palakuru M and Yarrakula K 2019a. Study on paddy phenomics ecosystem and yield estimation using space-borne multi sensor remote sensing data. *Journal of Agrometeorology* **21**(2): 171-175.

Palakuru M and Yarrakula K 2019b. Study on paddy phenomics ecosystem and yield estimation using multi-temporal remote sensing approach. *Indian Journal of Ecology* **46**(2): 293-297.

Palakuru M, Yarrakula K, Chaube NR, Khadar Babu SK and Satyajirao YR 2019c. Identification of rice crop phenological parameters using dualpolarized SCATSAT-1 (ISRO, India) scatterometer data. *Environ Sci Pollut Res*, DOI: 10.1007/s11356-018-3692-5.

Palakuru M and Yarrakula K 2020a. A comparison study of space borne Dual Polarization Difference Index (Sea Wind SCATSAT-1 Scatterometer) and NDVI (MODIS) on paddy crop growth. *Indian Journal of Geomarine Science* **49**(9): 41-47.

Palakuru M, Adamala S and Bachina HB 2020b Spatial mapping of rice crop evapotranspiration in Godavari command area. *Indian Journal of Ecology* **47**(2): 361-364.

Palakuru M, Khadar Babu SK and Renganayaki P 2020c. Estimation of rice crop biophysical parameters using multi-temporal SENTINEL-2 MSI sensor data. *Indian Journal of Ecology* **47**(1): 53-57.

Palakuru M, Krishna Reddy YV, Adamala S and Bachina HB 2020d. Hydrological appraisal of nariganipalli watershed (India) using spatial information technology. *Indian Journal of Ecology* **47**(2): 281-285.

Palakuru M, Adamala S and Bachina HB 2020e. Modeling yield and backscatter using satellite derived biophysical variables of rice crop based on artificial neural networks. *Journal of Agrometeorology* **22**(1): 41-47.

Palakuru M, Adamala S, Bachina HB, Lakshmi B and Krishna Reddy YV 2018. Application of space-born remote sensing to analyze forest cover in Chittoor (India) area. *International Journal for Research in Applied Science and Engineering Technology* **6**: 884-890.

Palakuru M, Khadar Babu SK and Chaube NR 2021. Exploring potential of C band synthetic aperture radar imagery to investigate rice crop growth mechanism and productivity. *Environmental Science and Pollution Research* **28**(31): 42001-42013.

Shimada M 2005. Long-term stability of L-band normalized radarcross section of Amazon rainforest using the JERS-1 SAR. *Canadian Journal of Remote Sens*ing **31**(1): 132-137.

Singh RP and Dadhwal VK 2003. Comparison of space-basedmicrowave polarization difference index and normalized difference vegetation index for crop growth monitoring. *Indian Journal of Radio and Space Physics* **32**: 193-197.

Suchandra B, Cotton J, Fore A, Raj Kumar et al 2019. An assessment of the performance of ISRO's SCATSAT-1 Scatterometer. *Current Science* **117**(6): 959-972.

Received 23 July, 2021; Accepted 12 November, 2021

Indian Journal of Ecology (2021) 48(6): 1658-1669

Manuscript Number: 3429
NAAS Rating: 5.79

Consul Multiphasic 3.5a Package for Modeling of Groundwater Protection from Amoxicillin using Modified Bentonite

Zahra Abdel Sahib and Said Tab Ali

Department of Environmental Engineering, University of Baghdad, Iraq
E-mail: friend.star222@gmail.com

Abstract: This study investigates the performance of modified bentonite (MB) as a reactive medium in the permeable reactive barrier (PRB) for remediation of simulated groundwater contaminated with amoxicillin. It is evident that the natural bentonite (NB) modified with hexadecyl trimethyl ammonium (DK1) can effectively remove amoxicillin from aqueous solution. The effect of different parameters such as contact time, initial pH of the solution, agitation speed, initial amoxicillin concentration and MB dosage was studied. The maximum removal (97%) of amoxicillin using MB for 4 hr, pH 11, 250 rpm, 50 mg l^{-1}, and 0.6 g 100 ml^{-1}, respectively. The adding glass waste (GW) to the reactive medium (MB) led to an increase the hydraulic conductivity and decrease the effectively of amoxicillin removal, at the same time. The isotherm study showed that th sorption of amoxicillin onto GW&MB mixture fitted the Freundlich isotherm model with coefficient of determination (R2) equal to 0.9432 The leaching test indicated that the dissolution of amoxicillin bearing-MB is very low. A two-dimensional groundwater numerical model was developed under equilibrium condition using COMSOL Multiphysics 3.5a software to evaluate the performance of GW&MB-PRB in two configurations namely continuous (C-PRB) and funnel and gate (FG-PRB). The experimental results proved that the GW and MB-PRB was efficient in the restriction of contaminant plume and both configurations of PRBs can be used successfully to treat amoxicillin-contaminated groundwater with operation time equal to 87 and 75 day for C-PRB and FG-PRB, respectively.

Keywords: COMSOL Multiphysics 3.5a, Groundwater, Amoxicillin

The contamination of groundwater by organic and inorganic compounds has been considered since the industrial revolution. Groundwater is generally more reliable for use than surface water (Faisal and Abd Ali 2017a). The most common technology used for remediation of groundwater has been ex-situ pump-and-treat system. This system extract groundwater to the surface then treats it through different approaches such as adsorption and either re-introduce the treated water to the subsurface or discharge it to a storm drain. This technique is difficult, costly, and ineffective most of the time in removing enough contamination to restore the groundwater to drinking water standards in acceptable time frames (Faisal and Abd Ali 2017b). Accordingly, permeable reactive barriers (PRBs) technology was the alternative method used to remediate groundwater contaminated with different types of contaminants (Faisal and Abd Ali 2016). It is found to be more cost-effective than a pump and treat and has been a demonstrated potential to diminish the spread of contaminants (Abd Ali et al 2019). PRB technology may be installed as a continuous reactive barrier (C-PRB) or as a funnel-and-gate system (FG-PRB). Due to the fact that one of the most important stages of designing a PRB is choosing appropriate filler for the barrier, many research centers are searching for new reactive materials in order to improve the effectiveness of decontamination (Faisal and Ali 2015). Activated carbon can be used as a reactive medium (sorbent) in PRB because of its effectiveness in removal of a wide variety of organic and inorganic pollutants from different media, but it still very expensive. Therefore, the production of low-cost sorbents becomes the aim of many researchers (Sulaymon et al 2015). Natural clay is acquiring prominence as low-cost adsorbents over the last a few decades due to their local and abundant availability and the capability to undergo modification to enhance the surface area, adsorption capacity and range of applicability (Monvisade And Siriphannon, 2009). Among natural clays, bentonite has been proven to be a promising adsorbent for contaminate removal. The presence of a net negative charge on the surface confines the use of bentonite for the effective removal of contaminate (An and Dultz 2007, QU 2008). In addition, the adsorption capacity of natural bentonite is hampered by its limited surface area. All these factors have led to the need for research and development in the field of modification of clay surfaces to enhance their adsorptive properties. Surface modified bentonites have high potential to provide an alternative to the most widely used activated carbon. Therefore, in order to ameliorate the adsorption properties and the range to the applicability, a number of physical and chemical methods have been investigated to

modify the bentonites, including heat treatment, acid activation, treating with cationic or anionic surfactants and polymer modification (Al-Asheh et al 1999). Accordingly, the main objective of this study is to investigate the possibility of modification of natural bentonite using hexadecyl trimethyl ammonium (DK1) to use it as a reactive material in PRB technology for remediation of amoxicillin contaminated groundwater. In addition, two-dimensional groundwater numerical model was developed under the equilibrium condition using COMSOL Multiphysics 3.5a software to evaluate the performance of PRB in two configurations namely continuous (C-PRB) and funnel and gate (FG-PRB).

MATERIAL AND METHODS

The bentonite used in this study was local bentonite in natural form (calcium base). It was supplied by the State Company of Geological Survey and Mining (Baghdad) as pieces of rocks. These rocks were washed with distilled water several times, dried at 90C°, crushed to granules of different sizes, then sieved using sieves to produce bentonite granules of sizes (250-500) µm. The physical characteristics and composition of the natural bentonite (NB) were analyzed in the laboratories of the State Company of Geological Survey and Mining; the results were listed in (Table 1). The sandy soil was used as an aquifer in a numerical groundwater model to simulate amoxicillin transport in groundwater because it represents the worst case in the speed of the arrival of the pollutant into the groundwater. This soil had a particle size distribution ranged from 63 µm to 0.71 mm (porosity = 0.41) with an effective grain size, d_{10}, of 110 µm, a median grain size, d_{50}, of 180 µm, a uniformity coefficient, Cu = d_{60}/d_{10}, of 1.73, and hydraulic conductivity of 0.0022 cm s^{-1}.The amoxicillin was selected as a contaminant: To simulate the water's amoxicillin contamination. It was obtained as trihydrate from local market and used without any further treatment. The aqueous solutions of amoxicillin that mimic contaminated water were prepared by dissolving 0.05 gram of Amoxicillin in one liter of distilled water in order to obtain a concentration of 50 mg L^{-1}. The initial pH of each of the solutions was adjusted by the addition of HNO_3 or NaOH solution. The remain amoxicillin concentration in the solution were measured using double beam UV-visible spectrophotometer (PG Instruments, Model UV T80, England) at λmax = 230 nm.

Table 1. Characteristics of natural Iraqi bentonite

Characteristics	Value
Physical	
d_{gm}, mm	0.35
Moisture content, %	4.57
Bulk density, kg/m^3	845
Specific surface area, m^2g^{-1}	63.5
CEC, meq $100g^{-1}$	65
Composition (wt %)	
Silica (SiO_2)	57
Aluminum (Al_2O_3)	13.5
Ferric oxide (Fe_2O_3)	4.5
Magnesium oxide(MgO)	2.35
Calcium oxide (CaO)	8
Sodium oxide (Na_2O)	0.7
Potassium oxide (K_2O)	0.4
Titanium oxide (TiO_2)	0.75
Loss on ignition (L.O.I)	12.8

Preparation of modified bentonite: The modified bentonite (MB) was chosen as a reactive medium for simulation of groundwater remediation using PRB technology in this study. It was prepared by adding 10 g of natural bentonite (NB) to 100 mL of distilled water. The mixture was mixed for 2 hr in order to swell and become homogeneous (Jeeva and Wan Yaacob 2018). Then a desired amount of surfactant hexadecyl trimethyl ammonium (DK1) was added in weight ratios of (0.25-0.45 g DK1 g^{-1} NB), after that, the mixing process continues for 2 hr. The resulting samples (mixtures) called the modified bentonite (organ-oclay), they were washed with distilled water several times to remove excess salts, and then dried at 105 C° in an oven. The produced samples of the modified bentonite were ground and sieved with a size range from 250 to 500 µm (Kıranşan et al 2014). Some properties of MB have been measured at the Petroleum Research and Development Center such as bulk density =931 kg/m^3, porosity = 0.67, and hydraulic conductivity = 0.00011 cm sec^{-1}.

Characteristics of organo-bentonite: The characteristics of the prepared organo-bentonite were typified by applying the following testes: Fourier-transform infrared spectroscopy (FTIR): A BRUKER FTIR spectrophotometer (Japan) was used to record the FTIR spectra of the natural and modified bentonite (before and after amoxicillin sorption). Samples for the spectral analysis were prepared by mixing bentonite with KBr for use as the reference, and the spectra obtained fell within the range of 4000–400 cm^{-1}.

Scanning electron microscopy analysis (SEM): Scanning electron microscopy is central to micro structural analysis and therefore important to any investigation relating to the processing, properties, and behavior of materials that involves their microstructure. Therefore, the natural and modified bentonite was examined using SEM (Inspect S50 Model, FEI/ Netherlands). It performed at The Technological University-Nanoscale Research Center.

Surface area: Surface area is an important factor in determining the active sites that will be occupied with the contaminants. Specific surface area was determined by surface area analyzer the BET method from the nitrogen adsorption at 77 K, using an automatic Micrometrics ASTM D 3663, USA. It performed at the Ministry of Science and Technology.

Distilled water leaching of amoxicillin - bearing modified bentonite: To confirm the ability of the modified bentonite to maintain the amoxicillin that removed from the contaminated solution. Amoxicillin - bearing modified bentonite specimens were subjected to a distilled water leaching procedure, conducted in accordance with "German Standard Methods DIN 38414 Part 4".The leachates were analyzed for the amoxicillin.

Batch Mode Sorption Experiments: The adsorption of amoxicillin by modified bentonite was studied using batch experiments under different conditions, the batch removal experiments were carried out by adding specified amount of the modified bentonite to 100 mL of amoxicillin synthetic solution with initial concentration of 50 mg L^{-1}, then the mixture was shaken using thermostatic shaker (Edmund Buhler SM25, German). For practical purposes, batch experiments were implemented with different contact time (0-5 hr), initial pH of solution (3-12), agitation speed (0-250 rpm), and sorbent dosage (0.1-0.8 g 100 mL^{-1}). A fixed volume(20 mL) of the solution was withdrawn from each flask, and filtered using filter paper type (Whatman No. 40) to separate the adsorbent from the aqueous solution, then the filtered solution was analyses to determine the remain amoxicillin concentration. The amount of amoxicillin adsorbed onto modified adsorbent, qe (mg g^{-1}), was calculated from the mass balance Eq. 1(Masood and Abd Ali 2019):

$$q_e = \frac{(C_O - C_e)V}{m} \qquad (1)$$

Where *qe* is the amount of amoxicillin adsorbed per unit mass of adsorbent (mg/g), C_o and C_e (mg L^{-1}) are initial and equilibrium amoxicillin concentration, *V* (L) is the volume of amoxicillin solution, and *m* (g) is the adsorbent mass. The removal efficiency (*R%*) of amoxicillin onto modified bentonite at time t was calculated by Eq.2 (Abd Ali et al 2019):

$$R\% = \frac{(C_o - C_e)}{C_o} \times 100 \qquad (2)$$

Sorption isotherms: Sorption process is usually described through isotherm models, which is the equilibrium relationship between the adsorbate concentration in the fluid phase and the adsorbate concentration on the adsorbent particles at a given temperature (Abd Ali and Ismail 2020). The sorption data for amoxicillin is fitted with two isotherm models as follows:

Freundlich model: This model was originally empirical in nature but was later interpreted as the sorption to heterogeneous surfaces or surfaces supporting sites with various affinities. It is assumed that; the stronger binding sites are initially occupied; and the binding strength decreasing with increasing degree of site occupation, can be quantified by the following equation 3 (Abd Ali 2019):

$$q_e = K_F C_e^{1/N} \; N > 1 \qquad (3)$$

Where K_F (mg g^{-1}) (l $mg^{-1})^{1/N}$ is the Freundlich sorption coefficient and *N* is an empirical coefficient indicative of the intensity of the adsorption.

Langmuir model: "The Langmuir adsorption model Eq. 4 is valid for single-layer adsorption. It is based on the assumption that maximum adsorption corresponds to a saturated monolayer of solute molecules on the adsorbent surface, that the energy of adsorption is constant, and that there is no transmigration of adsorbate in the plane of the surface (Abd Ali 2020).

$$q_e = \frac{q_m b C_e}{1 + bC_e} \qquad (4)$$

Where q_e (mg g^{-1}) is the solute adsorbed amount per unit of adsorbent weight at equilibrium, (q_m) is the maximum adsorption capacity, C_e (mg l^{-1}) is the equilibrium concentration of the solution in the bulk solution, and *b* is the constant related to the adsorption free energy.

Two-dimensional model development: A two-dimensional groundwater model of aquifer demonstrates that the COMSOL Multiphysics applied to unidirectional fluid flow and 2D transient solute transport through an unconfined aquifer. Although the velocity of flow has a component in the transverse direction (Y), the unidirectional fluid flow in the X direction was assumed in the present simulation which is fair for such situation (Khebchareon 2012). The model determines the spatially and temporally extent of the solute plume in the subsurface of the physical model adopted in the present study. The model aquifer is contained within the square shape (50 m × 50 m) for continuous-PRB (C-PRB) and funnel and gate-PRB (FG-PRB), as illustrated in (Fig. 1). The continuous PRB (C-PRB) model aquifer contained three parts. The first part represented by 30 m length of the sandy soil measured from the left side of the aquifer, the second part represented by 3 m (thickness) barrier placed beside the soil, and 17 m of the sandy soil represented the third part was placed beside the barrier. The contaminant solution with an initial concentration and velocity of 0.05 kg/m^3 and 3.45 m d^{-1}, respectively, was introduced through the model aquifer from line source (10 m long) which was located at left side of the aquifer. This source was simulated a continuous release of contamination, therefore, at zero time, the concentration of

the pollutant in all aquifer model, except the line source, is zero then the concentrations of pollutant start to increase with the increase of time indicating the spread of the pollutant in the aquifer model. The concentrations of amoxicillin at points of interest were monitored in front of, within, and behind the PRB, these points are very important because they clarify the difference in pollutant concentrations before, during, and after treatment thus demonstrating the efficiency of the barrier.

Transport of amoxicillin through the model aquifer: The transport of contaminant in the porous media can be described mathematically by the one-dimensional advection-dispersion equation Eq.5. This equation signifies that the transport of dissolved contaminant is governed by three mechanisms namely; advection, dispersion and sorption. The advection is the migration of contaminant with flowing water, while dispersion is the migration of contaminant due to concentration gradient and varied pathways (Travis and Webb 1978). "

$$D_x \frac{\partial^2 C}{\partial x^2} - V_x \frac{\partial C}{\partial x} = \frac{\partial C}{\partial t} + \frac{\rho_b}{n} \frac{\partial (q)}{\partial t} \qquad (5)$$

Where *n* is the porous medium porosity, *V* is the velocity of pore water m min^{-1}, *q* is the sorbed amount of contaminant onto the sorbent substance mg/g, *D* is hydrodynamic dispersion coefficient and ρb bulk density Kg/m^3. The description of *q* can be (incorporated) with; Eq.5 the subsequent can be present as follows:

$$D_x \frac{\partial^2 C}{\partial x^2} - V_x \frac{\partial C}{\partial x} = R \frac{\partial C}{\partial t} \qquad (6)$$

Where *R* is the retardation factor that has the effect of retarding the transport of adsorbed species relative to the advection front, it can be calculated by the following equation: " "

$$R = 1 + \frac{\rho_b}{n} \frac{\partial q}{\partial C} \qquad (7)$$

Eq.6 can be re-written to describe the two-dimensional contaminant transport as follows:

$$D_x \frac{\partial^2 C}{\partial x^2} + D_y \frac{\partial^2 C}{\partial y^2} - V_x \frac{\partial C}{\partial x} = R \frac{\partial C}{\partial t} \qquad (8)$$

For the flow of contaminated groundwater through the sandy soil (aquifer), the value of R will be assumed equal to 1 which is reasonable for this type of soil (assumed as non-reactive medium). On the other hand, the sorption of amoxicillin on modified bentonite (PRB) is governed by sorption isotherm that matches the batch experimental data (higher R^2). To present a numerical solution, Eq. (8) in combination with initial and boundary conditions (Table 2) can be solved using COMSOL Multiphysics 3.5 software which is based on finite element method.

Longitudinal dispersion coefficient: The effect of hydrodynamic dispersion is to cause a plume of contamination to elongate in the direction of advection as well as to develop a gradient of decreasing concentration from the center to the margins of the plume. However, the values of longitudinal dispersivity (α_L) used in the present study for PRB (organo-bentonite) and aquifers (sandy soil) were estimated using the following equation (Fetter 1999):

$$\alpha_L = 0.83 (\log L)^{2.414} \qquad (9)$$

where L is the length of the flow path (m).

Tortuosity (τ) is a measure of the effect of the shape of the flow path followed by water molecules in a porous medium. It is calculated depending on the porosity of the medium (n) as follows (Abd Ali et al 2019):

$$\tau = n^{m-1} \qquad (10)$$

(Archie 1942) reports values for m [Eq. (10)] of 1.8–2 for

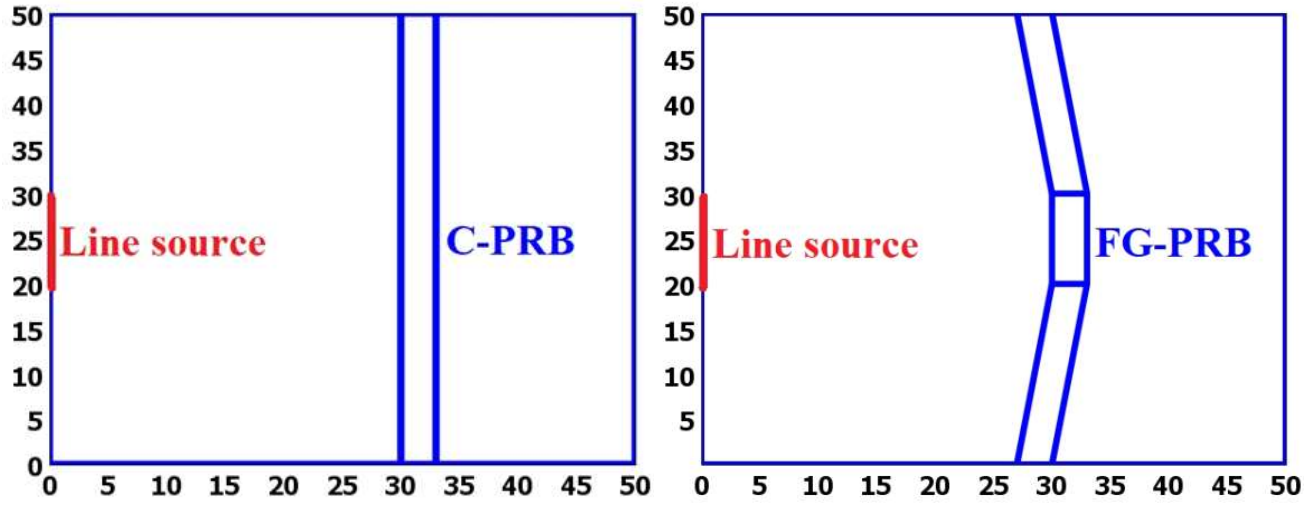

Fig. 1. Schematic diagram of the model aquifer with PRBs as plotted by COMSOL multiphysics 3.5a (all dimensions in m)

consolidated sandstones, 1.3 for unconsolidated sand in a laboratory experiment, and 1.3–2 for partly consolidated sand. For theoretical or conceptual work the value m = 2 is considered, which may be justified if there is no further information as cited by Holzbecher (Holzbecher 2007).

RESULTS AND DISCUSSION

Modification of natural bentonite: In order to determine the best ratio of (DK1/NB) to produce the modified bentonite (MB) that achieve the highest amoxicillin removal percent, different samples of MB were prepared and tested through mixing various amounts of DK1 with specified quantity of NB (0.25-0.45g DK1 g^{-1} of NB) under specified conditions (C_o=50 mg L^{-1}, time=5hr, pH=7, agitation speed=200 rpm, dosage=0.4g MB 100mL^{-1}) at 25°C, as illustrated in (Fig. 2). It was seen that removal percent of amoxicillin increases with the decreasing amount of DK1, this behavior can be attributed to presence of the cations of the modified bentonite and of amoxicillin that generate the electrostatic repulsion force (Shin 2008). Therefore, the ratio of 0.45 g DK1 g^{-1} NB was chosen as the best one for modification of natural bentonite which achieves the maximum amoxicillin removal percent of 70.1%.

Characterization of modified bentonite: The characteristics of the natural and modified bentonite were examined through several analyses as follows:

Fourier-transform infrared analysis (FTIR): FTIR analysis permits spectrophotometric observation and gives means for the identification of surface functional groups present on the adsorbent. These spectra were measured within the range 400-1500 cm^{-1} (Fig. 3). It was performed for natural and modified bentonite. The broad absorption bands that can be identified on the natural bentonite at strong band at 911 cm^{-1} represents the Si-O-Si groups of the tetrahedral sheets (Huang et al 2017). After the modification of natural bentonite, an asymmetric stretching mode of Si-O-Si has shifted from 911 to 877 cm^{-1}. The additional peaks at 1473 cm^{-1} in modified bentonite, which are absent in natural bentonite, indicate the presence of C-N vibration in tertiary amines (Pavia 2010, Jeeva and Wan Yaacob 2018). While the FTIR analysis of modified bentonite before and after sorption illustrates the shifted peaks at 903.39, 763.73 and 451.81 cm^{-1} which indicates the adsorption of amoxicillin on the silanol group.

Scanning electron microscopy analysis (SEM): The surface morphology and microstructure of natural bentonite before and after modification by DK1 was displayed using SEM revealed significant changes in the surface morphology of the natural bentonite after modifying with DK1 (Fig. 4). The

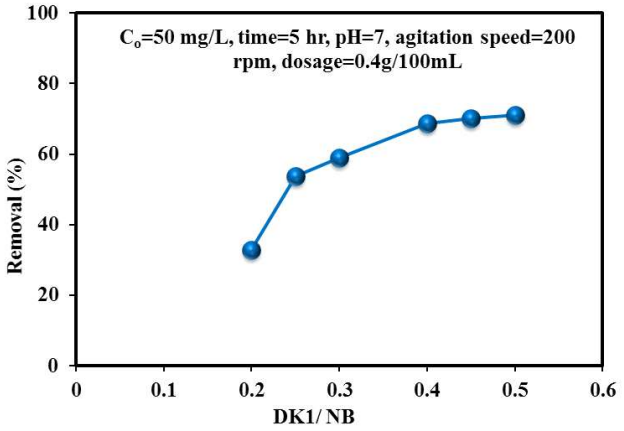

Fig. 2. Effect of the ratio of DK1 bentonite^{-1} for the sorption of amoxicillin

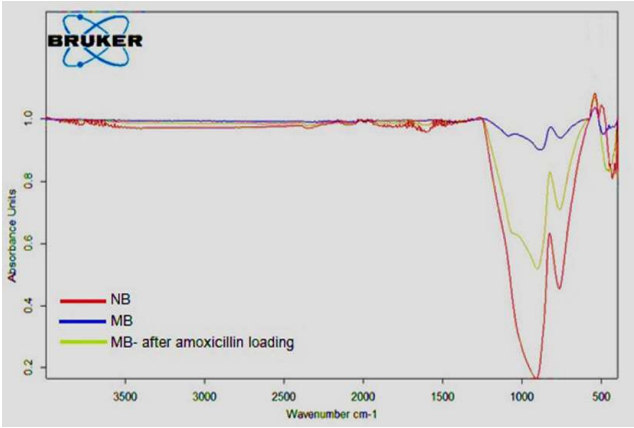

Fig. 3. FTIR analysis of natural and modified bentonite before and after amoxicillin loading

Table 2. Boundary and initial conditions used in the model aquifer

Item	Location	Type/Value	
Boundary settings	Upper boundary	No flux/symmetry	
	Lower boundary	No flux/symmetry	
	Left side boundary	Line source	C_o = 0.05 kg/m^3
		Except for the line source (10m)	No flux/symmetry
	Right side boundary	Advective flux	
Initial condition	(X, Y)	Initial concentration = 0	

natural bentonite has porous structure, rough and irregular appearance with scattered and different sizes of block structure, while the surface morphology of modified bentonite was smooth and accompanied by a small number of holes (Fig. 4). This fluffy appearance probably occurs due to the reduction in certain amorphous phases originally associated within the bentonite because DK1 has generally covered the surface of the bentonite (Anirudhan and Ramachandran 2015, Huang et al 2016)

Surface area: The specific surface area is a crucial indicator of adsorption capacity. The results of this test showed that the surface area of the modified bentonite was lower than natural bentonite. The surface area of natural bentonite is found to be 67.3m^2 g^{-1}. This value was decreased to 48.6m^2 g^{-1} for modified bentonite; this can be attributed to the agglomeration property of bentonite after modification by DK1. In addition, the organic molecules of surfactant entered into the interlayers of bentonite and overlapped its surface, that blocked the channel between the layers, reducing the surface area and pore volume (Ibrahim and Abd Ali 2020, Jeeva and Zuhairi 2018, Siregar et al 2018).

Distilled water leaching of amoxicillin-bearing MB: According to the "German Standard Methods", the leaching test indicated that the dissolution of amoxicillin-bearing MB is generally very low (below the limits of detection). This result confirms that MB can be effective reactive material in PRB by bonding strongly with the contaminant and prevent it to turn into a liquid phase again.

Influence of Batch Operating Parameters on the Amoxicillin Sorption

Effect of equilibrium time: Effect of contact time on amoxicillin removal using 0.4g of MB added to 100 mL of amoxicillin solution for batch tests at 25ºC demonstrates that amoxicillin removal percentage significantly increased with an increase in contact time (Fig. 5). The sorption rate was rapid at the initial stage and gradually slowed down afterwards (Alshammari et al 2020). The slower sorption was likely due to the decrease in sorption sites on the surface of the adsorbent. About 70 % of amoxicillin removed by MB after 4 hr; while the concentrations of amoxicillin were kept relatively constant at contact time greater than 4 hr (Abd Ali 2019). This means that there was no significant change in residual amoxicillin concentrations after this time up to 5 hr.

Effect of initial pH of the Solution: The effect of the initial pH of the solution on the amoxicillin sorption was investigated in the range of pH 3–12 (Fig. 6). The removal percent of amoxicillin increased from 5 to 82 % as pH rose from 2.0 to 11.0 and then remained constant when the pH increased to 12. This behavior can be due to the cation-exchange mechanism, where low valence cations in bentonite were exchanged by protonated functional groups within amoxicillin since amoxicillin has a positive charge at a low pH solution. This phenomenon occurs due to the ionization of its functional groups, identified as carboxyl (pKa: 2.68), amine (pKa: 7.49) and phenolic hydroxyl (pKa: 9.63) (Jin et al 2014). However, an increase in the sorption of amoxicillin onto MB

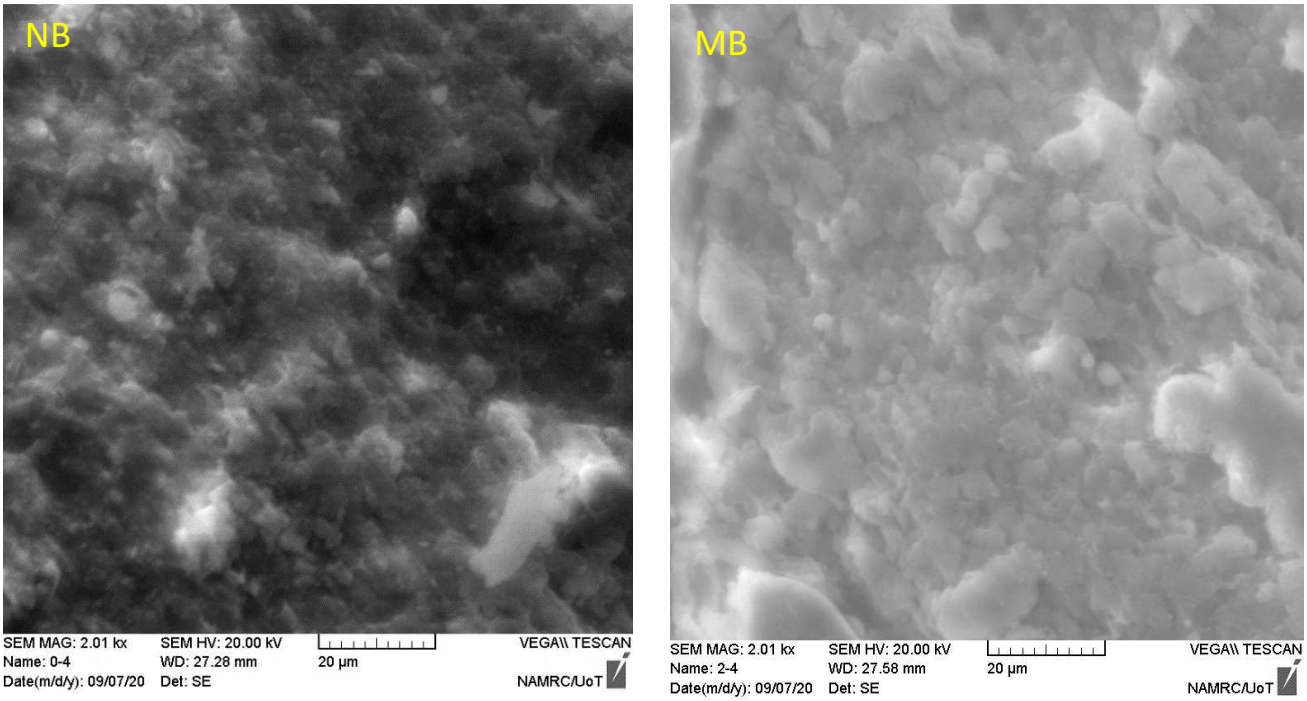

Fig. 4. SEM images of natural bentonite and modified bentonite

was observed when the solution pH increased, which is due to the charge of amoxicillin shifting into neutral molecules. Consequently, amoxicillin molecules were sorbed onto the MB by interacting with the surfactant using the partition mechanism (Zhu et al 2000). Furthermore the sorption of amoxicillin onto MB remained near constant when the pH rose from 11 to 12, resulting in amoxicillin shifting into a negative charge as the solution pH (Adriano et al 2005), and leading to a reduced interaction between amoxicillin and MB. It is concluded that sorption of amoxicillin onto MB in aqueous solution was influenced by the solution pH. It is possible that sorption mechanisms of amoxicillin onto MB are based on physical processes such as ion-exchange and partition mechanisms.

Effect of agitation speed: The agitation speed test is not crucial for the application in the PRB, but it is an important element in the batch experiments to find the best speed achieve the highest removal to reduce the time of experiments, otherwise, the experiments can take longer time. The effect of agitation speed on removal percent of amoxicillin was studied by varying the agitation speed from 0 (without shaking) to 250 rpm and keeping other parameters equal to best ones obtained in the previous steps. The 22 % of the amoxicillin was removed before shaking and the amoxicllin uptake increases with the increase in shaking rate (Fig. 7). There was gradual increase in uptake when agitation speed was increased from zero to 250 rpm at which about 85% of amoxicillin have been removed. These results can be associated to the fact that with the increase in the agitation speed improves the diffusion of amoxicillin towards the surface of the adsorbent. Thus, proper contact is developed between amoxicillin in solution and the binding sites, which promotes effective transfer of sorbate to the sorbent sites (Faisal and Ali 2015).

Effect of initial amoxicillin Concentration: The increase in the initial concentration of amoxicillin from 50 to 250 mg L^{-1} decreased removal percent from 85 to 65 % (Fig. 8). This represents the saturation of the active sites available on the MB to interact with amoxicillin, so with decreasing concentration the more favorable sites became involved in the process (Ali and Abd Ali 2020).

Effect of MB dosage: The effect of MB dosage on the removal percent of the amoxicillin was examined at different dosages. These dosages were ranging from 0.1 to 0.8 g MB added to 100 mL of the amoxicillin solution as presented in Figure 9. This fig showed that the increase of the MB dosage from 0.1 to 0.6 g at fixed initial amoxicillin concentration will lead to improving the removal percent because of a higher dosage of MB in the solution leads to greater availability of sorption sites. It's also clear that after a dosage of 0.6 g, the

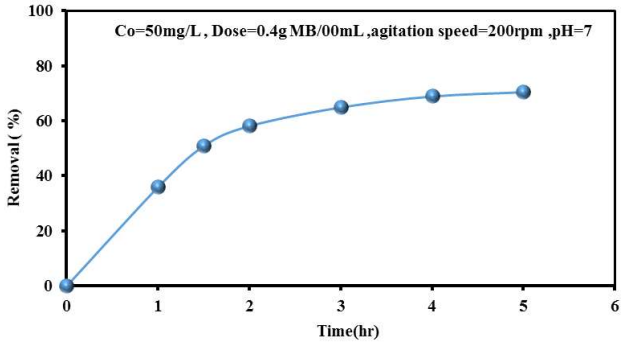

Fig. 5. Removal efficiency of amoxicillin on MB as a function of contact time

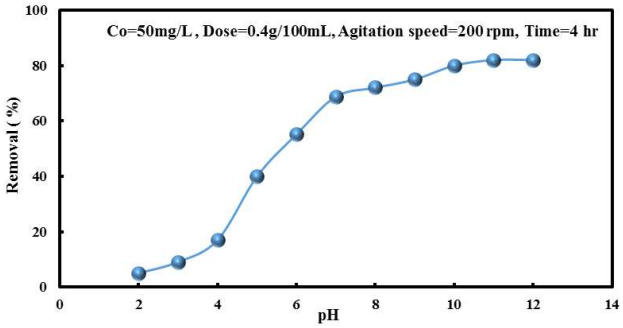

Fig. 6. Effect of initial pH on removal efficiency of amoxicillin by modify bentonite

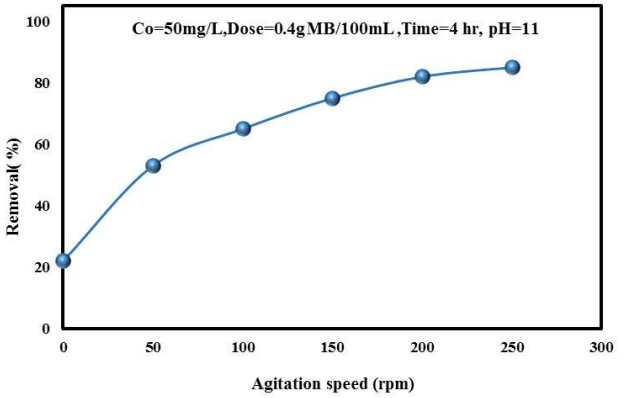

Fig. 7. Effect of agitation speed on removal percent of amoxicillin

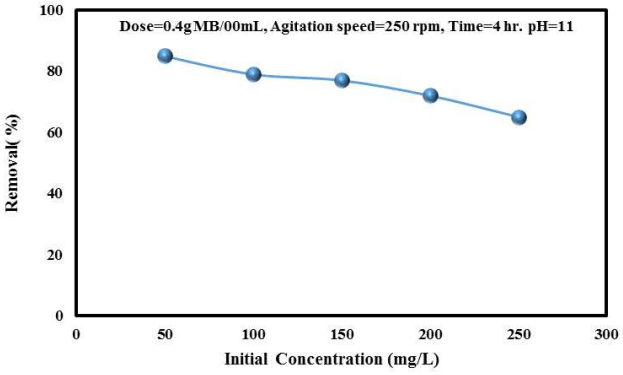

Fig. 8. Effect of initial concentration on removal percent of amoxicillin

removal percent was not changed. Hence, even with the further addition of MB, the removal percent of amoxicillin remain constant (97%). It is important to note that the bentonite has low hydraulic conductivity in comparable with other common reactive media (Chen et al 2018). This property has negative effects, especially when use it as reactive material in PRB because it leads to clogging the barrier and hinder the water flowing through it. Therefore, to make the simulation of groundwater remediation using PRB, which represents the core of interest in this study, closer to reality. The value of the hydraulic conductivity of bentonite should be increased to more than conventional levels by mixing the bentonite with coarse materials such as gravel, coarse sand, or tire chips (Mishra et al 2011, Spears 2014). Based on the principle of environmental preservation of waste and reuse, the glass waste (GW) was collected, washed, crushed, and sieved into (250-500 µm), then it was used as the inert filler material by mixing it with MB (GW/MB=1/1) to increase the hydraulic conductivity value which leads to preventing the blockage of barrier as illustrated in (Table 3). However, the effect of mixture of MB and GW dosage on the removal percent of the amoxicillin was examined at the same conditions of MB as illustrated in (Fig. 9). It can be seen that adding of glass waste granules to the reactive material (MB) led to raising the hydraulic conductivity of the reactive medium from 0.00011 to 0.0098 cm s^{-1} and reduce in its effectiveness from 97% to 60%, at the same time, as shown in (Fig. 9, Table 3). This is a logical result due to mixing a reactive material (MB) with an inert substance (GW).

Sorption Isotherms: The parameters which gave the higher removal percent of amoxicillin (60%) using mixture of GW and MB were pH of 11, agitation speed of 250 rpm, time of 4 hr, initial concentration of 50 mg L^{-1}, and GW and MB dosage of 0.7 g 100 mL^{-1}. The results of the sorption experiment were fitted with the previously described linearized form of two isotherm models. The fitted parameters and coefficient of determination (R^2) for each model are illustrated in Table 4. In comparison with the two models, the Freundlich isotherm model provided the higher coefficient of determination, therefore the Freundlich isotherm model was used to describe the amoxicillin sorption in the partial differential equation (PDE) governing the transport of a amoxicillin in two-dimension (2D) continuous model which is solved using COMSOL Multiphysics 3.5a. Considering the sandy soil (aquifer) as a non- reactive medium (inert) is one of the main aspects of the present study.

Transport of amoxcilline through aquifer model: The predicted contour plot of transport modeling results of amoxicillin-contaminated groundwater across the aquifer model in two different cases (without-PRB and GW and-PRB) after 1, 3 and 80 days indicate that the contaminant plume is hindered by the barrier which led to the fact that the concentrations reaching the outlet of the aquifer model region with presence of PRB were lower than that of the first case (without PRB) for the same velocity and travel time (Fig. 10).

Performance of PRB: After reaching the PRB, the amoxicillin-contaminated groundwater is treated and its contaminant concentration is reduced by the sorption process. Theoretical results for this simulation were gained in term of the relationship between amoxicillin concentration and PRB operation time. Relationships between time and concentration of amoxicillin-contaminated groundwater coming into (inflow) and leaving (outflow) the PRB at the points of (30, 25) and (33, 25), respectively, are presented in (Fig. 11). The main results that can be drawn from this fig are

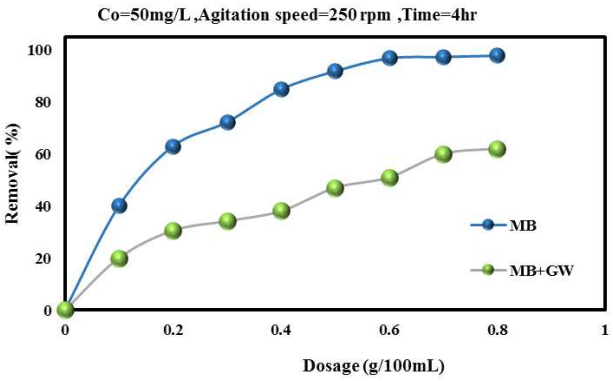

Fig. 9. Effect of sorbent dosage on removal percent of amoxicillin

Table 3. Hydraulic conductivity of materials used in the present study

Designation	K (cm sec^{-1})
NB	0.000004
MB	0.00011
GW	0.065
GW & MB (1/1)	0.0098

Table 4. Parameters of isotherm models for sorption of amoxicillin onto mixture of GW and MB

Model	Parameters	GW & MB
Langmuir	Q max (mg g^{-1})	61.2288
	b (L mg^{-1})	0.0034
	R^2	0.7645
Freundlich	K_F (mg g^{-1})(L mg^{-1})	0.1455
	N	0.9203
	R^2	0.9432

the GW and MB-PRB can be used successfully to treat amoxicillin-contaminated groundwater and the PRB start to saturate with increasing the travel time, this means that the functionality of barriers will be decreased with time due to the decreasing of barrier functionality in retardation of pollutant. The performance of the PRB is the time required to preserve the contaminant concentration down gradient of the barrier is less than the maximum contaminant level (MCL) that could be present in drinking water (zero value was adapted to MCL for amoxicillin). Accordingly, the operation time for GW and MB-PRB is equal to 87 days as long as the outflow amoxicillin concentration from GW and MB-PRB began to increase at this time, as illustrated in (Fig. 11). It can be seen that the concentration of amoxicillin entering the GW and MB-PRB was constant at about 0.048 kg/m3 which is less than the concentration at the source (i.e., 0.05 kg/m3). This is probably because of the effect of dispersion, this result is consistent with the results of some research, such as (Ziad et al 2019, Abd Ali et al 2019).

Amoxicillin Removal within PRBs: Amoxicillin concentration and time relationship within the thickness of GW and MB-PRB showed that the amoxicillin concentration in the front parts of the PRB (e.g., 1 m) increases very rapidly than the internal parts of the PRB (e.g., 2 or 3 m (Fig. 12)). The increment in amoxicillin concentration at the front parts of the PRB refers that the reactive materials have been lost its sorption ability in treating amoxicillin at the front part of barrier rather than the inner part, at the front parts of the PRB; it would be in contact with an incoming contaminant of high concentration, due to that the reactive materials at these parts would be reached its maximum sorption capacity early and the amoxicillin concentrations start to increase. On the other hand, the reactive materials at the end of the PRB would be reached its maximum sorption capacity in a longer time than the front ones because it would be in contact with incoming contaminated groundwater with lower concentrations in most of the times of simulation.

Comparison between two configurations of PRB: There are two configurations of PRB namely continuous (C-PRB)

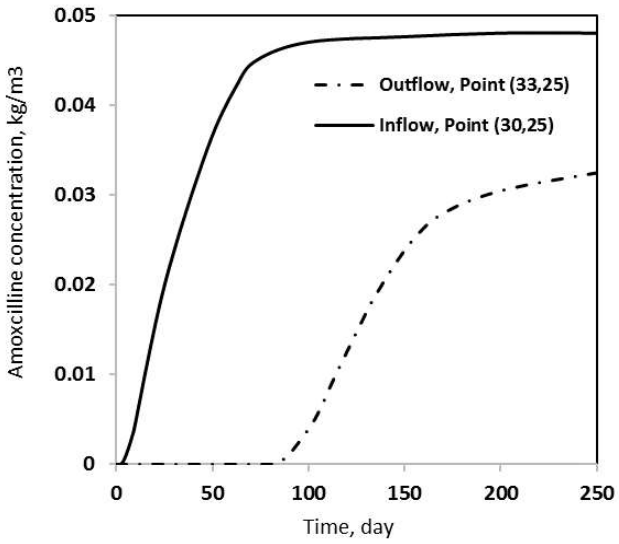

Fig. 11. Amoxicillin concentration and time relationship

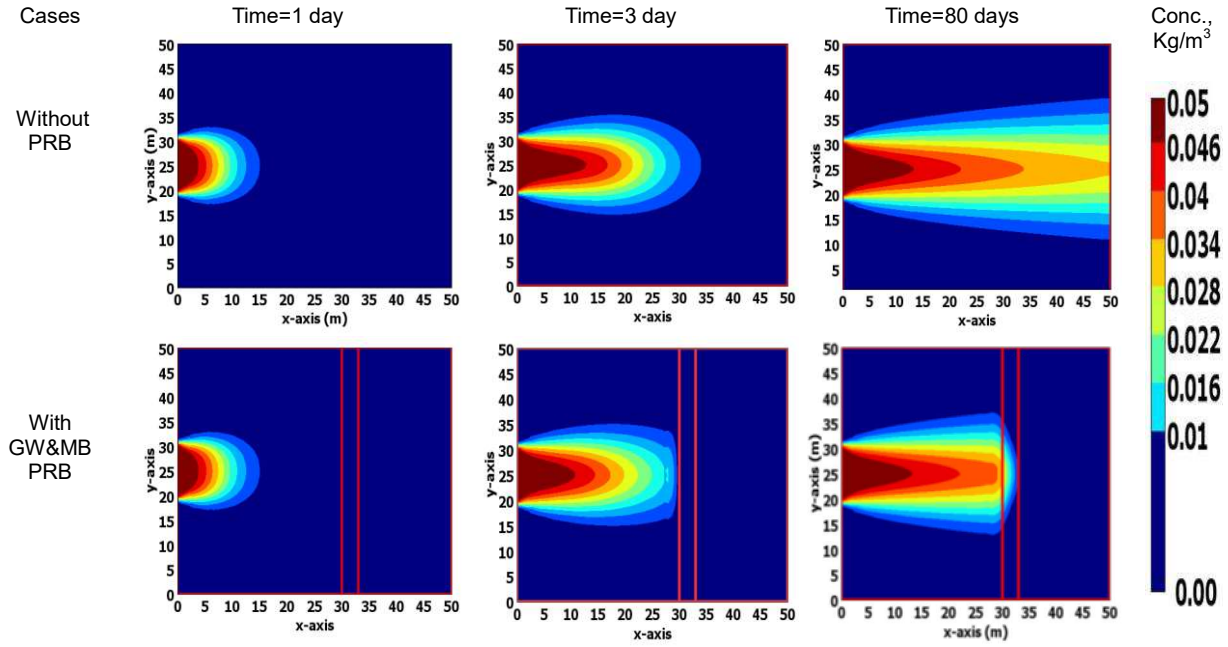

Fig. 10. Contour plot of amoxicillin concentration across the aquifer model after 1, 3 and 80 days

and funnel and gate (FG-PRB) permeable barrier as shown in Fig. 1). In the C-PRB, the reactive media (GW&MB) was placed along the barrier (i.e., 50 m long) with thickness of 3 m, while for FG-PRB, shorter reactive media was installed only in the permeable gate part of the barrier (i.e., 10 m long) with the same thickness of 3 m, and the impermeable material that has low hydraulic conductivity such as ebonite was installed in the impermeable funnel parts, therefore groundwater flow and contaminant transport were intentionally allowed through the gate part only (Fig. 10) describes the predicted contour plot of transport of amoxicillin-contaminated groundwater with Co = 0.05 kg/m3 and velocity = 3.45 m d^{-1}

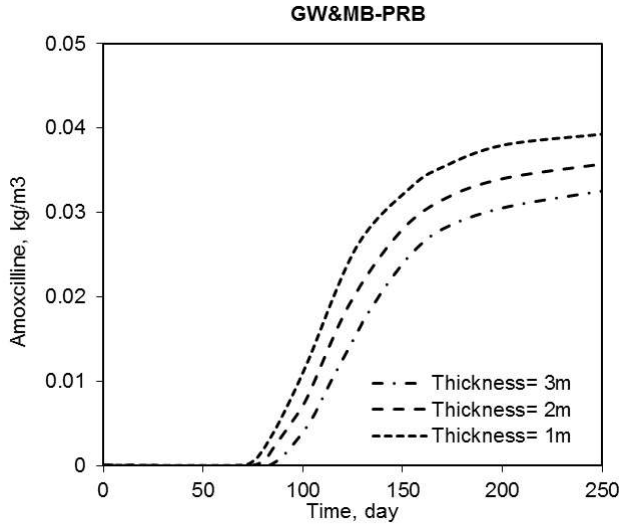

Fig. 12. Amoxicillin concentration and time relationship within the thickness of barrier

across the model aquifer in two cases (C-PRB, and FG-PRB) after 1, 3, 80, and 125 day. It is clear that the direction of the transport process of amoxicillin is from high concentration gradient on the left-hand side to the lower ones on the right-hand side, and the amoxicillin-contaminated groundwater is transported from the contaminated site to the PRBs within 80 day without exceeding the barrier, which mean that the propagation of contaminated plume is restricted by the reactive media (GW and MB) in the barrier region. For two configurations of PRBs, the typical results for this simulation

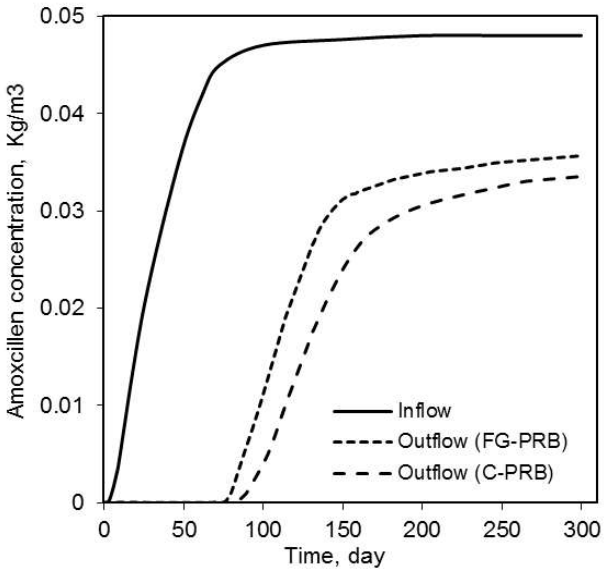

Fig. 14. Amoxicillin concentration and time relationship before (inflow) and after (outflow) treatment for C-MS-PRB and FG-MS-PRB

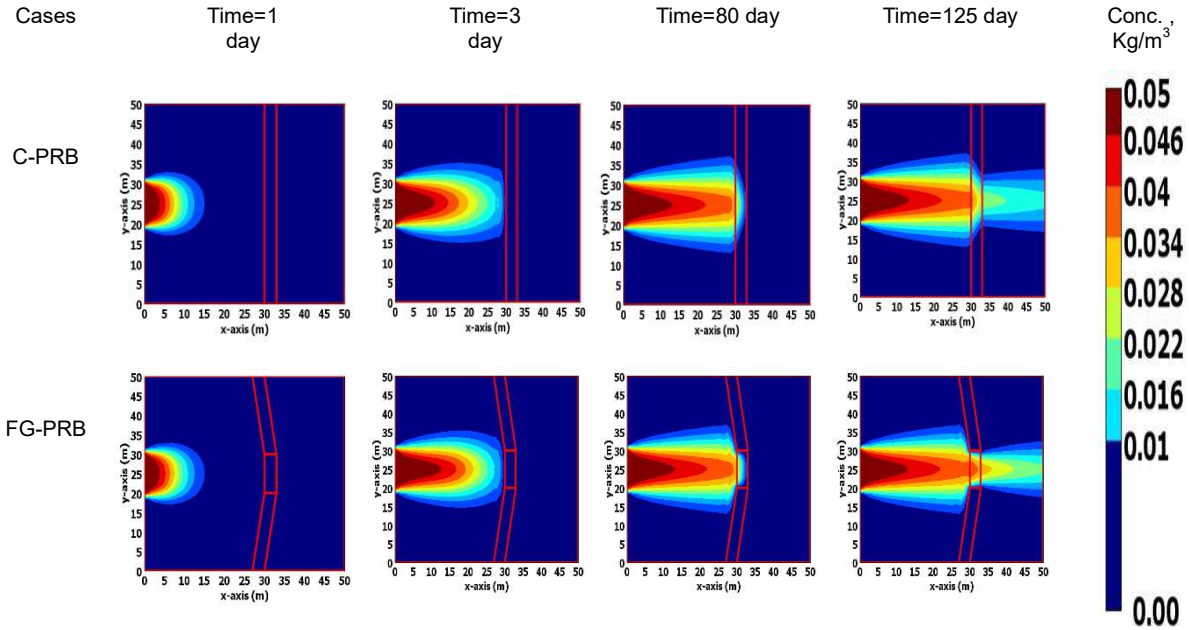

Fig. 13. Contour plot of amoxicillin concentration across the model aquifer after various times

were obtained in term of the relationship between amoxicillin concentration and PRB operation time. The relationship between time and concentration of amoxicillin entering (inflow) and leaving (outflow) the PRBs is shown in (Fig. 14). The main results that can be drawn from this figure that both configurations of PRBs can be used successfully to treat amoxicillin-contaminated groundwater, and the PRBs starts to saturate with increasing the travel time and this means that the amoxicillin retardation factor was reduced, indicating a decrease in the percentage of barrier functionality. In addition, the C-PRB has a higher operation time (87 day) in comparison with FG-PRB (75 day), as shown in (Fig. 14). This result can be attributed to the fact that the C-PRB has more quantity of the reactive material compared to FG-PRB, so it takes a longer time to reduce its functionality; therefore, the C-PRB has longer operation time than FG-PRB.

CONCLUSION

Contact time, initial pH of the solution, sorbent dosage, agitation speed, and initial concentration of the contaminant were most of the parameters affected on the amoxicillin sorption process using a mixture of GW and MB. The best values of these parameters that will achieve the maximum removal efficiency (60%) were 4 hr, 11, 0.7 g 100 mL^{-1}, 250 rpm, 50 mg L^{-1}. Adding the glass waste to the reactive material (MB) led to raising the hydraulic conductivity of the reactive medium and reduces its effectiveness at the same time. Amoxicillin sorption data on the mixture of GW and MB were correlated reasonably well by the Freundlich isotherm model with coefficient of determination (R2) equal to 0.9432. FTIR analysis proved that the sorption of amoxicillin onto modify bentonite was achieved depended on Si-O-Si functional groups. The two-dimensional numerical model confirmed that the GW&MB-PRB was efficient in the restriction of amoxicillin plume and both configurations of PRBs can be used successfully to treat amoxicillin - contaminated groundwater with operation time equal to 87 and 75 d for C-PRB and FG-PRB, respectively.

REFERENCES

Abd Ali ZT 2019. Green synthesis of graphene-coated sand (GCS) using low-grade dates for evaluation and modeling of the pH-dependent permeable barrier for remediation of groundwater contaminated with copper. *Separation Science and Technology*: 1-12. h.

Abd Ali ZT 2020. Combination of the artificial neural network and advection-dispersion equation for modeling of methylene blue dye removal from aqueous solution using olive stones as reactive bed. *Desalination and Water Treatment* **179**: 302-311.

Abd Ali ZT, Flayeh HM and Ibrahim MA 2019. Numerical modeling of performance of olive seeds as permeable reactive barrier for containment of copper from contaminated groundwater. *Desalination and Water Treatment* **139**: 268-276. https://doi.org/10.5004/dwt.2019.23305.

Abd Ali ZT and Ismail ZZ 2020. Experimental and modeling study of water defluoridation using waste granular brick in a continuous up-flow fixed bed. *Environmental Engineering Research* **26**. 190506–0. https://doi.org/10.4491/eer.2019.506.

Adriano WS, Veredas V, Santana CC and Gonçalves LRB 2005. Adsorption of amoxicillin on chitosan beads: Kinetics, equilibrium and validation of finite bath models. *Biochemical Engineering Journal* **27**: 132-137.

Al-Asheh S, Banat F and Mohai F 1999. Sorption of copper and nickel by spent animal bones. *Chemosphere* **39**: 2087-2096.

Ali AF and Abd Ali ZT 2020. Sustainable use of concrete demolition waste as reactive material in permeable barrier for remediation of groundwater: batch and continuous study. *Journal of Environmental Engineering* **146**: 04020048. https://doi.org/10.1061/(ASCE)EE.1943-7870.0001714.

Alshammari M, Al Juboury MF, Naji LA, Faisal AAH, Zhu H, Al-Ansari N and Naushad M 2020. Synthesis of a novel composite sorbent coated with siderite nanoparticles and its application for remediation of water contaminated with congo red dye. *International Journal of Environmental Research* **14**: 177–191.

An J-H and Dultz S 2007. Adsorption of tannic acid on chitosan-montmorillonite as a function of pH and surface charge properties. *Applied Clay Science* **36**: 256-264.

Anirudhan TS and Ramachandran M 2015. Adsorptive removal of basic dyes from aqueous solutions by surfactant modified bentonite clay (organoclay): Kinetic and competitive adsorption isotherm. *Process Safety and Environmental Protection* **95:** 215–225.

Chen JN, Benson CH and Edil TB 2018. Hydraulic conductivity of geosynthetic clay liners with sodium bentonite to coal combustion product leachates. *Journal of Geotechnical and Geoenvironmental Engineering*. https://doi.org/10.1061/(ASCE)GT.1943-5606.0001844.

Faisal AAH and Abd Ali ZT 2016. Groundwater protection from lead contamination using granular dead anaerobic sludge biosorbent as permeable reactive barrier. *Desalination and Water Treatment* **57**: 3891-3903.

Faisal AAH and Abd Ali ZT 2017a. Using sewage sludge as a permeable reactive barrier for remediation of groundwater contaminated with lead and phenol. *Separation Science and Technology (Philadelphia)*, Taylor andFrancis **52**: 732-742.

Faisal AAH and Abd Ali ZT 2017b. Remediation of groundwater contaminated with the lead–phenol binary system by granular dead anaerobic sludge-permeable reactive barrier. *Environmental Technology* **38**: 2534–2542.

Faisal AAH and Ali ZTA 2015. Using granular dead anaerobic sludge as permeable reactive barrier for remediation of groundwater contaminated with phenol. *Journal of Environmental Engineering* **141.** 04014072. https://doi.org/10.1061/(ASCE)EE.1943-7870.0000903.

Fetter CW 1999. *Contaminant hydrogeology*, Prentice-Hall, New Jersey.

German Standard Methods for the Examination of Water. Waste Water and Sludge and Sediments (Group S), Determination of Leachibility by Water (S4), DIN 38414, Part 4

Holzbecher E 2007. *Environmental modeling: Using MATLAB®*, *Environmental Modeling: Using MATLAB®*. https://doi.org/10.1007/978-3-540-72937-2.

Huang R, Hu C, Yang B and Zhao J 2016. Zirconium-immobilized bentonite for the removal of methyl orange (MO) from aqueous solutions. *Desalination and Water Treatment* **57**: 10646-10654. Huang Z, Li Y, Chen W, Shi J, Zhang N, Wang X, Li Z, Gao L and Zhang Y 2017. Modified bentonite adsorption of organic pollutants of dye wastewater. *Materials Chemistry and Physics* **202**: 266–276.

Ibrahim SM and Abd Ali ZT 2020. Using of modified-bentonite as low-cost sorbent for removal of methylene blue dye from aqueous solution. *Association of Arab Universities Journal of*

Engineering Sciences **27**: 45–54.

Jeeva M and Wan Yaacob WZ 2018. Comparison study on the adsorption of a synthetic textile dye using bentonite and surfactant modified bentonite. *Bulletin of the Geological Society of Malaysia* **65:** 107–117.

Jeeva M and Zuhairi WYW 2018. Adsorption of acid orange 33 dye by bentonite and surfactant modified bentonite. *Asian Journal of Chemistry*. https://doi.org/10.14233/ajchem.2018.21309.

Jin X, Zha S, Li S and Chen Z 2014. Simultaneous removal of mixed contaminants by organoclays - Amoxicillin and Cu(II) from aqueous solution. *Applied Clay Science*. https://doi.org/10.1016/j.clay.2014.09.040.

Khebchareon M 2012. Crank-Nicolson Finite Element for 2-D groundwater flow, advection-dispersion and interphase mass transfer: I. Model. *International Journal of Numerical and Analysis and Modelling*

Masood ZB and Abd Ali ZT 2019. Numerical modeling of two-dimensional simulation of groundwater protection from lead using different sorbents in permeable barriers. *Environmental Engineering Research* **25**: 605–613.

Received 24 June, 2021; Accepted 20 November, 2021

Monvisade P and Siriphannon P 2009. Chitosan intercalated montmorillonite: Preparation, characterization and cationic dye adsorption. *Applied Clay Science* **42**: 427–431.

QU J 2008. Research progress of novel adsorption processes in water purification: A review. *Journal of Environmental Sciences* **20:** 1-13.

Shin WS 2008. Competitive sorption of anionic and cationic dyes onto cetylpyridinium-modified montmorillonite. *Journal of Environmental Science and Health Part A*, **43**: 1459-1470.

Siregar SH, Wijaya K, Kunarti ES, Syoufian A and Suyanta 2018. Preparation and characterization of montmorillonite-cetyl trimethylammonium bromide. *Asian Journal of Chemistry* **30**: 25-28.

Sulaymon AH, Faisal AAH and Abd Ali ZT 2015. Performance of granular dead anaerobic sludge as permeable reactive barrier for containment of lead from contaminated groundwater. *Desalination and Water Treatment* **56**: 327-337.

Travis CC and Webb GF 1978. Cosine families and abstract nonlinear second order differential equations. *Acta Mathematica Academiae Scientiarum Hungaricae* **32:** 75-96.

Indian Journal of Ecology (2021) 48(6): 1670-1678

Manuscript Number: 3430
NAAS Rating: 5.79

Water Quality Assessment of Kela and Ejersa Rivers Using Benthic Macroinvertebrates, Ethiopia

Mekonnin Dula, Girum Tamire* and Gezahegn Degefe

Department of Biology, Debre Berhan University, Debre Berhan
**E-mail: tamiregirum1@gmail.com*

Abstract: Assessment of water quality of Kela and Ejersa Rivers was carried out from March 2019 to June 2019. Benthic macroinvertebrates were collected from 5 different sampling sites randomly using 500-µm mesh kick-net. A total of 684 benthic macroinvertebrates was recorded from the rivers, from which Chironomidae, Syrphidae and Perlidae were the three most abundant taxa collected. The result showed that site K1, K2 and E1 recorded the highest number of benthic macro invertebrate with the highest value of Shannon index and lowest value of Hilsenhoff family biotic index (H-FBI) which indicated good water quality while site E2 and E3 showed the lowest number of benthic macro invertebrate with the lowest value of Shannon-Wiener diversity index and highest value of Hilsenhoff family biotic index (H-FBI) which indicated poor water quality. The result obtained from community loss index showed that the degree of dissimilarity increases from site K1 (0.96) to site K2 (1.14), site E1 (1.34), site E3 (1.58) and site E2 (1.73) respectively which indicated the ecosystem disturbance at these study sites. The present study indicated that various anthropogenic activities are impacting the water quality of Kela and Ejersa Rivers, which needs management measures on these rivers.

Keywords: Benthic macro invertebrate, Kela river, Ejersa river, Water quality

Rivers are ecosystems of great ecological value with a rich fauna that consists of communities with a complex structure and high biological value. However, they are vulnerable to changes in the environment, particularly to anthropogenic disturbances (Qui and Liu 2016, Best and Darby 2020). This problem in turn could transform permanent systems to seasonal or in worst cases to disappearance. In consequence, the biodiversity of many of them will be reduced and their biogeochemical cycles will be altered. One of the major impacts that affect rivers is the pollution of their waters by both domestic and industrial waste (Benetti and Garrido 2010). In addition, agriculture, with intensive use of fertilizers and pesticides, has contributed significantly to eutrophication and contamination of aquatic ecosystems (Ndimele and Jimoh 2011). Another impact on running waters is the deliberate modification of streams by building dams and reservoirs, which alter the ecological characteristics of their basins (Gregory 2006). According to Islam et al (2019) changes in riverbanks can enhance erosion which in turn can cause severe consequences on socio-economic situations of riverside communities. Recently, benthic macroinvertebrates are the most common faunal assemblages for bio assessment and provide more reliable assessment of long term ecological changes in the quality of an aquatic system. The benthic macroinvertebrates respond differentially to biotic and abiotic factor in their environment. Consequently, the structure of macro invertebrate has long been used as bio indicators to assess the quality of a water body (Duran 2006). More recently detailed work on the use of benthic macroinvertebrates as indicator of water quality on some selected river in Ethiopia was worked out by Degefe et al (2017). Some other studies were also carried out by Tasew (2007) and Beneberu and Mengistou (2010).

Kela and Ejersa Rivers are located in areas with various degrees of anthropogenic impacts and both rivers were not included in above or other similar studies though they face unique environmental challenges due to untreated effluents from Soap and detergent factories, abattoirs and other small scale industries. In addition, local communities living around these rivers, rely on this untreated river for drinking, irrigation and other household purposes. Therefore, the present study was conducted to fill the gap by assessing water quality using benthic macro invertebrate to identify and determine the pollution status of these rivers.

MATERIAL AND METHODS

Sampling area: Woliso (which was also used to be known as Ghion, after being given by Emperor Haile Selassie I) is a town in central Ethiopia. The location of Woliso is 080 46' N latitude and 370 58' E longitude, being situated at 2,063 m asl. The wettest month is July and the mean annual rainfall is 1200 mm. The average minimum, maximum and mean annual temperatures of Woliso are about 13.6, 25 and 19.30C, respectively. The study was conduct on Kela and Ejersa River.

Ejersa River is located at the Western part of Woliso town, which is about 1Km far from the center of Woliso town flowing Southwest direction of the town and is finally joined Gibe basin. Ejersa River is used by the communities inhabiting around downstream for drinking, to irrigate their farm lands, for their cattle and other domestic use. The watershed of Ejersa River is highly exposed to several anthropogenic interventions including: agricultural, domestic, sewage from prison institution, abattoir, Woliso Campus and residential activity. Large quantities of untreated municipal sewage, from prison institution and abattoir effluents are directly discharged to Ejersa River. Among this wastewater together with agricultural activities cover all the watershed of the river and are more likely to affect the habitat qualities of the river (Fig. 1). Kela river is located at the same direction with Ejersa river from the center of Woliso town, Oromia region, Ethiopia, which is about 2.5Km far from the center of Woliso town Flowing Southwest direction of the town, the river is finally joined Gibe basin. This river is used by the communities for drinking, to irrigate their farm lands, for their cattle and other domestic use (Fig.1). In total five sampling sites from the two rivers were selected by considering the relative sources of pollution to the river and represent different anthropogenic activities between March and May 2019. Two sampling Sites were selected from Kela river, site K1 (upstream) and site K2 (downstream). Three sampling sites were selected from Ejersa river, Site E1 (upstream), Site E2 (middle stream) and E3 (downstream). The selections of sampling sites were based on land uses (woodlands, agriculture, transport system, urban areas, and industrial activities) (Table 1).

Sampling processing: Samples were taken following the Wadeable Rivers protocols for streams (USEPA 2007) using a 500-µm mesh kick-net for 1minute in an area measuring approximately 1 m2 (Brua et al 2011). Sieves of 500-µm mesh size were used to separate organisms from sediments. Large debris were removed from the samples after carefully washing off the attached organisms into a bucket and the water filtered through 250-µm mesh size sieves after hand sorting to separate the organisms from debris. Samples were taken randomly over a river length of 100 m at each site, put and preserved in 4% formalin. Macroinvertebrate identification was done to the family level using keys of Hering et al (2006) and Flinders et al (2008).

Metrics selection: Shannon diversity index was calculated as:

$$H' = -\sum_{i=1}^{S} pi\,lnpi$$

Where "Pi" is the proportion of individuals in the "i^{th}" taxon of the community and "S" is the total number of taxa in the community.

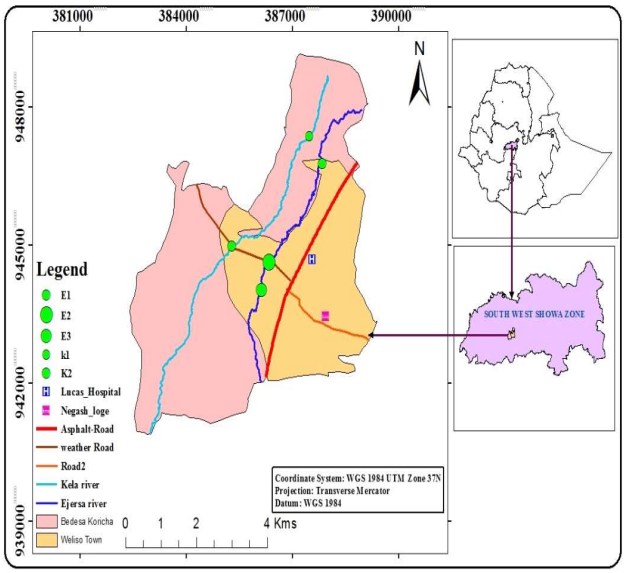

Fig. 1.

Each macro invertebrate taxa can tolerate a specific range of contamination, which is referred to as their pollution tolerance. Once this level is exceeded, the taxa are no longer present in that area of the stream. Highly sensitive taxa, or those with a low pollution tolerance, are only in streams with good water quality. Each family was assigned a biotic score between 0 for organisms very intolerant of organic wastes to 10 for organisms very tolerant of organic wastes (Table 2).

To analyze the degree of organic load among the study sites, Hilsenhoff-family biotic index was computed using Hilsenhoff (1987).

$$FBI = \frac{\sum XiTi}{N}$$

Where*:* xi= number of individuals within a taxon

Ti= tolerance value of a taxa

N=total number of organisms in the sample

To measure the loss of benthic taxa and dissimilarity between sample sites, community loss index (CLI) was used. Values range from 0 to infinity and increase as the degree of dissimilarity between the sites increases (Plafkin et al 1989).

Community loss index was calculated as:

$$CLI = \frac{D - A}{E}$$

where, A- is the number of taxa common to both sites, D- Is the total number of taxa present in reference site and E- total numbers of taxa present in the study sites. In addition to this percentage of diptera, ephemeroptera, oligochaeta, trichoptera, coleoptera, odonata, plecoptera were calculated.

Data analysis: SPSS software and Microsoft Excel sheet on computer were used to analyze data obtained from the two rivers.

RESULTS AND DISCUSSION

Benthic Macroinvertebrate Composition and Abundance

During March to June 2019, a total of 7 orders and 24 families with the total number of 684 macroinvertebrates were recorded from the two rivers and five sampling sites. The benthic macroinvertebrates were dominated by *Diptera* (44.2%) followed by *Odonata*, *Ephemeroptera*, *lecoptera*, *Oligochaeta, Coleoptera*, *Trichoptera* and *Hemiptera* had low benthic macro invertebrates' composition (Table 4). A total of 132 individual benthic macro invertebrate from 20 taxa were collected from site E1 and identified to family level. The most abundant taxa collected were *Chironomidae* 34 (25.5) followed by *Syrphidae* 15 (11.4), *Oligochaeta*, *Perlidae* and Baetidae (Table 3). *Empididae, Ephydridae, Simuliidae, Tipulidae, Leptophlebiidae, Heptageniidae, Caenidae, Capniidae, Gyrinidae, Dytiscidae, Elmidae, Naucoridae, Lestidae, Leech and Gomphidae* were the least benthic macroinvertebrates' composition (Table 4). In Site E2 a total of 102 individuals and 7 Taxa were recorded and the benthic macro invertebrates collected were dominated by the *Chironomidae* 51 (50%) followed by Syrphidae and *Lestidae*. The family *Ephydridae*, *Caenidae, Oligochaeta and Leech* were the least benthic macro invertebrates' composition in this sampling site (Table 4). A total of 112 individual benthic macro invertebrate from 9 Taxa were collected from Site E3. The most abundant taxon collected from this site were *Chironomidae* 48 (42.9) followed by *Syrphidae*, *Lestidae* and

Table 2. Ranking of bio-index values using benthic macro invertebrates

Shannon-Wiener Diversity Index(H')	Ranking
> 3.25	Very light pollution
2.20-3.25	Light pollution
1.40-2.20	Low moderate pollution
0.80-1.40	High moderate Pollution
0.10-0.80	Heavy pollution
< 0.10	Very heavy pollution

Table 3. Evaluation of water quality using the Hilsenhoff family-level biotic index (H-FBI)

Family biotic	Water quality	Degree of organic pollution index
0.00-3.75	Excellent	Organic pollution unlikely
3.76-4.25	Very good	Possible slight organic pollution
4.26-5.00	Good	Some organic pollution probable
5.01-5.75	Fair	Fairly substantial pollution likely
5.76-6.50	Fairly poor	Substantial pollution likely
6.51-7.25	Poor	Very substantial pollution likely
7.26-10.00	Very poor	Severe organic pollution likely

Table 1. Description of the sampling sites

Rivers	Site code	Altitude (m)	Latitude (E)	Longitude (N)	Distinguishing feature
Kela River	K1	2108	8°33'49"	37°59'21"	• Upstream site of the river. • Found in rural part of the town. • Covered with grasses and old trees. • This site is relatively less disturbed. • Utilized for drinking (reference site).
	K2	2165	8°35'12"	38°0'37"	• Downstream site of the river. • Utilized for cattle watering, washing and bathing. • Subsistence agriculture and depleted forest cover.
Ejersa River	E1	2070	8°33' 4"	37°58'23"	• Upstream site of the Ejersa river. • Covered by distinctive vegetation and grasses. • Utilized for cattle watering, washing and bathing . • Subsistence agriculture and depleted forest cover
	E2	2032	8°32'56"	37°58'11"	• Middle stream site of the river, Human settlement and Highly exposed to several anthropogenic interventions, sewage from prison institution, abattoir and residential activity. • Covered with grasses, shrubs and Eucalyptus trees.
	E3	2025	8°32'35"	37°57'57"	• Downstream Site, at the back of woliso food complex factory. • Covered with grasses, shrubs and acacia. • Utilized for cattle watering, washing and bathing. • Influenced by several anthropogenic interventions. • Subsistence agriculture and depleted forest cover.

Caenidae. Empididae, Ephydridae, *Simuliidae, Oligochaeta and Leech* were rarely observed families (Table 4). In site K1 a Total of 183 individuals and 23 taxa of benthic macro invertebrate were collected. Among the collected individuals the most abundant taxa were *Chironomidae* 37(20.21%) followed by *Perlida*e , *Aeshnidae* , and *Baetidae*. *Elmidae, Gyrinidae, Capniidae, Leptophlebiidae, Heptageniidae, Caenidae, Philopotamidae, Leptoceridae*, *Dytiscidae, Naucoridae, Gomphidae, Lestidae, Leech, Oligochaeta, Macromiidae, Empididae, Tipulidae, Simuliidae, Syrphidae and Ephydridae* families had lower abundance in this sampling site (Table 4). From the total of 155 benthic macroinvertebrate and 23 taxa collected in site K2 ,the most abundant taxa were *Chironomidae* 25 (16.12%) and *Aeshnidae* 25 (16.12%) followed by Perlidae and *Oligochaeta*. The family *Empididae, Ephydridae, Simuliidae, Syrphidae, Tipulidae, Leptophlebiidae, Heptageniidae, Baetidae, Caenidae, Capniidae, Leptoceridae,*

Table 4. Benthic macroinvertebrate family collected from each of the two river during the two sampling periods

Order/Family	Sites										Total No.
	E1		E2		E3		K1		K2		
	March	June	March	June	March	June	March	June	March	June	
Diptera											
Chironomidae	23	11	33	18	31	17	27	10	16	9	195
Empididae	2	1	0	0	1	0	2	0	1	1	8
Ephydridae	1	0	2	1	6	2	2	0	1	0	15
Simulidae	0	1	0	0	3	1	1	2	2	0	10
Syrphidae	10	5	17	8	18	6	0	0	0	0	64
Tipulidae	1	1	0	0	0	0	3	0	3	2	10
Ephemeroptera											
Leptophlebidae	4	1	0	0	0	0	5	3	3	3	19
Heptageniidae	4	3	0	0	0	0	4	4	4	1	20
Baetidae	6	3	0	0	0	0	7	5	6	1	28
Caenidae	2	1	4	3	7	2	1	1	2	0	23
Plecoptera											
Perlidae	10	5	0	0	0	0	17	8	15	6	61
Capniidae	1	1	0	0	0	0	6	1	2	3	14
Trichoptera											
Leptoceridae	0	0	0	0	0	0	2	0	1	0	3
Philopotamidae	0	0	0	0	0	0	4	2	4	1	11
Coleoptera											
Gyrinidae	1	1	0	0	0	0	3	5	2	3	15
Dytiscidae	2	1	0	0	0	0	3	0	2	2	10
Elmidae	1	0	0	0	0	0	7	2	3	1	14
Hemiptera											
Naucoridae	1	0	0	0	0	0	2	0	1	1	5
Odonata											
Lestidae	4	2	7	1	8	3	1	0	1	1	28
Gomphidae	2	0	0	0	0	0	5	2	3	1	13
Aeshnidae	0	0	0	0	0	0	10	9	20	5	44
Macromiidae	0	0	0	0	0	0	3	3	4	1	11
Oligochaeta	11	4	4	2	2	2	5	1	6	4	41
Leech	1	4	1	1	3	0	4	1	5	2	22
Total	87	45	68	34	79	33	124	59	107	48	684

Philopotamidae, Gyrinidae, Dytiscidae, Elmidae, Naucoridae, Lestidae, Gomphidae, Macromiidae and Leech had lower abundance (Table 4). From the total benthic macroinvertebrate collected from each of the two river, *Chironomidae* 195 (28.5%), *Syrphidae* and *Perlidae* were the top three most abundant taxa collected from the five sampling site (Table 5). Family *Chironomidae* (Red), *Ephydridae*, *Caenidae, Oligochaeta, Lestidae and Leech* were distributed through all sampling site. From the EPTC (Ephemeroptera, Plecoptera, Trichoptera and Coleoptera) family Perlidae 61 (8.91%), *Aeshinidae* 44 (6.43%), *Baetidae*

Table 6. Top three abundant taxa from each of the two rivers

Rivers	Family	Total No.	Per cent abundance
Ejersa	*Chironomidae*	51	50
	Syrphidae	25	24.5
	Oligochaeta	15	11.4
Kela	*Chironomidae*	37	20.21
	Aeshinidae	25	16.12
	Perlidae	25	13.7

Table 5. Calculated mean of benthic macroinvertebrate family for each of the two river during the study period

Order/Family	Sites					Total
	E1	E2	E3	K1	K2	
Diptera						
Chironomidae	17	25.5	24	18.5	13	97.5
Empididae	1.5	0	0.5	1	1	4
Ephydridae	0.5	1.5	4	1	0.5	7.5
Simulidae	0.5	0	2	1.5	1	5
Syrphidae	7.5	12.5	12	0	0	32
Tipulidae	1	0	0	1.5	2.5	5
Ephemeroptera						
Leptophlebidae	2.5	0	0	4	3	9.5
Heptageniidae	3.5	0	0	4	2.5	10
Baetidae	4.5	0	0	6	3	13.5
Caenidae	1.5	3.5	4.5	1	2.5	13
Plecoptera						
Perlidae	7.5	0	0	12.5	3.5	23.5
Capniidae	1	0	0	3.5	1	5.5
Trichoptera						
Leptoceridae	0	0	0	1	11	11.5
Philopotamidae	0	0	0	3	2.5	5.5
Coleoptera						
Gyrinidae	1	0	0	4	2.5	7.5
Dytiscidae	1.5	0	0	1.5	2	5
Elmidae	0.5	0	0	4.5	2	7
Hemiptera						
Naucoridae	0.5	0	0	1	1	2.5
Odonata						
Lestidae	3	4	5.5	0.5	1	14
Gomphidae	1	0	0	3.5	2	6.5
Aeshnidae	0	0	0	9.5	13	22
Macromiidae	0	0	0	3	2.5	5.5
Oligochaeta	7.5	3	2	3	5	20.5
Leech	2.5	1	1.5	2.5	3.5	11

28 (4%) and *Lestidae* 28 (4%) were the top three most abundant taxa collected from the five sampling sites. Family *Leptophlebiidae, Heptageniidae, Baetidae Perlidae, Capniidae, Gyrinidae, Dytiscidae, Elmidae Naucoridae and Gomphidae* were distributed in the E1, K1 and K2 sampling sites but they were not collected from E2 and E3 site which indicated the stress of aquatic environment in site (E2 and E2) (Table 7).

Richness of EPT is a widely used metric type in many biomonitoring systems as the components (Ephemeroptera, Plecoptera and Trichoptera) are well known for their sensitivity to anthropogenic impacts (Suhaila et al 2014). In this study, the EPTC Taxa and Hemiptera were not recorded at Site E2 and E3 during the period of the study. The lowest benthic Macro invertebrate composition and the absence of sensitive benthic Macro invertebrate species at site E2 and E3 may be attributed to the impact of uncontrolled discharge of industrial and municipal waste into the river at this site which indicates poor water quality which agrees with the study of Sitotaw (2006). Akalu et al (2011)also observed the same trend. EPT Taxa in general are highly sensitive to environmental degradation (Suhaila et al 2014). The dominance of the dipterans with respect to number of individuals and species in this study is in agreement with Edokpayi et al (2010). The dominance of dipterans in the system as in other aquatic ecosystems may be attributed to their morphological and physiological adaptations to the various habitats, availability of food and sustained reproduction (Jacobus et al 2019). From dipterans the red *Chironomidae* were distributed among all river quality classes. However, the average abundances for different quality classes showed that remarkably high abundances were recorded only at polluted sites, site E2 and E3. The percentage contribution is important to identify the level of impact that each stressor causes. This finding agreed well with the study of Lakew (2014) and Degefe et al (2017). The percentage of *Syrphidae* were the second most abundant families from dipterans next to chironomidae which was abundant at fairly poor water qualities, site (E1) and at very poor water qualities, Site (E2 and E3). This may be because, the family *syrphidae* were among the pollution tolerant benthic macro invertebrates.

Shannon-Wiener diversity index (H')

Shannon-Wiener function varied among the study site. Site K1 (2.78), K2 (2.73) and E1 (2.47) had the highest diversity index than E2 (1.42) and E3 (1.68) (Table 8). This reflects the evenly distribution of these organisms with light pollution of water quality. The diversity of benthic macroinvertebrate is known to be highly variable in rivers with response to disturbance, nutrients availability and the presence of suitable habitat (Iyagbaye et al 2017). Rana et al (2016) indicated that land use has considerable impact on diversity of aquatic invertebrates. Higher diversity also results when many species have equal or near-equal opportunity of co-existence. A decrease in diversity and corresponding increase in abundance of a limited number of species is a common community response to environmental disturbance. As the aquatic stress decreases, the number of macro invertebrate increases. Nutrient enrichment and organic loading decreases macro invertebrate richness by removal of sensitive taxa mostly insect orders like the mayflies (Ephemeroptera), the stoneflies (Plecoptera), the

Table 7. Observed values of metrics in Ejersa and Kela rivers

Metrics	Sites				
	E1	E2	E3	K1	K2
Total No. of individual	132	102	112	183	155
Total No. of taxa (family)	20	7	9	23	23
Relative abundance (%)	19.3	14.91	14.4	26.8	22.7
Diptera (%)	42.42	77.5	75.9	25.7	22.6
Ephemeroptera (%)	18.2	6.9	8	16.4	12.9
Plecoptera (%)	12.9	-	-	17.5	16.8
Trichoptera (%)	-	-	-	4.4	3.9
Coleoptera (%)	4.54	-	-	10.9	8.4
Odonata (%)	6	7.84	9.82	0.54	1.3
Oligochaeta (%)	11.4	5.9	3.6	3.3	6.5
Shannon diversity Index (H)	2.47	1.42	1.68	2.8	2.73
Family Biotic Index (FBI),	6.28	8.48	8.28	4.39	4.49
Community Loss Index (CLI)	1.34	1.73	1.58	0.96	1.14

caddisflies (Trichoptera) and Hemiptera. This could be the reason why macroinvertebrates difference among sites occurred in this study. Taxa richness decreased substantially at polluted sites and those species lost were usually pollution-intolerant. This supports the accepted view that sensitive species are reduced when water quality deteriorates (Enawgaw and Lemma 2019).

Hilsenhoff Family Biotic Index (H-FBI): Hilsenhoff family biotic index (H-FBI) were lowest at site K1 (4.4), K2 (4.5). The predicted water qualities at this sampling site were good, indicating some organic pollution probable. Most of the benthic macro invertebrates were relatively pollution intolerant, indicating the relatively clean water quality. At site E1 (6.3), H-FBI were lower than E2 and E3 but higher than

Table 8. Total number of benthic macroinvertebrates collected at the Ejersa and Kela River from the five sampling site 2019

Order/Family	Sites											
	E1		E2		E3		K1		K2		Total	
	Total No.	Abundence (%)	Total No.	Abundence (%)	Total No.	Abundence (%)	Total No.	Abundence (%)	Total No.	Abundence (%)	Total No.	Abundence (%)
Diptera												
Chironomidae (Red)	34	25.8	51	50	48	42.9	37	20.21	25	16.12	195	28.5
Empididae	3	2.8	-	-	1	0.9	2	1.09	2	1.3	8	1.2
Ephydridae	1	0.8	3	2.94	8	7.14	2	1.09	1	0.64	15	2.2
Simulidae	1	0.8	-	-	4	3.6	3	1.63	2	1.3	10	1.5
Syrphidae	15	11.4	25	24.5	24	21.42	-	-	-	-	64	9.4
Tipulidae	2	1.5	-	-	-	-	3	1.63	5	3.22	10	1.5
Ephemeroptera												
Leptophlebiidae	5	3.8	-	-	-	-	8	4.4	6	3.9	19	2.8
Heptageniidae	7	5.3	-	-	-	-	8	4.4	5	3.22	20	2.92
Baetidae	9	6.8	-	-	-	-	12	6.6	7	4.51	28	4.09
Caenidae	3	2.8	7	6.9	9	8	2	1.09	2	1.3	23	3.4
Plecoptera												
Perlidae	15	11.4	-	-	-	-	25	13.7	21	13.54	61	8.91
Capniidae	2	1.5	-	-	-	-	7	3.82	5	3.22	14	2.04
Trichoptera												
Leptoceridae	-	-	-	-	-	-	2	1.09	1	0.64	3	0.43
Philopotamidae	-	-	-	-	-	-	6	3.3	5	3.22	11	1.6
Coleoptera												
Gyrinidae	2	1.5	-	-	-	-	8	4.4	5	3.22	15	2.2
Dytiscidae	3	2.8	-	-	-	-	3	1.63	4	2.9	10	1.5
Elmidae	1	0.8	-	-	-	-	9	4.91	4	2.9	14	2.04
Hemiptera												
Naucoridae	1	0.8	-	-	-	-	2	1.09	2	1.3	5	0.73
Odonata												
Lestidae	6	4.54	8	7.84	11	9.82	1	0.54	2	1.3	28	4.09
Gomphidae	2	1.51	-	-	-	-	7	3.82	4	2.9	13	1.9
Aeshnidae	-	-	-	-	-	-	19	10.4	25	16.12	44	6.43
Macromiidae	-	-	-	-	-	-	6	3.3	5	3.22	11	1.6
Oligochaeta	15	11.4	6	5.9	4	3.6	6	3.3	10	6.5	41	6
Leech	5	3.8	2	2	3	2.7	5	2.73	7	4.51	22	3.21
Total Number of Taxa	20		7		9		23		23			
Total No. ind	132		102		112		183		155		684	

site K1 and K2. The water qualities at E1 sampling were poor with substantial pollution due to several anthropogenic interventions, sewage from prison institution, abattoir and residential activity and large quantities of untreated municipal sewage. The anthropogenic factors have severe impact on water quality of riverine system (Kumar 2019). The Site E2 (8.5) was highest H-FBI values which indicate very poor water qualities with severe organic pollution likely. The most of contributing families of benthic macro invertebrate in this sampling site were highly tolerant to organic pollution. The further downstream, site E3 (8.3) of contaminated area has shown lower Hilsenhoff Family biotic index (H-FBI) than site E2 but higher than site K1, K2 and E1. The predicted water qualities at this sampling site were also very poor indicating severe organic pollution likely (Table 8).

The diversity of Coleoptera and Odonata increases in healthy aquatic system especially in slow flowing and pool dominated streams Bonada et al 2007). This study also showed that diversity of Coleoptera and Odonata increases in E1, K1 and K2 sites which were relatively healthy sites. In general, the diversity of pollution tolerant benthic macroinvertebrates was more dominant at Ejersa river especially at very poor water qualities, site (E2 and E3) and more sensitive taxa of benthic macro invertebrate were more dominant at Kela river, at K1 and K2 sampling sites. The overall result of this study showed that site K1, K2 and E1 recorded the highest number of benthic Macro invertebrate with the highest value of Shannon-Wiener diversity index and lowest value of Hilsenhoff-family biotic index (H-FBI) which indicate good water quality while site E2 and E3 showed the lowest number of benthic Macro invertebrate with the lowest value of Shannon index and highest value of Hilsenhoff family biotic index (H-FBI) which indicate poor water quality.

Community loss index (CLI): The degree of dissimilarity increases from site K1 (0.96) to K2 (1.14), E1(1.34), E3 (1.58) and E2 (1.73) (Table 9). Therefore, the calculated community loss index (CLI) indicated the ecosystem disturbance at these study sites (Table 8). The Community Loss Index (CLI) measures the loss of benthic taxa in a study site with respect to a reference site. Values range from 0 to “infinity” and increase as the degree of dissimilarity between the sites increases and decrease with increasing water quality to maintain healthy aquatic ecosystem.

CONCLUSIONS

The difference in diversity of benthic macroinvertebrate between the two rivers can be attributed to the variation in degree of anthropogenic impacts such as agricultural, domestic, and abattoirs. The Ejersa river runs almost entirely through the urban area of Woliso, which is highly exposed, to several anthropogenic interventions while Kela River runs mostly through rural and semi-urban areas. This site was relatively less disturbed and point source of pollution was absent.

REFERENCES

Akalu S, Mengistou S and Leta S 2011. Assessing human impacts on the Greater Akaki River, Ethiopia using macroinvertebrates. *SINET: SINET: Ethiopian Journal of Science* **34**: 89-98.

Beneberu G and Mengistu S 2010. Benthic macroinvertebrate metrics in relation to physico-chemical parameters in selected rivers of Ethiopia, pp. 161-171. **In**: S Mengistou and B Lemma (eds), *Proceedings of Ethiopian Fishery and Aquatic Science Association*, Addis Ababa printing press, Addis Ababa.

Benetti C and Garrido J 2010. The influence of stream habitat and water quality on water beetles assemblage in two rivers in North west Spain. *Vie et milieu* **60**: 53-63.

Best J and Darby S 2020. The pace of human induced change in large rivers: Stresses, resilience, vulnerability to extreme events. *One earth* **2**(6): 510-514.

Bonada N, Rieradevall M and Prat N 2007. Macroinvertebrate community structure and biological traits related to flow permanence in a Mediterranean river network. *Hydrobiologia* **589**: 91-106.

Brua R, Culp J and Benoy G 2011. Comparison of benthic macroinvertebrate communities by two methods: Kick- and U-net sampling. *Hydrobiologia* **658**(1): 293-302

Degefe G, Tamire G, Mohammed S and Haile A 2017. Evaluation of the use of some benthic macro-invertebrate multimetric indices associations with environmental variables in ecological assessment of some Ethiopian rivers. *Hydro Nepal Journal of Water Energy and Environment* **20**: 49-54.

Duran M 2006. Monitoring water quality using benthic macro invertebrates and physico-chemical parameters of Behzat stream in Turkey. *Polish Journal of Environmental Studies* **15**: 709-717.

Edokpayi K, Olowoporoku A and Uwadiae R 2010. The hydrochemistry and microbenthic fauna characterstics of an urban draining creek. *International Journal of Biodiversity and Conservation* **2**(8): 196-203.

Enawgaw Y and Lemma B 2019. Ecological Conditions and Benthic Macroinvertebrates of Lake Tinishu Ababya, Ethiopia. *Oceanography & Fisheries Open access Journal* **10**(2): 55-82.

Flinders CA, Horwitz RJ and Belton T 2008. Relationship of fish and macro invertebrate community in the mid-Atlantic islands: Implication for integrated assessments. *Ecol.indicators* **8**(5): 518-598.

Gregory KJ 2006. The human role in changing river channels. *Geomorphology* **79**: 172-191.

Hering D, Feld C, Moog O and Ofenbock T 2006. Cook book for the development of a Multimetric Index for biological condition of aquatic ecosystems: experiences from the European AQEM and STAR projects and related initiatives. *Hydrobiologia* **566**: 311-324.

Hilsenhoff W L 1987. An improved biotic index of organic stream pollution. *Great Lakes Entomol* **20**: 31-39

Islam T, Azman A, Singh P, Ali I, Akhtar T, Rafatullah M, Ismail N and Hossain K 2019. Socio-economic vulnerability of riverbank erosion of displaces: Case study of coastal villages in Bangladesh. *Indian Journal of Ecology* **46**(1): 36-38.

Iyagbaye L, Iyagbaye R and Omoigberale M 2017. Assessment of benthic macroinvertebrates of freshwater ecosystem: A case study of Ovia River, Nigeria. *European Scientific Journal* **13:** 26-40.

Jacobus LM, Macadam CR and Sartori M 2019. Mayflies

(Ephemeroptera) and their contributions to ecosystem services. *Insects* **10**: 170-180

Kumar S and Nautiyal P 2019. State of benthic macroinvertebrate community in Bhagirathi river ecosystem impacted by hydroelectric projects. *Indian Journal of Ecology* **46**(4): 760-767.

Lakew A 2014. *Development of biological monitoring systems using benthic invertebrates to assess the ecological status of central and southeast highland rivers of Ethiopia*. Ph.D. Thesis. University of Natural Resources and Life Sciences, Vienna.

Ndimele P and Jimoh A 2011. Water Hyacinth (*Eichhornia crassipes* [Mart.] Solms.) in Phytoremediation of heavy Metal Polluted Water of Ologe lagoon, Lagos, Nigeria. *Research journal of Environmental Sciences* **5**(5): 424-433.

Plafkin JL, Barbour MT, Porter KD, Gross SK and Hughes RM 1989. *Rapid bioassessment protocols for use in Streams and Rivers: Benthic macroinvertebrate and Fish*. U.S. Environmental Protection Agency Office of Water, Washington D.C.

Qui S and Liu H 2016. Natural and anthropogenic hazards in the Yellow River Delta, China. *Natural Hazards* **85:** 1907-1911.

Rana A, Bhardwaj SK and Thakur M 2016. Surface Water Quality and Associated Aquatic Insect Fauna under Land Uses in Solan (District Solan) Himachal Pradesh. *Indian Journal of Ecology* **43**(1): 58-64.

Sitotaw B 2006. *Assessment of benthic macroinvertebrate structure in relation to environmental degradation in some Ethiopian rivers.* M.Sc. Thesis. Addis Ababa University.

Suhaila AH, Che Salmah MR and Nurul A 2014. Seasonal abundance and diversity of aquatic insects in rivers from Gunung Jerai Forest Reserve, Malaysia. *Sains Malaysiana* **43**(5): 667-674.

Tasew A 2007. *Assessment of Biological integrity using physico-chemical parameters and Macro invertebrate community index*. M.Sc. Thesis, Addis Ababa University, Addis Ababa, Ethiopia.

USEPA 2007. *National Rivers and Streams Assessment Field Operations Manual, EPA-841-B-07–009 U.S.* Environmental Protection Agency, Office of Water, Washington, D.C.

Received 22 April, 2021; Accepted 20 October, 2021

Indian Journal of Ecology (2021) 48(6): 1679-1684

Manuscript Number: 3431
NAAS Rating: 5.79

Repercussions of Urbanization on Surface Water Quality in Northern Hilly State of India

Diksha Rana and S.K. Bhardwaj

Department of Environmental Science
Dr. YS Parmar University of Horticulture and Forestry, Nauni, Solan-173 230, India
E-mail: diksharana.031@gmail.com

***Abstract*:** Water is one of the most precious resource and essential needs of life. Only 0.3 % water resources are usable in the world and with ever increasing population, urbanisation is leading to the poor quality of water resources which is a major concern of today's life. Hilly states of India are not untouched from growing population and resultant repercussions of the urbanisation; thus this study is a pioneer in accessing water quality in urban areas of Himachal Pradesh. Three areas were chosen depending upon the level of urbanisation and water samples were collected during monsoon and post monsoon season. Different water quality parameters such as pH, electrical conductivity (EC), turbidity, total dissolved solids (TDS), biological oxygen demand (BOD), chemical oxygen demand (COD) and dissolved oxygen (DO) were analysed by using standard methods. All the parameters were observed significantly different in surface water quality in selected urban areas. However, all the water parameters were within permissible limits as prescribed by ICMR but these tend to increase with years and urbanisation. Seasonal effect on water properties was significant. The pH, turbidity, BOD and COD was higher during monsoon as compared to post monsoon, whereas EC, DO and TDS were lower in monsoon as compared to post monsoon. Therefore study concluded that urbanisation had started impacting the surface water quality. Henceforth, further surveillance for quality assessment of water sources in urban areas is the need of the hour.

Keywords: Surface water quality, Urbanisation, BOD, pH

The global population estimates are around 7.9 billion people, representing a doubling of the global population in less than 50 years (UNDESA 2019). It is estimated that more than 55% of the global population live in cities and that 394 of the world's cities have a population exceeds 1 million inhabitants (UN 2011). Furthermore, it is anticipated that 83% of the developed world and 53% of the developing world will live in urban areas by 2030 (Cohen 2004). The population residing in urban areas in India is also increasing day by day, according to the 1901 census it was 11.4% increasing to 28.53% by the 2001 census, and is now currently 34% in 2017 (Worldbank 2019). According to a survey by UN, 40.76% of India's population is expected to reside in urban areas by 2030; the expansion of urban areas,population growing at rapid rate continues to pose a significant threat to natural dynamics, resource availability and environmental quality (Vorosmarty et al 2010). Poor water quality in urban areas is a major concern, especially with increasing population growth and uncertainty over the impacts of climate change on controlling factors of water quality such as temperature and environmental flow (Acreman and Ferguson 2010, Arnell et al 2015). Water is a valuable natural resource and safe water is a precondition for health and development. However, increasing population, urbanization and modernization in developing countries has created a significant risk on water quality (Rana et al 2016, Shridharan and Nathan 2017). Increasing anthropogenic activities, land use changes, discharge of sewage and municipal waste into water bodies have deteriorated water quality in some urban areas (Meitei et al 2004). Industrial and domestic sectors in urban areas contribute significantly to water contamination which renders the water unsafe for human consumption. Commercial farming and injudicious use of pesticides and fertilizers also contributes to the water quality deterioration. This poor quality water leads to water scarcity in urban areas. Himachal Pradesh is having 61 urban/sub urban habitation, which are further growing rapidly and releasing about hundreds tonnes of solid waste to the environment. Consequently, various anthropogenic activities like construction of roads, establishment of industries and educational institutes, deforestation, changes in cropping pattern and excessive use of chemical fertilizers and pesticides in the field for better crop yield has led to change in the land use pattern, which has degraded the water quality. Moreover, the waste water effluents are discharged directly to the water bodies without any treatment. The district Kangra is the most populous district of Himachal Pradesh and keeping in view the different urban local bodies and level of

urbanization one municipal corporation, one municipal council and Nagar Panchayat was selected to study the quality of water in these areas in order to evaluate the repercussions caused by urbanization.

MATERIAL AND METHODS

Site description: The Kangra district has altitude that varies from 500 metres above mean sea level (amsl) to around 5000 metres amsl. Kangra district lies between 31˚ 21′ to 32˚ 59′ North latitude and 75˚ 47′ 55″ to 77˚ 45′ East longitude. It is the most populous district of Himachal Pradesh with total population of about 1,510,075 with total geographical area of 5,739 sq. km, which is 10.31 per cent of the total area of the state. It is situated on the southern escarpment of the Himalayas. The entire area of the district is traversed by the varying altitude of the Shivalik, Dhauladhar and the Himalayas from north-west to south-east.

Experimental details: To study the effect of urbanization on the water quality in the selected municipal areas during the year 2019 and 2020, water samples were randomly collected from surface water sources during monsoon (July-August) and post monsoon (October-November) seasons. In total there were six treatment combinations (3 x 2 x 1) which were replicated three times in randomized block design factorial.

Water sampling and analysis: Surface (streams and rivers) water samples were collected in acid washed one litre plastic bottles as per standard procedure from 10 to 12 cm below the water surface for detailed chemical analysis. The water samples were then analysed for the following parameters using standard methods (APHA 2012).

pH: Water pH was determined by using pH meter (Model 1013 of EIA make) and was expressed in the scale of 0-14.

EC and TDS: EC and TDS (Model -1601 of EIA make) expressed in µS cm^{-1} were determined by using EC meter to make the measurement.

Turbidity: Turbidity (Model- 331 of EIA make) was determined by standard Nephelometric method and expressed in Nephelometric Turbidity Unit (NTU).

Biological oxygen demand (BOD): BOD was estimated by using 5 day BOD test as outlined in 5210B method (APHA2012).

Chemical oxygen demand (COD): COD was estimated by oxidizing water samples with hot $H_2SO_4$of potassium chromate with silver sulphate as the catalyst. The water sample was digested at 148°C in preheated thermometer (TR 320) for about 120 minutes. The concentration of Cr^{3+}ions was determined photometrically by using Spectroquant pharo 300 (Merck make) instrument and expressed as mg l^{-1}.

Dissolved Oxygen (DO): DO was measured by DO meter of Mark make and was expressed in mg l^{-1}.

Statistical analysis: The data obtained from the analysis of water samples was subjected to statistical analysis using SPSS software. The obtained results were compared with permissible limits of BIS: Indian Standards (IS 10500: 1991) (Table 1) and World Health Organization (Anonymous 2012, Kumar and Puri 2012).

RESULTS AND DISCUSSION

pH: The surface water pH in different urban areas ranged from 7.04 to 7.27 which was normal and within the permissible limits as prescribed by BIS (Table 2).

Electrical conductivity: The surface water EC in different urban areas ranged from 0.177 to 0.252 dS m^{-1} which was normal and within the permissible limits as prescribed by BIS (Table 3).

Total Dissolved Solids (TDS): The surface water TDS in different urban areas ranged from 141.06 to 269.12 mg l^{-1} which was normal and within the permissible limits as prescribed by BIS (Table 4).

Turbidity: The surface water turbidity in different urban areas

Table 1. Permissible limits of drinking water quality parameters

Parameters	BIS: Indian Standards		World Health Organization
	Desirable limit	Permissible limit	Maximum allowable concentration
pH	6.5-8.5	No relaxation	6.5-8.5
Electrical Conductivity (dS m^{-1})	--	300	--
Turbidity (NTU)	5	10	5
TDS (mg l^{-1})	500	2000	1000
BOD (mg l^{-1})	2	5	--
COD (mg l^{-1})	--	250	--
DO (mg l^{-1})	--	6	--

ranged from 3.22 to 4.89NTU which was normal and within the permissible limits as prescribed by BIS (Table 5).

Biochemical Oxygen Demand (BOD): The surface water BOD in different urban areas ranged from 1.557 to 2.585 mg l^{-1} which was normal and within the permissible limits as prescribed by BIS (Table 6).

Chemical Oxygen Demand (COD): The dissolved oxygen in all the urban areas was normal and ranged from 43.73 to 52.27 mg l^{-1}within the permissible limits as prescribed by BIS (Table 7).

Dissolved Oxygen (DO): The dissolved oxygen in all the urban local bodies was normal and ranged from 8.68 to 10.55

Table 2. Seasonal variation of pH in surface water sources of urban areas

Seasons/ Urban areas	Monsoon	Post monsoon	Mean	Monsoon	Post monsoon	Mean	Monsoon	Post monsoon	Mean
		2019			2020			Pooled	
Municipal Corporation (Dharamshala)	7.07	6.89	6.98	7.15	7.07	7.11	7.11	6.98	7.04
Municipal Council (Palampur)	7.26	7.01	7.13	7.37	7.25	7.31	7.31	7.13	7.22
Nagar Panchayat (Baijnath-Paprola)	7.22	7.10	7.16	7.42	7.36	7.39	7.32	7.23	7.27
Mean	7.18	7.00		7.31	7.23		7.25	7.11	
CD (p=0.05)									
Urban areas		0.05			0.04			0.03	
Seasons		0.04			0.03			0.02	
Urban areas x Seasons		NS			NS			NS	

Table 3. Seasonal variation of EC (dS m^{-1}) in surface water sources of urban areas

Seasons/ Urban areas	Monsoon	Post monsoon	Mean	Monsoon	Post monsoon	Mean	Monsoon	Post monsoon	Mean
		2019			2020			Pooled	
Municipal Corporation (Dharamshala)	0.153	0.160	0.156	0.195	0.200	0.198	0.174	0.180	0.177
Municipal Council (Palampur)	0.262	0.269	0.266	0.217	0.261	0.239	0.240	0.265	0.252
Nagar Panchayat (Baijnath-Paprola)	0.240	0.281	0.261	0.243	0.244	0.244	0.242	0.262	0.252
Mean	0.218	0.236		0.219	0.235		0.219	0.236	
CD (p=0.05)									
Urban areas		0.011			0.006			0.006	
Seasons		0.009			0.005			0.005	
Urban areas x Seasons		0.016			0.008			0.008	

Table 4. Seasonal variation of TDS (mg l^{-1}) in surface water sources of urban areas

Seasons/ Urban areas	Monsoon	Post monsoon	Mean	Monsoon	Post monsoon	Mean	Monsoon	Post monsoon	Mean
		2019			2020			Pooled	
Municipal Corporation (Dharamshala)	5.84	5.51	5.68	4.91	3.29	4.10	5.38	4.40	4.89
Municipal Council (Palampur)	4.59	2.77	3.68	3.92	2.71	3.32	4.26	2.74	3.50
Nagar Panchayat (Baijnath-Paprola)	3.50	2.82	3.16	3.77	2.79	3.28	3.64	2.80	3.22
Mean	4.64	3.70		4.20	2.93		4.42	3.31	
^{CD}0.05									
Urban areas		0.75			NS			0.45	
Seasons		0.61			0.55			0.36	
Urban areas x Seasons		NS			NS			NS	

mg l^{-1}within the permissible limits as prescribed by BIS (Table 8).

The low pH might be because of influx of freshwater from the Dhauladhar ranges which may lead to dilution of salts in water and subsequently reduce the pH of surface water sources. Rainfall contributing to dilution effect leads to replenishment of water sources during monsoon season and subsequent perceptible moderation in pH of water quality

Table 5. Seasonal variation of turbidity (NTU) in surface water sources of urban areas

Seasons/ Urban areas	Monsoon	Post monsoon	Mean	Monsoon	Post monsoon	Mean	Monsoon	Post monsoon	Mean
		2019			2020			Pooled	
Municipal Corporation (Dharamshala)	116.43	126.85	121.64	156.58	164.36	160.47	136.51	145.61	141.06
Municipal Council (Palampur)	174.25	181.75	178.00	160.16	179.43	169.79	167.20	180.59	173.90
Nagar Panchayat (Baijnath-Paprola)	265.65	284.10	274.88	252.99	273.74	263.37	259.32	278.92	269.12
Mean	185.45	197.57		189.91	205.84		187.68	201.71	
CD (p=0.05)									
Urban areas		8.22			18.65			9.28	
Seasons		6.71			15.22			13.12	
Urban areas x Seasons		NS			NS			NS	

Table 6. Seasonal variation of BOD (mg l^{-1}) in surface water sources of urban areas

Seasons/ Urban areas	Monsoon	Post monsoon	Mean	Monsoon	Post monsoon	Mean	Monsoon	Post monsoon	Mean
		2019			2020			Pooled	
Municipal Corporation (Dharamshala)	2.953	2.141	2.547	2.850	2.397	2.623	2.901	2.269	2.585
Municipal Council (Palampur)	1.986	0.933	1.460	1.867	1.530	1.698	1.926	1.232	1.579
Nagar Panchayat (Baijnath-Paprola)	1.817	1.210	1.513	1.670	1.530	1.600	1.743	1.370	1.557
Mean	2.252	1.428		2.129	1.819		2.190	1.624	
CD (p=0.05)									
Urban areas		0.707			0.209			0.341	
Seasons		0.577			0.171			0.278	
Urban areas x Seasons		NS			NS			NS	

Table 7. Seasonal variation of COD (mg l^{-1}) in surface water sources of urban areas

Seasons/ Urban areas	Monsoon	Post monsoon	Mean	Monsoon	Post monsoon	Mean	Monsoon	Post monsoon	Mean
		2019			2020			Pooled	
Municipal Corporation (Dharamshala)	53.87	50.43	52.15	55.80	48.96	52.38	54.84	49.70	52.27
Municipal Council (Palampur)	48.77	45.37	47.07	47.48	41.32	44.40	48.12	43.35	45.74
Nagar Panchayat (Baijnath-Paprola)	47.80	39.81	43.81	46.18	41.14	43.66	46.99	40.47	43.73
Mean	50.15	45.20		49.82	43.81		49.98	44.51	
CD (p=0.05)									
Urban areas		3.79			4.64			2.67	
Seasons		3.10			3.79			2.18	
Urban areas x Seasons		NS			NS			NS	

Table 8. Seasonal variation of DO (mg l^{-1}) in surface water sources of urban areas

Seasons/ Urban areas	Monsoon	Post monsoon	Mean	Monsoon	Post monsoon	Mean	Monsoon	Post monsoon	Mean
		2019			2020			Pooled	
Municipal Corporation (Dharamshala)	9.28	11.71	10.49	9.64	11.57	10.61	9.46	11.64	10.55
Municipal Council (Palampur)	8.33	9.97	9.15	8.52	10.58	9.55	8.43	10.28	9.35
Nagar Panchayat (Baijnath-Paprola)	7.97	9.37	8.67	7.63	9.77	8.70	7.80	9.57	8.68
Mean	8.53	10.35		8.60	10.64		8.56	10.49	
CD (p=0.05)									
Urban areas		1.057			1.059			0.677	
Seasons		0.863			0.865			0.553	
Urban areas x Seasons		NS			NS			NS	

parameters in the post-monsoon season is responsible for variation in pH in different seasons (Sunitha et al 2016, Trivedi et al 2010). Landfill leachate, impervious surface runoff and agricultural runoff can increase the EC levels due to anthropogenic activities along with other natural source impacting EC such as varied geological formations and rocks present in the concerned area (Vatanpour et al 2020).The higher value of TDS is due to prevailing drainage systems in urbanized watersheds; the influence of construction activities, evaporation, temperature and due to presence of excess of free CO_2 product as a result of decomposition process coupled with the mixing of sewage and domestic waste (Utang and Akpan 2012, Vatanpour et al 2020). The higher turbidity might be ascribed due to frequent rains and corresponding increased surface runoff leading to silting of the water sources, suspended and colloidal matter such as clay, finely divided organic, inorganic matter, microscopic organisms and developmental activities which might have loosened the soil thereby, increases the turbidity (Polkowska et al 2007, Balamurugan & Sivakumar 2015).The increased BOD may be due to the accumulation of leaves and woody debris, vegetation, dead plants and animals, animal manure, wastewater treatment plants, feedlots, illegal release of waste water into sources, food-processing units; failing septic systems, urban water runoff and degradation of organic matter and untreated domestic effluents. Further sedimentation and accumulation of waste into the water bodies resulted in higher BOD (USEPA 2011, Shimba 2017). The presence of inorganic and organic non-biodegradable content of pollutants, illegal release of domestic waste, unscientific disposal of urban solid and sewage waste as well as industrial effluent and sewage water into the surface water bodies leads to high levels of COD. The higher COD during monsoon may be due to more dilution of pollutants in water sources or presence of inorganic and organic non-biodegradable content of pollutants (Vieira et al 2013).The higher DO might be due to heavy rainfall in Dharamshala, more input of freshwater from the Dhauladhar ranges and also due to less temperature.

CONCLUSION

The urbanisation has started significantly affecting the water quality as illustrated by the seasonal variations in the hilly state of India. The repercussions of the urbanization such as population density, anthropogenic activities, tourism incursion, construction, dumping and disposal of sewage water and domestic waste directly into the surface water sources might be responsible for introducing pollutants or unwanted substances in the nearby water sources which are leading to deterioration of the water quality. Although the quality parameters lies within standard limits but further regular monitoring and surveillance for quality assessment of water sources, in the wake of detrimental activities caused by urbanisation, is needed. As the urbanization is inevitable part of growth, growth in harmony to normal rate of replenishment of resources and reliance on sustainable livelihood and practicing conservation of nature and resources is recommended.

REFERENCES

Acreman MC and Ferguson AJD 2010. Environmental flows and the European water framework directive. *Freshwater Biology* **55** (1): 32-48.

Anonymous 2012. *Indian standard 10500 of drinking water specification*. Bureau of Indian Standards, New Delhi, India. 32.

APHA 2012. *Standard methods for the examination of waste water*. Washington DC. 161.

Arnell NW, Halliday SJ, Battarbee RW, Skeffington RA and Wade AJ 2015. The implications of climate change for the water environment in England. *Progress in Physical Geography* **39**(1): 93-120.

Balamurugan C and Sivakumar R 2015. The seasonal variation of water quality parameters in Vaigai River at Madurai, Tamilnadu, India. *International Journal of Computer and Organization Trends* **5**(2): 59-67.

Cohen B 2004. Urban growth in developing countries: a review of current trends and a caution regarding existing forecasts. *World Development* **32**(1): 23-51.

Kumar M and Puri A 2012. A review of permissible limits of drinking water. *Indian Journal of Occupational and Environmental Medicine* **16**: 40-44.

Meitei NS, Bhargava V and Patil PM 2004. Water quality of Purna river in Purna town Maharashtra state. *Journal of Aqua Biology* **19**: 77-78.

Polkowska Z, Skarzynska K, Dubiella-Jackowska A, Staszek W and Namiesnik J 2007 Evaluation of pollutant loading in the runoff water from a major urban highway (Gdansk Beltway, Poland). *Global Nest Journal* **9**: 269-275.

Rana A, Bhardwaj SK and Thakur M 2016. Surface water quality and associated aquatic insect fauna under different land-uses in Solan (district Solan). Himachal Pradesh. *Indian Journal of Ecology* **43**(1): 58-64.

Shimba MJ 2017. Spatial and seasonal variations in surface water quality of the Mkondoa River, Tanzania. *Journal of Soil Science and Environmental Management* **8**(9): 148-154.

Shridharan M and Nathan DS 2017. Groundwater quality Assessment for domestic and agriculture purposes in Puducherry region. *Applied Water Science* **7**: 4037-4053.

Sunitha V, Khan JA, Prasad M and Reddy MR 2016. Seasonal variation of groundwater quality in parts of YSR and Anantapur Districts, Andhra Pradesh, India. *International Journal of Engineering Research and Application* **6**(6): 5-8.

Received 10 July, 2021; Accepted 10 November, 2021

Trivedi P, Bajpai A and Thareja S 2010. Comparative study of seasonal variation in physicochemical characteristics in drinking water quality of Kanpur, India with reference to 200 MLD filtration plant and ground water. *Nature and Science* **8**: 11-17.

UN (United Nations) 2011. *World urbanization prospects: the 2011 revision*. New York, USA United Nations Department of Economic and Social Affairs (Population Division).

USEPA 2011. *Environmental protection Agency Exposure factors Hand book*, www.epa. gov/ o opt/exp.

Utang PB and Akpan HE 2012. Water Quality Impediments to Sustainable Aquaculture Development Along Selected Segments of the New Calabar River, Niger Delta, Nigeria. **4**: 34-40.

Vatanpour N, Malvandi AM, Talouki HH, Gattinoni P and Scesi L 2020. Impact of rapid urbanization on the surface water's quality. A long-term environmental and physico-chemical investigation of Tajan river, Iran (2007–2017). *Environmental Science and Pollution Research* **27**: 8439-8450.

Vieira R, Fernandes JN and Barbosa AE 2013. Evaluation of the impacts of road runoff in a Mediterranean reservoir in Portugal. *Environment Monitor Assess* **185**: 7659-7673.

Vorosmarty CJ, McIntyre PB, Gessner MO, Dudgeon D, Prusevich A, Green P, Glidden S, Bunn SE, Sullivan CA, Reidy LC and Davies PM 2010. Global threats to human water security and river biodiversity. *Nature* **467**(7315): 555–561.

World bank 2019. Urban population (% of total) data. World bank.org.

United Nations, *Department of Economic and Social Affairs, Population Division (2019). World Population Prospects 2019: Highlights* (ST/ESA/SER.A/423)

Indian Journal of Ecology (2021) 48(6): 1685-1691

Manuscript Number: 3432
NAAS Rating: 5.79

Delineation of Groundwater Potential Zone in Foothill of Western Himalayan State

Pravidhi Sharma, R.K. Aggarwal and S.K. Bhardwaj

Department of Environmental Science, Dr Y S Parmar University of Horticulture and Forestry
Nauni, Solan-173 230, India
E-mail: vidhusharma461@gmail.com

***Abstract*:** The present study emphasizes on the integrated remote sensing and GIS approach for delineation of the groundwater potential zone in foothill situated between Northern latitudes of 30°52' to 31°04' and Eastern longitudes of 76°40' to 76°55' falling in the Survey of India Toposheets no. 53A/12, 53A/16, 53B/9 and 53B/13. The thematic maps of influencing parameters viz. LULC, slope, geology, drainage, soil, aspect and lineament were prepared in Arc GIS. By integrating the information derived from the maps five zones having high, high to moderate, moderate, moderate to low and low to poor groundwater potential were distinguished. The overall results showed that maximum region came under high and moderate groundwater potential zone. Potential zones were further validated with 15 locations (hand pump and bore well) which, were randomly selected in the study area. Plotting of these points on groundwater potential zone map revealed that maximum points fell in high groundwater potential zone and one point was found in moderate groundwater potential zone thereby verifying that, zone I identified by remote sensing analysis was the zone holding maximum groundwater potential. This study will help policy makers in making appropriate water conservation strategies for the actual groundwater potential zones in the study area.

Keywords: Groundwater, Remote sensing, Potential zones, GIS

Groundwater, which is one of the world's most precious and significant natural resource for the sustenance of life is controlled by geological and meteorological factors (Hutti and Nijagunappa 2011, Biswas et al 2012). Over the years, increase in population, urbanization and expanding agriculture has raised dependency on this valuable natural resource which is further expected to increase in future and the requirement in 2050 is estimated about more than three times to the present level due to increase in population (Gupta and Deshpande 2004). The groundwater is the largest available source of fresh water lying beneath the ground and has become crucial not only for targeting of groundwater potential zones, but also monitoring and conserving this important resource. Of the 37 Mkm^3 of freshwater estimated to be present on the earth, about 22% exists as groundwater, which constitutes about 97% of all liquid freshwater potentially available for human use. In India, 65% of the total geographical area is covered by hard rock formations and occurrence of groundwater in such rocks is essentially confined to fractured and weathered horizons (Saraf et al 2007). Therefore, an extensive hydrogeological investigation is required for thorough understanding of the groundwater conditions (Pandey et al 2013, Singh and Pandey 2014). To maintain the water table condition in balance and to restrict the surface runoff going waste, various measures for artificial groundwater recharge can be implemented in such zones. Till now, several conventional methods such as geological, hydro-geological, geophysical and photo-geological techniques are employed to delineate groundwater potential zones (Srivastava and Bhattacharya 2006) but these methods are very costly and time-consuming. Remote sensing with its advantage of spatial, spectral and temporal availability of data covering large and inaccessible areas within short time has become a very handy tool in assessing, monitoring and conserving groundwater resources. In recent years, extensive use of satellite data along with conventional maps and rectified ground truth data has made it easier to establish the baseline information for groundwater potential zones (Chowdhury et al 2010). GIS is considered as a powerful tool in integration and analysis of multi-thematic layers in delineating groundwater prospect and deficit zones (Ganapuram et al 2009, Selvam et al 2012). Several workers have used GIS techniques to delineate groundwater potential zone (Owolabi et al 2020, Ayyandurai and Venkateswaran 2021). Singh et al (2017) also conducted a study for delineation of the groundwater potential zone in Shimla city area and Suryabhagvan (2017) in the Bata river basin Himachal Pradesh using GIS technology. The Nalagarh valley is delimited between the Siwalik Hills with northeast (NE) and Sirsa river in southwest (SW). Sirsa River is the main river that flows through the

central part of the Nalagarh valley. Sirsa watershed occupies the whole Nalagarh valley, parts of Solan, Kasauli in Himachal Pradesh. The total catchment area of Sirsa River is about 250 km^2. Out of this, the Nalagarh valley alone occupied 230 km^2. Farmers are largely dependent on this river water for irrigating agricultural fields. But in past few years increased industrialization and urbanization activities has put immense pressure on surface as well as on groundwater resources. As per the state's Economic Survey report for the year 2013-2014, there were 39,819 industrial units registered with the Industries Department within the state on a permanent basis, which has led to the heavy extraction from the river as well as groundwater. The groundwater level in the valley of river Sirsa is thereby depleting at an alarming rate. Therefore, there is an urgent need to look for alternative water resources and delineate potential groundwater zones so that agricultural, industrial and domestic water needs are properly fulfilled. The present study was carried out with an objective to demarcate potential groundwater zones suitable for different artificial recharge structures with the help of GIS and remote sensing technology.

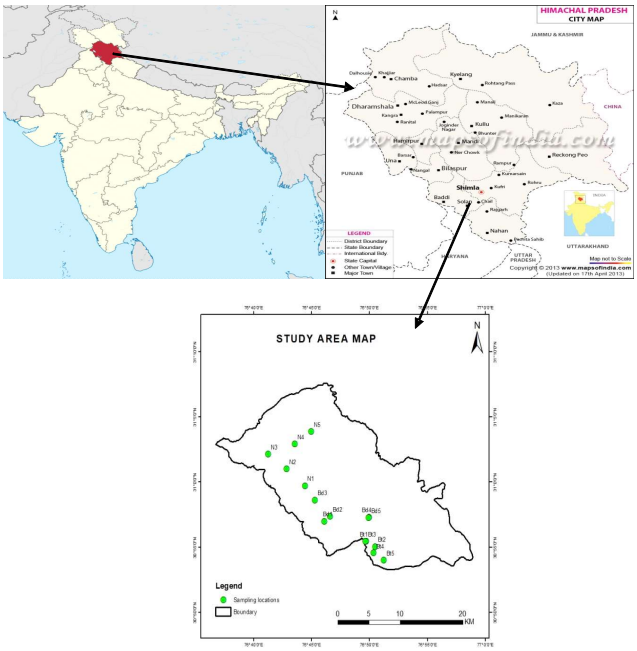

Fig. 1. Location map of study area

MATERIAL AND METHODS

Study region: The study area lies between Northern latitudes of 30°52' to 31°04' and Eastern longitudes of 76°40' to 76°55'. The climate of the Nalagarh valley varies from humid to semi-arid type which is subjected to mesothermal climatic condition. The mean minimum and mean maximum temperatures observed in the study area was around 4°C and 28°C. The average annual rainfall of the valley is about 1129.3 mm with approximately 64 rainy days and receives heavy rainfall during the southwest monsoon period, between June to mid-September due to southwest monsoon whereas enjoys moderate precipitation by western disturbances in the month of December to March (Fig. 1).

Data processing: In the present study, Arc GIS 10.0 software has been used for generating Geo-database and maps. It was used for creating maps; compiling geographic data; image interpretation; classification and further analysis.

Preparation of thematic maps: Firstly the base map has been created from SOI toposheets No.53A/12, 53A/16, 53B/9 and 53B/13 in scale 1:50,000. The base map reflected watershed boundary and some major settlements randomly selected. The watershed boundary of the study area was marked by locating contours and drainage lines available on the SOI topographic map. UTM Zone 43 projection coordinate system has been used for georeferencing. In this projection system the coordinates can be assigned in metric and geographic units both. After this further vectorization of geo-database of study area which includes its boundary, drainage, soil, slope, aspect, geology, lineament, and land use/land cover was done to generate digital input maps.

Drainage map: The drainage map was generated by overlaying the digitized study area boundary on the georeferenced toposheets No.53A/12, 53A/16, 53B/9 and 53B/13 in Arc GIS 10.0. After study area boundary map properly got overlayed on toposheets, the drainages falling within boundary map were manually digitized and the drainage map was prepared.

Soil, geology and lineament map: The soil, geology and lineament map of the study area was digitized from the groundwater prospect map of Nalagarh valley prepared under Rajiv Gandhi National Drinking Water Mission project work. These maps were scanned, rectified and then digitized using Arc GIS software.

Land use and landcover map: LULC maps were prepared from LISS 3 satellite images on scale 1:50,000 which was classified in the Arc GIS 10.1 using supervised classification method or more commonly known as pixel based classification method.

Slope and aspect map: The slope and aspect map was prepared with the help of ArcGIS 10.1 Spatial Analyst Tool-Surface-Slope using DEM of the study area.

Ground truthing: To check the accuracy of the results obtained from remote sensing study, a field survey in the study area was conducted. For this 15 hand pumps and bore

wells were randomly selected in the study area and their latitude and longitude were recorded through GPS. Locations (latitude and longitude) of these bore wells and hand pumps were then plotted on the groundwater potential map in order to examine the reliability of the zones identified from remote sensing study (Fig. 11).

RESULTS AND DISCUSSION

Drainage map: The valley is drained by numerous perennial and ephemeral streams emerging from the north-east flank passing through industrial belt often loaded with industrial and sewage discharges and transverse flow across the valley, to join Sirsa River. The important streams (tributary rivers) among them are Chikni, Phula, Ratta, Balad and Surajpur. All the tributaries (small river) of Sirsa river flow in north-east direction to south-west direction and are almost parallel to each other. These streams are fed by numerous secondary streams which form a dendritic type of drainage pattern which is clearly visible in the map. The drainage density was higher towards the upper hilly regions, thereby less infiltration and, hence low groundwater potential zone (Fig. 3).

Soil and geology map: The thematic layer of soil revealed four main soil classes viz., clay, clay loam, sandy clay loam and sandy loam and majority of area was dominated by sandy loam soil covering an area of 139.67 km^2(32.97%) and study area fell under sandy clay loam and sandy loam type of soil indicating that these areas have high and moderate to low groundwater potential based on the recharge potential and infiltration rate of soil type present (Fig. 4, Table 1). The different geology classes were identified as lower swales, quaternary and upper swales (Table 2). Majority of the study area was under lower swales (273.05 km^2) i.e 61.5% of the total area comprising mainly of sandstone with the intercalation of clay beds. The Lower Shiwalik sandstone was mainly fine to medium grained with pebbles. The Upper Siwalik formation mainly comprised of the areas on the area adjoining to Haryana and few patches on the north of Nalagarh in the central part of the study area. The quaternary contributed to about 33.2% covering 147.38 km^2. Very less

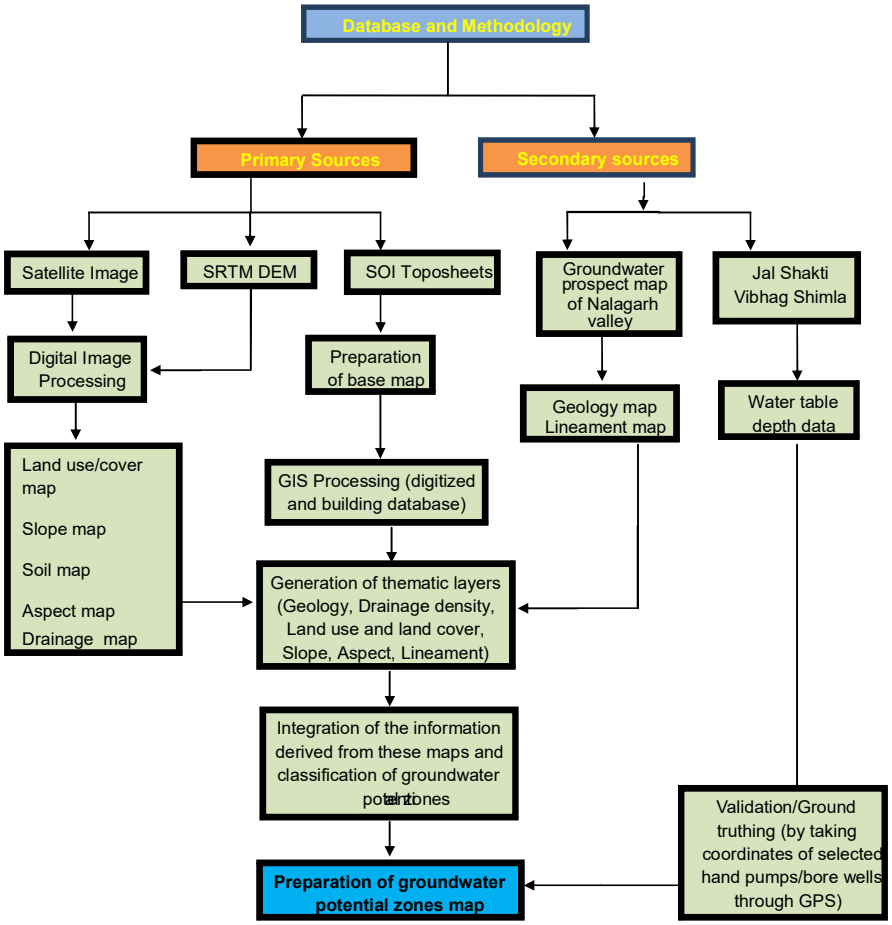

Fig. 2. Flow chart of methodology adopted for identification of potential groundwater zones

area was under upper swales (23.58 km^2) covering south-west portion of the valley. Major part of the Sirsa river basin is covered by alluvium soil with Holocene and Pre-Holocene deposits (quaternary) thereby having excellent recharge conditions because ground water mainly occurs in porous unconsolidated alluvial formation (valley fills) comprising sand, silt, gravel, cobbles and pebbles. Most of the sampling points taken for present study were also under quaternary, therefore making it the area under high groundwater potential zone (Fig. 5).

Land use and landcover map: There were six different classes agriculture, built up, forest, grassland/ grazing land, wasteland and water bodies (Fig. 6). Majority of the area was covered by forests (202.52 km^2) followed by wasteland, agriculture, water bodies, built-up and least by grassland and grazing land. Agriculture and forests were considered to be best for groundwater recharge as the vegetation cover tends to increase infiltration and reduces runoff. Based on the identified land use classes and their respective influence on groundwater occurrence, holding capacity and recharge the study area was classified into high, high to moderate, moderate, moderate to low and low to poor groundwater potential zone.

Slope and aspect map: On the basis of slope, study area was divided into six classes (Table 3). Majority of the study area was under gentle sloping which covered an area of 125 km^2 (28.22%) followed by very gentle slope covering which forms one of the most suitable areas for groundwater recharge and high groundwater potential zone as they reduces runoff and increase infiltration (Fig. 7). The aspect map showed about 14 per cent (62.62 km^2) and 16 per cent (70. 63 km^2) area was covered by southern and south-western aspect respectively (Fig. 8).

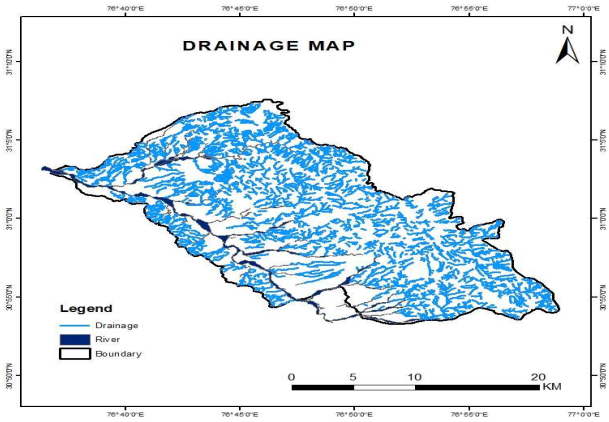

Fig. 3. Drainage map

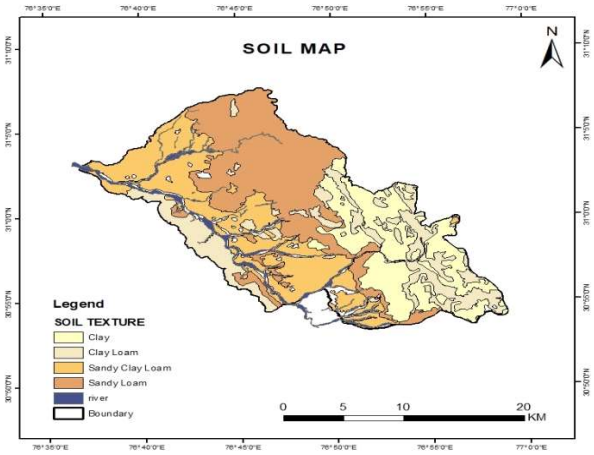

Fig. 4. Soil map

Table 1. Rate of infiltration in the different soil texture

Soil texture	Infiltration rate mm/hr
Clay	1-5
Clay loam	5-10
Sandy clay loam	10-15
Sandy loam	20-30

Table 3. Slope categories used to prepare slope map of the study area

Slope category	Slope (%)
Very gentle sloping	1-3
Gentle sloping	3-5
Moderately sloping	5-10
Moderately steep sloping	10-15
Steep sloping	15-35
Very steep sloping	>35

Table 2. Geological sequence of the Nalagarh valley

Rock	Lithology	Age
Holocene deposits (Quaternary)	Modern alluvium and river sediments (assorted mixture of boulder, cobble, pebble, sand and silt)	Recent
Pre-Holocene deposits	River terrace	Upper Pleistocene
Lower Siwalik	Grey sandstones and purple clays	Upper Miocene
Upper Siwalik	Boulder conglomerates, sand rocks and clays	Lower Pleistocene

Source: Geology and Mineral Resources of Himachal Pradesh (2012)

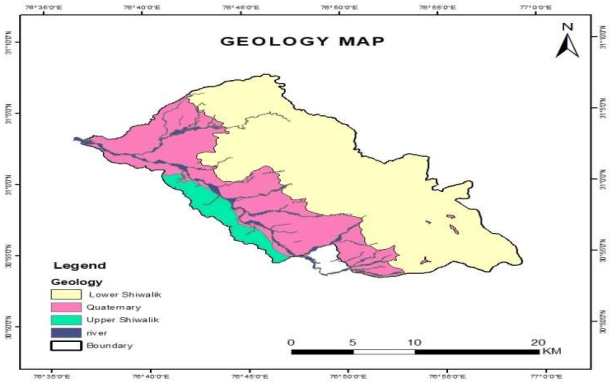

Fig. 5. Geology map

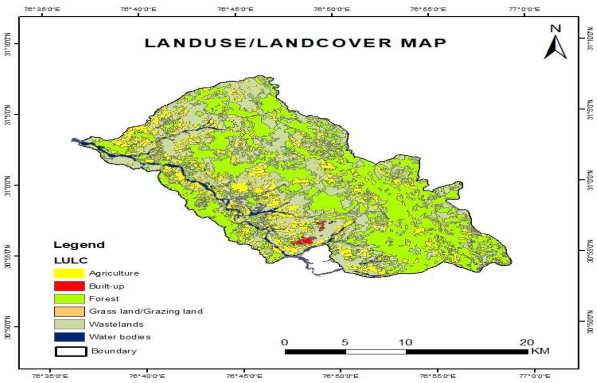

Fig. 6. Landuse and landcover map

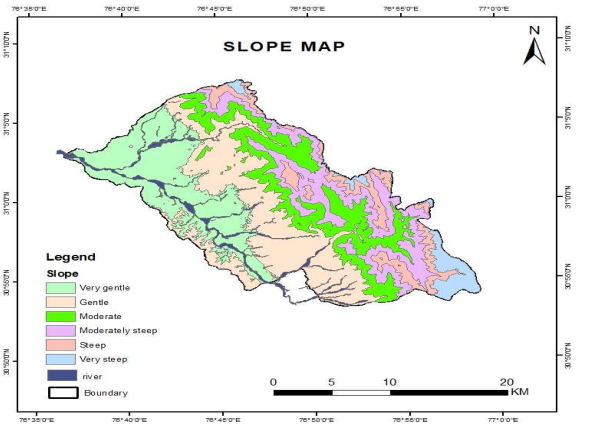

Fig. 7. Slope map

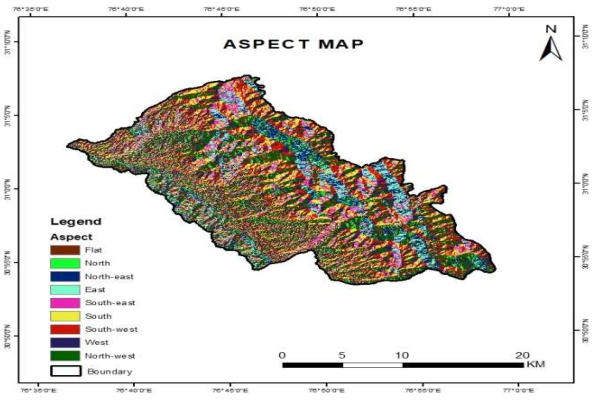

Fig. 8. Aspect map

Lineament map: The lineaments have been identified throughout the area as Pedi plain or valley floor (VF), shallow flood plain which was considered significant from

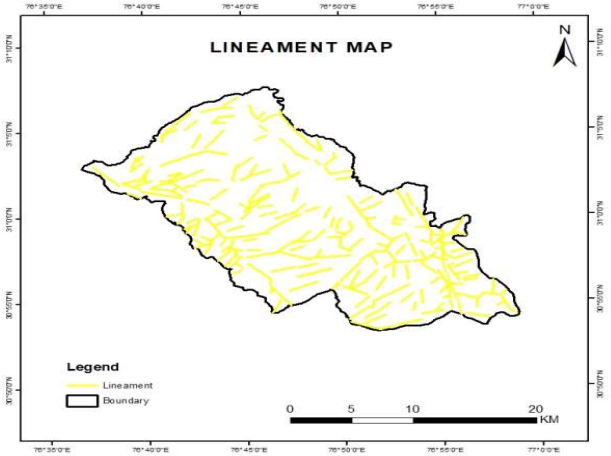

Fig. 9. Lineament map

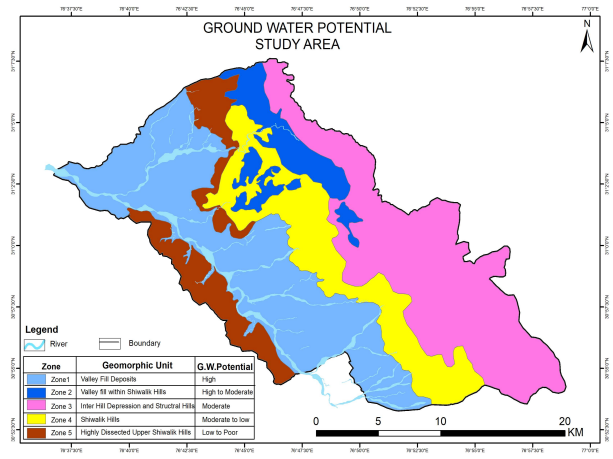

Fig. 10. Groundwater potential zones map

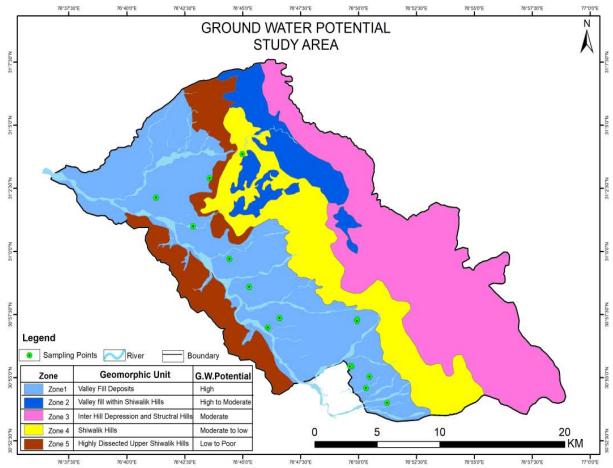

Fig. 11. Sampling points taken in the study area for ground truthing

groundwater occurrence point of view while those across the high-drainage density and high-slope area or in the area occupied by clay zones were of less significance as there could be high runoff along them and these may acted as only conduit to transmit infiltrated rain water (Fig. 9)

Groundwater potential zones map: Based on the investigation carried out in the study area and by integrating the information derived from the maps of the parameters affecting the groundwater occurrence prepared in Arc GIS tool i.e drainage, slope, aspect, soil, geology, land use land cover and lineament, the study area was classified into five different groundwater potential zones namely high, high to moderate, moderate, moderate to low and low to poor. Maximum area accounting 34.2% (151.83 km^2) of the total area was occupied by moderate potential zone (zone III) and 30.77% (136.58 km^2) by high potential zone. High to moderate potential zone occupy 10.02% of total predicted potential zones, while low to poor potential zone accounted to 17.25% of the area. Small portion of 7.78% of the study area came under moderate to low potential zone (Fig. 10). The maximum of the region came under high and moderate groundwater potential zone.

Ground truthing/ field validation of remotely sensed groundwater potential zones: The results obtained were validated with 15 handpump/ bore well randomly selected in the study area and their latitude and longitude were also recorded. These points were plotted on groundwater potential zone map with the help of Arc GIS tool in order to check where these points fall on the map. The maximum of the points fell in zone I (high groundwater potential zone) and one point in zone III (moderate groundwater potential zone) thereby verifying that, zone I identified by remote sensing analysis is the zone holding maximum groundwater potential (Fig. 11).

CONCLUSION

The present study demonstrated that the integrated use of geospatial and geophysical techniques is an efficient tool for assessing groundwater potential, based on which suitable locations for groundwater withdrawal could be identified. The potential zone map prepared revealed that the region along the Sirsa river (zone I) holds maximum groundwater potential as compared to the regions far from the river. Ground truthing survey conducted also validated these results derived from potential zone map which showed that maximum hand pump and tube well points fell within the high potential zone. The results of the present study can serve as guidelines for planning future artificial recharge projects in the study area in order to ensure sustainable groundwater utilization.

AKNOWLEDGEMENTS

The authors are grateful to Dr. S S Randhawa, Principal Scientific Officer, HIMCOSTE, State Centre on Climate Change, Shimla (H.P) for providing digital processing and GIS facilities and for their unstinted support in GIS analysis during this work.

REFERENCES

Ayyandurai R and Venkateswaran S 2021. Appraisal of groundwater potential zonation mapping in coastal track of Cuddalore district using geospatial techniques in Tamil Nadu, India. *Indian Journal of Ecology* **48:** 1011-1018.

Biswas S, Jana A and Sharma SP 2012. Delineation of groundwater potential zones using satellite remote sensing and geographic information system techniques: A case study from Ganjam district, Orissa, India. *Research Journal of Recent Sciences* **1**: 59-66.

Chowdhury A, Jha MK and Chowdary V M 2010. Delineation of groundwater recharge zones and identification of artificial recharge sites in West Medinipur district, West Bengal, using RS, GIS and MCDM techniques. *Environment Earth Sciences* **59**: 1209-1222.

Foster S 1998. Groundwater assessing vulnerability and promoting protection of a threatened resource, pp. 79-90. In Proceedings of the *'8th Stockholm Water Symposium'*, August 10-13, 1998, Sweden (Stockholm: International Water Institute).

Ganapuram S, Vijaya Kumar GT, Murali Krishna IV, Kahya E and Cuneyd Demirel M 2009. Mapping of groundwater potential zones in the Musi basin using remote sensing data and GIS. *Advances in Engineering Software* **40**: 506-518.

Gupta SK and Deshpande RD 2004. Water for India in 2050: First order assessment and available option. *Current Science* **86**: 1216-1224.

Hutti B and Nijagunappa R 2011. Identification of groundwater potential zone using geoinformatics in Ghataprabha basin, North Karnataka, India. *International Journal of Geomatics and Geosciences* **2**: 191-109.

Owolabi ST, Madi K, Kalumba MA and Orimoloye RI 2020. A groundwater potential zone mapping approach for semi-arid environments using remote sensing, GIS and AHP techniques: A case study of Buffalo catchment, Eastern cape, South Africa. *Arabian Journal of Geoscience* **13**: 1184.

Pandey AC, Singh SK, Nathawat MS and Saha D 2013. Assessment of surface and subsurface waterlogging, water level fluctuations and lithological variations for evaluating groundwater resources in Ganga Plains. *International Journal of Digital Earth* **6**(3): 276-296.

Saraf AK, Choudhury PR, Roy B, Sarma B, Vijay S and Choudhury S 2004. GIS based surface hydrological modelling in identification of groundwater recharge zones. *International Journal of Remote Sensing* **25**(24): 5759-5770.

Selvam S, Magesh NS, Sivasubramanian P, Soundranayagam J P, Manimaran G and Seshunarayana T 2014. Deciphering of groundwater potential zones in Tuticorin, Tamil Nadu, using remote sensing and GIS techniques. *Journal of the Geological Sociey of India* **84**: 597-608.

Singh SK, Kanga S and Mishra SK 2017. Delineation of groundwater potential zone using geospatial techniques for Shimla city, Himachal Pradesh, India. *International Journal for Scientific Research and Development* **5**: 225-234.

Singh SK and Pandey AC 2014. Geomorphology and the controls of geohydrology on waterlogging in Gangetic Plains, North Bihar, India. *Environmental Earth Sciences* **71**(4): 1561-1579.

Srivastava PK and Bhattacharya AK 2006. Groundwater assessment through an integrated approach using remote

sensing, GIS and resistivity techniques: A case study from a hard rock terrain. *International Journal of Remote Sensing* **27**: 4599-4620.

Suryabhagavan KV 2017. Application of remote sensing and GIS for groundwater potential zones identification in Bata River Basin, Himachal Pradesh, India. *Journal of Geomatics* **11**: 66-76.

Received 20 July, 2021; Accepted 22 November, 2021

Indian Journal of Ecology (2021) 48(6): 1692-1697

Manuscript Number: 3433
NAAS Rating: 5.79

Bioindication Assessment of Drinking Water Toxicity in Large Cities of Ukraine

Svitlana Skok and Denys Breus

Kherson State Agrarian and Economic University, Ukraine, 73006, Kherson, Stritens'ka str. 23,
E-mail: skok_sv@ukr.net

Abstract: Intense anthropogenic impact on drinking water sources contributes to the load on aquifers, which leads to deterioration of groundwater quality. Modern practice of water economy proves that the use of traditional methods of assessing the ecological status of waters does not fully reflect the real state of the biological properties of drinking water. In present study modern method of biotesting using test organisms was proposed and proved efficiency for assessing the quality of drinking water. Bioassays are toxic, mutagenic and carcinogenic properties of the aquatic environment, differentiating sources of drinking water in accordance with the requirements of water consumption. Comprehensive toxic and environmental assessment of drinking water was calculated as an average arithmetic toxicity index, determined by daphnia and onions. The drinking water quality in the city of Kherson (Ukraine) was allocated 7 functional zones with different degrees of anthropogenic load. According to the analysis it was observed that inadequate quality drinking water was observed at the industrial zone, toxic properties drinking water at residential area of multi-storey, individual buildings and transport load area and the best drinking water were in residential area of mixed development and residential area of multi-storey buildings with a local water supply system. Use of ecological and toxicological test objects in bioindication system with various levels of organization allowed assessing the ecological status of underground sources water in accordance with the requirements of drinking water supply. According to the bioindication classification, drinking water pollution scale determined an extremely high degree of anthropogenic load within the historic center test site.

Keywords: Drinking water quality, Groundwater, Test sites, Biotesting

In the context of intensive development of society, the problem of providing quality drinking water is one of the main environmental and socio-economic issues of sustainable development around the world. High-quality water supply is complicated by the uneven distribution of water resources on the continental parts of the globe, their intensive pollution by wastewater from agriculture (Pichura et al 2015, Zelenskaya et al 2018), industry and the utilities sector (Breus et al 2018, Breus et al 2019). Water scarcity is observed in 30% of North and South America, 33% in Europe, 60% in Asia, and 99% in Australia and Africa (Stadnyk 2010).In most residential areas of the world, the main source of drinking water supply is surface water, which due to intense anthropogenic impact does not meet the established quality requirements (Pichura et al 2020a, Haroon et al 2021). In this regard, to improve the quality of water, groundwater is used (by 2/3 of Europe's population), which is more protected from external negative influences and is characterized by a stable chemical composition. However, the main feature of their use for the purposes of the national economy is low development: only 8% of the projected groundwater reserves and 13% of the approved operational. The number of these reserves decreases every year due to the violation of their production regimes, which leads to depletion and pollution of aquifers, the restoration of which to its natural state is work-consuming and time-consuming. Given the intense anthropogenic pressure on all components of the environment and global climate change, issues related to environmental protection, including the provision of quality drinking water to the population have been raised in international forums, such as Aqua Ukraine, The United Nations Environmental Forum, Indo-European Water Forum in New Delhi etc., And for most countries of the world this problem has become one of the main priorities of public health policy to achieve their sustainable development (Pichura et al 2020b, Ondieki et al 2021). For high-quality water supply, there is a growing need to use an improved system for assessing the toxic and ecological status of drinking water using bioindication methods based on the specific response of test organisms to the content of toxic substances in the aquatic environment. For a long time, bioindication methods were used only to determine the quality of natural and wastewater, but with the adoption of European and national standards for human health protection from adverse effects of water pollution, the need for their use in assessing groundwater quality (Manickavasagam 2019, Larionova et al 2017). The aim of the article is to study the quality of drinking water and determine its toxicity using the method of bioindication assessment on the example of the city of Kherson (Ukraine).

MATERIAL AND METHODS

Studies of the toxicity of drinking water from underground sources in the city of Kherson (Ukraine) were conducted by biotesting using Daphnia *Magna straus* and onion *Allium cepa* L. (Vergolyas 2016). Drinking water samples were taken according to DSTU ISO 5667-11: 2005. Water sampling points for research were carried out in areas of the city that differ in relief, hydrological regime of underground layers, the level of destruction of the territory and depending on the depth of wells at different test sites (Fig. 1).

I test site - residential area of multi-storey buildings;

II test site - industrial zone;

III test site - residential area of mixed development;

IV test site - transport load area;

V test site - the area of the historic center;

VI test site - a residential area of multi-storey buildings with a local water supply system;

VII test site - a residential area of individual buildings.

To establish a toxico-ecological assessment of drinking water using daphnia, 8 water samples were taken from each landfill. In a container of water was placed 10 daphnia, the experiment was repeated three times. The number of live individuals was recorded after 24, 36, 48, 72, 92 hours. The criterion for the toxicity of drinking water was the number of dead daphnia in relation to the control.

For each investigated landfill and drinking water sampling site, the toxicity index was calculated according to the following formula:

$I = 100 (I_1 – I_0)/I_1$

I_1-I_0 - the number of live daphnia in the control and experiment at a fixed time of exposure to the test sample of drinking water with the test object.

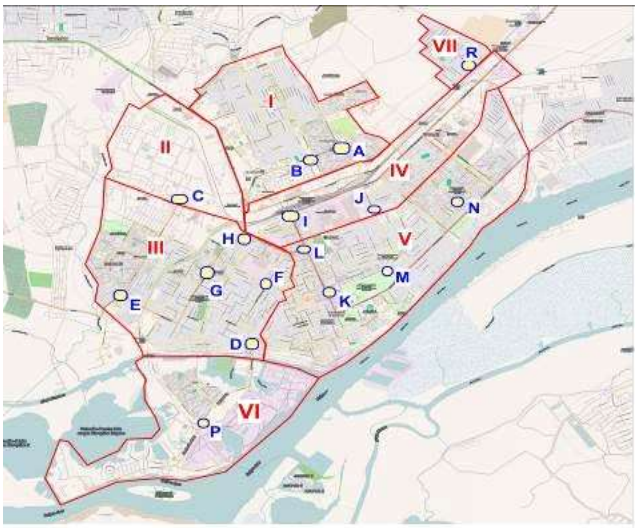

Fig. 1. Map-scheme of spatial distribution of test sites in Kherson

When conducting experiments to determine the toxicity of selected samples of drinking water, all exposure factors were unchanged. The following levels of drinking water toxicity were taken into account:

It <20 - the allowable degree of toxicity;

It = 21 - 50 - toxic water;

It> 51 - highly toxic water.

Water classes were determined according to the gradation scale of toxicity and bioindication classification of the level of drinking water pollution (Table 1).

Statistical analysis of the study results was to establish correlations between the time of toxic effects of drinking water and the survival of daphnia. For the reliability of the results of the study to determine the integrated toxicity of drinking water on the studied landfills, onions were used. For this the bulb was placed in a test tube with water. The number of test tubes with bulbs was 45 pieces, 5 pieces for each test sample of drinking water, taking into account the control sample. After 96 hours, measurements of the average length and number of roots in onion bunches were performed for each variant of the experiment. The criterion for drinking water toxicity was inhibition of onion root growth compared to control.

The comprehensive toxic-environmental assessment of drinking water was calculated as the arithmetic mean of the toxicity index, for the two selected test items. When conducting experiments to determine the toxicity of selected drinking water samples, all abiotic factors of possible influence on biotesting were unchanged.

RESULTS AND DISCUSSION

The main source of drinking water supply in the city of Kherson (Ukraine) is the groundwater of the Upper Sarmatian aquifer at a depth of 80-100 m. Their formation in the urban area is under the influence of natural and anthropogenic factors. Natural factors influencing the quality composition of groundwater in the urban area of Kherson (Ukraine) are the infiltration of precipitation and surface water within the Dnieper River basin, the inflow of groundwater from the Ukrainian Crystal Shield. However, in the conditions

Table 1. Bioindication classification scale for assessing water sources by pollution classes

Water quality class	Characteristics of the level of pollution
I	Weak
II	Moderate
III	High
IV	Highly dangerous
V	Dangerous

of unbalanced land use in the southern regions of Ukraine, irrational use of water resources in all spheres of the economy, the main factors influencing the quality of groundwater are anthropogenic (Breus et al 2020, Breus et al 2021). At the same time, the quality of drinking water becomes a limiting factor that affects the health of the population. The progressive growth of the level of anthropogenic pressure on the aquatic environment, the systematic inflow of pollutants into water supply sources, requires a rapid assessment of the ecological condition of water sources with low time consumption and little financial resources. In this regard, the suitability of water from underground sources for drinking purposes, determining the level of their toxicity within the urban system of the city of Kherson (Ukraine) was carried out on the basis of biotesting using invertebrates and plant bioassays. Biological testing was performed for three days, which allowed determining the level of acute toxicity of drinking water. During the experiment, the assessment of drinking water toxicity was performed on the basis of recording the number of live daphnia (Table 2).

Samples of drinking water of the VII test site in terms of survival of daphnia were 80%, and the level of toxicity of drinking water is acceptable. No significant morphological changes in the body were observed in dead individuals. Live daphnia actively moved in the water column during the entire exposure of the test. The amount of daphnia in drinking water samples of the III test site at the end of the experiment was 70%. The bodies of the dead were light. After 96 hours, the appearance of new daphnia was observed, which indicated the presence of phytoestrogens in drinking water samples, which determined the fertility of females. According to the toxicity index, water is assessed as toxic. The magnitude of the deviation of daphnia survival in all test samples of drinking water from the control sample was different for all studied landfills. .According to the biotesting, it was observed that the average time of death of 50% daphnia in test water samples at the V test site was 40 hours, II test site - 65 hours, IV test site - 85 hours. Therefore, according to the calculations of the toxicity index and reactions of daphnia to the content of pollutants in drinking water, low drinking water quality was observed at the II and V test sites. The biotesting of drinking water using the test object of daphnia, the intra-territorial zoning of the studied urban system was carried out (Fig. 2). It is proved that with increasing testing time the number of live daphnia decreases in all studied samples of drinking water. The rate of variation in mortality of test individuals is equal to 92% and depends on the time of toxic action of drinking water. Bioindication assessment of drinking water quality using daphnia allows to establish the level of toxicity of waters with different content of pollutants. However, the reliability of the result of such biotesting is only 35%. The single bioassay is not a universal and unified method in assessing the suitability of water in accordance with the requirements of drinking water supply. Therefore, it was expedient to establish a reliable assessment of the state of drinking water in Kherson (Ukraine) by means of biotesting using onions *Allium cepa* L (Table 3). According to the testing of drinking water using the test object *Allium cepa* L., was observed that the highest index of drinking water toxicity at the I test site. Germination of onion roots in all tested water samples throughout the experiment had inhibited growth. The length of onions in drinking water at the V test site had low values relative to the control sample. Only one sample out of five had a clear germination of onion roots. Drinking water is rated as highly toxic.

Progressive germination of onion roots was observed in the tested samples of drinking water at the VI test site, and green shoots appeared on the first day of the experiment. According to the toxicity index, water is toxic in the samples of

Table 2. Assessment of the level of drinking water toxicity by daphnia

Test site	Arithmetic mean survival rates of daphnia, hours							I_t	Level of toxicity
	1	6	24	36	48	72	96		
I test site residential area - multi-storey buildings	10	10	10	10	9	9	9	10	Permissible degree of toxicity
II test site - industrial zone	9	9	6	5	4	4	3	70	Strongly toxic
III test site - residential area mixed development	10	9	9	9	8	8	7	30	Toxic
IV test site – transport loaded area	10	10	10	9	9	7	6	40	Toxic
V test site - area of the historic center	9	8	8	3	3	3	1	90	Highly Toxic
VI test site - industrial zone with local water supply system	10	10	9	9	9	9	9	10	Permissible degree of toxicity
VII test site - area of individual construction	10	10	9	8	8	8	8	20	Permissible degree of toxicity
Control sample	10	10	10	10	10	10	10	0	Non-Toxic

the IV test site, inhibition of root growth of the test object was observed. One in five had the growth of green shoots. Three test samples of drinking water had the same root germination, but they had a tortuous shape. In this test site, the toxicity index of drinking water ranges from 20-50, so the water is rated from toxic to highly toxic. Three test drinking samples at the III test site had a clear and uniform germination of onion roots. Germination of green shoots was observed in four samples. Water from underground sources of this landfill according to the results of biotesting on onions is high quality.

Slow and inhomogeneous germination of onion roots was observed in drinking water samples of the II test site. One sample showed the germination of green shoots 2.5 cm long. According to the toxicity index, drinking water was assessed as toxic. In VII test site, four samples of onions had a clear germination of roots. The appearance of green shoots with a length of 9, 5, 9, 8, 6 (cm) was observed. The obtained value of the length of the onion roots is close to the control sample of drinking water. Water is rated on the toxicity index as non-toxic. Homogeneous and clear root germination was noted in the control sample. In four samples there was growth of the green shoots, 7 cm long, and 5 pieces. Drinking water is of excellent quality. According to the results of the study, the intra-territorial zoning of the studied urban area according to the index of drinking water toxicity was carried out (Fig. 3).

The ambiguity of the obtained results of drinking water quality assessment by the values of daphnia survival and germination of onion roots showed that living organisms, depending on the level of their organization, react differently to the content of pollutants in drinking water. Therefore, when establishing an integrated environmental assessment of drinking water, the reactions of various test objects are comprehensively taken into account (Table 4). The low-quality drinking water was observed at I, IV, V test sites, toxic properties were characterized by drinking water at II, VII test sites, quality drinking water by biotesting - at III and VI test sites. Based on the test results using both biological indicators, the zoning system of the city of Kherson (Ukraine) was zoned according to the generalized index of drinking water toxicity. The account of the basic features of adaptation processes, level of sensitivity, and resistance of test organisms at carrying out biotesting should be carried out taking into account the established terms and time of testing.

At the same time there is an expediency of carrying out the general assessment of toxicity of waters on the content of pollutants. In this case, taking into account the changes in the

Table 3. Biotesting of drinking water in Kherson (Ukraine) by test object *Allium cepa L.*

Test Site	The total number of roots, pcs.	Average length of roots, cm (M)	Relation to control (%)	Toxic index I_t
I test site - residential area multi-storey buildings	40	0,36	14	85,6
II test site - industrial zone	57	1,70	68	32,0
III test site - residential area- mixed development	77	2,20	88	12,0
IV test site - transport loaded area	38	1,20	48	52,0
	78	2,00	8	20,0
V test site - historic center area	41	0,66	26	73,6
VI test site - an industrial zone with a local water supply system	124	2,40	96	4,0
VII test site - a zone of individual construction	92	1,90	76	24,0
Control Sample	72	2,50	-	0

Table 4. Comprehensive toxic and ecological assessment of drinking water in Kherson (Ukraine)

Test site	I_t (by *Daphnia magna straus*)	I_t (by *Allium cepa L.)*	I_t (Average)	Toxico-ecological assessment of drinking water
I test site – a residential area of multi-storey buildings	10	85	48	Toxic
II test site – industrial zone	70	32	51	Highly Toxic
III test site – residential area of mixed development	30	4	17	Non-Toxic
IV test site – transport loaded area	60	20	40	Toxic
V test site – historic center area	90	73	80	Highly Toxic
VI test site – an industrial zone with a local water supply system	10	4	7	Non-Toxic
VII test site – a zone of individual construction	20	24	22	Toxic
Control Sample	0	0	0	Non-Toxic

Table 5. Bioindication classification scale for assessing water sources by pollution classes

Test site	Toxicity Index, I_t	Toxicity rating	Water quality class	Characteristics of the level of pollution
Residential area with multi-storey buildings	48	Toxic	III	High
Industrial area	51	Highly Toxic	III	High
Residential area with mixed buildings	17	Non-Toxic	I	Weak
Transport loaded area	40	Toxic	II	Moderate
City area and historical center	80	Highly Toxic	IV	Highly dangerous
Industrial zone with local water supply system	7	Non-toxic	I	Weak
Residential area with a standalone buildings	22	Toxic	II	Moderate

reaction of daphnia and onions in drinking water samples, the level of toxicity of drinking water at certain territorial landfills was determined. Due to the use of several test objects in the bioindication system for determining the quality of drinking water, the issue of developing a single scale for biological assessment of aquatic toxicity is relevant. According to the gradation scale of toxicity and drinking water quality classes, the level of drinking water pollution was set for each test site (Table 5).

The variability of toxic-ecological assessment according to the reactions of test organisms, bioindication differentiation of pollution level was established, which characterizes the ecological state of groundwater sources and their compliance with the established requirements for household and drinking needs. Thus, the transport load zone (IV test site) is a transitional zone between moderate and high levels of drinking water pollution. While drinking water taken from the residential area of individual buildings (VII test site) is in the range of pollution from moderate to weak. Extremely dangerous level of pollution is characteristic of the functional zone of the city and historical center (V test site). Intensive anthropogenic pressure on the territory, location of administrative institutions, the presence of dense multi-storey buildings, and the development of transport infrastructure led to unsatisfactory environmental conditions, which create conditions for the formation of poor-quality drinking water of the test site. Bioindication assessment of drinking water allows us to determine the consequences of systematic and volley pollution of water sources by the reaction of test objects of the average "pollution effect" over time. In addition, biological methods provide an assessment of the intensity of the processes of self-healing of groundwater after the action of the pollutant.

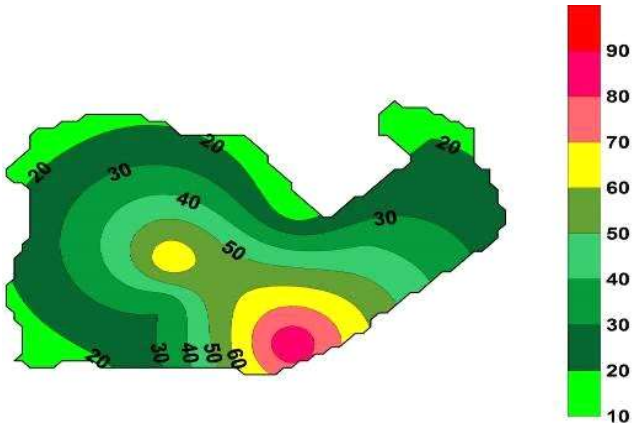

Fig. 2. Zoning of the urban system of the city of Kherson (Ukraine) according to the toxicity index (test object Daphnia magna straus)

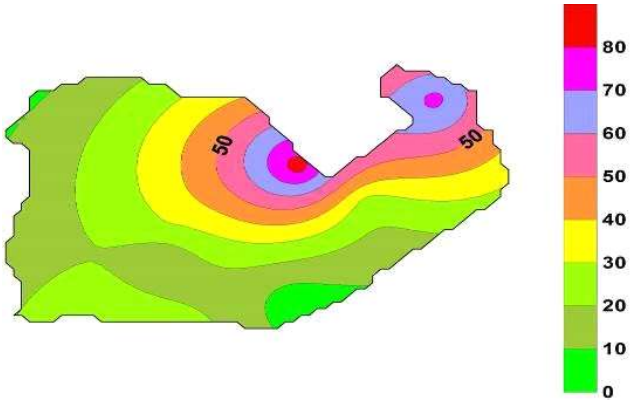

Fig. 3. Zoning of the urban system of the city of Kherson (Ukraine) according to the index of drinking water toxicity (test object *Allium cepa* L)

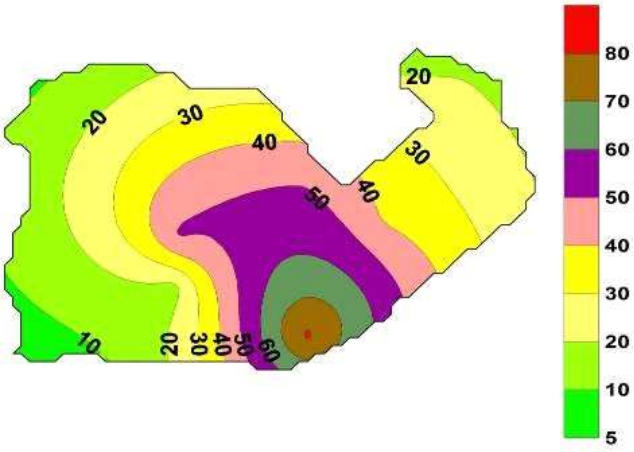

Fig. 4. Zoning of the urban system of the city of Kherson (Ukraine) according to the generalized index of drinking water toxicity

CONCLUSIONS

The biotesting is a fast and reliable method of assessing the quality of drinking water, which should be used for systematic environmental control over the quality of water supply sources. Assessment of drinking water toxicity was made based on morphological changes, survival rates of daphnia and biometric indicators of germinated onions. It was established that low-quality drinking water was present at II, V test sites, toxic properties of drinking water at I, IV, VII test sites, quality drinking water according to the results of biotesting was found - at III and VI test sites.The general index of drinking water toxicity for all studied test sites was calculated, according to which the intra-territorial zoning of the studied urban area was carried out. According to the conducted ecotoxicological and bioindication assessment of the state of drinking water sources, the level of drinking water pollution was determined at all test sites in the city of Kherson (Ukraine). The use of bioindication research will contribute to the development of scientifically sound measures to improve the quality of drinking water within the studied urban area.

REFERENCES

Breus DS, Dudyaeva OA, Evtushenko OT and Skok SV 2018. Organic agriculture as a component of the sustainable development of the kheson region (Ukraine), pp. 691-697. **In**: L. Lavrysen, Jurgen H. Breuste and Krassi Rumchev (eds), Proceedings of *18th International Multidisciplinary Scientific GeoConference SGEM 2018*, July 2-8, 2018, Albena, Bulgaria.

Breus DS and Skok SV 2021. Spatial modelling of agro-ecological condition of soils in steppe zone of Ukraine. *Indian Journal of Ecology* **48**(3): 627-633.

Breus DS, Yevtushenko OT, Skok SV and Rutta OV 2019. Retrospective studies of soil fertility change on the example of the Kherson region (Ukraine), pp. 645-652. **In**: Valeriy Bondur, Raimonds Ernsteins and Viktor Savinuh (eds), Proceedings of *19th International Multidisciplinary Scientific GeoConference SGEM 2019*, June 30-July 6, 2018, Albena, Bulgaria.

Breus DS, Yevtushenko OT, Skok SV and Rutta OV 2020. Method of forecasting the agro-ecological state of soils on the example of the South of Ukraine, pp. 523-528. **In**: Ojaris Sparitis, Valeriy Bondur and Mirko Orlic (eds), Proceedings of *20th International Multidisciplinary Scientific GeoConference SGEM 2020*, August 18-24, 2020, Albena, Bulgaria.

Haroon R Mian, Guangji Hu, Kasun Hewage, Manuel J Rodriguez and Rehan Sadiq 2021. Drinking water quality assessment in distribution networks: A water footprint approach. *Science of The Total Environment* **775**: 145844.

Larionova NV, Lukashenko SN, Lyakhova ON, Aidarkhanov AO, Subbotin SB and Yankauskas AB 2017. Plants as indicators of tritium concentration in ground water at the Semipalatinsk test site. *Journal of Environmental Radioactivity* **177:** 218-224.

Manickavasagam S, Sudhan C, Bharathi and Aanand S 2019. Bioindicators in aquatic environment and their significance. *Journal of Aquaculture in the Tropics* **34**(1/2): 73-79.

Ondieki JK, Akunga DN, Warutere PN, Omanga Kenyanya 2021. Bacteriological and physico-chemical quality of household drinking water in Kisii Town, Kisii County, Kenya. *Heliyon* **7**(5): e06937

Pichura VI, Pilipenko Yu V, Lisetskiy FN and Dovbysh OE 2015. Forecasting of Hydrochemichal Regime of the Lower Dnieper Section using Neurotechnologies. *Hydrobiological Journal* **51**(3): 100-110.

Pichura V, Potravka L, Skok S and Vdovenko N 2020a. Causal regularities of effect of urban systems on condition of hydro ecosystem of Dnieper river. *Indian Journal of Ecology* **47**(2): 273-280.

Pichura VI, Potravka LA, Skrypchuk PM and Stratichuk NV 2020b. Anthropogenic and climatic causality of changes in the hydrological regime of the Dnieper River. *Journal of Ecological Engineering* **21**(4): 1-10.

Stadnyk ME 2010. Freshwater safety: essence, threats and ways to overcome them. *Scientific Bulletin of Lviv State Department of Internal Affairs* **2**: 145-155 (in Ukrainian).

Vergolyas M R 2016. Ecotoxicological assessment of drinking water quality on test organisms. *Sciences of Europe* **8**(8): 4-8.

Zelenskaya E, Pichura V and Domaratsky Y 2018. Priorities of agroecological monitoring of the composition of soil trace elements taking into account the peculiarities of its formation over time. *Journal of Engineering and Applied Sciences* **13**: 5807-5813.

Received 07 July, 2021; Accepted 10 November, 2021

Indian Journal of Ecology (2021) 48(6): 1698-1704

Manuscript Number: 3434
NAAS Rating: 5.79

Impact Assessment of Invasive Alien Plants on Soil Organic Carbon (SOC) Status in Disturbed and Moderately Disturbed Patches of Hailakandi District in an Indo Burma Hotspot Region

Zingthoi Khuppi Sakachep and Prabhat Kumar Rai*

Department of Environmental Science
Mizoram University, (A Central University), Aizawl, Mizoram-796 004, India
**E-mail: pkraimzu@gmail.com*

***Abstract*:** Invasive alien plants introduced in novel ecosystem either accidentally or intentionally can perturb the diversity of native plants and concomitantly influence the soil nutrient dynamics. The present study aimed to investigate the impact of the invasive alien plants (IAPs) on the native vegetation diversity and the soil in forestry/agro-forestry ecosystems of Hailakandi District, Assam. This region is of extreme ecological relevance as it underlies in an Indo Burma hotspot region. In this study, an ecological investigation is performed along disturbance gradient to emphasise the plant-plant and plant-soil interrelationship. A total of 68 plant species were recorded in vegetation analysis during the ecological assessment of IAPs. The similarity index in herbs and the shrubs layer were 0.56 and 0.46, respectively. Meanwhile in soil analysis, the soil organic carbon (SOC) and the soil organic matter (SOM) were noted higher in the moderately disturbed site, when compared with the disturbed site. The study further observed that land use change significantly influences and plays a crucial role for the landscape spread of IAPs. Also, they alter native vegetation composition and cause depletion in SOC and SOM. This plant invasion ecology studies therefore predicted that land use changes increased pressure on the natural ecosystems, especially during the monsoon season.

Keywords: Invasive alien plants, Plant-plant interactions, Plant- soil interactions, Indo-Burma hotspot, Land use change

In current Anthropocene era, biological invasion is among most severe ecological threat and widely considered as key challenge for biodiversity conservation. In Indian biodiversity perspective, 40% of flora is identified as aliens (Rai 2012, Iyer et al 2019). Invasive alien plants (IAPs) are well adapted to diverse ecosystem due to the fast growth, adapted life cycle events, hardiness, and quick rates of reproduction (Sekar 2012, Kopelson 2014, Rai and Singh 2021). Their landscape spread is particularly devastating to forest ecosystem by forming a dense monoculture ground cover, thereby, suppressive to native and endemic forestry/agro-forestry vegetation (Zhang et al 2019).

Indian subcontinent with four global biodiversity hotspots is rich and importantly among these three i.e., the Western Ghats, Himalayas, and the Indo-Burma importantly accounts for 11% of the world's plant diversity (Rai 2015, Iyer et al 2019). In this aspect, Indo-Burma hotspot is comprised with rich diversity of ethno-medicinal plants linked with human health (Rai and Lalramnghinghlova 2011a, b). The impact of the IAPs are not only limited to the habitat destruction of native plants. Rather, their adverse effects extend to soil process (Ehrenfeld 2003, Rai 2021), as IAPs trigger the changes in biogeochemical cycling and soil nutrient dynamics (Rai 2013, Bjeckner et al 2007, Rai and Singh 2020). Interestingly, these alterations in soil attributes can vary across different seasons. In this respect, the effects of IAPs on Soil Carbon (SC) storage and sequestration are of major concern (Peltzer et al 2010) as soils are the largest terrestrial organic carbon pool (Rai 2009, Craig et al 2015). In this aspect, widespread changes in atmospheric carbon dioxide (CO_2) concentrations induced due to the plants invasions could have important climate change implications (Rai 2018, Rai and Singh 2020). The plants diversity and or the distribution may lead to changes in the soil C and due to which the Net Primary Productivity (NPP) also get affected (Raizada et al 2008). The fragmentation of forest ecosystem due to IAPs impacts the soil C-content by influencing the NPP in the invaded areas (Williamson and Fitter 1996, Raizada et al 2008).

Anthropogenic disturbances can remarkably exacerbate the problem of IAPs spread. For example, Honnay et al (1999) determined that the forest disturbances boost the IAPs diversity. Likewise, the age old traditional practice of unregulated shifting cultivation can also perturb the soil quality and environmental sustainability (Rai 2009, 2017). Therefore, the human interferences play the vital role in conversion of intact forest ecosystem into disturbed fragmented ecosystem, thereby making the site ripe for the arrival of IAPs. In this sense, Mukaromah and Imron (2018) concluded that there is luxuriant growth of the IAPs at the

disturbed sites when compared with undisturbed sites. The dominance of IAPs over the native plants is ascribed to their aggressive nature, quick multiplication than native plants and as a result of which they cover an extensive area with-in a short period of time (Rai and Singh 2020a, Ruati and Rai 2021).

Plants invasion transform the habitat and alters the surface soil physical-chemical attributes (Lone et al 2019) due to the modification of various biogeochemical cycling pattern in soil (Jordan et al 2011). Hailakandi district of Assam borders the state of Mizoram and is an integral component of Indo-Burma global biodiversity hotspot. Nevertheless, IAPs of this ecologically sensitive site is scantily documented, especially in relation to their impacts on soil attributes. Further by the increased infestation of IAPs, depletion of native biodiversity thereby, influences the SOC and the SOM. Since our previous ecological investigation on IAPs-native plant interactions of this region revealed remarkable impacts on vegetation indices (Sakachep and Rai 2021), therefore, the present work aims to study the changes in SOC and SOM to expand the horizon of invasion biology of this biodiversity rich region.

MATERIAL AND METHODS

Hailakandi district is situated in the southern part of Assam. It lies between 24° 22/ N and 25°8 /N Latitude and 92°24/ E and 93°15/ E Longitude and at the elevation of 21meter of the state. The geographical area of the district is 1327 km².

Important Value Index (IVI): The vegetative analysis is done by random quadrat method at the study sites and each plant species have been identified and IVI been calculated (Misra 1968).

IVI = Relative density + Relative frequency + Relative abundance

To study the similarity between the two communities Sorenson similarity index was used (Sorensen 1948)

$$\beta = \frac{2c}{S_1 + S_2}$$

Where, S_1= number of species in community 1, S_2= number of species in community 2 and c = number of species common to both communities.

Soil analysis: Soil sample was collected from August, 2016 to April, 2018 at seasonal interval (Monsoon, Post-monsoon and Pre-monsoon). The air-dried and fine sieved soil samples (0.2mm size fractions) were used for the analysis of SOC and SOM by using the method of Walkley and Black (1934).

Statistical analysis*:* The statistical analyses were performed by using SPSS (16.0.) and MS excel.

RESULTS AND DISCUSSION

From the phyto-sociological study 68 species from 53 genera and 30 families were recorded. Sorenson similarity index in the disturbed and moderately disturbed sites recorded are 0.58 and 0.46 in herbs and shrubs layers, respectively (Fig. 1 and 2). Asteraceae family members (*C. odorata* and *M. micrantha*) native to the Tropical America were reported asdominant IAPs at both the sampling sites. In this context, Nath et al (2019) reported that Manas National Park (MNP), about 15-20% of the park area and more than 30% of grassland is under the threat of *C. odorata* and *M. micrantha.* In present study, IVI value for *M. micrantha* at disturbed site was noted 23.17. While in moderately disturbed site a relatively lower IVI (18.68) value when compared with the disturbed site (Fig.2). In the ecological perspective, the IVI index reflected the plant distributions at the selected sites. Interestingly, *M. micrantha* was observed to grow well in diverse habitats in present study, ranging from the roadsides to the edges of forests, followed by *Ageratum conyzoides, Parthenium hysterophorus, Euphorbia hirta* and other in herbs layer. This distribution pattern of IAP was in corroboration with the other study performed by Maja et al (2008).Global researches also listed *M. micrantha* as one of

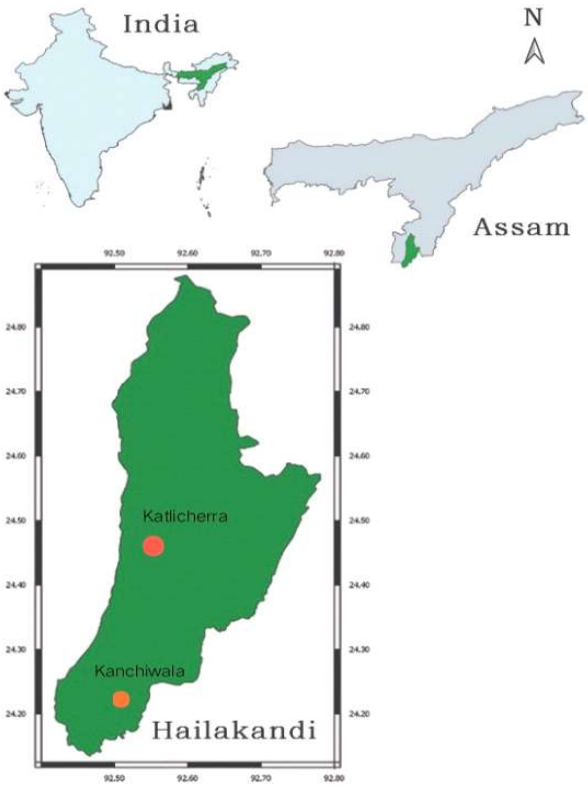

Fig. 1. Location map of study sites: Katlicherra (Disturbed) and Kanchiwala (Moderately Disturbed)

the top 100 global invaders (Lowe et al 2000) expanding its range in Indian subcontinent, especially in NE India (Iyer et al 2019).

Chromolaena odorata was recorded at the disturbed site (IVI= 69.42) and the moderately disturbed site (IVI= 19.83). It has already been evidenced that *C. odorata* reduces the diversity of native plants by forming a thick covers (Sapkota 2007, Awanyo et al 2011) and by acting as stronger competitors with better resource (nutrient) use efficiency in the non-native range (Qin et al 2013). Likewise, *C. odorata* was observed as one of the severe IAP in the Manas National Park, with co-dominance of *Lantana camara, Urena lobata* and *Melatoma malabathrium* (Lahkar et al 2011). The natural forest is not usually invaded, but forest degradation allows the weed like IAPs to establish by suppressing the recruitment of tress (Mandal and Joshi 2014). Nevertheless due to the land use changes and the human interference includes degradation of natural resources, shifting cultivation etc in the district. Dattagupta and Gupta (2013) observed that due to the human interference there is a continued degradation in natural forest in Cachar district.

Secondly, IAPs have rapid uptake capacity of more efficiently in low available resources environment then the native plants (Funk and Vitousek 2007). In the disturbed soil IAPs thrive in the short period of time due to the aggressive nature and it inhibits the growth of the native plants. Thus, for the future aspect the conversion of the forest land needs to be controlled to overcome from the risk of plant invasion (Zhuo et al 2020). In relation to seasonal variations in soil attributes due to plant invasion at disturbed site, the present study reported that SOC in different seasons were 0.65±0.05%, 0.96±0.06%, and 1.26±0.04% during monsoon, post monsoon and pre monsoon seasons, respectively. These seasonal trends in SOC were noted in the surface layer (0-15cm). However, the sub layers (15-30cm) were noted with SOC values of 0.53±0.02%, 0.82±0.05%, and 1.15±0.03% during monsoon, post monsoon and pre monsoon season, respectively. In the year 2017-2018 the lowest SOC and the SOM were recorded during monsoon season 0.61±0.08% and 1.05±0.14% in the soil surface layer. Sakachep and Rai (2019) demonstrated that the nutrient runoff, especially during monsoon season ascribed to heavy rainfall and soil erosion.

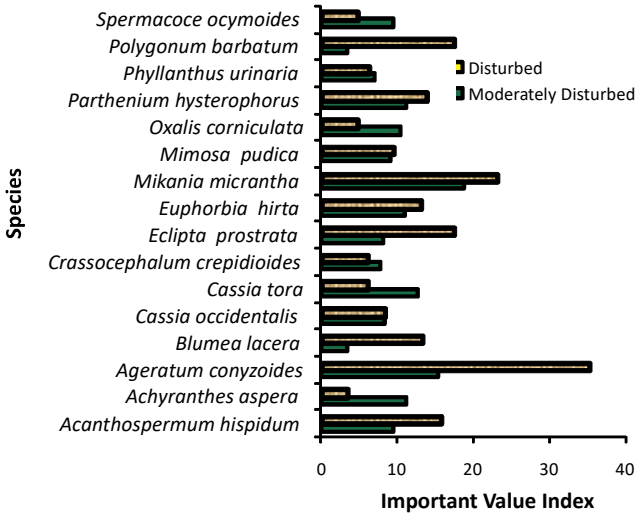

Fig. 2. IVI of some common species in herbaceous layer between disturbed and moderately disturbed patches of Hailakandi district, Assam

Table 1. ANOVA of SOC and SOM for the effect of sites in the study site. (df= Degree of freedom, F= Fisher's statistic value)

Parameters		Sum of Squares	Df	Mean Square	F	Sig.
Soil organic carbon	Between groups	5.203	1	5.203	72.818	.000
	Within groups	5.001	70	.071		
	Total	10.204	71			
Soil organic matter	Between groups	15.478	1	15.478	72.838	.000
	Within groups	14.875	70	.212		
	Total	30.352	71			

Table 2. ANOVA of SOC and SOM for the effect of season in the study site

Parameters		Sum of Squares	df	Mean Square	F	Sig.
Soil organic carbon	Between groups	4.387	2	2.193	26.013	.000
	Within groups	5.818	69	.084		
	Total	10.204	71			
Soil organic matter	Between groups	13.051	2	6.526	26.026	.000
	Within groups	17.301	69	.251		
	Total	30.352	71			

While in moderately disturbed site (2016-2017) in the surface layer during monsoon, post monsoon and pre monsoon were 1.00±0.05%, 1.35±0.04% and 1.73±0.07%, respectively. The sub-surface the recorded values were 0.90±0.06%, 1.35±0.04% and 1.66±0.03%, respectively. In

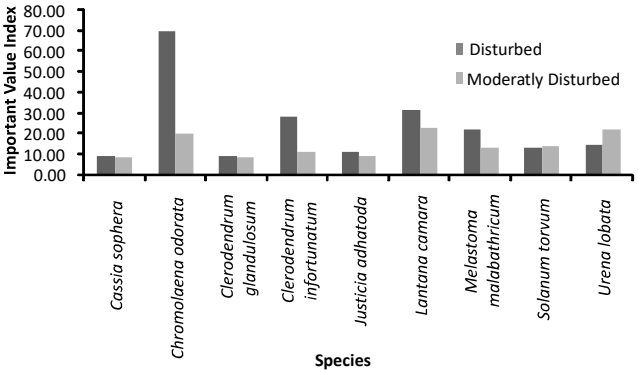

Fig. 3. IVI of some common species in shrubs layer between disturbed and moderately disturbed patches of Hailakandi district, Assam

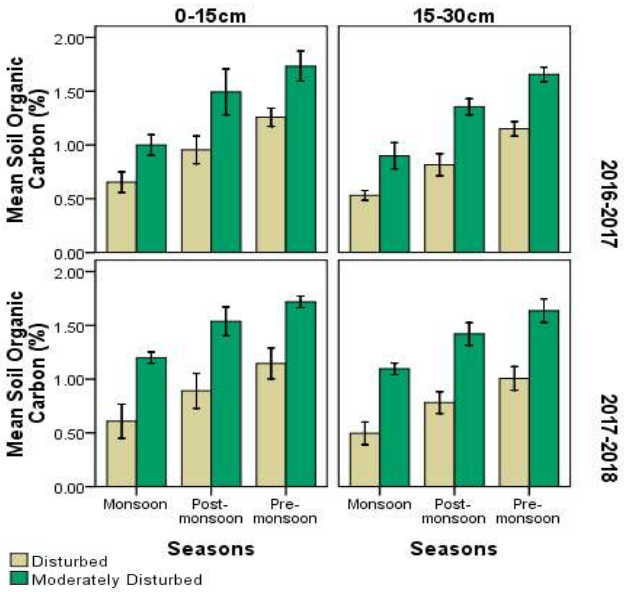

Fig. 4. SOC along with depths, seasons, years and sites by using mean ± standard deviation in Hailakandi District, Assam

Table 3. Descriptive summary of the SOC (%) in the study site

Sites	Years	Seasons	Depths	Mean	SD	CV	Min	Max
Disturbed (Katlicherra)	2016-2017	Monsoon	0-15cm	0.65	0.05	0.07	0.60	0.69
			15-30cm	0.53	0.02	0.04	0.51	0.55
		Post monsoon	0-15cm	0.96	0.06	0.07	0.88	1.00
			15-30cm	0.82	0.05	0.06	0.76	0.86
		Pre- monsoon	0-15cm	1.26	0.04	0.03	1.23	1.31
			15-30cm	1.15	0.03	0.03	1.11	1.18
	2017-2018	Monsoon	0-15cm	0.61	0.08	0.13	0.52	0.68
			15-30cm	0.50	0.05	0.11	0.44	0.55
		Post-monsoon	0-15cm	0.89	0.08	0.09	0.83	0.98
			15-30cm	0.78	0.05	0.06	0.73	0.83
		Pre-monsoon	0-15cm	1.15	0.07	0.06	1.09	1.23
			15-30cm	1.01	0.06	0.05	0.95	1.06
Moderately Disturbed (Kanchiwalal)	2016-2017	Monsoon	0-15cm	1.00	0.05	0.05	0.95	1.04
			15-30cm	0.90	0.06	0.07	0.85	0.97
		Post monsoon	0-15cm	1.49	0.11	0.07	1.42	1.62
			15-30cm	1.35	0.04	0.03	1.32	1.40
		Pre- monsoon	0-15cm	1.73	0.07	0.04	1.67	1.81
			15-30cm	1.66	0.03	0.02	1.63	1.69
	2017-2018	Monsoon	0-15cm	1.20	0.03	0.02	1.17	1.23
			15-30cm	1.10	0.03	0.02	1.07	1.12
		Post-monsoon	0-15cm	1.54	0.07	0.04	1.49	1.61
			15-30cm	1.42	0.05	0.04	1.36	1.46
		Pre-monsoon	0-15cm	1.72	0.03	0.02	1.69	1.75
			15-30cm	1.64	0.05	0.03	1.58	1.69

Table 4. Descriptive summary of the SOM (%) in the study site

Sites	Years	Seasons	Depths	Mean	SD	CV	Min	Max
Disturbed (Katlicherra)	2016-2017	Monsoon	0-15cm	1.13	0.08	0.07	1.03	1.19
			15-30cm	0.92	0.04	0.04	0.88	0.96
		Post monsoon	0-15cm	1.64	0.11	0.07	1.52	1.72
			15-30cm	1.41	0.09	0.06	1.31	1.48
		Pre- monsoon	0-15cm	2.17	0.07	0.03	2.11	2.25
			15-30cm	1.98	0.06	0.03	1.92	2.03
	2017-2018	Monsoon	0-15cm	1.05	0.14	0.13	0.90	1.17
			15-30cm	0.86	0.09	0.11	0.76	0.95
		Post-monsoon	0-15cm	1.54	0.14	0.09	1.43	1.70
			15-30cm	1.35	0.09	0.06	1.26	1.43
		Pre-monsoon	0-15cm	1.97	0.12	0.06	1.88	2.12
			15-30cm	1.74	0.10	0.05	1.64	1.83
Moderately Disturbed (Kanchiwala)	2016-2017	Monsoon	0-15cm	1.72	0.08	0.05	1.63	1.79
			15-30cm	1.55	0.11	0.07	1.47	1.67
		Post monsoon	0-15cm	2.57	0.18	0.07	2.45	2.79
			15-30cm	2.34	0.07	0.03	2.28	2.41
		Pre-Monsoon	0-15cm	2.99	0.11	0.04	2.89	3.11
			15-30cm	2.85	0.06	0.02	2.81	2.92
	2017-2018	Monsoon	0-15cm	2.07	0.04	0.02	2.02	2.11
			15-30cm	1.89	0.05	0.02	1.84	1.93
		Post-Monsoon	0-15cm	2.65	0.12	0.04	2.56	2.78
			15-30cm	2.45	0.09	0.04	2.35	2.52
		Pre-Monsoon	0-15cm	2.96	0.05	0.02	2.92	3.01
			15-30cm	2.82	0.09	0.03	2.73	2.92

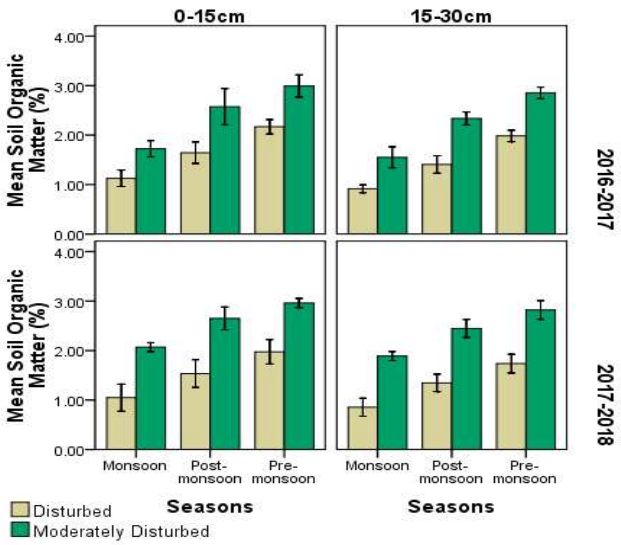

Fig. 5. SOM along with depths, seasons, years and sites by mean and standard deviation Hailakandi District, Assam

the year 2017-2018 the lowest SOC recorded were 1.20±0.03% and 1.10±0.03% in surface layer and sub-soil, respectively followed by post monsoon and pre-monsoon (Fig. 4, Table 3). While SOM value was noted highest 2.96±0.05% during pre-monsoon and lowest during monsoon 2.07±0.04%. The output of one way ANOVA analysis for SOC and SOM on the effect of sites, the significance value were<0.001 (i.e., p=<0.001) and F (1, 70)=72.818 and 72.838 respectively. Further the significance value of one way ANOVA for SOC and SOM on the effect of seasons were <0.001 and (2, 69)=26.013 and 26.026, respectively.

In the plant-soil interaction the diversity shrubs play vital role as compare to the herbaceous layer in a various cycling. Shrubs play very important role for the nutrient conservation (Mishra et al 2020). Wei et al (2017) determined that the SOC and the SOM decrease, possibly due the low Net Primary Production (NPP) and the high soil respiration losses.

CONCLUSION

Results of invasion ecology demonstrated that disturbed sites were dominated by few species such as *A. conyzoides, C. odorata, M. micrantha,* and *L. camara,* which resulted in depletion of species diversity. This depletion in species diversity was relatively low at moderately disturbed sites. Successful invasion of the IAPs like *C. Ododrata* and *L. Camara* were due to the availability of sufficient light at the disturbed site for the growth as the *C.odorata* and *L. Camara* can grow very well in the high intensity of light. Secondly, IAPs such as *M. micrantha* and *L. camara* grow well in diverse range of habitats and blocks the succession. The adverse impact on ecological succession results in the reduction of species richness through intense competition of resources like light and nutrients. Further, IAPs make the habitat quality, especially soil resource more favourable for itself. From the study it can further be concluded that the land use changes and the human interferences are prime factors driving the IAPs at the study site. The disturbance facilitated plant invasion which ultimately affects the SOC. Prior detection strategies and planning should need to be taken to manage IAPs in this Indo- Burma hotspot region to overcome from the IAPs.

ACKNOWLEDGEMENT

Authors are thankful to Mr.Tapan Deb, Divisional Forest Office, Hailakandi district, Assam, for providing necessary support and guidance for the identification of the plant species and National fellowship for ST for providing the financial support to complete the study. Dr. P.K. Rai thanks the financial assistance received from Department of Biotechnology (DBT) vide research project no.BT/PR24917/NER/95/907/2017 and Department of Science and Technology (DST) vide research project no.DST/TMD/EWO/WTI/2K19/EWFH/2019 C.

REFERENCES

Awanyo L, Attuah EM and McCarron M 2011. Rehabilitation of forest Savannas in Ghana: The impact of land use, shade and invasive species on tree recruitment. *Applied Geography* **31**(1): 181-190.

Craig ME, Pearson SM and Fraterrigo JM 2015. Grass invasion effects on forest soil carbon depend on landscape-level land use patterns. *Ecology* **96**(8): 2265-2279.

Bjerknes A, Totland O, Hegland SJ and Nielsen A 2007. Do alien plant invasions really affect pollinations success in native plant species? *Biological Conservation* **138**(12): 1-12.

Dattagupta S and Gupta A 2013. Traditional processing of timber forest production in Cachar, Assam, India. *Indian Journal of Traditional Knowledge* **13**(2): 427-433.

Ehrenfeld JG 2003. Effects of exotic plant invasions on soil nutrient cycling processes. *Ecosystems* **6**: 503-523.

Funk J and Vitousek PM 2007. Resources-use efficiency and plant invasion in low-resource systems. *Nature* **446**: 1079-1081.

Honnay O, Endels P, Vereecken H and Hermy M 1999. The role of the patch area and habitat diversity in explaining native plant species richness in disturbed sub urban forest patches in northern Belgium. *Diversity and Distributions* **5**(4): 129-141.

Iyer SG, Banerjee AK and Bhowmick AR 2019. Making choices that matter-use of statistical regularization in species distribution modelling for identification of climatic indicators: A case study with *Mikania micrantha* Kunth in India. *Ecological Indicators* **98**: 92-103.

Jordan NR, Larson DL and Huerd SC 2011. Evidence of qualitative differences between soil-occupancy effects of invasive vs. Native grassland plants species. *Invasive Plant Science and Management* **4**(1): 11-21.

Kopelson H 2014. The impacts of Invasive plant species on human health. *City Wild* **6**: 1-14

Lahkar BP, Talukdar BK and Sarma PK 2011. Invasive species in grassland habitat: an ecological threat to the greater one-horned rhino (*Rhinoceros unicornis*). *Pachyderm* **49**: 33-39.

Lone PA, Dar JA, Subashree K, Raha D, Pandey PK, Ray T and Khare PK 2019. The impact of plant invasion on physical, chemical and biological aspects of ecosystems: A review. *The Journal of the Society* for *Tropical Plant Research* **6**(3): 528-544.

Lowe S, Browne M, Boudjelas S and De Pooter M 2000. *100 of the World's Worst Invasive Alien Species: A selection from the Global Invasive Species Database*. Available athttps://www.iucn.org/content/100-worlds-worst-invasive-alien-species-a-selection-global-invasive-species-database. Accessed 10th January, 2021.

Maja W, Zerbe S and Kuo Y 2008. Distribution and ecological range of alien plants species *Mikania micrantha* Kunth (Asteraceae) in Taiwan. *Journal of Ecology and Field Biology* **31**(4): 277-290.

Mandal G and Joshi SP 2014. Invasion establishment and habitat suitability of *Chromolaena odorata* (L.) King and Robinson over time and space in the western Himalayan forest of India. *Journal of Asian-Pacific Biodiversity* **7**(4): 391-400.

Mishra V, Yadav AS and Mathur R 2020. Leaf nutrient dynamics of shrubs in a tropical dry deciduous forest in Rajasthan in North-West India. *Tropical Ecology* **61**: 196-202.

Misra B 1968. *Ecological Work Book.* New Delhi, India: Oxford and IBN, pp.31-51.

Mukaromah L and Imron MA 2020. Invasive plant species in the disturbed forest of Batukahu Nature reserve, Bali, Indonesia. *Biotropia* **27**(1): 22-23.

Nath A, Sinha A, Lahkar BP and Brahma N 2019. In search of aliens: Factors influencing the distribution of *Chromolaena odorata* L. and *Mikania micrantha* Kunth in the Terai grasslands of Manas National Park, India. *Ecological Engineering* **131**: 16-26.

Peltzer DA, Allen RB, Lovett GM, Whitehead D and Wardle DA 2010. Effects of biological invasions on forest carbon sequestration. *Global Change Biology* **16**: 732-746.

Qin RM, Zheng YL, Valiente-Banuet A, Callaway RM, Barclay GF, Pereyra CS and Feng YL 2013. The evolution of increased competitive ability, innate competitive advantages, and novel biochemical weapons act in concert for tropical invader. *New Phytologist* **197**(3): 979-988.

Rai PK 2018. *Phytoremediation of emerging contaminants in wetlands.* CRC Press Taylor and Francis Group, Boca Rotan, London, New York.

Rai PK 2017. Ethnoagriculture in North East India: Pros, Cons and eco-sustainable model. In Ethnobotany of India Volume 3 North East India and Andaman and Nicobar island CRC Press (Apple Academic Press), 394 p.

Rai PK 2009. Comparative assessment of soil properties after bamboo flowering and death in a tropical forest of Indo-Burma hot spot. *Ambio* **38**(2): 118-120.

Rai PK 2012. Assessment of multifaceted environmental issues and model development of an Indo-Burma hot spot region *Environmental Monitoring & Assessment* **184**: 113-131.

Rai PK 2013. *Plant invasion ecology: Impacts and sustainable management*. Nova Science Publisher New York, 196p.

Rai PK 2015. Paradigm of plant invasion: Multifaceted review on sustainable management. *Environmental Monitoring and Assessment* **187:** 759.

Rai PK and Singh JS 2020. Invasive alien plant species: Their impact on environment, ecosystem services and human health. *Ecological Indicators* **111**: 106020.

Rai PK and Singh MM 2020a. Fe- wetland plant's chemical ecology of a Ramsar site in an Indo-Burma hotspot: *In-situ* bio-accumulation and phytoremediation implications. *Nature Environment Pollution Technology* **19**(4): 1607-1615.

Rai, PK.,and Lalramnghinghlova, H 2011a. Threatened and less known ethnomedicinal plants of an Indo-Burma hotspot region: conservation implications. *Environmental Monitoring and Assessment* **178**: 53-62.

Rai PK and Lalramnghinghlova H. 2011b. Ethnomedicinal plants of India with special reference to an Indo-Burma hotspot region: an overview *Ethnobotany Research Application* **9**: 379-420.

Rai PK 2021. Environmental degradation by invasive alien plants in the anthropocene: Challenges and prospects for sustainable restoration. *Anthrpocene Science* (ANPS) https://doi.org/10.1007/s44177-021-00004-y

Rai PK and Singh JS 2021. Plant invasion in protected areas, the Indian Himalayan region and the North East India: Progress and prospects. *Proceedings of the Indian National Science Academy* **87**(1): 19-35.

Raizada P, Raghubanshi AS and Singh JS 2008. Impact of invasive alien plants species on soil processes: A review. *Proceeding of National Academic of Sciences*. India Section B. **78**(4): 288-298.

Ruati VL and Rai PK 2021. The impact of *Tithonia diversifolia* (Hemsl.) A. Gray on phytosociology in Aizawl, Mizoram. *Ecology Environment and Conservation* **27:** S209-S214.

Received 05 July, 2021; Accepted 12 November, 2021

Sakachep ZK and Rai PK 2019. Status of soil nutrients in inner line reserve forest of Hailakandi, Assam. *Natural Resource Management for Sustainable Development.* Today and Tomorrow's Printers and Publishers. New Delhi, pp. 449-452.

Sakachep ZK and Rai PK 2021. Influence of invasive alien plants on vegetation of Hailakandi district, Assam, North-East, India. *Indian Journal of Ecology* **48**(1): 261-266.

Sapkota L 2007. Ecology and management issues of *Mikania micrantha* in Chitwan national park, Nepal. *Banko Janakari* **17**(2): 27-39.

Sekar KC 2012. Invasive alien plants of Indian Himalayan region-diversity and implication. *American Journal of Plant Sciences* **3**: 177-184.

Sorenson T 1948. A method of establishing groups of equal amplitudes in plant sociology based on similarity of species content. *Kongelige Danske Videnskabernes Selskab, Biologiske Skrifter* (Copenhagen) **5**: 1-34.

Walkley A and Black IA 1934. An examination of the degtjareff method for the determining soil organic matter and a proposed modification of chromic and titration method. *Soil Sciences* **37**(1): 29-38.

Wei H, Xu J, Quan G, Zhang J and Qin Z 2017. Invasion effects of *Chromolaena odorata* on soil carbon and nitrogen fractions in a tropical Savanna. *Ecosphere* **8**(5): 1-16.

Williamson MH and Fitter A 1996. The characteristics of successful invaders. *Biological conservation* **78**: 163-170.

Zhang P, Li B, Wu J and Hu S 2019. Invasive plants differentially affect soil biota through litter and rhizosphere pathway: meta-analysis. *Ecology Letters* **20**: 200-210.

Zhou Q, Wang Y, Li X, Liu Z, Wu J, Musa A, Ma Q, Yu H, Cui X and Wang L 2020. Geographical distribution and determining factors of different invasive ranks of alien species across China. *Science of the Total Environment* **722**: 1379.

Indian Journal of Ecology (2021) 48(6): 1705-1708

Manuscript Number: 3435
NAAS Rating: 5.79

Effect of Micronutrients Application on Growth, Yield and Quality of Guava (*Psidium guajava* L.)

Shahroon Khan, Ashwani Kumar and Jeet Ram Sharma

Department of Horticulture, CCS Haryana Agricultural University, Hisar-125 004, India
E-mail: shahroonkhan25@gmail.com

Abstract: The study was conducted to evaluate the effects of foliar application of micronutrients (zinc sulphate, boric acid and manganese sulphate) alone and in combination on growth, yield and quality of guava cv. Hisar Safeda. The treatments were set up in randomized blocks [T1 (0.5% $ZnSO_4$) T2 (0.5 $ZnSO_4$ + 0.2% $MnSO_4$), T3 (0.5% $ZnSO_4$ + 0.3% H_3BO_3), T4 (0.3% H_3BO_3), T5 (0.3% H_3BO_3 + 0.2% $MnSO_4$), T6 (0.2% $MnSO_4$), T7 (T1 + T4 + T6), T8 (Control)] replicated three times. In general, application of zinc sulphate, boric acid and manganese sulphate alone increased in fruit set, fruit weight, fruit yield, ascorbic acid and pectin content of fruit over control, while, higher increase was evident in boric acid application. The combined foliar application of 0.2% $MnSO_4$ + 0.3% H_3BO_3 + 0.5% $ZnSO_4$ showed higher impact for increase in traits like plant height, fruit retention (72.34%), fruit weight (113.3 g), fruit yield (72.03 kg/tree), ascorbic acid (191.8 mg/100g) and pectin content (0.76%) as compared to control as well as their application alone.

Keywords: Ascorbic acid, Boric acid, Micronutrients, Pectin content, Yield

Guava (*Psidium guajava* L.) is one of the most important fruit in India with high nutritive value. It is widely adapted fruit crop, which can be grown in diverse climate conditions in India. Guava occupies in India, 2.64 lakh hectares with annual production of 40.5 lakh tonnes and productivity 15.30 MT/ha (Anonymous, 2018). Likewise, In Haryana, the area under guava crop is 12.09 thousand hectares with production of 1.37 lakh tonnes and productivity 11.33 MT/ha (Anonymous, 2018). Nutritional deficiencies in fruit crops significantly hamper the physiological process of plants thus reducing yield and quality. Application of micronutrients has received a greater attention for fruit crop production in view of their general deficiency in soils. Foliar application of micronutrients is advantageous over soil application as it helps in uniform distribution of fertilizers, low application rates and quick response to applied nutrients (Kumar et al 2015). Imbalances in micronutrient management may lead to reduced yield and poor fruit quality whereas, micronutrients density in fruit plants favour growth attributes and health benefits to the consumer. It is evident from earlier studies that combine foliar application of zinc sulphate, boric acid and copper (Sau et al 2018) and zinc sulphate, boric acid and magnesium (Giram et al 2021) significantly improved growth, yield and quality of guava. Therefore, the objective of the present study was to evaluate the effect of individual and combined foliar application of zinc sulphate, boric acid and manganese sulphate on plant growth, fruit yield and quality attributes under Haryana condition.

MATERIAL AND METHODS

The field experiment was performed during 2015-16 & 2016-17 at "CCS Haryana Agricultural University, Hisar (Haryana)" located at 215.2 m above the sea level with co-ordinates 75º 46' E longitudes, 29º10'N latitude and has typical semi-arid climate with extremely cold winters and very hot summers season. The maximum day temperatures during May-June around 45ºC and as low as freezing temperature in December-January are common. There was a lot of variance in overall rainfall and distribution in this area. The total rainfall received during the year 2015-16 and 2016-17 were 529.6 and 505.9 mm respectively. Almost 80% of the precipitation happens *i.e.*, July to September. The experiment was in randomized block design with eight treatments [T1 (0.5% $ZnSO_4$) T2 (0.5 $ZnSO_4$ + 0.2% $MnSO_4$), T3 (0.5% $ZnSO_4$ + 0.3% H_3BO_3), T4 (0.3% H_3BO_3), T5 (0.3% H_3BO_3 + 0.2% $MnSO_4$), T6 (0.2% $MnSO_4$), T7 (0.2% $MnSO_4$ + 0.3% H_3BO_3 + 0.5% $ZnSO_4$), T8-Control (only water spray)] replicated three times. The trees foliar applications were given in March and July. The soil texture in the experimental field was sandy loam. At the start of the experiment, the productivity of the soil in the experimental orchard field was calculated. The samples were obtained, at various depths (0-15, 15-30 and 30-60 cm).and dried in the shade, sieved at 2 mm, and tested for soil physiochemical property. The soil of the orchard was sandy loam with soil pH 7.6, electrical conductivity 0.29 dSm^{-1}, organic carbon 0.45 per cent, DTPA-extractable zinc 1.53 (mg kg^{-1}), available boron 1.81 (mg/kg)

and DTPA-extractable manganese 6.79 (mg kg^{-1}) at soil depth 0-15 cm. Different quality parameters were estimated by extracting juice of fruits in the juice extractor. Total soluble solids were determined using a hand refractometer and expressed as ºBrix. The acidity was determined by titrating 5 ml of juice against 0.1 N NaOH solution using phenolphthalein as an indicator (A.O.A.C 1990). Total sugars and reducing sugars were estimated by Hulme and Narain method (1931). Subtraction of reducing sugars from the total sugars gave the values of non-reducing sugar after multiplying the value with the factor (0.95) as suggested in A.O.A.C. method (1990).

RESULTS AND DISCUSSION

Growth and flowering parameters: The plant height and canopy spread of guava increased with the foliar application of micronutrients with respect to control (Table 1). In pooled data, the maximum per cent increase in plant height (6.10), canopy spread East-West (8.04) and North-South (7.93) was recorded with the application of 0.2% $MnSO_4$ + 0.3% H_3BO_3 + 0.5% $ZnSO_4$, whereas minimum recorded in control. Improvement in stem girth with application of micronutrients individual or in combination was non-significant. In individual treatments, 0.5% $ZnSO_4$ indicated the maximum increase in plant height and canopy spread. Similar results were also observed by Goswami et al (2012) and Sau et al (2018) in guava. This might be due to effect of zinc, which is the main component in biosynthesis of tryptophan, might led to more synthesis of auxin, which is responsible for overall plant growth (Kumar et al 2017). Number of flower per branch, fruit set and fruit retention increased with the foliar application of micronutrients. The maximum number of flowers per branch (27.0), fruit set (64.43%) and fruit retention (72.34%) was obtained when plant was supplemented with 0.2% $MnSO_4$ + 0.3% H_3BO_3 + 0.5% $ZnSO_4$ whereas, in individual treatments, application of 0.3% H_3BO_3 recorded maximum number of flowers per branch. This might be due to role of boron in translocation of carbohydrates, auxin synthesis, increased pollen viability and fertilization (Kumar et al 2017). Earlier studies by several researchers in guava also indicated the same trend (Shukla et al 2009, Yadav et al 2014).

Yield and Quality parameters: The foliar application of zinc sulphate, boric acid, and manganese sulphate alone and their combinations exhibited remarkable influence on yield and quality parameters of guava. The maximum number of fruits (635.9), fruit weight (113.3 g) and fruit yield (72.03 kg $tree^{-1}$) was with combination of 0.2% $MnSO_4$ +0.3% H_3BO_3 + 0.5% $ZnSO_4$, which was significantly higher than control (Table 2). Among individual treatments, foliar application of 0.3% H_3BO_3 recorded significantly higher number of fruits in comparison to other treatments and may be due to more fruit set and higher fruit retention. These results obtained were similar to the findings earlier workers in guava (Mahaveer et al 2016, Sau et al 2018). Genie et al (2013) reported increased in fruit set, fruit retention and yield of guava is due to beneficial role of boron in pollen grain germination and pollen tube development. The Zn also play an important role in fruit bud formation and fruit drop reduction by synthesis of tryptophan and regulate the translocation of metabolites to the site of bud development.

The maximum TSS (12.05 ºBrix) was obtained with the foliar application of 0.5% Zinc sulphate over control (Table 2). All combine application of micronutrients influenced TSS except foliar application of 0.2% $MnSO_4$. The acidity was decreased with the foliar application of micronutrient alone and their combinations during both the years. The lowest acidity was with foliar application of 0.5% zinc sulphate, while maximum acidity was in control. The decrease in the acidity is

Table 1. Effect of foliar application of micronutrients on plant growth and flowering parameters in guava

Treatments	Growth parameters (Per cent increase over control)				Flowering parameters		
	Plant height	Stem girth	E-W Canopy spread	N-S Canopy spread	Number of flower per branch	Fruit Set (%)	Fruit retention (%)
0.5%$ZnSO_4$	6.02	2.94	7.90	7.81	24.34	60.96	68.97
0.5% $ZnSO_4$ + 0.2% $MnSO_4$	5.96	2.92	7.78	7.71	24.83	61.74	69.61
0.5% $ZnSO_4$ + 0.3% H_3BO_3	5.93	2.90	7.73	7.68	25.67	62.88	70.49
0.3% H_3BO_3	5.90	2.88	7.67	7.58	26.00	63.59	71.52
0.3% H_3BO_3 + 0.2% $MnSO_4$	5.87	2.88	7.58	7.55	24.50	60.94	69.11
0.2% $MnSO_4$	5.81	2.87	7.49	7.45	21.67	58.90	67.82
0.2% $MnSO_4$ + 0.3% H_3BO_3 + 0.5% $ZnSO_4$	6.10	2.95	8.04	7.93	27.00	64.43	72.34
Control	5.75	2.85	7.44	7.32	19.34	55.56	65.83
CD (p=0.05)	0.12	NS	0.28	0.26	3.39	1.93	2.82

Table 2. Effect of foliar application of micronutrients on yield and quality parameters of guava

Treatments	Yield parameters			Quality parameters						
	Number of fruit per tree	Weight of fruit (g)	Fruit Yield (Kg/tree)	TSS (ºBrix)	Acidity (%)	Total Sugars (%)	Reducing sugars (%)	Non-reducing sugars (%)	Ascorbic acid (mg/100 g)	Pectin content (%)
0.5% $ZnSO_4$	569.4	107.0	60.91	12.05	0.42	7.12	4.12	3.00	182.0	0.70
0.5% $ZnSO_4$ + 0.2% $MnSO_4$	579.2	107.6	61.85	11.80	0.45	6.96	4.04	2.92	183.4	0.72
0.5% $ZnSO_4$ + 0.3% H_3BO_3	592.0	112.3	66.44	11.54	0.48	6.74	3.91	2.83	185.5	0.73
0.3% H_3BO_3	609.7	110.7	67.50	11.37	0.50	6.59	3.82	2.77	189.1	0.74
0.3% H_3BO_3 + 0.2% $MnSO_4$	583.0	107.7	62.80	11.42	0.50	6.63	3.85	2.78	183.2	0.72
0.2% $MnSO_4$	557.8	104.8	59.18	11.24	0.53	6.52	3.78	2.74	177.7	0.68
0.2% $MnSO_4$ + 0.3% H_3BO_3 + 0.5% $ZnSO_4$	635.9	113.3	72.03	11.72	0.46	6.83	3.95	2.88	191.8	0.76
Control	544.5	98.9	53.84	11.04	0.55	6.36	3.70	2.66	170.8	0.66
CD (p=0.05)	19.9	2.62	1.73	0.27	0.03	0.16	0.15	0.12	4.30	0.02

obvious due to increased TSS. Similarly, foliar application of micronutrients significantly increased total sugars, reducing sugars, and non-reducing sugars over control during both the years. The maximum total sugars (7.12%), reducing sugars (4.12%) and non-reducing sugars (3.00%) were obtained with the foliar application of 0.5% zinc sulphate as compared to control. The zinc nutrient is very helpful in photosynthetic process that led to the accumulation of carbohydrates and activates many enzymes which help metabolized the carbohydrates into simple sugars. The present study corroborates the earlier findings of Sau et al (2018) and Yadav et al (2018) in guava. The maximum ascorbic acid with the foliar application of 0.2% $MnSO_4$ + 0.3% H_3BO_3 + 0.5% $ZnSO_4$, which was significantly higher than individual treatments except 0.3% H_3BO_3 as compared to control (Table 2). Pooled data showed maximum pectin content achieved through the foliar combinations 0.2% $MnSO_4$ + 0.3% H_3BO_3 + 0.5% $ZnSO_4$ as compared to control. In individual treatments, the highest pectin content was observed with 0.3% H_3BO_3. Similar findings were reported by Sau et al (2018), and Yadav et al (2018) in guava.

CONCLUSION

The foliar application of 0.2% $MnSO_4$ + 0.3% H_3BO_3 + 0.5% $ZnSO_4$, individual or in combination impacted significantly in terms of increase in plant growth parameters, fruit yield, total soluble sugars, ascorbic acid, pectin content and reduction in acidity. However, the combine foliar application of 0.2% $MnSO_4$ + 0.3% H_3BO_3 + 0.5% $ZnSO_4$, was superior over individual micronutrient application as well as control treatment. Hence, it can be concluded that combine foliar application of 0.2% $MnSO_4$ + 0.3% H_3BO_3 + 0.5% $ZnSO_4$, should be recommended to increase the fruit yield and better quality in guava.

REFERENCES

Anonymous 2018. *Horticultural Statistics at a Glance*. Ministry of Agricultural & Farmers Welfare, GOI, New Delhi.

AOAC 1990. *Official Methods of Analysis*. Association of Official Analytical Chemists, 15th Edn, Washington, D.C, USA.

Ganie MA, Akhter F, Bhat M.A, Junaid JM, Shah MA, Bhat AH and Bhat TA 2013. Boron a critical nutrient element for plant growth and productivity with reference to temperate fruits. *Current Science* **104**(1): 76-85.

Giram KS, Shinde SJ, Jaiswal SB and Pavankumar LG 2021. Influence of foliar application of micronutrients on physical and yield attributes of mrig bahar guava (*Psidium guajava* L.) cv. Sardar. *The Pharma Innovation* **10**(10): 911-913.

Goswami AK, Lal S and Misra KK 2012. Integrated nutrient management improves growth and leaf nutrient status of guava cv. Pant Prabhat. *Indian Journal of Horticulture* **69**(2): 168-172.

Hulme AC and Narain R 1931. The ferrycyanide method for determination of reducing sugars. A modification of Hagedom-Jersen-Hanes Technique. *Biochemical Journal* **25**(4): 1051-1061.

Kumar J, Kumar R, Rai R and Mishra DS 2015. Response of 'Pant Prabhat' guavatrees to foliar sprays of zinc, boron, calcium and potassium at different plant growth stages. *The Bioscan* **10**(2): 495-498.

Mahaveer S, Dubalgunde SV, Ooty P and Sangma PD 2016. Effect of foliar application of micronutrients on yield and economics of guava (*Psidium guajava* L.) cv. L-49. *International Journal of Agriculture, Environment and Biotechnology* **9**(2): 221-224.

Sachin, Arvind K, Vipin K, Tripathi SK and Mukesh K 2019. Effect of application of micronutrients on physical quality parameters of guava (*Psidium guajava* L.) cv. Lalit. *Annals of Horticulture* **12**(2): 130-133.

Sau, S, Sarkar S, Ghosh B, Ray K, Deb P and Ghosh D 2018. Effect of foliar application of B, Zn and Cu on yield, quality and economics of rainy season guava cultivation. *Current Journal of Applied Science and Technology* **28**(1): 1-10.

Sheoran OP, Ton, DS, Kaushik LS, Hasija RC and Pannu RS 1998. Statistical software package for agricultural research workers. *Recent Advances in information theory, Statistics & Computer Applications,* Department of Mathematics Statistics, CCS HAU, Hisar 139-143.

Shukla AK, Sarolia DK, Kumari B, Kaushik RA, Mahaver LN and Bairwa HL 2009. Evaluation of substrate dynamics for integrated nutrient management under high density planting of guava (*Psidiumguajava* L.) cv. Sardar. *Indian Journal of Horticulture*, **66**(4): 461-464.

Singh Y, Thakur N and Meena NK 2018. Studies on the effect of foliar spray of Zn, Cu and B on growth, yield and fruit quality of sweet orange (*Citrus sinensis* L.) cv. Mosambi. *International Journal of Chemical Studies* **6**(5): 3260-3264.

Yadav A, Ram RB, Verma RS, Kumar V and Yadav RK 2018. Effects of foliar application of micronutrients on bio-chemical attributes of winter season guava (*Psidium guajava* L.) cv. Lalit. *Journal of Pharmacognosy and Phytochemistry* **7**(2): 3196-3197.

Yadav RK, Ram RB, Kumar V, Meena ML and Singh HD 2014. Impact of micronutrients on fruit set and fruit drop of winter season guava (*Psidium guajava* L.) cv. Allahabad Safeda. *Indian Journal of Science and Technology* **7**(9): 1451-1453.

Received 18 August, 2021; Accepted 22 November, 2021

Indian Journal of Ecology (2021) 48(6): 1709-1714

Manuscript Number: 3436
NAAS Rating: 5.79

Species Diversity and Composition of Spiders (Arachnida: Araneae) of Different Micro-habitats in Nilgiri Foothills, Western Ghats, Tamil Nadu, India

Vijay Kumar Yadav, John T.D. Caleb[1] and R. Revathi[2]

Department of Forestry, Mewar University, Gangrar, Chittorgarh-312901, India
[1]No. 27, Saravana Nagar, Manigantapuram, Thirumullaivoyal, Chennai-600 062, India
[2]Forest College and Research Institute, Mettupalayam, TNAU, Coimbatore-642110, India
E-mail: yadavvijaykumar3@gmail.com

***Abstract*:** Spider diversity and composition was assessed by various field surveys in the campus and its surroundings of Forest College and Research Institute, Mettupalayam, located in foothills of Nilgiris, Western Ghats, Coimbatore district, Tamil Nadu from January 2019 to June 2019. Four micro-habitats identified for the study purpose were *Jatropha* plantation & surrounding (JPS), *Melia dubia* plantation and surrounding (MPS), campus buildings and garden (CBG) and campus forest nursery (CFN). A total of 410 individuals of spiders were collected from 16 families, 42 genera and 55 species. Tukey Post Hoc multiple comparison test showed that mean spider density was significantly higher in CBG site as compare to other micro-habitats, followed by MPS and CFN, however, maximum 39 spiders species were recorded in MPS. Mean species richness was significantly higher in CFN, followed by MPS and CBG micro-habitats. Spider species were grouped in seven different feeding guilds, in which stalkers was dominant guild (40%), followed by orb-web builders (25%). Diversity indices, Shannon-Wiener, Simpson, Margalef and Pilou's Evenness Indexs, were calculated as 3.44, 0.95, 8.98, and 0.86 respectively. Maximum value for relative diversity indices (RDi) was for family – Salticidae (33.33 RDi for genera and 30.91 RDi for species). These results show that micro-habitats play an important role in composition and survival of spiders.

***Keywords*:** Diversity, Institute campus, Micro-habitat, Species composition, Spider

In agro-ecosystems, spiders are also considered as active biological control agents and considered as important food source of other animals like lizards and birds. Food energy can be transmitted through spiders from lower level to higher level (Sebastian and Peter 2009). Currently, the world population of spiders accounts for 128 families, 4209 genera and about 49,235 taxonomically recognized species (World Spider Catalog 2021), out of which Tamil Nadu represents 250 spider species belonging to 131 genera and 33 families (Caleb and Karthikeyani 2021). Western Ghats is one of the hotspots of India, comes under the state of Tamil Nadu and occupying an area of about 27,069 km^2 (Karthikeyani et al 2017). The Forest College and Research Institute (FC&RI) campus is situated at Nilgiris foothills, opposite to Jakanari Reserved Forest (JRF), Western Ghats is well known for its enriched floral and faunal diversity. However, the spider diversity in the campus and its surroundings remained unexplored. Therefore, the present study aims to explore diversity, composition, and abundance of spiders in different micro-habitats.

MATERIAL AND METHODS

Study area: Forest College and Research Institute (11.19' N & 77.56' E; 300 m altitude) is situated at the foothills of Nilgiris on the Kotagiri road over a sprawling expanse of 200 ha of reserved forest with diverse ecological habitats and vegetation types. The annual rainfall is up to 830 mm. The average maximum and minimum temperature of the area are 32.2°C and 23.2°C respectively. As all selected micro-habitats were close to each other, hence don't have any significant difference in environmental conditions.

Methodology: The study was carried out from January, 2019 to June, 2019. All surveys were conducted in the morning from 7.00 am to 9.00 am and in the evening from 4.00 pm to 6.00 pm. Spiders were collected from four micro-habitats of the campus according to their vegetation types. Samples were collected from 10 x 10 m quadrats, laid randomly for each site and adopted standard sampling techniques such as sweep netting, beating sheets, active searching and hand picking. Description of the selected micro-habitats of campus is as follows:

***Jatropha* plantation and surroundings (JPS):** It was dominated with *Jatropha curcus* plantation with grasses. The boundary of plantation was covered with multistoried vegetation. An area of plantation was two hectares without any human activity except seed collection and irrigation. Canopy height of the plantation was up to two meters. This habitat plays an important role for survival of ground runners,

orb-web builders, stalkers and foliage hunters.

***Melia dubia* plantation and surroundings (MPS)**: This micro-habitat, with an area of two hectares, was dominated with *Melia dubia* plantation, and used for the agroforestry purpose like the area presents between trees are utilized for cultivation of agricultural crops. Canopy height of the plantation was between six and eight meters, thus provides more space for orb-web builders, ground runners, stalker, foliage hunter and ambushers.

Campus buildings and garden (CBG): Buildings are the important micro-habitats for spiders, as spiders usually come in buildings in search of prey. Canopy height of the garden vegetation was between two and four meters.

Campus forest nursery (CFN): Forest nursery had different types of vegetation with different layers like herbs, shrubs, seedlings, saplings and trees. Canopy height of this vegetation was between less than one meter and five meters. A permanent water source was available there for plants; hence moisture was the key factor at this site for attracting different prey insects as well as spiders. Spiders were observed under the stereozoom microscope and identified using standard taxonomic keys and field guides (Tikader 1970, Tikader 1977, Tikader 1980, Tikader 1982, Tikader 1987, Sebastian and Peter 2009, Mondal et al 2020)

Statistical analysis: The diversity of spiders was estimated using different indices viz., The Shannon-Wiener index (H1), Simpson index (λ), Margalef Richness and Pielou's Evenness Index (J') by using PAST software and other analysis was done with the help of MS Excel office 2007 (Hammer et al 2001). The relative diversity (RDi) of families was calculated using as Torre-Cuadros et al (2007), Yadav and Chauhan 2018.

$$RDi = \frac{\text{Number of spider genus or species in a family}}{\text{Total number of genus or species}} \times 100$$

All analysis were performed using IBM-SPSS 16.0 version (SPSS 2007).

RESULTS AND DISCUSSION

The total of 410 spider specimens were identified belonged to 55 species, 42 genera and 16 families (Araneidae, Corinnidae, Cheiracanthiidae, Filistatidae, Hersiliidae, Liocranidae, Lycosidae, Oxyopidae, Philodromidae, Pholcidae, Salticidae, Sparassidae, Tetragnathidae, Thomisidae, Uloboridae and Zodariidae) Table 1). The higher species diversity (Shannon-Wiener diversity index) was for both MPS and CFN micro-habitats (3.13) while Simpson diversity index was maximum for CFN (0.95). Mahalakshmi and Jeyaparvathi (2014) and Rain et al (2016) recorded Shannon-Wiener diversity index between 1.42-2.48 and 2.96-3.14 respectively. These are similar to present study might be due to similarity in the number of spider species. Bhat et al (2013) and Rain et al (2016) recorded Simpson diversity index for spiders were 0.82 and 0.89 respectively. This result is also showing similarity with present study. Margalef diversity index was higher (7.94) for MPS whereas Pilou's Evenness Index was higher (0.93) for CFN. The Margalef diversity index (8.98) was calculated for all micro-habitats of FC&RI. Mahalakshami & Jeyaparvathi (2014) and Krishnaveni & Kandeepan (2018) recorded that Margalef diversity index ranged from 4.12-4.98 and 8.42. The main reason for differences in values of Margalef diversity index is possibly variation in numbers of spider species. The maximum value for relative diversity (RDi) was for family Salticidae (33.33 genera and 30.91 species), followed by the family Araneidae (16.67 genera and 16.36 species) (Table 2).

Maximum 39 species were recorded in MPS, followed by 29 species in JPS and 26 species in CFN and CBG respectively. Identified species were grouped in seven different feeding guilds: ambushers, foliage hunters, ground runners, orb-web builders, crevice-web builders, space-web builders and stalkers (Uetz et al 1999). The stalkers constituted the dominant guild (40%), followed by the orb-web builders (25%). The lowest were oambushers, crevice-web builders and space-web builders (2%) (Table 2). The family Salticidae was the most diverse (14 genera and 17 species), followed by Araneidae (seven genera and nine species). Nine families were recorded with single representative (one genus and one species) included Corinnidae, Cheiracanthiidae, Filistatidae, Hersiliidae, Liocranidae, Philodromidae, Pholcidae, Thomisidae and Uloboridae (Table 1). Thus, a total of 16 spider families distributed among 42 genera and 55 species were recorded in the campus (Yadav et al 2018a). There is no previous study on spider's diversity in FC&RI campus and its surroundings so far. Caleb and Karthikeyani (2021) enlisted 250 spider species belonging to 131 genera and 33 families from the state of Tamil Nadu. However, the present study recorded 55 spider species belonged to 46 genera and 16 families. The highest spider diversity was recorded from the MPS micro-habitat (39 species), followed by the JPS and CFN micro-habitats (29 species each).

Tukey Post Hoc multiple comparison test for mean spider density between different micro-habitats (F_3, 25 = 7.68; p = 0.001) showed significant similarity between JPS & CBG; MPS & CBG; CBG & CFN, whereas, there were non-significantly different among other micro-habitats. The mean spider density was significantly higher in CBG micro habitat as compare to the other micro-habitats, which was followed by MPS and CFN. Therefore, collage buildings and garden (CBG) are playing the major role in spiders' diversity.

Table 1. Checklist of spiders species composition in micro-habitats of in campus of Forest College and Research Institute, Coimbtore, Tamil Nadu

Species name	Species composition in different micro habitat (%)				
	JPS	MPS	CBG	CFN	TSC
Family: Araneidae					
Argiope aemula (Walckenaer 1841)	0.49	0.00	0.73	0.98	2.20
A. anasuja Thorell 1887	0.24	0.24	0.24	1.46	2.20
Cyclosa sp.	0.00	0.24	0.00	0.00	0.24
Cyrtophora cicatrosa (Stoliczka 1869)	0.49	1.22	2.68	1.95	6.34
C. citricola (Forsskal 1775)	0.00	1.22	1.71	0.49	3.41
Eriovixia excelsa (Simon 1889)	0.98	0.49	0.00	0.00	1.46
Gasteracantha geminata (Fabricius 1798)	0.00	0.49	1.22	0.24	1.95
Neoscona sp.	0.00	0.98	0.49	0.00	1.46
Nephila pilipes (Fabricius 1793)	0.00	0.00	0.49	1.22	1.71
Family: Corinnidae					
Corinnomma severum (Thorell 1877)	0.98	0.24	0.24	0.00	1.46
Family: Cheiracanthiidae					
Cheiracanthium sp	0.00	0.24	0.98	0.24	1.46
Family: Filistatidae					
Pritha sp.	0.00	0.24	0.00	0.24	0.49
Family: Hersiliidae					
Hersilia savignyi (Lucas 1836)	0.00	0.98	0.24	0.49	1.71
Family: Liocranidae					
Oedignatha sp.	0.49	0.00	0.00	0.00	0.49
Family: Lycosidae					
Hippasa greenalliae (Blackwall 1867)	1.95	0.98	0.24	0.49	3.66
Hippasa madraspatana Gravely 1924	0.49	1.22	0.00	0.00	1.71
Lycosa sp.	0.49	0.24	0.00	0.49	1.22
Wadicosa fidelis (O. Pickard-Cambridge 1872)	0.98	0.49	0.00	0.49	1.95
Family: Oxyopidae					
Hamataliwa sp.	0.24	0.49	0.00	0.00	0.73
Oxyopes birmanicus Thorell 1887	0.24	0.73	0.00	0.98	1.95
O. javanus Thorell 1887	1.71	2.68	1.22	1.46	7.07
O . shweta Tikader 1970	0.49	1.22	0.00	0.49	2.20
Peucetia viridana (Stoliczka 1869)	2.93	6.83	0.24	0.00	10.00
Family: Philodromidae					
Philodromus sp.	0.24	0.24	0.00	0.00	0.49
Family: Pholcidae					
Crossopriza lyoni (Blackwall 1867)	0.00	0.00	14.15	0.00	14.15
Family: Salticidae					
Bianor balius Thorell 1890	0.98	1.22	0.00	0.00	2.20
Carrhotus sp.	0.24	0.49	0.49	0.00	1.22
C. viduus (Koch 1846)	0.24	0.24	0.00	0.49	0.98
Cyrba ocellata (Kroneberg 1875)	0.73	0.49	0.00	0.00	1.22
Hyllus semicupreus (Simon 1885)	0.00	0.49	0.98	0.24	1.71

Cont...

Table 1. Checklist of spiders species composition in micro-habitats of in campus of Forest College and Research Institute, Coimbtore, Tamil Nadu

Species name	Species composition in different micro habitat (%)				
	JPS	MPS	CBG	CFN	TSC
Langona tigrina (Simon 1885)	0.00	0.49	0.00	0.98	1.46
Menemerus bivittatus (Dufour 1831)	0.24	0.00	0.49	0.24	0.98
Myrmarachne prava (Karsch 1880)	0.00	0.24	0.98	0.49	1.71
Myrmaplata plataleoides	0.00	0.49	0.73	0.00	1.22
Myrmarachne sp.	0.00	0.24	0.24	0.00	0.49
Pellenes sp.	0.24	0.00	0.00	0.00	0.24
Phintella vittata (Koch 1864)	0.24	0.49	0.24	0.00	0.98
Plexippus paykulli (Audouin 1826)	0.00	0.00	0.98	0.00	0.98
Stenaelurillus lesserti Reimoser 1934	0.24	0.00	0.49	0.24	0.98
Stenaelurillus sp.	0.00	0.00	0.00	0.24	0.24
Telamonia dimidiata (Simon 1899)	0.24	0.49	0.98	0.24	1.95
Thyene imperialis (Rossi 1846)	0.00	0.00	0.00	0.49	0.49
Family:Sparassidae					
Heteropoda sp.	0.24	0.00	0.49	0.00	0.73
Olios lamarcki (Latreille 1806)	0.00	0.00	0.00	0.49	0.49
Olios milleti (Pocock 1901)	0.00	0.24	0.00	0.24	0.49
Olios sp. 1	0.24	0.00	0.00	0.00	0.24
Olios sp. 2	0.00	0.24	0.00	0.00	0.24
Family: Tetragnathidae					
Leucauge decorata (Blackwall 1864)	0.98	0.73	1.95	1.46	5.12
L. tessellata (Thorell 1887)	0.00	0.00	0.00	0.49	0.49
Tetragnatha sp.1	0.00	0.24	0.00	0.00	0.24
T. sp.2	0.00	0.00	0.00	0.24	0.24
Family: Thomisidae					
Thomisus sp.	0.00	0.24	0.00	0.00	0.24
Family: Uloboridae					
Uloborus sp.	0.00	0.24	0.00	0.00	0.24
Family: Zodariidae					
Hermippus sp.	0.24	0.00	0.00	0.00	0.24
Tropizodium sp.	0.00	0.24	0.00	0.00	0.24

JPS (*Jatropha curcas* plantation and surroundings), MPS (*Melia dubia* plantation and surroundings), CBG (Campus buildings and garden), CFN (Campus forest nursery) and TSC (Total % species Composition)

Buildings provide edges and more space to survive the spiders. Attraction of spiders towards buildings may be availability of prey insects which attracted towards the light of night lamps or due to less pressure of predators on spiders. Thus, buildings are the most important habitat for spider density. Tukey Post Hoc multiple comparison test was also used for mean spider species richness between different micro-habitats (F_3, 25 = 12.92; p = 0.000) showed significant similarity between JPS & MPS; JPS & CBG; JPS & CFN, whereas, there was non-significant difference among other micro-habitats. Based on these observations mean spider species richness was significantly higher in CFN micro-habitat as compare to the other micro-habitat, which was followed by MPS and CBG. It may be due to availability of multi-storied vegetation and moisture which was attracted a number prey insects and provide a suitable environment and space for their survival (Table 3).

CONCLUSION

The study showed that great variety of spider exists in

Table 2. Guilds of structure and relative diversity (RDi) of spider species in campus of Forest College and Research Institute, Coimbatore, Tamil Nadu

Families	Guilds	RDi	
		Genus	Species
Araneidae	Orb-web builder	16.67	16.36
Corinnidae	Ground Runners	2.38	1.82
Cheiracanthiidae	Foliage hunter	2.38	1.82
Filistatidae	Crevice Web Builder	2.38	1.82
Hersiliidae	Foliage hunter	2.38	1.82
Liocranidae	Ground Runners	2.38	1.82
Lycosidae	Ground Runners	7.14	7.27
Oxyopidae	Stalkers	7.14	9.09
Philodromidae	Ground Runners	2.38	1.82
Pholcidae	Space-web builder	2.38	1.82
Salticidae	Stalkers	33.33	30.91
Sparassidae	Foliage hunter	4.76	9.09
Tetragnathidae	Orb-web builder	4.76	7.27
Thomisidae	Ambusher	2.38	1.82
Uloboridae	Orb-web builder	2.38	1.82
Zodariidae	Ground Runners	4.76	3.64

Table 3. Spider density (N / 100 m^2) and species richness in different micro-habitat in campus of Forest College and Research Institute, Coimbatore, Tamil Nadu

Parameters	Sites	Mean	Std. Deviation	Tukey Post Hoc multiple comparison test
Density /100 m^2	JPS	9.50^a	5.398	F_3, 25 = 7.68; p = 0.001
	MPS	16.00^a	2.000	
	CBG	29.00^b	13.620	
	CFN	15.00^a	5.244	
Species richness /100 m^2	JPS	3.63^a	0.744	F_3, 25 = 12.92; p = 0.000
	MPS	5.57^b	0.976	
	CBG	5.20^b	0.447	
	CFN	5.80^b	0.447	

Significant difference at $p < 0.05$ level represented with similar superscript on the mean values

the different micro-habitats and it varies with the different strata of vegetation. There is little human interference in spider habitat and need to research on individual species as the climatic conditions supports the spider fauna to multiply their population. Research work on the biology of spiders including their web construction, food and feeding habitats, physiology, reproduction and life history can be done that may lead to open new door for the conservation of spider species.

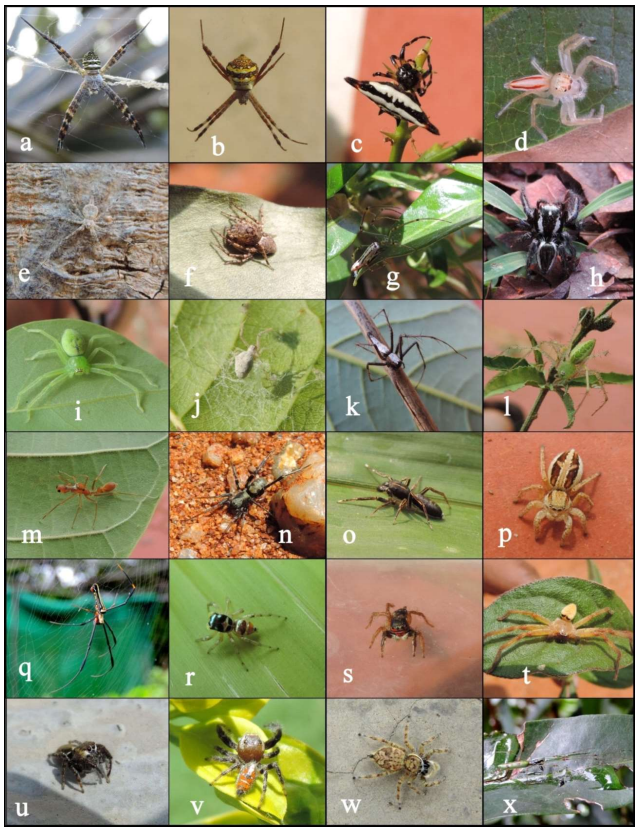

Plate 1. Some important spiders recorded from different micro-habitats of the Nilgiri Foothills, Tamilnadu; (a) *Argiope aemula* (b) *Argiope anasuja* (c) *Gasteracantha geminata*, (d) *Telamonia dimidiata*, (e) *Hersilia savignyi* (f) *Hamataliwa* sp. (g) *Leucauge decorata* (h) *Carrhotus viduus* (I) *Olios milleti*, (j) *Uloborus* sp. (k) *Oxyopes shweta* (l) *Peucetia viridana* (m) *Myrmaplata plataleoides* (n) *Corinnomma severum* (o) *Cyrba ocellata* (p) *Langona tigrina* (q) *Nephila pilipes*, (r) *Phintella vittata* (s) *Stenaelurillus lesserti* (t) *Olios lamarcki*, (u) *Bianor balius* (v) *Thyene imperialis*, (w) *Menemerus bivittatus* (x) *Tetragnatha* sp

REFERENCES

Bhat S, Srikumar KK and Raviprashad TN 2013. Seasonal diversity and status of spiders (Arachnida: Araneae) in cashew ecosystem. *World Applied Science Journal* **22**(6): 763-770.

Caleb JTD and Karthikeyani R 2021. JoTT Checklist of the spiders of Tamil Nadu (v1.0), 10 February 2020. https://threatenedtaxa.org/index.php/JoTT/checklists/spiders/TamilNadu. Accessed on 16.03.2021.

Hammer O, Harper DAT and Ryan PD 2001. PAST: Paleontological statistical software package for education and data analysis. *Palaeontologia Electronica* **4**(1): 1-9.

Karthikeyani R, Caleb JTD, Gajbe UA and Muthuchelian K 2017. Checklist of spiders (Arachnida: Araneae) of the State of Tamil Nadu, India. *Munis Entomology & Zoology* **12**(1): 180-193.

Krishnaveni K and Kandeepan C 2018. Biomonitoring of diversity and compostition of spider collection at Sirumalai hills, Dindigul district, Tamil Nadu. *International Journal of Zoology Studies* **3**(1): 44-47.

Mahalakshmi R and Jeyaparvathi S 2014. Diversity of spider fauna in the cotton field of Thailakulam, Virudhunagar District, Tamil

Nadu. *International Journal of Zoology Studies* **1**(1): 12-18.

Mondal A, Chanda D, Vartak A and Kulkarni S 2020. *A Field Guide to the Spider Ganera of India*, Ayan Mondal, Burdwan, West Bengal, India, p 408.

Nobre T, Carolia M and Oliveira N G 2000. Comparison of sampling techniques for vineyard foliage spiders (araneae). *Ekologia (Bratislava)* **19**(3): 201-206.

Rain FF, Howlader AJ and Bashar K 2016. Diversity and abundance of spider fauna at different habitats of Jahangirnagar University Campus, Bangladesh. *Journal of Entomology and Zoology Studies* **4**(5): 87-93.

Sebastian P A and Peter K V 2009. *Spiders of India*, University Press (India) P.L., Hyderabad, India, p 614.

SPSS 2007. SPSS for Windows, version 16.0. Chicago, SPSS. Inc.

Tikader BK 1970. Spider fauna of Sikkim. Rec. *Zoological Survey of India* **64**: 1-83.

Tikader BK 1977. Studies on spider fauna of Andaman and Nicobar Islands, Indian Ocean. Rec. *Zoological Survey of India* **72**: 153-212.

Tikader BK 1980. Thomisidae (Crab-spiders). Fauna of India (Araneae)**.** *Zoological Survey of India* **1**: 1-247.

Tikader BK 1982. Family Araneidae (Argiopidae), typical orb weavers - Fauna of India (Araneae). *Zoological Survey of India* **2**: 1-293.

Tikader BK 1987. *Handbook of Indian Spiders*, Zoological Survey of India, Culcutta, p 251.

Torre-Cuadros MDLAL, Herrando-Perez S and Young KR 2007. Diversity and structure patterns for tropical montane and premontane forests of central Peru, with an assessment of the use of higher-tax on surrogacy. *Biodiversity and Conservation* **16:** 2965-2988.

Uetz GW, Halaj J and Cady AB 1999. Guild structure of spiders in major crops. *Journal of Arachnology* **27:** 270-280.

World Spider Catalog 2021. *World Spider Catalog*. Version 22.0. Natural History Museum Bern, online at http://wsc.nmbe.ch, accessed on {16.03.2021}. doi: 10.24436/2.

Yadav VK, Chauhan PS, Revathi R and Chauhan DS 2018a. Diversity of spiders in Forest College and Research Institute, Nilgiri Foothills, Western Ghat, Mettupalayam, Coimbatore, Tamil Nadu, pp. 113. **In:** *National Conference on Livelihood and Food Security (LFS-2018)* 27-28 January, 2018 at Bihar Veterinary College, Patna.

Yadav VK and Chauhan PS 2018b. Avifaunal diversity and status of Jhalawar Forest Division, South-Eastern Rajasthan, India. *Indian Journal of Ecology* **45**(1): 107-116.

Received 12 July, 2021; Accepted 12 November, 2021

Indian Journal of Ecology (2021) 48(6): 1715-1720

Manuscript Number: 3437
NAAS Rating: 5.79

Diversity of Weed Flora in Citrus of the Oranian Phytogeographical Sector

Karima Hanitet, Nadia Bemmansour[1] and Zoheir Mehdadi

Plant Biodiversity Laboratory: Conservation and Valorization, Faculty of Natural and Life Sciences, Djillali Liabes University, Sidi Bel Abbès 22000, Algeria
[1]Laboratory of Genetics and Plant Improvement, Faculty of Biological Sciences and Agricultural Sciences, Mouloud Mammeri University, Tizi Ouzou, Algeria
E-mail: karihan213@gmail.com

Abstract: The study of citrus weeds in citrus groves in the north-western tell of Oranie (western Algeria) is based on 200 phytoecological surveys carried out in different sites , taking into account certain agro-ecological variables according to the round-field sampling method. The flora recorded in all the sites in our study area includes 101 weed species belonging to 31 families and 87 genera. The species inventoried are mainly represented by therophytes, whose presence rate is estimated at 74.5%, reflecting unfavourable climatic conditions. Phytogeographical, the species inventoried belonging in particular to the Mediterranean element have a present rate of 43%. The weeds inventoried are classified according to their frequency and abundance. The analysis of the agronomic importance of the species based on their relative frequency and average coverage has been established. The projection of species on an infestation diagram made it possible to differentiate between 6 groups of species.

Keywords: Weeds, Citrus groves, Phytoecological surveys, Tell North Oranian, Thérophytes, Biological types

Among the many pests of crops, weeds play a very important role. The term weed is accepted as a synonym, although its botanical meaning refers to a plant accidentally introduced without the knowledge of man. Weeds or weeds compete with the plants we want to develop. In some cases, their seeds contaminate the crop and reduce its value. Losses caused by these weeds are estimated at 9.7% of world agricultural production and are in the order of 10 to 56% in Africa. However, numerous researches carried out to highlight the influence of weeds in crops have highlighted the existence of constantly evolving relationships related to different parameters: climatic conditions, cultivation techniques used, type of crop, and especially type of infestation and weed emergence period (Traoré and Mangara 2009). Abdelkrim (2004) and Kazi Tani (2010) carried out the most important phytosociological works on weeds in perennial crops (orchards and vineyards) in Algeria to characterize them botanically, ecologically and agronomically. It also aims to understand how this flora develops and spreads under the effect of the natural environment. In present study the relationships that may exist between weeds and the environment is assessed in the most discriminating descriptors of the environment in terms of their distribution.

MATERIAL AND METHODS

Study area: The study area is part of the Oranian (western Algeria) phytogeographic sector where five sampling sites were selected: Oran, Mohammadia, Sig, Tlemcen, and Maghnia (Fig. 1). In general, the climate of the five study sites is semi-arid with a temperate winter, with mean annual rainfall ranging from 246.5 to 332 mm. The mean annual maximum temperature (M) is 34.21°C. The mean annual temperature is 18°C. The hottest month is August with 32.1°C and 33.53°C for Oran and Tlemcen and July with 34.87°C and 36.38°C for Maghnia and Mascara respectively. The coldest month is January with 5.40°C for Oran, 5.33°C for Tlemcen, 4.23°C for Maghnia and 4.12°C for Mascara. The dry season lasts 7 to 8 months from spring to autumn.

Inventory of the weed flora: For the inventory of the weed flora, 200 phytoecological surveys over the entire study area (Oran, Mascara, Mohammedia, Sig, and Tlemcen), in citrus orchards, during the spring period of the year 2015-2016 were carried out to take into account the variability of ecological and agronomic factors. The floristic survey technique used was the field tour technique, which provides information on the various species in the plot (Lebreton et al 2005). The surveys were carried out on representative areas of about 100 m^2 (minimum area) that were homogeneous from a floristic standpoint. Each species inventoried is assigned an abundance-dominance coefficient (from + to 5). The inventoried species were distributed according to botanical family, Raunkiær biological type, and biogeographical status using the new flora of Algeria and the southern desert regions

of Quézel and Santa (1962-1963) and the weed species of Mamarot and Rodriguez (2014). The abundance-dominance index was transformed into mean and soil cover (%) according to the scales mentioned in Table 1.

The dominance of a species is the surface area covered by it, hence its total abundance (Kazi Tani 2011). To calculate species dominance, transformed the abundance-dominance coefficients of Braun-Blanquet (1951) and modified by Marnotte (1984) to obtain the soil cover (%) for each weed species. Concerning the "major and minor weeds" method of Baker (1974) and Guillerm (1990) was followed and adapting the classes defined by Le Bourgeois and Guillerm (1995). The projection of species on a graph with the relative frequency on the abscissa and the mean abundance on the ordinate (both of which represent a fundamental concept in weed science), makes it possible to differentiate between species according to their degree of infestation and therefore their agronomic importance. The mean abundance of a species in a set of surveys is represented by its mean abundance/dominance index, AD moy(e). This corresponds to the average of the abundance/dominance indices of the species AD(e), calculated with the number of surveys in which the species is present N rel (e). The abundance/dominance index is an index from 1 to 100 corresponding to the ground cover scale. The use of an average index gives the species a weight similar to that shown on the graph, and makes it easy to delineate the areas corresponding to the different groups.

Soil analysis: The physico-chemical parameters were determined from soil samples taken at a depth of approximately 10 cm from each study site: texture, pH, electrical conductivity, organic matter content, active limestone content, and total nitrogen content.

Data analysis: The data obtained were processed by correspondence factor analysis (C.F.A.) to highlight possible correlations between the species identified in study sites (ecological and pedological parameters). These parameters make it possible to specify the ecological and pedological conditions that contribute to the composition of weed groups in the study area.

RESULTS AND DISCUSSION

Weed fauna: Across the study area, identified 101 weed species belonging to 87 genera and 31 families (Fig. 2). The family Poaceae is the most species-rich with 17 species or 16.83 % of the total number, followed by the family Asteraceae with 13 species or 12.87 % and the families Brassicaceae and Fabaceae with 9 species or 8.91 % and the family Apiaceae with 6 species or 5.94 %. The other families are divided between 1 and 4 species with a contribution of 0.99% to 3.96%. From a floristic point of view, weed flora is characterized by a relatively large number of families. The main families recorded in our study area are Asteraceae, Fabaceae, and Poaceae. These same families are also the most represented in the Oranian weed flora (Kazi Tani, 2010) and the Indian citrus weed flora (Kiran Kumar and Kiran Babu 2019). The presence of Poaceae in the middle of an annual crop induces more complex competition for water, nutrients, and light resources and also makes possible chemical or cultural control of these weeds difficult (Fenni 2003). These results are very close to those reported by Hseini et al (2007) showing that the Asteraceae family still occupies the top ranks with 601 species in the spontaneous flora of Morocco.

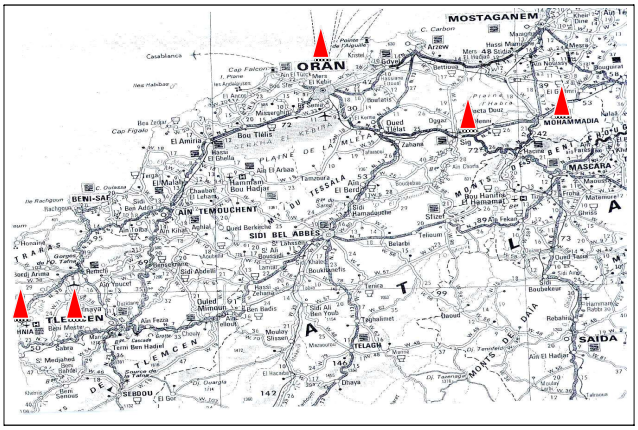

Fig. 1. Location of sampling sites (red triangles). Geographic map of Oranie from the National Institute of Cartography of Oran (1/500 map)

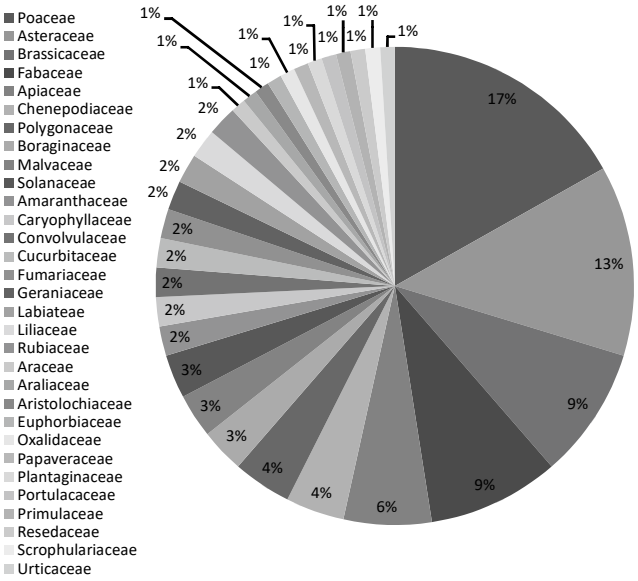

Fig. 2. Global spectrum of the main families identified in our study region

The presence of Poaceae in the middle of an annual crop determines more complex competition phenomena in terms of water, nutrients and space factors, and also makes possible chemical or cultural control of these weeds difficult (Fenni 2003). *Fabaceae* have a strong competition for water from the crop, due to their deep root system, and also allow high nitrogen availability in the soil (Fenni 2003). This family is represented in the Algerian flora by 55 genera (Hannachi 2010). In addition to these, *Brassicaceae*, *Caryophyllaceae*, *Apiaceae*, and *Boraginaceae* are also well represented in the (agricultural) weed flora of Oran, where they maintain more or less the same ranking order as in the Algerian flora (Kazi Tani et al 2010).

Biogeographic distribution: Phytogeographical, the weed flora of the Oranie is characterized by a heterogeneous set of elements of very diverse origin. The 101 species in the floristic list are divided into 28 class's characteristic of one or more regions. The study of the biogeographical affiliation of the weeds listed shows that the strict Mediterranean element is dominant with 27 Mediterranean species, i.e. 26.73% of the total number, followed by the Mediterranean-Irano-Turanian species 15, i.e. 14.85%, and 9 cosmopolitan species represented by 8.91% of the total number. The European-Mediterranean was with 5.94% of species, European-Siberian-Mediterranean and Paleo-Temperate with 4.95% of species, Eurasian with 3.96% species and the North American element, Thermocosmpolite with 2.97% species. The other biogeographic elements are very poorly represented. The importance of Mediterranean elements in the weed flora of our zone confirms the fact that the studied area belongs to the Mediterranean flora and these results are similar to the study of crop weed communities in the phytogeographic sector of Oran by Kazi Tani (2010). The relative importance of Eurasian, a paleo-temperate, and cosmopolitan element in the weed flora of crops in the Mediterranean basin was also observed by Fenni (2003).

Table 1. Transformation of abundance-dominance into percent coverage and ground cover

Abundance-dominance index	Overlay class	E.C.E.B	Ground cover (%)	Average recovery (%)
+	0-1	1	1	0,5
1	01-10	2	7	5.5
2	10-25	3	15	17,5
3	25-50	5	50	37,5
4	50-75	7	85	67,5
5	75-100	9	100	87,5

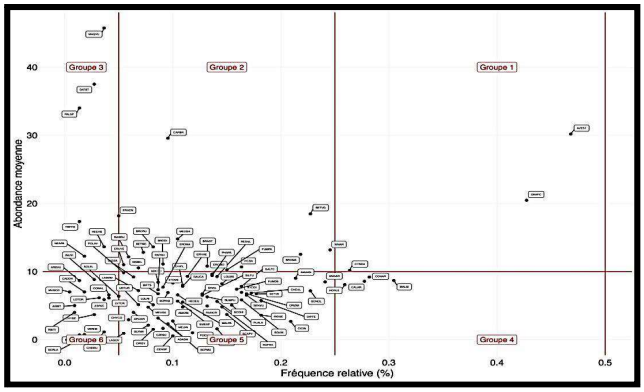

Fig. 3. Species infestation diagram (Species are represented by their OPPO code)

Global biological spectrum: The dominance of therophytes in all the sites visited is about 72.27% of the total number. This contribution is lower than that previously established at 69% for citrus flora in eastern Morocco (Chafik 2013),the therophytes are75 % in Oranian (KaziTani *et al* 2010) and Rachgoune and Oulhassa Region of Tlemcen Algeria 45% (Ghalem and Hassani 2020).The geophytes are represented by 15 species, i.e. 14.85% of the total population. Hemicryptophytes and chamephytes constitute 10.89 and 0.99% respectively. In most cases of geophytes, vegetative propagation becomes their only mode of survival. *Cynodon dactylon* L is one of the main perennial weeds that pose a problem for arboriculture (Fenni, 2003). Although tillage perfectly destroys woody species (phanerophytes and chamephytes) or herbaceous stumpy species (hemicryptophytes), it has a much more nuanced action on biological types adapted to disturbances such as perennials with high vegetative multiplication power (geophytes) or especially annual plants (therophytes). For the latter, the destructive action is largely offset by the beneficial effect of burying the seeds. Benarab (2007) mentioned that therophytes complete their cycles very quickly, taking advantage of the spring rains to germinate, and they complete their cycle before the summer drought and thus spend the summer and winter as seeds. This high rate of annuals indicates cultural habitats that are often disturbed by agronomic interventions (Fenni, 2003). Repeated tillage tends to eliminate perennial species in the annual profile. Hammada (2007 observed that abundance of therophytes can be due to seasonal submerged habitats, conducive to the development of annual plants with rapid germination and growth.

Agronomic importance of species: The analysis of our weeds allowed us to distinguish 6 groups of species reflecting their potential for harmfulness and therefore their agronomic importance (Fig. 3 , Table 2).

Group 1: General major weeds: These are the most harmful species in the region (very common species due to

Table 2. Agronomic importance of the main weed species

Code Bayer	*Espèces*
Group 1: General major weeds	
AVEST	*Avena sterilis*L.
OXAPC.	*Oxalis cernua* Thumb
CYNDA	*Cynodon dactylon*L.
Group 2: Major regional weeds	
SINAR	*Sinapis arvensis*L.
BETVG	*Beta vulgaris*L.
BROMA	*Bromus madritensis*L.
VICSA	*Vicia sativa*
FUMPA	*Fumaria parviflora* Lamk
BRADT	*Brachypodium distachyum* L.
MEDPO	*Medicag ohispida*Gaertn.
BRODI	*Bromus rigidus* Roth
BRORU	*Bromus rubens* L
BETMC	*Beta macrocarpa*Guss
EKBEL	*Ecballium elaterium* Rich
RASRU	*Rapistrum rugosum*L
ERUVE	*Eruca vesicaria*L
ERACN	*Eragrostis cilianensis* All
CAPBR	*Capsella bursa-pastoris* L
Group 3: Major local weeds	
DATST	*Datura stramonium* L
HEEHE	*Hedera helix* L
NEAPA	*Neslia paniculata* L
MAQVU	*Marrubium vulgare* L
PALSP	*Pallenis spinosa*L
TRRTO	*Trifolium tomentosum L.*
Group 4: General weeds	
MALSI	.*Malva sylvestris* L
CONAR	*Convolvulus arvensis* L
CALAR	*Calendula arvensis* L
HORLE	*Hordeum murinum* L
Group 5: Regional weeds	
ANGAR	*Anagallis arvensis*L
AMAAN	*Amaranthus angustifolius* Lamk
SONOL	*Sonchus oleraceus* L
CICIN	*Cichorium intybus* L
DIPTE	*Diplotaxis tenuifolia* L
RAPRA	*Raphanus* raphanistrum L
SOLNI	*Solanum* nigrum L.
RIDSE	*Ridolfia segetum*Moris
ORZMI	*Oryzopsis miliacea* (L.
CHEAL	*Chenopodium album* L
GALTC	*Galium tricorne* Witth
FUMDE	*Fumaria densiflora* DC
SETVE	*Setaria verticillata* (L.) P.B
SCAPV	*Scandix pecten-veneris* L
PLALA	*Plantago lanceolata* L
SENVU	*Senecio vulgaris* L
BYODI	*Bryonia dioica* Jacq
SILFU	*Silene fuscata* Link

Cont...

Table 2. Agronomic importance of the main weed species

Code Bayer	*Espèces*
LOLMU	*Lolium multiflorum* Lam
SINAL	*Sinapis alba* L
RUMPU	*Rumex pulcher* L
SCOHI	*Scolymus hispanicus*
MALPA	*Malva parviflora* L
SCPMU	*Scorpiurus muricatus* L
FOEVU	*Foeniculum vulgare* Mill
EMESP	*Emex spinosa* L.
RUMCR	*Rumex crispus* L
STEME	*Stellaria media* L
HEOEU	*Heliotropium europaeum* L
AMARE	*Amaranthus retroflexus* L
MEUIN	*Melilotus indica*L.
ASASM	*Astragalus sesameus* L
CENSP	*Centaurea sphaerocephala* L
CZRSC	*Coronilla scorpioides* Koch
MEUSU	*Melilotus sulcata* Des
SORHA	*Sorghum halepense* L.
BIFTS	*Bifora testiculata* Roth
ABKDO	*Arundo donax* L
URTUR	*Urtica urens* L
APUGR	*Apium* gravolens L.
SLYMA	*Silybum marianum* L.
CIRSY	*Cirsium syriacum*L.
CHYCO	*Chrysanthemum coronarium* L
DIGSA	*Digitaria sanguinalis* L
POLAV	*Polygonum aviculare* L.
LAMAM	*Lamiumam plexicaule* L.
EROMA	*Erodium malachoides* L.
EHIPL	*Echium plantagineum* L
EROMO	*Erodium moschatum* Burm.
PHAPA	*Phalaris paradoxa* L
RESAL	*Reseda alba* L
SOLEL	*Solanum eleagnipholium var*
LAGOV	*Lagurus ovatus* L
POROL	*Portulaca oleracea* L
Group 6: Minor weeds	
CHEMU	*Chenopodium* murale L
SCRLA	*Scorzonera laciniata* L
BOROF	*Borago officinalis* L
VERHE	*Veronica hederaefolia* L
RBITI	*Rubia tinctorum*
CHYSE	*Chrysanthemum segetum* L.
ARIBT	*Aristolochia boetica*
ASPAC	*Asparagus acutifolius* L
LOTOR	*Lotus ornithopodioides* L
CADDR	*Lepidium draba* L
LVTCR	*Lavater acretica* L
ARSVU	*Arisarum vulgare* Targ.-Tozz
INUVI	*Inula viscosa* L
CHEAL	*Chenopodium album* L
MUSCO	*Muscari comosum* L

great adaptation to the agricultural environment which gives them a very high potential for invading particularly *Avena sterilis* L., *Oxalis cernua*, and *Cynodon dactylon*.

Group 2: Major regional weeds: These are species with wide or medium ecological amplitude whose presence is linked to ecological factors of a regional nature (crop, soil, and climate). Their abundance is regularly high, conferring them the status of species frequently codominant of the communities in which they participate. This group consists of 15 species including *Sinapis arvensis*, *Beta vulgaris, Bromus madritensis, Vicia sativa, Fumaria parviflora, Brachypodium distachyum, Medicago hispida, Bromus rigidus, Bromus rubens, Beta macrocarpa, Ecballiume laterium, Rapistrum rugosum. Eruca vesicaria , Eragrostis cilianensis , Capella bursa-pastoris.*

Group 3: Major local weeds: They have a very narrow ecological range. They only occur in certain environmental conditions that are poorly represented and for which they are ecological indicators. In these environmental conditions, they are very abundant and constitute an important agronomic constraint, namely *Datura stramonium, Hedera helix, Neslia paniculata, Marrubium vulgare , Pallenis spinosa* and *Trifolium tomentosum.*

Group 4: General weeds: They are very ubiquitous but do not pose any particular problem in the current phytotechnical context. They are species to be monitored, due to their wide distribution, when the context is modified by an evolution of the cropping system that could lead to a disruption in interspecific competitive relationships. *Hordeum murinum*, a xerophilic and nitrophilic species present in all types of soils and all types of crops.

Group 5: Regional weeds: They have average ecological amplitude but do not constitute an agronomic constraint due to their limited abundance. On the other hand, they can serve as indicators of regional ecological conditions. *Reseda alba* and *Cichorium intybus*, are clearly related to orchards. *Sinapis alba*, was more ruderal and xerophilic than arvicultural. It has become more infested probably because of the prolonged drought of the last 30 years.

Group 6: Minor weeds: They are infrequent and scarce and are in no way a hindrance to cultivation. They are rare, foreign, pioneer, or residual species from a previous situation, quite often heritage species to maintain biodiversity. They can be inferred from ecological conditions that are very poorly represented, which gives them the status of indicator species.

The analysis of the agronomic importance of weed species is studied based on the relationship between relative frequency and mean species abundance. The most damaging agronomic species were *Avena sterilis* L., *Oxalis cernua* and *Cynodon dactylon. Cynodon dactylon* is a thermophilic species that prefers dry, bright, and very warm silty to sandy loamy soils in orchards and vineyards. the latter species is very drought resistant and that its rhizomes, which are difficult to eradicate, can survive up to a moisture content of about 10% of their total weight, which has made it one of the most threatening exotic weeds (originally introduced as a forage plant) for agriculture in subtropical regions (e.g. South Africa) .*Convolvulus arvensis* is ranked among the top fifteen "weeds" of spring and summer crops (Kazi tani 2011). Traoré and Mangara (2009) observed climate is the dominant abiotic factor in the distribution of species, followed by soil type, rainfall, substrate type and texture. *Papaver rhoeas* is classified by Fried et al (2008) as an indicator species of cultural practices and not of soil-climatic conditions. *Papaver rhoeas* is frequent and abundant in the southern zone of Skikda, which is a somewhat dry area, is almost absent in the northern zone (Hannachi, 2019). The presence of *Plantago* indicates clayey, acidic, and poorly drained soil. The development of appropriate weed control techniques requires knowledge of the composition of the weed flora (Lebreton and al 2005). However, Fried et al (2008) found that soil pH and texture are the most important factors structuring weed communities in temperate regions (France). Some studies have pointed out that agricultural practices are the main driver for weed diversity and abundance in agro-ecosystems (Rauber et al 2018 in Al-Qahtan 2018).Among the indicator species for cultural practices and not soil and climate conditions, the presence of *Plantago* indicates clay, acidic and poorly draining soil are key factors. Clavien and Delabays (2006) concluded that these, benefits from long-lasting seed dormancy potential and seeds are produced in large quantities.

CONCLUSION

The study of the agronomic importance of weeds allowed us to distinguish 6 groups of species reflecting their pest potential, it highlighted the species of greatest concern in citrus orchards. These are particularly *Avena sterilis, Oxalis cernua*, and *Cynodon dactylon*. The intensification of agriculture has created new conditions for which few weed species are equipped. However, the process of adjustment to these new environmental conditions has recently started. Through this work, knowledge was built up on weeds in the Oranie and would be desirable to further develop it by expanding the sampling area, increasing the number of surveys and exploring different crops (olive groves, fruit trees, vines, cereals, field vegetable crops and greenhouse crops) and fallow land.

REFERENCES

Abdelkrim H 2004. Contribution à l'étude écologique et phytosociologiques des adventices des cultures et des jachères dans le secteur phytogéographique de l'Algérois (Algérie). *Phytocoenologia* **34**(2): 287-326.

Al-Qahtani SM 2018. Effect of soil properties on the diversity and distribution of weeds in citrus farms in Arid Region of Saudi Arabia, *Applied Ecology and Environmental Research* **17**(1): 723-732.

Benarab H 2007. *Contribution à l'étude des mauvaises herbes des vergers de la région nord de Sétif.* Thèse Magister, Biol. Vég., UFA, Sétif, 73p.

Braun-Blanquet J 1951. *Pflanzensoziologie* (2eéd.). Springer, Vienne, 631 p.

Chafik Z, Taleb A, Bouhache M and Berrichi A 2013. Weed flora of western Morocco agrosystems: case of the Moulouya perimeter. *Revue Marocaine de Protection des Plantes* **4**: 27-44.

Clavien Y and Delabays N 2006. Inventaire floristique des vignes de Suisse romande: connaître la flore pour mieux la gérer. *Revue suisse Vitic. Arboric. Hortic* **38** (6): 335 341.

Fenni M 2003. *Etude des mauvaises herbes des céréales d'hiver des hautes plaines constantinoises. Ecologie, dynamique, phénologie et biologie des bromes*. Thèse doctorat d'état, Université de Sétif, p 165.

Fried G, Norton LR and Reboud X 2008. Environmental and management factors determining weed species composition and diversity in France. *Agriculture*, *Ecosystems* and *Environment* **128**: 68-76.

Fried G, Chauvel B and Reboud X 2008. Évolution de la flore adventice des champs cultivés au cours des dernières décennies : vers la sélection de groupes d'espèces répondant aux systèmes de culture. *Innovations Agronomiques* **3:** 15-26.

Ghalem S and Hassani F 2020. Phytobiological and morphological diversity of a *Malvaceous Lavatera* Maritima in Rachgoune and Oulhassa Region of Tlemcen Algeria. *Indian Journal of Ecology* **47**(2): 575-578.

Hammada S 2007. *Etude sur la végétation des zones humides du Maroc. Catalogue et Analyse de la Biodiversité Floristique et Identification des principaux Groupements Végétaux.* Thèse Doc En Sci. Eco. Univ MOHAMMED V – AGDAL, Faculté des sciences, Rabat, 187p

Hannachi A 2019. Ecological study for groups of citrus weeds in the Skikda region, Algeria, *Journal of Research in Weed Science* **2:** 216-223

Hannachi A 2010. *Étude des mauvaises herbes des cultures de la région de Batna :Systématique, Biologie et Écologie*. Mag. Agro. Univ Ferhat Abbas-Setif UFAS (ALGERIE). Faculté des sciences dept : agro.124 p

Hseini S, Kahouadji A, Lahssissene H and Tijane M 2007. Analyses floristique et ethnobotanique des plantes vasculaires médicinales utilisées dans la région de Rabat (Maroc occidental). Département de Biologie, Faculté des Sciences. Univ Mohammed V. Agdal, Rabat, Maroc, *LAZAROA*, pp 93-100

Kiran Kumar K and Kiran Babu P 2019. Diversity of Weed Flora in Citrus at ICAR-Regional Research Centre for Citrus, Biswanath Chariali, Assam, India. *International Journal of Current Microbiology and Applied Sciences* **8**(4): 2100-2107.

Kazi Tani C 2011. *Contribution à l'étude des communautés d'adventices des cultures du secteur phytogéographique oranais (Nord-Ouest algérien): Aspects botanique, agronomique et phyto- écologique*. Thèse Doc. En Sc., Univ. Tlemcen, Algérie, p227 + Annexes.

Kazi Tani C, Le Bourgeois T and Munoz F 2010. Contribution à l'étude des communautés d'adventices des cultures du secteur phytogéographique Oranais (nordouest algérien): Aspects botanique, agronomique et phyto-écologique. *Flora Mediterranea,* **20** : 29-46.

Lebreton G and LE Bourgois T 2005. Analyse de la flore adventice de la lentille à Cilaos – Réunion. *Cirad*-Ca / 3P ; UMR PVBMT, 20 p.

Mamarot J and Rodriguez A 2014. *Mauvaises herbes des cultures*. 4emeEd ACTA. Paris (France), 569 p.

Rauber RB, Demaría MR, Jobbágy EG, Arroyo DN and Poggio SL 2018. Weed communities in semiarid rainfed croplands of Central Argentina: comparison between corn (Zea mays) and soybean (Glycine max) crops. *Weed Science* **66**: 368-378.

Traoré and Mangara 2009 . Étude Phytoécologique des Adventices dans les Agro Écosystèmes Oléicoles de la Mé et de Dabou. *European Journal of Scientific Research* ISSN1450-216X 31 **4**: 519-533.

Received 23 May, 2021; Accepted 05 November, 2021

Indian Journal of Ecology (2021) 48(6): 1721-1725

Manuscript Number: 3438
NAAS Rating: 5.79

Clonal Variation in Gas Exchange Traits Linked to Water Use Efficiency in Eucalyptus

M. Karthikeyan, K.T. Parthiban[1], P. Boominathan, S. Umesh Kanna and C. Cinthia Fernandaz

Department of Agroforestry, [1]Forest College and Research Institute
TNAU, Mettupalayam-641 301, India
E-mail: karthikeyanforestry@gmail.com

***Abstract*:** Eucalyptus is the most widely planted species around the tropics for its potential as a raw material for pulp and paper, plywood and other wood related products. With declining rate of fresh water resources around the globe and rising demand for wood and wood-related products from the industries, there is an increased need to develop genotypes or clones with higher water use efficiency (WUE) leading to enhanced biomass accumulation per unit amount of water transpired. Eucalyptus proves to be a sustainable species which could meet out the wants and needs of industrial sector in a short interval. Although Eucalyptus is known for its multifarious utility, there is a huge concern over its water use efficiency and the associated genetic resources. Against this background, fifteen superior eucalyptus clones were used to study the genetic variation in gas exchange and physiological traits linked to water use efficiency including intrinsic WUE, instantaneous WUE and intrinsic carboxylation efficiency that provides a baseline information for the selection of clones suitable for arid and semi-arid regions. Significant variation was observed for physiological traits among the fifteen clones wherein, the clone EU UG 10 was found to be superior with enhanced net photosynthetic rate (An) coupled with WUE, followed by the clone ET 46. Besides, it also showed higher instantaneous WUE over the other clones. Thus, identified clones will be suited for water limited condition by producing higher biomass per unit amount of water transpired. This study also demonstrated the variability among the clones for physiological traits associated with gas exchange parameters which forms basis for further advancement in the tree improvement program.

***Keywords*:** Eucalyptus, Clonal variations, Gas exchange parameters, Water use efficiency

Eucalyptus species has long been inseparable from the commercial race owing to its potential usage as a prime source of raw material for many products and could thrive along varying environmental gradients which make it an environmentally and commercially sustainable species. Projections on climate change stipulates an increase in global mean temperature and CO_2 levels, erratic precipitation pattern and uneven global surface temperature which concomitantly increases the surface evaporation resulting in the limitation of atmosphere and soil water holding capacity (Hatfield and Dold 2019). Diminishing fresh water supplies and increase in frequent drought periods around the world, enabled the researchers to develop better drought tolerant genotypes without compromising biomass productivity. Although several physiological traits proclaim to have a pivotal role in drought tolerance, WUE seems to be pertinent that produces higher biomass per unit amount of water transpired. Plant level carbon and water balance are indicated by water use efficiency (WUE), which is defined as the carbon assimilation to water loss ratio (Kang and Kang 2019). Information on water use efficiency for various crops such as rice, millets, maize are enormous compared to tree species in which physiological traits linked to water use efficiency is inadequate. Due to the difficulty in meeting out the raw material demand from pulp, paper and plywood industry in short term, development of highly productive clones with higher biomass with efficient water use through genetic improvement program is imperative (Vijayakumar et al 2015). The clones which are closely related can show variations for their physiological traits the proportion of the biomass produced since the variation is resulted from genetic and environmental interaction. Both interspecific and intraspecific genotypes may have enough trait variation that paves way for various unique features within and between the them (Boyden et al 2008). Eucalyptus being second most widely planted species around the globe could meet the demand of such industries which prevail to be a significant source of biomass as an exotic tree in the tropics. However, the potential productivity and WUE raise concern over the commercial aspects of this species (Kaur and Monga 2021). Response of plants in-terms of physiological process to varying environmental gradients and changing climate could be instantaneously revealed at the leaf-level (Hatfield and Dold 2019). Leaf-level gas exchange parameters found to be the best method for determining the real-time measurement in physiological traits, which includes photosynthetic rate,

stomatal conductance, transpiration rate, instantaneous WUE, intrinsic WUE. Hence, the study was conducted among the selected clones of eucalyptus to find the variation for leaf gas exchange parameters and physiological traits linked to water use efficiency.

MATERIAL AND METHODS

The experiment was conducted with fifteen eucalyptus clones as a pot culture study at Forest College and Research Institute, Mettupalayam located at 11˚ 19'N latitude and 77˚ 56'E longitude. The gas exchange parameters were measured using an infrared gas analyzer (IRGA, LI-6400XT, LI-COR Biosciences, USA). Fifteen different clones from four different species *viz. Eucalyptus camaldulensis, Eucalyptus tereticornis, Eucalyptus hybrid* and *Eucalyptus urograndis* were taken and grown under well-watered conditions. Observations were taken between 9.30 a.m. and 11.30 a.m. The physiological parameters such as net photosynthetic rate (An), stomatal conductance (g_s), transpiration rate (E) and intercellular CO_2 concentration (Ci) were observed using portable photosynthesis system. Intrinsic WUE (iWUE) was calcaulted from net photosynthetic rate (An) to stomatal conductance (g_s) and ratio of net photosynthetic rate (An) and the transpiration rate (E) was used to calculate the instantaneous WUE of a plant. Besides, intrinsic carboxylation efficiency was also measured using ratio of net photosynthetic rate (An) and the intercellular CO_2 concentration (Ci). The experiment was carried out in a completely randomized block design following the standard procedure.

RESULTS AND DISCUSSION

Greater variability for net photosynthetic rate (An) (µmol/m^2 /s): Net photosynthetic rate (An) (µmol/m^2/s) is an important physiological parameter which determining the dry matter accumulation in plants. The photosynthetic rate differs among the plants belonging to different taxa between varieties and within the same species. In this study, the data revealed that the eucalyptus clones differed significantly due to various physiological traits. Among the clones, the net photosynthetic rate ranged between 13.91- 20.05 µmol/m^2/s and observed to be higher in the clone EU UG 10 and lower in EH 05 (Table 1) compared to other clones. Warrier and Vekataramanan (2010) reported that the net photosynthetic rate (An) among the fifty-nine eucalyptus clones was ranged between 10.05 to 37.80 µmol/m^2/s. The change in net photosynthetic rate may be attributed to the influence of surrounding air temperature and the CO_2 concentration gradient that could modulate the rate of transpiration and stomatal conductance which in turn affects the ary matter accumulation (Zhang 2020). The photosynthetic rate differed among different ages, groups and also the changes in photosynthetic response curve was better observed on *Eucalyptus globulus* and *Eucalyptus nitens*, while the former had narrower photosynthetic response than the latter which

Table 1. Key physiological parameters of selected *Eucalyptus* clones

Clones	Net photosynthetic rate (An) (µmol m^{-2} s^{-1})	Stomatal conductance (g_s) (mol m^{-2} s^{-1})	Transpiration rate (E) (mmol m^{-2} s^{-1})	Leaf temperature (˚C)
EH 01	18.65^{b}	0.34^{c}	11.63^{j-k}	33.27^{g}
ET 46	19.73^{a}	0.45^{a}	6.67^{b}	33.52^{e-f-g}
ET 56	17.31^{d-e}	0.40^{ab}	9.77^{g}	33.43^{f-g}
ET 03	16.54^{e-f}	0.43^{a}	11.00^{h}	33.92^{e}
ET 01	17.07^{d-e}	0.42^{a}	12.07^{k}	33.80^{e-f}
EH 02	15.57^{g}	0.34^{b-c}	11.30^{h-j}	34.68^{d}
EH 03	18.42^{b-c}	0.26^{d-e}	9.47^{f-g}	35.47^{c}
EH 04	15.98^{f-g}	0.12^{g}	8.08^{c-d}	36.34^{b}
EC 07	17.78^{c-d}	0.24^{d-e}	8.58^{d-e}	34.56^{d}
EC 413	18.27^{b-c}	0.21^{e-f}	11.00^{h}	33.46^{e-f-g}
EH 05	13.91^{h}	0.27^{d}	7.69^{c}	35.18^{c}
E 13	18.25^{b-c}	0.23^{d-e-f}	9.09^{e-f}	36.51^{b}
DF 97	15.72^{f-g}	0.14^{g}	11.63^{j-k}	36.36^{b}
EUUG 10	20.05^{a}	0.44^{a}	4.37^{a}	38.78^{a}
EUUG 11	15.25^{g}	0.17^{f-g}	8.37^{d}	36.51^{b}
S. Ed	0.41	0.03	0.28	0.22
CD (p=0.05)	0.83	0.06	0.57	0.46

Means followed by small superscript letter in a column do not differ significantly as per DMRT (p≤0.05); All the values are means of 3 replications

had better response over the optimum growth temperature indicating different acclimation trajectory under different growth environments viz. green house and field grown plants (Battaglia and Loughhead 1996).

Effect of leaf temperature on stomatal conductance (mol/m/s): Stomatal conductance (g_s) is considered as vital trait that correlates with net photosynthetic rate (An) and also found to be good indicator of plant water status/stress (Urban et al 2017). In the present study, the stomatal conductance significantly differed among the clones and values ranged between 0.12 mol m^{-2} s^{-1} and 0.45 mol/m^2/s, wherein the clones EH 04 and ET 46 showed a maximum and minimum respectively. Kallarackal and Somen (1998) revealed that significant differences were observed among the different species of Eucalyptus viz., *Eucalyptus tereticornis, E. camaldulensis* and *E. pellita* for stomatal conductance where the lowest was found in *E. urophylla* and highest in *E. camaldulensis*. The differences might be due to their stomatal aperture response to excessive water loss to maximize photosynthesis. Increased stomatal conductance due to increase in temperature led to increased photosynthesis which may attribute to short heat waves under well-watered conditions (Urban et al 2017).

The leaf temperature was ranging from 33.27˚C to 38.78˚C (Table 1). The leaf temperature was found higher in clone EUUG 10 with value of 38.78˚C, while clone EH 01 recorded lower value of 33.27˚C. Although the clone EUUG 10 showed higher leaf temperature, incidentally it also showed higher photosynthetic rate which might be due to contribution from non-transpiring leaves as evidenced from study in poplar species by Urban et al (2017). Reduction in leaf temperature by about 9˚C was seen in well–watered poplar species due to the evaporative cooling of the non-transpiring leaves which consequently affects the ratio of net photosynthesis and stomatal conductance. Grossiord et al (2020) reported that increased vapour pressure deficit (VPD) could also influence the stomatal conductance and subsequent reduction in the photosynthesis. Stomatal conductance was observed to be the most limiting trait rather than mesophyll conductance (g_m) under plant stress conditions as per studies conducted in poplar species.

Intercellular CO_2 concentration of leaves (Ci) is a critical parameter in photosynthesis. Table 2 and corresponding Figure 2 showed values for intercellular CO_2 concentration (Ci) ranged between 87.33 µl l^{-1} and 276.67 µl l^{-1}. Clone EU UG 10 registered the minimum value and the maximum value was recorded by clone ET 01. In the present study, higher CO_2 concentration in the intercellular spaces of the leaves is correlated with increasing stomatal conductance which considerably affects the rate of photosynthesis.

Transpiration rate reflects stomatal conductance: Transpiration is one of the crucial gas exchange traits associated with plant growth and productivity and also has linear relation with photosynthesis. Among the 15 clones, transpiration rate ranged between 4.37 and 12.07 mmol m^{-2} s^{-1}as shown in table 1. Clone EUUG 10 registered the minimum value (4.37 mmol m^{-2} s^{-1}) followed by ET 46 (6.67 mmol m^{-2} s^{-1}) and the maximum value was recorded by clone ET 01 (12.07 mmol m^{-2} s^{-1}). The clones with lower transpiration rate showed the considerable growth rate morphologically even under well-watered conditions indicating their efficiency towards water use. Clones with these traits might be utilised under drought prone areas or in areas of water-deficit.

Under the non-drought conditions, the stomatal conductance and transpiration rate of mulberry leaves decreased slightly with increased CO_2 concentration, but the net photosynthetic rate (An) increased significantly (Liu et al 2019).Increase in transpirational loses could be accompanied by increase in vapor pressure deficits (VPD) which further increased stomatal responses to rapid water loss from moist soils causing plant water stress (Grossiord et al 2020).

Intrinsic carboxylation efficiency-non-stomatal factor affecting photosynthetic rate: The net ratio of the photosynthetic rate to the intercellular CO_2 concentration is termed as intrinsic carboxylation efficiency (Hamerlynck et al

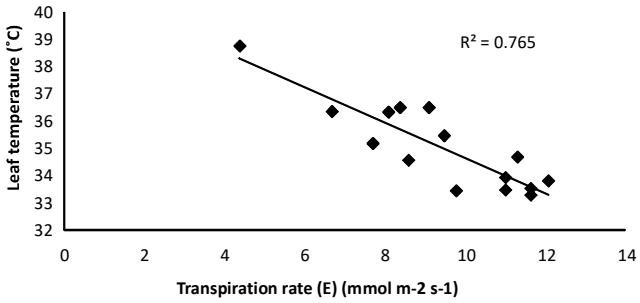

Fig. 1. Correlation between transpiration rate and leaf temperature

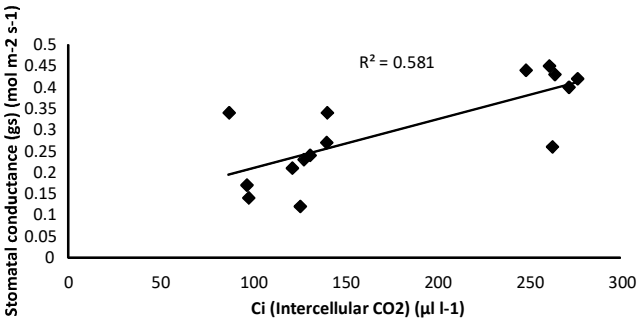

Fig. 2. Correlation between intercellular CO_2 concentration and stomatal conductance

2000). The intrinsic carboxylation rate was the highest in the EUUG 10 (0.227) followed by EUUG 11 (0.159) and the lowest was recorded in clone ET 01 (0.062) followed by clone ET 03 (0.063). The higher and lower carboxylation efficiency of the clones could be attributed to changes in the activity of Rubisco enzymes. Warrier and Venkataramanan (2010) reported the clones of eucalyptus observed with superior growth rate correlated with favourable physiological characteristics including high photosynthesis, carboxylation efficiency and water use efficiency.

Instantaneous and Intrinsic WUE: Instantaneous water use efficiency was estimated as the ratio of net photosynthetic rate to the transpiration rate Petite et al (2000). The higher value of instantaneous WUE, the greater the performance of the plants to divert water for photosynthesis than the transpiration. Table 2 showed that the clones EUUG 10, EC 07, DF 97 and E 13 recorded higher values for instantaneous WUE and clones EH 02, ET 03 and EH 01 recorded lower values. Instantaneous water use efficiency was higher in clone EUUG10 with a maximum of 4.53 (µmol $mmol^{-1}$) and minimum in EH 02 (1.38) (µmol $mmol^{-1}$). In the present study, instantaneous water use efficiency was found to be correlated with carboxylation efficiency indicating the importance of diffusion of CO_2 into the carboxylation site leading to higher photosynthetic rate.

The ratio of net photosynthetic rate (An) to stomatal conductance (g_s) is referred to as intrinsic water use efficiency (µmol mol^{-1}) (iWUE = An/g_s) show the photosynthetic characters independent of evaporative demand. High intrinsic WUE indicated the better carbon assimilation leading to higher productivity under water limited conditions. Table 2 showed that intrinsic WUE ranged between 38.71 and 136.31 µmol mol^{-1} while the maximum was observed in clone EH 04 and minimum in clone ET 03. Saravanan et al (2018) reported that net photosynthetic rate directly related to the changes in stomatal conductance correlated with high rates of iWUE of eucalyptus clones. Polley et al (1996) concluded that higher intrinsic (WUE) was analogous with productivity in *Prosopis glandulosa* and *Acacia smallii.* Tricker et al (2005) observed that restricted stomatal opening will results in the decreased stomatal conductance and lower transpiration rate, hence increased plant water use efficiency.

The correlation analysis showed that there is significant correlation between the measured traits. Transpiration rate showed significant positive correlation with stomatal conductance indicating that both traits are considered important for the rate of CO_2 assimilation leading to higher biomass productivity. Similarly, intercellular CO_2 concentration showed a strong positive correlation with the stomatal conductance indicating the rate of CO_2 entering through the stomatal apertures controls the rate of opening and closing of the stomata. Intrinsic WUE showed a strong negative correlation with the stomatal conductance prove the

Table 2. Water use efficiency (WUE) of selected *Eucalyptus* clones

Clones	Intercellular CO_2 (Ci) (µl l^{-1})	Intrinsic water use efficiency (µmol mol^{-1}) (An/g_s)	Instantaneous water use efficiency (µmol $mmol^{-1}$) (An/E)	Intrinsic carboxylation efficiency (µmol m^{-2} s^{-1} (µl l^{-1})$^{-1}$ (An/Ci)
EH 01	248.67^{b}	43.38^{f-g}	1.60^{g-h}	0.075^{g}
ET 46	261.33^{a-b}	44.13^{f-g}	1.72^{e-f}	0.077^{g}
ET 56	272.00^{a-b}	43.15^{f-g}	1.77^{e-f}	0.064^{g}
ET 03	264.33^{a-b}	38.71^{g}	1.50^{h-i}	0.063^{g}
ET 01	276.67^{a}	40.86^{f-g}	1.41^{i-j}	0.062^{g}
EH 02	140.67^{c}	45.31^{f-g}	1.38^{j}	0.112^{e-f}
EH 03	263.00^{a-b}	72.04^{d}	1.95^{d}	0.070^{g}
EH 04	126.00^{c}	136.31^{a}	1.98^{c-d}	0.127^{d-e}
EC 07	131.33^{c}	75.37^{c-d}	2.07^{c}	0.135^{c-d}
EC 413	121.67^{c-d}	89.66^{c}	1.66^{f-g}	0.152^{b-c}
EH 05	140.33^{c}	51.14^{f}	1.81^{e}	0.102^{f}
E 13	128.00^{c}	81.36^{c-d}	2.01^{c-d}	0.144^{b-c-d}
DF 97	98.00^{d-e}	110.75^{b}	2.36^{b}	0.161^{b}
EUUG 10	87.33^{e}	59.19^{e}	4.53^{a}	0.227^{a}
EUUG 11	97.00^{d-e}	91.98^{c}	1.82^{e}	0.159^{b}
S. Ed	12.21	5.89	0.06	0.01
CD (p=0.05)	24.94	12.03	0.12	0.02

Means followed by small superscript letter in a column do not differ significantly as per DMRT (p≤0.05); All the values are means of 3 replications

Table 3. Correlation of physiological traits for the selected *Eucalyptus* clones

	An/Ci	An	g_s	E	T_l	Ci	iWUE	WUE
An/Ci	1							
An	0.050	1						
g_s	-0.582*	0.411	1					
E	-0.767**	0.128	0.545*	1				
T_l	0.786**	-0.075	-0.546*	-0.875**	1			
Ci	-0.905**	0.295	0.763**	0.688**	-0.695**	1		
iWUE	0.525*	-0.225	-0.923**	-0.466	0.493	-.0638*	1	
WUE	0.750**	0.356	-0.149	-0.830**	0.779**	-0.471	0.164	1

*Correlation is significant at the 0.05 level; **Correlation significant at the 0.01 level
An/ci = Carboxylation efficiency'; An = Photosynthetic rate; g_s = Stomatal conductance; E= Transpiration rate; T_l = Leaf Temperature; Ci = Intercellular CO_2 concentration; iWUE = intrinsic Water Use Efficiency; WUE = An/E (Instantaneous Water Use Efficiency)

fact that stomatal regulations are important in terms of maintaining the WUE under water limited conditions.

CONCLUSION

Wider variability for gas exchange and physiological traits linked to water use efficiency among the fifteen eucalyptus clones was recorded. Among the clones studied, EU UG 10 and ET 46 were found to be promising clones in terms of higher biomass and water use efficiency associated traits. Understanding water use efficiency and its contributing traits is essential for further tree improvement in eucalyptus and to develop clones tolerant to drought and high temperature in view of climate change. Besides, this could also reduce the trade-off between the water and carbon relations ultimately reducing the risk of plantation failure. Our data suggest that, the gas exchange traits at the leaf level/plant level have to be validated at whole stand/field level for further physiological dissection of traits in contributing plant productivity under irrigated or water deficit conditions.

REFERENCES

Battaglia M, Beadle C and Loughhead S 1996. Photosynthetic temperature responses of *Eucalyptus globulus* and *Eucalyptus nitens*. *Tree physiology* **16**(1-2): 81-89.

Boyden S, Binkley D and Stape JL 2008. Competition among eucalyptus trees depends on genetic variation and resource supply. *Ecology* **89**(10): 2850-2859.

Grossiord C, Buckley TN, Cernusak LA, Novick KA, Poulter B, Siegwolf RT and McDowell NG 2020. Plant responses to rising vapor pressure deficit. *New Phytologist* **226**(6): 1550-1566.

Hamerlynck EP, Huxman TE, Nowak RS, Redar S, Loik ME, Jordan DN, Zitzer SF, Coleman JS, Seemann JR and Smith SD 2000. Photosynthetic responses of *Larrea tridentata* to a step-increase in atmospheric CO_2 at the Nevada desert FACE facility. *J Arid Environ* **44**: 425-436.

Hatfield JL and Dold C 2019. Water-use efficiency: advances and challenges in a changing climate. *Frontiers in Plant Science* **10**: 103.

Received 09 August, 2021; Accepted 25 November, 2021

Kallarackal J and Somen CK 1998. *Water relations and rooting depth of selected eucalypt species.* Kerala Forest Research Institute, Peechi, Thrissur, India.

Kang W and Kang S 2019. On the use of alternative water use efficiency parameters in dryland ecosystems: a review. *Journal of Ecology and Environment* **43**(1): 1-8.

Kaur A and Monga R 2021. *Eucalyptus* trees plantation: A review on suitability and their beneficial role. *International Journal of Bio-Resource & Stress Management* **12**(1): 21-27.

Liu X, Zhang H, Wang J, Wu X, Ma S, Xu Z and An B 2019. Increased CO_2 concentrations increasing water use efficiency and improvement PSII function of mulberry seedling leaves under drought stress. *Journal of Plant Interactions* **14**(1): 213-223.

Petite MA, Moro GB, Murua GC, Lacuesta M and Rueda MA 2000. Sequential effects of acidic precipitation and drought on photosynthesis and chlorophyll fluorescence parameters of *Pinus radiata* D. Don seedlings. *Journal of Plant Physiol* **156:** 84-92.

Polley H W, Johnson H B and Mayeux H S 1996. Carbon Dioxide on Seedling Growth of Mesquite and Huisache. Vol. 338, p. 246. In: Las Cruces, NM, *Proceedings of Shrubland Ecosystem Dynamics in a Changing Environment*, May 23-25, 1995. Intermountain Research Station, Forest Service, US Department of Agriculture.

Saravanan S 2018. Gas exchange characteristics and water use efficiency in eucalyptus clones. *Journal of Stress Physiology and Biochemistry* **14**(3): 49-58.

Tricker PJ, Trewin H, Kull O, Clarkson GJ, Eensalu E, Tallis MJ and Taylor G 2005. Stomatal conductance and not stomatal density determines the long-term reduction in leaf transpiration of poplar in elevated CO_2. *Oecologia* **143**(4): 652-660.

Urban J, Ingwers MW, McGuire MA and Teskey RO 2017. Increase in leaf temperature opens stomata and decouples net photosynthesis from stomatal conductance in *Pinus taeda* and *Populus deltoides* x *nigra*. *Journal of Experimental Botany* **68**(7): 1757-1767.

Vijayakumar R, Buvaneswaran C, Warrier R and Jayaraj RSC 2015. Clonal variation in Eucalyptus with reference to biochemical parameters. *Eurasian Journal of Forest Science* **3**(1): 14-21.

Warrier KC and Venkataramanan KS 2010. Gas exchange characteristics in *Eucalyptus* clones. *Indian Journal of Plant Physiology* **15**(3): 226.

Zhang P, Zhang Z, Li B, Zhang H, Hu J and Zhao J 2020. Photosynthetic rate prediction model of newborn leaves verified by core fluorescence parameters. *Scientific Reports* **10**(1): 1-11.

Indian Journal of Ecology (2021) 48(6): 1726-1731

Manuscript Number: 3439
NAAS Rating: 5.79

Impacts of Seasonal Variation on Habitat Selection by Sichuan Golden Snub-nosed Monkey: A Case Study of Tangjiahe National Nature Reserve

Majda Aouititen, Aravinda Ravibhanu[1], Wancai Xia, Dayong Li[2] and Xiaofeng Luan

Beijing Forestry University, School of Ecology and Nature Conservation, Beijing 100083, China
[1]Department of Research & Innovation – Eco Asronomy Inc, Colombo, Sri Lanka
[2]Institute of Rare Animals and Plants Chinese, West Normal University, Nanchong, Sichuan 637009, China
E-mail: majda_578@yahoo.fr

Abstract: The habitat selection for a group of *R. roxellana* at Tangjiahe National Nature Reserve during two seasons of 2010 was analysed with direct observation and vegetation survey. Eleven ecological variables were measured in seventy-five sites using 20 m 20 m plots. The research aims to document the impacts of seasonal variation in *R. roxellana* habitat selection. *R. roxellana* selected the deciduous broadleaf forest and mixed conifer-broadleaf forest for both seasons and have extended the altitude range between less than 2000 m and beyond 2500 m during the winter, and they restrict it to 2000~2500 m for the summer season. *R. roxellana* have selected as winter habitat trees with DBH of 11~30 cm with a height of 10~29 m, canopy coverage of 25~49%, with a water distance of 0~300 m. However, during summer *R. roxellana* preferred canopy coverage of 25 to 74%. The water source was at <100 m and trees with DBH of 0 ~ 10 cm, 11 ~ 20 cm, and height of 10 ~ 19 m. The seasonal availability of food resources was the main factor influencing the habitat selection behavior of *R. roxellana.*

Keywords: Climate change, Endangered species, *Rhinopithecus roxellana*, Primate

Golden snub-nosed monkeys are found only in mountainous, temperate forests in China (Milton et al 2005). Previous studies describe *R. roxellana* as an endangered species with three geographically isolated populations of monkey found in Qinling, Sichuan-Gansu, and Shennongjia (Dayong et al 2006). These primates have a preferred elevation range between 1,500m and 4,100 m, known for their strong seasonality and cold, snowy winters (Kirkpatrick 2001, Li et al 2008). The average annual temperature of *R. roxellana*'s habitat rage selection starts from 6℃ with a minimum of -8°C in January and a maximum of 22°C in July (*Zhang* et al 2016). The home range size of the *R. roxellana* group usually exhibits seasonal variance due to changes in food availability throughout the year (Zhou et al 2007, Zhang et al 2011, Albert et al 2013). The stability of trees, unit cohesion, and the monitoring potential were essential criteria for *R. roxellana*'s selection of preferred habitat (Dayong et al 2006). In concordance with research on other primates have shown that their home-range selection is impacted by specific ecological and behavioral factors, which may change from one season to another. These may include factors such as food availability (*Zhang* et al 2006, Zhou et al 2007), water source distance (Scholz et al 2004) and intergroup relationships (Benadi et al 2008). These factors as well have been affected by climate change. For establishing an adequate protection plan for monkeys' habitat, it is necessary to understand the species home ranges. However, more studies conducted about behavioral ecology are needed (Zhou et al 2007). These are the reasons that lead us to undertake a study on this issue. Previous studies have shown that environmental variables will affect the structure and composition of local plant communities, contributing to primates' ecological resources and conditions (Dunn et al 2008, Amare and Bhardwaj 2016, Srinivas and Krishnamurthy 2016, Simimole and Joice 2016). That will lead to a bifurcation of survival strategies; some primates may choose a wide strategy as they develop large home ranges traveling across large swaths of land searching for food (Milton et al 2005, Boubli et al 2008, Mourthé 2014). The other primates with a tall strategy live on smaller home ranges, restricting their ranges to areas of higher quality habitats to find their preferred foods (Nagy et al 1979, Strier 1992, Mourthé 2014). This paper aims to study the effects of the seasonal variation on *R. roxellana's* habitat selection for both, Winter and Summer seasons.

MATERIAL AND METHODS

Study area: The study was conducted in winter and summer seasons at Tangjiahe National Nature Reserve, located in the northwest corner of Qingchuan County on the Sichuan Basin's northern edge, East longitude 104º 36'~104º 52' North latitude 32º 30'~32º 41' (Fig. 1); a total area of 1359.12 km^2 which is known as one of the 25 biodiversity hotspots

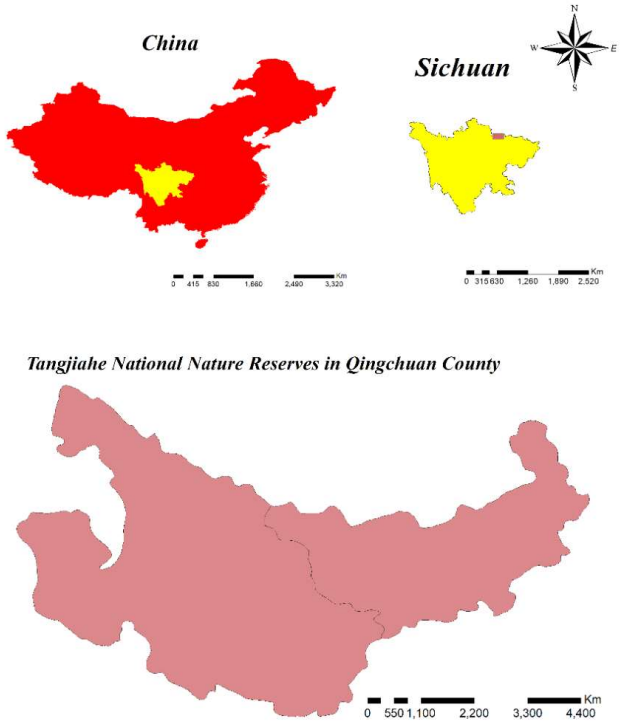

Fig. 1. Location of the Tangjiahe, national nature reserves in Qingchuan County, Sichuan Province, China

worldwide (Mittermeier et al 1998). The highest elevation is around 3864 m, the lowest elevation is about 1100 m, and the relative elevation difference is estimated to be 2764 m (Hu Jinchu 2005). The study area belongs to the humid subtropical climate, with noticeable vertical changes; and four seasons with abundant rainfall. The average annual temperature is 13.7ºC, the annual average sunshine hours is 1303 hours, the annual rainfall is 1100~1200 mm and the relative humidity is 78% (Hu Jinchu 2005). The vertical spectrum order of vegetation has mountainous evergreen broad-leaved forest belts, evergreen, mixed deciduous forest, coniferous and broad-leaved mixed forest; the subalpine coniferous forest includes 267 families, 969 genera, and 422 species of plants (Hu Jinchu 2005). It provides a high-quality living environment for rare wild animals such as giant pandas, golden monkeys, takins and has bred the rich life of Tangjiahe Diversity (Hu Jinchu 2005).

Data collection: The first survey was conducted during the winter season from January 2010 to the beginning of March 2010, and the second survey was during the summer season starting from Jun 2010 until the end of August 2010. Based on monkey group observations, recorded daily activities, and used a GPS device to record their location. During the research phase, a total of seventy-five sites where a group of monkey's activities was recorded in order to document the impact of seasonal variation on a group of the Golden Snub-Nosed Monkeys selection habitat. Stratified random sampling was conducted (Mueller-Dombois and Ellenberg, 1974) and eleven ecological variables were measured in around seventy-five sites using 20 m 20 m plots, where our group of monkeys was frequently observed. These variables included the type of habitat vegetation, DBH (diameters of breast height of trees), canopy cover, tree height, elevation, slope degree, slope aspect, slope type, and distance to the water source as the tree and arbor density.

To ensure that different measurement standards will not produce different results for the same variables, proposed a specific division for each ecological factor as follow:

Slope: Different slopes are divided according to the measured angle; there are five levels, namely 0~5, 6~20, 21~30, 31~40,> 41

Aspect: Divide the aspect into five levels: sunny slope, semi-sun slope, shade slope, semi-shady slope, and no aspect.

Altitude: The altitude where the golden monkey or its traces are found, divided into three levels: <2000m, 2000~2500 m, >2500 m.

Canopy closure: divided into 4 levels, 0~0.24, 0.25~0.49, 0.50~0.74, 0.74~1.00.

Habitat type: Divided into five levels, evergreen broad-leaved forest, evergreen and deciduous broad-leaved mixed forest, deciduous coniferous, broad-leaved forest, and broad-leaved mixed forest, and coniferous forest.

Water source distance: The golden monkey or its traces are found to be away from the water; the distance of the source is divided into <100m, 100~300 m, >300m.

Average DBH of trees: The average DBH of all trees in the trace plots, divided into five grades, namely 0~10~ cm, 11~20 cm, 21~30 cm, 31~50 cm,> 50 cm.

Slope shape: It is divided into five grades: uniform slope, convex slope, concave slope, compound slope, and non-slope.

Shrub coverage: Divided into 4 levels, namely 0~0.24, 0.25~0.49, 0.50~ 0.50~ 0.74, 0.75~1.00.

Average tree height: The average tree height of all trees in the tracepoint plot, divided into four levels: 5-9 m, 10-19 m, 20-29 m, and >30 m.

Tree density: The number of trees (trees) in the trace plot, divided into

Data processing: The Vanderploeg selection coefficient Wi and Scavia selection index Ei were used to measure Sichuan golden snob-nosed monkeys' preference for Habitat (habitat selection characteristics). The method used was as follows (Li Dayong et al 2006, Wang Jianhong et al 2006).

$$Wi= (ri/Pi) / \sum(ri/Pi)$$

$$Ei= (Wi-1/n)/ (Wi+1/n)$$

Among them, Wi is the selection coefficient, Ei is the

selection index, i is the eigenvalue, n is the total number of eigenvalues, Pi is the number of quadrats with i characteristics in the environment, and ri is the number of quadrats with i characteristics selected by the Sichuan Golden Monkey.

Ei the value is between -1 and 1(Manly et al 2002).

-1<Ei<0 means our monkeys avoids it (indicated by N.P.),

Ei= -1 means our monkeys will not choose it (indicated by N),

0<Ei<1 means likely selected by our monkeys (indicated by P),

Ei = 1 (indicated by S.P.) means a special preference,

Ei = 0 means random selection (indicated by R).

RESULTS And Discussion

Sichuan Golden Monkey's habitat during the winter season of 2010: The group of monkeys found during the winter season is mainly active in the evergreen deciduous broad-leaved mixed forest and the deciduous broad-leaved forests with an altitude starting from < 2000 m till >2500 m, located on sunny slopes, with a canopy closure of 25to 49% and a slope of 6° to 20° and 21° to 30. The main slope shapes selected were the convex slopes and the composite slopes. The shrub coverage is 25 ~ 49%; water source distances found to be around <100 m and 100 ~ 300 m, The group of monkeys chosen trees with an average DBH of 11 ~ 20 cm, 21 ~ 30 cm, and do not choose woods with a DBH of less than 11 cm and more than 30 cm. Choose trees with an average height of 10 ~ 19 m, 20 ~ 29 m and ovoid habitat with trees high below 5 m and above 30 m. The prefers density of trees woods was between 20~ 40 and >40 nd avoids woods with a density of less than 20 (Table 1).

Sichuan Golden Monkey's habitat selection during the summer season of (2010): During the summer season of 2010, group of monkeys was mainly active in the evergreen deciduous broad-leaved mixed forest and the deciduous broad-leaved forests. However, avoid the evergreen broad-leaved forest, coniferous and broad-leaved mixed forest, and the coniferous forest with an altitude of 2000~2500 m, and avoid elevations less than 2000 m and more than >2500 m, located on sunny and semi-sunny slopes; still, they avoid semi-shady foggy slope, with a canopy coverage of 25 to 49%, 50 to 74% and a slope degree of 21° to 30°. The main slope shapes selected were uniform and composite slopes; the shrub coverage is 25 ~ 49%; water source distances were around <100 m, monkeys chose trees with an average DBH of 0 ~ 10 cm, 11 ~ 20 cm, and do not choose trees with a DBH 21~30 cm, 31~50 cm, and less than 50 cm. They Choose trees with an average height of 10 ~ 19 m. In fact, do not select habitats with trees high of 20 ~ 29 m, below 5 m and above 30 m; the density of trees prefers woods between 20~ 40; still, they avoid woods with a density of less than 20 and more than 40 (Table 2).

The habitat selection for wild animals is often affected by environmental factors in the ecosystem and their diet demands (Sun Ruyong 2000, Morrison et al 2006). Studies previously have documented the impacts of seasonal variation on the Sichuan golden snub-nosed monkey's habitat selection (Hu Jinchu 2005). The present study indicates monkey's group selected different ecological variables in a selected habitat that differ from one season to another. The altitude, habitat aspect, and the distance from water source played a significant component in the selection of both winter and summer habitat by *R. roxellana* in Tangjiahe National Nature Reserve. Besides, the slope type and its degree with the forest canopy coverage have a significant impact on the distribution of monkey's population during both seasons. The stability of trees, unit cohesion, and the monitoring potential, were shown to be important criteria for *R. roxellana*'s selection of a preferred habitat. The influence of seasonal variations on the type of habitat selected is not evident since our group of monkeys has selected for both seasons in the same habitat type, which were evergreen deciduous broad-leaved mixed forest and the deciduous broad-leaved forests. When the living conditions become harsh during the winter season, *R. roxellana* has changed its diet and monkeys extend home range altitude starting from less than 2000 m to beyond 2500 m and during summer, when food starts to be abundant, *R. roxellana* restricted their habitat altitude to 2000 ~ 2500 m again. The same observation was recorded for the distance from the water source selected by our monkeys. The home range size of *R. roxellana* group usually exhibits seasonal variance due to changes in food availability throughout the year (Albert et al 2013). As it is challenging for them to find food during the winter season, monkeys have chosen to be relatively far away from the river < 100 m, 100 ~ 300 m but not from the food resources, as the summer season known to be rich in food resources monkeys have then restricted the distance that separates them from the river source of water to < 100 m. Guo Qiang and Xie Jiahua (2002) observed that climatic conditions may substantially affect the ecological factors that affect monkey's habitat selection. However, the difference in the choice of slope type in both seasons may be related to the wind direction and its strength, as r monkeys use the trees to stand in, to move around, and to sleep in, as a result, a relative none-windy slope type will be selected.

Table 1. Habitat selection of *Rhinopithecus* at Tangjiahe National Reserve in winter (2010)

Ecological variables	Eigenvalue (I)	Pi	Wi	Ei	Habitat selection
Aspect	Sunny slope clear	38	0.54	0.46	P
	Semi-sun slope overcast	12	0.17	-0.08	NP
	Shade slope snow	2	0.02	-0.82	NP
	Semi-shady slope foggy	10	0.14	-0.18	NP
	No aspect	9	0.13	-0.21	NP
Slope degree	0°≈5°	6	0.07	-0.48	NP
	6°≈20°	44	0.5	0.43	P
	21°≈30°	29	0.33	0.25	P
	31°≈40°	6	0.07	-0.48	NP
	>41°	3	0.03	-0.74	NP
Type of habitat	Evergreen broad-leaved forest	0	0	-1	N
	Evergreen and deciduous broad-leaved mixed forest	56	0.61	0.51	P
	Deciduous broad-leaved forest	22	0.24	0.09	P
	Coniferous and broad-leaved mixed forest	14	0.14	-0.18	NP
	Coniferous forest	1	0.01	-0.91	NP
Slope shape	Uniform slope	16	0.1	-0.33	NP
	Convex slope	33	0.38	0.31	P
	Concave slope	13	0.15	-0.14	NP
	Composite slope	24	0.27	0.15	P
	Non-slope	8	0.1	-0.33	NP
Canopy	0~0.24	13	0.13	-0.53	NP
	0.25~0.49	77	0.78	0.54	P
	0.50~0.74	8	0.08	-0.52	NP
	0.74~1.00	1	0.01	-0.92	NP
Shrub overcast	0~0.24	17	0.21	-0.09	NP
	0.25~0.49	56	0.68	0.16	P
	0.50~0.74	8	0.09	-0.47	NP
	0.74~1.00	2	0.02	-0.85	NP
Elevation (m)	<2000m	39	0.37	0.06	P
	2000~2500 m	61	0.57	0.27	P
	>2500 m	6	0.06	0.69	P
Distance from water (m)	<100m	33	0.39	0.08	P
	100~300 m	43	0.51	0.21	P
	>300m	24	0.29	-0.07	NP
Average diameter of tree (cm)	0~10~ cm	0	0	-1	N
	11~20 cm	48	2.76	0.87	P
	21~30 cm	38	2.18	0.83	P
	31~50 cm	1	0.06	-0.54	NP
	> 50 cm	0	0	-1	N
Average height of tree (m)	5-9 m	1	0.01	-0.92	NP
	10-19 m	65	0.72	0.49	P
	20-29 m	24	0.27	0.04	P
	>30 m	0	0	-1	N
Arbor density	<20	19	0.254	-0.13	NP
	20~40	13	0.173	0.31	P
	>40	43	0.573	0.27	P

I. Eigenvalue, Pi. The number of quadrats with i characteristics in the environment, Wi. Selection factor, Ei. Selection Index, P: likely to be selected, N: not selected, N.P: avoid it; Pi, the number of sample units under the i^{th} class; ri, the number of units used by snow leopards under the i^{th} class

Table 2. Habitat selection of *Rhinopithecus* during summer at Tangjiahe National Reserve (2010)

Ecological variables	Eigenvalue (i)	Pi	Wi	Ei	Habitat selection
Aspect	Sunny slope clear	5	0.5556	0.47059	P
	Semi-sun slope overcast	3	0.3333	0.25	P
	Shade slope snow	0	0	-1	N
	Semi-shady slope foggy	1	0.1111	-0.2857	NP
	No aspect	0	0	-1	N
Slope degree	0°≈5°	0	0	-1	N
	6°≈20°	1	0.167	-0.0899	NP
	21°≈30°	3	0.5	0.42857	P
	31°≈40°	1	0.167	-0.0899	NP
	>41°	1	0.167	-0.0899	NP
Type of habitat	Evergreen broad-leaved forest	0	0	-1	N
	Evergreen and deciduous broad-leaved mixed forest	7	0.6	0.5	P
	Deciduous broad-leaved forest	4	0.4	0.33333	P
	Coniferous and broad-leaved mixed forest	0	0	-1	N
	Coniferous forest	0	0	-1	N
Slope shape	Uniform slope	2	0.33	0.24528	P
	Convex slope	0	0	-1	N
	Concave slope	0	0	-1	N
	Composite slope	4	0.67	0.54023	P
	Non-slope	0	0	-1	N
Canopy	0~0.24	0	0	-1	N
	0.25~0.49	3	0.75	0.5	P
	0.50~0.74	1	0.25	0	P
	0.74~1.00	0	0	-1	N
Shrub overcast	0~0.24	0	0	-1	N
	0.25~0.49	3	1	0.6	P
	0.50~0.74	0	0	-1	N
	0.74~1.00	0	0	-1	N
Elevation (m)	<2000m	2	0.18	-0.2941	NP
	2000~2500 m	8	0.73	0.37736	P
	>2500 m	1	0.09	-0.5714	NP
Distance from water (m)	<100m	4	1	0.50376	P
	100~300 m	0	0	-1	N
	>300m	0	0	-1	N
Average diameter of tree (cm)	0~10~ cm	1	0.25	0.11111	P
	11~20 cm	3	0.75	0.57895	P
	21~30 cm	0	0	-1	N
	31~50 cm	0	0	-1	N
	> 50 cm	0	0	-1	N
Average height of tree (m)	5-9 m	0	0	-1	N
	10-19 m	4	1	0.6	P
	20-29 m	0	0	-1	N
	>30 m	0	0	-1	N
Arbor density	<20	0	0	-1	N
	20~40	1	1	0.50376	P
	>40	0	0	-1	N

See Table 1 for details

CONCLUSION

Seasonal variation effects on the climatic conditions, food resources distribution, and monkeys' feeding preference may be the leading factors affecting habitat selection behavior. Among them, the distribution of food resources is the most crucial factor. The more studies will be needed for a further clear understanding of *R. roxellana* selection of habitat.

ACKNOWLEDGMENTS

We are thankful to Tangjiahe National Nature Reserve's personnel help for all their help and guidance and we would like to show gratitude to team for their high monitoring quality of this research. We want to address our sincere appreciation for all the motivation and support received from Mrs. Jamila Semlal.

FUNDING SOURCES

This work was supported by the National Natural Science Foundation of China (No. 32070454), the National Key Program of Research and Development, Ministry of Science and Technology (No. 2016YFC0503200), the Biodiversity Survey and Assessment Project of the Ministry of Ecology and Environment, China (2019HJ2096001006).

REFERENCES

Albert A, Huynen MC, Savini T and Hambuckers A 2013. Influence of food resources on the ranging pattern of northern pig-tailed macaques (*Macaca leonina*). *International Journal of Primatology* **34**(4): 696-713.

Amare T and Bhardwaj DR 2016. Effect of lopping on stand structure and tree species composition of *Quercus glauca* Thunb. Forests of Himachal Pradesh, India. *Indian Journal of Ecology* **43**(1): 218-223.

Benadi G, Fichtel C and Kappeler P 2008. Intergroup relations and home range use in Verreaux's sifaka (*Propithecus verreauxi*). *American Journal of Primatology* **70**(10): 956-965.

Boubli JP and Tokuda M 2008. Socioecology of black uakari monkeys, *Cacajao hosomi*, in Pico da Neblina National Park, Brazil: The role of the peculiar spatial-temporal distribution of resources in the Neblina forests. *Primate Report* **75**: 3-10.

Curtis DJ and Zaramody A 1998. Groupsize, homerange use, and seasonal variation in the ecology of Eulemur mongoz. *International Journal* of *Primatology* **19**: 811-835.

Dayong Li, Cyril CG, Baoping R, Qihai Z, Ming L, Zhengsong P and Fuwen WEI 2006. Characteristics of night-time sleeping places selected by golden monkeys (*Rhinopithecus bieti*) in the Samage Forest, Baima Snow Mountain Nature Reserve. *China, Integrative Zoology* **1:** 141-152.

Received 12 June, 2021; Accepted 10 November, 2021

Hu J 2005. Comprehensive scientific investigation report of Tangjiahe Nature Reserve in Sichuan Chengdu. *Sichuan Science and Technology Press* **1**:5-11.

Kirkpatrick RC, Zou RJ, Dierenfeld ES and Zhou HW 2001. Digestion of selected foods by Yunnan snub-nosed monkey *Rhinopithecus bieti* (Colobinae). *American Journal of Physical Anthropology* **114**: 156-62.

Li DY, Grueter CC, Ren BP, Long YC, Li M, Peng ZS and Wei FW 2008. Ranging of Rhinopithecus bieti in the Samage Forest, China. II. Use of land cover types and altitudes. *International Journal of Primatology* **29**: 1147-1173.

Milton K, Giacalone J, Wright SJ and Stockmayer G 2005. Do frugivore population fluctuations reflect fruit production? Evidence from Panama In: Dew JL, Boubli JP, editors. *Tropical Fruits and Frugivores, Dordrecht, The Netherlands* **1**: 5-35.

Mittermeier RA 1988. Primate diversity and the tropical forest', in E.O. Wilson (ed.), Biodiversity. *Washington DC: National Academy Press* **1**: 145-154.

Morrison ML, Marcot BG and Mannan RW 2006. *Wildlife-habitat relationships: Concepts and applications.* 3rd ed. Washington: Island Press **1**: 10-20.

Mourthé I 2014. Response of frugivorous primates to fruit supply changes in a northern Amazonian forest. *Brazilian Journal of Biology* **74**: 720-727.

Mueller-Dombois D and Ellenberg H 1974. Aims and methods of vegetation ecology. *John Wiley and Sons New York* **1**: 547-549.

Nagy KA and Milton K 1979. Energy metabolism and food consumption by wild howler monkeys (*Alouatta palliata*). *Ecology* **60**: 475-480.

Scholz F and Kappeler PM 1992. Effects of seasonal water scarcity on the ranging behavior of Eulemur fulvus rufus. *International Journal of Primatology* **25**(3): 599-613.

Simimole S and Joice VT 2016. Temporal variation of phytoplankton in Idukki Reservoir, Kerala. *Indian Journal of Ecology* **43**(1): 22-27.

Srinivas SG and Krishnamurthy YL 2016. Distribution of *Litsea floribunda* (Lauraceae), A Dioecious tree endemic to Western Ghats of India. *Indian Journal of Ecology* **43**(1): 224-228

Strier KB 1992. Atelinae adaptations: behavioral strategies and ecological constraints. *American Journal of Physical Anthropology* **88**: 515-524.

Sun R 2002. Principles of Animal Ecology. *Beijing Normal University Press* **3**: 10-20.

Wang J, Huang H and Teng J 2006. Habitat selection of giant pandas in the western section of Baishuijiang Nature Reserve in Gansu. *Sichuan Zoology* **5**(4): 771-775.

Zhang P, Hu KJ, Yang B and Yang HD 2016. Snub-nosed monkeys (*Rhinopithecus* spp.): Conservation challenges in the face of environmental uncertainty. *Science Bulletin* **61**(5): 345-348.

Zhang P, Li BG, Watanabe K and Qi XG 2011. Sleeping cluster patterns and retiring behaviors during Winter in a free-ranging band of the Sichuan snub-nosed monkey. *Primates* **52**(3): 22.

Zhang P, Watanabe K, Li B and Tan Chia L 2006. Social Organization of Sichuan snub-nosed monkeys (*Rhinopithecus roxellana*) in the Qinling Mountains Central China. *Primate* **47**(4): 374-382.

Zhou QH, Huang CM, Li YN and Cai XW. 2007- Ranging behavior of the Francois' langur (*Trachypithecus francoisi*) in the Fusui Nature Reserve, China. *Primates* **48**(4): 320-323.

Indian Journal of Ecology (2021) 48(6): 1732-1735

Manuscript Number: 3440
NAAS Rating: 5.79

Effect of Spacing and Fertility Levels on Growth, Yield and Economics of Green Gram (*Vigna radiata* L) under Rainfed Conditions

S.K. Sharma, Kuldeep Singh, Kautilya Chaudhary and S.K. Thakral

Department of Agronomy
Chaudhary Charan Singh Haryana Agricultural University, Hisar-125 004, India
E-mail: sksharma67@rediffmail.com

***Abstract*:** Field experiments were conducted at CCS Haryana Agricultural University, Hisar during *Kharif* season of 2018 and 2019 to study the effect of spacing and fertility levels on growth, yield parameters, yield and economics of green gram. The experiment was laid out in factorial randomized block design with 3 spacings *viz.* S_1:22.5 × 10 cm, S_2:30 × 10 cm and S_3: 45× 10 cm and 3 fertility levels *viz*. F_1:100 % RDF (20-40 kg NP ha^{-1}), F_2:125 % RDF (25-50 kg NP ha^{-1}) and F_3:150 % RDF (30-60 kg NP ha^{-1}). Green gram sown at spacing of 45 x 10 cm registered significantly higher seed yield (824 kg ha^{-1}), yield attributing parameters, RWUE (5.29 kg ha^{-1} -mm), net returns (Rs 39940 ha^{-1}) and BC ratio (3.10) compared to other spacings during *Kharif* season. Application of 100 % recommended dose of fertilizers (20-40 kg NP ha^{-1}) recorded significantly higher seed yield (748 kg ha^{-1}), yield attributing parameters, rain water use efficiency (4.85 kg ha^{-1} -mm), net returns (Rs 34461 ha^{-1}) and BC ratio (2.80) compared to 125 and 150 % recommended dose of fertilizers.

Keywords: BC ratio, Fertility levels, Green gram, Net returns, Spacings, Seed yield

Green gram [*Vigna radiata* (L.) Wilczek] is one of the important pulse crops of India and is becoming the best alternative to meet the food need of the large population of developing countries due to its nutritional superiority and nitrogen fixing characters (Raza et al 2012). In India, total pulses were grown in an area of 29.36 million ha, with the production of 24.50 million tons and average productivity of 835 kg ha^{-1} during 2017-18 (Anonymous 2018). Among pulses, green gram is grown in an area of 4.07 million ha, with the production of 1.90 million tons and average productivity of 467 kg ha^{-1} during 2017-18 (Anonymous 2018). The green gram foliage left over after picking of mature pods can either be fed to livestock or it may plough in situ as a green manure to enrich soil with organic matter under rainfed conditions. Green gram crop have direct effect of spacing (planting geometry) due to availability of moisture and nutrient dependency on spacing (Singh et al 2011). The optimum spacing favours the plants to grow in their both aerial and underground parts through efficient utilization of solar radiation and nutrients and thus increase grain yield (Miah et al 1990). Green gram gives low seed yield and poor growth performance mainly due to poor management and low soil fertility. Being a leguminous crop, green gram does not need a high dose of nitrogenous fertilizer. However 20 kg N ha^{-1} as a starter dose is required for good crop growth and accelerated nodulation. It has already been established that supply of nitrogen is very important for the growth of legume which is able to fix atmospheric nitrogen through activity of micro-organism (Rhizobium) inhabiting in its root nodules (Singh et al 2011).

Balanced fertilization is necessary to increase productivity of green gram. Regular and judicious use of primary nutrients not only helps in raising good crop yield but can help farmers to gain higher profit. But, a large number of farmers in the region are not applying a dose of fertilizers to this crop. Nitrogen due to leaching and vitalization, and phosphorus due to fixation may not be available adequately at flowering and pod formation stages of crop and result in shading of flowers and pods (Hangsing et al 2020). The crop needs more nitrogen at the reproductive phase and the nutrient uptake after flowering either becomes slow or stops due to inactivation of roots. The optimum supply of nitrogen and phosphorus significantly influenced on growth and yield of green gram. Therefore, yield of green gram may increase with the balanced combination of nitrogenous and phosphatic fertilization. Usually grain legumes are grown on marginal land under rainfed conditions. On the other hand, the optimum doses of nutrients for green gram crop was determined long back but thereafter, the fertility status, crop varieties and other inputs have undergone a considerable change, so there is a need to give fresh look to fertilizer requirement of green gram in the light of introduction of new varieties. Hence, to evaluate correct spacing and fertility levels on growth and yield of green gram, the present investigation was undertaken to find out the optimum spacing and fertilizers dose for green gram under rainfed conditions.

MATERIAL AND METHODS

The field experiment was conducted at Dryland Agriculture Research Farm, CCS Haryana Agricultural University, Hisar situated in the sub-tropics at 29^{0}10' N latitude and 75^{0}46' E longitude and 215.2 m above mean sea level during two *Kharif* (rainy) seasons of 2018 to 2019. The total rainfall received during the crop growth period was 209.9 and 189.9 mm while during *Kharif* season (Jun-Sep) it was 381.6 and 305.9 mm during 2018 and 2019, respectively with average of 347.7 mm, which was 1.74 per cent higher over the mean normal rainfall (337.8). Month wise it was 26.4, 24.3 and 21.1% higher in June, July and September and 48 % deficit in August over the mean monthly normal rainfall, respectively (Table 1). The total dry spells occurred during the crop growth period were two and one coinciding with flowering and pod formation stages of green gram during 2018 and 2019, respectively (Table 2).

Soil of the experimental site was sandy loam in texture, low in organic carbon (0.27%), low in available N (132 kg ha^{-1}), medium in available P (13.1 kg ha^{-1}) and medium in available K (274 kg/ha). The experiment was laid out in factorial randomized block design with three replications. Total nine treatment combinations comprising three spacings *viz.* S_1:22.5 x 10 cm, S_2:30 x 10 cm and S_3: 45 x 10 cm and 3 fertility levels *viz*. F_1:100 % RDF (20-40 kg NP ha^{-1}), F_2:125 % RDF **(**25-50 kg NP ha^{-1}) and F_3:150 % RDF (30-60 kg NP ha^{-1}). Green gram variety MH 421 was sown on 6th July and 10th July and harvested on 15th September and 22nd September during 2018 and 2019, respectively. Fertilizers were applied through DAP and urea. The other agronomic practices were followed as per package of practices during the crop growth period. At maturity, the observations on ancillary characters were recorded on five randomly selected plants in each plot. The crop was harvested separately from the net plots, and thereafter seed and stover yields were recorded. Since similar trend was noticed during both the years, the data pertaining to all the two years were pooled. The prevailing market price of inputs as per treatment in the experiment was considered for working out the cost of cultivation. Net returns (Rs ha^{-1}) was calculated by deducting the cost of cultivation (Rs ha^{-1}) from gross returns, while BC ratio was worked out as a ratio of gross returns (Rs ha^{-1}) to cost of cultivation (Rs ha^{-1}). All the results were then analyzed statistically.

RESULTS AND DISCUSSION

Effect of spacing: Spacing at 45×10 cm recorded the maximum plant height (44.6 cm), followed by 30×10 cm spacing and the shortest plant height was observed at 22.5×10 cm spacing at the time of harvesting of green gram. The probable reason for tallest plant height at 45×10 cm spacing could be more utilization of energy properly in branching because there was less competition of light while in case of 22.5×10 cm spacing, there was insufficient utilization of light energy by the plant and due to the inter plant shading along the row. The results corroborate the findings of Sonani (2016). The highest number of branches per plant (6.5) was at spacing of 45×10 cm and the lowest at 22.5×10 cm spacing respectively. Significantly highest number of pods per plant (22.2) was recorded at spacing of 45 x 10 cm over other spacing. This might be due to better utilization of available growth resources *viz*. nutrient, moisture and solar radiation to a greater extent and accumulation of photosynthates. Similar trend were observed by Mandal (2012). Number of seeds per pod was also influenced significantly by different spacing and the highest (8.9) was recorded under spacing of 45×10 cm, followed by 30×10 cm spacing and the lowest at 22.5×10 cm spacing. Different spacing differed significantly 1000 seed weight of green gram. However, maximum 1000 seed weight (33.4 g) was achieved at the spacing of 45 × 10 cm followed by spacing of 30×10 cm and the lowest value (29.4 g) was recorded at 22.5×10 cm spacing. Similar findings were observed by earlier workers (Sathyamoorthi et al 2008, Kabir and Sarkar 2008). The higher values of the parameters may be explained in term of rapid growth, more branching and dry matter production. It is also corroborated with the findings of Kabir and Sarkar (2008). The maximum seed yield (824 kg ha^{-1}), stover yield (1284 kg ha^{-1}) and RWUE (5.29 kg ha^{-1}-mm) were at spacing of 45×10 cm followed by spacing at 30 x 10 cm and 22.5×10 cm. The highest seed yield at 45× 10 cm

Table 1. Rainfall recorded at experimental site

Season	Actual rainfall (mm)		Mean	Normal Rainfall (mm)
	2018	2019		
June	47.0	98.7	72.8	57.6
July	193.5	104.2	148.8	119.7
August	23.2	85.7	54.4	104.7
September	117.9	17.3	67.6	55.8
Kharif (Jun-Sep)	381.6	305.9	343.7	337.8

Table 2. Dry spell during crop growing season

Year	Dry spell		Stage of the crop
	Duration (days)	Dates and months	
2018	11	10-08-18 to 20-08-18	Flowering
	12	22-08-18 to 03-09-18	Pod formation
2019	16	18-08-19 to 02-09-19	Flowering and Pod formation

spacing resulted mainly due to highest growth and yield parameters of green gram under 45 x 10 cm spacing. Rasul et al (2012) and Wubetu (2018) also mentioned similar trend.

Effect of fertilizers: The plant height (43.5 cm) number of branches per plant (6.3), number of pods per plant (21.6), number of seeds per pod (8.7) and 1000 seed weight (33 g) were significantly higher with application of 100 % recommended dose of fertilizers (20-40 kg NP ha^{-1}) being at par with 125 % RDF (25-50 kg NP ha^{-1}) compared to 150 % RDF (30-60 kg NP ha^{-1}) (Table 2, 3). The highest values of the parameters was at 100 % recommended dose of fertilizers (20-40 kg NP ha^{-1}) is due to stimulation of root growth of the crop as balanced combination of nitrogen and phosphorus plays an important role in various physiological process including root development, nodulation and N- fixation, better utilization of available growth resources *viz*., nutrient, moisture and solar radiation to a greater extent and accumulation of photosynthates under rainfed conditions. The results corroborate the findings of earlier workers (Kadam and Khanvikar 2015, Sipai et al 2015, Sathyamoorthi et al 2008). Application of 100 % recommended dose of fertilizers (20-40 kg NP ha^{-1}) was at par with 125 % RDF (25-50 kg NP ha^{-1}) and gave significantly higher seed (748 kg ha^{-1}) and stover yield (1161 kg ha^{-1}) of green gram compared to 150 % RDF (30-60 kg NP ha^{-1}). Highest RWUE (4.85 kg ha^{-1} - mm) was with the application of 100 % recommended dose of fertilizer (20:40 kg NP ha^{-1}) and the lowest value (3.95 kg ha^{-1} - mm) was observed with the application of 150% RDF (30-60 kg NP ha^{-1}). The higher seed and stover yield of green gram might be due to the primary role of balanced combination of nitrogen and phosphorus in photosynthesis by way of rapid energy transfer and thereby increased photosynthetic efficiency and thus increased the availability of photosynthesis. This resulted in increase in seed and stover

Table 3. Effect of treatments on growth and yield attributes of green gram (Two years pooled data)

Treatments	Plant height (cm)	Branches $plant^{-1}$	Pods $plant^{-1}$	Seeds pod^{-1}	1000 seed weight (g)
Spacing					
S_1: 22.5 × 10 cm	37.7	5.2	17.8	7.2	29.4
S_2: 30 × 10 cm	41.0	5.9	19.4	7.9	31.2
S_3: 45 × 10 cm	44.6	6.5	22.2	8.9	33.4
CD (P=0.05)	2.8	0.4	1.5	0.5	2.1
Fertility levels					
F_1:100 % RDF (20-40 kg NP ha^{-1})	43.5	6.3	21.6	8.7	33.0
F_2: 125 % RDF (25-50 kg NP ha^{-1})	41.5	6.0	20.0	8.4	31.6
F_3: 150 % RDF (30-60 kg NP ha^{-1})	38.3	5.4	17.8	7.0	29.4
CD (P=0.05)	2.8	0.4	1.5	0.5	2.1

Table 4. Effect of treatments on crop yield and economics of green gram

Treatments	Grain yield (kg ha^{-1})	Stover yield (kg ha^{-1})	Gross returns (Rs ha^{-1})	Cost of cultivation (Rs ha^{-1})	Net returns (Rs ha^{-1})	BC Ratio	RWUE (kg/ha-mm)
Spacing							
S_1: 22.5 × 10 cm	534	823	38241	20350	17891	1.87	3.50
S_2: 30 × 10 cm	722	1117	51597	19450	32147	2.65	4.67
S_3: 45 × 10 cm	824	1284	58940	19000	39940	3.10	5.29
CD (P=0.05)	47	73					
Fertility levels							
F_1:100 % RDF (20-40 kg NP ha^{-1})	748	1161	53511	19050	34461	2.80	4.85
F_2: 125 % RDF (25-50 kg NP ha^{-1})	718	1114	51360	19600	31760	2.62	4.64
F_3: 150 % RDF (30-60 kg NP ha^{-1})	614	949	43907	20150	23757	2.18	3.95
CD (P=0.05)	47	73					

yield of green gram under rainfed conditions. Kundu et al (2013), Khan et al (2017), Kalsaria et al (2017) and Hangsing et al (2020) reported almost similar results. Interaction effect between spacing and fertility levels was non-significant for all characters.

Economics: Higher net returns (Rs. 39940 ha^{-1}) and BC ratio (3.10) were recorded when green gram was sown at the spacing of 45×10 cm (Table 4). Application of 100 % recommended dose of fertilizers (20-40 kg NP ha^{-1}) recorded higher net returns(Rs. 34461 ha^{-1}) and BC ratio (2.80) among all the fertility levels.

CONCLUSION

The present study exhibited that sowing at 45×10 cm and 100 % recommended dose of fertilizers (20:40 NP NP ha^{-1}) increased the yield attributing parameters and yield of green gram. Similarly, maximum net returns, BC ratio and RWUE was also observed under 45×10 cm spacing and 100 % recommended dose of fertilizers in green gram under rainfed conditions.

REFERENCES

Anonymous 2018. DES, Ministry of Agri. & FW (DAC&FW), Govt. of India.

Hangsing N, Tzudir L and Singh AP 2020. Effect of spacing and levels of phosphorus on the growth and yield of green gram (*Vigna radiata*) under rainfed condition of Nagaland. *Agricultural Science Digest* **40**(2): 139-143.

Kabir MH and Sarkar MAR 2008. Seed yield of mungbean as affected by variety and plant spacing in *Kharif*-I season. *Journal of Bangladesh Agriculture University* **6**(2): 239-244.

Kadam SS and Khanvilkar SA 2015. Effect of phosphorus, boron and row spacing on growth of summer green gram (*Vigna radiata*). *Journal of Agriculture and Crop Science* **2**: 7-8.

Kalsaria RN, Vekariya PD, Hadiyal JG and Ichchhuda PK 2017. Effect of spacing, fertility levels and bio-fertilizers on growth and yield of summer green gram (*Vigna radiata* L. Wilczek). *Journal of Pharmacognosy and Phytochemistry* **6**(5): 934-937.

Received 18 June, 2021; Accepted 10 November, 2021

Khan MMS, Singh VP and Kumar A 2017. Studies on effect of phosphorus levels on growth and yield of *kharif* mungbean (*Vigna radiata* L. wilczek). *International Journal of Pure applied Biosciences* **5**(4): 800-808.

Kundu R, Mandal J and Majumder A 2013. Growth and production potential of green gram (*Vigna radiata*) influenced by rhizobium inoculation with different nutrient sources. *International Journal of Agriculture, Environment and Biotechnology* **6**(3): 344-350.

Miah MHN, Karim MA, Rahman MS and Islam MS 1990. Performance of nizersail mutants under different row spacings. *Bangladesh Journal of Training and Development* **3**(2): 31-34.

Mandal J, Mallick R and Banerjee H 2012. Growth and yield of green gram (*Vigna radiata*) as affected by row spacing and foliar application of nutrients. *Research on Crops* **13**(2): 525-528.

Rasul F, Cheema MA, Sattar A, Saleem MF and Wahid MA 2012. Evaluating the performance of three mungbean varieties grown under varying inter-row spacing. *Journal of Animal and Plant Sciences* **22**(4): 1030-1035.

Raza MH, Sadozai GU, Baloch MS, Khan EA, Din I and Wasim K 2012. Effect of irrigation levels on growth and yield of mungbean. *Pakistan Journal of Nutrition* **11**(10): 876-879.

Sathyamoorthi K, Mohamed Amanullah E, Pazhanivelan S and Vaiyapun K 2008. Root growth and yield of Green gram [*Vigna radiata* (*L.*)Wilczek] as influenced by increased plant density and nutrient management. *Journal of Applied Sciences Research* **1**(7): 917-924.

Singh G, Ram H, Sekhon HS, Aggrawal N, Kumar M, Kaur P, Kaur J and Sarma P 2011. Effect of nitrogen and phosphorus application on productivity of summer mungbean sown after wheat. *Journal of Food Legumes* **24**: 327-329.

Singh G, Sekhon HS, Singh G, Brar JS, Bains TS and Shanmugasundaram S 2011. Effect of plant density on growth and yield of mungbean genotype under different environments in India and Taiwan. *International Journal of Agricultural Research* **6**(7): 573-583.

Sipai, AH, Jat, JS, Rathore, BS, Kuldeep, S, Jodha and Singh, J 2015. Effect of phosphorus, sulphur and biofertilizer on productivity and soil fertility after harvest of moongbean grown on light textured soil of Kachchh. *Asian Journal of Soil Science* **10**: 228-236

Sonani, VV, Gurjar, R, Parmar, HC and Patel RR 2016. Effects of sowing dates and *spacing* on summer *green gram*. *Green Farming* **7**(1): 194-196.

Wubetu A 2018. Effect of intra and inter row spacing on yield and yield components of mungbean (*Vigna radiata*). *Journal of Biology, Agriculture and Healthcare* **8**(12): 2224

Indian Journal of Ecology (2021) 48(6): 1736-1739

Manuscript Number: 3441
NAAS Rating: 5.79

Assessment of Variation for Pterostilbene in Heartwood of *Pterocarpus marsupium* Roxb., a Vulnerable Medicinal Tree from Central India

Naseer Mohammad, Hari Om Saxena[1], Raj Singh Yadav and Ganesh Pawar[1]

Genetics and Tree Improvement Division; [1]NWFP Section, Silviculture, Forest Management and Agroforestry Division, Tropical Forest Research Institute (ICFRE), Jabalpur - 482 001, India
E-mail: naseer35518@gmail.com

Abstract: Variation studies for the Pterostilbene, a highly reliable quality control marker for antidiabetic *Pterocarpus marsupium* was carried out to identify the appropriate populations for conservation. Heartwood core samples were extracted from different forest divisions of Madhya Pradesh and subjected to quantification employing HPLC technique. Analysis revealed that highest average percent of pterostilbene was recorded in samples from Sara (0.47%) followed by Lamta (0.42) and Barha (0.41). Bahoriband population recorded highest range of variation i.e., 0.12- 0.97% for pterostilbene followed by Lamta (0.15-0.98%) whereas, lowest was recorded in samples from Barha population (0.11-0.56). In consonant with the range, estimates of the coefficient of variations also exhibited similar trend. Highest CV was recorded in samples from Bahoriband followed by Lamta and lowest in Barha. Considering vulnerable status of *P. marsupium* and importance of heartwood, Bahoriband and Lamta populations are the suitable candidates for conservation as both harbours large variation for pterostilbene.

Keywords: Indian kino, Marker, Conservation, Heartwood, Endangered

Pterocarpus marsupium Roxb., commonly known as 'Bijasar', is one of the most important medicinal trees in Ayurvedic system of medicine used for the treatment of diabetes mellitus (Anonymous 2001). In India, it is commonly found in dry deciduous tropical forests of Madhya Pradesh, Maharashtra, Chhattisgarh, Odisha, Andhra Pradesh, Karnataka, Kerala, Tamil Nadu, West Bengal and Uttar Pradesh (Kirtikar and Basu 1999). All the plant parts of *P. marsupium* have medicinal importance, but heartwood has great demand due to its antidiabetic properties (Kirtikar 1987, Maurya et al 2004). Phytochemical assessments revealed that heartwood contains pterostilbene and marsupin (Mathew et al 1977) and both were more effective against hyperglycemia on comparison with metformin (Manickam et al 1997). Annual demand of heartwood and stem bark of *P. marsupium* is estimated about 200-500 MT (NMPB 2021).

Phytochemical variation is a common phenomenon in medicinal plants and quantitative variation of a particular compound usually varies in the plant material from different locations due to environmental, genotype and G×E interactions (Dhami and Mishra 2015). Export potential of medicinal plants in national and international market is highly depends on the variation of active ingredients with respect to different environmental conditions (Sandeep et al 2015). WHO and modern herbal pharmacopoeia also emphasized the need of standardization of herbal drugs with respect to their active chemical markers (Sharma et al 2010, Vasudevan 2009). Thus, quality standardization of medicinal plants in terms of their chemical markers is the need of the hour to ensure reproducible quality of herbal drugs for their safety and efficacy (Goldman 2001, Kushwaha et al 2010).

Although heartwood extract of *P.marsupium* is reported to have many pharmacological compounds such as pterostilbene, marsupsin, pterosupin, liquiritigenin, etc. (Dhayaney and Sibi 2019). Pterostilbene is considered as the most reliable chemical marker compound for quality assessment of heartwood of *P. marsupium* due to various biological activities such as anti-hyper-glycemic, hypolididemic, anti-cancer, anti-diabetic and antifungal, (Annapurna et al 2018).

Tropical deciduous forest of central India is known for harboring vast genetic diversity and variation. *P. marsupium* was reported to be one of the important species commonly found in this forest. However, due to over-exploitation coupled with poor natural regeneration, this species has been included in IUCN Red List of Threatened Species (IUCN 2017). Therefore, present investigation was undertaken to assess the variations in pterostilbene content in heartwood samples of *P. marsupium* collected from different locations of Madhya Pradesh.

MATERIAL AND METHODS

Sampling and extraction of wood cores: For the study, we sampled 42 trees randomly from seven different localities

(Fig. 1, Table 1) of Madhya Pradesh. Wood core samples were extracted at breast height. Haglof three-thread increment borer (Ben Meadows Company, USA) was used for extraction of wood core. Care has been taken to remove mosses, aroids, and the outer bark at beast height where the trunk was cored. Dried heartwood samples were fine powdered using pulverizer machine and used for estimation of pterostilbene by HPLC technique.

Extraction of plant materials: 30 ml methanol was added into 1 gm fine dried heartwood powder and refluxed on a water bath for 30 minutes. The same operation was repeated twice with methanol (2×30 ml) and filtrates were combined and made up to 100 ml with methanol. All the extracts solutions were made following similar procedure.

Preparation of standard solution: Pterostilbene standard was procured from M/s Sigma Aldrich, India (purity ≥ 97%) and diluted with methanol to 0.1 mg/ml concentration. Working solution having concentration range of 0.03 -0.15 µg/0.5 ml was prepared by further diluting with methanol.

Estimation of pterostilbene: HPLC instrument was calibrated for all parameters viz. pumps, manual injector and detector. The HPLC-515 series system supplied by Alliance HPLC System, USA having C-18 column equipped with a Photo Diode Array (PDA) detector was used for detection. Chromatographic conditions were as follows: Mobile Phase- a mixture of acetonitrile and 0.1% (v/v) phosphoric acid in water in the ratio 55:45, injection volume-20 µl, flow rate-1.0 ml/min and wavelength - 313 nm. Test samples were filtered through 0.2 µm pore size syringe filter before HPLC analysis.20 µl from working standard solution of pterostilbene was injected and calibration curve was generated by linear regression based on the peak areas. Linearity was obtained over a concentration range of 1.2-6.0 ng per injection with a $R^2 = 0.99$.

20µl of each heartwood extract was injected into HPLC system. Samples were run for 15 minutes since the retention time of pterostilbene was 9.94±0.5 min. Specificity ascertained by comparing the peak purity of standard and samples through their HPLC chromatograms (Fig. 2). Peak corresponding to pterostilbene in the sample was confirmed by comparing the spectrum obtained by using photo diode array detector, which was completely in agreement with the standard. The content of pterostilbene in samples was calculated by linear regression.

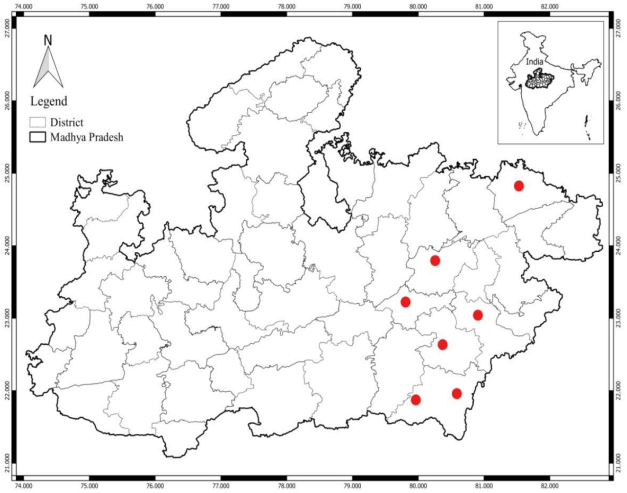

Fig. 1. Sampling locations heartwood core of *P. marsupium* from Madhya Pradesh, a central Indian state

Table 1. Details of the sample plots laid for regeneration study of *P. marsupium* at different forest divisions of Madhya Pradesh

Name of forest division	Details of sampling site (Range & Compt. No)	GPS coordinates of sampling site
Mandla	Sara / RF-324	22º 23' 30.1" N 80º 23' 12.8" E
Balaghat	Birsa / P-1671	21º 58' 41.5" N 80º 46' 50.2" E
Balaghat	Lamta/ P-1388	22º 00' 18.7" N 80º 08' 04.5" E
Jabalpur	Barha/ RF-259	23º 18' 22.8" N 80º 28' 20.6" E
Dindori	Chada/ RF-563	22º 33' 21.6" N 81º 22' 20.9" E
Katni	Bahoriband/ P-189	23º 48' 38.5" N 79º 51' 51.1" E
Rewa	Semariya/ P-166	24º 54' 06.2" N 81º 13' 25.9" E

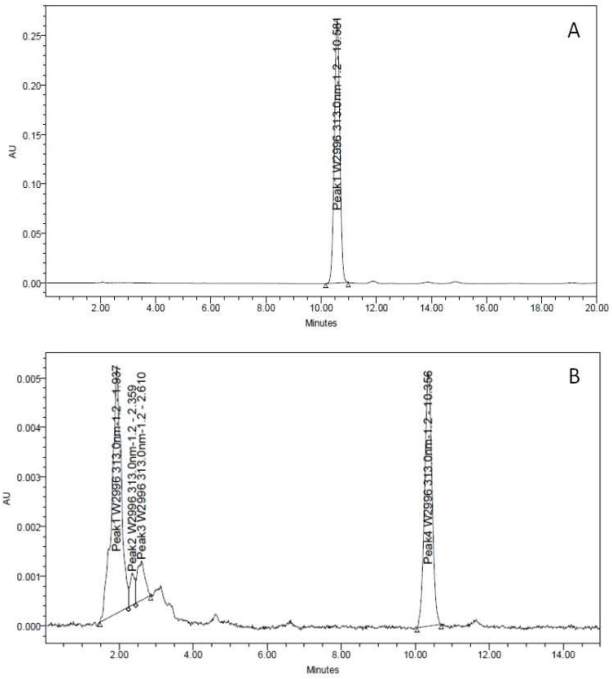

Fig. 2. HPLC chromatograms of (A) Pterostilbene standard and (B) *P. marsupium* heartwood extract

Data analysis: Data was analysed for basic descriptive statistics using SYSTAT Ver 13.1 Software (Systat Software, San Jose, CA).

RESULTS AND DISCUSSION

Chemical markers are crucial for the quality control of herbal medicines, including authentication of genuine species, harvesting the best quality raw materials, evaluation of post harvesting handling and detection of harmful or toxic ingredients (Mukherjee and Wahil 2006). Pterostilbene which is reliable marker for *P. marsupium* is a natural polyphenolic compound which having anti-diabetic properties and also reported to modulates the suppression of multidrug resistance protein 1 and triggers autophagic and apoptotic mechanisms in cisplatin-resistant human oral cancer CAR cells via AKT signaling (Chang et al 2018).

Randomly chosen six heartwood sample from each study site was analyzed for pterostilbene content. Analysis revealed that the highest content of pterostilbene was found in sample # 19 of Lamta locality (0.978%) followed by sample # 4 of Bahoriband (0.969%) and sample # 25 of Birsa (0.836%) location, respectively (Table 2). Locality-wise basic descriptive statistic for the pterostilbene content is presented in Table 3. Critical perusal of the table revealed that highest average percent of pterostilbene was recorded in samples from Sara (0.47%) followed by Lamta (0.42) and Barha (0.41).

Highest range of variation for pterostilbene was recorded in samples from Bahoriband i.e., 0.12-0.97% followed by Lamta (0.15-0.98%). Lowest range of variation was recorded in samples from Barha (0.11-0.56). In consonant with the range, estimates of the coefficient of variations also exhibited similar trend. Highest CV was recorded in samples from Bahoriband followed by Lamta and lowest in Barha. The variation in pterostilbene content among various locations of central India may be correlated with various environmental factors in addition to genetic factors which influence the growth of a plant and secondary metabolite production (Pothitirat and Gritsanapan 2006,

Table 2. Estimates of the Pterostilbene (%) in different samples of *P. marsupium* collected from study site

Study site	Pterostilbene (%)	Study site	Pterostilbene (%)
Bahoriband	0.292	Lamta	0.978
	0.304		0.727
	0.124		0.255
	0.969		0.149
	0.209		0.218
	0.210		0.167
Chada	0.219	Birsa	0.836
	0.225		0.192
	0.192		0.192
	0.672		0.249
	0.231		0.298
	0.177		0.199
Sara	0.203	Barha	0.109
	0.724		0.562
	0.326		0.494
	0.612		0.466
	0.700		0.348
	0.273		0.473
Semariya	0.266		
	0.207	Mean : 0.037	
	0.209	SE: 0.04	
	0.248	SD: 0.24	
	0.708		
	0.510		

Table 3. Population-wise descriptive statistics for the Pterostilbene (%) estimated from heartwood samples collected from different study site

Study site	Pterostilbene (%)					
	Mean	Standard deviation	Standard error	Range	Coefficient of variation	Coefficient of dispersion
Bahoriband	0.35	0.31	0.13	0.12-0.97	0.88	0.68
Chada	0.29	0.19	0.08	0.18-0.67	0.67	0.41
Sara	0.47	0.23	0.09	0.20-0.72	0.49	0.44
Semariya	0.36	0.21	0.08	0.21-0.71	0.57	0.53
Lamta	0.42	0.35	0.14	0.15-0.98	0.84	1.00
Birsa	0.33	0.25	0.1	0.19-0.84	0.77	0.6
Barha	0.41	0.16	0.07	0.11-0.56	0.4	0.22

Critical difference value - N/A
Overall coefficient of variation - 66.99

Anandaraj et al 2014, Sandeep et al 2015). Irrespective of locations, the overall coefficient of variation was recorded to be 66.99%. Looking to the vulnerable status of the species and importance of pterostilbene i.e. quality heartwood, populations of Bahoriband and Lamta are the suitable candidates for conservation as both harbours large variation for pterostilbene.

CONCLUSION

Present investigation revealed that there is adequate variation for the pterostilbene content in heartwood samples collected from different forest divisions of Madhya Pradesh. Samples from Katni Forest Division (Location–Bahoriband) and Balaghat Forest Division (Location-Lamta) have high variation for pterostilbene content. We conclude that these forest divisions should be targeted for conservation as well as growing stock of this valuable species.

ACKNOWLEDGEMENTS

The authors are thankful to the Director, Tropical Forest Research Institute, Jabalpur, Madhya Pradesh for providing necessary facilities for the study. Authors are also grateful to the Madhya Pradesh State Forest Department for providing access to forest areas and necessary assistance in field work. Investigation is financially supported by Indian Council of Forestry Research and Education, Dehradun under the project Id -240/TFRI/2017/Biod-1(19).

REFERENCES

Anandaraj M, Prasath D, Kanadiannan K, John Zachariah T, Srinivasan V, Jha AK, Singh BK, Singh AK, Pandeye VP, Singh SP, Shoba N, Jana JC, Ravindra Kumar K and Uma Maheswar K 2014. Genotype by environment interaction effects on yield and curcumin in turmeric (*Curcuma longa* L.). *Industrial Crops and Products* **53**: 358-364.

Annapurna MM, Venkatesh B and Teja GR 2018. Development of a validated stability indicating liquid chromatographic method for the determination of pterostilbene. *Indian Journal of Pharmaceutical Education and Research* **52**(4S): S63-S70.

Anonymous. 2001. *The Ayurvedic Pharmacopoeia of India*, First Edition, Govt. of India, Ministry of Health and Family Welfare, Dept. of Indian System of Medicine & Homeopathy, New Delhi. **1**(1):12-13.

Received 12 September, 2021; Accepted 30 November, 2021

Chang HP, Lu CC, Chiang JH, Tsai FJ, Juan YN, Tsao JW, Chiu HY and Yang JS 2018. Pterostilbene modulates the suppression of multidrug resistance protein 1 and triggers autophagic and apoptotic mechanisms in cisplatin-resistant human oral cancer CAR cells via AKT signaling. *International Journal of Oncology* **52**: 1504-1514.

Dhami N and Mishra AD 2015. Phytochemical variation: How to resolve the quality controversies of herbal medicinal products? *Journal of Herbal Medicine* **5**(2): 118-127.

Dhayaney V and Sibi G 2019. *Pterocarpus Marsupium* for the treatment of diabetes and other disorders. *Journal of Complement Med Alt Healthcare* **9**(1): 555754.

Goldman P 2001. Herbal medicines today and the roots of modern pharmacology. *Ann Intern Medicines* **135**: 594-600.

IUCN 2017. World Conservation Monitoring Centre 1998. *Pterocarpus marsupium*. IUCN Red List Threat. Species. 2017, Version 2017.2.

Kirtikar B 1987. *Indian medicinal Plants*, 2nd Ed, New Delhi, 1:826-827.

Kirtikar KR and Basu BD 1999. *Indian Medicinal Plants*, Vol-I. Naya Prakashan, Kolkata, Pp. 828-829.

Kushwaha SKS, Kushwaha N, Maurya N and Rai AK. 2010. Role of markers in the standardization of herbal drugs: A review. *Archives of Applied Science Research* **2**(1): 225-229.

Manickam M, Ramanathan M, Jahromi MA, Chansouria JP and Ray AB 1997. Antihyperglycemic activity of phenolics from *Pterocarpus marsupium. Journal of Natural Product* **60**: 609-610.

Mathew J, Subba Rao AV and Subba Rao NV 1977. Photooxidation of pterostilbene from *Pterocarpus marsupuim* Roxb. *Current Science* **46**: 337-338.

Maurya R, Singh R, Deepak M, Handa SS, Yadav PP and Mishra PK 2004. Constituents of *Pterocarpus marsupium*: An ayurvedic crude drug. *Phytochemistry* **65**(7): 915-920.

Mukherjee PK and Wahil A 2006. Role of markers in the standardization of herbal drugs: a review. *Drug Information Journal* **40**: 131-139.

NMPB. 2021. https://www.nmpb.nic.in/medicinal_list. Accessed on 01.07.2021.

Pothitirat W and Gritsanapan W 2006. Variation of biotic components in *Curcuma longa* in Thailand. *Current Science* **91**(10): 1397-1400.

Sandeep IS, Sanghamitra N and Mohanty S 2015. Differential effect of soil and environment on metabolic expression of turmeric (*Curcuma longa* cv. Roma). *Indian Journal of Experimental Biology* **53**: 406-411.

Sharma P, Kaushik S, Jain A and Sikarwar SM. 2010. Preliminary phytochemical screening and HPTLC fingerprinting of *Nicotiana tabacum* leaf. *Journal of Pharm Research* **3**(5): 1144-1145.

SYSTAT Version 13.1 (2021) Systat Software, Inc., San Jose, California.

Vasudevan H 2009. DNA fingerprinting in the standardization of Herbs and Neutaceuticals. *The Science Creative Quarterly* **4**: 56-59.

Indian Journal of Ecology (2021) 48(6): 1740-1746

Manuscript Number: 3442
NAAS Rating: 5.79

Cytogenetic Investigations and Karyological Relationships of Eight *Medicago* species (Fabaceae)

Z.A. Turki and M.M. Hegazy

Department of Botany and Microbiology, Faculty of Science, Menoufia University, Shebeen El Koom, Egypt
E-mail: marwahegazy204@gmail.com

***Abstract*:** A karyological study was conducted of eight taxa of the genus *Medicago* L. namely *M. sativa*, *M. glutinosa*, *M. x varia* and *M. polychroa*, *M. hemicycle*, *M. falcate*, *M. suffruticosa* and *M. hybrid* of *Medicago sativa-falcata* complex. Cytological tools used as an attempt to found new traits which may be significant in classifying the taxa of the complex. The measured chromosomal parameters were, short arm, long arm, and total length of chromosomes, mean relative length percentage and mean centromeric index percentage of each chromosome and total genome length. Satellite chromosomes and chromosome type were detected and the chromosomal formula for each taxon was provided. The basic chromosome numbers in the eight studied taxa varied between; x=8, for diploid (2n=16); *M. hemicycle*, *M. falcate*, *M. suffruticosa* and *M. hybrid* and tetraploid (2n=32); *M. sativa*, *M. glutinosa*, *M. x varia* and *M. polychroa*. Karyotype characters were significant to identify the studied taxa. Detailed karyotype analysis allows to group the different species and to postulate relationships among them. The present study supports putting the taxa *M. sativa*, *M. suffruticosa* and *M. hybrid* in one group and treating *M. glutinosa*, *M. x varia, M. polychroa*, *M. hemicycle* and *M. falcate* as a distinct species rather than considering them as subspecies of *M. sativa*.

***Keywords*:** Alfalfa, Cytotaxonomy, Fabaceae, Falcago, Falcatae, Karyotype, *Medicago*, *Medicago sativa-falcata* complex, Polyploidy

Medicago L. is one of the largest genera in family Fabaceae with 87 species including shrubs and herbs (Small 2011). Species are annual, biennial and perennials, widely distributed from the Mediterranean to central Asia (Nixon 2006). Taxonomically, genus *Medicago* belongs to tribe Trifolieae, sub-tribe Trigonellinae. *Medicago* species are variously grouped based on morphological and floral characters (Small 2011). Relationships within the genus are not yet sufficiently resolved, contributing to difficulty in understanding the evolution of a number of distinguishing characteristics such as aneuploidy and polyploidy, life history, structure of cotyledons, and number of seeds per fruit (Lesins and Lesins 1979). In addition to the morphology, Cytogenetical studies based on chromosomal information may provide more information and are useful for taxonomy, phylogeny and evolution, of the genetic and breeding in *Medicago* plants (Sadeghian et al 2014). Both number and morphology of chromosomes were investigated extensively (Agarwal, 1983; Falistocco et al 1995, Calderini et al 1996, Bauchan and Hossain 1997). Small (2011) demonstrated number of problems concerning the reliability of chromosome number reports of the genus *Medicago* viz. misidentification, errors of technique (somatic chromosomes are small in *Medicago* and not easy to count. also, satellite chromosomes may be miscounted as additional chromosomes) and tendency to verify previous counts. In several species there are both diploid (2n=16) and tetraploid (2n=32) populations. The *Medicago sativa-falcata* complex includes subspecies that are partially sympatric and potentially freely hybridizing in nature (İlhan et al 2016). The complex was first recognized in Lesins and Gillies (1972). The complex is in the section Falcago and subsection Falcatae (Quiros & Bauchan 1988). Largely due to the millennia long economic importance, the taxa have been in the center of attention. Sharma and Datta (2020) examined the effect of heavy metal i.e. lead on *Medicago sativa*. They founded that the toxicity increased with increase in concentration of lead. Therefore, they called for an urgent strategy to mitigate lead pollution for the sake of food safety.

The taxa encompassed in the complex contain both diploids (2n = 2× = 16) and tetraploids (2n = 2× = 32), and gene flow can occur within and between ploidy levels. The most up-to-date list of taxa in the *M. sativa-falcata* complex include: *M. sativa* subsp. *caerulea* (2n), *M. sativa* subsp. *falcata* (2n and 4n), *M. sativa* subsp. x *hemicycla* (2n), *M. sativa* subsp. *glutinosa* (2n), *M. sativa* subsp. *sativa* (4n), *M. sativa* subsp. x *varia* (4n), and *M. sativa* subsp. *glomerata* (4n) (Şakiroğlu and İlhan 2020). These subspecies represent the primary gene pool for alfalfa improvement (Humphries et al 2021, İlhan et al 2016, Şakiroğlu and İlhan 2020). These taxa have been given the hierarchy of species by some authors (Lesins and Lesins 1979) and of subspecies by others (Gunn et al 1978). Morphological traits such as flower color, pod shape, pollen shape along with the cytogenetic state of ploidy have

traditionally been considered as the focal criteria for classification of taxa included in the complex. The polyploidy in the complex has been investigated extensively by researchers in different disciplines (Sakiroglu and Kaya 2012). *Medicago sativa-falcata* complex has also been proposed as a model in polyploidy evolution studies (Havananda et al 2011). The objectives are chromosome count, to revise the taxonomy, understanding the delimitation and affinities of some *Medicago* species by the use of cytological analysis.

MATERIAL AND METHODS

The present study carried out on eight *Medicago* species (*M. sativa*, *M. glutinosa*, *M. hemicycle*, *M. falcate*, *M. x varia*, *M. polychroa*, *M. suffruticosa* and *M. hybrida*). The seeds were obtained from the Institute of Plant Genetics and Crop Plant Research (IPK) Germany. The cytological investigations were conducted at the cytogenetic lab of the National Gene Bank (NGB) at Agricultural Research Center (ARC) Giza, Egypt during 2018 to 2021 (Table 1). The eight *Medicago* species were karyotyped to determine their chromosome number and morphology. Somatic chromosomes were studied in root meristems of germinating seeds. Using data taken from the average of five metaphases of the species under study chromosomes lengths and centromeric index percentage of the 16 chromosomes at *M. hemicycle*, *M. falcate*, *M. suffruticosa* and *M. hybrid* and 32 chromosomes at *M. sativa*, *M. glutinosa*, *M. x varia* and *M. polychroa*, and the mean were calculated for each species.

Seeds were germinated on moistened filter paper in petri dishes at 4°C in cooling incubator. Healthy roots of proper length (1-1.5 cm, collected at 7 am to 8 am) were pre-treated with ice water and incubated in ice box overnight, fixed (3: 1 ethanol - glacial acetic acid for overnight) hydrolysed (0.1 N HCl for 3-5 min at 60°C) and stained by squashing the meristemtic regions in a drop of 1% acetic orcein mixed with a drop of 45% acetic acid. The cover slip was placed on it and the slides were placed on a levelled surface of table and pressed firmly to get a good spread of chromosomes and observed. Scattered metaphase plates prepared for the species were analyzed through Image Analyzing System. Metaphase plates observed and photographed using a verticals fluorescence microscope (Leica DM2500 Wetzlar, Germany) equipped with a cooled monochrome digital camera (Leica DFC340FX) at 100X magnification under oil immersion and those photographs were transferred directly to computer. Chromosome images were analysed and Chromosome counting, measurements and karyotype has performed from at least 5 plates (in each species) using the automated Karyotype and FISH software processing (Leica CW4000) system.

Metaphase chromosomes of each taxon were arranged in a decreasing order of size and keeping in view the centromere position that constitutes a karyotype. The length of short arm chromosomes (p) and the lengths of long arm chromosomes (q) were measured and total length (TL) of each chromosome was calculated (p + q). The relative length (RL) of the chromosomes was calculated [RL = (TL/sum TL) ×100]. The centromeric index (CI %) was also estimated by [CI % = (p/TL) ×100] according to Peruzzi and Eroğlu (2013). The mean centromeric index (MCI) was calculated to represent the centromeric index value of particular chromosome pair. MCI was also determining the position of centromere, the chromosome was considered metacentric when the centromeric index was ranged between 45.0 and 50.0 and telocentric when this value was zero (Hassan and Abd El-Gawad 2013). Idiograms were drawn based on mean centromeric index and arranged in order of decreasing size. The karyotypic formula was established, karyograms were obtained with the help of a Photoshop program. Morphometric data were statistically analyzed in a completely randomized design with five replicates.

RESULTS AND DISCUSSION

The basic chromosome number of X = 8 was found in all of the eight species.. The chromosome count of these species in mitotic metaphase of the meristemtic root cells revealed the presence of two types, 2n=16 and 2n=32 (Tables 2-5). Based on the observed chromosome number, the eight studied *Medicago* species were divided into two groups: Group one (*M. hemicycle*, *M. falcate*, *M. suffruticosa*, *M. hybrida*) exhibited a chromosome set of 2n=2x=16, named as diploid, while Group two (*M. sativa*, *M. glutinosa*, *M. x varia*, *M. polychroa*) exhibited a chromosome set of 2n=4x=32, named as tetraploid (Fig. 1).

Karyotype of the eight *Medicago* species: Chromosome sets of eight (x=8) were highly variable in their lengths among the different studied species. The first chromosome pair is the longest one in the complement of all species and length

Table 1. Details of species and source used in study

Species	Source and accession number	Origin
M. sativa	IPK/ 1771588	Deutchland
M. glutinosa	IPK/ 1772029	Unknown
M. hemicycla	IPK/ 1771973	Unknown
M. falcata	IPK/ 1772209	Unknown
M. x varia	IPK/ 1771590	Germany
M. polychroa	IPK/ 1773054	Soviet Union
M. suffruticosa	IPK/ 1772161	Unknown
M. hybrida	IPK/ 1772201	Unknown

Table 2. Karyotype characteristics of the studied *Medicago* species

Species	x	2n	K.F.	SAT. chromosome
M. sativa	8	32	$L_{16}^{m} + M_{16}^{m}$	Ch. 8
M. glutinosa	8	32	$L_{16}^{m} + M_{16}^{m}$	Ch. 1
M. hemicycla	8	16	$L_{8}^{m} + M_{8}^{m}$	Ch. 2
M. falcata	8	16	$L_{8}^{m} + M_{8}^{m}$	Ch. 3
M. x varia	8	32	$L_{16}^{m} + M_{16}^{m}$	Ch. 3,4
M. polychroa	8	32	$L_{16}^{m} + M_{16}^{m}$	—
M. suffruticosa	8	16	$L_{8}^{m} + M_{8}^{m}$	—
M. hybrida	8	16	$L_{8}^{m} + M_{8}^{m}$	—

Basic chromosome (x), Somatic chromosome number (2n), karyotype formula (K.F.) (L: Large, M: Medium, m: Metacentric), Satellite (SAT)

ranged from 5.11 to 9.16 µm in *M. polychroa* and *M. suffruticosa*, respectively (Table 3) and a mean relative length (MRL) of 15.40 to 19.24% in *M. sativa* and *M. falcate*, respectively (Table 4). The last chromosome pair is the shortest one in the complement of all species and length ranged from 1.47 to 4.27 µm (*M. glutinosa* and *M. suffruticosa*, respectively, Table 3) and a mean relative length (MRL) ranged from 4.24 to 9.30% (*M. x varia* and *M. sativa*, respectively, Table 4). The retrieved results showed that the total genomic length ranged from 30.14 µm in *M. polychroa* to 52.8 µm in *M. suffruticosa* (Table 4). The overall analysis indicated that chromosomes vary in size, large and medium and as detailed in the karyotype formula of each species. Five species exhibited satellite chromosome viz; the eighth chromosome pair of *M. sativa*, the first chromosome pair of

Table 3. Mean average of karyomorphological for chromosome pairs (1–8) in *Medicago* species

Species	Chromosome pairs							
	1	2	3	4	5	6	7	8
Long arm length (µm)								
M. sativa	3.27	3.05	2.95	2.63	2.63	2.53	2.42	1.89
M. glutinosa	3.47	3.37	2.63	2.31	2	2	1.79	0.80
M. hemicycla	2.63	2.21	2.11	2	1.89	1.89	1.79	1.47
M. falcate	3.47	3.37	2.63	2.11	2	2	1.79	0.748
M. x varia	3.37	3.37	2.63	2.11	2.1	2	1.79	0.74
M. polychroa	2.61	2.21	2.22	2	1.89	1.89	1.79	0.77
M. suffruticosa	4.63	4.47	4.23	3.2	3.79	3.16	2.53	2.32
M. hybrid	3.47	3.05	2.55	2.63	2.63	2.53	2.42	1.89
Short arm length (µm)								
M. sativa	2.84	2.51	2.51	2.22	2.22	2.2	2	1.8
M. glutinosa	3.05	2.95	2.42	2.12	1.69	1.5	1.37	0.67
M. hemicycla	2.53	2.11	2	1.89	1.89	1.79	1.68	1.11
M. falcate	3.05	2.95	2.42	2	1.79	1.47	1.37	0.72
M. x varia	3.05	2.85	2.45	2.02	1.79	1.9	1.77	0.73
M. polychroa	2.5	2.11	2.2	1.89	1.89	1.79	1.68	0.7
M. suffruticosa	4.53	3.97	3.4	2.72	3.2	2.7	2	1.95
M. hybrid	2.84	2.51	2.11	2.5	2.2	2	2	1.71
Total chromosome length (µm)								
M. sativa	6.11	5.56	5.46	4.85	4.85	4.73	4.42	3.69
M. glutinosa	6.52	6.32	5.05	4.43	3.69	3.5	3.16	1.47
M. hemicycla	5.16	4.32	4.11	3.89	3.78	3.68	3.47	2.58
M. falcate	6.52	6.32	5.05	4.11	3.79	3.47	3.16	1.47
M. x varia	6.42	6.22	5.08	4.13	3.89	3.9	3.56	1.47
M. polychroa	5.11	4.32	4.42	3.89	3.78	3.68	3.47	1.47
M. suffruticosa	9.16	8.44	7.63	5.92	6.99	5.86	4.53	4.27
M. hybrid	6.31	5.56	4.66	5.13	4.83	4.53	4.42	3.6

M. glutinosa, the second chromosome pair of *M. hemicycle*, the third chromosome pair of *M. falcate* and both the third and fourth chromosome pairs of *M. x varia* (Table 2, Fig. 2). The chromosomes are clearly heterogeneous with respect to their mean relative lengths (MRLs), and were arranged from the longest to the shortest (Table 3 and Fig. 2, 4). In all chromosomes, centromeres acquired metacentric positions (Table 5 and Fig. 2, 5).

By using SPSS statistics software program version 16.0 Cluster analysis constructed on the basis of karyotype similarities to illustrate the relationship between the studied *Medicago* species using the between groups method (Fig. 3). The dendrogram shows two major groups. The first group includes five species (*M. glutinous*, *M. falcata*, *M. x varia*, *M. hemicycle*, *M. polychroa*). The second is composed by the three species (*M. sativa*, *M. hybrid*, *M. suffruticosa*).

Chromosome numbers and morphology were performed by analysis of dividing root tips of germinating seeds. In *M. sativa*, count of 2n = 32 chromosomes is in agreement with numerous indications for this taxon (Okumura et al 1995, Savova et al 1996). Deviating chromosome count of 2n = 16 was reported by Nazarova (2004). In *M. glutinosa*, count is in accordance with indications of tetraploid chromosome numbers made by several authors with 2n = 32 (Magulaev 1992). In *M. hemicycle*, our count of 2n = 16 chromosomes is in

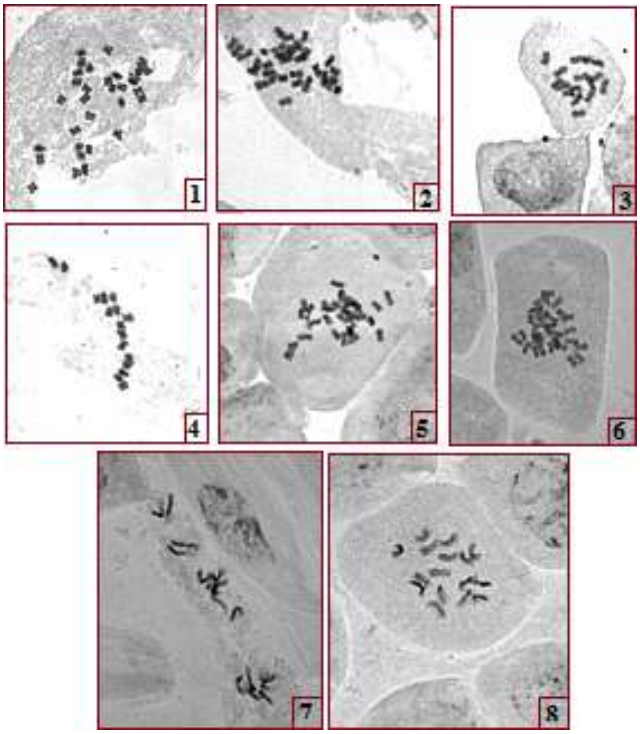

Fig. 1. Representative photomicrographes of well-spread mitotic metaphase, indicating number of chromosomes in the eight studied *Medicago* species. (1) *M. sativa*, (2) *M. glutinosa*, (3) *M. hemicycle*, (4) *M. falcate*, (5) *M. x varia*, (6) *M. polychroa*, (7) *M. suffruticosa*, (8) *M. hybrid*

Table 4. Mean relative length percentage of each chromosome pair with respect to the total genome in *Medicago* species

Species	Chromosome pairs								
	1	2	3	4	5	6	7	8	Total genome µm
M. sativa	15.40	14.02	13.76	12.23	12.23	11.92	11.14	9.30	39.67
M. glutinosa	19.10	18.51	14.79	12.98	10.81	10.25	9.26	4.31	34.14
M. hemicycle	16.65	13.94	13.26	12.55	12.20	11.87	11.20	8.33	30.99
M. falcate	19.24	18.65	14.90	12.13	11.18	10.24	9.32	4.34	33.89
M. x varia	18.52	17.94	14.65	11.91	11.22	11.25	10.27	4.24	34.67
M. polychroa	16.95	14.33	14.66	12.91	12.54	12.21	11.51	4.88	30.14
M. suffruticosa	17.35	15.98	14.45	11.21	13.24	11.10	8.58	8.09	52.8
M. hybrid	16.16	14.24	11.94	13.14	12.37	11.60	11.32	9.22	39.04

Table 5. Mean centromeric index percentage of each chromosome pair in *Medicago* species

Species	Chromosome pairs							
	1	2	3	4	5	6	7	8
M. sativa	46.48	45.14	45.97	45.77	45.77	46.51	45.25	48.78
M. glutinosa	46.78	46.68	47.92	47.86	45.80	42.86	43.35	45.58
M. hemicycla	49.03	48.84	48.66	48.59	50.00	48.64	48.41	43.02
M. falcata	46.78	46.68	47.92	48.66	47.23	42.36	43.35	49.05
M. x varia	47.51	45.82	48.23	48.91	46.02	48.72	49.72	49.66
M. polychroa	48.92	48.84	49.77	48.59	50.00	48.64	48.41	47.62
M. suffruticosa	49.45	47.04	44.56	45.95	45.78	46.08	44.15	45.67
M. hybrida	45.01	45.14	45.28	48.73	45.55	44.15	45.25	47.50

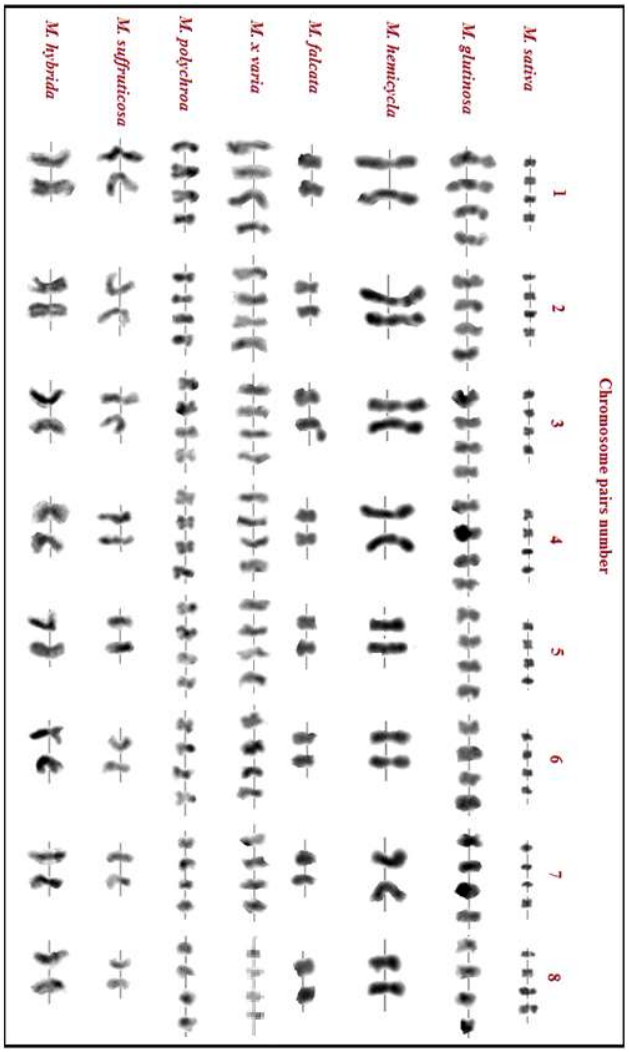

Fig. 2. Karyotypes of the eight studied *Medicago* species. *M. sativa*, *M. glutinosa*, *M. x varia* and *M. polychroa* are tetraploids (2n=4x=32). *M. suffruticosa*, *M. hybrid*, *M. hemicycla* and *M. falcate* are diploids (2n=2x=16)

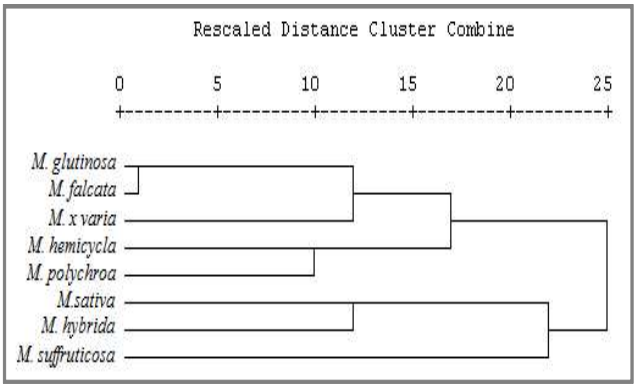

Fig. 3. Dendrogram of eight species of *Medicago* by analyzing karyotypic parameters

agreement with McLennan et al (1966). A deviating count was reported by Clement (1962) with tetraploid chromosome number of 2n = 32. In *M. Falcata*, our count of 2n = 16 chromosomes agrees with indications made by several authors (Jahan et al 1994, Savova et al 1996). Deviating count of 2n =32 chromosomes reported by others (Lovkvist and Hultgard 1999). In *M. x varia*, count of 2n = 32 chromosomes in accordance with indications for this species made by several authors (Karshibaev 1992, Zhang et al 1993, Savova et al 1996). Deviating count of 2n =16 chromosomes reported by others (Clement 1962). Bolkhovskikh et al (1969) recorded three different chromosome numbers in *M. x varia*; 2n = 16, 2n = 32 and 2n = 36.

In *M. polychroa* our count is in accordance with indications of tetraploid chromosome numbers made by several other authors with 2n = 32 (Clement 1962). In *M. suffruticosa*, count of 2n = 16 chromosomes is in agreement with numerous indications for this taxon (Lesins and Lesins 1979, Galland 1988). In *M. hybrida* count is in accordance with indications of diploid chromosome numbers made by several other authors with 2n = 16 (Lesins 1969). The present study compare the karyotypes of several diploid and tetraploid species of the genus *Medicago*. *M. hemicycla*, *M. falcata*, *M. suffruticosa* and *M. hybrida* were reported to be the diploid species (2n=2x=16) while, *M. sativa*, *M. glutinosa*, *M*. x *varia* and *M. polychroa* were found to be the tetraploid species (2n=4x=32) . Statistical analysis of Karyograms prepared from somatic chromosomes has provided some information on taxonomic relationships between the studied taxa. Firstly, the species; *M. sativa*, *M. suffruticosa* and *M. hybrid* were closely grouped together, the results supports grouping them in one group in agreement with several authors. Urban (1873) grouped *M. sativa*, *M. suffruticosa* and *M. hybrid* in section Falcago. Small (1981) put the three species in one group. Small and Jomph (1989) grouped the three species under section Medicago. Lesins & Lesins (1979) grouped *M. sativa*; *M. glomerata* and *M. Falcata* in subsection Falcatae under section Falcagowhile, *M. hybrid*, *M. suffruticosa* were grouped in section Suffruticosa.

Statistical analysis for the studied species based on karyological characters shows that the taxa; *M. glutinosa*, *M. hemicycle*, *M. falcate*, *M. x varia* and *M. polychroa* are grouped in a distinct group away from *M. sativa*. Sinskaya (1961) denoted *M. caerulea*, *M. hemicycla*, *M. falcata*, and *M. sativa* as distinct species. The division of taxa was based on morphology and hierarchical grouping was based on ploidy, assuming that the taxa within the same ploidy level were more closely related (Şakiroğlu and İlhan 2020).

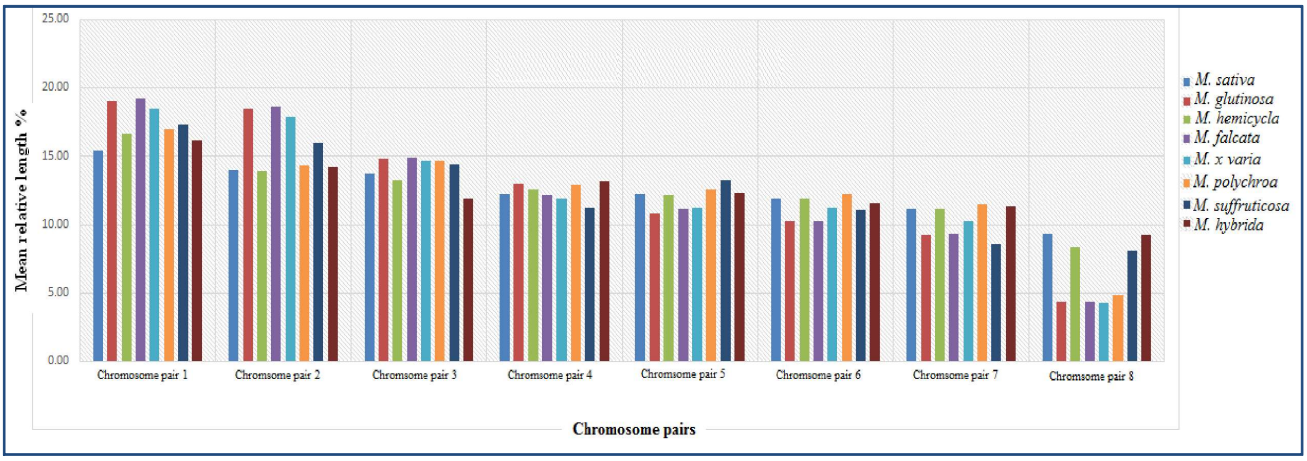

Fig. 4. Mean relative length percentage of each chromosome pair of the eight sets of chromosomes in the different studied *Medicago* species

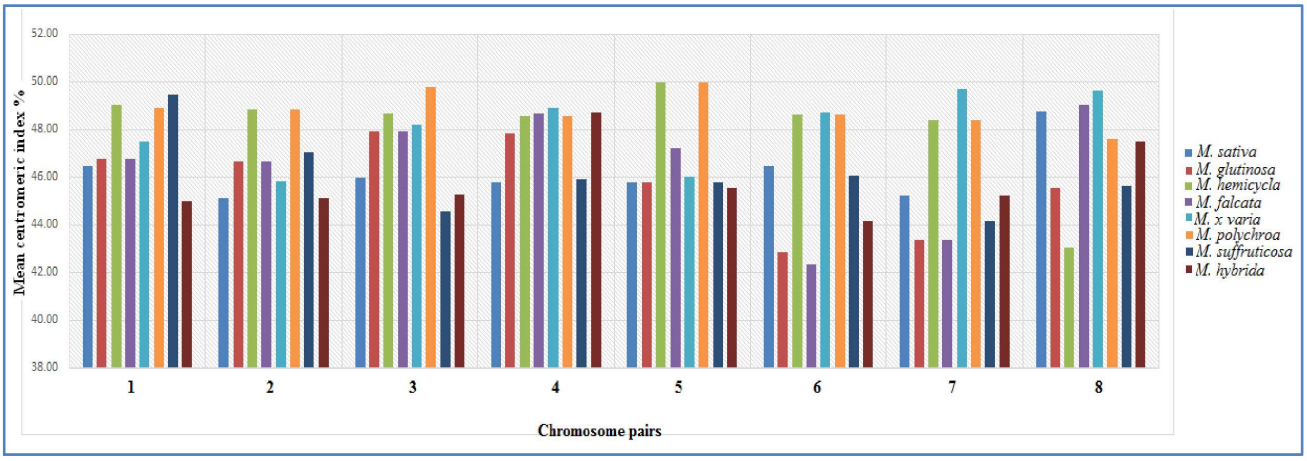

Fig. 5. Mean centromeric index percentage of each chromosome pair of the eight sets of chromosomes in the different studied *Medicago* species

REFERENCES

Agarwal K 1983. Cytological studies in the genus *Medicago* Linn. *Cytologia* **48**(4): 781-793.

Bauchan GR and Hossain MA 1997. Karyotypic analysis of C-banded chromosomes of Diploid Alfalfa: *Medicago sativa* ssp. *Caerulea* and ssp. *Falcata* and Their Hybrid. *Journal of Heredity* **88**(6): 533.

Bolkhovskikh ZV, Grif VG, Zakharyeva OI and Matveeva TS 1969. *Chromosome numbers of flowering plants* (A.A. Fedorov, ed.). Nauka, Leningrad, p 926.

Calderini O, Pupilli F, Cluster PD, Mariani A and Arcioni S 1996. Cytological studies of the nucleolus organizing regions in the *Medicago* complex: Sativa-coerulea-falcata. *Genome* **39**(5): 914-920.

Clement WM and Lehman WF 1962. Fertility and cytological studies of a dihaploid plant of Alfalfa, *Medicago sativa* L. 1. *Crop Science* **2**(6): 451-453.

Falistocco E, Falcinelli M and Veronesi F 1995. Karyotype and C-banding pattern of mitotic chromosomes in alfalfa, *Medicago sativa* L. *Plant Breeding* **114**(5): 451-453.

Galland N 1988. *Recherche sur l'origine de la flore orophile du Maroc étude caryologique et cytogéographique. Travaux de l'Institut Scientifique, Université Mohammed V. Série Botanique* **35**: 1-168.

Gunn CR, Skrdla WH and Spencer HC 1978. *Classification of Medicago sativa L. using legume characters and flower colors.* United States Department of Agriculture, Agriculture Research Service.

Hassan NA and Abd-El Gawad MH 2013. Morphological karyotype analysis of eleven pomegranate cultivars. *American-Eurasian Journal of Agricultural & Environmental Sciences* **13**(11): 1562-1567.

Havananda T, Brummer EC and Doyle JJ 2011. Complex patterns of autopolyploid evolution in alfalfa and allies (*Medicago sativa*; Leguminosae). *American Journal of Botany* **98**(10): 1633-1646.

Havananda T, Brummer EC, Maureira-Butler IJ and Doyle JJ 2010. Relationships among diploid members of the *Medicago sativa* (Fabaceae) species complex based on chloroplast and mitochondrial DNA sequences. *Systematic Botany* **35**(1): 140-150.

Humphries A, Ovalle C, Hughes S, del Pozo A, Inostroza L, Barahona V, Yu L, Yerzhanova S, Rowe T, Hill J, et al 2021. Characterization, preliminary evaluation and pre-breeding of diverse alfalfa crop wild relatives originating from drought-stressed environments. *Crop Science* **61**: 69-88.

Ilhan D, Li X, Brummer EC, Sakiroˇglu M 2016. Genetic diversity and population structure of tetraploid accessions of the Medicago sativa–falcata Complex. *Crop Science* **56**: 1146-1156.

Jahan B, Vahidy AA and Ali SI 1994. Chromosome numbers in some taxa of Fabaceae mostly native to Pakistan. *Annals of the Missouri Botanical Garden* **81**: 792-799.

Karshibaev HK 1992. Chromosome numbers of some Fabaceae in Uzbekistan. *Tezisy 3 Soveshchanie Po Kariologii Rastenii* **27**: 1-2.

Lesins and Lesins 1979. *The Genus Medicago (Leguminosae)*. The Hague, Boston, London: Dr W. Junk.

Lesins K 1969. Relationship of taxa in genus *Medicago* as revealed by hybridization. IV. *M. hybrida* x *M. suffruticosa*. *Canadian Journal of Genetics and Cytology* **11**: 340-345.

Lesins KA and Gillies CB 1972. Taxonomy and cytogenetics of *Medicago*. P. 53-86. In Hanson CH (ed.) *Alfalfa Science and Technology*. ASA-CSSA-SSSA, Madison, Wisconsin.

Lövkvist B and Hultgård UM 1999. Chromosome numbers in south Swedish vascular plants. *Opera Botanica* **137**: 1-42.

Magulaev AY 1992.Chromosome numbers in some species of vascular plants of the northern Caucasus flora. *Botaniceskij Zurnal* **77**(10): 88-90.

Mclennan HA, Armstrong JM and Kasha KJ 1966. Cytogenetic behavior in alfalfa hybrid by diploid crosses. *Canadian Journal of Genetics and Cytology* **8**: 544-555.

Nazarova EA and Ghukasyan AG 2004. *Chromosome numbers of flowering plants of Armenian flora*. Yerevan. p 171 (in Russ.)

Nixon K 2006. Diversity of life .org (DOL), Cornell University, from http://www. Plantsystematics.org.

Okumura K, Takai T, Kanbe M and Gau M 1995. Variations in pollen production and seed set of male sterile alfalfa some clones. *Breeding Science* **45**: 25-29.

Peruzzi L and Eroğlu HL 2013, Karyotype asymmetry: again, how to measure and what to measure? *Comparative Cytogenetics* **7**(1): 1-9.

Quiros CF and Bauchan GR 1988. The genus *Medicago* and the origin of the *Medicago sativa* complex. In AA Hanson [ed.], DK Barnes and RR Hill, Jr. [co-eds.], *Alfalfa and Alfalfa Improvement, Agronomy Monograph* **29**: 93–124. American Society of Agronomy, Crop Science Society of Agronomy, and Soil Science Society of Agronomy, Madison, Wisconsin, USA.

Şakiroğlu M and İlhan D 2020. *Medicago sativa* species complex: Re-visiting the century old problem in the light of molecular tools. *Crop Science* **61**: 827-838.

Sakiroglu, Muhammet and Kaya MM 2012. Estimating genome size and confirming ploidy levels of wild tetraploid alfalfa accessions (*Medicago sativa* subsp.× *varia*) using flow cytometry. *Turkish Journal of Field Crops* **17**: 151-156.

Salehi M, Hesamzadeh Hejazi SM and Tabaei aghdaei SR 2014. Cytogenetic studies of two *Dracocephalum* (Lamiaceae) species and populations in Iran. *International Journal of Biosciences* **4**(9): 100-108.

Savova D, Mazyad PRA and Felber F 1996. Cytogeography of *Medicago falcata* L. and *M. sativa* L. in Switzerland. *Botanica Helvetica* **106**: 197-207.

CP Sharma and Datta S 2020. Biochemical analysis of lead induced stress in fodder plants pearl millet (*Pennisetum glaucum* L.) and alfalfa (*Medicago sativa* L.). *Indian Journal of Ecology* **47**(4): 984-987.

Sinskaya EN 1961. *Flora of Cultivated Plants of the USSR: XIII. Perennial Leguminous Plants,* Part 1, Israel Program of Scientific Translations, Jerusalem.

Small E and Jomphe M 1989. A synopsis of the genus *Medicago*. *Canadian Journal of Botany* **67**: 3260-3294.

SMALL E 1981. Numerical analysis of major groupings in *Medicago* employing traditionally used characters. *Canadian Journal of Botany* **59**: 1553-1577.

Small E 2011. *Alfalfa and relatives: Evolution and classification of Medicago*. NRC Research Press, Ottawa, Ontario, Canada.

Urban I 1873. *Prodromus einer Monographie der Gattung Medicago* L. *Verhandlungen des Botanischen Vereins für die Provinz Brandenburg* **15**: 1-85.

Zhang ZP, Wu LH and Kang YF 1993. Analyses of karyotypes in four forage species of *Medicago*. *Botanical Research* **1**: 55-59.

Received 12 July, 2021; Accepted 12 November, 2021

Indian Journal of Ecology (2021) 48(6): 1747-1754

Manuscript Number: 3443
NAAS Rating: 5.79

Ecological Studies on Southern Secondary Moist Deciduous Forest of Shendurney Wildlife Sanctuary, Kollam, Kerala, India

Halliru Bilyaminu, K. Vidyasagaran, S. Gopakumar and Nadan Vijaykumar[1]

Department of Natural Resources Management, Kerala Agricultural University, Thrissur-680 656, India
[1]Parassinikkadavu Snake Park, Kannur-670 001, India
Email: bilyaminhalliru@gmail.com

Abstract: The current ecological studies conducted to examine the tree species diversity, richness, structure, and composition of the moist deciduous forest of Shendurney Wildlife Sanctuary, in Kollam district of Kerala state of India. The stratified random sampling method was employed and enumerated all the trees ≥ 10 cm diameter at breast height. Fifty-eight species of trees belonging to twenty-five families and forty-eight genera were recorded. The forest is dominated by *Terminalia paniculata*, *Aporosa cardiosperma*, and *Olea dioica*. The family Euphorbiaceae dominated the forest with a maximum Importance Value Index of 52.99, followed by Combretaceae 41.23 and Malvaceae 32.73. The Shannon-Weiner index (H') is 3.68, with Simpson's value 0.92. The density was 876.97 $ha^{-1.}$ and the basal area of 26.88 m^2ha^1. The size class distribution displayed a completely L shape pattern. The significant number of species belonging to the lower girth class category (≥10-30 cm) contributed to 43.1% of the total number of species. Out of the 58 species recorded, fifty-six species are contagiously distributed, and two species are randomly distributed. The present study can provide vital information for proper monitoring, planning, and management of phytodiversity of the moist deciduous forest of Shendurney Wildlife Sanctuary.

Keywords: Floristic composition and structure, Phytodiversity, Species diversity moist deciduous

Forest is a complex ecosystem consisting of fauna and flora existing together and interacting with the components of their environment and supporting human life on earth. The role of forest ecosystems cannot be over-emphasized; forest remained a vital and integral component for human sustenance. Forest ecosystems have proven to be exceptionally significant globally; they act as a rich reservoir for biological and genetic diversity. The tropical forest ecosystem is one of the complex and diverse terrestrial ecosystems globally, favoring diverse life forms and possessing exceptional self-maintenance. Anthropogenic perturbation, climate change, and uncontrolled grazing lead to failure in the capacity of these forests' ecosystems. India is among the 12 mega-biodiversity centers globally, characterized by a greater diversity of faunal and floral match with distinguishing climatic, topographic, and ecological factors with about 18,664 taxa of vascular plants 5725 endemics (Nayar, 1996). The Western Ghats is a UNESCO World Patrimony. It is one of the eight "hottest hotspots" of biological diversity globally, harboring over 3500 flowering plants from the 17000 species accounted for in India (Myers et al 2000). The Western Ghats estimated to accommodate about 4000 species of flowering plants (Nayar 1997), out of which about 1500 endemic to the region (Chatterjee 1939). Thus, the forests of the region comprise some of the perfect representatives of non-equatorial evergreen tropical forests. They are home to at least 325 globally endangered flora, fauna, birds, amphibians, reptiles, and fish species (Mittermeier 2011). Southern Western Ghats is considered one of the richest in terms of floral diversity and endemism, constituting about 3900 species, out of the 4000 species found in the Western Ghats area of about 12000 Km^2 distributing over the area of the Southern parts of the states of Kerala, Tamil Nadu and Karnataka (Nayar 1996). The science of plant studies is enormous for analyzing and understanding forest ecosystem structural, dynamic, and composition. Plants communities are described by their dominant growth, species diversity, forms, and structure (Sharma 1998).

Champion and Seth (1968) classified southern secondary moist deciduous forests as (2A/C3), which is primarily dominated by the deciduous species and predominated by evergreen species at understorey strata. The lower storey's evergreen species give the forest a more or less evergreen appearance for most of the year. However, their frequency of distribution is far too low (KFD 2014). These forests are located in almost the part of the Sanctuary, mainly below 600 m altitudes. Compared to the moist mixed deciduous forests, secondary moist mixed deciduous forest area receives high rainfall (KFD 2014). These forest types are mostly confined to the low elevation, which is susceptible to various disturbances. Anthropogenic disturbances have

resulted in significant tropical forest degradation and, as a result, a reduction in global biodiversity (Alroy 2017, Barlow et al 2016). In addition, natural and human-induced factors alter the diversity, structure, and composition of tropical forests at different geographic scales (Burslem and Whitmore 1999). Therefore, in tropical forests, the studies on plant diversity for understanding the status and extent of disturbance and various threats have attracted many researchers (Pandey and Shukla 1999, Misra et al 2004, Sahu et al 2008). Because of this circumstance, it is paramount to study and understand the interaction between the tree species and ecosystem function in which they inhibit (Younes 1992). Shendurney Wildlife Sanctuary is a protected area. Despite its floristic richness, ecological studies have not been conducted mainly at ecosystem types levels. Hence, there is a tremendous need to assess the status and the threat that may require a long-term managerial approach. This study aimed to evaluate and examine tree species diversity and richness and floristic structure composition of the moist deciduous forest of Shendurney Wildlife Sanctuary of Kerala, part of the southern Western Ghats region.

MATERIAL AND METHODS

The study was conducted in Shendurney wildlife sanctuary, Kollam district of Kerala, India, located between the geographical extremes of 8°44' and 9° 14' N latitude and 76° 59' and 77° 16' E longitude, Thenmala, Kollam district Kerala state (Fig. 1). The climate of the study is hot and humid, with a moderate amount of rainfall. The mean annual rainfall of the study area ranges from 1300-3000 mm, with the highest amount in July. The study area has no pronounced variation in the temperature, seasonal and diurnal, with the maximum daytime temperature exceeding 33°C in the hottest month.

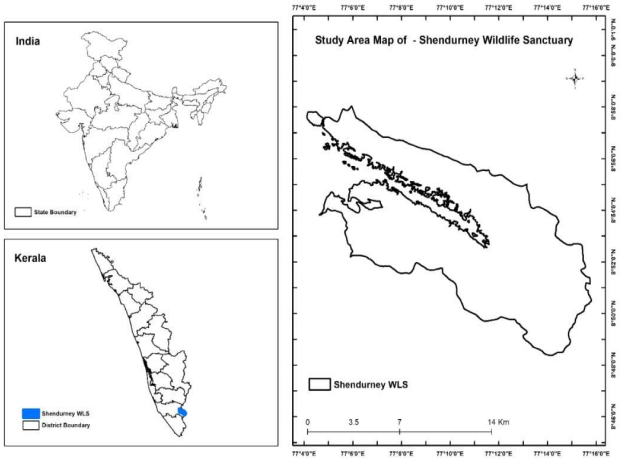

Fig. 1. Map showing the study area

Vegetation sampling: The phytosociological analysis data was collected in 2019-2020 following a preliminary survey. The structural analysis of plant communities was carried out following the standard method (Mueller-Dombois and Ellenberg, 1974). The sample plots were collected based on the stratified random sampling method. Random quadrates of size 20 m × 20 m were laid from the forest. All the trees with DBH ≥ 10 cm were enumerated.

Floristic structure and diversity: The structural attributes such as girth class distribution of tree species were evaluated. The phytosociological observations such as a relative density (rd), relative frequency (rf), relative basal area (rba), and importance value index (IVI) were enumerated using the expression given by Curtis and McIntosh (1950) as follows. The different diversity indices of the tree species were also calculated. The various species diversity indices were analyzed using the PAST (Paleontological Statistics) software 4.03 version. The cluster analysis was done using the Biodiversity R software Version. 3.6.2.

RESULTS AND DISCUSSION

Tropical forest ecosystems are among the most globally endowed terrestrial ecosystems in terms of species richness and diversity. The present study recorded fifty-eight species with DBH ≥ 10 cm (Table 1). Out of these seven species are endemic to the Western Ghats region of India, two species are endangered, two species belong to the near-threatened category, while four species are vulnerable to extinction in the future. The dominant species are *Terminalia paniculata* represented by the 215 individuals, followed by *Aporosa cardiosperma* (256 individuals), *Olea dioica* (84 individual species), and *Tabernaemontana alternifolia* (79 individuals). Species whose number of individuals is greater than 30 are *Careya arborea, Macaranga peltata, Xanthophylum arnottianum, Schleichera oleosa,* and *Holarrhena pubescens*. Forty-nine species were represented by less than 30 individuals species (Table 1). The species importance value index was maximum for *Terminalia paniculata* (26.67) followed by *Aporosa cardiosperma* (26.08), *Olea dioica* (12.67) *Bombax ceiba* 10.70, and *Tabernaemontana alternifolia* (10.48) (Table 8). Twenty-five families were represented by in the ≥ 10 cm GBH class. The family Euphorbiaceae showed the maximum family index value (FIV) of 52.99 followed by Combretaceae (FIV=41.23), Malvaceae (FIV= 32.73), Apocynaceae (FIV=24.89), Fabaceae (FIV=24.54), and Rubiaceae (FIV=21.18). Eight families showed a family index value of greater than ten (Table 2).

The girth class distribution was recorded for trees with a

Table 1. The phytosociological parameters of Southern Secondary Moist Deciduous Forest of Shendurney Wildlife Sanctuary, Kollam

Species name	AB	AB/F	Ds	RD	PF	RF	BA	RBA	IVI
Terminalia paniculata	7.68	0.10	141.45	16.13	73.68	7.07	9.44	3.47	26.67
Aporosa cardiosperma	9.85	0.14	168.42	19.20	68.42	6.57	0.84	0.31	26.08
Olea dioica	3.50	0.06	55.26	6.30	63.16	6.06	0.84	0.31	12.67
Bombax ceiba	1.22	0.05	7.24	0.83	23.68	2.27	20.70	7.60	10.70
Tabernaemontana alternifolia	4.65	0.10	51.97	5.93	44.74	4.29	0.72	0.26	10.48
Bombox insigne	1.00	0.38	0.66	0.08	2.63	0.25	25.78	9.47	9.80
Careya arborea	2.75	0.07	28.95	3.30	42.11	4.04	4.69	1.72	9.06
Spondias pinnata	1.00	0.38	0.66	0.08	2.63	0.25	22.99	8.45	8.77
Schleichera oleosa	1.94	0.04	21.71	2.48	44.74	4.29	1.98	0.73	7.50
Dillenia pentagyna	2.90	0.11	19.08	2.18	26.32	2.53	7.36	2.70	7.40
Lagerstreomia microcarpa	1.70	0.06	11.18	1.28	26.32	2.53	9.79	3.59	7.40
Dalbergia sissoides	1.78	0.08	10.53	1.20	23.68	2.27	10.08	3.70	7.18
Lagerstroemia speciosa	1.60	0.12	5.26	0.60	13.16	1.26	13.50	4.96	6.82
Terminalia elliptica	1.80	0.14	5.92	0.68	13.16	1.26	12.81	4.70	6.64
Pterocarpus marsupium	2.43	0.13	11.18	1.28	18.42	1.77	9.73	3.57	6.62
Macaranga peltata	4.40	0.17	28.95	3.30	26.32	2.53	1.88	0.69	6.52
Xanthophyllum arnottianum	3.09	0.11	22.37	2.55	28.95	2.78	0.61	0.22	5.55
Tetrameles nudiflora	2.17	0.14	8.55	0.98	15.79	1.52	7.43	2.73	5.22
Alstonia scholaris	2.43	0.13	11.18	1.28	18.42	1.77	5.13	1.88	4.93
Bridelia retusa	3.13	0.15	16.45	1.88	21.05	2.02	2.19	0.80	4.70
Terminalia bellirica	1.40	0.11	4.61	0.53	13.16	1.26	7.59	2.79	4.58
Mallotus philippensis	5.00	0.38	16.45	1.88	13.16	1.26	3.64	1.34	4.48
Pterygota alata	2.25	0.21	5.92	0.68	10.53	1.01	7.29	2.68	4.36
Phyllanthus emblica	1.33	0.06	7.89	0.90	23.68	2.27	3.02	1.11	4.28
Holarrhena pubescens	5.33	0.34	21.05	2.40	15.79	1.52	0.94	0.34	4.26
Strychnos-nux-vomica	2.00	0.10	10.53	1.20	21.05	2.02	2.74	1.01	4.23
Dalbergia latifolia	1.75	0.17	4.61	0.53	10.53	1.01	7.12	2.62	4.15
Haldina cordifolia	2.17	0.14	8.55	0.98	15.79	1.52	4.47	1.64	4.13
Grewia tiliifolia	1.70	0.06	11.18	1.28	26.32	2.53	0.81	0.30	4.10
Stereospermum colais	1.56	0.07	9.21	1.05	23.68	2.27	1.92	0.71	4.03
Buchanania Lanzan	2.00	0.13	7.89	0.90	15.79	1.52	4.37	1.60	4.02
Macarangia indica	4.40	0.33	14.47	1.65	13.16	1.26	2.29	0.84	3.75
Wrightia tinctoria	2.43	0.13	11.18	1.28	18.42	1.77	1.31	0.48	3.53
Mitragyna parvifolia	2.17	0.14	8.55	0.98	15.79	1.52	2.73	1.00	3.49
Terminalia crenulata	2.50	0.16	9.87	1.13	15.79	1.52	1.92	0.70	3.34
Lannea coromandelica	1.50	0.29	1.97	0.23	5.26	0.51	6.82	2.50	3.23
Cinnamomum malabatrum	2.00	0.11	9.21	1.05	18.42	1.77	1.09	0.40	3.22
Mallotus tetracoccus	4.20	0.32	13.82	1.58	13.16	1.26	0.93	0.34	3.18
Sterculia guttata	1.83	0.12	7.24	0.83	15.79	1.52	1.15	0.42	2.76
Cassia fistula	1.50	0.29	1.97	0.23	5.26	0.51	5.48	2.01	2.74
Vitex altissima	1.00	0.05	4.61	0.53	18.42	1.77	1.21	0.44	2.74
Miliusa tomentosa	1.25	0.12	3.29	0.38	10.53	1.01	3.65	1.34	2.73
Tamarindus indica	1.00	0.38	0.66	0.08	2.63	0.25	6.44	2.37	2.69

Cont...

Table 1. The phytosociological parameters of Southern Secondary Moist Deciduous Forest of Shendurney Wildlife Sanctuary, Kollam

Species name	AB	AB/F	Ds	RD	PF	RF	BA	RBA	IVI
Diospyros buxifolia	1.20	0.09	3.95	0.45	13.16	1.26	2.04	0.75	2.46
Hymenodictyon orixense	1.40	0.11	4.61	0.53	13.16	1.26	1.75	0.64	2.43
Ixora brachiata	2.60	0.20	8.55	0.98	13.16	1.26	0.27	0.10	2.34
Sterculia balanghas	1.00	0.38	0.66	0.08	2.63	0.25	5.09	1.87	2.20
Hydnocarcpus pentandrus	2.75	0.26	7.24	0.83	10.53	1.01	0.93	0.34	2.18
Hymenodictyon obovatum	4.33	0.55	8.55	0.98	7.89	0.76	0.62	0.23	1.96
Chionanthus mala-elengi	2.50	0.24	6.58	0.75	10.53	1.01	0.40	0.15	1.91
Ailanthus triphysa	1.00	0.38	0.66	0.08	2.63	0.25	3.90	1.43	1.76
Wrightia arborea	1.00	0.38	0.66	0.08	2.63	0.25	3.57	1.31	1.64
Pongamia pinnata	6.00	2.28	3.95	0.45	2.63	0.25	1.38	0.51	1.21
Litsea coriacea	3.00	0.57	3.95	0.45	5.26	0.51	0.55	0.20	1.16
Naringi crenulata	1.00	0.13	1.97	0.23	7.89	0.76	0.46	0.17	1.15
Elaeocarpus tectorius	1.00	0.19	1.32	0.15	5.26	0.51	1.17	0.43	1.08
Melicope-lunu-ankeda	3.00	1.14	1.97	0.23	2.63	0.25	1.40	0.52	0.99
Elaeocarpus serratus	1.00	0.38	0.66	0.08	2.63	0.25	1.27	0.47	0.80

AB- Abundance; Species density; RDs – Relative density of the species; PF- Percent Frequency of the species; RFs- Relative frequency of the species; BAs- Basal area of the species; RBA – Relative basal area; IVI- Importance value index of the species

girth ≥ 10 cm. The distribution of the trees showed a completely L-shaped distribution with decreasing density with increasing girth size. The lower girth class (10-30 cm) occupied a more significant number (574 species), representing 43.10 % of all individuals trees followed by 31-60 cm (445 species), representing 33.4% and 61-90 cm (164 species) representing 12.3%. On the other hand, the lowest number (15 species) of individuals species representing 1.1%, was recorded in the >210 girth class distribution. The tree species density was recorded as 876.97 individuals per hectare.

The cluster analysis grouped the whole ecosystem into five groups based on the compositional similarities. Plot 1, 2, 3, 4,7,8,9, 11, 12, 13, 19, 24, 25, 27, 28, 29, 30, 31, and 37 were clustered as one group. Plot 5, 6, and 23 as another cluster. Plot 18, 20, 21, 22, 23, 32, 34, 35, and 36 as one clustered. Plot 10 is an independent cluster, while plot 14, 15, 16, 26, and 38 is one cluster. The divisive coefficient similarity value as 0.52 (Fig. 3). The detrended correspondence analysis identified different species assemblages as follows: *Pterocarpus marsupium, Terminalia elliptica, Careya arborea,* and *Aporosa cardiosperma* as one assemblages. *Terminalia paniculata*, *Lagerstreomia microcarpa, Dillenia pentagyna, Vitex altissima* and *Bridelia retusa* as an assemblage. *Diospyros buxifolia*, *Macaranga peltata*, *Cinnomomum malabatrum* as an assemblage, and *Xanthophyllum arnottianum*, *Hydnocarpus pentandrus*, *Miliusa tomentosa, Bombox ceiba,* and *Alstonia scholaris* (Fig. 4).

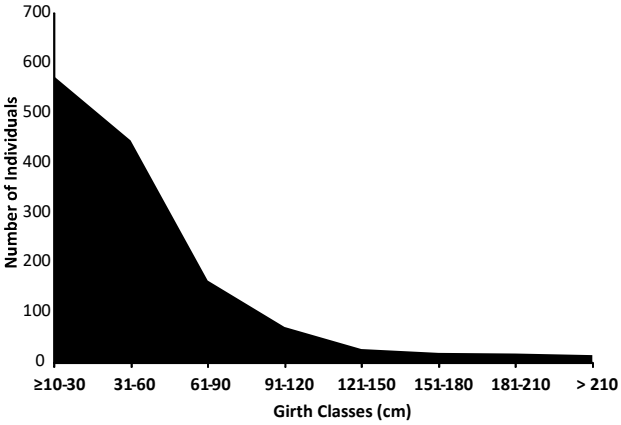

Fig. 2. The girth class distribution of trees species

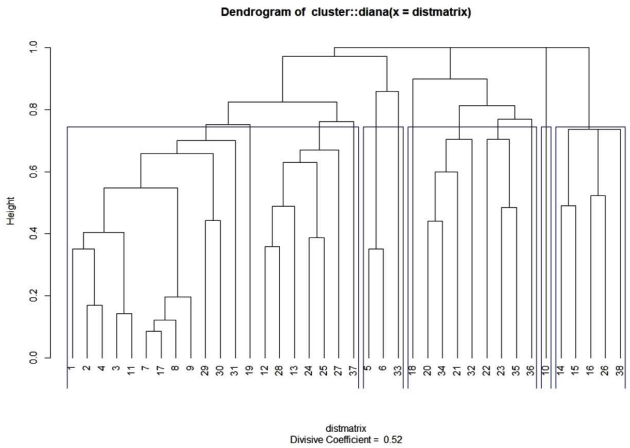

Fig. 3. Divisive cluster analysis of different plots in the study area

Different community indices were assessed to understand the overall state of the biodiversity in the study area. The Shannon-Weiner index (H), was estimated as (3.22), Simpson index (1-D) was found to be (0.92), dominance (D) was estimated as (0.10), and Margalef, Evenness and Equitability index (J) the value was estimated as (7.92, 0.43 and 0.80), respectively (Table 3). The abundance-frequency ratio showed that species displayed both contagious and uniform patterns of distribution (Table 1).

The tree species richness in the present study was fifty-eight species, with the domination of *Terminalia paniculata* and *Aporosa cardiosperma* (Table 1). A similar species richness and species domination pattern was reported in the moist deciduous forest of Kodayar Western Ghats (Sundarapandian and Swamy 2000). Naidu and Kumar (2016) recorded 129 species from Eastern Ghats' tropical deciduous forest; 125 species were recorded in the tropical moist deciduous forest of Odisha (Reddy et al 2007). Murthy et al (2016) also observed a similar domination pattern of *Terminalia paniculata* and *Aporosa cardiosperma*, in the moist deciduous forest of Uttara Kannada Western Ghats. Kumar et al (2010), in their studies in the deciduous forest of Western India, recorded 93 species. Relatively, the number of species diversity reported in the current investigation is modest. The stand density (876.97 stems ha^{1}) recorded in the present study is comparably higher than the range reported (Kumar et al 2010, Panda et al 2013, Reddy et al 2007, Sahu et al 2007) but similar to that reported (Naidu and Kumar 2016, Sahoo et al 2017, Sahoo et al 2020). The diameter distribution represents the impact of disturbances within the forest (Denslow 1995) and can spot trends in regeneration patterns (Poorter et al 1996). The pattern of girth class distribution of the current study manifested typical L shape distribution. The present study observed species density decreased with increasing in girth class. A similar trend was recently reported by Sahoo et al (2020) in the moist deciduous forest of Eastern Ghats, Odisha. The subsequent dropped in the stem density with increasing girth classes has also been recorded by Ganesh et al (1996) for evergreen forest KMTR of the Western Ghats region. In the present

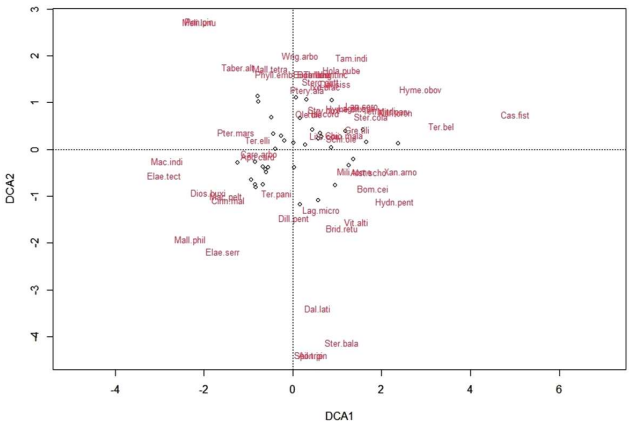

Fig. 4. Detrended correspondence analysis for tree species assemblages

Table 2. Family Importance Value (FIV) of moist deciduous forest of shendurney wildlife sanctuary

Family	FIV
Euphorbiaceae	52.99
Combretaceae	41.23
Malvaceae	31.73
Apocynaceae	24.84
Fabaceae	24.59
Rubiaceae	21.18
Anacardiaceae	16.03
Oleaceae	14.58
Lecythidaceae	9.06
Sapindaceae	7.5
Dilleniacaceae	7.4
Lythraceae	7.4
Xanthophyllaceae	5.55
Tetramelaceae	5.22
Lauraceae	4.37
Loganiaceae	4.23
Bignoniaceae	4.03
Lamiaceae	2.74
Annonaceae	2.73
Ebenaceae	2.46
Sterculiaceae	2.2
Flacourtiaceae	2.18
Rutaceae	2.14
Elaeocarpaceae	1.88
Simaroubaceae	1.76

FIV: Family importance value

Table 3. Different community indices of moist deciduous forest of Shendurney

Community indices	Mean
Shannon H'	3.22
Simpson Index (1-D)	0.92
Dominance Index	0.1
Evenness_e^H/S	0.43
Equitability_J	0.8
Margalef	7.92

study, the decline in stem density in the lower girth classes is noticeable. This is in agreement with the investigation of Muthuramkumar et al (2006). The lack of individuals in the larger size classes in the present study could be due to the locals' disturbance were giant trees are exploited for timber and construction. As a result, the forest has limited species that grow larger than these diameters (Hadi et al 2009).

The basal area was 26.88 m^2 ha^1, comparatively lower than the ranges recorded (Reddy et al 2007, Murthy et al 2016). Comparably within the range reported (Sahoo et al 2017, Saho et al 2020). Higher than reported (Bijalwan et al 2009, Kumar et al 2010, Panda et al 2013). Therefore, the basal area reported in the present study is within the range reported in several studies in moist deciduous forests. Moreover, the relatively lower basal area cover reported in the deciduous forest could be due to a more significant proportion of 574 species (43.1%) of tree species belonging to the lower girth class category (10-30 cm) and few (15 species) representing 1.1 % in the girth class category of >210 cm. The familial importance value showed that Euphorbiaceae and Combretaceae were the dominant families of the present study. The families Combretaceae and Euphorbiaceae showed the highest importance value index in the tropical deciduous forest of Eastern Ghats (Naidu and Kumar 2016). Sundarapandian and Swamy (2000) also reported that the family Combretaceae is the most important in the moist deciduous forest of Kodayar forest, the Western Ghats. A similar familial dominance was reported by Pragasan and Parsatharathy (2010) in Southern Western Ghats. Few other studies reported that the family Euphorbiaceae was the most diverse in tropical moist deciduous forests (Panda et al 2013). The present study conformed with several other studies.

The pattern of species distribution in forest communities is measured as the ratio of abundance and frequency. The values ranged as < 0.025, between 0.025 and 0.05 random, and value > 0.05, showing the clumped or contagious pattern of species distribution (Curtis and Cottam 1956). The distribution of the species in the present study was recorded as more contagious than random or regular distribution. Out of the fifty-eight species, fifty-seven are contagiously distributed, and only one species were randomly distributed. Sahu et al (2012) recorded fifty-two species that showed contagious distribution and five species randomly distributed out of the fifty-seven species in the moist deciduous forest of Malyagiri of the Eastern Ghats region. The clumped or contagious pattern of species distribution portrays natural vegetation (Odum 1971, Verma et al 1999). The random pattern of distribution is portrayed by the species exposed to large recurrent disturbances (Armesto et al 1986).

The Shannon index reported in the present study was 3.22, higher than the range reported (Panda et al 2013) in the tropical moist deciduous forest of the Eastern Ghats; Murthy et al (2016) in the moist deciduous forests of Uttara Kannada of Western Ghats and recently (Ramya et al 2020) Karamadai reserve forest of Western Ghats, However, the value was within the range reported (Sahoo et al 2017, Sahoo et al 2020) but lower than reported (Reddy et al 2007, Reddy et al 2008, Naidu and Kumar 2016). Simpson index value as 0.92, which was higher than the range of value reported in the deciduous forests of Uttara Kannada of Western Ghats (Murthy et al 2016). However, our value is similar to 0.96-0.97 (Naidu and Kumar 2016); 0.94 (Reddy et al 2008). The Margalef value (7.90) reported in the current work is lower than reported by Kumar et al (2010) in the deciduous forest of western Ghats but higher than recently reported by Ramya et al (2020) in the moist deciduous forest of Karamadai of Western Ghats region. Our Margalef value is within the range reported in moist deciduous and dry deciduous forests of Mudhumalai (Reddy et al 2008). The Margalef index is an important diversity index that measures species richness, and it is notably sensitive to the sampling size (Magurran 2005).

CONCLUSION

The study on tree species diversity, structure, and composition is crucial for planning, monitoring, and management of forests ecosystem. The current study on moist deciduous forest of Shendurney Wildlife sanctuary reported that this forest is rich in tree species dversity. However, the fact that these forest are mostly found in the lower altitude area, are therefore, proximate to various degree of local disturbances such as fire, grazing and logging for constructions. Moreover, the limited number of individual species belonging to the higher girth classes were reported which could be associated to the anticipated local disturbances. Therefore, managerial approach should be put in place to protect and conserve this vulnerable ecosystem. The finding of this research can be crucial to management decision making process.

REFERENCES

Alroy J 2017. Efect of habitat disturbance on tropical forest biodiversity. *Proceedings of the National Academy of Sciences of the United States of America* **114**(23): 6056-6061.

Armesto JJ, Mitchell JD and Villagran C 1986. A comparison of spatial patterns of trees in some tropical and temperate forests. *Biotropica* **41:** 1-11.

Barlow J, Gareth D, Lennox FJ, Berenguer E, Lees AC and Ralph Mac Nally R 2016. Anthropogenic disturbance in tropical forests can double biodiversity loss from

deforestation. *Nature* **7610**: 144-147.

Bijalwan A, Swamy SL, Sharma CM, Sah VK and Singh RK 2009. Phytosociological analysis of overstorey and understorey woody perennials along with aspects in balamdi watershed of mixed dry tropical forest in chhattisgarh plain. *Indian Journal of Tropical Biodiversity* **17**(1):47-58.

Burslem DFRP and Whitmore T 1999. Species diversity, susceptibility to disturbance and tree population dynamics in tropical rain forests. *Journal of Vegetation Science* **10**(6): 767-776.

Champion HG and Seth SK 1968. A revised survey of the forest types of India. Govt. *India Publ*. Delhi.

Chatterjee D 1939. Studies on the endemic flora of India and Burma.

Curtis JT and Mcintosh RP 1950. The interrelations of certain analytic and synthetic phytosociological characters. *Ecology* **31**(3): 434-455.

Curtis JT and Cottam G 1956. Plant Ecology Workbook, *Laboratory Field Manual*. Burgess.

Denslow JS 1995. Disturbance and diversity in tropical rain forests: the density effect. *Ecological Applications* **5**(4): 962-968.

Ganesh T, Ganesan R, Devy MS, Davidar P and Bawa KS 1996. Assessment of plant biodiversity at a mid-elevation evergreen forest of Kalakad–Mundanthurai Tiger Reserve, Western Ghats, India. *Current Science* **71**: 379-392.

Hadi S, Ziegler T, Waltert M and Hodges JK 2009. Tree diversity and forest structure in northern Siberut, Mentawai Islands, Indonesia. *Tropical Ecology* **50**(2): 315-327.

KDF [Kerala Forest Department] 2014. Management Plan of Shendurney Wildlife Sanctuary 2013-2014 to 2020-2021 http://www.forest.kerala.gov.in/index.php/forest/forest-management/management-plans Accessed on 29-05-2021.

Kumar JN, Kumar RN, Bhoi RK and Sajish PR 2010. Tree species diversity and soil nutrient status in three sites of tropical dry deciduous forest of Western India. *Tropical Ecology* **51**(2): 273-279.

Magurran AE 2005. Biological diversity. *Current Biology* **15**(4): R116-R118.

Mishra BP, Tripathi OP, Tripathi RS and Pandey HN 2004. Effect of anthropogenic disturbance on plant diversity and community structure of a sacred grove in Meghalaya, northeast India. *Biodiversity and Conservation* **13**: 421-436.

Mittermeier RA, Turner WR, Larsen FW, Brooks TM and Gascon C 2011. Global biodiversity conservation: The critical role of hotspots. In *Biodiversity hotspots* (pp. 3-22). Springer, Berlin, Heidelberg.

Mueller-Domboise D and Ellenberg H 1974. *Aims and methods of vegetation ecology.* Wiley, New York, 547p.

Murthy IK, Bhat S, Sathyanarayan V, Patgar S, Beerappa M, Bhat PR, Bhat DM, Ravindranath NH, Khalid MA, Prashant M and Iyer S 2016. Vegetation structure and composition of tropical evergreen and deciduous forests in Uttara Kannada District, Western Ghats under different disturbance regimes. *Tropical Ecology* **57**(1):77-88.

Muthuramkumar S, Ayyappan N, Parthasarathy N, Mudappa D, Raman TS, Selwyn MA and Pragasan LA 2006. Plant community structure in tropical rain forest fragments of the Western Ghats, India. *Biotropical Journal of Biological Conservation* **38**(2):143-160.

Myers N, Mittermeier RA, Mittermeier CG, Da Fonseca GA and Kent J 2000. Biodiversity hotspots for conservation priorities. *Nature* **403**(6772): 853-858.

Naidu MT and Kumar OA 2016. Tree diversity, stand structure, and community composition of tropical forests in Eastern Ghats of Andhra Pradesh, India. *Journal of Asia-Pacific Biodiversity* **9**(3): 328-334.

Nayar MP 1996. *Hot spots of endemic plants of India, Nepal and Bhutan*. Tropical Botanic garden and research Institute.

Nayar MP 1997. Biodiversity challenges in Kerala and science of conservation biology. *Biodiversity of Tropical Forests the Kerala Scenario, STEC, Kerala, Trivandrum*, pp.7-80.

Odum EP 1971. *Fundamentals of Ecology*. W.B. Saunders Co., Philadelphia, 574p.

Panda PC, Mahapatra AK, Acharya PK and Debata AK 2013. Plant diversity in tropical deciduous forests of Eastern Ghats, India: A landscape level assessment. *International Journal of Biodiversity and Conservation* **5**(10): 625-639.

Pandey SK and Shukla RP 1999. Plant diversity and communitypatterns along the disturbance gradient in plantation forests of sal (Shorea robusta Gaertn.). *Current Science* **77**: 814-818.

Poorter L, Bongers F, van Rompaey RS and de Klerk M 1996. Regeneration of canopy tree species at five sites in West African moist forest. *Forest Ecology and Management* **84**(1-3): 61-69.

Pragasan LA and Parthasarathy N 2010. Landscape-level tree diversity assessment in tropical forests of southern Eastern Ghats, India. *Flora-Morphology, Distribution, Functional Ecology of Plants* **205**(11): 728-732.

Ramya EK and Mownika SSS 2020. Phytosociological assessment of tree vegetation in tropical moist deciduous forest of Veerakkal area, Nilgiris, Western Ghats, India. *Indian Journal of Ecology* **47**(2): 480-484.

Reddy CS, Pattanaik C, Mohapatra A and Biswal AK 2007. Phytosociological observations on tree diversity of tropical forest of Similipal Biosphere Reserve, Orissa, India. *Taiwania* **52**(4): 352-359.

Reddy CS, Ugle P, Murthy MSR and Sudhakar S 2008. Quantitative structure and composition of tropical forests of Mudumalai Wildlife Sanctuary, Western Ghats, India. *Taiwania* **53**(2): 150-156.

Sahoo T, Panda PC and Acharya L 2017. Structure, composition, and diversity of tree species in tropical moist deciduous forests of Eastern India: A case study of Nayagarh Forest Division, Odisha. *Journal of Forestry Research* **28**(6): 1219-1230.

Sahoo T, Acharya L and Panda PC 2020. Structure and composition of tree species in tropical moist deciduous forests of Eastern Ghats of Odisha, India, in response to human-induced disturbances. *Journal of Environmental Sustainability* **3**(1): 69-82.

Sahu SC, Dhal NK, Reddy CS, Pattanaik C and Brahmam M 2007. Phytosociological study of tropical dry deciduous forest of Boudh district, Orissa, India. *Research Journal of Forestry* **1**(2): 66-72.

Sahu PK, Sagar R and Singh JS 2008. Tropical forest structure and diversity in relation to altitude and disturbance in a Biosphere Reserve in central India. *Applied Vegetation Science* **11**: 461-470.

Sahu SC, Dhal NK and Mohanty RC 2012. Tree species diversity, distribution and population structure in a tropical dry deciduous forest of Malyagiri hill ranges, Eastern Ghats, India. *Tropical Ecology* **53**(2): 163-168.

Sharma R 1998. *A Study of the effect of long-term protection against grazing on the grassland vegetation at Udaipur*. Ph.D. Thesis, submitted to Mohan Lal Sukhdia University, Udaipur.

Sundarapandian SM and Swamy PS 2000. Forest ecosystem structure and composition along an altitudinal gradient in the Western Ghats, South India. *The Journal of Tropical Forest Science* **12**: 104-123.

Verma RK, Shadangi DK and Totey NG 1999. Species diversity under plantation raised on a degraded land. *Malaysian For* **62**(2): 95-106.

Younes T 1992. Ecosystem function of biodiversity: A progress report on the IUBS-SCOPE-UNESCO Programme. *Bull Inter* **24**: 16-21.

Received 12 August, 2021; Accepted 22 November, 2021

Indian Journal of Ecology (2021) 48(6): 1755-1759

Manuscript Number: 3444
NAAS Rating: 5.79

Conjoint Effect of Organic Formulations and Inorganic Fertilizers on Growth, Yield and Quality in Strawberry (*Fragaria × ananassa* Duch.)

Praveen Verma, Jitender K. Chauhan, D.P. Sharma, N.C. Sharma and Uday Sharma

Dr YS Parmar University of Horticulture and Forestry, Nauni, Solan-173 230, India
E-mail: praveenver2014@gmail.com

***Abstract*:** The present investigations were focused on investigating the possibilities of supplementing chemical fertilizers with organic fertilizers to maintain environment including preserving beneficial soil microbes, soil properties and sustaining crop productivity at Dr Y S Parmar University of Horticulture and Forestry, Nauni, Solan, Himachal Pradesh. The experiment consisting of 7 treatments. Application of FYM and N, P, K fertilizers was done during field preparation and after transplanting. Application of jeevamrit was done in 5 equal split doses at monthly intervals starting at 15 days after transplanting as soil application. Ghanjeevamrit was applied in two equal split doses at transplanting and at the initiation of flowering. Among different treatments, T_4(75% of T_1+ 25% RDN through Jeevamrit + Ghanjeevamrit in the ratio 1:1) resulted in better growth, flowering, yield and fruit quality in strawberry.

***Keywords*:** Organic formulations, jeevamrit, Ghanjeevamrit, Strawberry

The currently cultivated strawberry (*Fragaria × ananassa* Duch.) is hybrid crop developed by crossing two species, *Fragariachiloensis* and *Fragaria virginiana*. This crop can be a good option for many small scale and part-time farming operations because of high potential for significant profit.Among the various factors which contribute towards the growth and yield of strawberry, nutrition is an important aspect of crop production (Iqbal et al 2008). Ensured balanced nutrient proportion by enhanced nutrient response efficiency and maximized crop productivity is attained from integrated nutrient management comprises of inorganic, organic and microbial sources of nutrients. It also helps in minimizing the existing gap between the nutrient removal through continuous use of chemical fertilizers and supply through slow release of fertilizers. The extensive use of chemical fertilizers adversely affects the soil health and results in decreased crop productivity and quality (Das et al 2015). Modern day intensive crop cultivation results in huge application of chemical fertilizers which are not only in short supply but also expensive and pollute the environment, soil and water. Therefore, in the present study emphasis was given to explore the possibilities of supplementing the chemical fertilizers with organic formulations.

MATERIAL AND METHODS

The present study was carried outat an elevation of 1250 m above mean sea level at Dr YS Parmar University of Horticulture and Forestry, Nauni, Solan, Himachal Pradesh, during the years 2018-19 and 2019-20.The plants were planted at 30 × 60 cm spacing during October in both years. Grass mulching (10 cm) was done during January month of each year. The experiment consisted of 7 treatments with 3 replications (Table 2). Application of FYM and N, P, K fertilizers was done during field preparation and after transplanting. Jeevamrit and Ghanjeevamrit were prepared following the procedure laid out by Palekar (2006). Field application of jeevamrit was done in 5 equal split doses at monthly intervals starting at 15 days after transplanting as soil application. Ghanjeevamrit was applied in two equal split doses at transplanting and at the initiation of flowering.Jeevamrit and Ghanjeevamrit were analyzed for its chemical properties as per standard procedures suggested by Nyang'auet al (2016) (Table 1).

Plant growth: Plant height was measured with a measuring scale from the crown level to the apex of primary leaves and the trait was expressed in centimetres (cm). Plant spread was measured in both the directions i.e. East-West (E-W) and North-South (N-S) and the mean was taken as the actual plant spread. The numbers of leaves were recorded from fifteen plants from each replication at the end of harvest. The leaf area was recorded from 10 leaf samples from each replication using leaf area meter (LI-COR 3000). The number of runners produced was counted before uprooting the plant for fresh plantation. The average number of crowns per plant was recorded at the end of growing season.

Chlorophyll content: Fully grown leaves from the current

season's growth were collected during the morning hours, during third week of June immediately and were then kept in the refrigerator at 0°C to avoid degradation of chlorophyll pigment. Chlorophyll extraction and estimation was done by using DMSO (Hiscox and Israelstam 1979) and absorbance was recorded on UV-VIS spectrophotometer at 645 nm and 663 nm wavelength against a DMSO blank for chlorophyll a and b, respectively. The total chlorophyll content was recorded using formula and expressed as (mg g^{-1} of fresh weight).

Flowering and fruiting: Total numbers of flowers were recorded at the time of flowering from ten marked plants and the results were expressed as number of flowers per plant. The numbers of fruits i.e. primary, secondary and tertiary were counted per pedicel at the time of fruit maturity. Total numbers of flowers per plant from ten plants were recorded at five days interval. The per cent berry set per plant was worked out as, Fruit set (%) = (Number of berry set / Number of flowers) × 100. The total numbers of berries from ten randomly selected plants were recorded flush wise, pooled at the end of fruiting and their average was worked out and expressed as grams/ plant. The yield per hectare was calculated on the basis of yield recorded in kg per plot and expressed in t/ ha.

Fruit quality: Ten berries from each treatment were taken randomly and fruit length and diameter was measured in centimetre (cm). The total soluble solids content in fruits were determined by Erma hand refractometer (0-32 ºB).Physico-chemical analysis of fruits for evaluation ofquality was done as per standard procedures (AOAC 1980).

Table 1. Chemical properties of Jeevamrit and Ghanjeevamrit

Chemical properties	Jeevamrit	Ghanjeevamrit
pH	4.99	6.73
EC (dSm^{-1})	3.08	1.63
N (%)	1.71	1.68
P (%)	0.19	0.25
K (%)	0.32	0.63

RESULTS AND DISCUSSION

Plant growth: The pooled data over two years showed maximum (21.50 cm) plant height in T_2, which was statistically at par with treatments T_1, T_3, T_4 and T_6, respectively. The minimum plant height was recorded in T_5 and T_7.The plant spread was observed to vary among different treatments. The maximum plant spread in T_1which was statistically at par with T_2, $T_3$and T_4, respectively .Number of leaves per plant was maximum in $T_3$and minimum in T_5, T_6 and T_7. The leaf area was maximum and minimum in T_2 and T_1. There was no significant difference among all treatments. The numbers of runners per plant was maximum in T_1 which was statistically at par with treatments T_2, T_3 and T_4, respectively and were minimum in T_5, $T_6$and T_7. The pooled data elucidate that number of crown per plant were maximum in T_1, $T_2$and T_3 and minimum in T_4, T_5, T_6 and T_7. The total chlorophyll content was maximum in treatment T_3 and was minimum in treatment T_6. Analysis of variance showed no significant difference among all other treatments. The increase in plant height, plant spread, number of leaves/plant, leaf size, leaf area, fresh weight of leaves and dry weight of leaves with the application of fertilizers and organic manure has also been reported by Nowsheen et al (2006) and Yadav et al (2010) in strawberry. The increase in leaf area might be due to increased nitrogen availability generated by nitrogen content available in organic formulations and inorganic fertilizers. The increase in vegetative growth and other parameters might be due to the inoculation of plant beneficial microorganisms through organic formulations in the root zone and nitrogen content available in inorganic fertilizers. The increased vegetative growth might have been production of plant growth regulators by microorganism in rhizosphere. The increased vegetative growth is attributed to the increased biological nitrogen fixation. Better development of root system possibly by synthesis of plant growth hormones like IAA, GA and Cytokinins might have attributed for better growth parameters (Kumar 2006, Palekar 2006, Sreenivasa et al 2010). Increase in number of runners per plant might be due to increased growth of plant in terms of height and number of leaves, which accumulated more photosynthates and thereby increased runners and leaf area per plant.

Table 2. Treatment details

T_1(Control)	100% RDF through inorganic fertilizers (50 tonnes FYM, 80 kg N, 40 kg P, and 40 kg of K per hectare)
T_2	75% T_1 + 25% RDN through Jeevamrit
T_3	75% T_1 + 25% RDN through Ghanjeevamrit
T_4	75% T_1 + 25% RDN through Jeevamrit + Ghanjeevamrit in the ratio 1:1
T_5	50% T_1 + 50% RDN through Jeevamrit
T_6	50% T_1 + 50% RDN through Ghanjeevamrit
T_7	50% T_1 + 50% RDN through Jeevamrit + Ghanjeevamrit in the ratio 1:1

Flowering and fruiting: Numbers of flowers per plant was maximum in T2 which was statistically at par with treatments T1, T3 and T4 .Number of fruits per plant was maximum in treatments T_2 and T_4 which was statistically at par with treatments T_1, T_3, and T_5 .The highest per cent fruit set was recorded in treatment T_4 and lowest in$T_6$with no significant difference among all other treatments. The maximum yield per plant and per ha wasinT_4which was statistically at par with T_1, $T_2$and T_3.Theapplication of inorganic fertilizers and organic formulations has given increase in the yield of strawberry fruits.. Application of integrated nutrients accelerates the development of inflorescence, leaf number, which positively turned in to increased number of flowers and fruits in the plants. The increased number of flowers might have also owed to number of crowns per plant. The increase in yield might be due to increased fruit set per plant and fruit weight.

Fruit quality: Fruit length was maximum in $T_4$and minimum inT_6 and T_7 with no significant difference among all other treatments. Maximum fruit breadth was recorded in T4 which was statistically at par with T_1, T_2, T_3, $T_5$and T_7. The pooled data for fruit weight over the year observed highest fruit weight in T_4 which was statistically at par withT_1, T_2 and T_3. The maximum TSS was inT_3 which was statistically at par with T_1, $T_2$and T_4, respectively. Highest titratable acidity was recorded in $T_4$and lowest in T_6. The pooled data over the year recorded that TSS/acid ratio was maximum in$T_3$and minimum in $T_7$with no significant difference among all other treatments. The total sugars content was maximum inT_3 which was statistically at par with treatments T_1, T_2 and T_4 and was minimum in T_6 and reducing sugars was maximum inT_1 and minimum inT_6. Maximum content of non-reducing sugars was inT_3 which was at par with T_2, T_4, T_6 and T_7, respectively. There was no significant difference in anthocyanin content, ascorbic acid and total phenols among different treatments under study.

During present investigation, it was observed that the physico-chemical parameters of strawberries were significantly increased by different treatment combinations of inorganic fertilizers and organic formulations. Increase in physico-chemical properties of strawberries with adoption of integrated nutrient management may be attributed to the quick metabolic transformation of starch and pectin into soluble compounds and rapid translocation of sugars from leaves to the developing fruits. The improvement in fruit quality parameters with the integrated application of

Table 3. Plant growth parameters of strawberry as influenced by inorganic fertilizers and organic formulations

Treatment	Plant height (cm)			Plant spread (cm)			Number of leaves per plant			Leaf area (cm^2)		
	2019	2020	Pooled	2019	2020	Pooled	2019	2020	Pooled	2019	2020	Pooled
T_1	20.67	21.50	21.08	24.67	27.08	25.87	18.3	20.7	19.5	42.15	42.39	42.27
T_2	20.83	22.17	21.50	24.67	25.83	25.25	17.7	21.3	19.5	46.79	44.05	45.42
T_3	19.50	20.83	20.17	23.83	26.26	25.05	18.7	20.7	19.7	43.64	43.87	43.75
T_4	18.83	20.83	19.83	23.67	25.88	24.78	17.7	20.3	19.0	43.97	44.20	44.08
T_5	17.33	18.67	18.00	20.33	23.26	21.80	15.0	19.0	17.0	43.87	44.10	43.98
T_6	18.67	19.50	19.08	22.50	24.78	23.64	14.7	19.3	17.0	44.30	44.54	44.42
T_7	16.50	19.50	18.00	20.50	21.06	20.78	15.0	18.7	16.8	43.17	43.41	43.29
CD (p=0.05)	2.01	1.57	1.71	2.41	1.40	1.86	NS	NS	NS	NS	NS	NS

Table 4. Number of runners, number of crowns and total chlorophyll content of strawberry as influenced by organic formulations

Treatment	Number of runners per plant			Number of crowns per plant			Total chlorophyll content (mg g^{-1})		
	2019	2020	Pooled	2019	2020	Pooled	2019	2020	Pooled
T_1	6.0	6.2	6.1	3.0	3.3	3.2	0.62	0.63	0.63
T_2	4.7	4.8	4.8	3.0	3.3	3.2	0.65	0.63	0.64
T_3	5.0	5.2	5.1	3.0	3.0	3.0	0.67	0.64	0.65
T_4	4.3	4.5	4.4	2.3	3.0	2.7	0.65	0.66	0.66
T_5	3.3	3.5	3.4	2.0	2.0	2.0	0.65	0.64	0.64
T_6	3.0	3.2	3.1	2.0	2.0	2.0	0.62	0.64	0.63
T_7	3.3	3.5	3.4	2.0	2.0	2.0	0.65	0.64	0.64
CD (p=0.05)	1.69	1.67	1.68	0.68	0.57	0.80	NS	NS	NS

Table 5. Flowering, fruit set and yield parameters of strawberry as influenced by inorganic fertilizers and organic formulations

Treatment	Number of flowers plant^{-1}			Number of fruits plant^{-1} Fruit set (%)			Fruit set (%)			Yield per plant (g)			Yield hectare^{-1} (tonnes)		
	2019	2020	Pooled	2019	2020	Pooled	2019	2020	Pooled	2019	2020	Pooled	2019	2020	Pooled
T_1	25.3	25.7	25.5	21.0	21.3	21.2	82.69	82.96	82.83	298.10	305.69	301.90	16.56	16.98	16.77
T_2	27.3	26.3	26.8	22.7	21.3	22.0	82.97	81.15	82.06	320.07	307.49	313.78	17.78	17.08	17.43
T_3	26.0	26.7	26.3	21.7	21.3	21.5	83.03	80.12	81.57	304.10	301.38	302.74	16.89	16.74	16.82
T_4	26.7	25.7	26.2	22.3	22.0	22.2	83.66	85.73	84.69	321.51	314.66	318.09	17.86	17.48	17.67
T_5	22.7	24.0	23.3	18.3	19.3	18.8	80.56	80.48	80.52	220.64	234.98	227.81	12.26	13.05	12.66
T_6	20.7	21.7	21.2	16.7	17.3	17.0	80.00	79.84	79.92	201.37	210.40	205.89	11.19	11.69	11.44
T_7	20.7	22.3	21.5	16.7	18.0	17.3	80.45	80.63	80.54	200.91	219.32	210.12	11.16	12.18	11.67
CD (p=0.05)	4.32	2.31	3.43	4.74	2.92	4.03	NS	NS	NS	60.64	67.81	63.14	3.37	3.77	3.51

Table 6. Fruit size, weight and TSS of strawberry as influenced by organic formulations

Treatment	Fruit length (cm)			Fruit breadth (cm)			Fruit weight (g)			TSS (˚B)		
	2019	2020	Pooled	2019	2020	Pooled	2019	2020	Pooled	2019	2020	Pooled
T_1	3.52	3.50	3.51	2.65	2.69	2.67	14.18	14.29	14.24	9.7	9.5	9.58
T_2	3.53	3.50	3.52	2.73	2.73	2.73	14.13	14.33	14.23	10.5	9.7	10.08
T_3	3.52	3.52	3.52	2.58	2.59	2.58	14.02	14.12	14.07	10.7	10.3	10.50
T_4	3.54	3.53	3.54	2.83	2.75	2.79	14.41	14.33	14.37	9.7	9.5	9.58
T_5	3.46	3.45	3.46	2.73	2.63	2.68	12.13	12.16	12.15	9.2	9.0	9.08
T_6	3.44	3.43	3.44	2.36	2.36	2.36	12.10	12.13	12.12	8.3	8.7	8.50
T_7	3.47	3.41	3.44	2.66	2.34	2.50	12.03	12.19	12.11	8.2	8.5	8.33
CD (p=0.05)	NS	NS	NS	0.37	0.40	0.38	0.76	2.03	1.40	1.13	1.26	1.14

Table 7. Titratable acidity and sugar content of strawberry as influenced by organic formulations

Treatment	Titratable acidity (%)			TSS/acid ratio			Total sugars (%)			Reducing sugars (%)		
	2019	2020	Pooled	2019	2020	Pooled	2019	2020	Pooled	2019	2020	Pooled
T_1	0.31	0.32	0.31	32.73	30.34	31.54	5.93	5.98	5.95	3.68	3.61	3.64
T_2	0.24	0.36	0.30	44.40	27.24	35.82	6.18	6.14	6.16	3.71	3.60	3.66
T_3	0.26	0.37	0.31	43.24	31.27	37.25	6.30	6.09	6.20	3.75	3.73	3.74
T_4	0.31	0.36	0.33	32.30	27.57	29.93	6.05	5.91	5.98	3.73	3.62	3.68
T_5	0.22	0.41	0.32	41.23	24.36	32.80	5.99	5.86	5.92	3.74	3.65	3.70
T_6	0.24	0.35	0.29	35.01	26.61	30.81	5.93	5.84	5.88	3.70	3.57	3.63
T_7	0.24	0.36	0.30	34.79	24.31	29.55	5.83	6.03	5.93	3.65	3.68	3.66
CD (p=0.05)	NS	NS	NS	NS	NS	NS	0.26	0.27	0.26	NS	NS	NS

Table 8. Fruit quality parameters (physico-chemical) of strawberry as influenced by inorganic fertilizers and organic formulations

Treatment	Non-reducing sugars (%)			Anthocyanin content (mg 100 g^{-1})			Ascorbic acid (mg 100 g^{-1})			Total phenols (%)		
	2019	2020	Pooled	2019	2020	Pooled	2019	2020	Pooled	2019	2020	Pooled
T_1	2.14	2.25	2.19	26.00	25.20	25.60	65.10	70.68	67.89	47.11	51.71	49.41
T_2	2.35	2.41	2.38	27.60	33.60	30.60	66.03	67.89	66.96	51.23	51.47	51.35
T_3	2.42	2.24	2.33	30.00	32.00	31.00	69.75	66.96	68.36	55.29	55.49	55.39
T_4	2.20	2.18	2.19	32.00	30.40	31.20	68.82	66.03	67.43	55.29	55.53	55.41
T_5	2.13	2.09	2.11	28.00	27.60	27.80	67.89	66.96	67.43	47.02	49.39	48.20
T_6	2.12	2.16	2.14	34.00	22.80	28.40	68.82	69.75	69.29	47.96	48.69	48.32
T_7	2.07	2.23	2.15	28.00	22.80	25.40	65.10	66.96	66.03	46.99	48.99	47.99
CD (p=0.05)	NS	NS	NS	NS	NS	NS	NS	NS	NS	NS	NS	NS

inorganic and organic sources of nutrients have been reported by several workers (Rana and Chandel 2003, Yusuf et al 2003, Sahoo and Singh 2005, Singh and Singh 2009, Iqbal et al 2009 and Gupta and Tripathi, 2012). The increase in ascorbic acid content might be due to the increased efficiency of microbial inoculants to fix atmospheric nitrogen, increase in availability of phosphorous and secretion of growth promoting substances which accelerated the physiological process like carbohydrates synthesis etc. These results are similar with the findings of earlier workers.

CONCLUSION

The application of organic formulations with organic and inorganic sources of nutrients significantly influences the crop performance. In the present study, increase in crop performance among different treatments, application of 75% T_1 + 25% RDN through Jeevamrit + Ghanjeevamrit in the ratio 1:1 resulted in better growth, flowering, yield and fruit quality in strawberry.

REFERENCES

AOAC 1980. *Association of Official Analytical Chemists. Official Methods of Analysis*. Hortwitz, W. (ed.), 13th ed. Washington, D.C. 1015 p.

Ahmadi E, Honnabyraiah MK, Alur AS, Adiga JD and Rao V 2017. Impact of integrated nutrient management on yield and quality parameters of strawberry (*Fragaria* × *ananassa* Duch.) *Cv*. "Sabrina" under polyhouse. *International Journal of Current Microbiology and Applied Sci*ences **6**: 3481-3487.

Das D, Dwivedi BS, Meena MC, Singh VK and Tiwari KN 2015. Integrated nutrient management for improving soil health and crop productivity. *Indian Journal of Fertilisers* **11**: 64-83.

Gupta AK and Tripathi VK 2012. Efficacy of Azotobacter and vermicompost alone and in combination on vegetative growth, flowering and yield of strawberry (*Fragaria* × *ananassa* Duch.) cv. Chandler. *Progressive Horticulture* **44**: 256-261.

Iqbal U, Wali VK, Kher R and Jamwal M 2009. Effect of FYM, urea and Azotobacter on growth, yield and quality of strawberry cv. Chandler. *Notulae Botanaicae Horti Agrobotanici* **37**: 139-143.

Received 12 July, 2021; Accepted 12 November, 2021

Iqbal U, Wali VK, Kher R and Sharma A 2008. Impact of integrated nutrient management on strawberry yield and soil nutrient status. *Applied Biological Research* **10**: 22-25.

Kumar Vasanth HHA 2006. Jeevamrut slurry preparation. *Siri Samruddhi* pp. 4-5.

Kushwah MS, Singh D, Singh S and Bairwa M. 2018.Effect of Integrated Nutrient Management on growth, yield and quality traits of strawberry (*Fragaria* x *ananassa* Duch.) cv. Chandler. *Journal of Pharmacognosy and Phytochemistry* **1**: 712-715.

Nowsheen N, Singh SR, Aroosa K, Masarat J and Majeed S 2006. Yield and growth of strawberry cv. Senga Sengana as influenced by integrated organic nutrient management system. *Environment and Ecology* **24**: 655-659.

Nyang'au J, Gatebe E, Nyagah C and Ahenda S 2016. Evaluation of biogas slurry as an alternative organic fertilizer: A case study in Kenya. *International Journal of Extensive Research* **9**: 10-14.

Palekar S 2006. *Shoonya Bandovalada Naisargika Krushi*. Swamy A and AgriPrakashana. Bangalore. 214p.

Pradeep B and Saravanan S 2018. Effect of different biofertilizers and organic manures on yield and quality of strawberry (*Fragaria* × *ananassa* Duch.) cv. Chandler. *Journal of Pharmacognosy and Phytochemistry* **7**:151-155.

Rana RK and Chandel JS 2003. Effect of biofertilizers and nitrogen on growth, yield and fruit quality of strawberry. *Progressive Horticulture* **35**: 25-30.

Sahoo SK and Singh DB 2005. Effect of different levels of biofertilizers on growth, yield and quality of strawberry (*Fragaria* × *ananassa* Duch) cv. Sweet charley. *Orissa Journal of Horticulture* **33**: 82-85.

Singh A and Singh JN 2009. Effect of biofertilizers and bio regulators on growth, yield and nutrient status of strawberry cv. Sweet Charlie. *Indian journal of Horticulture* **66**: 220-222.

Sreenivasa MN, Negara MN and Bhat SN 2010. Beejamruth: A source for beneficial bacteria. *Karnataka Journal of Agricultural Sciences* **17**: 72-77.

Umar I, Wali VK, Ravisher and Marital J 2009. Effect of FYM, Urea and Azotobacter on growth, yield and quality of strawberry cv. chandler. *Not Bot Horticulture Agro botanicaea Cluj* **37**: 139-143.

Yadav SK, Kocher UU and Yadav RP 2010. Integrated nutrient management for strawberry cultivation. *Indian Journal of Horticulture* **67**: 445-449.

Yusuf A, Iqbal M, Shah SZA and Ahmed MJ 2003. Effect of different combinations of nitrogen, phosphorous and farm yard manure on yield and quality of strawberry. *Sarhad Journal of Agriculture* **19**: 185-188.

Indian Journal of Ecology (2021) 48(6): 1760-1765

Manuscript Number: 3445
NAAS Rating: 5.79

Seed Traits and Germination in *Syzygium caryophyllatum* (L.) Alston: An Endangered Species of the Western Ghats

A. Joglekar, M. Tadwalkar, P. Ghate[1], R.P. Gunaga[2] and A. Patwardhan[1*]

Annasaheb Kulkarni Department of Biodiversity, M.E.S. Abasaheb Garware College, Pune-411 004, India
[1]Research and Action in Natural Wealth Administration (RANWA), Kothrud, Pune-411 052, India
[2]College of Forestry, Navsari Agricultural University, Navsari-396 450, India
**E-mail: ankurpatwardhan@gmail.com*

Abstract**:** *Syzygium caryophyllatum* (L.) Alston is one of the ecologically important tree species of Western Ghats, a global biodiversity hotspot. According to the IUCN assessment, this species belonged to the 'Endangered' category. Present study was designed to assess the fruit and seed traits as well as germination pattern in *S. caryophyllatum*. Reproductive phenology observations revealed that flowering period spread over four months from March to June; while, overall fruiting period ranged between May to July. Individual fresh fruit weight ranged from 0.74 to 3.45 g with highly positive skewed distribution. Seed weight varied from 0.04 to 0.59 g with 83 per cent of seeds being represented in seed weight class of 0.04 to 0.34 g. Seed germination initiated after 13th day of sowing and overall germination success was 90 per cent in germination chamber @ 28-35°C temperature and 70-75% relative humidity. However, natural regeneration was very poor in the study area necessitating the need for further focused studies to understand factors that delimit the population build-up of the species.

Keywords: *Syzygium caryophyllatum,* Endangered species, Seed traits, Seed germination, Natural regeneration

Syzygium, an Old-World Genus, is one of the largest generic groups of family Myrtaceae with about 1200 species (Parnell et al 2007). Fifty-two species of *Syzygium* have been recorded from the Western Ghats, one of the global biodiversity hotspots; of which, 26 species have been listed in IUCN red list (Ramasubbu et al 2016). *Syzygium* exhibits different life forms that range from large sized canopy trees, small to medium sized understorey trees/shrubs and is distributed widely across evergreen to deciduous forest types. *Syzygium* species provide various ecosystem services, pollination being one of the most significant ones. Majority of the *Syzygium* species possess high economic potential in terms of timber, fuel wood and medicinal properties. 'Honey' branded in the name of '*Syzygium* honey' is one of the most popular traded commodities. *Syzygium* is also found as one of the most dominant and abundant genera in the protected and reserved forests of Northern Western Ghats (NWGs, Kanade et al 2008, Joglekar et al 2015, Tadwalkar et al 2020). *Syzygium caryophyllatum* (L.) Alston is one such species that is categorized as 'Endangered' as per IUCN assessment. This medium sized evergreen tree species prefers forest edge as habitat and is sparsely distributed along the margins of evergreen forests and in nearby open patches (Stalin 2015). Though listed as endangered, very few studies have been conducted on current population status, reproductive biology and ecological importance of *S. caryophyllatum*. Seed traits studies have an important role in understanding dispersal potential, germination success, seedling survival and establishment and community composition (Gunaga 2011, Poschlod 2013, Osuri et al 2016, Hegde et al 2018, Tadwalkar et al 2020). Regeneration which is a fundamental in maintenance of natural population of the species needs to be studied to understand population structure especially for the species which is already 'Endangered' (Gunaga et al 2011, Mirgal et al 2013, Patwardhan et al 2016). Present study focused on all the important life cycle events of the *S. caryophyllatum* like flowering and fruiting, fruit and seed traits and most importantly germination success under controlled conditions and present natural regeneration status of the species in the study area.

MATERIAL AND METHODS

Field studies were conducted at 'Amboli' forests of Northern Western Ghats (15°57 N latitude, 74°00E longitude and altitude of 697 m), a part of Sahyadri- Konkan Ecological Corridor (CEPF 2007, Patwardhan et al 2016; Plate 1). Rainy season spans primarily over June to September with occasional pre-monsoon showers in May. The area receives >6000 mm rainfall annually during this period. Present study was conducted for the period from 2017 to 2019. The taxonomic identification of *S. caryophyllatum* was confirmed by referring to the taxonomic literature (Singh et al 2001) and referring to the herbaria.

Fruit and seed traits assessment*:* Flowering and fruiting (reproductive phenology) of *S. caryophyllatum* was regularly monitored during monthly field visits to study area. Buds and open flower duration were recorded under flowering period; while, immature fruits and mature fruits duration was recorded under fruiting period. Mature fruits with dark purple to black colour (Plate 2) were collected from crown of the standing trees using telescopic cutting pole from distantly placed six trees. The fruits collected (N=230) were immediately subjected to the measurement of various traits such as fruit weight (g), fruit length (mm), fruit breadth (mm), pulp weight (g), seed weight (g), seed length (mm) and seed breadth (mm) using pocket balance and digital vernier caliper on the field. Individual tree wise record was maintained. Tree wise numbered fruits were manually de-pulped and then shade dried. Measurements of seeds were taken using precision balance (CONTECH-CA SERIES Model and SHIMADZU ATY224) and vernier caliper in the laboratory. Pulp weight (g) was calculated as a difference between fruit and seed weight. Pulp to seed ratio was also calculated.

Natural regeneration: Natural regeneration was assessed by quadrat method of sampling. Ten quadrats of 10 m x 10 m were randomly laid in open forest patches where adult population was recorded. In addition to this, 13 permanently laid vegetation study quadrats (20 m x 20 m) were also assessed for species regeneration status. In total, 0.62 ha was surveyed for natural regeneration count. Regeneration status was assessed by classifying individuals into four classes based on girth and height *viz.,* Class I (<40 cm height), Class II (40-100 cm height), Class III (> 100 cm height, and < 10 cm Girth at breast height (GBH)) and Class IV (GBH between 10-15 cm).

Germination trials*:* Bulk fruit collection was carried out from distantly located trees. Each seed was measured for its weight and numbered separately. Germination trials were conducted for two consecutive years. Total 300 seeds were subjected to germination trials (100 seeds in year 2017 and 200 seeds in year 2018). Germination trials were conducted in germination chamber under controlled conditions of temperature (28-35°C) and relative humidity (70-75%). No external nutrient support was provided to seeds while performing germination trials. Since seeds of *Syzygium* are considered as recalcitrant in nature, seeds were sown within four days of fruit collection at a depth of 0.5-1.0 cm in the germination trays (1 seed per germination well) filled with moistened cocopeat. No pre-sowing treatment was given to the seed. Regular moistening of the germination tray was carried out till the last day of observation. Germination was marked as positive after seeing radicle emergence. Days required for radicle emergence were grouped into class of 10 days. The number of days required to attain 50 per cent germination in each trial was also recorded. Germination success was monitored upto 90 days from the date of sowing. The summary statistics for the fruit and seed measurements was calculated. Pearsons' correlation coefficients were computed for natural log transformed fruit and seed traits. All statistical analysis was conducted using PAST (version 4.0) and JASP (Version 0.14.1).

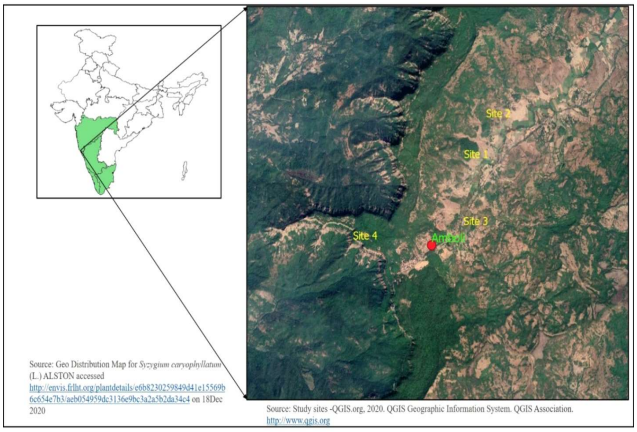

Plate 1. Study area map with species population locations

RESULTS AND DISCUSSION

In *S. caryophyllatum*, flowering and fruiting was observed for a period of five months spreading across March to July. Bud initiation started in the first half of the March and peak flowering was observed in the last week of April. Fruit formation started in the month of May and mature fruits were

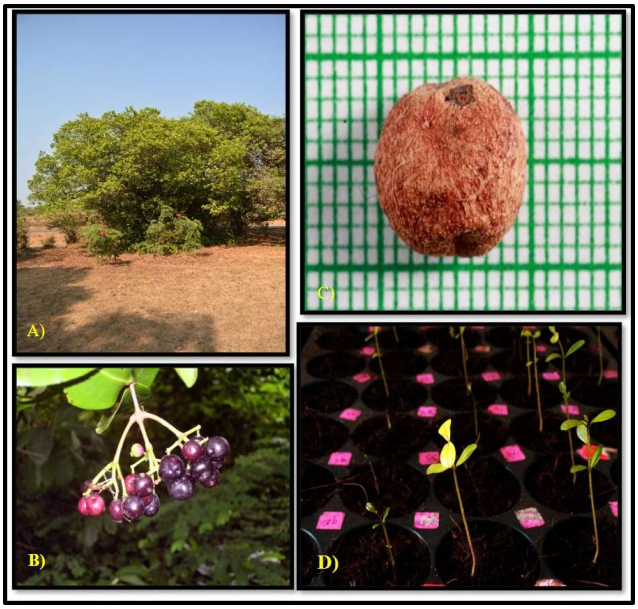

Plate 2. Profile of *S. caryophyllatum*- A) Entire plant, B) Fruits, C) Seed, D) Seedlings

observed in rainy season from mid-June to mid-July (Fig. 1). Fruits of *S. caryophyllatum* are single seeded berries with a round shape. Unripe fruits are green and pink in colour and turn dark purple or black at the time of maturity (Plate 2). Red vented bulbul (*Pycnonotus cafer*) was observed feeding on mature fruits. Average fruit weight was 1.52 g (±0.45) and exhibited positively skewed distribution (skewness= 1.24). Average fruit length and breadth were 11.04 and 13.02 mm respectively. Seed weight ranged across one order of magnitude with average of 0.25 g. Average pulp weight was 1.27 (Table 1). Out of six classes, 83 per cent of the seeds were distributed between 0.04 to 0.34 g (Fig. 2).

There was significant variation in fruit weight (1.02 to 2.19 g), fruit length (9.77 to 12.94 mm), fruit breadth (12.18 to 14.36 mm), seed weight (0.14 to 0.43 g), seed length (4.86 to 6.71 mm), seed breadth (6.79 to 9.25 mm) and pulp weight (0.83 to 1.76 g) recorded among six accessions (Table 2). Natural log transformed fruit and seed traits showed highly significant correlation ($p<0.001$) with each other; however, correlation coefficient values between seed length with fruit traits were relatively low (Table 3). Out of 23 quadrats (0.62 ha) assessed for the regeneration status of the species, regeneration of *S. caryophyllatum* was seen only in 7 quadrats and representing 21 recruits only. Highest number of recruits were found in class IV (N=9), followed by Class II (N=5) and class III (N=5); however, it was least in Class I (only two recruits). Sixty seven per cent regenerating individuals were recorded near adult trees in open forest. It was interesting to note that regeneration was not observed in the adjoining closed forest quadrats. Out of total 300 sown seeds, 90 per cent of seeds showed successful germination. The germination percentage recorded during 2017 and 2018

Table 1. Descriptive statistics of fruit and seed traits of *S. caryophyllatum* (N=230)

Descriptive statistic	Fruit weight (g)	Fruit length (mm)	Fruit breadth (mm)	Seed weight (g)	Seed length (mm)	Seed breadth (mm)	Pulp Weight (g)	Pulp to seed ratio
Minimum	0.74	7.85	9.67	0.04	3.73	4.86	0.56	2.22
Maximum	3.45	15.41	16.73	0.59	8.52	10.61	3.14	35.21
Mean	1.52	11.04	13.02	0.25	5.88	7.85	1.27	5.98
Std. error of mean	0.03	0.08	0.08	0.01	0.06	0.07	0.02	0.21
Variance	0.20	1.64	1.65	0.01	0.91	1.25	0.14	10.57
Standard deviation	0.45	1.28	1.28	0.11	0.95	1.12	0.38	3.25
Median	1.44	10.91	12.97	0.23	5.83	7.88	1.20	5.20
25thpercentile	1.22	10.12	12.09	0.17	5.26	7.07	1.01	4.12
75thpercentile	1.7	11.76	13.78	0.31	6.52	8.70	1.44	6.74
Skeweness	1.239	0.627	0.217	0.904	0.219	-0.086	1.282	4.052
Kurtosis	2.078	0.654	0.078	0.570	-0.275	-0.412	2.917	29.094
Geom. mean	1.46	10.97	12.95	0.22	5.80	7.77	1.22	5.44
Coeff. Var (%)	29.68	11.61	9.86	44.77	16.22	14.25	29.82	54.35

Table 2. Variation in fruit and seed traits among six accessions of *S. caryophyllatum*

Tree accession	Fruit weight (g)	Fruit length (mm)	Fruit breadth (mm)	Seed weight (g)	Seed length (mm)	Seed breadth (mm)	Pulp weight (g)
SCAP-01	1.46	11.19	12.79	0.24	5.70	7.86	1.22
SCAP-02	1.33	10.29	12.26	0.14	4.86	6.81	1.18
SCAP-03	2.19	12.94	14.36	0.43	6.70	9.25	1.76
SCAP-04	1.02	9.77	12.18	0.18	5.34	6.79	0.83
SCAP-05	1.37	10.73	12.87	0.25	6.71	8.45	1.12
SCAP-06	1.52	10.92	13.10	0.24	5.68	7.61	1.28
Mean	1.48	10.97	12.93	0.25	5.83	7.79	1.23
SEm (±)	0.11	0.30	0.39	0.02	0.14	0.18	0.10
CD ($p<0.05$)	0.33	0.94	1.23	0.05	0.44	0.55	0.30
CV (%)	12.27	4.75	5.27	10.74	4.19	3.89	13.43

SCA= *Syzygium caryophyllatum* Amboli population; SEm = Standard Error of Mean; CD= Critical Difference; CV= Coefficient of variation

was 89 and 91 per cent, respectively. Germination was highest in smaller seeds (with less seed weight) than bigger ones. Seed germination initiated after 13th day of sowing and extended up to 83rd day. There was a difference between the time period for 50 per cent germination, where number of days for 50 per cent germination was 19 days for the year 2017 as against 46 days for the year 2018 (Table 4). Maximum germination was observed within 13 to 20 days of sowing. Plant growth abnormalities such as twin shoot formation was seen for a few germinated seeds. Between twin shoots, taller shoot of the seedling showed blackening at the tip and no further leaf production, whereas dwarf shoot showed delayed leaf development.

There are very few studies available on fruit and seed traits of woody species of Western Ghats. *Syzygium*, a dominant genus of the Western Ghats, is also under-researched for fruit and seed traits. Sivasubramaniam and Selvarani (2012) recorded fruit weight of *S. cumini* within range of 2 to 5 g. Moreover, tree to tree variation in *S. caryophyllatum* for fruit and seed traits was also recorded indicating genotypic effect. Such variability has also been recorded for threatened species like *Dysoxylum binectariferum* (Gunaga et al 2015) and *Mammea suriga* (Gunaga and Vasudeva 2009). Tree to tree variation for germination success was also recorded in this species. Such genotypic variation was also recorded in *Melia dubia, Sterculia urens* for germination attributes (Chauhan et al 2019, Bhuva et al 2019). Data shows that *S. caryophyllatum* can be classified as an intermediate fruit and seed size as compared to other *Syzygium* species in study area (Table 5). *S. caryophyllatum* showed fruit initiation and maturation coinciding with pre-monsoon and rainy season in the study area. Season of fruit maturation can be considered as suitable for *in-situ* germination of pulpy and recalcitrant nature species. Despite profuse fruiting, very poor natural (*in-situ*) regeneration of the species was observed. Reverse-J pattern, a characteristic of healthy regeneration dynamics was also not seen in the *S.caryophyllatum*. The disproportionate regeneration across classes and poor regeneration in class I indicates non favorable conditions for

Table 4. Germination observation of *S. caryophyllatum*

Year of experiment	Number of seeds sown	50% germination period	Germination success
2017	100	19 days	89 %
2018	200	46 days	91 %
Mean	-	32.5 days	90 %

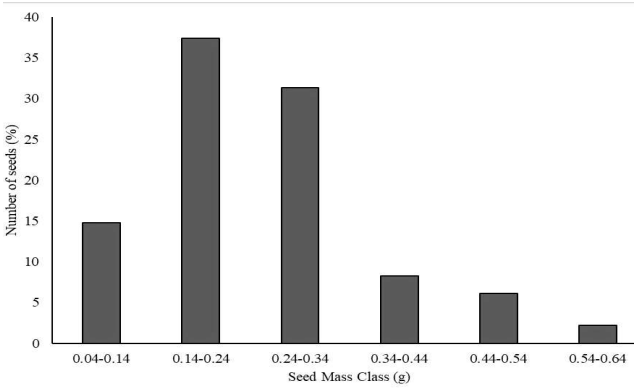

Fig. 2. Distribution of seeds across different seed weight classes (N=230)

Fig. 1. Phenogram of flowering and fruiting of *S. caryophyllatum*

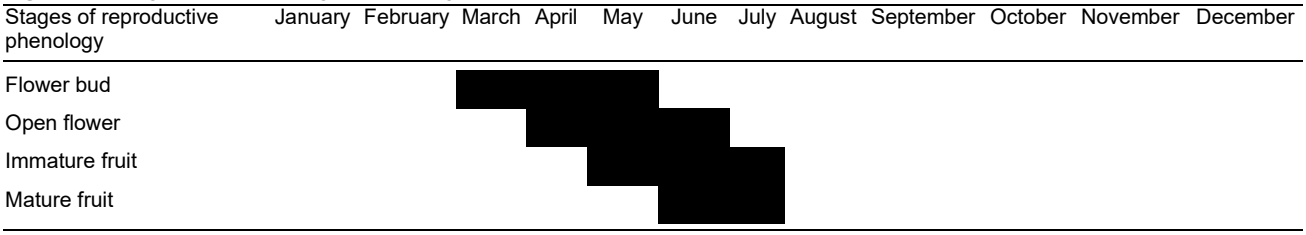

Table 3. Correlation between natural log transformed weight, length and breadth of *S. caryophyllatum*

Traits	Fruit weight	Fruit length	Fruit breadth	Seed weight	Seed length	Seed breadth
Fruit weight	—					
Fruit length	0.851*	—				
Fruit breadth	0.877*	0.733*	—			
Seed weight	0.651*	0.682*	0.577*	—		
Seed length	0.436*	0.509*	0.431*	0.789*	—	
Seed breadth	0.611*	0.649*	0.536*	0.906*	0.782*	—

* $p < .001$

Table 5. Fruit and Seed weight of *Syzygium* species from Amboli, Maharashtra

Species	Fruit weight (g) Mean ± SD	Seed weight (g) Mean ± SD	Pulp weight Mean ± SD	Pulp to seed ratio Mean ± SD	Remarks
Syzygium caryophyllatum (L.) Alston	1.52 ± 0.45	0.25 ± 0.11	1.27 ± 0.38	5.98 ± 3.25	Prefers forest edge
S. cumini (L.) Skeels	1.82 ± 0.62	0.40 ± 0.15	1.41 ± 0.59	4.03 ± 2.57	Dominant species along NWG crestline and in Amboli forest
S. hemisphericum (Wight) Alst.	7.32 ± 3.43	1.77 ± 0.85	5.54 ± 2.80	3.64 ± 3.15	Canopy species in Amboli forest
S. phillyraeoides (Trim.) Sant.	0.83 ± 0.35	0.27 ± 0.14	0.55 ± 0.29	2.60 ± 1.78	Understorey species in evergreen forests
S. zeylanicum (L.) DC.	0.33 ± 0.06	0.05 ± 0.01	0.28 ± 0.05	6.26 ± 3.16	Riparian species

natural regeneration and disturbances in ecological process due to climatic and/or biotic factors (Gunaga et al 2011, Mirgal et al 2013, Hegde et al 2018). Species showed clumped distribution in the study area mainly along stream banks which makes habitat inimical to the seedling establishment (Patwardhan et al 2016). During regeneration studies, it was difficult to differentiate whether class III and IV individuals were separate or were vegetative outgrowth of the same adult clump (GBH>15 cm). No seed germination was observed on the ground; but two fruits showed radicle emergence on the plant itself like vivipary. Long term natural regeneration monitoring can be the next step to understand factors affecting natural germination and overall demographic structure of the species (Patwardhan et al 2016, Hegde et al 2018). Though very poor natural regeneration in the forest was observed, species showed 90 per cent *ex-situ* germination success under controlled conditions without any presowing tratement. *S.caryophyllatum* showed twin shoot formation like *S. cumini* (Sivasubramaniam and Selvarani 2012) and *S. mundagom* (Jose et al 2009). The double embryony is also reported in *S. cumini* (Wanage et al 2012). Large scale germination trials to check relation between seed weight and germination success and to examine possibility of polyembryony can form the future step of action in standardization of mass multiplication protocols. Further, studies on possible causes for lack of natural regeneration are needs to be attmepted, especially in endangered species like *S. caryophyllatum* in the Sahyadri- Konkan Ecological Corridor.

CONCLUSION

Fruit and seed size data of an endagered species like *S. caryophyllatum* can be used as an important addition to the global seed database. Poor regeneration on field and high germination success under controlled germination conditions of temperature and humidity without any kind of treatment is one of the intersting finding of the study. Long term comparitive study for *in-situ* in the field and *ex-situ* germination in the nursery may be taken up to identify and understand limiting and promoting factors for germination and further ecological attributes. Further, seedling establishment of nursery plants in *in-situ* conditions is a crucial step in conservation of endangered species through introduction of species in suitable habitat.

ACKNOWLEDGEMENTS

Authors thank forest officials of Amboli forest division for their cooperation and guidance throughout the study period also to, Amboli Biodiversity Management Committee and Malabar Nature Conservation Club for their support .

REFERENCES

Bhuva DC, Gunaga RP, Thakur NS and Bhusara JB 2019. Seed and germination attributes in *Sterculia urens* Roxb. populations in South Gujarat. *Journal of Tree Sciences* **38**(1): 23-27.

CEPF 2007. Ecosystem profile: Western Ghats and Sri Lanka Biodiversity Hotspot- Western Ghats Region. Critical Ecosystem Partnership Fund, 100pp. https://www.cepf.net/sites/default/files/western-ghats-ecosystem-profile-english.pdf

Chauhan RS, Thakur NS, Gunaga RP, Bhuva DC and Jadeja DB 2019. Assessment of germination attributes in Candidate Plus Trees (CPTs) of Malabar Neem (*Melia dubia* Cav.). *Indian Journal of Ecology* **46**(2): 335-339.

Geo Distribution Map for *Syzygium caryophyllatum* (L.) ALSTON accessed http://envis.frlht.org/plantdetails/e6b8230259849d41e15569b6c654e7b3/aeb054959dc3136e9bc3a2a5b2da34c4accessedon 18Dec 2020.

Gunaga RP 2011. Influence of seed size on seed germination and seedling vigour in *Calophyllum inophyllum*: an important multipurpose tree of coastal region. *Journal of Indian Society of Coastal Agricultural Research* **29**(2): 35-38.

Gunaga RP and Vasudeva R 2009. Seed traits and half-sib family variation for seed germination and early seedling vigour in Suragi (*Mammea suriga*), an important aromatic tree species of the Western Ghats. *Journal of Non-Timber Forest Products* **16**(4): 285-290.

Gunaga RP, Manjunath AV, Gunaga SV and Vasudeva R 2015. Tree to tree variation in seed traits and germination in *Dysoxylum binectariferum* Hook. F. *The Indian Forester* **141** (5): 578-580.

Gunaga RP, Wanage SS, Ganiger RV, Rane AD, Narkhede SS, Bhave SG, Vasudeva R, Patwardhan A and Sai Prakash 2011. Stand dynamics and regeneration status of *Nothapodytes nimmoniana* Graham. in Open and Close forests of Western Ghats of Maharashtra. *In:* Proceedings of national seminar on Forest resources: Diversity, Utilization and Conservation held

at UAS Bangalore, Pp. 44-47.

Hegde HT, Gunaga RP, Thakur NS, Jha SK and Dobriyal MJ 2018. Population structure and regeneration of Mahua (*Madhuca longifolia* var. *latifolia* (Roxb.) A. Chev.) in disturbed and undisturbed sites. *Indian Journal of Ecology* **45**(4): 724-727.

Joglekar A, Tadwalkar M, Mhaskar M, Chavan B, Ganeshaiah KN and Patwardhan A 2015. Tree species composition in Koyna Wildlife Sanctuary, Northern Western Ghats of India. *Current Science* **108**(9): 1688-1693.

Jose PA, Mohanan N and Hussain A 2009. Occurrence of twin seedlings in *Humboldtia vahliana* Wight and *Syzygium mundagom* (Bourd.) Chithra - Two Endemic Trees of Southern Western Ghats. *Indian Forester* **135**: 290-292.

Kanade R, Tadwalkar M, Kushalappa C and Patwardhan A 2008. Vegetation composition and woody species diversity at Chandoli National Park, Northern Western Ghats, India. *Current Science* **95**(5): 637-646.

Mirgal AB, Rane AD, Gunaga RP, Narkhede SS and Bhave SG 2013. A note on stand dynamics of *Antiaris toxicaria*, a rare plant of Konkan Region of Western Ghats. *The Indian Forester* **139**(12): 1161-1162.

Osuri AM and Sankaran M 2016. Seed size predicts community composition and carbon storage potential of tree communities in rain forest fragments in India's Western Ghats. *Journal of Applied Ecology* **53**(3): 837-845.

Parnell Jan, Craven LA and Biffin E 2007. Matters of scale: Dealing with one of the Largest Genera of Angiosperms, pp. 251-273. In: Hodkinson TR and Parnell JNL (eds). *Reconstructing the Tree of Life: Taxonomy and Systematics of Species Rich Taxa*. Edition: Systematics Association Special Volume Series 72. Taylor and Francis, CRC Press. Boca Raton.

Patwardhan A, Pimputkar M, Mhaskar M, Agarwal P, Barve N, Gunaga R, Mirgal A, Salunkhe C and Vasudeva R 2016. Distribution and population status of threatened medicinal tree *Saraca asoca* (Roxb.) De Wilde from Sahyadri-Konkan ecological corridor. *Current Science* **111**(9): 1500-1506.

Poschlod P, Abedi M, Bartelheimer M, Drobnik J, Rosbakh S and Saatkamp A 2013. Seed ecology and assembly rules in plant communities. *Vegetation ecology* **2**: 164-202.

QGIS.org 2020. QGIS Geographic Information System. QGIS Association. http://www.qgis.org

Ramasubbu R, Divya C and Anjana S 2016. A Note on the taxonomy, field status and threats to three endemic species of *Syzygium* (Myrtaceae) from the Southern Western Ghats, India. *Journal of Threatened Taxa* **8**(11): 9384-9390.

Singh NP, Lakshminarsimha P, Karthikeyan S and Prasanna PV 2001. *Flora of Maharashatra State*. Botanical Survey of India, Vol. 1 and 2.

Sivasubramaniam K and Selvarani K 2012. Viability and vigor of Jamun (*Syzygium cumini*) Seeds. *Brazilian Journal of Botany* **35**(4): 397-400.

Stalin N and Swamy PS 2015. Prediction of suitable habitats for *Syzygium caryophyllatum*, an endangered medicinal tree by using species distribution modelling for conservation planning. *European Journal of Experimental Biology* **5**(11): 12-19.

Tadwalkar M, Joglekar A, Mhaskar M and Patwardhan A 2020. Woody species diversity from proposed ecologically sensitive area of Northern Western Ghats: Implications for biodiversity management. *Journal of Threatened Taxa* **12**(9): 16048-16063.

Wanage SS, Mirgal AB, Gunaga RP, Rane AD, Narkhede SS and Bhave SG 2012. A report on double embryos in *Syzigium cumini*, an important tropical wild fruit tree. *Journal of Non-Timber Forest Products* **19**(2): 151-152.

World Conservation Monitoring Centre 1998. *Syzygium caryophyllatum*. The IUCN Red List of Threatened Species 1998:e.T38036A10094391. https://dx.doi.org/ 10.2305/IUCN.UK.1998.RLTS.T38036A10094391.en. Downloaded on 24 April 2021.

Received 20 July, 2021; Accepted 12 November, 2021

Indian Journal of Ecology (2021) 48(6): 1766-1771

Manuscript Number: 3447
NAAS Rating: 5.79

Characterization of Few Fabaceous Plants towards their Medicinal Application

Neena Bagchi, Amit Sharma and Santosh K. Sar[1]

Department of Botany, Dr. C.V. Raman University, Kota, Bilaspur-495 113, India
[1]Department of Applied Chemistry, BIT, Durg- 490 006, India
E-mail: neenabagchi08@yahoo.com

***Abstract*:** The chemical characterization of the leaves of *Bahunia variegata, Cassia fistula* and *Dalbergia sissoo* of Fabaceae family were carried out to evaluate its bioactive potential. Fresh leaves of these plants were collected, dried and powdered for analysis. The proximate analysis of the leaves showed that the proportion of moisture content, volatile matter, ash content and fixed carbon were 5, 63, 18 and 14% respectively in *Bahunia variegata.* 4, 48.47, 11.88 and 35.65% respectively in *Cassia fistula* and 4, 70.25, 15.84 and 9.91% respectively in *Dalbergia sissoo*. The results of FTIR revealed the strong bonds between C-H, C-H, C=C, N-O, O-H, S=O, C-H, C-Br in *Bahunia variegata*, C-H, C-H, C=C, N-O, C-N, S=O, C-Cl, C-Br in *Cassia fistula.* C-H, C-H, C=C, N-O, S=O, C-O, S=O, C-H in *Dalbergia*. Moreover the result of TGA depicts that the highest weight loss occurred at temperature of 489.09°C in *Bahunia*, 497.91°C in *Cassia* and at 487.51°C in *Dalbergia* with a degradation rate of 10.00 K/min. The samples were also subjected to SEM and EDS analysis which is used to investigate the microstructure and the chemistry of range of material. With the execution of all these studies, the medicinal plants might become pharmacologically important and also confirm the medicinal practices used by earlier studies.

Keywords: Proximate analysis, FTIR, TGA, SEM, *Bahunia variegata, Cassia fistula, Dalbergia sissoo*

Medicinal plants are the major sources of herbal drugs and there is growing interest in the field of research for identification and isolation of biologically active compound from plant (Pye et al 2017). These plants are widely used for the treatment of various diseases associated to traditional medicine from different parts of the world (Mownika et al 2021). Due to the advancement in scientific approach and instrumental analysis, multinational pharmaceutical sectors took interest to develop potential drugs from plant sources for the improvement of different health issues. Verification of the folklore practices using medicinal plants, development of medicine and the treatment of patients is the main target of ethno- pharmacology (Anand 2019). Elements present in the plant show significant function for their pharmacological properties as they determine its potential to treat various diseases and usage in drug development (Mathai et al 2021). Extensive research is being assured for safety, quality, efficacy and stability for herbal drug preparation and hence characterization of medicinal plants has become an important aspect for drug development (Adhikari et al 2017).

The main objective of this study is the characterization of leaves of *Bahunia variegata, Cassia fistula and Dalbergia sissoo* to know its bioactive potential as these are known traditional medicinal plants used for the treatment of large number of diseases. *Bahunia variegata* Linn. commonly known as Kachnar is a medicinal plant from fabaceae family. The leaves of this plant are traditionally used for the treatment of bacterial infection, fungal infection, intestinal worms, diarrhea, inflammation, bronchitis, leprosy, liver disorder, skin disease, tumors, ulcers, and wounds. It is laxative in nature and is used for treating pile. (Khare et al 2018). It can be used as an alternative medicine against different bacterial pathogens if various pathogens become resistant or attain resistance to antibodies (Nariyal 2017). *Cassia fistula* commonly known as golden shower belongs to fabaceae family and its leaves possess antioxidant, antidiabetic, antimicrobial, antipyretic, antitumor, antiulcer properties (Mandloi et al 2018). *Dalbergia sissoo* is an indigenous plant which belongs to fabaceae family commonly known as shisham. The medicinal properties of this plant leaf include antioxidant, anti-inflammatory and estrogenic properties (Bijauliya et al 2017).There are many folklore and herbal practices in India but most of them are without scientific authentication. Thus with the execution of proximate analysis, FTIR, TGA, SEM and EDS, the above three plants may be identified as pharmacologically important and confirm all medicinal practices used in earlier studies. Also they could give answers to many health related problems we face in the modern world.

MATERIAL AND METHODS

Leaves of *Bahunia variegata, Cassia fistula and*

Dalbergia sissoo were collected from Durg district of Chhattisgarh in May-June 2020. Chhattisgarh is located in the central part of India. The geographical location is 17°46' N to 24°5' N latitude and from 80°15' E to 84°20' E longitude. Climate and weather condition is mainly dry and hot. During summer season the temperature varies from 42°C to 45°C. During winter, temperature falls down. The soil of Chhattisgarh is mainly known by its red color and the vegetation of this state is very rich where forest area covers about 44 percent.

Leaves of three different sample plants of each medicinal plant from different location were collected and care was taken to select the leaves of healthy plants, which were washed and dried in shade. The dried leaves were grinded in electric grinder to get a fine powder. It was then sieved to get 105 micron size particle for further use. This was followed by storing it in air tight bottles. Chemical Characterization of the plants was carried out with the help of different specialized standard laboratory equipment. Proximate analysis, FTIR, TGA, SEM and EDS of the sample were analyzed. Proximate analysis was carried out as per methods of Kathiresan Prabhu et al 2011. Moisture was determined by heating a known quantity of dried sample to 105- 110°C for one hour and percentage was calculated by loss in weight. To know the volatile matter, the dried sample of about 1 gm was heated in a silica crucible for 7 minutes at a steady temperature of 625°C in a muffle furnace. To get the ash percentage, 1 gm of sample was dried at 100- 105°C for one hour and ignited in a muffle at 600 - 625°C, which was carbon free and is weighed.

FTIR: In this technique, infrared light is used to scan the test sample which identifies the chemical bonds present in a molecule. The FTIR analysis measures the vibrations of bonds within chemical functional groups and generates a spectrum that can be called as finger-print of the sample (Mandloi 2018). The result by FTIR is extremely accurate and reproducible.

TGA: Thermo gravimetric analysis is an accurate procedure for studying the thermal stability and decomposition pattern of food polymers. It was done with the help of Module: TGA 1 SF/1100/321,02.11.2015 13:58:28. Method: 25-600@10N240ml dt 1.00s [1] 25.0.600.0°C, 10.00K/min, N_2 40.0 ml/min. Synchronization enabled.

SEM: A scanning electron microscope scans a focused electron beam over a surface to create an image. The electrons in the beam interact with the sample, produces various signals that can be used to obtain information about the surface topography and composition.

EDS: Energy dispersive X-ray spectroscopy is an analytical technique used for the elemental analysis or chemical characterization of a sample.

RESULTS AND DISCUSSION

The proximate analysis, FTIR, TGA, SEM, and EDS can be used as supporting tools for evaluation of the quality of the samples. The proximate composition of *Bahunia variegata, Cassia fistula and Dalbergia sissoo* (Table 1) indicated that the ash content was high (18%) in the leaves of *Bahunia variegata,* low moisture content of 5%, volatile mater content of 63% and carbon content 14 per cent. Similarly *Cassia fistula* has ash content 11.88 %, low moisture content (4%), volatile mater content (48.47%) and high carbon content of 35.65%. *Dalbergia sissoo* has ash content (15.84 %), low moisture content of 4%, Volatile mater content of 70.25% and carbon content of 9.91 per cent.

Flavonoid and alkaloid were highly present in leaves of these medicinal plants (Table 2). The moderate amount of saponin and terpenoid was identified in their leaves. The presence of tannin and anthocyanin was also recorded. The good amounts of carbohydrate and proteins were noted in leaves of these medicinal plants. Since the leaves of these medicinal plants contain flavanoids, it has anti-allergic, anti-cancer, anti-microbial and anti-tumor properties (Mohiuddin 2019). Due to the presence of high concentration of flavanols, xanthones, tannins and proanthocyanidins, it protects free radical mediated damage. Secondary metabolites present in the plants, produce some biological activity in man and animals which is responsible for their medicinal uses and therefore it becomes good remedy in traditional use. Presence of tannins is reported to heal wound, inflame the mucus membrane and arrest the bleeding. Moreover tannin containing plant extracts were used against stomach and duodenal tumors, diarrhea and diuretics. Due to the presence of these secondary metabolites, the plants are responsible for the antimicrobial activity against some microorganisms (Mandloi et al 2018). Saponin has the ability to stimulate the cell-mediated immune system and can enhance the production of antibodies. It exhibit medicinal properties such as anti-inflammatory, antibacterial, antifungal, antiviral, insecticidal, anticancer and cytotoxic activity (Aziz et al 2019). Due to the presence of immense amount of calcium, the plant reduces the risk of osteoporosis and arthritis in older people.

Table 1. Proximate composition of *Bahunia variegata, Cassia fistula and Dalbergia sissoo* (%)

Proximate composition	*Bahunia variegata*	*Cassia fistula*	*Dalbergia sissoo*
Moisture	5	4	4
Volatile matter	63	48.47	70.25
Ash	18	11.88	15.84
Carbon	14	35.65	9.91

FTIR of *Bahunia variegata, Cassia fistula and Dalbergia sissoo*

The results of FTIR revealed the strong bonds between C-H, C-H, C=C, N-O, O-H, S=O, C-H and C-Br in *Bahunia variegata*, C-H, C-H, C=C, N-O, C-N, S=O, C-Cl and C-Br in *Cassia fistula* and C-H, C-H, C=C, N-O, S=O, C-O, S=O and C-H in *Dalbergia sissoo* (Fig. 1).

In the leaves of *Bahunia variegata,* presence of functional group, alkane was confirmed by the strong absorption band between 3000-2840 at 2916.43 and 2848.71 cm^{-1}, while alkene C=C was confirmed by the strong stretching band between 1662-1626 at 1627.24 cm^{-1}. Presence of nitro compound was confirmed by the N-O stretching observed between 1550-1500 at 1545.85 cm-1. Phenol can be confirmed by the O-H bending at 1315.85 between 1390-1310 and sulfoxide by S=O stretching band observed between 1070-1030 at 1031.72 cm^{-1}. 1, 2, 3-trisubstituted compound was confirmed by the C-H bending between range 780+20 at 777.91. Halo compound of C-Br stretching can be observed between 690-515 at 667.25 cm^{-1}. Similarly, in the leaves of *Cassia fistula,* different absorption band and stretching shows the presence of alkane, alkene, nitro compound, sulfoxide and halo compound. The functional group amine can be confirmed by the C-N stretching at 1245.15. Likewise, in the leaves of *Dalbergia sissoo,* alkane, alkene and nitro compounds were confirmed. Sulphone and alkyl aryl ether were confirmed by the S=O stretching at 1314.82 and C-O stretching band at 1243.26 cm^{-1} respectively. Sulfoxide and 1, 2-disubstituted C-H bending was also found (Fig. 1).

Table 2. Phytochemical analysis of *Bahunia variegata, Cassia fistula and Dalbergia sissoo*

Phytochemical	*Bahunia veriegata*	*Cassia fistula*	*Dalbergia sissoo*
Alkaloid	+	+	+
Flavonoid	+	+	+
Saponin	+	+	+
Terpenoid	+	+	+
Glycoside	+	-	+
Tannin	+	+	+
Anthraquinone	+	+	-
Oxyanthraquinones	-	+	-
Oxalic acid	-	+	-
Phytobatannins	+	+	-
Sterols	+	+	+
β-sitosterol	+	-	-
Quercetin	+	-	-
Apigenin	+	-	-
Xanthones	-	+	-
Carbohydrate	+	+	+
Protein	+	+	+
Phenols	+	-	+
Lignin	+	-	-
Reducing Sugar	+	+	+
Crude Fat	-	+	+
Crude fibre	-	+	+
Neoflavene	-	-	+
Isoflavone	-	-	+

Functional groups play an important role in the formation of biological molecules such as protein, DNA, carbohydrates and lipids. Amino acids and amines are important constituents of protein synthesis and play a vital role in the physiology of living organisms. Some examples of sulfoxide occurring in nature are allin, allicin that were found in garlic and is of much ayurvedic importance. Their Sulphur derivative compounds were used to prepare disinfectants and dermal cream. Functional groups are important components of drug molecule. From the medicinal chemistry perspective, these functional groups provide the specific properties and behaviour that allow the drug molecule to show their pharmacokinetic and pharmacodynamic effects (Harrold et al 2018).

TGA of leaves of *Bahunia variegata, Cassia fistula and Dalbergia sissoo*

The leaves of *Bahunia variegata* were subjected to Thermo gravimetric analysis. A descending Z shaped curve is obtained from TGA curve (Fig. 2). It depicts the weight of

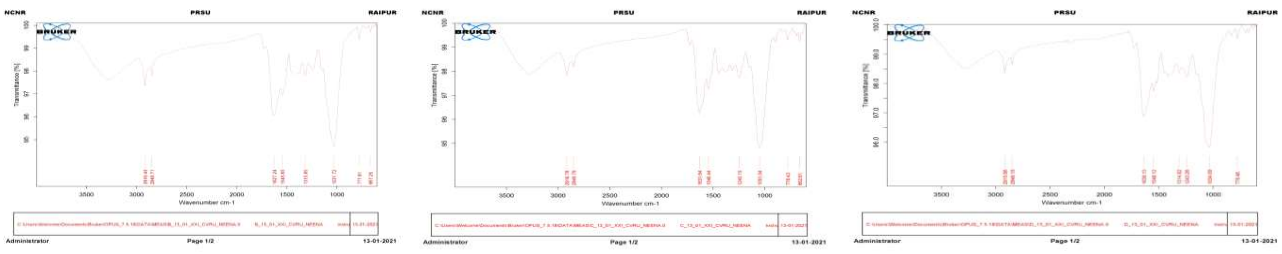

Fig. 1. FTIR of *Bahunia variegata, Cassia fistula and Dalbergia sissoo* (leaf)

the sample in three stages. Initial weight of the sample taken was 6.1520 mg. In TGA graph the initial decomposition of the biomass occurred at onset temperature of 49.69 °C to eliminate the moisture content and the volatile matter present in the biomass and its end set is 95.91°C. In this first step 89.4221% of residue remains and loss of 0.6508 mg of biomass occurred. In the second step 3.017 mg of biomass has decomposed and 40.3811% of residue remains in which onset temperature is 251.34°C and end set temperature is 320.60°C. In the third step 1.5053 mg of decomposition of biomass (carbon content) took place between onset 463.19°C and end set 489.09°C in which residue is 15.9119%. After that the remaining is the ash component.

Similarly the leaves of *Cassia fistula* show the decomposition of the sample in different stages. In TGA graph the initial decomposition of the biomass occurred at onset temperature of 46.69 °C to eliminate the moisture content and the volatile matter present in the biomass and its end set is 95.30°C. In this first step 90.88% of residue remains and loss of 0.602 mg of biomass occurred. In the second step highest decomposition of 3.05 mg of biomass has occurred and 45.09% of residue remains in which onset temperature is 237.47°C and end set temperature is 322.93°C. In the third step 2.36 mg of biomass decomposed and remains 0.64 mg. Residue is 9.55% in which onset is 458.73° C and end set 497.91°C. After that the remaining is the ash component.

Thermo gravimetric analysis of *Dalbergia sissoo*, depicts the loss of weight of the sample in different stages (Fig. 2). In TGA graph the initial decomposition of the biomass occurred at onset temperature of 44.46 °C to eliminate the moisture content and volatile matter present in the biomass and its end set is 95.38°C. In this first step 89.9632% of residue remains and loss of 0.497 mg of biomass occurred. In the second step, highest decomposition of 2.6355 mg of biomass has occurred and 36.7424% of residue remains in which onset temperature is 237.64 °C and end set temperature is 328.12 °C. In the third step decomposition of 1.2071 mg of biomass (carbon content) has occurred between onset 454.03 °C and end set 487.51°C in which residue is 12.3674%. The remaining is the ash component.

The curve of weight loss gives information about the thermal stability of the sample, changes in the sample composition and kinetic parameters for chemical reaction. Also it is useful for quality control and identification. Moreover

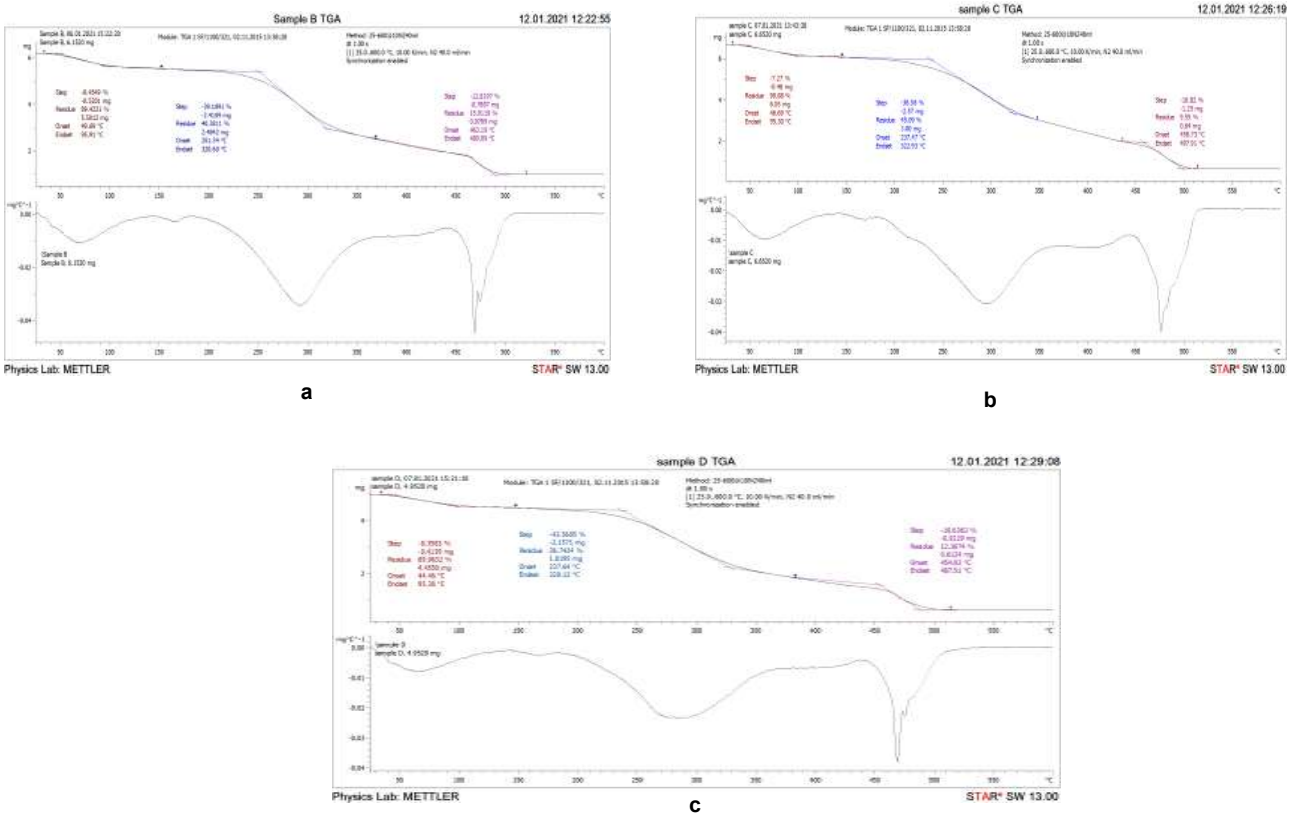

Fig. 2. Graph between weight and temperature to show the decomposition rate of a. *Bahunia variegata,* b. *Cassia fistula and* c. *Dalbergia sissoo* (leaf)

the estimated lifetime, oxidative stability, decomposition and rate of reaction could be understood. At the initial stage, due to the loss of moisture, weight of the sample is reduced. As the temperature increases further, the sample weight loss occurs due to the decomposition of organic matter and polymer decomposition. The most apparent point of weight loss of the sample can be done with the help of a derivative weight loss curve.

Scanning Electron Microscopy **(**SEM) provides high resolution images of the sample by a focused electron beam across the surface and detects the backscattered electron signal. The surface characteristics of the particles play a very critical role in the field of pharmaceuticals. The surface morphology of the particles derived from *Bahunia variegata, Cassia fistula and Dalbergia sissoo* leaves (Fig. 3) shows some roughness, grooves and pores. SEM has been used to obtain physicochemical characteristics, such as the particle size, crystalline form, roughness and pores which play an important role in the dissolution rate and bioavailability of a pharmaceutical formulation (Silva et al 2018).

The weight and atomic percentage of some elements found in *Bahunia variegata, Cassia fistula and Dalbergia sissoo* obtained from EDS are given in Table 3. It is a known fact that metals and minerals in the permissible level play very important role in the biological system of plants and animals. Carbon, oxygen, hydrogen and nitrogen are the major constituents of tissues in humans. Ca, Mg, Na, K, P, Cl and S are nutritionally important elements. Fe is an essential component of hemoglobin, myoglobin and cytochrome. (Prashant et al 2015). Ca is necessary for permeability of membrane, transmission of nerve impulses, muscle contraction etc. Copper plays very important role in our metabolism as it helps enzymes to function properly. (Birma 2018). Potassium and sodium are semi major elements which exist in the ionic state and maintain osmotic pressure and membrane potential. Silicon is beneficial for normal development of connective tissue and skeletal health (Uribe et al 2020).

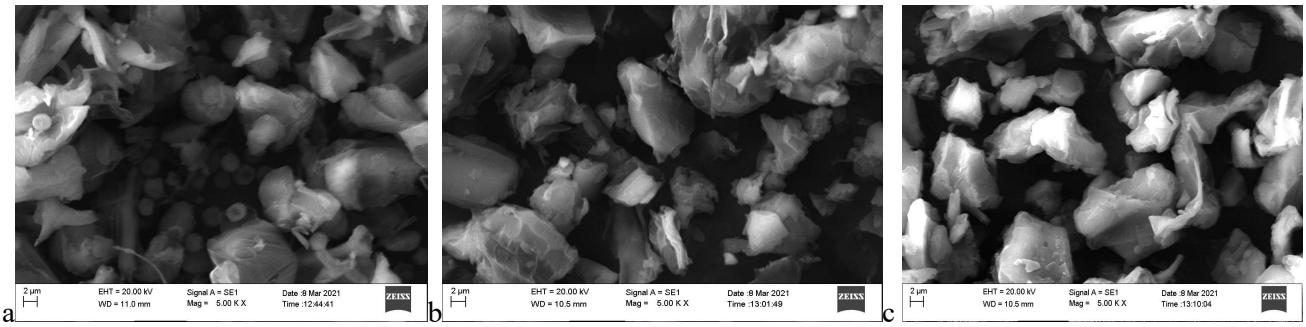

Fig. 3. Monograph of the particle of a. *Bahunia variegata*, *b. Cassia fistula* and *c. Dalbergia sissoo* leaves using scanning electron microscope of a 500K X

Table 3. Elemental content of *Bahunia variegata, Cassia fistula and Dalbergia sissoo* leaves

Element	*Bahunia variegata* (%)		*Cassia fistula* (%)		*Dalbergia sissoo* (%)	
	Weight	Atomic	Weight	Atomic	Weight	Atomic
Carbon (C)	18.04	23.94	23.68	30.18	21.35	27.60
Nitrogen (N)	5.48	6.24	1.33	1.46	2.83	3.14
Oxygen (O)	65.41	65.16	68.78	65.80	67.76	65.79
Sodium (Na)	0.01	0.01	-	-	-	-
Magnesium (Mg)	0.84	0.55	0.43	0.27	0.78	0.50
Silicon (Si)	1.12	0.64	0.46	0.25	0.60	0.33
Chlorine (Cl)	-	-	-	-	0.59	0.26
Potassium (K)	1.74	0.71	2.20	0.86	2.48	0.98
Calcium (Ca)	5.57	2.22	2.87	1.10	2.97	1.15
Iron (Fe)	0.74	0.21	0.17	0.05	0.30	0.08
Sulphur (S)	0.30	0.15	0.07	0.03	0.34	0.16
Copper (Cu)	0.74	0.18	-	-	-	-
Total	100	100	100	100	100	100

CONCLUSION

The uses of SEM, EDS, TGA, FTIR, Proximate analysis have gained a wide interest and importance within the pharmaceutical industries for testing of raw material, process monitoring and quality control of the product. It also provides us detailed information of the sample, its authenticity and the wide applicability of the instrumental techniques. FTIR spectrum was used to identify the functional group of the active component and due to the presence of the above functional groups found in the medicinal plants, it might be helpful for treatment of diseases. With the help of analysis of TGA, thermal stability of the plant, oxidation, moisture, volatile content of materials, loss of moisture, drying, corrosion and desorption of the material could be studied which are pharmacologically important. The presence of phytochemicals directly influences the quality of secondary metabolites and they can also serve as active constituents of herbal medicines. Proximate analysis is helpful for the identification of genuineness which plays key role in authentication of plant such as the ash value shows the qualitative standards and purity of the sample. In this study higher ash value shows higher mineral content whereas high carbon content shows high calorific value in the leaves of *Bahunia variegata, Cassia fistula and Dalbergia sissoo.* The multiple benefits of these medicinal plants are miracles of nature. A systematic study is required for identification, cataloguing and documentation of plants that gives a meaningful direction for the promotion of our traditional knowledge of herbal medicinal plant. Numerous studies have been conducted on these plants but the above data were missing and hence it may be concluded that the data obtained could be useful for the discovery of novel herbal drugs to treat various diseases of animals as well as human beings. It may also be helpful for further studies that are needed in this direction to explore more pharmacological actions of these plants.

REFERENCES

Adhikari PP and Paul SB 2018. History of Indian traditional medicine: A medical inheritance. *Asian Journal of Pharmaceutical and Clinic Research* **11**(1): 421-426.

Anand Utpal NJH 2019. A comprehensive review on medicinal plants as antimicrobial therapeutics: Potential avenues of biocompatible drug discovery. *Southern Illinois University Carbondale* **9**(11): 258.

Aziz MMA, Ashour AS and Melad ASG 2019. A review on saponins from medicinal plants: chemistry, isolation, and determination. *Journal of Nano medicine Research* **7**(4): 282-288.

Bijauliya RK, Jain SK, Alok S, Dixit VK, Singh D and Singh M 2017. *Dalbergia* sissoo Linn.: An overview morphology, phytochemistry and pharmacology. *International Journal of Pharmaceutical Sciences and Research* **8**(4): 1522-1533.

Birma Eid I 2018. Levels of essential elements in different medicinal plants determined by using inductively coupled plasma mass spectrometry. *Journal of Analytical Methods in Chemistry.* Volume 2018, Article ID 7264892, 6 pages. https://doi.org/10.1155/2018/7264892.

Harrold Marc W and Zavod Robin M 2018. *Basic concepts in medicinal chemistry*. Edition 2: Chapter- 2, American Society of Health-System Pharmacists, p 21-66.

Kathiresan Prabhu, Kakar PK, Shiva Hemlata, Kathiresan P and Ghatuary SK 2011. A comparative study on proximate analysis conducted on three Viburnum Linn. Species. *DEr Pharmacia Sinica* **2**(3): 200-206.

Khare P, Kishore K and Sharma DK 2018. Historical aspects, Medicial uses, phytochemistry and pharmacological review of *Bahunia variegata*. *Asian Journal of Pharmacy and Pharmacology* 4(5): 546-562.

Mandloi R, Solanki P, Chauhan R and Baviskar M 2018. Phytochemical Screening of *Cassia fistula* Bark and Leaves Ethanolic Extracts and FTIR analysis. *International Journal for Research Trends and Innovation* **3**(1): ISSN: 2456-3315.

Mathai RV, Mitra JC and Sar SK 2021. Quantitative analysis of elements in some efficacious medicinal plants by using ICPMS and IRMS method. *Indian Journal of Ecology* **48**(4): 1068-1074.

Mohiuddin AK 2019. Medicinal and Therapeutic values of *Sesbania grandiflora*. *Journal of Pharmacology and Clinical trials* 2019 (1) Short Communication.

Mownika S, Sharmila S and Ramya EK 2021. Documentation of ethno medicinal plants used for treating rheumatoid arthritis disorder by aboriginal communities of Manar beat, Karamadai Range, Western Ghats, India. *Indian Journal of Ecology* **48**(1): 78-85.

Nariyal V and Sharma P 2017. Kachnar (*Bahunia variegata*) as a medicinal herb: A systematic review. *International Journal of Advance Research* **5**(9): 587-591.

Prashant L, Kattapagari KK, Chitturi RT, Reddy VR and Prasad LK 2015. A review on role of essential trace elements in health and disease. *Journal of Dr, NTR University of Health Sciences* **4**(2): 75-85.

Pye CR, Bertin Lokey JM, Gerwick SR, Linington RG and Retrospec HW 2017. Retrospective analysis of natural products provides insights for future discovery trends. *Proc. Natl. Acad. Sci.* USA 114, 5601–5606

Silva Michelli dos Santos, Gonring Karla Loriatto, Ricky Cassio Santos da Silva, Fonseca Matheus Cecilio, Borges Marcella Matos Cordiro 2018. Fourier transform infrared spectroscopy, thermogravimetric analysis, scanning electron microscopy as supporting tools in quality control of antiparasitics. *Quim. Nova* **41**(3): 258-267.

Uribe P, Johansonsson A, Jugdaohsingh R, Powell Jonathan J, Magnusson C, Davila M, Westerlund A and Ransjo M 2020. Soluble silica stimulates osteogenic differentiation and gap junction communication in human dental follicle cells. *Scientific Reports*. https: //doi.org/10.1038/s41598-020-66939-1.

Received 06 June, 2021; Accepted 12 November, 2021

Indian Journal of Ecology (2021) 48(6): 1772-1779

Manuscript Number: 3447
NAAS Rating: 5.79

Generation of Paddy Straw Composts in Rice Based Integrated Farming System and Evaluating in Organic Production of Fodder Maize

K.V. Athira, B. Sudha[1*], Jacob John[1], Shalini Pillai P and R.V. Manju

College of Agriculture, Kerala Agricultural University Vellayani-695 522, India
[1]Integrated Farming System Research Station (IFSRS), Karamana-695 002, India
**E-mail: sudha.b@kau.in*

Abstract: The experiment was carried out in a rice based integrated farming system (IFS) at the Integrated Farming System Research Station, Kerala Agricultural University (KAU), Thiruvananthapuram, India in establishing the potential of IFS in supporting organic crop nutrition. In this study, nutrient rich composts were generated from discarded paddy straw by way of co-composting using organic inputs *viz.*, cow dung, goat manure and poultry manure generated from livestock components within farm. These composts were evaluated for major properties and were utilized for organic nutrition of test crop Fodder Maize grown as summer crop in paddy field. Nutrient rich compost generated by co composting paddy straw with goat manure and poultry manure (4:1:1 on volume basis) when used in organic nutrition of fodder maize, could produce higher and comparable yields as that with the KAU recommended integrated nutrient management practice. Two other composts (generated from paddy straw: cow dung : goat manure ; paddy straw: cow dung : poultry manure in the ratio 4:1:1 on volume basis) also produced quality composts and could register comparable growth and yield of fodder maize as that with the recommended nutrient management. Status of major soil nutrients N, P and K after the harvest of test crop was improved under organic crop nutrition using the above mentioned composts. The study therefore highlights the potential of IFS in ensuring bio recycling within farms for supporting organic crop production, registering higher crop yields and improving the soil nutrient status.

Keywords: Fodder maize, Organic nutrition, Paddy straw compost, Growth, Yield, Crude Protein

The input intensive farming practices are mostly associated with environmental degradation and there is an urgent thrust for ecofriendly farming practices. Organic farming as an ecofriendly farming technique and its diverse benefits especially on long term maintenance of soil health are well established (Bhatia et al 2016). Integrated farming systems which combine agriculture with allied enterprises mostly dairying well support organic farming through generation of considerable quantities of organic resources recyclable as quality organic manures for crop nourishment (Sudha et al 2020). Livestock especially dairy is an integral component of IFS. High cost of concentrate cattle feeds is a major constraint contributing to escalated cost of production rendering dairy farming a non-economic activity. This necessitates generation of adequate quantities of green fodder within farms. Among different fodder crops, fodder maize is much important owing to its higher production potential, wider adaptability, quick growing nature, succulence, palatability and excellent fodder quality. Most important is that being a short duration crop, it can also fit well in different cropping systems. Onte et al (2019) have detailed the favourable impacts of organic nutrition on fodder yield and soil quality.

Rice based IFS generate large quantities of crop residues mainly straw. Though straw is quite useful as dry fodder, a large fraction of straw goes waste as a result of improper storage and drying. Harvest during rainy season limits the chances of spreading and drying of straw resulting in mouldy growth, considerably reducing its feed value. This straw unfit as feed material is often discarded as bio waste in fields. With the increasing trend towards organic farming, recycling of all such organic resources generated in a farm assumes greater importance. Rice straw owing to its bulky volume, slow decomposition and short term negative effect of nitrogen immobilization is difficult to be recycled as such to soils (Buresh and Sayre 2007). Wide C: N ratio, high lignin (11-24%) and silica (7-20%) content makes degradation of rice straw a difficult process (Kumar et al 2008, Hu et al 2016). Composting of straw is an alternate option to recycle the nutrients contained in it. With improved composting technologies, the prospects of nutrient recycling from rice straw are immense. Co-composting with nitrogen rich organic inputs is a proven technology in generating nutrient rich manures from rice straw (George 2019). Especially in an IFS, the dung and droppings obtained from livestock mainly cow dung, goat manure, poultry manure etc and green leaf

manures like glyricidia could be utilized as nitrogen sources for co-composting in generating quality inputs in support of organic crop production. This in turn will lead to favourable impacts on soil health in the long run. Based on the above, an experiment was carried out at Kerala Agricultural University, India in generating nutrient rich composts through co-composting of paddy straw (discarded as agro waste in field) along with organic inputs viz., cow dung, goat manure, poultry manure etc generated in IFS. Further, these composts were utilized for organic nutrition of fodder maize grown as summer crop in paddy field. The study recorded the effects of organic nutrition using different paddy straw composts on the growth, yield and quality aspects of fodder maize apart from changes in soil properties.

MATERIAL AND METHODS

The experiment was carried out at the Integrated Farming System Research Station, Kerala Agricultural University (KAU), Karamana, Thiruvananthapuram, Kerala located at 8 28' 25"N Latitude and 76 57 '32"E Longitude. The experimental site was lowland (5 m above mean sea level).

Generation of paddy straw composts: The experiment on generation of paddy straw composts was laid out in completely randomised design with 8 treatments and three replications. Different paddy straw composts generated in the experiment (July-November 2019) through co-composting (Table 1). Their major chemical properties and major and micro nutrient status are listed in Table 2, 3. Partially shredded rice straw of variety *Uma* obtained from rice harvest at IFSRS, Karamana and stored for one month was used for compost preparation. Rice straw was uniformly sprinkled with water and was turned and kept overnight. Further, it was mixed with different organic manures in 4:1 or 4:1:1 ratios (on volume basis) and was filled in concrete pits of size 1 m^3 as per the treatments (Table 1). Sufficient moisture levels were maintained in the composting material by periodic sprinkling of water. The materials were turned twice a week to ensure aeration and uniform decomposition. Maturity of composts was determined initially based on visual observation and then confirmed upon C: N ratio narrowed down to less than 20:1 2016). Mature composts were sieved, shade dried and stored and were used for field evaluation.

Samples obtained from each treatment on maturity were mixed with water in the ratio 1:5 and pH were measured using pH meter with glass electrode (Jackson 1973). Compost - water solution used for determination of pH was again used for estimating electrical conductivity (EC) using conductivity meter (Jackson, 1973). The carbon content of compost samples was determined using weight loss on ignition method (FAI, 2017) and total N content using microkjeldhal method (Jackson, 1973). The ratio of carbon to total nitrogen was worked out and expressed as C: N ratio. Composts were also analysed for major nutrients P (Nitric - perchloric acid digestion (9:4) and spectrophotometry using Vanadomolybdate phosphoric yellow colour method) and K(Nitric-perchloric acid digestion (9:4) and flame photometry) and micronutrients Fe, Cu, Mn, Zn (Nitric-perchloric acid digestion (9:4) and Atomic Absorption Spectrophotometry (Jackson 1973) and B using Spectrophotometer-Azomethane-H method (Roig et al1996).

Field experiment: The field experiment on evaluation of paddy straw composts was laid out in randomised block design with 8 treatments and three replications. FYM @ 10 t ha^{-1} was applied as basal organic dose uniformly for all the treatments. In treatment T_8, soil test data based application of chemical fertilizers as per KAU recommendation (120: 60: 40 kg ha^{-1}) was followed apart from the basal dose. In treatments T_1 to T_7, crop nutrition using composts 1 to 7 respectively generated in the composting trial were used for crop nourishment. These were supplied on N equivalent basis to substitute the recommended inorganic N requirement and were sufficient to meet the P and K requirements as well.

Table 1. Co - composting of organic resources to generate paddy straw composts

Treatment	Co- composting technique
T_1	Rice straw + cow dung (4:1)
T_2	Rice straw + goat manure (4:1)
T_3	Rice straw + poultry manure (4:1)
T_4	Rice straw + cow dung + goat manure (4:1:1)
T_5	Rice straw + cow dung + poultry manure (4:1:1)
T_6	Rice straw + goat manure + poultry manure (4:1:1)
T_7	Rice straw + cow dung + glyricidia leaves (4:1:1)
T_8	Natural composting (Rice straw alone as control)

* Paddy straw and organic manures mixed in volume basis (v:v)

Table 2. Different paddy straw composts generated and their major properties

Treatments	C:N ratio	pH	EC
T_1	12.90	8.08	0.80
T_2	11.43	8.16	0.80
T_3	11.69	7.83	0.77
T_4	10.67	8.03	0.67
T_5	10.69	7.78	0.73
T_6	10.23	7.78	0.63
T_7	11.16	7.98	0.67
T_8	19.50	8.04	0.90
CD (p = 0.05)	0.79	NS	NS

The soil type of the experimental site was riverine alluvium of sandy clay loam texture and was moderately acidic (5.9), with normal electrical conductivity (0.24 dS m^{-1}) and high organic carbon (1.7%). Available N was low (259 kg ha^{-1}), P high (32 kg ha^{-1}) and available K was medium (125 kg ha^{-1}). Fodder maize (variety *African Tall*) was the test crop and the experiment was carried out in summer rice fallows (01-03-2020 to 09- 05-2020). The plot size was 3m x 3m. Healthy seeds of African tall were dibbled at 5-6 cm depth with 2 seeds per hole at a spacing of 30 cm between rows and 15 cm between plants. Harvesting was done at 70 DAS at lush green stage of crop.

Observations on growth parameters viz., plant height, leaf number and dry matter production were periodically recorded. Uprooted plant samples were first sundried and then oven dried at 65^0c till attainment of constant weight and the dry matter production was worked out in kg ha^{-1}. Physiological attributes contributing to growth and yield including Leaf Area Index/LAI (Watson 1947), Spad Chlorophyll Meter Reading (SCMR), a measure of chlorophyll content (using chlorophyll meter SPAD 502 plus) etc were also recorded. Uptake of major nutrient N (N content in plant x DMP) was worked out in kg ha^{-1}. The crude protein content in forage, an important quality parameter was worked out as the product of N content of plant sample and a constant factor 6.25 (Simpson et al 1965).

RESULTS AND DISCUSSION

Properties of paddy straw composts (C:N ratio, pH and EC): Different properties of paddy straw composts viz., C:N ratio, pH and EC were estimated (Table 2). The C: N ratio of all the composts was within the acceptable limit of 20:1. Favourably lower C: N ratio was r with T_6 (10.23) and it was comparable with T_5 and T_4. Natural composting of rice straw without addition of any organic manure/nitrogen source recorded wider C: N ratio of 19.5. The pH of all the paddy straw composts generated through co- composting with different organic manures showed no significant difference and was in slightly alkaline range. EC values also showed non-significant difference among treatments and were in the normal range. The initial C: N ratio of the partially shredded paddy straw used for composting was 39: 1. Reduction in C: N ratio is considered as a criterion of maturity of compost. Lowering of C: N ratio of paddy straw by the addition of animal manures is a reliable composting method to generate quality compost (Cayuela et al 2009). C: N ratio of paddy straw used for co-composting was considerably narrowed down in the end product. This could be related with the fact that during co-composting, carbon is used up as an energy source for microbial metabolism and the intense microbial activity results in a decrease in carbon content of the composting material. Simultaneous addition of N rich organic manures increases the N level as well as the activity of N fixing bacteria (Raj and Antil 2011). Because of these reasons C: N ratio narrows down. Paddy straw co-composted with goat manure and poultry manure in the ratio 4:1:1 (T_6) registering a lower C: N ratio comparable to treatments $T_4$and T_5 could be related with the higher N content of these organic manures - goat manure (3.75 %), poultry manure (2.57%) and cow dung (1.45 %) as ascertained from initial analysis of manures. George, (2019) also observed that paddy straw compost with a narrow C: N ratio (10.32) could be obtained by co-composting paddy straw with two organic sources *viz*., poultry manure and cow dung. The wider C: N ratio recorded with natural composting (T_8) could be attributed to the non-addition of N sources**.** Microbial proliferation and nitrogen enrichment might have been less under this treatment**.**

Nutrient Status of Composts

Major nutrients: Co-composting using different organic manures as nitrogen source could significantly influence the

Table 3. Major and micro nutrient content of the different paddy straw composts

Treatments	Major nutrients (%)			Micronutrients (mg kg^{-1})				
	N	P	K	Fe	Cu	Mn	Zn	B
T_1	2.59	0.55	2.39	1239.83	18.17	447.08	148.47	14.10
T_2	2.88	0.73	2.60	1299.50	19.62	645.73	161.50	16.83
T_3	2.78	0.79	2.45	1875.17	22.52	834.17	177.40	17.63
T_4	3.04	0.89	2.94	3031.83	31.90	908.75	244.85	17.93
T_5	2.99	0.93	2.86	3187.00	35.25	1053.75	244.67	18.77
T_6	3.30	0.98	3.22	3201.66	45.58	1096.17	280.40	19.97
T_7	2.93	0.82	3.00	1788.33	24.48	900.00	211.85	17.53
T_8	1.20	0.35	1.95	807.16	12.65	413.75	43.10	12.97
CD (p = 0.05)	0.23	0.09	0.16	778.87	8.45	177.16	71.19	0.90

total N, P and K content of rice straw composts. Rice straw co-composted with goat manure and poultry manure in the ratio 4:1:1 on volume basis (T_6) had the maximum content of major nutrients (Table 3).This treatment recorded the highest N content of 3.30 per cent and was statistically on par with treatments T_4 (3.04 %) and T_5 (2.99 %). Considerable enhancement in the content of N was thus noticed as compared to that of paddy straw (0.22%) used for composting. Concentrations of primary nutrient P in rice straw composts also were well above the initial content (0.15 %) in rice straw. With nitrogen, T_6 recorded the highest P content (0.98 %) and was comparable to T_5 (0.93 %) and T_4 (0.88 %). Significantly higher potassium content of 3.22 per cent was recorded with treatment T_6 and was comparable to T_7 (3.00 %) *i.e*., co-composting of rice straw with cow dung and glyricidia leaves. The initial potassium content of rice straw was 1.38 per cent. The compost generated with goat manure and poultry manure as N sources (T_6) recorded significantly higher N and P contents, which could be related with the higher N and P content of these two manures over cow dung. Naturally, when used as organic sources in composting, these manures enriched the N and P content of final product. The N and P contents of goat manure were respectively 3.75 and 0.34 per cent and that of poultry manure were 2.57 and 0.24 per cent as ascertained from initial analysis of manures. Cow dung had lower N, P contents of 1.45 and 0.2 per cent respectively. Higher and comparable N content recorded with treatments T_4 and T_5 could be related with the fact that goat manure /poultry manure were included as one of the nitrogen sources along with cow dung. These results are in conformity with Qian et al (2014) and Sanusi et al (2018) who obtained composts having higher nutrient content through co composting rice straw with goat manure and poultry manure.

The total K content was found to be higher for treatment T_6(3.22 %), but comparable to T_7(3.00 %) *i.e.,* co-composting of rice straw with cow dung and glyricidia leaves in 4:1:1 ratio on volume basis. Higher K content registered in composts T_6 and T_7 could be attributed to the richness of K in goat manure (1.22%), poultry manure (0.95 %) and glyricidia leaves (1.18%). Apart from the abovementioned enriching effect, these manures might have contributed to the buildup of microbial organisms thereby enhancing mineralization of K from the composting substrate. Shak et al. (2014) also observed the beneficial effects of K enrichment of composts on co-composting of rice straw with goat manure and poultry manure. Daphal (2018) reported similar enhancement in potassium content on co composting wheat straw with glyricidia leaves. Treatment T_8 *i.e.* paddy straw compost generated through natural composting recorded significantly lower N (1.2 %) P (0.35 %) and K (1.95%) contents compared to other composts. This could be attributed to the non-addition of organic manures to paddy straw resulting in lesser enrichment of nutrients. Similar to this result, Chan et al (2016) reported that the non-addition of organic manures to carbon rich composting substrates resulted in low nutrient composts attributed to lower microbial activity and hence less mineralization of N.

Micronutrients: Paddy straw samples at the start of experiment contained micronutrients viz., Fe (262.75 mg kg^{-1}), Cu (27.10 mg kg^{-1}), Mn (637.10 mg kg^{-1}), Zn (31.10 mg kg^{-1}) and B (4.24 mg kg^{-1}). Statistical analysis of the data generated on the content of micronutrients in different paddy straw composts revealed that co-composting methods had a significant influence on the content of all these micronutrients. Treatment T_6 (paddy straw co-composted with goat manure and poultry manure in the ratio 4:1:1 on volume basis) had a distinct advantage with regard to content of micronutrients Fe (3201.66 mg kg^{-1}), Cu (45.58 mg kg^{-1}), Mn ((1096.17 mg kg^{-1}), Zn ((280.40 mg kg^{-1}), B content (19.97 mg kg^{-1}) comparable or closely followed by treatments T_5 and T_4. Organic manures like goat manure and poultry manure are rich in plant nutrients including micronutrients (Aziza and Averbeke, 2010) and when co-composted with paddy straw could enhance the content of micronutrients in the final product Also, the N rich nature of these composts could have resulted in flourishing of microbes which could accelerate the rate of mineralization of nutrients from the composting substratum (Jusoh et al 2013). T_8 (natural composting of rice straw) registered lower content of micronutrients and was comparable to $T_1$and T_2mostly. Fe content was much low with T_8 and was on par with T_1) and T_2). Similarly, Cu content was lower for T_8 comparable to T_1 and T_2.T_8 also registered lower Mn content, comparable to T_1. Significantly lowest Zn and B contents were also with T_8

Growth Attributes of Fodder Maize as Influenced by Different Paddy Straw Composts

Plant height, leaf count, dry matter production: Growth attributes including plant height, leaf number, dry matter production (DMP) etc were recorded at 40 days of sowing (DAS) and at harvest (Table 4). Plants nourished under INM (T_8), basal dose of FYM @ 10 t ha^{-1} and NPK fertilizers on soil test basis recorded enhancement in all the growth attributes in both the stages. Organic nutrition using paddy straw composts (Treatments T_6, T_4 and T_5) proved equally good as INM and recorded comparable plant heights, leaf count and DMP. It could be assumed that integrated nutrient management as provided by T_8 as well as organic nutrition using composts prepared under treatments T_6, T_4 and T_5were equally effective in well nourishing the crop. The composts

mentioned above had favourable C: N ratios (Table 2) and higher content of micronutrients (Table 3) in improving crop growth in terms of plant height and leaf count. Speedy mineralization of nutrients from these composts might have provided nutrients in time for better crop growth. Coupled with adequate micronutrients, this could provide a well-balanced nutrient package resulting in better growth. Borase et al (2018) reported improvement in growth attributes of fodder maize under supply of micronutrients Zn and B. The crop span was short (70 days) and a speedy mineralisation of nutrients could definitely influence crop growth (Alade et al 2019).

Higher and comparable DMP was recorded in T_8 and $T_6$and could be attributed to the enhancement in growth in terms of plant height and leaf count which naturally reflected in higher DMP. Taller plants with more leaves having increased photosynthetic area could produce more dry matter (Mahdi 2012) and an increase in dry matter accumulation in fodder maize under INM was reported by Bharat et al (2017). The results also suggest that certain paddy straw composts (T_1 and T_2) generated with less addition of organic manure (4:1), couldn't perform well as T_6, wherein organicmanures were added at higher rates (4:2). T_1 and T_2 had wider C: N ratios compared to T_6suggesting more time for nutrient mineralization. Also these composts had lesser content of micronutrients compared to T_6justifying their relatively poor performance in influencing growth attributes.

Leaf Area Index, SCMR, N uptake: LAI was significantly influenced by different treatments at 40 DAS and at harvest (Table 5). At 40 DAS, LAI was higher with treatment $T_8$and it was comparable to T_6 andT_4 and closely followed by T_5. LAI was lower and comparable in treatments T_1) at this stage. At harvest, LAI was significantly higher with T_8 and was comparable to treatments T_6, T_4 and T_5. Lowest leaf area index was recorded with T_1at harvest. Crop nutrition followed under different treatments could significantly influence the LAI of test crop at 40 DAS and at harvest. At both these stages, plants nourished under integrated nutrient management (T_8) recorded significantly higher LAI and it was comparable to T_6, T_4 and T_5which were based on organic nutrition using paddy straw composts. Elfeel and Abohssan (2016) also reported a similar observation. Performance of organic nutrition in a manner comparable to INM could be related with the narrower C: N ratios and higher content of micronutrients in the composts supplied (Table 2 and 3). A narrow C:N ratio suggests faster mineralization of plant nutrients thereby ensuring timely nutrient availability to crops resulting in improved growth. The higher micronutrient contents in these composts had a favourable influence on various physiological reactions within plants leading to better nutrient uptake and enhanced crop growth.

SCMR is a measure of greenness of the leaves and is related to the chlorophyll content which in turn decides photosynthesis and crop yield. Application of different paddy straw composts could produce a significant influence on the SCMR of fodder maize at 60 DAS (Table 5). At 60 DAS, significantly higher SCMR of 48.70 was with treatment T_8 (basal FYM, followed by application of chemical fertilizers) and it was on par with treatments $T_6$and T_4, followed by T_5. Significantly, lower SCMR of 37.08 was recorded in plants under T_1, comparable to T_3 and T_2.Integrated nutrient management (T_8) recording higher SCMR could be related with the higher nutrient availability to crops. It could be assumed that the higher micronutrient status of composts (Table 3) also helped in improving the chlorophyll content of crop. Among micronutrients - Fe, Mn and Zn play a significant role in influencing chlorophyll content. Fe has definite role in the biosynthesis of chlorophyll and its precursors, while Mn

Table 4. Effect of different paddy straw composts on major growth attributes of fodder maize

Treatments	Plant height (cm)		No. of leaves		DMP (kg ha^{-1})	
	20 DAS	40 DAS	20 DAS	40 DAS	40 DAS	At harvest
T_1	94.57	145.95	7.67	10.78	4196	9988
T_2	100.94	165.81	8.11	11.11	4370	10116
T_3	98.81	158.04	7.78	11.00	4230	10035
T_4	113.30	176.74	9.11	12.45	5133	13111
T_5	113.05	172.15	9.00	12.22	5001	13024
T_6	115.15	174.81	9.22	12.56	5243	13309
T_7	105.94	168.21	8.11	11.55	4898	11037
T_8	118.34	180.87	9.33	12.67	5393	13580
CD (p =0.05)	5.38	12.24	1.20	1.03	178	305

DMP – Dry Matter Production

and Zn support chlorophyll production through the activation of certain enzymes (James et al 2008)

Yield and crude protein content of fodder maize: Among different treatments, T_8 (basal dose of 10 t ha^{-1} of FYM followed by NPK fertilizers) registered higher yield of 35.56 t ha^{-1}(Table 5). Chopra et al (2016) and Narkhede and Khandare (2016) also reported enhancement in crop yield with INM. The yield obtained from T_8 was however comparable to organic treatments T_6, T_4, T_5 and T_7. These composts had narrower C: N ratio (Table 2) enabling faster mineralization of plant nutrients. This could especially benefit crops with shorter duration including the test crop fodder maize. The micronutrient content was more in compost supplied in treatments T_6, $T_4$and T_5(Table 2) which could have influenced the crop physiology in a better manner leading to better yield performance. In the present study, growth parameters including plant height, leaf number, dry matter production were significantly improved under treatments T_6, $T_4$and T_5(Table 4). The physiological parameters in support of crop growth including LAI and SCMR (Table 5) also recorded significant improvement under the above treatments. All these could be related with better crop growth leading to enhanced yields. Mithare et al (2019) reported that leaf area influences interception and utilization of solar radiation by crops which in turn could influence dry matter accumulation and ultimately fodder yield. Lower yields recorded under $T_1$and T_3could be well related with their lower nutrient content, especially micronutrients. These treatments, only one part of organic manure was added to four parts of cow dung and it could therefore be assumed that the microbial build up in these composts could have been less in influencing many enzymatic changes in soil that could lead to better nutrient release. Growth and physiological parameters recorded were also comparatively poor with regard to these treatments.

Crude protein content of fodder is well related with the N uptake of crop. Being a structural component of amino acids, nitrogen plays a direct role in protein synthesis thereby influencing the quality of fodder. Significantly higher crude protein content was recorded (Table 5) in the treatment T_8 based on INM principles and it was found comparable to T_6, T_4 and T_5 maintained under organic nutrition. The improvement in crude protein content could be attributed to the increased uptake of major nutrient N as observed for these treatments .Rice straw composts generated under T_6, $T_4$and T_5had higher amount of micronutrients *viz*., Fe, B and Zn (Table 6) which have a very important role to play in the uptake of major nutrients including N. Organic crop nutrition therefore performed in a good manner with regard to nutrient availability and uptake, comparable to the well balanced INM provided by T_8. Similar findings of improved crop performance with organic nutrition were reported by Black (2019).

Soil Properties of Cropped Field as Influenced by Organic Nutrition using Different Paddy Straw Composts

pH, organic carbon, available nutrients: The initial pH of the soil was 5.9 indicating that the soil was moderately acidic. After the experiment it ranged from 5.71 to 6.23. Maintenance of soil pH after the experiment could be attributed to the buffering action of organic manure applied as basal FYM and different paddy from 1.7 to 1.76 per cent, denoting the maintenance of organic matter in soil and no depletion of carbon reserves. In the case of organic carbon a very minor increase was observed, which could be attributed to the addition of carbonaceous organic inputs.

The available N status of the soil was 259.24 kg ha^{-1}. After the experiment it ranged from 267.33 kg $ha^{-1}$to 287.5 kg ha^{-1} suggesting no depletion but maintenance of soil N. The initial available P content of the soil was 32.26 kg ha^{-1}. After the experiment, P status in all the treatments were found

Table 5. Effect of different paddy straw composts on major physiological attributes supporting growth of fodder maize, uptake of nitrogen (kg ha^{-1}) yield and crude protein content of fodder maize

Treatments	LAI		SCMR	Uptake of N	Green fodder yield (t ha^{-1})	Crude protein (%)
	40 DAS	At harvest	At 60 DAS	At harvest		
T_1	2.02	5.03	37.08	275.0	29.89	7.94
T_2	2,53	5.31	40.49	271.11	31.05	8.08
T_3	2.23	5.26	39.12	275.33	29.94	8.00
T_4	3.36	5.76	45.09	283.33	32.67	8.17
T_5	3.25	5.71	44.84	283.33	32.23	8.11
T_6	3.45	5.88	46.12	287.50	33.11	8.19
T_7	2.81	5.32	41.10	279.17	32.20	8.08
T_8	3.67	5.91	48.70	267.33	33.56	8.26
CD (p =0.05)	0.35	0.20	3.84	NS	2.03	0.14

Table 6. Effect of different paddy straw composts on major soil properties of cropped field

Treatments	Major nutrients (%)			pH	OC (%)
	N	P	K		
T_1	275.00	29.19	129.57	5.92	1.76
T_2	271.11	30.86	129.70	6.20	1.75
T_3	275.33	31.69	129.63	5.86	1.75
T_4	283.33	33.56	132.08	5.91	1.74
T_5	283.33	32.53	131.38	6.05	1.74
T_6	287.50	34.19	132.42	5.93	1.73
T_7	279.17	31.69	131.98	6.23	1.72
T_8	267.33	30.02	121.83	5.71	1.70
CD (p = 0.05)	NS	0.67	0.43	NS	NS

maintained at higher levels denoting maintenance of soil P. Available P was the highest in T_6 comparable to T_4. Initially the soil had an available potassium content of 125.15 kg ha^{-1}. Potassium levels higher in comparison to initial status were observed in all the treatments except T_8 (121.83 kg ha^{-1}). Among different treatments, T_6 (rice straw co-composted with goat manure and poultry manure in the ratio 4:1:1) registered higher available potassium content of 132.42 kg ha^{-1} comparable to T_4 (132.08 kg ha^{-1}). It could thus be generalized that soil nutrient status in terms of major plant nutrients was replenished under organic nourishment attributed mainly to the slow release of nutrients from compost. It could also be assumed that flourishment of microbes under organic nutrition might also have contributed to soil buildup of available plant nutrients through mineralization reactions. Singh et al (2016) reported the beneficial effects on soil properties maintained under organic nutrition. In a similar study, Albert and Frimpong (2018) experimented with compost application in maize crop and confirmed slow release of nutrients thereby maintaining soil fertility.

CONCLUSION

The study suggests that organic recycling could efficiently be carried out in rice based integrated farming systems in support of organic nutrition of component crops. Crop residues like paddy straw which are difficult to be degraded could be converted to quality composts through co composting with organic manures like goat manure/poultry manure /cow dung generated in integrated farms. Livestock being an integral component of IFS, these recycled organic inputs could be utilized for organic nourishment of fodder crops like maize. Results of the study recorded that nutrient rich compost could be generated by co composting paddy straw with goat manure and poultry manure (4:1:1 on volume basis) and when used in organic nutrition of component crop fodder maize, could produce similar yields as compared to the recommended integrated nutrient management practice. Composts generated from paddy straw: cowdung: goat manure (4:1:1 on volume basis) and paddy straw: cowdung: poultry manure (4:1:1 on volume basis) also produced quality composts and could register comparable growth and yield of fodder maize as that with the recommended integrated nutrient management practice. The soil properties including nutrient status of the cropped field were also favourably maintained under organic nutrition. The study therefore emphasizes the potential of IFS in supporting organic nutrition and improving soil health.

REFERENCES

Alade AA, Azeez JO, Ajiboye GA, Adewuyi S, Olowoboko TB and Hussein SM 2019. Influence of animal manure on soil nitrogen indices and maize growth. *Russian Agricultural Sciences* **452**: 175-185.

Albert KM and Frimpong KA 2018. Biochar and/compost applications improve soil properties, growth and yield of maize grown in acidic rainforest and coastal savannah soils in Ghana. *International Journal of Agronomy* available at https://doi.org/10.1155/2018/6837404

Azeez JO and Averbeke VW 2010. Nitrogen mineralisation potential of three animal manures applied on a sandy clay loam soil. *Bioresource Technology* **10**: 5645-5651.

Bharath T, Vidyasagar GE, Rao VP, Reddy SN and Madhavi A 2017. Effect of INM on growth and physiological parameters of maize in maize-groundnut cropping system in southern Telangana region. *International Journal of Pure and Applied Bioscience* **5**(4): 418-424.

Bhatia R, Mehta SK, Godara AK, Mehta VP and Ghanghas BS 2016. Organic paddy cultivation in Haryana: Constraints analysis. *Indian Journal of Ecology* **43**(Special Issue-1): 78-82

Black B 2019. *The relationship between nutrients.*OMEX Agriculture Inc., Canada, p 80

Borase CL, Lomte DM, Thorat SD and Dhond AS 2018. Response of kharif maize (*Zea mays* L.) to micronutrients. *Journal of Pharmacology and Phytochem*istry **7**(3): 482-484.

Buresh R and Sayre K 2007. *Implications of straw removal on soil fertility and sustainability* **In**: APAARI (ed), Proceedings of *Expert Consultation on Biofuels*, August 27-29, 2007, IRRI, Los Banos, Philippines,pp. 34-44

Cayuela ML, Sinnico T and Mondini C 2009. Mineralization dynamics

and biochemical properties during initial decomposition of plant and animal residues in soil. *Applied Soil Ecology* **4**: 118-127.

Chan TM, Selvam A and Wong JWC 2016. Reducing nitrogen oss and salinity during 'struvite' food waste composting by zeolite amendment. *Bioresources Technol*ogy **200**: 838-844.

Chopra S, Samnotra RK, Kumar M and Kumar S 2016. Integrated nutrient management practices influencing the productivity of potato under subtropical plains of Jammu, India. *Indian Journal of Ecology* **43**(Special issue 1): 428-431.

Daphal PN 2018. *Characterization of enriched compost prepared from different crop residues.* M.Sc. (Ag.) thesis, Dr. Panjabrao Deshmukh Krshi Vidyapeeth, Akola, India.

Elfeel AA and Abohassan RA 2016. Compost effects on leaf area index and seed production enhancement in an important arid land leguminous tree (*Acacia tortilis* subsp. raddiana). *Legume Res*earch **39**(5): 748-754.

FAI [Fertilizer Association of India] 2017. *The Fertilizer (Control) Order, 1985.* The Fertilizer Associoation of India, New Delhi. p 305

George MA 2019. *Bio recycling of paddy straw for quality manure production*. M.Sc. (Ag.) thesis, Kerala Agricultural University, Thrissur, India

Hu Z, Lane R and Wen Z 2009. Composting clam processing wastes in a laboratory and pilot scale in vessel system. *Waste Management* **29**: 180-185.

Jackson ML 1973. *Soil Chemical. Analysis.* Prentice Hall of India Pvt. Ltd., New Delhi, India p 991

James RA, Von Caemmerer S, Condon, AT, Zwart AB and Munns R 2008. Genetic variation in tolerance to the osmotic stress component of salinity stress in drum wheat. *Functional Plant Biology* **35**: 111-123.

Jusoh MLC, Manaf LA and Latiff PA 2013. Composting of rice straw with effective microorganisms (EM) and its influence on compost quality. *Iranian Journal of Environmental Health Science and Engineering* **10**(17): 1-9.

Kumar A, Gaind S and Nain L 2008. Evaluation of thermophilic fungal consortium for paddy straw composting. *Biodegradation* **19**(3): 395-402.

Mahdi S, Hasan B and Singh L 2012. Influence of seed rate, nitrogen and zinc on fodder maize (*Zea mays*) in temperate conditions of western Himalayas. *Indian Journal of Agronomy* **57**: 85-88.

Manna MC, Subbarao A, Sahu A and Singh UB 2012. *Compost Handbook: Research-Production-Application*. Fertilizer Development and Consultation Organisation, New Delhi, India, p132

Mithare P, Biradar US, Jawarkar P, Vaishali M, Ashwini S, Kamlakar A and Karbari A 2019. Performance of different sources of livestock and poultry waste as organic manures on growth and yield of fodder maize (*Zea mays*). *International Journal of Current Microbiology and Applied Science* **8**(11): 2319-7706.

Narkhede WN and Khandare RN 2016. Evaluation of organic and integrated nutrient management on productivity, economics and soil health in soybean (*Glycine max*) onion (*Allium cepa*) Cropping sequence. *Indian Journal of Ecology* **43**(Special issue 1): 404-409

Onte S, Singh M, Meena VK, Kumar S, Meena BL and Dutta S 2019. Organic nutrient management in context to sustainable fodder production: A review. *International Journal of Current Microbiology and Applied Sci*ences **8**(9): 2434-2449

Qian X, Shen G, Wang Z, Guo C, Liu Y, Lei Z and Zhang Z 2014. Co-composting of livestock manure with rice straw: Characterization and establishment of maturity evaluation system. *Waste Manage*ment **34**: 530-535.

Raj D and Antil RS 2011. Evaluation of maturity and stability parameters of composts prepared from agro-industrial wastes. *Bioresources Technol*ogy **102**: 2868-2873.

Roig A, Lax A, Costa F, Cegarra J and Hernandez T 1996. The influence of organic materials on the physical and physico-chemical properties of soil. *Agriculture Mediterranean* **117**: 309-318.

Sanusi S, C'hng YH, Osman OS and Zain MN 2018. Production, characterization and phytotoxicity evaluation of compost produced from rice straw and goat manure slurry. *Research Journal of Applied Sciences* **13**(9): 559-567.

Shak KPY, Wu TY, Lim SL and Lee CA 2014. Sustainable reuse of rice residues as feedstocks in vermicomposting for organic fertilizer production. *Environmental Science and Pollution Research* **2**: 1349-1359.

Shyam C and Kaur S 2016. Crop residue management: A sustainable way to control weeds in rice. *Indian Journal of Ecology* **43**(Special issue 1): 83-87.

Singh S, Jhorar BS, Sheoran HS, Bhat MA, Dinesh and KS Grewal 2016. Prospects of long-term FYM application on physical properties of sandy loam soil under pearl millet-wheat rotation. *Indian Journal of Ecology* **43**(Special issue 1): 420-423.

Simpson JE , Adair CR, Kohler GO, Dowson EH, Donald HA, Kester EB and Klick JJ 1965. *Quality Evaluation Studies of Foreign and Domestic Rices*. USDA, USA. p 186.

Sudha B, John J, Meera AV and Sajeena A 2020. INM in rice based integrated farming system model for food security and enhanced productivity. *Indian Journal of Ecology* **47**(3): 630-633.

Vigneswaran S, Kandasamy J and Johir MAH 2016. Sustainable operation of composting solid waste management. *Procedia Environmental Sci*ences **35**: 408-415.

Watson DJ 1947. Comparative physiological studies in the growth of field crops: Variation in assimilation rate and leaf area between species and varieties and within and between years. *Annals of Botany* **11**: 41-76.

Received 09 June, 2021; Accepted 12 November, 2021

Indian Journal of Ecology (2021) 48(6): 1780-1788

Manuscript Number: 3448
NAAS Rating: 5.79

Antimicrobial Activity of Endophytic Microorganisms Isolated from *Allium Sativum*

U. Dutta, D. Khajuria and J.D. Bandral

Division of Microbiology, Division of FST, SKUAST-Jammu-180 009, India
E-mail: deepikakhajuria02@gmail.com

***Abstract*:** Endophytes are endosymbionts, may be fungus or bacteria, that live inside the plants without showing any disease symptomps. These microorganisms produced a plethora of chemical substances that is beneficial for the growth and development of their host. *Allium sativum* contain compound with antimicrobial, anticancer and antioxidant activity. In present study, 20 bacterial and 15 fungal endophytes were isolated from healthy leaves and bulbs of *Allium sativum* which were collected from different locations of Jammu. All isolates were screened for their antimicrobial activity against human pathogens *Pseudomonas aeruginosa* (MTCC741) and *Salmonella typhimurium* (MTCC98) and plant pathogens *Rhizactonia solani* and *Macrophomina phaseolina*. Out of 20 bacterial endophytes ALR-2, ALR-3 , ABC-6 and ABC-7 showed significant results against *S. typhi.* ALM-5 , ABC-6 and ABC-7 isolates showed significant results against *P.aeruginosa* whereas ALM-5 , ALG-9 , and ABC-6 , showed t against *R. solani*. Among fifteen fungal endophytes, the isolates ALFR-1, ALFG-3, ALFR-6, ABFM-6 and ABFR-8 showed best results against *P. aeruginosa*ALFG-3, ALFR-6, ABFM-6 and ABFR-8 isolates showed significant results against *S. typhi* whereas ALFR-1 (39.60%) and ABFR-8 (31.85%) significantly inhibit the mycelial growth of *Rhizactonia solani*. None of the bacterial and fungal endophyte showed antimicrobial activity against *M. phaseolina.* The effective bacterial isolates were identified on the basis of their morpho taxonomic and biochemical characteristics and the isolates identified belonged to *Pseudomonas* sp., *Bacillus* sp. and *Burkholderia* sp. whereas based on morpho taxonomic characteristic the effective fungal isolates were identified as *Alternaria* sp., *Aspergillus* sp. *Phoma* sp. *Cladosporium* sp. and *Fusarium* sp.

Keywords: *Allium sativum*, Endophytes, Human pathogens, Plant pathogens

India has a long tradition of using medicinal plants and herbal medicines to cure human illnesses. For the majority of our population in rural and tribal areas, medicinal plants are the only readily accessible health care option. Tribal life, tradition, and culture have remained nearly unchanged for hundreds of years. Traditional herbal medicines, which are used by various cultures, are effective in treating certain skin diseases. They are safe, reliable, and accessible and in many situations, they are the only choice for care drugs derived from the medicinal plant play an important role in the prevention and treatment of human diseases (Agarry et al 2005, Adhikari et al 2021) as they are cost effective, easily available and with negligible side effects and also a chief source of secondary metabolites. *Allium sativum* L. (garlic), belong to the family Amaryllidaceae, contains compounds with potent medicinal properties. India is the largest producer of garlic after China and produces 23,869.27 metric tons of garlic per year. Garlic is one of the most important plants in herbal medicine. Recent studies have shown the virtues of garlic in cancer prevention (Woo et al 2014). Some studies have also demonstrated its strong capacity to protect the cardiovascular system (Stabler et al 2012). Allicin is the most vital compound in the garlic having great antimicrobial and anti-oxidant properties. Other compounds like ajoene, alliin, etc are also present in the garlic and they have a great healing effect on our circulatory, digestive and immunological systems (Macphetson et al 2005). Medicinal property of any plant depends on the accumulation of endophytic microorganisms having metabolites bearing antimicrobial properties, in its different organs. Almost all vascular plant species examined to date were found to anchorage endophytic bacteria and fungi (Zhang et al 2006). In 1866, De Bary, first defined the endophytes as the organisms that colonize the internal plant tissue (Gr. *endon*, within; *phyton*, plant) and the first endophytic fungus was isolated from *Lolium persicum* (Persian darnel) and identified by Freemanin 1904. Endophytes are microorganisms that colonize living internal tissue of the plant without showing any disease symptoms. The bioactive metabolites present in the endophytes showed antimicrobial property against pathogenic microorganisms (Maria et al 2005). Madhaiyan et al (2004) observed that some endophytes shows increased resistance to human and plant pathogens thus making them ideal candidates for biological control. Other beneficial effects of endophytes to plants include nitrogen fixation (Barraquio et al 1997) increased drought resistance (Nowak et al 1995), thermal protection (Redman et al 2002), survival under osmotic stress (Creus et al 1998) and have potential to degrade several pollutants (Doty 2008).

MATERIAL AND METHODS

Collection of plant material: The medicinal plant used in this study was *Allium sativum,* which was collected from the four different locations of Jammu division namely Chatha, R.S Pura, Muthi and Gangyal. The samples were brought to the lab in perforated polythene bags and stored in refrigerator for further use.

Isolation of entophytes: Fresh samples of *Allium sativum* was taken for the isolation of endophytes. Samples (bulbs and leaves) were briefly washed under running tap water for 10 minutes and cut into 2-3 cm long pieces. Then these pieces were surface sterilized with 70% alcohol for 1 minute, 1.0% sodium hypochlorite (NaOCl) (v/v) for 1 minute and further cleaned by passing through two sets of sterile distilled water. The sterile samples were placed on plate containing Potato Dextrose Agar (PDA) media with 200 mgL^{-1} concentration of streptomycin to suppress the bacterial contamination in case of fungal endophytes and plates were incubated at 25±2℃ till the fungal mycelia start growing, whereas in case of bacterial endophytes, sterile samples were placed on Nutrient Agar (NA) media and incubated at 28±2°C till the bacteria start growing. The endophytic fungi and bacteria were transferred into fresh agar slants and stored at 4°C for the further studies. To confirm that the surface disinfection process was successful, sterility checks were conducted for each sample (bulbs and leaves) to monitor the effectiveness of the disinfection procedures. For these checks, 0.1 ml from the final rinse was plated out onto Petri plates of potato dextrose agar and nutrient agar. The absence of bacteria and fungi after 6 days of incubation during the sterility checks was taken to confirm sterility and confirm the isolated microbes were endophytic (Strobel etal 1996).

Test microorganisms: A total of four test microorganism counting two human pathogens such as *Pseudomonas aeruginosa* (MTCC741) and *Salmonella typhimurium* (MTCC98) were procured from IMTECH-Chandigarh, India and two plant pathogens such as *Rhizactonia solani* and *Macrophomina phaseolina* were taken from Division of Plant Pathology, SKUAST-J, Chatha, Jammu.

Standardisation of test microorganisms: To standardized the test microorganism, 0.5 Mc Farland standard was used as reference to adjust the turbidity of microbial suspension so that their number will be within a given range. The microbial suspensions were prepared in nutrient broth and are compared either visually or by measuring the absorbance with 0.5 Mc Farland standard which gives approximate cell density of 1.5 x 108 CFU/ml, having absorbance of 0.132 at wavelength of 600 nm(Andrews 2001).

Antimicrobial property of isolated endophytes: Antimicrobial properties of isolated endophytes (fungi / bacteria) were performed on the basis of following methods:

Agar well diffusion method: Screening of bacterial endophytes against test microorganisms was done by using Agar well diffusion method given by Perez et al (1990). The bacterial endophytes were grown in nutrient broth for 24 hours and then centrifuged at 8000rpm for 5 minutes for supernatant of bacterial endophyte. Molten Nutrient Agar (NA) media was poured into Petri plates and allowed to set. A sterile swab was used to evenly distribute human and plant pathogenic culture over the NA medium. The plates were allowed to dry for 15 minutes. Four wells were created using 6mm cork borer. Then in the wells supernatant of endophytic bacteria was added with the help of micropippete and incubated at 37±2°C for human pathogens and 28±2°C for plant pathogens for overnight and zones of inhibition were recorded with the help of scale.

Disc diffusion method: Antimicrobial activity of fungal endophytes against human pathogens was performed by using Disc diffusion method given by (Zhang et al 2009). The Petri dishes containing Nutrient Agar media for the growth of bacteria was prepared and 100 µL of human pathogenic culture was spread over the surface of the agar media using sterile cotton swab. Nine-millimeter diameter of actively growing fungal culture discs from PDA plates were cut using a sterile cork borer and placed on the surface of the nutrient agar media seeded with test bacteria. These plates were sealed with parafilm and kept in refrigerator at 4°C for 12 hours for complete diffusion of antimicrobial compounds, thereafter they were incubated at 37±2°C for next 12 hours. After incubation the diameter of the inhibition zone was measured in millimeter by using scale.

Dual culture method: Antimicrobial activity of fungal endophytes against plant pathogens was done by using dual culture method (Li et al 2003). In this method, the Petri dishes were poured with potato dextrose agar medium (PDA). 6mm disc of plant pathogen was cut with the help of cork borer and placed 1cm away from the edge on the one side of the plate and on the other side of the plate six mm disc of fungal endophyte was placed. A plate inoculated with plant pathogen served as control. Three replicates of control and treated plates were used and then all plates were sealed with parafilm and kept at 25±2°C for 3-5 days. The mycelial growth of inhibition was recorded using formula:

$$I = 100 \times (C-T)C^{-1}$$

Where, I = Mycelial growth inhibition percentage
C = Mycelial growth of control
T= Mycelial growth of an endophyte (Hajieghrari et al 2010)

Identification of Isolated Endophytes

Bacterial endophytes: Bacterial endophytes were identified

on the basis ofmorphotaxonomic and biochemical tests.

Morphological identification: Individual bacterial colony were streaked on the plates with the help of sterilized inoculation loop and incubated at 28±2°C for 24 hours and colony characteristics were observed visually viz, shape, colour and mucosity.

Gram staining: Gram's stain reaction is an important tool developed by Dr. Hans Christain Gram, a Danish Physician, in 1884 for the classification remains an important and useful technique till today. On the basis of Gram staining bacteria are grouped into Gram positive or Gram negative. The bacterial endophytes were examined for Gram reaction and cell shape. In this method, bacterial smears were prepared on grease free glass slides, out of the cultures taken from 24 hours old colonies, grown on nutrient agar. Smears were heat fixed and flooded with crystal violet for 30 seconds, then washed with water. Gram's iodine was applied on smear for 60 seconds and then washed with ethyl alcohol. Finally safranin was applied on the smear for 30 seconds and then washed by distilled water. After air drying it was observed under microscope, first it was observed under 10x and then a drop of immersion oil was placed on smear and observed under 100x magnification in order to record the microscopic characteristics (Bathlomew 1962).

Biochemical Identification: Different biochemical test viz, starch hydrolysis, triple sugar iron agar (TSIA), indole production, hydrogen sulphide production, methyl red test (MR test), Voges-Proskauer test (VP Test), citrate utilization test, lipid hydrolysis test and gelatin hydrolysis test was conducted to identify the selected isolates, as described in Bergey's Manual of Determinative Bacteriology (Holt et al 1994)

Identification of fungal isolates: Fungal isolates were identified on the basis of morph taxonomic characteristics.

Morphological characteristics: Fungal isolates were grown on Petri plates containing potato dextrose agar (PDA) media and then incubated at 25±2℃ for 5-6 days and colony characteristics were recorded visually viz. colour, margin, mycelial growth, etc.

Microscopic characteristics: Fungal isolates were stained using lactophenol cotton blue and then observed under microscope, firstly under 10x and then under 40x magnification and identified on the basis of mycelia and spore characteristics.

Statistical Analysis: Experimental data obtained from the investigation shall be analysed by using completely randomized design (Sheoran et al 1998).

RESULTS AND DISCUSSION

Isolation of endophytes: Twenty bacterial endophytes (ten from leaves and ten from bulbs) and fifteen fungal endophytes (seven from leaves and eight from bulbs) were isolated from the collected samples(Table 1) (Fig. 1 and 2). The isolation of endophytes from different parts of medicinal plants has been reported by various workers (Gonthier et al 2006, Ferreira et al 2008) whereas the isolation of endophytes from *Allium* sp. has been reported by various researchers (Zhang et al 2013, Mandyam and Jumpponen 2015).

Antimicrobial activity of bacterial isolates: Twenty bacterial endophytes were screened against *Salmonella typhi* and *Pseudomonas aeruginosa* (human pathogens) and *Rhizactonia solani* and *Macrophomina phaseolina* (plant pathogens) for their antimicrobial activity. Among the bacterial isolates, four isolates (ALR-2, ALR-3, ABC-6 and ABC-7) significantly inhibited the growth of *Salmonella typhi* and among these isolates, isolate ALR-2 showed maximum zones of inhibition (14.0mm), which was followed by ALR-3 (12.6mm) whereas the isolates ALM-5, ABC-6 and ABC-7 significantly inhibited the growth of *Pseudomonas*

Table 1. Endophytes from *Allium sativum*

Location	Bacterial isolate	Fungal isolate
Leaves		
R.S. Pura	ALR-1	ALFR-1
	ALR-2	ALFR-6
	ALR-3	ALFR-7
	ALR-7	
	ALR-10	
Gangyal	ALG-4	ALFG-3
	ALG-9	ALFG-2
Muthi	ALM-5	ALFM-4
	ALM-6	ALFM-5
	ALM-8	
Chatha	---------	----------
Bulbs		
R.S. Pura	ABR-1	ABFR-4
	ABR-2	ABFR-8
	ABR-5	
	ABR-9	
	ABR-10	
Chatha	ABC-6	ABFC-7
	ABC-7	
Gangyal	----------	ABFG-1
		ABFG-2
		ABFG-3
Muthi	ABM-8	ABFM-5
	ABM-4	ABFM-6
	ABM-3	

aeruginosa (Table 3). The bacterial isolates ALM-5, ALG-9 and ABC-6 significantly inhibited the mycelia growth of *Rhizoctonia solani* and among these isolates, ALM-5 showed maximum zones of inhibition (3.33mm) followed by ALG-9 (2.66mm) (Table 2) (Fig. 3). The bacterial endophytes did not show any antimicrobial activity against *Macrophomina phaseolina*.Isolation of antimicrobial compounds from endophytes helps to reduce the problem related with drug resistant microbes. Similar work has been done by various workers which describes that *Burkholderia, Pseudomonas* and *Bacillus* species showed antimicrobial activity against human and plant pathogens. (Chin et al 2000) revealed that *Pseudomonas* species are the best biocontrol agents and they are antagonistic to certain plant and human pathogens because of the production of phenazine type antibiotic products from them. Bloemberg and Lugtenberg (2001) describes that majority of the endophytic bacteria are Gram negative and belonged to *Pseudomonas* species, which are effective biocontrol agents similarly.

Antimicrobial activity of fungal endophytes: Among all the isolates, ALFG-3, ALFR-6, ABFM-6 and ABFR-8 significantly inhibited the growth of *Salmonella typhi* and among these isolates, ABFR-8 showed maximum zone of inhibition (6.33mm) followed by ABFM-6 (5.66mm). The

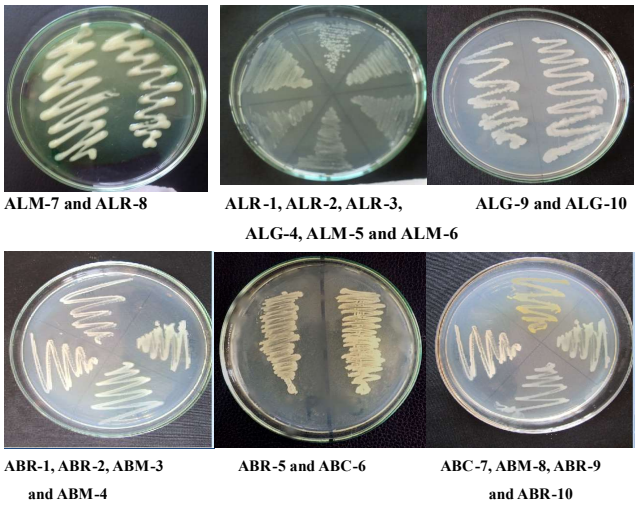

Fig. 2. Bacterial isolates from leaves and bulbs of *Allium sativum*

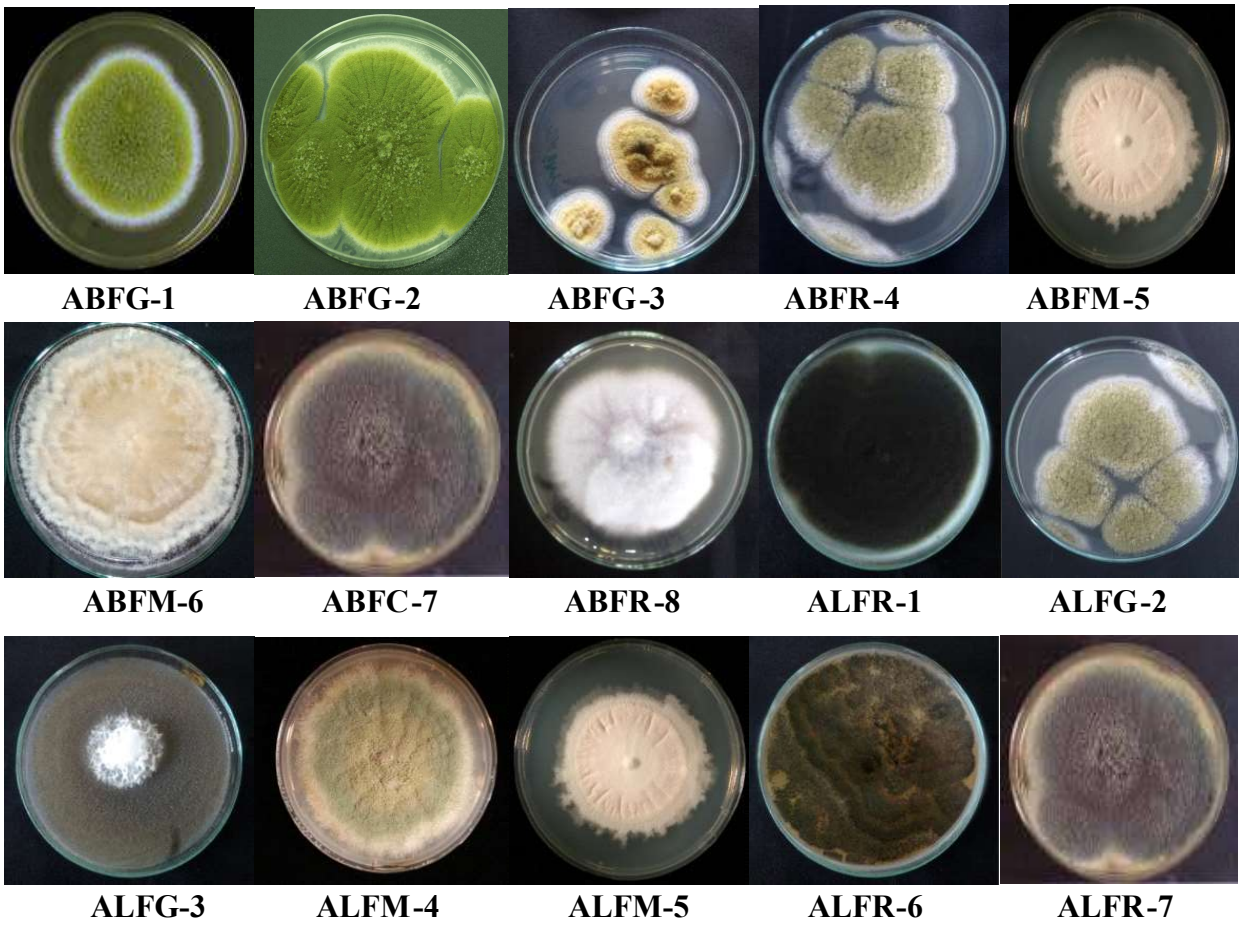

Fig. 1. Fungal isolates from bulbs and leaves of *Allium sativum*

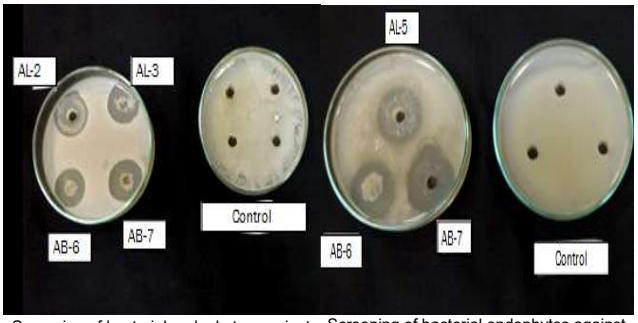

Screening of bacterial endophytes against *Salmonella typhi*

Screening of bacterial endophytes against *Pseudomonas aeruginosa*

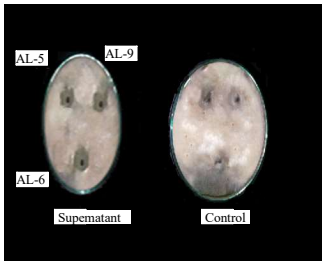

Screening of bacterial endophytes against *Rhizactonia solani*

Fig. 3 Antimicrobial activity of bacterial endophytes

Table 2. Effect of bacterial and fungal endophytes against *Rhizactonia solani*

Bactrial isolates	Zone of inhibition (mm)	Fungal isolate	Colony diameter (mm)	Mycelia growth inhibition (%)
Leaves				
ALR-1	0.00	ALFR-1	61	39.60
ALR-2	0.00	ALFG-2	90	0.00
ALR-3	0.00	ALFG-3	90	0.00
ALG-4	0.00	ALFM-4	90	0.00
ALM-5	3.33	ALFM-5	90	0.00
ALM-6	0.00	ALFR-6	90	0.00
ALR-7	0.00	ALFR-7	90	0.00
ALM-8	0.00			
ALG-9	2.66			
ALR-10	0.00			
Bulbs				
ABR-1	0.00	ABFG-1	90	0.00
ABR-2	0.00	ABFG-2	90	0.00
ABM-3	0.00	ABFG-3	90	0.00
ABM-4	0.00	ABFR-4	90	0.00
ABR-5	0.00	ABFM-5	90	0.00
ABC-6	2.33	ABFM-6	90	0.00
ABC-7	0.00	ABFC-7	90	0.00
ABM-8	0.00	ABFR-8	54	31.85
ABR-9	0.00			
ABR-10	0.00			
Control			90	0.00
CD (p=0.05)	0.71			0.79

isolates ALFR-1, ALFG-3, ALFR-6, ABFM-6 and ABFR-8 significantly inhibited the growth of *Pseudomonas aeruginosa* and among these isolates, isolate ALFG-3 showed maximum zone of inhibition (8.66mm) which was statistically at par with the isolate ABFR-8 (8.33mm), followed by ALFR-6 (7.66mm) and this isolate was statistically at par with isolate ALFR-1. The least zone of inhibition (6.66mm) was showed by the isolate ABFM-6. Among all the fungal isolates, ALFR-1 (39.60%) and ABFR-8 (31.85%) significantly inhibited the mycelial growth of *Rhizactonia solani* (Table 2) (Fig. 4). The fungal endophytes did not show any antimicrobial activity against *Macrophomina phaseolina*. Various bioactive metabolites were isolated from these species which possess antimicrobial property. (Melfei et al 2011) reported two new antimicrobial compounds, (10-oxo-10H-phenaleno [1,2,3-de]chromene-2-carboxylic acids and xanalteric acids I and II) and 11 known secondary metabolites obtained from extracts of the endophytic fungus *Alternaria* sp., isolated from the mangrove plant *Sonneratia* which showed activity against *E. faecalis, Pseudomonas aeroginosa* and *S. epidermidis* due to their extracellular metabolites production secreted by endophytes which were acted to pathogen cell membrane and damaged it (Akpas et al 2001). Chandrappa et al (2013) also reported that the ethyl acetate extract of *Aspergillus niger* showed maximum zone against *Shigella felxnen.* Wang (2012) isolated *Phoma* species from *Arisaema erubescens* and the isolated *Phoma* species produce a new compound α-tetralone which works

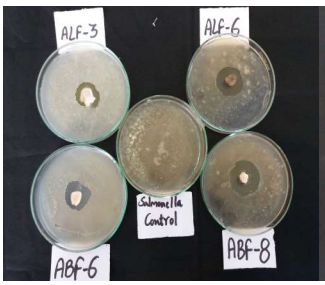

Screening of fungal endophytes against *Salmonella typhi*

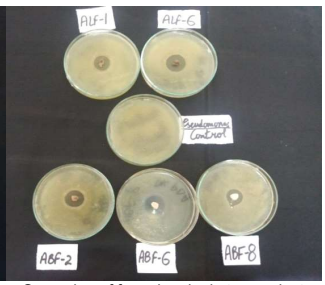

Screening of fungal endophytes against *Pseudomonas aeruginosa*

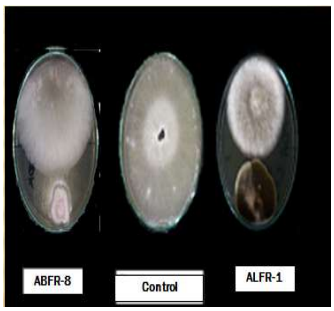

Screening of fungal endophytes against *Rhizactonia solani*

Fig. 4. Antimicrobial activity of fungal endophytes

as an antimiocrobial compound against certain bacterial and fungal pathogens. Kusari and Spiteller (2011) revealed the production of Hypericin and Emodin believed to be the main precursor of hypericin, by the endophytic fungus isolated antimicrobial activity against several bacteria and fungi.

Identification of bacterial endophytes: The effective bacterial endophytes which showed antimicrobial activity against human and plant pathogens were identified on the basis of morphotaxonomic and biochemical characterization. Isolates ALR-2 and ABC-6 were white in colour with shiny and circular colonies whereas ALR-3, ALM-5, ALG-9 and ABC-7 were pale yellow in colour with slimy, shiny and circular colonies. The microscopic characteristics of bacterial endophytes showed that the isolates ALR-2, ALR-3, ALM-5 and ABC-7 were Gram –ve and short rod whereas the isolates ALG-9 and ABC-6 were Gram+ve (Fig. 5).

Biochemical characterization of bacterial endophytes: The isolate ALR-2 showed positive results for citrate utilization, indole production, methyl red test and lipid hydrolysis. Isolate ALR-3 showed positive results for citrate utilization, indole production, methyl red test, TSIA test and

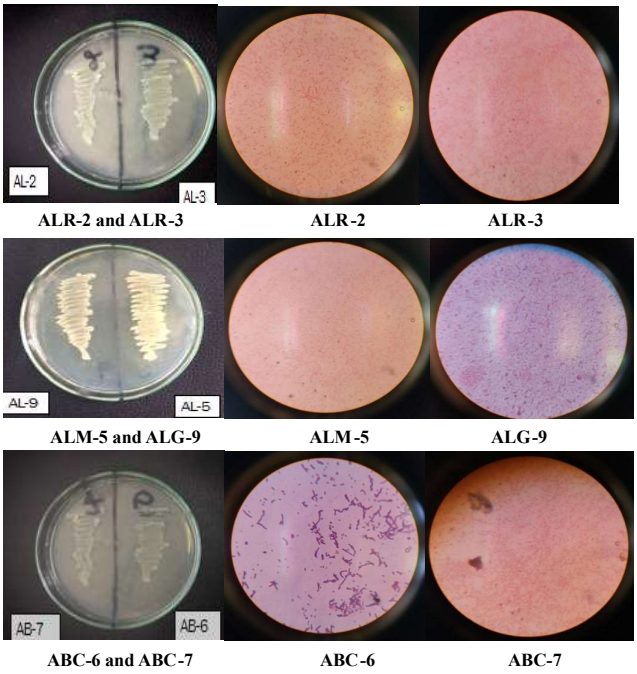

Fig. 5. Colony and microscopic characteristics of bacterial endophytes

Table 3. Effect of bacterial and fungal endophytes against human pathogens

Isolates		*Salmonella typhi*		*Pseudomonas aeruginosa*	
Bacterial	Fungal	Bacterial	Fungal	Bacterial	Fungal
Leaves					
ALR-1	ALFR-1	0.00	0.00	0.00	7.00
ALR-2	ALFG-2	14.00	0.00	0.00	0.00
ALR-3	ALFG-3	12.60	2.33	0.00	8.66
ALG-4	ALFM-4	0.00	0.00	0.00	0.00
ALM-5	ALFM-5	0.00	0.00	15.60	0.00
ALM-6	ALFR-6	0.00	2.66	0.00	7.66
ALR-7	ALFR-7	0.00	0.00	0.00	0.00
ALM-8		0.00		0.00	
ALG-9		0.00		0.00	
ALR-10		0.00		0.00	
Bulbs					
ABR-1	ABFG-1	0.00	0.00	0.00	0.00
ABR-2	ABFG-2	0.00	0.00	0.00	0.00
ABM-3	ABFG-3	0.00	0.00	0.00	0.00
ABM-4	ABFR-4	0.00	0.00	0.00	0.00
ABR-5	ABFM-5	0.00	0.00	0.00	0.00
ABC-6	ABFM-6	10.33	5.66	15.00	6.66
ABC-7	ABFC-7	12.33	0.00	15.00	0.00
ABM-8	ABFR-8	0.00	6.33	0.00	8.33
ABR-9		0.00		0.00	
ABR-10		0.00		0.00	
CD (p=0.05)		0.53	0.50	0.56	0.80

starch hydrolysis, whereas isolate ALM-5 positive results for citrate utilization, starch hydrolysis and indole production and ALG-9 for citrate utilization, TSIA test and lipid hydrolysis. Isolate ABC-6 showed positive results for citrate utilization, starch hydrolysis and indole production and isolate ABC-7 indicated positive results for citrate utilization, TSIA test, methyl red test, VP test and gelatin hydrolysis. None of the bacterial isolate showed positive result for H2S production. On the basis of gram staining and biochemical characterization, bacterial isolates were identified using ABIS online software and that isolated bacterial endophyte ALR-2, ALR-3 and ALM-5 belonged to the genus *Pseudomonas*, isolate ALG-9 and ABC-6 belonged to genus *Bacillus* and isolate ABC-7 belonged to the genus *Burkholderia* (Table 4) (Fig. 6).

Identification of fungal endophytes: On the basis of morphotaxonomic characteristics it was observed that isolate ALFR-1 belonged to the genus *Alternaria*, ALFG-3 belonged to genus *Phoma*, ALFR-6 belonged to genus *Aspergillus*, ABFM-6 belonged to the genus *Cladosporium* and ABFR-8 belonged to the genus *Fusarium* (Fig. 7).

Fig. 6. Biochemical characterization of bacterial endophytes

Table 4. Biochemical characterization of bacterial endophytes

Bacterial culture	Indole test	H2S production test	MR test	Starch hydrolysis test	Citrate test	Gelatin hydrolysis	VP test	Lipid hydrolysis test	TSIA Test	Genus ABIS
ALR-2	+ve	-ve	+ve	-ve	+ve	-ve	-ve	-ve	Whole slant red –alkaline	*Pseudomonas* sp.
ALR-3	+ve	-ve	+ve	+ve	+ve	-ve	-ve	+ve	Yellow butt – acidic Red slant - alkaline	*Pseudomonas* sp.
ALM-5	+ve	-ve	-ve	+ve	+ve	-ve	-ve	-ve	Whole slant red- alkaline	*Pseudomonas* sp.
ALG-9	-ve	-ve	-ve	-ve	+ve	-ve	-ve	+ve	Whole slant yellow- acidic	*Bacillus* sp.
ABC-6	+ve	-ve	+ve	+ve	+ve	-ve	-ve	-ve	Whole slant red- alakline	*Bacillus* sp.
ABC-7	-ve	-ve	+ve	-ve	+ve	+ve	+ve	-ve	Whole slant yellow- acidic	*Burkholderia* sp.

Table 5. Colony and microscopic characteristics of fungal endophytes

Fungal endophyte	Colony characteristics	Microscopic characteristics	Fungal genus
ALFR-1	Greenish black in colour, sporulated, embedded	Conidia septate, 2-3 septa	*Alternaria* sp.
ALFG-3	White fluffy centre with aerial mycelia, greyish margin, embedded	Oval shaped short conidia, conidiophores short, pycnidia dark	*Phoma* sp.
ALFR-6	Dark brown coloured, circular colony, powdery, embedded	Small conidia arise in chains	*Aspergillus* sp.
ABFM-6	Light brown centre, white margin, aerial mycelia, embedded	Oval shaped dark conidia,, large hyphae septate	*Cladosporium* sp.
ABFR-8	Whitish colony with slightly pink colour, fluffy growth, aerial mycelium	Sickle shaped macroconidia	*Fusarium* sp.

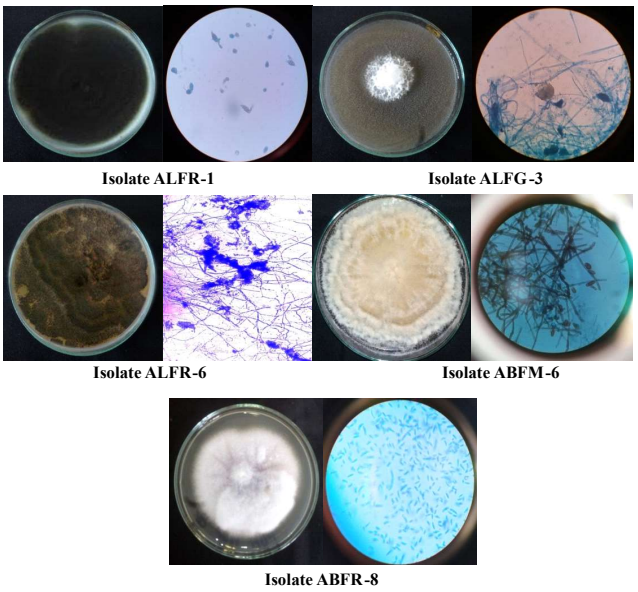

Fig. 7. Morphological and colony characteristics of effective fungal endophytes

CONCLUSION

In the present research work, twenty bacterial and fifteen fungal isolates were isolated from the *Allium sativum* and out of these isolates only six bacterial and five fungal isolates showed antimicrobial activity against human and plant pathogens but among all the effective isolates, bacterial isolate ABC-6 and fungal isolate ABFR-8 were effective against all the test pathogens except *Macrophomina phaseolina*. So, this study proved that *Allium sativum* contains biodiversity of endophytic microorganisms viz. bacteria and fungi that showed antimicrobial activity against human and plant pathogens and can be used in the pharmaceutical industry.

REFERENCES

Adhikari C, Devanand, Kumar T and Bishwas AJ 2021 Review on Ethno-medicinal plants used for healing skin ailments in Madhya Pradesh. *Indian Journal of Ecology* **48**(3): 709-715

Agarry OO, Olaleye MT, Bello and MCO 2005 Comparative antimicrobial activities of Aloevera gel and leaf. *African Journal of Biotechnology* **4**: 1413-1414.

Akpas E, Jacques P, Wathelet B, Paquot M, Fuchs R, Budzikiewicz H and Thonart P 2001 Influence of culture conditions on lipopeptide production by *Bacillus subtilis*. *Applied Biochemical and Biotechnology* **91**: 551-561.

Andrews JM 2001. Determination of minimum inhibitory concentration. *Journal of Antimicrobial Chemotherapy* **48**: 5-16.

Barraquio WL, Revilla L and Ladha JK 1997 Isolation of endophytic diazotrophic bacteria from wetland rice. *Plant Soil* **194**: 15-24.

Bathlomew JW 1962 Variables influencing results and precise definition steps in Gram staining as a means of standardizing the results obtained. *Stain Technology* **37**: 139-155.

Bloemberg GV and Lugtenberg BJ 2001 Molecular basis of plant growth promotion and biocontrol by rhizobacteria. *Current Opinion in Plant Biology* **4**: 343-50.

Chandrappa CP, Anitha R, Jyothi P, Rajalakshmi K, Seema MH, Govindappa M and Sharanappa P 2013 Phytochemical analysis and antibacterial activity of endophytes of *Embelia tsjeriam Cottam* Linn. *Research Article Biological Sciences* **3**: 467-473.

Chin AW, Bloemberg TF, Guido V, Mulders IH, Dekkers M and Linda 2000. Root colonization by phenazine-1-carboxamide-producing bacterium *Pseudomonas chlororaphis* PCL1391 is essential for biocontrol of tomato foot and root rot. *Molecular Plant Microbe Interaction* **13**(12): 1340-1345.

Creus CM, Sueldo RJ and Barassi C 1998 Water relations in *Azospirillum* inoculated wheat seedlings under osmotic stress. *Canadian Journal of Botany* **76**: 238-244.

De Bary A 1866 Morphologie und Physiologie der Pilze, Flechten and Myxomyceten. *Hofmeister's Handbook of Physiological Botany* **2:** 1831-1888.

Doty SL 2008 Enhancing phytoremediation through the use of transgenics and endophytes. *New Phytology* **179**: 318-333.

Ferreira A, Quecine MC, Lacava PT, Oda S, Azevedo JL, Araujo and WL 2008 Diversity of endophytic bacteria from *Eucalyptus* species seed and colonization of seedling by *Pantoea agglomerans*. *FEMS Microbiology Letter* **287**: 8-14.

Freeman EM 1904. The seed-fungus of *Lolium temulentum*, L. the Darnel. *Philosophical Transactions* **196:** 1-27.

Gonthier P, Gennaro M and Nicolotti, G. 2006. Effects of water stress on the endophyticmycota of *Quercusrobur*. *Fungal Diversity* **21**: 69-80.

Holt JG, Krieg NG, Sneathm PHA, Staley JT and Williams ST 1994 *Bergey's Manual of Determinative Bacteriology*, 9th edn. Baltimore, MD: Williams and Williams.

Kusari S and Spiteller M 2011. Are we ready for industrial production of bioactive plant secondary metabolites utilizing endophytes? *Natural Product Reports* **28**: 1203-1207.

Li G, Huang H and Acharya S 2003. Antagonism and biocontrol potential of *Ulocaldiumatrum* on Sclerotinia sclerotiorum. *Biological Control* **28**(1): 11-18.

Macpherson LJ, Geierstanger BH, ViswanathV, Bandell M, Eid SR, Hwang SW and Patapoutian A 2005 The pungency of garlic: Activation of TRPA1 and TRPV1 in response to allicin. *Current Biology* **15**(10): 929-934.

Madhaiyan M, Poonguzhali S and Senthilkumar M 2004 Growth promotion and induction of systemic resistance in rice cultivar Co-47 (*Oryza sativa* L.) by *Methylobacterium* sp. *Botanical Bulletin Academic Sinica* **45**: 315-324.

Mandyam KG and Jumpponen A 2015 Mutualis-parasitism paradigm synthesized from results of root-endophytic models. *Frontiers of Microbiology* **5**: 10-33

Maria GL, Sridhar KR and Raviraja NS 2005 Antimicrobial and enzyme activity of mangrove endophytic fungi of southwest coast. *Indian Journal of Agricultural Technology* **1**(20): 67-80.

Melfei E, Bungihan MA, Tan MK, Kogure N, Franzblau SG, Edison TE, Cruz D, Takayama H and Nonato MG 2011 Production of antimicrobial compounds from Alternaria species from *Sonneratia*.*Journal of Natural Medicine* **65**: 606-609.

Nowak J, Asiedu SK and Lazarovits G 1995 Enhancement of *in vitro* growth and transplant stress tolerance of potato and vegetable plantlets co-cultured with a plant growth promoting pseudomonad bacterium. In: Carre F, Chagvardieff P (eds) Proc. *International Symposium on Ecophysiology and Photosynthetic in vitro* Cultures, Aix-en-Provence, France CEA, Cadarache, France, pp. 173-180.

Perez C, Pauli M and Bazerque P 1990. An antibiotic assay by agar-well diffusion method. *Acta Biologiae et Medicine Experimentalis* **15**: 113-115.

Redecker D, Kodner R and Graham LE 2000. Glomalean fungi from

the Ordovician. *Science* **289**: 1920-1921.

Redman RS, Sheehan KB and Stout RG 2002. Thermotolerance generated by plant/fungal symbiosis. *Science* **298**:1581

Sheoron OP, Tonk DS, Kaushik LS, Hasija RC and Pannu RS 1998.*Statistical software package for agricultural research workers*. Recent advances in information theory, pp: 139-143

Stabler SN, Tejani AM, Huynh F and Fowkes C 2012. Garlic for the prevention of cardiovascular morbidity and mortality in hypertensive patients. *Cochrane Database of Systematic Reviews* **8**: 1-25.

Strobel G, Yang XS, Sears J, Kramer R, Sidhu RS and Hess WM 1996. Taxolfrom Pestalotiopsis microspora, an endophytic fungi of Taxuswallachiana. *Microbiology* **142**(2): 435-440.

Taylor JE, Hyde KD and Jones EBG 1999. Endophytic fungi associated with the temperate palm *Trachycarpus fortunei* within and outside its natural geographic range. *New Phytologist* **142**: 335-346.

Received 19 July, 2021; Accepted 12 November, 2021

Wang LW 2012. Bioactive metabolites from Phoma species, an endophytic fungus from the Chinese medicinal plant Arisaema erubescens. *Applied Microbial Biotechnology* **93**(3): 1231-1239.

Woo HD, Park S, Oh K, Kim HJ, Shin HR, Moon HK and Kim J 2014. Diet and cancer risk in the Korean population: A meta- analysis. *Asian Pacific Journal of Cancer Prevention* **15**(19): 8509-8519.

Zhang H, Mallik A and Zeng RS 2013. Control of Panama disease of banana by rotating and intercropping with Chinese chive (*Allium tuberosum*): Role of plant volatiles. *Journal of Chemical Ecology* **39**(2): 243-252.

Zhang HW, Song YC and Tan RX 2006 Biology and chemistry of endophytes. *Natural Product Reports* **23**: 753-771.

Zhang Y, Mu J, Feng Y, Kangt Y, Zhang J, Gu PJ, Whang Y, Ma LF and Zhu YH 2009. Broad-spectrum antimicrobial epiphytic and endophytic fungi from marine organisms: isolation, bioassay and taxonomy. *US National Library of Medicine National Institutes of Health* **7**(2): 97-12.

Indian Journal of Ecology (2021) 48(6): 1789-1792

Manuscript Number: 3449
NAAS Rating: 5.79

Improvement of Xylanase Activity of *Aspergillus* sp. by Physical and Chemical Mutagenesis

T. Venkatram Reddy, M. Rajashekhar[1], N. Kishore and D. Madhusudan Reddy*

Department of Microbiology,
[1]Department of Zoology, Palamuru University, Mahbubnagar- 509 001, India
**E-mail: dadireddy@gmail.com*

***Abstract*:** A xylan-degrading enzyme (endo ß-1, 4 xylanase, EC 3.2.1.8) cleaves ß-1, 4 glycosidic bond to produce xylose and is useful mainly in bio bleaching paper pulp, pharmaceutical and food industries. The purpose of the present investigation is to enhance xylanase production by subjecting indigenous xylanase producing strain *Aspergillus niger to* improvement by random mutagenesis by ultra-violet (UV) irradiation and *N*-methyl-*N*-nitrosourea (NMU) treatment. Mutants were screened as xylanase producers on the reddish zone of enzyme activity formation in PDA xylan agar plates. UV-12 mutant showed activities of 204.25 for submerged fermentation (Smf). UV-12 further mutated by NMU to produced NMU-10 mutant. Compared to wild strain, NMU-10 mutant produce 6.5 fold more activities in Smf. Thus these findings have more impact on enzyme economy for biotechnological applications of microbial xylanase.

***Keywords*:** Strain improvement, *Aspergillus niger,* UV-NMU mutation, Xylanase production

Xylan is the major hemicellulose constituent of hard wood and soft wood, and is the next most abundant renewable polysaccharide after cellulose and is a heterogeneous carbohydrate, consisting of ahomopolymeric backbone of ß-1, 4 linked D-xylopyranose units and short chain branches consisting *of* O-acetyl, a-L-arabinofuranosyland a-D-glucuronyl residues. Endo-xylanase (ß-1, 4-Dxylan-xylanohydrolase, EC 3.2.1.8) is the key enzyme for xylan depolymerization. Microbial xylanases are used in the animal feed, textile and food processing industries, and in the production of several valuable products like xylitol and ethanol (Salles et al 2005). Bio bleaching of pulps using xylanase is one of the most suitable applications in the pulp and paper industry to reduce and/or eliminate the use of chlorine and chlorine dioxide. There is a great interest in the enzymatic hydrolysis of xylan because of possible applications in ruminal digestion, waste treatment, fuel, chemical production and paper manufacture. These uses have placed a greater stress on increasing xylanase production (Lindberg et al 2007, Tapingkae et al 2008, Bakri et al 2008). A large number of bacteria and fungi are known to produce xylanases (Kulkarni et al 1999, Subramaniyan and Prema 2002). Filamentous fungi are industrially important producers of this enzyme due to extracellular release of xylanases, higher yield compared to yeast and bacteria and production of several auxiliary enzymes that are necessary for de-branching of the substituted xylans (Haltrich et al 1996). However, fungal xylanases are generally associated with concurrent production of celluloses. Among the microorganisms that have xylanolytic activity, *Aspergillus niger* is one of the well-known producer (Record et al 2003, Raana et al 2004, Maciel et al 2008). The strain improvement has been achieved through mutation, selection, or genetic recombination. In many cases, mutations are harmful, but occasionally may lead to a better adapted organism to its environment with improved bio catalytic performance. The potential of a microorganism to mutate is an important property conferred by DNA, since it creates new variations in the gene pool. The challenge is to isolate those strains which are true mutants that carry beneficial mutations (Parekh et al 2000). UV rays are important inducers of strain mutations. The pyrimidines (thymine and cytosine) are especially sensitive to modifications by UV ray's absorption. This may result in the production of thymine dimers that distort the DNA helix and block future replications (Sambrook et al 2000). Random mutagenesis can enhance enzyme productivity several fold than the parental strain. *N*-methyl-*N*-nitroso urea (NMU), an alkylating agent, has found a potential routine application for inducing mutagenesis in the genome of microorganisms. The same approach of NMU treatment and mutant selection was used in the present study. Purpose of the present investigation is to enhance Xylanase production by subjecting indigenous Xylanase producing strain *Aspergillus niger* to improvement by random mutagenesis by ultra-violet (UV) irradiation and *N*-methyl-*N*-nitrosourea (NMU) treatment.

MATERIAL AND METHODS

Microorganism and growth media: The wild-type strain *Aspergillus niger* was isolated from garden soil by serial dilution technique and *Aspergillus niger* was identified and isolated in pure form. In conformation screening by congo red test, based on the reddish zone of enzyme activity formation in oat spelt xylan agar plates and identified by physiological and morphological tests as depicted by Pitt and Hocking (1977). The isolates was grown on potato dextrose agar (PDA) at 30°C, and then stored at 4°C. PDA slants incubated for 7 days were used for the preparation of the inoculums.

Preparation of conidial suspension: Ten milliliters of 0.85% saline containing 0.1% Tween-80 was transferred to a 7 days old PDA slant culture of *Aspergillus niger*. The conidia were dislodged using an inoculation needle under aseptic conditions and the suspension was used for its conidia count in a Neuberger chamber by serial dilution and plating on PDA agar medium.

Isolation and Selection of Mutants

UV irradiation: Fifteen ml of the spore suspension containing 10^7 spores ml^{-1} was pipette aseptically into sterile petri-dish of 80 mm diameter having a flat bottom. The exposure of spore suspension to UV light was carried at distance of 15 cm away from UV lamp (15W, 2537A0). Radiation intensity was 350 µW cm^{-2} (Montiel-González et al 2004). The exposure times were 5, 10, 15, 20, 25 and 30 min each. UV exposed spore suspension was stored in dark overnight to avoid photo reactivation, then was serially diluted in saline and plated on PDA medium. The plates were incubated for 7 days at 30°C and the numbers of colonies in each plate were counted. Each colony was assumed to be formed from a single spore. Mutants were selected from the plates showing less than 1% survival rate and screened for xylanase production on PDA xylon agar medium.

NMU treatment: The best UV mutant was used for NMU treatment. The spore suspension was prepared in the same manner as described earlier and calculated the spore count in a Neubauer chamber. To 9 ml of spore suspension (106 spores ml^{-1}), 1 ml NMU solution (1 mg ml^{-1} in sterile water) was added. The reaction was allowed to proceed at 30^0C, 120 rpm. Samples were withdrawn from the reaction mixture at intervals of 20, 40, 60, 80 and 100 min and immediately centrifuged for 20 min at 6000 rpm and the supernatant solution was decanted. Cells were washed three times with sterile water and re-suspended in 10 ml of sterile saline. The samples were serially diluted in the same saline and plated over PDA as mentioned earlier. NMU mutants were selected from the plates showing less than 1% survival and screened for xylanase production on PDA xylon agar plates.

Xylanase production by submerged fermentation technique: Hyper producing mutant of UV, NTG treatment and a wild strains were inoculated separately in Smf. The liquid medium was prepared which contain NaNO3 1.0, NH4Cl 1.0, KH2PO4 1.0, CaCl2 1.0, MgSO4.7H2O 0.3, meat extract 5.0, Tween-80 1.5 ml, wheat bran 20.0, pH 5.0 and autoclaved at15.0 lbs/in^2 pressure (121°C) for 15 min. After cooling to an ambient temperature, the flasks were inoculated with 1.0 ml of the conidial suspension containing 1.2×106 conidia and incubated at 30°C in a rotary shaking incubator (200 rpm) for 72 h. The ingredients of the flasks were filtered and the filtrate was used for the estimation of xylanase. All the experiments were run parallel in triplicates.

Enzyme assay: Xylanase activity was determined by mixing 0.9 ml of 1% (w/v) birch wood xylan (prepared in 50 mM Na-citrate buffer, pH 5.3) with 0.1ml of suitably diluted enzyme and the mixture was incubated at 50°C for 5 min (Bailey et al 1992). The reaction was stopped by addition of 1.5 ml of 3, 5-dinitrosalicylic acid (DNS) and the contents were boiled for 5 min (Miller 1959). After cooling, the colour developed was read at 540 nm. The amount of reducing sugar liberated was quantified using xylose as standard. One unit of xylanaseis defined as the amount of enzyme that liberates 1 mmol of xylose equivalents per minute under the assay conditions. Cellulase (CMCase) activity was determined as above and amount of reducing sugar liberated was quantified using glucose as standard.

RESULTS AND DISCUSSION

UV mutation: The UV treatment with fungal spores showed 1% survival when treated for 25 min (Fig. 1). The plates having less than 1% survival rate was at 25 min UV exposure time. From UV mutagenesis total 15 mutants were selected on the basis of different morphology, shapes and colored mutants. Out of 15 mutants, only Uv-12 mutants showed higher clear zone diameter than wild type (Table 1). UV-12 showed maximum xylanase activities of 52.6 U ml^{-1} (in Smf). The wild strain produced xylanase activities of 19.3 U ml^{-1} (in Smf). Overall, 2.7 fold xylanase activity was enhanced from UV-12 mutant in Smf, when compared with wild strain.

NMU mutation: The UV mutant (UV-12) was selected and was subjected for further strain improvement by NMU treatment. NMU was considered to be very effective chemical mutagen. The 1% survival was observed in between 60-80 min incubation (Fig. 2). Total 15 mutants were selected on xylon agar plates. Among 15 mutants, one mutant (NMU-10) showed maximum clear zone (13 mm diameter) than UV-12 mutant while 8 mutants showed higher clear zone diameter than wild strain. NMU-10 showed maximum xylanase activities of 204.25 U ml^{-1} (in Smf). The xylanase yield of NMU-10 mutant was 3.8 fold higher in Smf

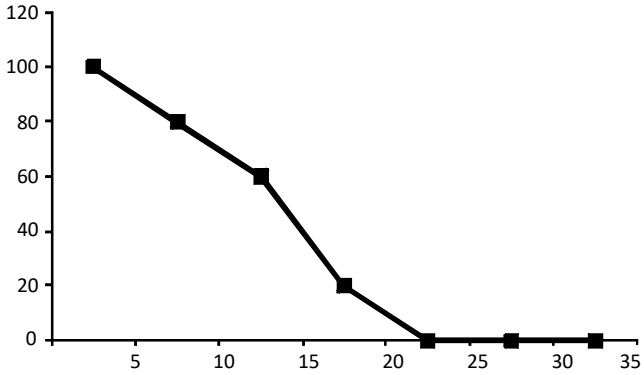

X- Axis :- Time (Mins), Y- Axis :- % survival

Fig. 1. UV irradiation on survival of *Aspergillus niger* at different time

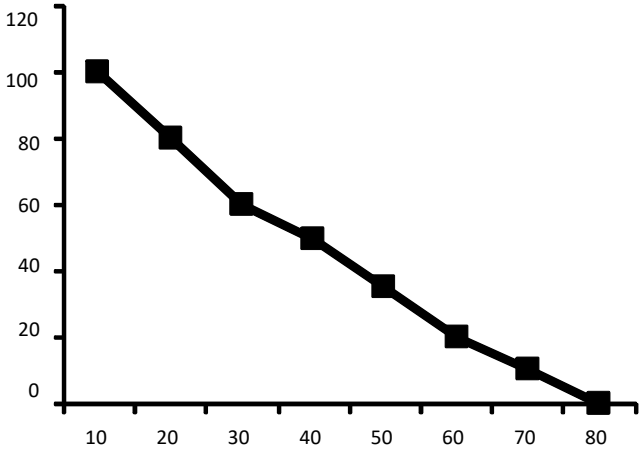

X- Axis :- Time (Mins)
Y- Axis :- %s Survival

Fig. 2. NMU treatment on survival of UV mutant of *Aspergillus niger* (UV-12) at different time

Table 1. UV mutant and xylanase activity

Isolates	Xylanase activity (U ml^{-1}) (Smf)
Wild strain	19.3
Uv-1	23.5
Uv-2	35.67
Uv-3	15.43
Uv-4	7.85
Uv-5	45.6
Uv-6	28.34
Uv-7	39.5
Uv-8	6.98
Uv-9	47.46
Uv-10	0
Uv-11	50.23
Uv-12	52.6
Uv-13	35.76
Uv-14	21.3
Uv-15	5.05

Table 2. NMU mutant and this xylanase activity

Isolates	Xylanase activity (U ml^{-1} in Smf)
Wild strain	19.3
Uv-12	52.6
NMU-1	77.58
NMU-2	85.7
NMU-3	115.4
NMU-4	187.56
NMU-5	65.62
NMU-6	105.45
NMU-7	193.5
NMU-8	166.98
NMU-9	147.65
NMU-10	204.25
NMU-11	175.23
NMU-12	142.73
NMU-13	135.83
NMU-14	111.35
NMU-15	25.05

than UV-12 mutant when compared to wild strain (Table 2).

CONCLUSIONS

A mutant, NMU-10 was obtained from a Mutant UV-12 of *Aspergillus niger*. It was screened as best potential because of its enhanced zone of clearance on PDA xylon agar plate. It was developed using UV irradiation followed by NMU treatment of the spores. Compared to wild strain, NMU-10 mutant showed 6 .5-fold higher xylanase productions in Smf. Thus the selected mutant has potential in minimizing the cost of enzyme for its biotechnological applications.

ACKNOWLEDGEMENT

This research work was sponsored by Palamuru University, which is gratefully acknowledged.

REFERENCES

Bailey MJ, Biely P and Poutanen K 1992. Inter laboratory testing of methods for assay of xylanase activity. *Journal of Biotechnology* **23:** 257-271.

Bakri Y, Al-Jazairi M and Al-Kayat G 2008. Xylanase production by a newly isolated *Aspergillus niger* SS7 in submerged culture. *Polish Journal of Microbiology* **57**(3): 249-251.

Bakri Y, Jacques P and Thonart P 2003. Xylanase production by *Penicillium canescens* 10-10c in solid-state fermentation. *Applied Biochemistry and Biotechnology* **108:** 737-748.

Bakri Y, Al-Jazairi M and Al-Kayat G 2008. Xylanase production by a newly isolated *Aspergillus niger* SS7 in submerged culture. *Polish Journal of Microbiology* **57**(3): 249-251.

Biely P 1985. Microbial xylanolytic system. *Trends in Biotechnology* **3:** 286-291.

Biswas SR, Jana SC, Mishra AK, Nanda G 1990. Production, Purification, and Characterization of Xylanase from a Hyperxylanolytic Mutant of *Aspergillus ochraceus. Biotechnology and Bioengineering* **35:** 244-251.

Camacho, NA and Aguilar OG 2003. Production, purification and characterization of a low molecular-mass xylanase from *Aspergillus* sp. and its application in baking. *Applied biochemistry and Biotechnology* **104:** 159-172.

Carmona EC, Pizzironi-Kleiner AA, Monteiro RTR, Jorge JA 1997.Xylanase production by *Aspergillus versicolor*. *Journal of Basic Microbiology* **38**(6): 387-394.

Chadha, BS, Jaswinder K, Rubinder K, Saini HS and Singh S 1999. Xylanase production by *Thermomyces lanuginosus* wild and mutant strains. *World Journal of Microbiology and Biotechnology* **15:** 195-198.

Costa-Ferreira M, Diass A, Maximo C, Morgado MJ, Sena-Martins G and Duarte JC 1994. Xylanolytic enzyme production by an *Aspergillus Niger* isolate. *Applied Biochemistry and Biotechnology* **44:** 231-242.

Das A and Nanda G 1995. Production of xylanolytic enzymes during growth on pulverized grass by *Aspergillus ochraceus. Letters in Applied Microbiology* 42.

Das, A and Ponty R 1981. Rapid strain selection for citric acid production. *Advances in Biotechnology* **1:** 51-55.

De vries RP and Visser J 2001. *Aspergillus* enzymes involved in degradation of plant cell wall polysaccharides. *Microbiology and Molecular Biology Reviews* **65**(4): 497-522.

Drazic M and Delac V 1970. Mutagenic action of N-methyl N-nitro N-nitroso guanidine. *Journal of Experimental Biology* **11:** 141.

Eriksson KEL 1985. Swedish developments in biotechnology related to the pulp and paper industry. *Tappi journa*l **68**: 46-55.

Eriksson KE and Kirk TK 1985. Biopulping, biobleaching and treatment of kraft bleaching effluents with white-rot fungi. In: Robinson CW (ed) *Comprehensive Biotechnology,* **3**. Pergamon Press, Toronto, pp 271–294

Ghose TK 1987. Measurement of cellulose activities. *Pure and Applied Chemistry* **59:** 257:268.

González AM, Viniegra-González G, Fernández FJ and Loera O 2004. Effect of water activity on invertase production by improved diploids strains of *Aspergillus niger*. *Process Biochemistry* **39**(12): 2085-2090.

Haltrich D, Nidetzky B, Kulbe KD, Steiner W and Zupancic S 1996. Production of fungal xylanases. *Bioresource Technology* **58**: 137-161.

Howard RL1, Abotsi E, Jansen van Rensburg EL and Howard S 2003. Lignocellulose biotechnology: Issues of bioconversion and enzyme production review. *African Journal of Biotechnology* **2**(12): 602-619.

Jeffries TW 1985. Emerging technology for fermenting D-xylose. *Trends in Biotechnology* **3:** 208-212.

Jurasek L and Paice MG 1988. Biological Bleaching of pulp, Proceedings. International *Pulp Bleaching Conference*, Orlando, June 5-9, p 11-13

Kadowaki MK and Souza CGM 1997. Xylanase production by *Aspergillu stamarii. Applied Biochemistry and Biotechnology* **66:** 97-106.

Received 25 July, 2021; Accepted 28 November, 2021

Kantelinen A, Ratto M, Sundqvist J, Ranua M, Viikari L and Linko M 1988. Hemicellulases andtheir potential role in bleaching. Proceeding of *International Pulp Bleaching Conference*, Tappi,

Kulkarni N, Shendye A and Rao M 1999. Molecular and biotechnological aspects of xylanases. *FEMS Microbiology Reviews* **23:** 411-456.

Lindberg JE, Lyberg K and Sands J 2007. Influence of phytase and xylanase supplementation of a wheat-based diet on ileal and total tract digestibility in growing pigs. *Livestock Science* **109**(1-3): 268-270.

Maciel GM, Vandenberghe LPS, Haminiuk CWI, Fendrich RC, Bianca BED, Brandalize1 TQS, Pandey A and Soccol CR 2008. Xylanase production by *Aspergillus niger* LPB 326 in solid-State fermentation using statistical experimental designs. Xylanase production by *A. niger* in SSF. *Food Technology and Biotechnology* **46**(2): 183-189.

Miller GL 1959. Use of dinitrosalicylic acid reagent for determination of reducing sugar. *Analytical Chemistry* **31**(3): 426-428.

Parekh S, Vinci VA and Strobel RJ 2000. Improvement of microbial strains and fermentation processes. *Applied Microbiology and Biotechnology* **54**: 287-301.

Pitt JI and Hocking AD 1977. Germination and growth of six *xerophilic fungi*, *Aspergillus flavus*, *Aspergillus ochraceus*, *Eurotium chevalieri*, *Chrysosphorium fastidium, Wallemia sebi* and *Xeromyces bisporus* were examined on media of a wide range of water activities. *Journal of General Microbiology* **101**(1): 35-40.

Raana K, Tasneem M, Haq I and Mukhtar H 2004. Effect of additional carbon and nitrogen on the production of xylanase by a mutant strain of *Aspergillus niger* GCBCX-20. *International Journal of Biology and Biotechnology* **1**(4): 529-533.

Record, E, Asther M, Sigoillot C, Paes S, Punt PJ, Delattre M, Haon M, Van Den Hondel CA, Sigoillot JC, Lesage-Meessen L and Asther M 2003. Overproduction of the *Aspergillus niger* feruloyl esterase for pulp bleaching application. *Applied Microbiology and Biotechnology* **62**: 349-355.

Salles BC, Medeiros RG, Bao SN, Silva Jr. FG and Filho EXF 2005. Effect of cellulase-free xylanases from *Acrophia lophoranainiana* and *Humicola gri seavarthermoidea* on eucalyptus kraft pulp. *Process Biochemistry* **40:** 343-349.

Sambrook J and Russell D 2000. Molecular Cloning. *A Laboratory Manual* Third edn. New York. Cold Spring Harbor Laboratory Press.

Siikaaho Ranua M and Viikari L 1992. Xylanases and mannanases in the treatment of pulp. In: KUWAHARA M and SHIMADA M. eds. *The 5th International Conference on Biotechnology in the Pulp and Paper Industry*. Uni Publishers, Tokyo, Japan, 1992, p. 139-143.

Subramaniyan S and Prema P 2000. Cellulase-free xylanases from Bacillus and other microorganisms. *FEMS Microbiology Letters* **183:** 1-7.

Tapingkae W, Yachai M, Visessanguan W, Pongtanya P and Pongpiachan P 2008. Influence of crude xylanase from *Aspergillus niger* FAS128 on the in vitro digestibility and production performance of piglets. *Animal Feed Science and Technology* **140**(1-2): 125-138.

Indian Journal of Ecology (2021) 48(6): 1793-1797

Manuscript Number: 3450
NAAS Rating: 5.79

Protective Role of Allicin Compared with Kcl administration on some Cardiac Markers, Electrolyte, Oxidative Status and Gene Expression of NOS in Ovariectomized Rabbits

Hayder S. Rwayyih and Luma Waleed Khaleel

Department of Physiology & Pharmacology, College of Veterinary Medicine
University of Baghdad, Iraq
E-mail: Haider_sabih91@yahoo.com

***Abstract*:** The present experiment was designed to study the protective role of Allicin on some cardiac markers, electrolyte, oxidative status and gene expression of NOS in Ovariectomized rabbits. Forty-two female Rabbits (7-8 weeks) were used in this study. Ovariectomy was performed on twenty-eight of female rabbits. The animals were divided equally in to four groups: Group one (GO_1): Ovariectomized rabbits received distilled water. Group two (GO_2): Ovariectomized rabbits received Allicin orally (10 mg/kg body weight).Group three (GO_3): Ovariectomized rabbits received Kcl orally (1.39g body weight). Group four (GO_4): Ovariectomized rabbits received Kcl orally (1.39g body weight) and Allicin orally (10 mg/kg body weight). The daily administration of Allicin for 60 days caused a significant decrease serum creatine phosphokinase (175.40 and 139.20) compared with in Ovariectomized groups (313.40 and 299.20, respectively). Allicin supplementation has a protective role concerning the increase in nitric oxide synthase. There was significant increase in NO3 (7.67and 7.25) compared with Ovariectomized (3.89 and 5.24 with distilled water and Kcl, respectively). GPX concentration was in groups with Allicin than in Ovariectomized rabbits received D.W and Kcl. The results confirm the protection action of Allicin ovariectomized rabbits against the effect of some aged cardiac markers.

***Keywords*:** Electrolyte, Oxidative status, Gene expression, NOS, Ovariectomized rabbits

Allicin was discovered as part of efforts to create thiamine derivatives in the 1950s, mainly in Japan. Allicin became a model for medicinal chemistry efforts to create other thiamine disulfides. The results included sulbutiamine, fursultiamine (thiamine tetrahydrofurfuryl disulfide) and benfothiamine. These compounds are hydrophobic, easily pass from the intestines to the bloodstream, and are reduced to thiamine by cysteine or glutathione (Bettendorff et al 2014). Allicin is an organosulfur compound obtained from garlic, a species in the family Alliaceae (Rani and Kumar 2014). It was first isolated and studied in the laboratory by Chester J. Cavallito and John Hays Bailey in 1944. The biosynthesis of Allicin commences with the conversion of cysteine into S-allyl-L-cysteine. Oxidation of this thioether gives the sulfoxide (alliin). The enzyme alliinase, which contains pyridoxal phosphate (PLP), cleaves alliin, generating allysulfenic acid (CH2=CHCH2SOH), pyruvate, and ammonium. At room temperature, two molecules of allysulfenic acid condense to form allicin (Alemkhoumaram et al 2019). The allicin generated is unstable and quickly changes into a series of other sulfur-containing compounds such as diallyl disulfide (Ilic et al 2012). Allicin is part of a defense mechanism against attacks by pests on the garlic plant. It is effective in reducing relapses and progression of disability. Shakir and Khalil (2015) concluded that alcoholic extract of dill seeds was increase in serum glutathione concentration (GSH) and effective in reducing the complications of diabetes mellitus such as nephropathy such as in allicin.

In the recent years, investigations in human and animal models have provided abundant evidence that age-dependent oxidative stress plays an important role in cardiovascular diseases (Dai et al 2011). Studies indicate that antioxidants prevent development of many cardiovascular diseases and may even improve course of diseases, such as atherosclerosis, hypertension, ischemia reperfusion, or heart failure. Allicin administration proved effective in preventing or at least delaying pathological processes in various experimental models in which ROS have been implicated (Zhu et al 2012). Gender differences in the risk of cardiovascular diseases are well recognized, with premenopausal female exhibiting a lower risk than age-matched male. Estrogen treatment improves endothelial dysfunction, a major contributor to the pathophysiology of cardiovascular disease, through up regulation of endothelial cell genes, such as endothelial nitric oxide syntheses (Janaszak-Jasiecka et al 2021). Therefore, in light of the above insights, present study was conducted to investigate

the potential influence of oral supplementation with Allicin on some aged related metabolic disorders in intact and ovariectomized rabbits .

MATERIAL AND METHODS

Animal and experimental design: This experiment was carried out in the animal house at the College of Veterinary Medicine, University of Baghdad during August, 2019 till June, 2020. Twenty eight Rabbits were used in this study and age ranged between 7-8 weeks, and r weight was around 820-1050 gram. These animals were kept under suitable environmental conditions of 20-25 0C in an air conditioned room and photoperiod of 12 hours daily (Gary and Donald 1997). Ovariectomy was performed to twenty eight of female rabbits. The animals were divided equally in to four groups as follows (GO_1): Ovariectomized rabbits received distilled water. Group two (GO_2): Ovariectomized rabbits received Allicin orally (10 mg/kg body weight). Group three (GO_3): Ovariectomized rabbits received Kcl orally (1.39 body weight). Group four (GO_4): Ovariectomized rabbits received Kcl orally (1.39g body weight) and Allicin orally (10 mg/kg body weight).

Ovariectomy operation technique: Ovariectomy for both ovaries was performed to all rabbits according the procedure followed by Meyer et al (2001). The animals were kept individually with post-operative care and pencil line streptomycin was injected intramuscularly for 5 days.

Allicin dose: Allicin capsule contain 180 mg allisure allicin powder. Allicinmax UK could be 90-180 mg and was taken daily. The dose for each rabbit was 10mg/kg body weight and was calculated according to Fawzi and Elsohaby (2017).

Parameters determination: The principle of Ichroma™ CK-MB uses a sandwich immunofluorescence assay conjugated Anti-CK-MB in a detection buffer binds to CK-MB in a sample to form an antigen-antibody complex (Lewandrowski et al 2002). ichroma™ Tn-I is based on a lateral flow immunoassay system using an antigen-antibody reaction with the fluorescence technology (Panteghini et al 2004). Lactate dehydrogenase is a hydrogen transfer enzyme that catalyzes the oxidation of L-lactate to pyruvate with the mediation of NAD+ as a hydrogen acceptor (Kurutas et al 2006). The sodium and the protein in the serum are precipitated with magnesium uranyl acetate. Potassium is determined spectrophotometrically through a kinetic coupling assay system using potassium dependent pyruvate kinase. Pyruvate generated is converted to lactate accompanying conversion of NADH to NAD. The corresponding decrease of optical density at 380 nm is proportional to the potassium concentration in the serum (Wu 2006). GPX catalyze the reaction with glutathione reductase (GR). Peroxynitrite interpose nitration of phenol that is form the nitrophenol, and formed the basis of the peroxynitrite test. Briefly, 10 µL serums was placed in glass tube and added to 5 mM phenol in 50 mM of sodium phosphate buffer (pH7.2) to the final volume of 2 mL and mix well. This was incubated for 2 h at 37 °C, and followed by addition 15 µL of 0.1 NaOH then it mixed. Primer Design the cDNA sequences of Nos3 gene were obtained from the NCBI GenBank database. RT-qPCR primers were designed using Primer Premier 3 software with melting temperature between 58 to 62oC, primer length between 18 to 23 nucleotides, and PCR amplicon length within 75 to 150 base pair. The standard curve method employs a dilution series of known template copy number in the qPCR assay (Applied Biosystems 2003).

Statistical analysis: All data were subjected to assess the significant differences among mean by using SAS (SAS 2010).

RESULTS AND DISCUSSION

There was significant decrease in CPK level in ovariectomized groups that received allicin (GO2 and GO4). The serum troponin level shows significant decrease in GO2 as compared (GO1) group. Moreover, the two groups that received allicin (GO2 and GO4) showed significantly lower serum troponin as compared with groups that not received allicin (GO1and GO3). There was significant decrease in serum lactate dehydrogenase level in groups that received allicin (GO2 and GO4) as compared with those groups that not received allicin (GO1 and GO3). These results show a significant decrease) of serum Na^+ in GO2 and GO4 ovariectomized rabbits as compared with control and group that received KCL. On the other hand, there is on difference between these later two groups (GO1 and GO3). KCL administration significantly increased in K^+ concentration as compared with control group. There was increase in GPX level in groups received allicin (GO2 and GO4) in comparison with groups that received D.W (GO1) and that received KC(GO3). The serum peroxynitrite concentration (MM/L) and shows a significant decrease in peroxynitrite level in groups that received allicin (GO2 and GO4) in comparison with groups that received D.W (GO1) and KCL (GO3). After 60 day interval of treatment, the quantitative expression of NOs3 in aorta tissue indicated significant increase in values of NOs3 gene expression in aorta tissues of group that received 10 mg/kg B.W allicin, 1.39 g/B.W KCL and both in comparison with in the GO1 group (Table 2).

Clinically, CK is assayed in blood as a marker of damage of CK-rich tissue such as in myocardial infarction (heart attack), muscular dystrophy and acute kidney injury (Parsanathan and Jain 2020). The ovariectomized rabbits

had shown raised concentration of CPK, troponin and lactate dehydrogenase in serum significantly after 60 day. One mechanism of low estrogen has direct and indirect effects include increases in the creatine phosphokinase activity in skeletal muscle (Allen et al 2010). Moreover, elevated CTn in heart failure is associated with decreased left ventricular ejection fraction. Its elevation diagnosed in acute infarction, severe pulmonary embolism causing acute heart overload and heart failure (Lee et al 2019). Recently, it has been reported that Mesterolone (anabolic androgenic steroid) administration to female rabbits induces an elevation in serum cpk and troponin. This indicated that effect was due to anti-estrogenic role (Asker and Al- Azawi 2021). The anabolic effect of mesterolone increased the activity of CK in skeletal muscle and increases the circulation insulin like growth factor (IGF-1) (Aboalola 2017).

Supplementation of allicin to the intact and ovariectomized rabbits at a dose of 10mg/kg body weight produced a significant amelioration in the heart damage markers. The present study shows a significant elevation in the beneficial antioxidant glutathione level in groups administrated with allicin and associated with regeneration of cardiac damage. Therefore, the reduced oxidative stress on the heart in allicin supplemented group with reduced ROS led the heart to spend less amount of energy which is shown by decreasing CPK level in blood (Noeman et al 2011). Supplementation of allicin to the intact and ovariectomized rabbits at a dose of 10mg/kg B.wt produced a significant amelioration in the heart damage markers. This is associated with decreasing in the level of serum lipid and ameliorating of oxidative stress in heart tissues (Gomes and Negrato 2014). The allicin may exert protective effects on the myocardium. Allicin is thought to have a high antioxidant capacity and as such may have the ability to scavenge free radicals and stimulate the expression and activities of certain antioxidant enzymes, thereby limiting the oxidative damage of cardiomyocytes exposed to conditions of stress or injury (Mendelsohn and Karas 1999). Therefore, the concentration of troponin decreased in the animals that were treated with allicin. Abnormalities of these electrolytes due to different causes can lead to a significant cardiac life threatening events. However, the ovariectomized rabbits used in this study are a desirable model with clinical feature of estrogen efficiency or menopausal. Elevated serum Na level in this animal could be attributed to the lack effect of estrogen on the renin-angiotensin system to regulated Na reabsorption (Medina et al 2020). Sodium and chloride serum levels are both carefully controlled by the kidneys, and acute and chronic excessive intake of both ions can cause adverse health effect. However, only serum sodium is thought to be strongly correlated to blood pressure levels and cardiovascular disease (Faraj 2015). A decrease in serum potassium (K) level has been suggested to be a fairly common observation in patients with acute coronary syndrome (ACS), which has been shown to increase the risk of cardiac events, including lethal ventricular arrhythmias (Sekiyama et al 2013).

Allicin also inhibit the renin angiotensin aldosterone system (RAAS) and prostaglandin synthesis. The change in this balance favors vasodilation. This is from garlic's inhibition of angiotensin converting enzyme (ACE) activity. The reductions in ACE activity results in a number of

Table 1. Protective role of allicin compared with KCl administration for 60 days on serum(CPK, Tn, Na, LDH, K, GPX and peroxynitrite) concentration in ovariectomized rabbits

Parameter/ Group	Serum CK level (IU L^{-1})	Serum troponin level (ng M^{-1})	Serum LDH (ng M^{-1})	Na concentration (mmol)	K concentration (mmol)	Glutathione peroxidase (M L^{-1})	Peroxynitrite concentration (MM L^{-1})
GO_1	313.40±2.78A	131.66±2.46B	198.20±2.33B	130.00±1.04A	3.68±0.10C	79.02±1.29D	1.92±0.01A
GO_2	175.40±1.88C	83.00±0.70D	91.40±1.43D	119.00±1.09C	4.34±0.11B	98.54±1.36A	1.07±0.003C
GO_3	299.20±6.22B	156.64±0.01A	312.60±8.00A	130.20±1.06A	4.70±0.08A	76.80±6.22C	1.91±0.007A
GO_4	139.20±2.47D	113.72±0.99C	137.00±0.89C	125.20±1.39B	4.70±0.08A	83.80±1.59B	1.34±0.005B

Values are presented as Means ± SE . Different capital letters refer significant differences between groups within one column at (P≤0.05).

Table 2. Relative Quantification of nitric oxide synthase (NOs3) gene expression in tissue of aorta after administration allicin in ovariectomized rabbits

Group/ Parameter	Go1 d.w	Go2 (10mg kg^{-1} bw allicin)	Go3 (1.39g bw kcl)	Go4 (1.39g bw kcl and 10 mg kg^{-1} bw allicin)
Tissue nitric oxide synthase3 (NO3)	3.89±0.02D	7.67±0.02A	5.24±0.01C	7.25±0.01B
LSD	0.06			

See Table 1 for details

favorable effects that cause reductions in blood pressure. These mechanisms could be summarized as s: The first effect is the reduction in angiotensin II (ATII), which is known to be a direct vasoconstrictor. Secondly, a reduction in ATII will decrease adrenal production of aldosterone In another study on the cardioprotective actions of allicin in ischemia and reperfusion, contributed to its ability to attenuate ACE activity (Boschitsch et al 2010). The decrease of estrogen level in ovariectomized rabbits could cause a generation of caused by hydroxyl radicals and causing subsequent damage to DNA, proteins, and membrane lipids. In most cells, H2O2 can be detoxified by catalase and glutathione peroxidase, the latter use GSH as co enzyme. Cell necrosis after mitochondrial GSH depletion has been ascribed to increased steady-state levels of reactive oxygen species that lead to mitochondria damage and dysfunction (Tan and Suda 2018). Allicin can enhance hepatic glutathione (GSH) and GSH-related enzyme system. Allicin selectively expresses the glutathione S-transferase (GST) gene in the murine gastrointestinal tract and liver (Andorfer et al 2004). The results suggest that 10 mg/Kg. B.W allicin may potentially enhance the antioxidation and detoxification capability of primary rabbits cardiac cells. Allicin increase the nuclear factor erythroid 2–related factor 2 (Nrf_2) expression and consequently their target genes (GPx), which led to decrease in hypertension, oxidative stress, ultimately improving cardiac structure and performance (Zhou et al 2014). Abed and Al-Azawi (2020) concluded that the increase in Nrf2 Mrna in animals treated with Anabolic Androgenic steroids (AAS) could associated with the oxidative stress caused by AAS because the antioxidant pathway of Nrf_2 is an emerging master of the defense against oxidative stress.

The molecular mechanisms associated with estrogenic modulation of hypertensive heart disease, and specifically Left ventricular diastolic dysfunction (LVDD), are complex, but reduced NO availability and altered NOS system component expression and activity have been implicated as potential contributors. Briefly, NO activity is the net result of a balance between its production by NOS and its inactivation by ROS (i.e., free radicals), such as superoxide (Rubanyi 1986). The ovariectomized rabbits in the present study had revealed a deceased in the expression of NO3 activity and this could be explained by the fact suggested that under various pathological states, both NO and superoxide are increased by NOS with a net balance being a decrease in NO activity. This concept of “uncoupling” of NOS has been implicated as a major factor responsible for endothelial dysfunction, diastolic dysfunction, and left ventricular (LV) remodeling (Silberman et al 2010).

The mechanism of allicin associated vasodilation is mainly attributed to its ability to increase the production of hydrogen sulfide (H2S), (Shouk et al 2014). It is known that red blood cells will produce H2S when provided with sulfur containing products. As mentioned earlier, allicin is degraded when taken with water to produce organic polysulfides. These garlic derived polysulfides contribute the sulfur needed by the RBC to increase the production of H2S. Upon its production, H2S will bind to and activate vascular KATPchannels, thereby resulting in hyperpolarization of the vascular smooth muscle cells (Sun et al 2015). Hyperpolarization of these cells causes vasodilation or vascular relaxation that facilitates a reduction in blood pressure.

In addition allicin has cardio protective effect through prevention of cardiac mitochondrial dysfunction caused by sever oxidative stress during ischemic reperfusion in animals. An increase in proteins expression of antisuperoxide indicators, catalase, GPx and SOD as markers of antioxidative activity was documented as possible mechanism of antioxidant activity of allicin (Abdel-Daim et al 2019).

REFERENCES

Abdel-Daim MM, Abushouk AI, Donia T, Alarifi S, Alkahtani S, Aleya L and Bungau SG 2019. The nephroprotective effects of allicin and ascorbic acid against cisplatin-induced toxicity in rats. *Environmental Science and Pollution Research* **26**(13): 13502-13509.

Abed SK and Al-Azawi TS 2020. Selenium enriched yeast modifies the effects of methandienone in male rabbits on the HPA axis and adrenal gland oxidative stress. *Al-Anbar Journal of Veterinary Sciences* **13**(2): ٩١-٩٩.

Alemkhoumaram MH, Keshtkar AH and Mirzaie Asl A 2019. Study of Agromorphological diversity, and path analysis of bulb yield and allicin content of Iranian garlic landraces under Hamedan Region. *Journal of Horticultural Science* **33**(3): 481-497.

Allen PJ, D'anci KE, Kanarek RB and Renshaw PF 2010. Chronic creatine supplementation alters depression-like behavior in rodents in a sex-dependent manner. *Neuropsychopharmacology* **35**(2): 534-546.

Andorfer JH, Tchaikovskaya T and Listowsky I 2004. Selective expression of glutathione S-transferase genes in the murine gastrointestinal tract in response to dietary organosulfur compounds. *Carcinogenesis* **25**(3): 359-367.

Applied Biosystems 2003. Creating standard curves with genomic DNA or Plasmid DNA templates for use in quantitative PCR. *ReVision*: 1–8.

Asker MH and Al-Azawi SS 2021. Alpha lipoic acid against the adverse action of mesterolone on cardiac and renal. *Biochemical and Cellular Archives* 21(1): 373-377.

Bettendorff L, Lakaye B, Kohn G and Wins P 2014. Thiamine triphosphate: A ubiquitous molecule in search of a physiological role. *Metabolic Brain Disease* **29**(4): 1069-1082.

Boschitsch E, Mayerhofer S and Magometschnigg D 2010. Hypertension in women: The role of progesterone and aldosterone. *Climacteric* **13**(4): 307-313.

Dai DF, Johnson SC, Villarin JJ, Chin MT, Nieves-Cintrón M, Chen T and Rabinovitch PS 2011. Mitochondrial oxidative stress mediates angiotensin II–induced cardiac hypertrophy and Gαq overexpression–induced heart failure. *Circulation Research*

108(7): 837-846.

Faraj HR 2015. Clinical study of some electrolytes (sodium, chloride and potassium) with patients in acute coronary syndrome (ACS) in Thi–Qar Governorate, Iraq. *International Journal of Current Microbiology and Applied Sciences* **4**(3): 700-705.

Fawzi EMV and Elsohaby I 2017. Prevalence of gastrointestinal nematodes and the role of allicin in treatment of cattle in Sharkia Governorate. *Zagazig Veterinary Journal* **45**(Supplementary 1): 109-117.

Gary LW and Donald DH 1997. A comparison Ketamine and a combination of ketamine xylazine for effective surgical anesthesia in rabbit. *Laboratory Animal Science* **26**(5): 804-806.

Gomes MB and Negrato CA 2014. Alpha-lipoic acid as a pleiotropic compound with potential therapeutic use in diabetes and other chronic diseases. *Diabetology & Metabolic Syndrome* **6**(1): 1-18.

Ilić D, Nikolić V, Stanković M, Nikolić L, Stanojević L, Mladenović-Ranisavljević I and Šmelcerović A 2012. Transformation of synthetic allicin: the influence of ultrasound, microwaves, different solvents and temperatures, and the products isolation. *The Scientific World Journal*. Retrieved from https://doi.org/10.1100/2012/561823

Janaszak-Jasiecka A, Siekierzycka A, Płoska A, Dobrucki IT and Kalinowski L 2021. Endothelial dysfunction driven by hypoxia: The influence of oxygen deficiency on NO bioavailability. *Biomolecules* **11**(7): 982.

Lee JH, Kim MS, Kim EJ, Park DG, Cho HJ, Yoo BS and Choi DJ 2019. KSHF guidelines for the management of acute heart failure: Part I. definition, epidemiology and diagnosis of acute heart failure. *Korean Circulation Journal* **49**(1): 1-21.

Lewandrowski K, Chen A and Januzzi J 2002. Cardiac markers for myocardial infarction. *American Journal of Clinical Pathology* **118**(Suppl 1): S93-S99.

Medina D, Mehay D and Arnold AC 2020. Sex differences in cardiovascular actions of the renin–angiotensin system. *Clinical Autonomic Research* **30**(5): 393-408.

Mendelsohn ME and Karas RH 1999. The protective effects of estrogen on the cardiovascular system. *New England Journal of Medicine* **340**(23): 1801-1811.

Meyer Jr, RA, Tsahakis PJ, Martin DF, Banks DM, Harrow ME and Kiebzak GM 2001. Age and ovariectomy impair both the normalization of mechanical properties and the accretion of mineral by the fracture callus in rats. *Journal of Orthopaedic Research* **19**(3): 428-435.

Noeman SA, Hamooda HE and Baalash AA 2011. Biochemical study of oxidative stress markers in the liver, kidney and heart of high fat diet induced obesity in rats. *Diabetology and Metabolic Syndrome* **3**(1): 1-8.

Parsanathan R and Jain SK 2020. Novel invasive and noninvasive cardiac-specific biomarkers in obesity and cardiovascular diseases. *Metabolic Syndrome and Related Disorders* **18**(1): 10-30.

Rani A and Kumar A 2014. Allium sativum: A global natural herb with medical properties. *Journal Academica* **4**(1): 33-37.

Rubanyi GM 1986. Superoxide anions and hyperoxia inactive endothelium-derived relaxing factor. *American Journal of Physiology* **250**: H815-H821.

SAS 2010. *SAS\STAT user Guide for Personal computer*. Release 9.1SAS Institute Inc., cary, N.C, USA.

Sekiyama H, Nagoshi T, Komukai K, Matsushima M, Katoh D, Ogawa K and Yoshimura M 2013. Transient decrease in serum potassium level during ischemic attack of acute coronary syndrome: paradoxical contribution of plasma glucose level and glycohemoglobin. *Cardiovascular Diabetology* **12**(1): 1-7.

Shakir WA and Khalil LW 2015. The protective role of alcoholic extract of Anethum graveolens seeds on renal function in alloxan induced diabetic rabbits. *The Iraqi Journal of Veterinary Medicine* **39**(2): 1-6.

Shouk R, Abdou A, Shetty K, Sarkar D and Eid AH 2014. Mechanisms underlying the antihypertensive effects of garlic bioactives. *Nutrition Research* **34**(2): 106-115.

Silberman GA, Fan THM, Liu H, Jiao Z, Xiao HD, Lovelock JD and Dudley Jr SC 2010. Uncoupled cardiac nitric oxide synthase mediates diastolic dysfunction. *Circulation* **121**(4): 519-528.

Sun Y, Huang Y, Zhang R, Chen Q, Chen J, Zong Y and Jin H 2015. Hydrogen sulfide upregulates K ATP channel expression in vascular smooth muscle cells of spontaneously hypertensive rats. *Journal of Molecular Medicine* **93**(4): 439-455.

Tan DQ and Suda T 2018. Reactive oxygen species and mitochondrial homeostasis as regulators of stem cell fate and function. *Antioxidants & Redox Signaling* **29**(2): 149-168.

Wu H, Cowing JA, Michaelides M, Wilkie SE, Jeffery G, Jenkins SA and Webster AR 2006. Mutations in the gene KCNV2 encoding a voltage-gated potassium channel subunit cause “cone dystrophy with supernormal rod electroretinogram” in humans. *The American Journal of Human Genetics* **79**(3): 574-579.

Zhou S, Sun W, Zhang Z and Zheng Y 2014. The role of Nrf2-mediated pathway in cardiac remodeling and heart failure. *Oxidative Medicine and Cellular Longevity.* Retrieved from https://doi.org/10.1155/2014/260429.

Zhu JW, Chen T, Guan J, Liu WB and Liu J 2012. Neuroprotective effects of allicin on spinal cord ischemia-reperfusion injury via improvement of mitochondrial function in rabbits. *Neurochemistry International* **61**(5): 640-648.

Received 12 July, 2021; Accepted 10 November, 2021

Indian Journal of Ecology (2021) 48(6): 1798-1801

Manuscript Number: 3451
NAAS Rating: 5.79

Natural Occurrence of *Euphorbia leaf curl virus* (EuLCV) Infecting Zinnia in India

Shikha Sharma, Vineet K. Sharma and Tapish Pawar

Department of Plant Pathology, Punjab Agricultural University, Ludhiana-141 004, India
E-mail: shikhasharma-coapp@pau.edu

***Abstract*:** In the year 2020, plants of *Zinnia elegans* were observed to be showing viral disease symptoms on campus of Punjab Agricultural University, Ludhiana. The plants exhibited puckering, thickening and curling of leaf lamina. Nucleic acid based detection of the associated pathogen was done *via* PCR. The sequencing of the desired amplicon from coat protein (CP) region of the virus confirmed the association of *Euphorbia leaf curl virus* (EuLCuV). The variable symptoms *viz.,* accession no. OK094316 shared 95.98 % nucleotide similarity with EuLCuV Fujian isolate. Polymerase chain reaction on the basis of phylogenetic as well as species demarcation tool, the isolate in the study was considered as *Euphorbia leaf curl virus* (EuLCuV). To best of our knowledge, this is the first report of occurrence of EuLCV in India on zinnia.

***Keywords*:** Begomovirus, Coat protein, PCR, Zinnia, *Euphorbia leaf curl virus*

Zinnia (*Zinnia elegans* Jacq.) is an ornamental flowering plant. The flower is named after a German Professor, Johann Gottfried Zinn (1727-1759) and has gained its popularity as garden annual in late 19th century. The flower can grow both as an annual as well as perennial species. However, in India, it is mostly cultivated as summer season annual. Zinnia is native to Mexico but its cultivation is extended up to USA from Texas and Colorado in the far north to Brazil and Chile in the far south (Ewart 1981). *Z. elegans* possess phytoremediation properties and has the potential to accumulates lead and cadmium in different parts of plant *viz.,* shoots, leaves and roots (Thamayanthi and Sharavanan 2012). Zinnia is susceptible to large number of biotic and abiotic stresses. Many pathogens infect zinnia and lead to huge economic losses. Among the fungal pathogens, *Alternaria alternata*, *Alternaria zinniae*, *Glomerella* sp. and *Fusarium* sp. are major seed-borne fungi. These pathogens infect the seeds and cause seed as well as seedling rotting. Species of *Xanthomonas* cause leaf spots in zinnia (Hernandez and Trujillo 2000). Among the viral pathogens, *Tomato aspermy virus* (TAV) was detected to infect zinnia and caused mosaic and chlorosis kind of symptoms (Kameya et al 1996). In India, a mosaic disease from zinnia was reported which was vectored by *Aphis gossypii* and *Myzus persicae* (Sastry et al 1973). Another viral disease *i.e* Zinnia mild mottle was reported to be transmitted by green peach aphid. The crop has also been reported to carry the *Watermelon mosaic virus* (WMV) infection in latent state. Around the world other diseases of zinnia are also reported which can cause huge economic losses (Farzadfar et al 2005).

Begomoviruses are a large group of plant DNA viruses which are transmitted in persistent manner by whitefly (Satter et al 2017). These viruses are major constraints causing huge economic losses to food and fibre crops worldwide, mainly in tropical and sub-tropical parts of the world (Varma and Malathi 2003, Tiwari et al 2008). Some begomoviruses were reported earlier to be associated with leaf curling symptoms *viz. Tobacco leaf curl virus*, *Cotton leaf curl virus*, *Ageratum enation virus* and *Alternanthera yellow vein virus* (Ha et al 2008, Kang et al 2004, Kumar et al 2010 and Storey 1931). *Euphorbia leaf curl virus* (EuLCV), belonging to the genus Begomovirus, has been identified in poinsettia (*Euphorbia pulcherrima*) and passion fruit (*Passiflora edulis*) plants cultivated in China and Taiwan (Cheng et al 2014, Wu et al 2011). In the present study, symptoms of virus infection were observed in flower beds of zinnia at Punjab Agricultural University, Ludhiana and attempt was made to characterize the associated pathogen with the disease.

MATERIAL AND METHODS

During 2020, monitoring and surveillance of the ornamental plants of university campus were undertaken. Plants of zinnia planted in campus of PAU, Ludhiana were found to exhibit viral disease symptoms. Leaf samples of five plants showing puckering, curling of leaf lamina and main vein thickening were collected and preserved at -80°C for the *in vitro* studies of the molecular characterization. Total DNA (Plant DNA+ Viral DNA) was extracted by using the Cetyltrimethylammonium Bromide (CTAB) method (Doyle and Doyle 1987). Isolated DNA was quantified with the help

of Eppendorf Bio-Spectrometer. Subsequently, total DNA was enriched with circular viral genome by using rolling circle amplification (RCA) with the help of Φ29 DNA polymerase as per manufacturer's protocol (GE Healthcare UK Limited). The RCA products were used as template for detection *via* Polymerase Chain Reaction (PCR) with universal degenerate primer (Rojas et al 1993). While the primer pairs Beta 01/ 02 (Briddon et al 2002) and Alpha UN 101/ 102 (Bull et al 2003) were used to amplify the betasatellite and alphasatellite, respectively. For characterization of main DNA associated, primer pair corresponding to coat protein of virus was further utilized. The PCR reaction was carried out by using the EmeraldAmp® GT PCR Master Mix（2× Premix). The amplified PCR products were visualized on the 1% Agrose gel stained with Ethidium Bromide. Desired amplicons were purified by using NucleoSpin Gel and PCR Clean-up kit (Macherey-Nagel, 95 Germany). Afterward, the purified PCR products were outsourced to AgriGenome Labs Pvt. Ltd. (Kerala) for bi-directional sanger sequencing. The raw reads thus obtained *via* sanger sequencing were analyzed and assembled using SeqMan (DNA Star Inc., Madison, USA). Overlapping contigs were prepared and searched in the BLASTn (Basic Local Alignment Searching Tool for nucleotides) algorithm available at NCBI. Top BLAST hits sequences were retrieved and aligned using the Clustal W algorithm available in MEGA X (Kumar et al 2018). The phylogenetic tree was constructed using the Neighbor-Joining method with 1000 bootstrap replicates. Pairwise nucleotide identity was determined by using the Sequence Demarcation Tool (SDT) version 1.2 (Muhire et al 2014).

RESULTS AND DISCUSSION

Leaf curling symptoms were recorded at PAU campus, Ludhiana (Fig. 1). At later stages, the plants showed severe puckering of leaves. In the nucleic acid-based detection assay (PCR) with coat protein specific primers, a desired amplicon of ~1200 bp was observed in all the subjected samples which suggested the association of begomovirus with infected zinnia samples. Sequencing of one sample was performed (Agri Genome, India). It was evident from the BLAST results that the virus species in study shared 99.99 per cent nucleotide identity with other begomovirus (s) species deposited in NCBI database. Top blast hits showing 100 per cent coverage and nucleotide sequence similarity >97 per cent were retrieved for further phylogenetic analysis. The partial CP gene of begomovirus isolate amplified in this study was analysed with 25 other begomoviruses including isolates of *Cherry tomato leaf curl virus* (CToLCV), *Tomato leaf curl virus* (ToLCV), *Papaya leaf curl virus* (PaLCuV), *Croton yellow vein mosaic virus* (CYVMV), *Pedialanthus leaf curl virus* (PeLCuV), *Ageratum enation virus* (AEV), *Tobacco curly shoot virus* (ToCSV), *Cestrum yellow leaf curling virus* (CmYLCV) and *Euphorbia leaf curl virus* (EuLCV) which shared >95 per cent nucleotide sequence identity. Phylogenetic tree analysis (MEGA X) of coat protein sequence of zinnia isolate (EuLCuV, OK094316) showed clustering with isolates of *Euphorbia leaf curl virus* isolate Fujian (Fig. 2). The pairwise sequence similarity analysis was done with SDT v1.2 for the demarcation of species and coloured matrix chart was generated (Fig. 3). It became evident from SDT analysis that virus infecting zinnia shared ~ 95 per cent nucleotide similarity with EuLCV Fujian isolate

Fig. 1. Naturally infected Zinnia plants showing puckering and curling

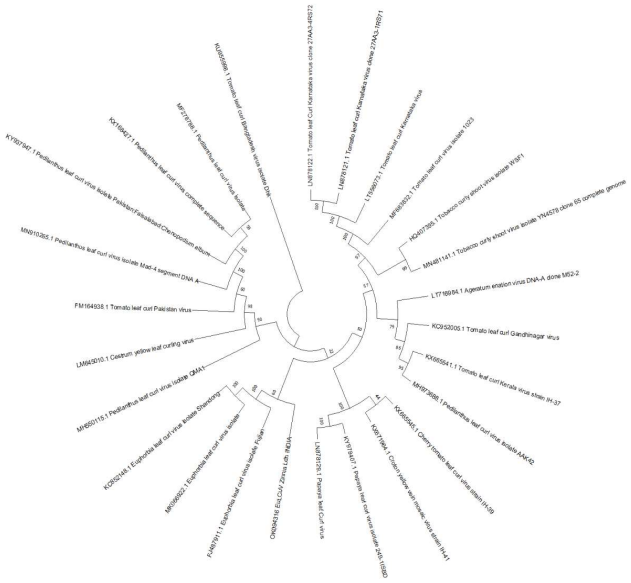

Fig. 2. A neighbour-joining phylogenetic tree obtained *via* MEGA X software from top BLAST hits of *Zinnia elegans* virus isolate (OK094316)

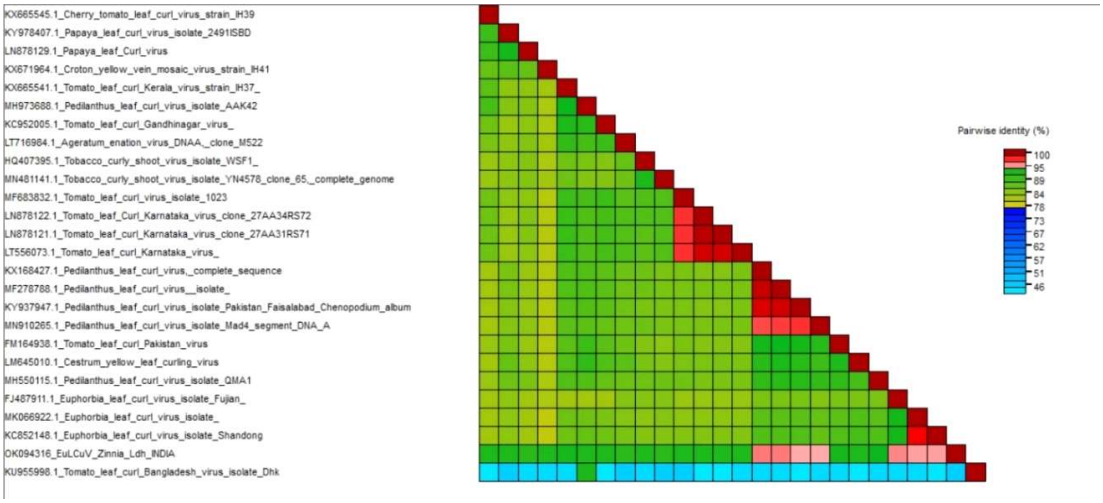

Fig. 3. Analysis of top BLAST hits with SDT 1.2 tool for begomovirus species demarcation

(FJ487911). However, the same level of nucleotide similarity was also shared with PeLCuV isolates (KX168427 and MF278728). Based on the new criterion (species demarcation cut-off value ≥ 91%) given by Brown et al (2015), it was concluded that the virus associated with zinnia leaf curl disease was EuLCV. Zinnia is susceptible to a number of viral diseases. Leaf curling, mosaic and mottling in zinnia are caused due to viral pathogens. *Zinnia leaf curl virus* has been reported from India to infect zinnia under natural ephiphytotic conditions (Pandey and Tiwari 2012). *Euphorbia leaf curl virus* (EuLCuV) has so far been reported from China, Taiwan and South Korea (Cheng et al 2014, Wu et al 2011).The virus has so far been reported to infect *Euphorbia pulcherrima* and *Passiflora* sp (NCBI database). A total of 24 full genome sequences are available in NCBI of EuLCuV. To best of our knowledge this is the first report of infection of zinnia by EuLCuV in India. Further, work on epidemiology and management of the zinnia disease complex and characterization of other strains of virus through full genome sequencing is required to be undertaken.

CONCLUSIONS

Zinnia plants showing puckering and curling types of symptoms were infected with EuLCuV. Further variability in symptomatology as well as severity of disease can vary depending on the association of different satellite molecules.

REFERENCES

Briddon RW, Bull SE, Mansoor S, Amin I and Markham PG 2002. Universal primers for PCR mediated amplification of DNA ß: A molecule associated with some monopartite begomoviruses. *Molecular Biotechnology* **20**: 315-318.

Brown JK, Zerbini FM, Navas-Castillo J, Moriones E, Ramos-Sobrinho R, Silva JCF, Fiallo-Olive E, Briddon RW, Herna´ndez-Zepeda C, Idris A, Malathi VG, Martin DP, Rivera-Bustamante R, Ueda S and Varsani A 2015. Revision of begomovirus taxonomy based on pairwise sequence comparisons. *Archives of Virology* **160**: 1593-1619.

Bull SE, Briddon RW and Markham PG 2003. Universal primers for the PCR-mediated amplification of DNA 1: A satelitte-like molecule associated with begomovirus-DNA beta complex. *Molecular Biotechnology* **23**(1): 83-86.

Cheng YH, Deng TC, Chen CC, Chiang CH and Chang CA 2014. First report of Euphorbia leaf curl virus and papaya leaf curl Guangdong virus on passion fruit in Taiwan. *Plant Disease* **98**(12): 1746.

Doyle JJ and Doyle JL 1987. A rapid DNA isolation for small quantities of fresh leaf tissue. *Phytochemical Bulletin* **19**: 11-15.

Ewart LC 1981. Zeroing in on zinnias. *American Vegetable Grower & Greenhouse Grower* **29**: 8-9.

Farzadfar S, Ohshima K, Pourrahim R, Golnaraghi AR, Jalali S and Ahoonmanesh A 2005. Occurrence of Turnip mosaic virus on ornamental crops in Iran. *Plant Pathology* **54**(2): 21-27.

Ha C, Coombs S, Revill P, Harding R, Vu M and Dale J 2008. Molecular characterization of begomoviruses and DNA satellites from Vietnam: Additional evidence that the New World geminiviruses were present in the Old World prior to continental separation. *Journal of General Virology* **89**: 312-326.

Hernandez Y and Trujillo G 2000. *Xanthomonas campestris* pv. zinniae infecting zinnia plants (Zinnia elegans Jacq.) in Venezuela. *Revista de la Facultad de Agronomia, Universidad del Zulia* **17**: 156-163.

Kameya MI, Suzuki Y, Hanada K, Ito S and Tanako S 1996. A new mosaic disease of zinnia caused by tomato aspermy virus. *Annals of Phytopathological Society of Japan* **62**: 175-176.

Kang SS, Athar M and Cheema SS 2004. Additional hosts for cotton leaf curl gemini-virus. *Agricultural Reserach Journal* **41**(1): 85-88.

Kumar S, Stecher G, Li M, Knyaz C and Tamura K 2018. MEGA X: molecular evolutionary genetics analysis across computing platforms. *Molecular Biology and Evolution* **35**(6): 1547.

Kumar Y, Hallan V and Zaidi AA 2010. First report of Ageratum enation virus causing leaf curl disease of Zinnia. *Journal of General Plant Pathology* **76**(6): 395-398.

Muhire BM, Varsani A and Martin DP 2014. SDT: A virus classification tool based on pairwise sequence alignment and identity calculation. *PLoS ONE*. https://doi.org/10.1371/journal.pone.0108277

Pandey N and Tiwari AK 2012. Identification of Zinnia leaf curl virus infecting *Zinnia elegans* in India. *ISABB Journal of*

Biotechnology and Bioinformatics **302**(1): 6-10.

Rojas MR, Gilbertson RL, Russel DR and Maxwell DP 1993. Use of degenerate primers in the polymerase chain reaction to detect whitefly transmitted Gemini viruses. *Plant Disease* **77**: 340-347.

Sattar MN, Iqbal Z, Tahir MN and Ullah S 2017. The prediction of a new CLCuD epidemic in the Old World. *Frontiers of Microbiology* **8**: 631.

Sastry KS, Sastry KSM and Singh SJ 1973. Studies on virus causing mosaic disease on *Zinnia elegans*. *Indian Journal of Mycology and Plant Pathology* **3**: 165-168.

Storey HH 1931. Tobacco leaf curl virus on Zinnia elegans. *Nature London* **128**:187.

Tewari JP 1976. *Zinnia elegans* Jacq., the latent host of watermelon mosaic virus. *Current Science* **45**: 37.

Received 12 July, 2021; Accepted 12 November, 2021

Thamayanthi D and Sharavanan PS 2012. Phyto-accmulation of cadmium polluted soil using Zinnia plants (*Zinnia elegans* L.). *International Journal of Current Science* (Special Issue) 311-315.

Tiwari AK, Snehi SK, Raj SK, Rao GP and Sharma PK 2008. Begomovirus; a major problem for cucurbitaceous crops in Eastern part of U.P. India. *Indian Journal of Virology* **19**(1): 124.

Varma A and Malathi VG 2003. Emerging gemini virus problems: A serious threat to crop production. *Annals of Applied Biology* **142**: 145-164.

Wu J, Zulfiqar A and Huang C 2011. Infectivity of Euphorbia leaf curl virus and interaction with Tomato yellow leaf curl China beta satellite. *Archives of virology* **156**(3): 517-521.

Indian Journal of Ecology (2021) 48(6): 1802-1808

Manuscript Number: 3452
NAAS Rating: 5.79

Screening the Virulence of *Metarhizium anisopliae* MT193505 against Spider Mite, *Tetranychus urticae* Koch

Dalia A. Waked and M. Eleawa

Plant Protection Research Institute, Agricultural Research Center, Dokki, Giza, Egypt
E-mail: dr.dalia188@yahoo.com

Abstract**:** *Tetranychus urticae* Koch is one of the most harmful pests of agricultural crops and management using synthetic acaricides is probably prone to different problems. Therefore, non- chemical measure are being developed as alternative option, avoiding those drawbacks. The present study aims at investigating the potential of the entomopathogenic fungus, *Metarhizium anisopliae* to control spider mite, *T. urticae* Koch. All fungal isolates were pathogenic to spider mite, causing mortality of 85.71% against *T. urticae* associated with LT_{50} values ranging from 3.12 and 6.52 days for 2.4 $x10^7$ and 2.4 $x10^9$ spore ml^{-1}. Concerning the factors affecting the activity of enzymes excreted by fungus, the optimum temperature was 30ºC and pH value was 6.0 for lipase and chitinase. The optimal incubation period was 5 and 7 days for lipase and chitinase, respectively. Chitinase gene on the fungus *M. anisopliae* was determined by PCR amplification achieves at annealing of 55ºC and appeared in a 900 bp fragment at gel marker. The adult mites of *T. urticae* treated by *M. anisopliae* culture were inspected by SEM that demonstrated the existence of colonies of *M. anisopliae* on the body surface of *T. urticae*, that could be recognize by many conidia.

Keywords**:** *M. anisopliae*, *T. urticae*, Spider mite, LT_{50}, Entomopathogenic fungus

Mites especially family tetranychidae are common agricultural pests that cause more economic losses than any other arthropod pest in many cases. The spider mite, *T. urticae* Koch is considered one of the major pests attacking different field and horticultural crops in Egypt. High numbers of *T. urticae* can decline the quality of the host plants very rapidly. Mite feeding may have both direct and indirect effects. Direct effects include defoliation, leaf fire, and even plant death. Reduced photosynthesis and transpiration are two indirect effects that may contribute to other problems in the plant. The amount of yield for that crop is also reduced as a result of this combination of effects on the host plant. In the last few years, many efforts have been done to mitigate the environmental pollution and death of natural enemies resulting from the use of pesticides to combat these pests has a negative impact on the ecosystem's ecological equilibrium and needed some alternative compounds for field crop protection. Entomopathogens fungi were a step among others. In addition to virulence of *M. anisopliae* against *T. urticae* also effect enzymes activities. The aim of this study is to evaluate of the factors affected lipase and chitinase activities of *Metarhizium anisopliae*.

MATERIAL AND METHODS

Culture of *Tetranychus urticae*: The colony of *T. urticae* was reared under laboratory conditions 27± 2ºC and 70 ± 5% R.H. at Plant Protection Research Institute, Giza, Egypt. Fungus was isolated from dead bodies of *T. urticae* which was obtained from leaves of maize crop and identification of isolated fungal species by Assiut University Mycological Centre (AUMC), Assiut, Egypt.

Harvesting of spores from agar to prepare the original treatment suspension: The spores of growing fungus were harvested by adding a mixture of 100 ml of sterile water + 50 ml of tween 80 to each petri- dish to reduce the surface tension of the spores suspension. The spores were harvested from the surface of agar by scraping with spatula into the mixture of water+ tween 80 then the crude suspension was collected in sterilized bottle the glass pearls were added to the bottle and shacked well using a laboratory horizontal shaker to separate the medium, mycelium and spores from each other. The big lumps of mycelium and growth media were removed from the suspension by using an ordinary tea sieve or muslin cloth.

Preparation of spore suspension: Determination of spore's concentration was made by using the Burker chamber (Hemocyte counter). The spores were harvested from the mass culture media of the fungus into sterile water containing 0.05% tween 80 (surfactant). Dilution was done to facilitate the spores suspension counting. One ml of initial spore's suspension was added to 9 ml of sterile water containing 0.05% tween 80 and then shacked well. Using 1/100 dilution rate was enough, taking the concentration of the initial suspension into consideration. A small drop of the

final dilution was put into the dish of Burker counter by using a Pasteur pipette. The dish should be full, but the water should not run out of it. A cover slip was carefully placed over the dish, so that the water drop spread over the sets of squares (the counting cells) after at least 2 min the spores sediment to the bottom of the counting cell, then the number of spores was counted under a microscope, in each of the nine squares surrounded by three lines, altogether nine squares surrounded in the upper counting cell and nine in the lower counting cell. The lines of the counter and the number of the counting squares can be differently arranged according to the type of the chamber. The counting was repeated for four times (4 drops) to obtain a good estimate of the spore concentration.

No. of spores in suspension = m x 2.5 x10^5 x d

Where: m= mean number of spores per one square, d= dilution rate

The volume of the square was usually at least in Burker chamber, 1/ 4000 ml, i.e. 2.5 x 10^5 is used in the formula.

Bioassay

Susceptibility of egg and adult female *T. urticae* to the entomopathogenic, fungi, *M. anisopliae:* To study the action of different conc. of *M. anisopliae* on eggs of *T. urticae* amount of adult females were transferred to leaf discs about 2.4 cm in diameter which were placed in petri – dish on moist cotton and were allowed to lay eggs on the lower surface of mulberry leaves discs for 24 hr. The adult females were removed after 24 hr. and the number of deposited eggs per disc was counted. The 70 eggs per discs surface were gently dipped separately in serial concentrations for about 5 seconds. In control test the leaf discs were dipped in water only. The treated eggs as well as the control were kept under constant temperature and 65% R.H. The egg not unhatched was calculated. The incubation period was calculated for eggs and immature survival to adulthood was observed daily and development was recorded and calculated the longevity and fecundity. The effect of *M. anisopliae* was evaluated against adult females of *T. urticae* using different age cultures (1, 3 and 7 days) at the concentrations, 2.4 x10^9, 2.4 x10^8 and 2.4 x10^7 spore ml^{-1}. Each concentration contained three different ages of the fungus that repeated 3 times. Every treatment was repeated seven times with 10 mites per replicate in the experimental arena, which consisted of 2 cm diameter mulberry leaf discs mounted on moist cotton in petri plates (9 cm diameter). All treatments sprayed until the leaf surface was only wet with very fine droplets, using a hand spray atomizer with a 50 ml capacity. The mortality per cent was calculated after 3, 7 and 10 days of treatment for each age of *M. anisopliae* and LT_{50} were calculated and the experiment incubated at 27 ± 2ºC.

Evaluation of the physical factors affecting lipase and chitinase activity: Fifty ml of basal medium is inoculated with one ml of 10^6 spores ml^{-1} and incubated for 96 hours in an orbital shaker at 150 rpm at three different temperatures (25,30, and 35ºC) to determine the optimum temperature for lipase and chitinase synthesis. To determine the best pH for lipase and chitinase activity, the above-mentioned basal media was buffered with 0.1 ml sodium phosphate to achieve pH of 5.0, 6.0, 7.0, and 8.0, respectively, while the control was a non-buffering basal medium. 50 ml of sterile growth medium inoculated for 96 hours at 150 rpm in an orbital shaker and 28ºC. Incubation period was screened for the tested fungi and its relation to enzyme activities.

Enzyme preparation: Treated mites at different concentrations, 2.4 x10^9, 2.4 x10^8 and 2.4 x10^7 spore ml^{-1} were treated with 50 mg from each concentration were repeated 3 times using a chilled glass Teflon homogenizer homogenized in distilled water (50 mg ml^{-1}). Homogenates were centrifuged at 5000 rpm for 20 minutes at 5°C. The deposits were discarded, and the supernatants were stored at -20°C until required.

Amylase enzyme activity: The digestion of amylase, starch and sucrose by amylase enzyme was estimated Ishaaya and Swiriski (1976). The group of free aldehydes produced by glucose after digestion with amylase, starch, and sucrose was determined.

Chitinase activity: This was estimated according to Ishaaya and Casida (1974).

Protease activity: The proteolytic activity of *T. urticae* was determined according to Birk et al (1962).

PCR: PCR is a quick and easy technique for amplification of a single section of DNA. Amplification usually happens as long as the fragment is present in the sample, regardless of the microorganisms' culture potential or viability.

Test fungi selection and PCR primer design: Chitinase gene product from fungus, *M. anisopliae* primers Chi2:chi2f–GACAAGCACCCGGAGCGC, chi2r-CTTGCTTGACACATTGGTAA. Were designed from the 18Sr RNA gene. Pure gene GENETAQ Green PCR Master Mix (2X) contains Taq DNA polymerase, optimized GENETAQ Green buffer, MgCL2, and dNTPs in a ready-to-use solution. Two tracking dyes and a density reagent are added to the Master Mix, allowing the PCR product to be directly applied to the gel. The dye in the master mix is consistent with downstream applications such as DNA sequencing, ligation, and restriction digestion and does not interfere with PCR results. Since there are fewer pipetting steps available for PCR setup, this ready-to-use formula saves time and prevents pollution. All of the properties of Taq DNA polymerase are preserved in the master blend. It can

amplify up to 6 kb of genomic DNA and up to 20 kb of viral DNA with high accuracy.

Images of GFP marked conidia by electron microscopy: This work carried out in the electronic microscope unit (SEM) at the Mansoura University, Egypt. The treated adult *T. urticae* with the *M. anisopliae* culture filtrate were examined by scanning electron microscope (SEM) by using high vacuum mode.

RESULTS AND DISCUSSIONS

The virulence of *M. anisopliae* showed a decrease in mobility and a cessation of feeding, and the body's fluid started oozing out. The mortality trend is positively correlated to both of the concentration and age of the culture (Table 1). The mortality until 10 days after treatment was 0% at one day age culture. Mortality started increasing as culture age increases the maximum mortality was 85.71% for 2.4 $x10^9$ spore ml^{-1} at 7 days, while the least mortality was 11.24% for 2.4 $x10^7$ at 3 days.

All concentrations of *M. anisopliae* caused significant mortality of *T. urticae* eggs reached 60% (Table 2) at concentration 2.4×10^9 spore ml^{-1} followed by 51.42% at concentration 2.4x10^8 spore ml^{-1} while the least concentration 2.4×10^6 spore ml^{-1} caused 25.71%. The incubation period for *T. urticae* eggs varied from 5.9 to 3.44 days. The life cycle was between 12 and 17.23 days for 2.4x10^6 and 2.4x10^9 spore ml^{-1} while it was 11.54 days in control. The longevity and fecundity were significantly affected and as compared to decreased than the control. There were significant differences in the fecundity and decreased to 37.13 eggs for high concentration, 2.4 x10^9 spore ml^{-1} compared with 18.11 eggs for control.

Evaluation of the physical factors affecting lipase and chitinase activity: Incubation temperatures varied in their effect on growth and activity of lipase and chitinase (Table 3). The activity of lipase was 88.2 u ml^{-1} at 30ºC and the chitinase activity was 76.51 u ml^{-1} for the same temperature. The biomass was 14.5 and 24.63 mg ml^{-1} for lipase and chitinase at 30ºC. Concerning the degree of the pH, under which the incubation is carried out, on the tested enzymes data in (Table 4) clarify that optimum pH varied from one enzyme to another and was 6 that have given the highest biomass (16.4 mg ml^{-1}) for lipase, the activity of which was 88.3 u ml^{-1} and in chitinase biomass was only 13.09 mg ml^{-1} and 82.25 u ml^{-1} of activity.

Data in Figure 1 and 2 show that different incubation

Table 1. Virulence of *M. anisopliae* against *T. urticae* against adult females

Treatment spore ml^{-1}	Age of fungus (days)	Mortality day after treatment (%)			
		3 days	7 days	10 days	LT_{50} days
2.4 $x10^7$	1	0.00±0.00^e	0.00±0.00^e	0.00±0.00^e	6.52
	3	11.42±0.51^d	20.00±0.74^c	45.71±1.87^d	
	7	18.57±0.63^d	28.57±0.89^c	52.85±2.04^c	
2. 4$x10^8$	1	0.00±0.00^e	0.00±0.00^d	0.00±0.00^e	7.61
	3	27.14±0.98^c	68.57±2.54^b	75.71±3.01^b	
	7	32.85±1.01^b	71.42±2.85^a	80.00±3.86^a	
2.4 $x10^9$	1	0.00±0.00^e	0.00±0.00^d	0.00±0.00^e	3.12
	3	34.28±1.04^b	74.28±3.06^a	81.44±3.97^a	
	7	48.57±1.23^a	80.00±4.11^a	85.71±4.35^a	
Control		0.00	0.00	0.00	

Means in columns followed by the same letter are not significantly different at 5%level (Duncan's multiple range tests). ± Standard Error

Table 2. Effect of entomopathogenic, fungus, *M. anisopliae* against *T. urticae* eggs and some biological aspects of *T. urticae* females

Conc. Spore ml^{-1}	Mortality (%)	Incubation period/days	Survival (%)	Life cycle (in days)	Development (%)	Longevity (days)	Fecundity (egg)
2.4x10^9	60.00	5.90	71.42	17.23	28.57	7.55^d	37.13^d
2.4x10^8	51.42	5.02	76.47	15.01	37.14	9.01^c	40.27^c
2.4x10^7	41.42	4.59	80.48	12.93	47.14	9.98^c	55.10^b
2.4x10^6	25.71	3.44	86.53	12.00	64.28	12.35^b	62.43^a
Control	7.14	3.16	95.38	11.54	88.57	15.26^a	68.11^a

Means in columns followed by the same letter are not significantly different at 5 per cent level (Duncan's multiple range tests)

periods affect lipase and chitinase activity of *M. anisopliae*, which activity of lipase and chitinase increased gradually from the first day of incubation period till sixth day for chitinase and fifth day for lipase. Chitinase activity ranged from zero to 0.88 u mg^{-1} from first to sixth day and for lipase activity from zero to 105.6 u ml^{-1} and begin to decrease at the seventh day to tenth day for chitinase and decrease at the sixth to tenth ranged from 102.99 to 18.6 u ml^{-1} for lipase. Resistance to a pesticides in insects, this is mostly attributed to the activity of enzymes that are either pesticide resistant or capable of degrading pesticides to nontoxic metabolites.

Chitinase activity: The change in the sensitivity of chitinase was revealed the activity to the fungus, *M. anisopliae* used (Table 5). The treatment with any of tested concentrations caused a variable level of the sensitivity towards the enzyme. All concentrations of *M. anisopliae* culture increased the activity of chitinase, the maximum activity was 526.35 u gm^{-1} for 2.4 $x10^9$ spore ml^{-1} while was 302.11 and 253.69 u gm^{-1} for 2.4 $x10^8$ and 2.4 $x10^7$ spore ml^{-1} respectively. The activity of chitinase in untreated mite (control) was 157.9 u gm^{-1}.

Amylase: There was slight inhibitions in different concentrations of *M. anisopliae* of *T. urticae*, 89.85 u gm^{-1} for 2.4 $x10^7$ spore ml^{-1}, while the enzyme activity increased to 111.73 u gm^{-1} and 190.13 u/mg for 2.4 $x10^8$ and 2.4 $x10^9$ spore /ml respectively, compared to the control with 60.87 u gm^{-1}.

Protease activity, as for the protease activity, which hydrolyzes protein caused available levels of activity. The activity was marked in 2.4 $x10^9$ spore ml^{-1} for *M. anisopliae* 432.30 u gm^{-1} while other concentrations were near similar which were 389.7 and 325.49 u gm^{-1} for 2.4 $x10^8$ and 2.4 $x10^7$ spore ml^{-1}, respectively.

Detection and Identification of chitinase gene in *M. anisopliae* by PCR: The aim of this study was to see if sequence analysis of internal transcribed spacers could help with this in *M. anisopliae* ribosomal DNA (rDNA) can be used to detect chitinase gene in fungus, *M. anisopliae*, which is responsible for death of *T. urticae* and semi nested PCR to detect this gene in fungal DNA. More recently, PCR- based marker system have become available. One of these has been called pure gene GENETAQ Green PCR Master Mix (2X). Standardization of PCR conditions for chitinase gene amplification by checking annealing temperature 55ºC using GENETAQ Green PCR technique, desirable amplification

Table 3. Lipase and chitinase activity, produced by *M. anisopliae* isolates influenced by different temperature

Temperature (°C)	Lipase		Chitinase	
	Biomass (mg ml^{-1})	Activity (u ml^{-1})	Biomass (mg ml^{-1})	Activity (u ml^{-1})
25	6.92	50.4	21.25	69.14
30	14.5	88.2	24.63	76.51
35	11.3	61.5	15.00	40.77

Table 4. Effect of pH values on lipase and chitinase activity were produced by *M. anisopliae*

pH values	Lipase		Chitinase	
	Biomass (mg ml^{-1})	Activity (u ml^{-1})	Biomass (mg ml^{-1})	Activity (u ml^{-1})
5	12.2	81.0	10.26	77.23
6	16.4	88.3	13.09	82.25
7	9.1	73.0	8.23	61.25
8	8.3	62.4	2.60	52.93

Table 5. Effect of different concentrations of *M. anisopliae* culture on the enzymes activity of *T. urticae*

Treatment spore ml^{-1}	Enzyme activity		
	Chitinase (u gm^{-1})	Amylase (u gm^{-1})	Protease (u gm^{-1})
2.4 $x10^7$	253.69±4.76^c	89.85±3.02^c	325.49±4.87^b
2.4 $x10^8$	302.11±4.98^b	111.73±3.87^b	389.70±4.15^b
2.4 $x10^9$	526.35±5.11^a	190.15±4.12^a	432.30±5.02^a
Control	157.90±3.97^d	60.87±2.43^d	207.59±4.23^c

Means in columns followed by the same letter are not significantly different at 5% level (Duncan's multiple range tests). ± Standard Error

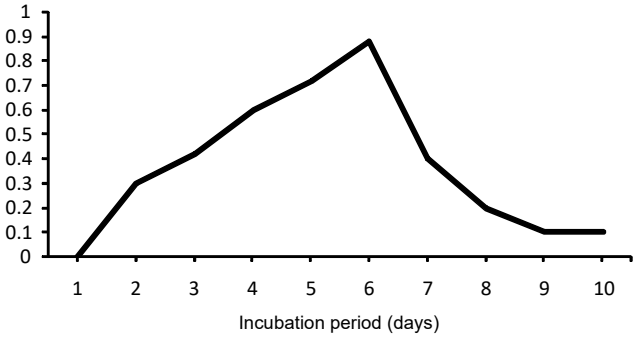

Fig. 1. Chitinase production by *M. anisopliae* as influenced by incubation period

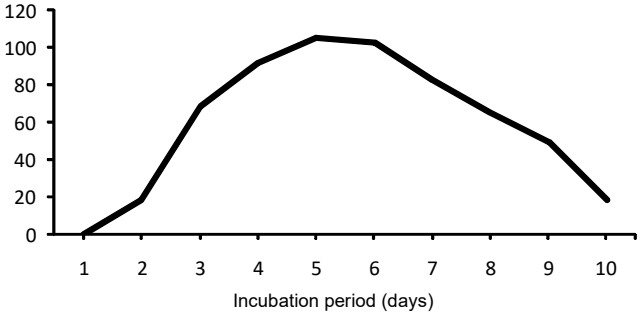

Fig. 2. Lipase production by *M. anisopliae* as influenced by incubation period

has been achieved at the annealing of 55ºC for chitinase gene amplification. The band of a 900 bp under uniform PCR conditions, a fragment corresponding to the chitinase gene (Fig. 3) was amplified. The PCR products' amplification was verified.

Ultra – structure of *T. urticae* infected with *M. anisopliae* by scanning electron microscope: Treated adult mites of *T. urticae* by the *M. anisopliae* culture were examined by using scanning electron microscope (SEM) to indicate the effect of the *M. anisopliae* culture filtrate on the cuticle of the mite to indicate any growth of the fungus mycelium on surface of treated mite *T. urticae* and observe any other symptom on treated mites. The result appeared in images A, B and C) clearly indicated the growth of colonies of the fungus, *M. anisopliae* on *T. urticae* recognized by many conidia (Fig. 5).

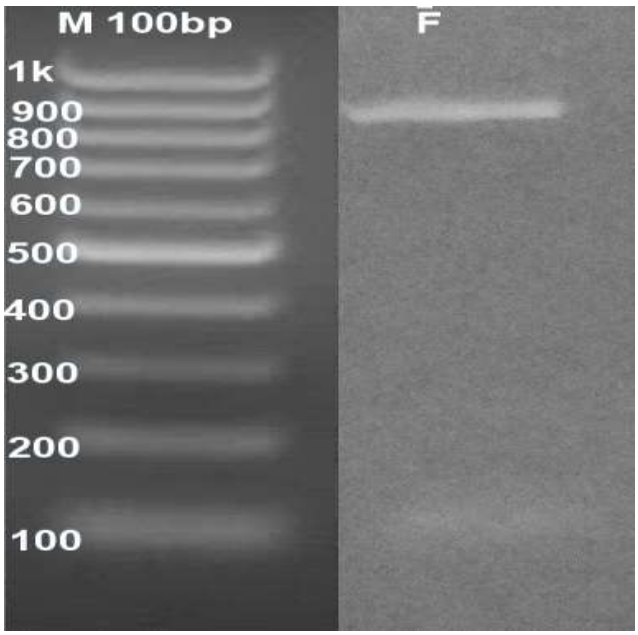

Fig. 3. PCR to detect the presence of chitinase gene on *M. anisopliae* MT193505 by using specific primer Chi2:chi2f-GACAAGCACCCGGAGCGC,chi2r-CTTGCTTGACACATT GGTAA

Biological control agents like pathogenic fungi are important in the natural control of many crop pests. *M. anisopliae* has a high effectiveness in causing mortality of the phytophagous mite, *T. urticae*. Mero et al (2011) illustrated that many entomopathogenic fungi were more effective against *T. urticae*. Nugroho and Bin Ibrahim (2004) used fungal pathogens as bio control agents are now recognized as an essential biological control factor in IPM programmes. Roza et al (2014) stated that *M. anisopliae* able to kill *T. urticae* eggs and adults and can be used as substitute or complement to synthetic chemicals most of which lack ovicidal activity. Dalia et al (2017) observed *M. anisopliae* was most potent toward eggs of *T. urticae* where caused unhatchability reached to 99%. Similar results were reported by Kakde (2011) in which *Fusarium oxysporum* gave maximum activity of lipase at 30ºC and Shimaa et al (2017) indicated that lipase production by *R. oryzae* R1 as influenced by different incubation temperature. The optimum temperature for lipase production was determined as 30ºC.

Brzezinska and Jankiewicz, (2012) are in general in harmonious with our results, indicating that for highest chitinase production by other fungi the optimum temperature ranged from 26 to 28ºC. Ghanem *et al*. (2010) indicated that optimum pH for chitinase production from *Asprigellus terrus* is pH 6.5. Huang et al (2009) recorded that the optimal pH for lipase produced by *M. anisopliae* was at pH 5.7. The incubation period is an important parameter for lipase

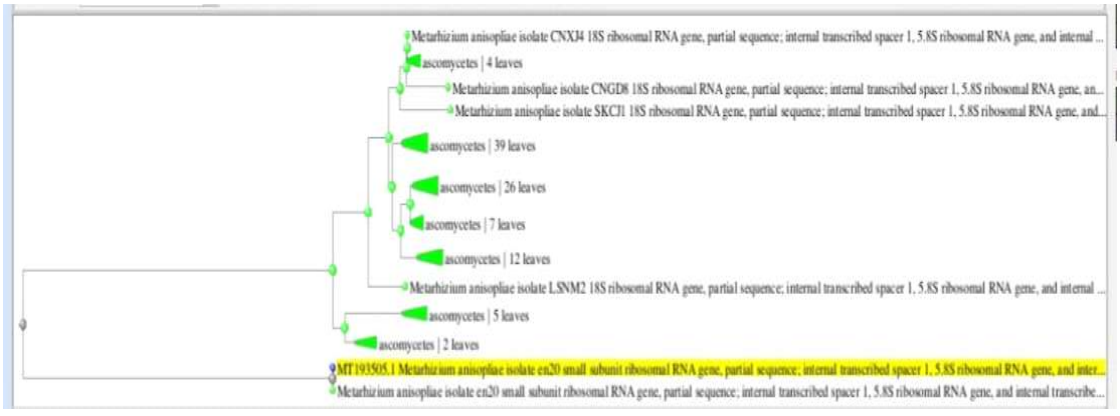

Fig. 4. Phylogenetic tree based on alignment of ITSI-5.8-ITS2 region to the closely related published sequence from NCBI Gene Bank. The tree constructed with fast minimum evolution method. The alignment showed that the retrieved sequence of the tested fungal strain was closely related to both *M. anisopliae* with accession No. FJ545297.1 and *M. brunneum* with accession no. CPO58932.1 with identity 90.5-90.7% and with query covers 97-100% for both species

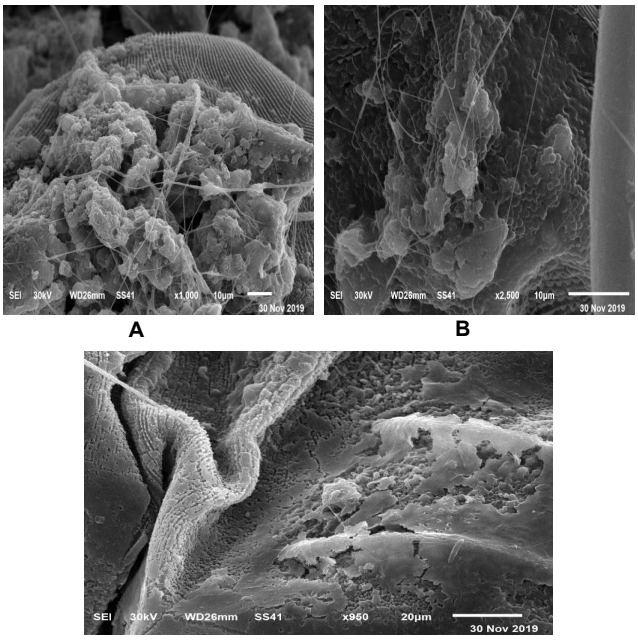

Fig. 5. Photo (A): Scanning electron micrograph of *M. anisopliae* mycelium and conidia growing on the body surface of infected *T. urticae*. Photo (B): Scanning electron micrograph of M. *anisopliae* hyphae and spores growing on the body surface of infected *T. urticae*. Photo (C): Scanning electron micrograph of degradation of cuticle layer of infected *T. urticae* by chitinase production from *M. anisopliae*

production from different microorganisms (Niaz et al 2014). Imandi et al (2013) revealed the highest activity of lipase production on the fourth day and decrease in activity may be due to metabolism changes such as nutrition consumption. Rodrigues et al (2015) recorded that the most efficient isolate that gave the highest lipase activity after fifth day of incubation period in mineral media. Lopez- LIorca et al (2002) used scanning electron microscopy and observed that Conidia of *M. anisopliae* germinated on all regions of the cuticle and once the fungal spores attach to the insects cuticle, they germinate sending out structures (hyphae) that penetrate in to the insects body and proliferate that led to function disorder and death (Abdelkader 2016). Scanning electron microscopy is a useful instrument for studying how *M. anisopliae* colonises and infects *T. urticae* and for observing the mode of action of entomopathogenic fungi. In addition, proposed the molecular studies of this isolate fungus detection and identification of chitinase gene by PCR.

CONCLUSION

The present study has underlined the significance of the entomopathogenic fungus *M. anisopliae* in controlling spider mite *T urticae* through reducing its mobility. The activity of lipase as well chitinase, which are liable for the infection process, is affected by some physical factors. Both enzymes showed similarity with respect to the optimum physical items, which are pH value (6.0) and incubation temperature 30ºC. The incubation period has shown different trend in relation to the activity of both enzymes. The results offered unique evidence for the chitinase gene on fungus *M. anisopliae* by using PCR at the band 900 bp as well as SEM that confirmed the growth of fungus mycelia on the surface of treated mite.

REFERENCES

Abd El- Kader MA 2016. *Usage of fungus Beauvaria bassiana in the control of Tropinota squalida, Sesamia cretica and Cassida vittata At Sharkia Governorate.* Ph.D. Thesis (Microbiology), Botany Department at Faculty of Science Zagazig University pp. 260.

Birk Y, Harpaz I, Ihasaya I and Bondi A 1962. Studies on the proteolytic activity of the beetles *Tenebrio* and *Tribolium*. *Journal of Insect Physiology* **8**: 417-429.

Brzezinnska MS and Jankiewicz U 2012. Production of antifungal chitinase by *Aspergillus nigar* LOCK62 and its potential role in the biological control. *Current Microbiology* **65**: 666-672.

Dalia MA Hassan, Marguerite A Rizk, Hassan M Sobhy, Wafai ZA Mikhail and Maha S Nada 2017. Virulent entomopathogenic fungi against the two-spotted spider mite *Tetranychus urticae* and some associated predator mites as non-target organisms. *Egyptian Academic Journal of Biological Sciences* **10**(6): 37-56.

Duncan DB 1955. *Multiple range and multiple F. tests*. *Biometrics* **11**: 1-41.

Ghanem KM, Al-Garni SM and Al-Makishah NH 2010. Statistical Optimization of culture conditions for chitinase production from fish scales wastes by *Aspergillus terrus*. *African Journal of Biotechnology* **9**(32): 5135-5146.

Huang C, Zong MH, Wu H and Liu QP 2009. Microbial oil production from rice straw hydro lysate by *Trichosporon fermentans*. *Bioresource Technology* **100**: 4535-4538.

Imandi SB, Karanam SK and Garapati HR 2013. Use of Placket-Burman design for rapid screening of nitrogen and carbon sources for the production of lipase in solid state fermentation by *Yarrowia lipolytica* from mustard oil cake (*Brassica napus*). *Brazilian Journal of Microbiology* **44**: 915-921.

Ishaaya I and Casida JE 1974. Dietary TH-6040 alters composition and enzyme activity of housefly larval cuticle. *Pesticide Biochemistry and Physiology* **4**: 484-490.

Ishaaya I and Swiriski E 1976. Trehalase, invertase and amylase activities in the black scale, *Saissetia oleae* and their relation to host adaptability, *Journal of Inset Physiology* **16**: 1025-1029.

Kakde RB 2011. Extracellular lipase enzyme production by seed-borne fungi under the influence of physical factors. *International Journal of Biology* **3**(1): 94-100.

Lopez-LIorca LV, Bordullo JJ, Salinas J, Monfort E and Lopez-Serna ML 2002. Use of light and scanning electron microscope to examine colonization of barley rhizosphere by the nematophagous fungus *Verticillium chramydosporium*. *Micron* **33**: 61-70.

Mero LB, Polanczyk RA, Pratissoli D, Carvalho JR and Franco CR 2011. Potential use of entomopathogenic fungi in the control of *Tetranychus urticae* Kock (Acari: Tetranychidae) in Papaya: Cultivar effect on pathogenicity. *Arquivos do Instituto Biologico* **78**(2): 267-272.

Niaz M, Iftikhar T and Qureshi FF 2014. Extracellular lipase production by *Aspergillus nidulans* (MBL- S-6) under

submerged fermentation. *International Journal of Agriculture and Biology* **16**: 536-542.

Nugroho I and Bin Ibrahim Y 2004. Laboratory bioassay of some entomopathogenic fungi against broad mite (*Polyphagotrasonemus latus* Banks). *International Journal of Agriculture and Biology* **6**(2): 223-225.

Rodrigues C, Cassini STA, Antunes PWP, Pinotti LM, Keller RP and Goncalves RF 2015. Lipase and surfactant production by fungi isolated of oily residues of environmental sanitation in liquid and solid phase reactors. *International Journal of Applied Science and Technology* **5**(3): 46-54.

Received 19 July, 2021; Accepted 12 November, 2021

Roza N, Mohammed D and Ferdu Azerefegne 2014. Pathogenicity of *Beauvaria bassiana* and *Metarhizium anisopliae*, to the two spotted spider mites, *Tetranychus urticae*, (Acari: Tetranychidae) at different temperatures and greenhouse conditions. *Ethiopian Journal of Agricultural Sciences* **24**: 51-58.

Shimaa E Helal, Hemmat M Abdelhady, Khadiga A Abou-Taleb, Mervat G Hassan and Mohamoud M Amer 2017. Evaluation of factors affecting the fungal lipase production using one factor at a time Approach and Response surface methodology. *Egyptian Journal of Microbiology* **52**: 1-16.

Indian Journal of Ecology (2021) 48(6): 1809-1814

Manuscript Number: 3453
NAAS Rating: 5.79

Assessment of the Diversity of Thrips species (Thysanoptera) in Solanaceous Vegetable Crops

Amit Kumar, Tamoghna Saha*, R. Rachana[1], Nithya Chandran[2] and K. Santosh[3]

Department of Entomology, Bihar Agricultural University, Sabour, Bhagalpur-813 210, India
[1]ICAR-NBAIR, Bengaluru-560 024, India
[2]Division of Entomology, ICAR-IARI, New Delhi-110 012, India
[3]Department of Plant Pathology, Bihar Agricultural University, Sabour, Bhagalpur-813 210, India
**E-mail: tamoghnasaha1984@gmail.com*

***Abstract*:** The study was done during 2019-20 to determine the species composition of thrips in solanaceous vegetable crops namely brinjal, chilli and tomato in southern part of Bihar. Diversity was calculated by Shannon-Weaver Index, Simpson index, Richness index and evenness by Pielou evenness index. Among the thrips species, the most abundant species was *Scirtothrips dorsalis* with 887 specimens were collected from solanaceous vegetable crops and considered as a serious pest species (741 from chilli and 146 from brinjal). The next most abundant species was *Thrips palmi* found with 769 specimens (292 from tomato, 287 from brinjal and 190 from chilli) and followed by *Frankliniella schultzei* reported with 106 specimens from brinjal crop only, and *Thrips tabaci* with 96 specimens only recorded from tomato crops. As far as the diversity index is concerned, the highest Shannon-Wiener index, Margelef richness index and Pielou's evenness index was recorded in the brinjal crop, and it was followed by tomato and chilli crops. The domination coefficient of thrips species was also studied and it revealed that *Scirtothrips dorsalis* and *Thrips palmi* were the most eudominant species, whereas, *Frankliniella schultzei* and *Thrips tabaci* were the subdominant species. The above findings would be useful in the development of monitoring programs and design of pest management strategies.

***Keywords*:** Thrips, Diversity, Relative abundance, Common solanaceous vegetable crops

Thrips are serious pests of a wide range of agricultural crops including ornamental, vegetables, and fruits in both greenhouses and open field cultivation throughout the world. Bunyaviridae are transmitted by thrips and cause significant losses in quality and yield of many vegetables, legume and ornamental crops in many tropical and subtropical regions (Pappuet al 2009, Mandal et al 2012). Among Thysanoptera, the family Thripidae is the most harmful genera for both field and greenhouse crops (Tommasini 2003) and most harmful genera are *Frankliniella* and *Thrips* (Mound 2012). Currently, species of *Frankliniella* and *Thrips* are present on all continents (Moritz 2002). They exhibit remarkable diversity in terms of habit and habitat. There are approximately 6000 described species thrips (Mound 2007) and diversity is higher in the warm tropical parts than in the colder regions of the world. Ananthakrishnan (1973) published mycophagous Thysanoptera of India and Palmer and Mound (1978) also reported nine genera of fungus-feeding Thysanoptera from the oriental region. Sen et al (1988) gave the keys and description of Thysanoptera of north-eastern India. However, even though it is a significant crop pest and virus vector, diversity of thrips from Bihar has not been fully explored. Hence, the present study was conducted to the assessment of temporal diversity of thrips species on common solanaceous vegetable crops of Bihar.

MATERIAL AND METHODS

The field experiment was carried out during *kharif* and *rabi* season during the period 2019-20 on solanaceous vegetable field of Bihar Agricultural College, Sabour, Bhagalpur. The insect samples (thrips) were collected crop wise from randomly selected twenty plants at weekly intervals and were kept separately in plastic vial filled with 70% ethanol. Morphological based identification of various characteristics including colour, size, number of antennal segments, distribution and number of setae across different parts of the body along the forewings was done according to key of Riley et al (2011). At laboratory, larvae and adult thrips specimens were separated under stereo zoom microscope and microscopic slides were arranged for identification using Hoyer's medium. A water-soluble mounted of individual population of thrips was fixed with ventral side upward in a drop of Hoyer's mount ant and species were identified using appropriate diagnostic keys (Ananthakrishnan and Sen 1980).

Mounting methodology: The specimens collected were removed from the collection media and were kept in 2 per cent NaOH for half an hour and were transferred to 60 per cent alcohol and were kept for at least one day and after that these were dehydrated through a series of alcohol (1 hour in

70 per cent alcohol, 20 minutes in 80 per cent, 10 minutes in 95 per cent and 5 minutes in absolute alcohol). Then the specimens were cleared in clove oil for five to ten minutes and were mounted on the microscopic slides by putting a drop of Canada balsam on the cover slip and then specimens were kept gently on it with the help of a fine needle. After that the antennae, legs and wings were spread gently. After mounting, the microscopic slides were kept in oven at 45 °C for 30 minutes. The identification was further confirmed by NBAIR, Bangalore. Collection was done once in a week, data was collected by examining 20 plants of each crops to determine the diversity, species richness, species evenness and analyzed by using Shannon-Weaver Diversity Index, and Simpson Index.

Then, relative abundance of thrips species were worked by the following formula developed by Kasprzak and Niedbala (1981):

$$\text{Relative abundance (\%)} = \frac{ni}{N} \times 100$$

Where, n_i = Total no. of individuals of each species. N = Total no. of individuals of all species

Diversity, evenness and dominance indices were worked out. The formulas used for diversity indices are as follows:

Simpson's index of dominance (Simpson 1949)

$$Simpson's\ index\ (Ds) = \sum_{i-1}^{s} \left(\frac{[ni(ni-1)]}{[N(N-1)} \right)$$

Where, n_i= number of individuals in the i^{th} species.

N = total number of individuals in the sample

Reciprocal of Simpson's index of diversity ($1/D_{s)}$) was exercised to articulate the diversity of species so that as the index goes up, so does the diversity.

Index of species diversity (Shannon and Weaver 1949)

Shannon – Weaver index (H') = -Σpi loge pi

Where, p_i= the proportion of individuals of species i (n_i/N)

n_i= number of individuals in the i^{th}species

Evenness index (Hill 1973)

Evenness index (J) = H'/ $\log_e$ S

Where, H' = Shannon – Weaver index

S = number of species

Margalef's richness index (Margalef, 1958) was computed with the formula:

α = (S – 1) / ln (N)

Where, S = the total number of species in the sample; and N = the total number of individuals in the sample.

RESULTS AND DISCUSSION

Occurrence of thrips in common solanaceous: The total number of collected thrips was 1,858 out of which 539 from brinjal, 931 from chilli and 388 specimens from tomato crops (Table 2). All recorded thrips species were found active throughout the cropping season up to the harvesting of the crops. The results showed that mostly four species of thrips belong to Thripidae and observed in solanaceous vegetable crops from 32 SMW of 2019 to 12 SMW, 2020 (Table 10). These species were *Thrips palmi* Karny (Fig. 5), *Frankliniella schultzei* Trybom (Fig 4), *Scirtothrips dorsalis* Hood (Fig. 6) and *Thrips tabaci* Lindeman (Fig. 7). The three solanaceous vegetable crops (brinjal, tomato and chilli) were infested with one or more species of thrips (539 in brinjal, 931 in chilli and 388 in tomato). *Thrips palmi* Karny and *Scirtothrips dorsalis* Hood were encountered mostly due to polyphagous behaviour and harboured on leaves and flower buds. The three thrips species were associated with brinjal crop (*T. palmi*, *F. schultzei* and *S. dorsalis*), two species were associated with both chilli (*T. palmi* and *S. dorsalis*) and tomato crops (*T. palmi*and *T. tabaci*) (Table 1). *T. palmi* was recorded from brinjal, chilli and tomato. *S. dorsalis* in brinjal and chilli crops, *F. schultzei* in brinjal only and *T. tabaci* in tomato. The maximum intensity was in *T. palmi* (53.25 %) followed by *S. dorsalis* and *F. Schultzei*, whereas, in chilli, maximum intensity was n *S. dorsalis* (79.51 %) followed by *T. palmi* ((Table 1). In tomato, the highest intensity was recorded in *T. palmi* (75.26 %) followed by *T. tabaci* (24.74 %). The incidence of thrips in brinjal crop was taken from 32 SMW (1st week of August) to 43 SMW (3rd week of December) (Fig 1). The peak population of these species

Table 1. Occurrence of thrips in solanaceous vegetable crops during *kharif* and *rabi* 2019-20

Name of the crop	Scientific name	Family	Season	Per cent intensity	Plant part harboured
Brinjal	*Thrips palmi* Karny	Thripidae	*Kharif*	53.25	Leaves and flower bud
	Frankliniella schultzei Trybom	Thripidae	*Kharif*	19.67	Leaves and flower bud
	Scirtothrips dorsalis Hood	Thripidae	*Kharif*	27.08	Leaves and flower bud
Chilli	*Scirtothrips dorsalis* Hood	Thripidae	*Kharif*	79.51	Leaves and flower bud
	Thrips palmi Karny	Thripidae	*Kharif*	20.41	Leaves and flower bud
Tomato	*Thrips palmi* Karny	Thripidae	*Rabi*	75.26	Leaves and flower bud
	Thrips tabaci Lindeman	Thripidae	*Rabi*	24.74	Leaves and flower bud

was on the 38 SMW (4th week of September) in *T. palmi* followed by *S. dorsalis* and *F. schultzei*. From 33 SMW, the population of thrips was increasing gradually and attained its peak population afterwards their population fell down and reached a minimum level during 43 SMW till the harvesting of the crop. The population of thrips was observed in the chilli crop from the 32nd SMW after transplanting. The peak population was in 39 SMW (Last week of September) afterwards, it decreased gradually up to 43 SMW (Fig. 2). *S. dorsalis* increased their population rapidly, comparatively *T. palmi*. Among all the solanaceous vegetable crops chilli was the most susceptible host of thrips. The population of thrips in tomato was first noticed on the 48th SMW (Last week of November) with species of *T. palmi* and *T. tabaci*. During the cropping season *T. palmi* was the most dominant species and it reached the peak population on the 10th SMW (1st week of March) and thereafter the population shows a decreasing trend (Fig. 3).

Relative abundance and temporal diversity of thrips species: The total of 1,858 specimens were collected during the first week of August, 2019 (32 SMW) to fourth week of March, 2020 (13 SMW) from solanaceous vegetable crops. Among the thrips species, the most abundant species was *Scirtothrips dorsalis* with 887 specimens were collected from solanaceous vegetable crops and considered as a serious pest species (741 from chilli and 146 from brinjal). The next most abundant species was *Thrips palmi* with 769 specimens (292 from tomato, 287 from brinjal and 190 from chilli) and

Table 3. Domination coefficient of different thrips species collected from solanaceous vegetable crops during 2019-20

Species of Thysanoptera	Total number of Thrips	Domination coefficient
Thrips palmi	769	41.38
Frankliniella schultzei	106	5.70
Scirtothrips dorsalis	887	47.73
Thrips tabaci	96	5.16
Total = 1,858		

Eudominant: ≥ 20.1%, Dominants: 10.1 – 20.0%, Subdominants: 5.1 – 10.0%, Precedents: 1.1 – 5.0%.

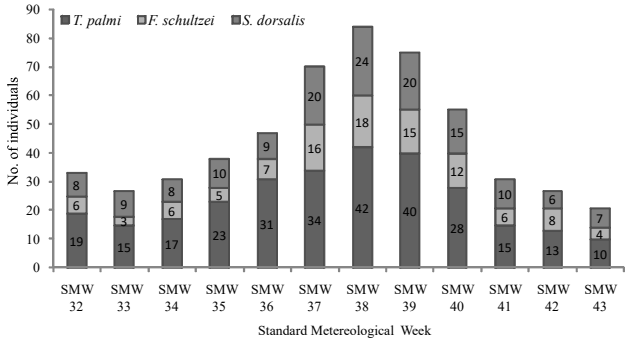

Fig. 1. Population dynamics of thrips in brinjal during *kharif*, 2019-20

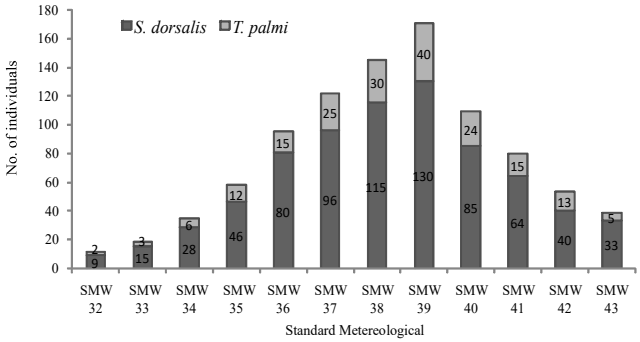

Fig. 2. Population dynamics of thrips in chilli during *kharif*, 2019-20

Table 2. Relative abundance and diversity of thrips species in solanaceous vegetable crops during *kharif* and *rabi* 2019-20

Index	Total number of thrips (adult) species collected from solanaceous vegetable crops					
	Brinjal	Relative abundance	Chilli	Relative abundance	Tomato	Relative abundance
Thrips palmi Karny	287	0.53	190	0.20	292	0.75
Frankliniella schultzei Trybom	106	0.20	-	-	-	-
Scirtothrips dorsalis Hood	146	0.27	741	0.80	-	-
Thrips tabaci Lindeman	-	-	-	-	96	0.25
Total individuals	539	-	931	-	388	-
Total number of species observed	03	-	02	-	02	-
Shannon-Weaver Index of Diversity (H'):	1.01	-	0.51	-	0.56	-
Simpson Dominance Index (D)	0.39	-	0.67	-	0.63	-
Margelef Species Richness Index (α)	0.32	-	0.15	-	0.17	-
Pielou's Species Evenness Index (J)	0.92	-	0.74	-	0.81	-

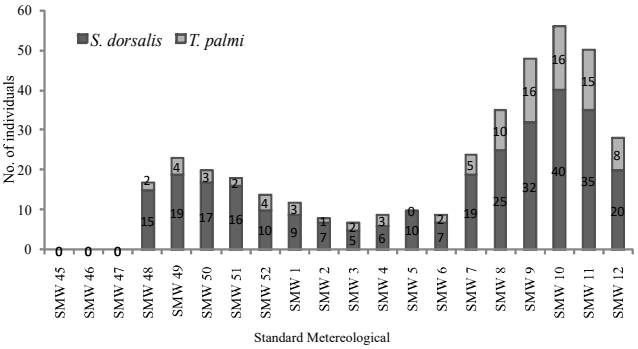

Fig. 3. Population dynamics of thrips in tomato during *rabi*, 2019-20

followed by *Frankliniella schultzei* and *Thrips tabaci* .The relative abundance revealed that for brinjal crop, thrips species *T. palmi*, *F. Schultzei* and *S. dorsalis* were 0.53, 0.20 and 0.27 %, respectively. In case of chilli crop, the relative abundance of thrips species *T. palm* and *S. dorsalis* were 0.20 and 0.80%, respectively. However in tomato crop, the relative abundance of thrips species *T. palmi* and *T. tabaci* were 0.75 and 0.25%, respectively (Table 2). *S. dorsalis* and *T. palmi* were the most eudominant species, whereas, *F. schultzei* and *T. tabaci* were the subdominant species (Table 3). Shannon-Weaver index (H'), Simpson index (D), Margelef species richness (a) and Pielou's species evenness index (J) in Brinjal were 1.01, 0.39, 0.32 and 0.92, respectively and in

Fig. 4. *Frankliniella schultzei*

Fig. 6. *Scirtothrips dorsalis*

Fig. 5. *Thrips palmi*

Fig. 7. *Thrips tabaci*

chilli crop were 0.51, 0.67, 0.15 and 0.74, respectively and in tomato crop were 0.56, 0.63, 0.17 and 0.81, respectively.

The highest Shannon-Weaver index value was in the brinjal crop of 1.01 and it was followed by tomato (0.56) and chilli (0.51). The dominance was measured by the Simpson dominance index and it shows the species dominance and diversity ranging from 0-1. In the case of the Simpson dominance index, the highest value was in chilli crop followed by tomato and brinjal crop. The species richness was measured using Margelef richness index and species richness was highest (0.32) in brinjal crop as compared to chilli and tomato crops (0.15 and 0.17). Pielou's evenness index is the measure of evenness of organisms. From the results, the maximum (0.92) evenness index occurred in brinjal crop and it was followed by tomato and chilli crops (0.81 and 0.74).

Incidence of thrips in brinjal, tomato and chilli crops: As far as diversity index is concerned, the highest Shannon-Weaver index value was recorded in brinjal crop of 1.01 and it was followed by tomato (0.56) and chilli (0.51). In Shannon-Weaver index (H'), higher the value obtained, higher is the diversity. Similarly Margelef richness index and species evenness index was also higher in brinjal crop as compared to tomato and chilli crop. The diversity index vary between 0-<1 for minimum diversity and 1 for maximum diversity (Anonymous 2000). In this study, the values were just higher than 1 i.e. 1.01 for brinjal crop. In this study, a total of 1,858 species of thrips were associated with common solanaceous vegetable crops and among the thrips species, the most abundant species was *Scirtothrips dorsalis* in solanaceous vegetable crops, next most abundant species was *Thrips palmi* followed by *Frankliniella schultzei* and *Thrips tabaci.* Sanjta and Chauhan (2015 reported that thirteen species of thrips were associated with different vegetable crops in Himachal Pradesh. Thrips species were *Thrips tabaci*, *T. flavus*, *T. palmi*, *T. carthami*, *T. alatus, Ayyariachaetophora*, *Anaphothrips sudanensis*, *Scirtothrips dorsalis*, *Megalurothrips peculiaris*, *Neohydatothrips samayankur*, *Aeolothrips sp., Haplothrips tenuipennis* and *Haplothrips tenuipennis.* Among all the thrips, *Thrips tabaci, T. flavus* and *T. palmi* were recorded as polyphagous pest and most abundant. During their study *Scirtothrips dorsalis* was associated with capsicum, *Haplothrips tenuipennis* with brinjal and tomato crops. Razi et al (2017) after a survey reported that the four species were affiliated to genus *Frankliniella (F. occidentalis, F. intonsa)* and two species were associated with the genus *Thrips (T. tabaci and T. flavus)* and they were collected from 14 vegetable crops. Kirk and Terry (2003) reported that *Frankliniella* species have worldwide distribution and it is the most abundant and harmful one. *T. tabaci* was also maximum in surveyed crops and sites and is a polyphagous and cosmopolitan species (Liu and sparks 2003). Mound (2005) reported that *T. palmi* is an Asian polyphagous thrips species which spread around the world during the 1980s. Shruthi et al (2017) observed that among the two different thrips species occurring on watermelon, *Thrips palmi* was more abundantly occurred in watermelon crop in all localities. Elimem et al (2017) mentioned that the most abundant thrips species are *T. palmi* with percentages of 25 and 23.53 %, followed by *Limothrips cerealium* with 18.75 and 17.65%, *T. tabaci* 12.5% and 17.65% and *Haplothrips* sp. 31.25 and 11.76% respectively in vine table grape orchard and wine cellar grape orchard.

CONCLUSION

The most abundant thrips in common solanaceous vegetable crops was *Scirtothrips dorsalis* followed by *T. palmi* and *F. schultzei*. The highest diversity, richness and evenness were recorded in the brinjal crop, and it was followed by tomato and chilli. The maximum dominance was noticed in chilli crop followed by tomato and brinjal crop.

REFERENCES

Ananthakrishnan TN 1973. *Mycophagous Tubulifera* of India. Loyola College Madras, Entomology Research Unit. *Occasional Publications* **2**: 144.

Ananthakrishnan TN and Sen S 1980. Taxonomy of Indian thysanoptera. *Zoological Survey of India (Handbook Series)* **1**: 1-234.

Anonymous 2000. Ecological sampling methods. *http://www.countrysideinfo.co.uk/ simpsons.htm*

Bhatti JS 1999. Enigmatic tentorium in adults of the Onion thrips, *Thrips tabaci*. *Thrips* **1**: 15-30.

Elimem M, Karouia W, Lahef C, Othmen SB, Limem E and Mliki Y 2019. Thrips species composition, biodiversity and seasonal dynamic populations in two vine grape orchards in the north-eastern region of Tunisia. *Journal of New Sciences* **64**(4): 4028-4039.

Hill MO 1973. Diversity and evenness: A unifying notation and its consequences. *Ecology* **54**: 427-432.

Kasprzak K and Niedbala W 1981. Wskazniki biocenotyczne stosowane Przy porzadkowaniu analize danych W budaniach ilosciowych. In Metody Stosowane W. Zoologii gleby (Gorny, M& Greun, L .Eds). PWN. Warszawa 397-416.

Kirk WDJ 1997. *Distribution, Abundance and Population Dynamics*. **In**: *Thrips as crop pests*. Lewis, T. (Eds.): 217-257. CAB International Wallingford, UK.

Kirk W D J and Terry I 2003. The spread of the western flower thrips *Frankliniella occidentalis. Agricultural and Forest Entomology* **5**: 301-310.

Lewis T 1973. *Thrips, their biology, ecology and economic importance*. Academic Press, London, UK, p 349.

Lewis T 1997. *Thrips as Crop Pests*. Lewis (Eds) Wellingford, Oxon, UK, New York, USA: CAB Int. p 349.

Liu TX and Sparks NA 2003. Injury and distribution of onion thrips in red cabbage heads. *Southwestern Entomologist* **28**: 77-79.

Mandal B, Jain RK, Krishnareddy M, Krishna Kumar NK, Ravi KS and Pappu HR 2012. Emerging problems of Tospo viruses (Bunyaviridae) and their management in the Indian

subcontinent. *Plant Disease* **96**: 468-479.

Margalef R 1958. Information Theory in Ecology. *General Systems* **3**: 36-71.

Moritz G 2002. The biology of thrips is not the biology of their adults: A development view. Thrips and Tospo viruses: Proc. **In**: *7th International Symposium on Thysanoptera 2001/07/2-7*, Italy. 259-267.

Mound LA 1972. Species complexes and the generic classification of leaf-litter thrips of the tribe Urothripini (Phlaeothripidae). *Australian Journal Zoology* **20**: 83-103.

Mound LA 2005.Thysanoptera: Diversity and interactions. *Annual Review of Entomology* **50**: 247-269.

Mound LA 2007. Thysanoptera (Thrips) of the World: A checklist. *http://www.ento.csiro.au/thysanoptera/ worldthrips.html.*

Mumford RA, Barker I and Wood KR 1996. The biology of the Tospo viruses. *Annals of Applied Biology* **128**: 159-183.

Palmer JM and Mound LA 1978. Nine genera of fungus-feeding Phlaeothripidae (Thysanoptera) from the Oriental Region. *Bulletin of the British Museum (Natural History) Entomology* **37**: 153-215.

Pappu HR, Jones RA and Jain RK 2009. Global status of tospo virus epidemics in diverse cropping systems: Successes achieved and challenges ahead. *Virus Research* **141**: 219-236.

Razi S, Bernard EC and Laamari M 2017. A survey of thrips and their potential for transmission of viruses to crops in Biskara (Algeria): First record of the species *Frankliniella intonsa* and *Thrips flavus. Tunisian Journal of Plant Protection* **12**: 197-205.

Riley DG, Joseph SV, Srinivasan R and Diffie S 2011. Thrips Vectors of Tospo viruses. *Journal of Integrated Pest Management* **2**(1): 1-10.

Sanjta S and Chauhan U 2015. Survey of Thrips (Thysanoptera) and their natural enemies in vegetables from Mid Hill of Himachal Pradesh. *The Ecoscan* **9**(3&4): 713-715.

Sen S, Pramanik NK and Gupta CK 1988. Thysanoptera fauna of north-eastern India. *Records of the Zoological Survey of India* (Occasional Paper) **10**: 100-123.

Shannon CE and Weaver W 1949. *The Mathematical Theory of Communication*. University of Illinois Press, Urbana, Illinois. p 144.

Simpson EH 1949.Measurement of diversity. *Nature* **163**: 688.

Shruthi CR, Narabenchi GB, Nirmala HR and Devaraju G 2017. Species composition, identification and relative abundance of *Thrips palmi* on watermelon. *International Journal of Pure and Applied Bioscience* **5**(5): 318-321.

Tommasini M 2003. *Evaluation of Orius species for biological control of Frankliniella occidentalis (Pergande) (Thysanoptera: Thripidae)*. Ph.D. dissertation, Wageningen University, Wageningen, p 63.

Tommasini MG and Maini S 1995. *Frankliniella occidentalis and other thrips harmful to vegetable and ornamental crops in Europe*. Wageningen Agricultural University Papers **95**: 1-42.

Received 22 June, 2021; Accepted 12 November, 2021

Indian Journal of Ecology (2021) 48(6): 1815-1820

Manuscript Number: 3454
NAAS Rating: 5.79

Evaluation of Hydrogel and *Trichoderma* based Formulations on Root Characteristics and Water Use Efficiency in Linseed under Rainfed Ecology

K. Dujeshwer, R.K. Singh[1] and N.R. Sandhya[2]

Faculty of Agricultural Sciences, GLA University, Mathura-281 406, India
[1]Department of Agronomy, Banaras Hindu University, Varanasi-221 005, India
[2]ICRISAT-International Crop Research [2]Institute for Semi- Arid Tropics, Hyderabad-500 050, India
E-mail: dkurrey73@gmail.com

Abstract: In India, climate change is expected to reduce the overall crop production. Increased global CO_2 emissions could result in erratic weather conditions, especially uncertain rainfall and temperature, which may lead to soil moisture stress in several crops. Hydrogel was efficient in altering the water holding capacity of soil by absorbing significant amount of water and releasing it under moisture stress conditions in soil., *Trichoderma* is multi-tasking fungus and proven to enhance root proliferation and nutrient uptake in several crops. The current study was aimed to assess the effect of super absorbent polymer (Hydrogel) and *Trichoderma* based formulations on root characteristics and water use efficiency (WUE) in linseed varieties under no irrigation condition. The experiment was conducted on four linseed varieties *viz.* Kartika, Deepika, Garima, and RLC-92 with six hydrogel based *Trichoderma* formulated treatments. The varieties Garima and RLC-92 recorded highest root area, root biomass, WUE and seed yield. Furthermore, the soil amendment with hydrogel @ 2 g m^{-2} + sowing of *Trichoderma* treated seed significantly improved the root area, root biomass, WUE, relative water content (RWC), soil microbial biomass carbon (SMBC) and seed yield over control. The super absorbent polymer (hydrogel) was able to improve physical property of soil i.e. water holding capacity (WHC), and the seed treatment with *Trichoderma* positively influenced root characteristics of linseed in the experimental location. Moreover, both the inputs showed potential to enhance crop yield. No negative impact of hydrogel was observed on *Trichoderma* population as well as growth and yield of linseed crop. Conclusively, soil amendment with hydrogel and seed treatment with *Trichoderma* fungus found effective in enhancing root growth and WUE in rainfed linseed at experimental location.

Keywords: Bio-inoculant, hydrogel, Linseed, Root biomass, Super absorbent polymer, Water use efficiency

Linseed (*Linum usitatissimum* L.) is a member of Linaceae family and commonly known as alsi, chikna or flaxseed in India and is considered to be native to India and eastern Mediterranean (Badole et al 2013). It is grown throughout the world including Canada, India, China, United States, Ethiopia and all over Europe (FAOSTAT 2018). Linseed has been a major source of industrial oil for products like paints, linoleum, polish, inks and cosmetic (Zhang et al 2007). Currently, linseed is important as a functional food from the point of view of its nutrition and pharmaceutical value, and its nutritious components include oil, protein, lignin, resolvable fiber, mineral and vitamins (Wu et al 2008). India is the second largest producer of linseed, next to Canada in the world with an area of 2.98 lakh ha, total production of 1.59 lakh tones per annum and productivity of 442 kg ha^{-1}. India has 18.8 per cent of world recorded linseed area but produces less than 10% of total world production (DoE&S 2019). Linseed is generally grown in rainfed/dry land areas where the residual moisture of previous crop is only source of water; thereby crop often suffers from the water stress conditions resulting in drastic decrease in productivity of crop. Development of micro-irrigation systems has considerably reduced the water requirement of the crops; moreover the performance of super absorbent polymers (SAPs) that absorb and retain huge amount of water and releases slowly, also demands attention. It absorbs water a minimum of 400- 1600 times of its dry weight and gradually releases it to growing plants (John 2011, Hu et al 2020). Use of hydrogel increases the amount of available moisture in the root zone, resulting in longer intervals between irrigations (Jain et al 2017). Hydrogels were reported to help reduce irrigation frequency by increasing moisture saturation especially in coarse-textured soils in arid and semi-arid regions (Kumar et al 2020). Amending soil with SAPs was also found to improve plant growth and increase both yield and WUE (El-Asmar et al 2017). *Trichoderma* sp. is a common component of rhizosphere soil and has been reported to suppress a great number of plant diseases, some strains also have been reported to colonize the root surface, enhancing root growth and development, crop productivity, resistance to abiotic stresses and the uptake and use of nutrients (Martinez-Medina et al 2011, Sureshrao et al 2016). *Trichoderma* species are highly opportunistic fungi isolated from diverse range of natural and artificial substrata and have shown adaptability to various ecological conditions. The

single application of *Trichoderma* as seed treatment is considered beneficial for the enhancement of root-related traits inducing vigorous plant root system (Dujeshwer et al 2021). Some strains of *Trichoderma* have ability to reduce the severity of plant diseases by inhibiting plant pathogens, mainly in the soil or on plant roots, through their high antagonistic and mycoparasitic potential (Grover et al 2011). Keeping the above facts in view, the present study was undertaken to evaluate the effect of hydrogel and *Trichoderma* on root parameters and WUE in linseed varieties under rainfed condition.

MATERIAL AND METHODS

A field experiment was conducted during *rabi* season of 2015 and 2016 to evaluate the effect of hydrogel and *Trichoderma* on root growth and WUE in linseed varieties at Agricultural Research farm (25.2568^{0}N, 82.9868^{0}E), Banaras Hindu University, Varanasi (U.P.). The experiment was laid out in split plot design (SPD) comprising three replications with four linseed varieties and six hydrogel and *Trichoderma* based formulation (Table 1). Seed soaking with hydrogel was done by mixing of required amount of hydrogel (Neethu et al 2018, Dar et al 2018) with same amount of water and seed for 12 hrs before sowing. Seeds were treated with *Trichoderma harzianum* @10 g kg^{-1} seed just before sowing of seed. Furrow application of hydrogel was done just before of direct seeding of seeds. Although, hydrogel is not soluble in water but it makes semi-translucent material with seed. The plants were established at 25 cm of row distance and a uniform dose of 40 kg N ha^{-1}, 20 kg P_2O_5ha^{-1}, and 20 kg K_2O ha^{-1} were applied as basal dose during both years of experiment. Seeds of requisite varieties were sown @ 30 kg ha^{-1}. Soil moisture content at the time of sowing was 65 per cent. The weekly mean minimum and maximum average temperature ranged between 14.8^{0}C to 29.4 ^{0}C and 14.6^{0}C to 28.9^{0}C during 2015 and 2016, respectively. The rainfall received during the period of experiment was 45.5 mm and 1.0 mm during 2015 and 2016, respectively.

The root area was recorded from three randomly selected plants in each plot from the sampling area. The uprooting of sample was performed with the help of core cutting equipment i.e. soil ring sampler along with the soil up to effective root zone (25 cm). The roots of the plant were washed in sieve with running water and effective root covering area (length and width) was measured. Root length was measured from root/shoot demarcation point to root tip (The roots biomass was recorded by drying of separated roots at 60^{0}C±5^{0}C for 48 hours in hot air oven thereafter dry weight of roots was recorded by an electronic digital balance and average dry weight plant^{-1} was worked out. The WUE in kg ha^{-1} mm^{-1} for a given treatment was calculated by dividing the seed yield with the respective total evapotranspiration (ET) of the cropping period. ET can be calculated by multiplication of pan evaporation (PE) value with Crop coefficient (K_c). K_c value for different crops is suggested by Allen et al (1998).

$$WUE = \frac{\text{Yield (Seed yield in kg)}}{ET}$$

ET = PE value x K_c

The RWC of plant is taken at maximum growth stage (90 DAS) and it is obtained using following equation given by Tian et al (2015).

Table 1. Details of treatments

Main plot: Varieties	Characteristics
V1: Kartika	Erect plant, upper top branching, non-lodging, shattering resistance and seed colour is brown. Suitable for early to medium late sown conditions. Maturity duration is 110-120 days and oil content is 37 per cent.
V2: Deepika	Erect plant, small flower and seed color is brown. Moderately resistant to rust, wilt and *Alternaria* blight. Maturity duration is 110-115 days and oil content is 39 per cent.
V3: Garima	Oil purpose variety. It performs well under irrigated as well as rainfed conditions. Oil content in seed is around 40%. Maturity duration ranges between 135-145 days.
V4: RLC-92	Erect plant, upper top branching, non-lodging, shattering resistance and seed colour is brown. Suitable for early, normal and late sown condition. Resistant to rust, wilt and moderately resistant to *Alternaria* blight and bud fly. Maturity duration is 110-115 days and oil content is 39 per cent.

Sub plots: Hydrogel & *Trichoderma*

H_1:	Control
H_2:	Seed soaking in hydrogel @ 42 g kg^{-1}seed
H_3:	Seed treatment with *Trichoderma* @ 10 g kg^{-1}
H_4:	Seed soaking in hydrogel @ 42 g kg^{-1}seed followed by seed treatment with *Trichoderma* @ 10 g kg^{-1}
H_5:	Soil amendment with hydrogel @ 2 g m^{-2}
H_6:	Soil amendment with hydrogel @ 2 g m^{-2} + sowing of *Trichoderma* treated seed

$$RWC\ (\%) = \frac{(FW-DW)}{FW} \times 100$$

Whereas, FW = Fresh weight of plant, DW = Dry weight of plant

SMBC was determined by using chloroform extraction fumigation method (Witt et al 2000). Yield was recorded at harvest.

Data analysis: The data were subjected to statistical analysis using STAR (Statistical Tool for Agricultural Research) software of International Rice Research Institute and R package. The parameters under study were tested for normality assumption and homogeneity of variances using Shapiro-Wilk's normality test. All the parameters were non-significant and hence null hypothesis of data is normal and variances are homogenous was accepted. The significant treatments were marked with Duncan's Multiple Range Test (DMRT) letter (Duncan 1955).

RESULTS AND DISCUSSION

Effect on root area (cm^2) and root biomass (g $plant^{-1}$): The root area and root biomass were recorded at 30, 60 and 90 DAS of crop growth and revealed significant differences among the varieties and also with hydrogel & *Trichoderma* based treatments (Fig. 1 and 2). Among the varieties, V_3 recorded significantly highest root area, V_1 and V_4 were on par with each other at all stages of observation. The lowest root area was recorded with V_2. The *Trichoderma* and hydrogel formulation treatments were also found significant during the observation. Data on root area revealed that H_3 recorded significantly highest root area and was comparable with treatment H_4, H_5 and H_6 at all the stages of observations (Fig. 1). None of the interaction between treatments and varieties was found significant on root area during the observations. The perusal of mean data revealed that the cultivar V_3 and V_4 recorded significantly superior on root biomass over V_1 and V_2 and remained at par with each other at 60 DAS and 90 DAS (Fig. 2). At 30 DAS, V_3 recorded higher root biomass over other varieties. V_1 and V_2 remained at par with each other during the observation. Among the treatments, H_6 recorded significantly highest root biomass and remained at par with H_3. Treatment H_2, H_4 and H_5 were at par with each other during the observation. The significantly lowest root biomass was found in H_1(Control). The interaction between V_3 and V_4 with treatments H_6 on root biomass was significant at 90 DAS. The higher root area and biomass were recorded by hydrogel and *Trichoderma* applied treatments that may indicate higher water availability at initial stage of root development and improved root extension by hydrogel (Akhter et al 2004). *Trichoderma* enhances drought tolerance, plant growth promotion including enhanced nutrient uptake and inhibition of deleterious root microflora (Harman et al 2004, Dujeshwer et al 2021) and also promotes plant root growth by controlling the population of pathogenic microorganisms in rhizosphere (Benítez et al 2004) by influencing plant physiology through mineral solubilization (Harman et al 2004, Li et al 2015) or by increased availability of phosphorus and possibly through hormones (Cuevas 2006, Banoni et al 2020).

Effect on water use efficiency (kg ha^{-1} mm^{-1}): The mean data pertaining to WUE in linseed showed significant differences on varieties as well as hydrogel, *Trichoderma* and combination of these two (Table 2). Variety V_4 recorded significantly highest WUE over other varieties and V_2 and V_3 at par to each. The lowest WUE was for V_1. The pooled data revealed significantly higher WUE by using H_6 over H_1. Treatments H_3, H_4 and H_5 remained at par with each other. The lowest WUE was found under H_1 (control). The interaction between the varieties and treatments was unable to reach any significance level. Hydrogel created a reservoir within the root zone and made moisture available to the plant when it needed. Better water uptake by plant can be ensured by changing physical properties of soil like better water holding capacity or by enhancing the root capacity to reach deeper layers of the soil. Hydrogel addition in soil was effective in improving soil moisture availability hence increased WUE and better plant establishment was recorded in hydrogel applied treatments (Akhter et al 2004, Abdallah 2019).

Effect on relative water content (%): The mean data pertaining to RWC indicated that varieties V_3 and V_4 were superior over V_1 and V_2. However, V_2 and V_4 were statistically comparable (Table 2). Lowest RWC was recorded in variety

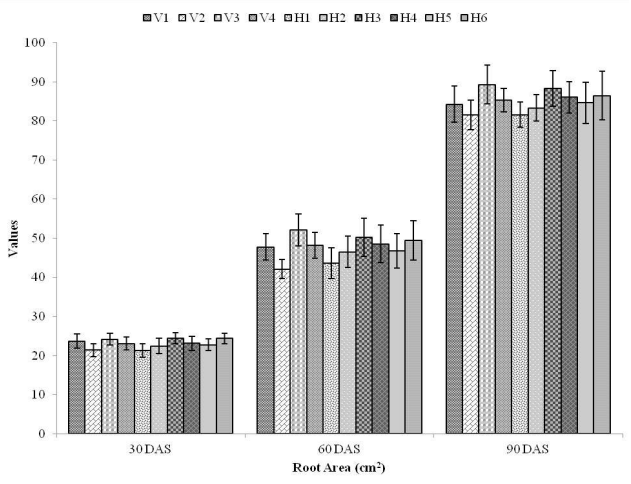

Error bar indicated the standard error

Fig. 1. Effect on *Trichoderma* and hydrogel formulations on root area (cm^2) in linseed

V_1. RWC was significantly different among various treatments. Treatment H_3 and H_6 recorded statistically superior and comparable RWC over H_1. Treatment H_2, H_3, H_4 and H_5 remained at par and the lowest RWC was recorded by H_1 (control). None of the interaction effect between varieties and treatments on RWC was significant during the experimentation. Different studies clearly indicated that the hydrogel reduces the downward movement of water, thereby reducing percolation. Additionally, amending the soil with hydrogels, particularly with small sized particles, markedly increased WHC and plant available water (PAW) induced better growth of water-stressed plant and significantly prolonged their survival. More available water to the plants resulted in higher RWC and PAW (Orikiriza et al 2013, Abdallah 2019).

Effect on soil microbial biomass carbon (mg C kg $^{-1}$ soil): The mean data on SMBC revealed that varieties were not significant (Table 2). Among the treatments, the maximum SMBC was recorded under H_3 and H_6 which remained statistically at par with each other and significantly superior over H_1. Treatment H_1, $H_2$and H_5were statistically at par. None of the interaction effect between varieties and treatments on SMBC was significant. Application of *Trichoderma* may change the biotic composition of rhizosphere by multiplying in significant number. *Trichoderma* is reported to increase the SMBC in the soil (Yadav et al 2009). *Trichoderma* bio-fertilizer effectively regulated soil chemistry and microbial communities, driving substantially improved above ground plant biomass as well as soil microbial biomass (Zhang et al 2018).

Effect on seed yield (kg ha^{-1}): The varieties have shown significant variation in seed yield (Table 2). V_4 recorded significantly highest seed yield over other varieties. Variety V_1, V_2 and V_3 remained at par with each other and V_1recorded lowest seed yield. Among the *Trichoderma* & hydrogel treatments, H_4 and H_6 recorded significantly highest seed

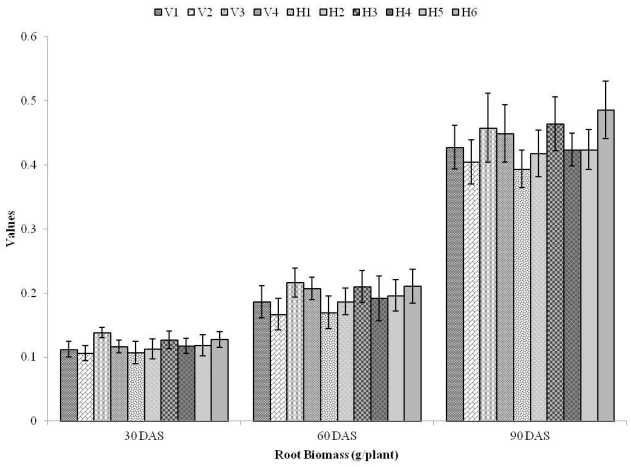

Error bar indicated the standard error

Fig. 2. Effect on *Trichoderma* and hydrogel formulations on root biomass (g plant^{-1}) in linseed

Table 2. Effect on *Trichoderma* and hydrogel formulations on WUE, RWC, SMBC and seed yield in linseed

Treatments	WUE (kg ha^{-1} mm^{-1})	RWC (%)	SMBC (mg C kg $^{-1}$ soil)	Seed yield (kg ha^{-1})
Varieties				
V_1: Kartika	3.39^{c}	66.8^{c}	182.7	1311.7^{c}
V_2: Deepika	3.49^{bc}	68.0^{bc}	185.0	1354.6^{bc}
V_3: Garima	3.60^{b}	69.8^{a}	186.3	1388.3^{b}
V_4: RLC-92	3.80^{a}	68.7^{ab}	184.6	1469.0^{a}
CD (P=0.05)	0.14	1.70	NS	54.3
Hydrogel and *Trichoderma* treatments				
H_1: Control	3.27^{c}	66.3^{c}	173.3^{c}	1258.7^{c}
H_2: Seed soaking in hydrogel @ 42 g kg^{-1}	3.47^{bc}	68.0^{abc}	173.6^{c}	1344.3^{b}
H_3: Seed treatment with *Trichoderma* @ 10 g ha^{-1}	3.62^{ab}	67.9^{bc}	200.6^{a}	1398.7^{ab}
H_4: Seed soaking in hydrogel @ 42 g kg^{-1} followed by seed treatment with *Trichoderma* @ 10 g ha^{-1}	3.70^{ab}	69.1^{ab}	188.4^{b}	1430.6^{a}
H_5: Soil amendment with hydrogel @ 2 g m^{-2}	3.58^{ab}	68.3^{abc}	176.3^{c}	1384.6^{ab}
H_6: Soil amendment with hydrogel @ 2 g m^{-2} + sowing of *Trichoderma* treated seed.	3.81^{a}	70.4^{a}	195.9^{a}	1468.4^{a}
CD (P≤0.05)	0.23	2.40	5.88	84.7
Interaction (P≤0.05)	NS	NS	NS	NS

Values with the same letter differ non significantly (p > 0.05). Different letters for each parameter show a significant difference (p < 0.05), NS= Not significant

yield and were at par with treatment H_3 and H_5 over H_1 (control). H_1 recorded significantly lowest seed yield. None of the interaction effect between varieties and treatments on seed yield was significant. Hydrogel and *Trichoderma* both affect the nutrient uptake indirectly by increasing moisture in the soil and subsequently ion mobility. Therefore, the availability of some nutrients either present in soil or added in the form of relatively insoluble fertilizers such as phosphates may increases (El-Hady et al 2003). Hydrogel and *Trichoderma* applied treatments resulted in higher WUE, RWC, root biomass and crop yield which may be attributed to more available water provided during critical growth period by hydrogel combined with higher root growth and nutrient uptake by *Trichoderma* application (Chaudhary et al 2020).

CONCLUSION

Trichoderma with hydrophilic polymer (hydrogel) was effective in enhancing root growth, root biomass, WUE and yield of linseed under rainfed ecology of Indo Gangetic plains (IGPs). Hydrogel manipulate the physical condition of soil, mainly water holding capacity. Sufficient amount of water combined with *Trichoderma* treatment promoted the root growth, plant growth and yield of crop. Both the input had no negative impact on plant growth, yield and beneficial soil micro-flora. Interaction effect of hydrogel and *Trichoderma* could not establish. Although the present result showed that *Trichoderma* and hydrogel could enhance growth and yield of linseed in the experimental location, hence the *Trichoderma* and hydrogel application can be recommended for Indo-Gangetic plains in Uttar Pradesh.

ACKNOWLEDGEMENT

The authors would like extend gratitude to University Grant Commission, New Delhi for the financial support.

REFERENCES

Abdallah AM 2019. The effect of hydrogel particle size on water retention properties and availability under water stress. *International Soil and Water Conservation Research* **7**: 275-285.

Akhter J, Mahmood K, Malik KA, Mardan A, Ahmad M and Iqbal MM 2004. Effects of hydrogel amendment on water storage of sandy loam and loam soils and seedling growth of barley, wheat and chickpea. *Plant, Soil Environment* **50**: 463-469.

Allen RG, Pereira LS, Raes D and Smith D 1998. *Crop Evapotranspiration-Guidelines for computing crop water requirement.* FAO United Nations Rome.

Badole SL, Zanwar, AA and Bodhankar SL 2013. Antihyperglycemic Potential of Secoisolaricinol Diglucoside, *Bioactive Food as Dietary Interventions for Diabetes,* Academic Press 53-57.

Benitez T, Rincon AM, Limon MC and Codon AC 2004. Biocontrol mechanisms of *Trichoderma* strains. *International Microbiology* **7**: 249-260.

Bononi L, Chiaramonte JB, Pansa CC, Moitinho MA and Melo IS 2020. Phosphorus-solubilizing *Trichoderma* spp. from Amazon soil improves soybean plant growth. *Scientific Report* **10:** 2858.

Chaudhary S, Sagar S, Lal M, Tomar A, Kumar V and Kumar M 2020. Biocontrol and growth enhancement potential of *Trichoderma* spp. against *Rhizoctonia solani* causing sheath blight disease in rice. *Journal of Environmental Biology* **41**: 1034-1045.

Cuevas VC 2006. Soil inoculation with *Trichoderma pseudokoningii* rifai enhances yield of rice. *Philippine Journal of Science* **135**(1): 31-37.

Dar SB, Mishra D, Zahida R and Afshana BB 2018. Hydrogel: To enhance crop productivity per unit available water under moisture stress agriculture. *Bulletin of Environment Pharmacology and Life Sciences* **6**: 129-135.

DoE&S 2019. Directorate of Economics and Statistics, Ministry of Agriculture and Farmers Welfare.

Dujeshwer K, Singh RK, Jatav HS, Lakpale R, Khan M, Rajput VD and Minkina T 2021. Hydrogel based *Trichoderma* formulations' effect on different varieties of rice under rainfed condition of Indo-Gangetic Plains. *Environment, Development and Sustainability,* doi.org/10.1007/s10668-021-01738-w.

Duncan DM 1955. Multiple range and multiple F-test. *Biometric* **11**: 1-42.

El-Asmar J, Jaafar H, Bashour I, Farran MT and Saoud IP 2017. Hydrogel banding improves plant growth, survival, and water use efficiency in two calcareous soils. *Clean-Soil, Air, Water* **45**(7): 1-9.

El-Hady OA, Abdel Hady BM, Rizk NA, El-Saify ES 2003. The potentiality for improving plant-soil-water relations in sandy soils using some synthesized AmNa (or K) ATEA hydrogels. *Egyptian Journal of Soil Sciences* **43**: 547-566.

FAOSTAT 2018. http://www.faostat.org.

Grover M, Ali SKZ, Sandhya V, Rasul A and Venkateswarlu B 2011. Role of microorganisms in adaptation of agriculture crops to abiotic stresses, *World Journal of Microbiology and Biotechnology* **27**: 1231-1240.

Harman GE, Petzoldt R, Comis A and Chen J 2004. Interactions between *Trichoderma harzianum* strain T22 and maize inbred line Mo17 and effects of this interaction on diseases caused by *Pythium ultimum* and *Colletotrichum graminicola*, *Phytopathology* **94**(2): 147-153.

Hu X, Wang Q, Liu Q, Li Z and Sun G 2020. Villus like nano composite hydrogels with a super high water absorption capacity. *Journal of Material Chemistry A* **25**: 12613-12622.

Jain NK, Meena HN and Bhaduri D 2017. Improvement in productivity, water-use efficiency, and soil nutrient dynamics of summer peanut (*Arachis hypogaea* L.) through use of polythene mulch, hydrogel and nutrient management. *Communication in Soil Science and Plant Analysis* **48**(5): 549-564.

John GF 2011. *Towards improved application of super absorbent polymers in agriculture and hydrology: A cross-disciplinary approach*. Dissertation, Auburn University.

Kumar R, Yadav S, Singh V, Kumar M and Kumar M 2020. Hydrogel and its effect on soil moisture status and plant growth: A review. *Journal of Pharmacognosy and Phytochemistry* **9:** 1746-1753.

Li R X, Cai F, Pang G, Shen QR, Li R and Chen W 2015. Solubilization of phosphate and micronutrients by *Trichoderma harzianum* and its relationship with the promotion of tomato plant growth. *PLoS ONE* **10**: 1-16.

Martinez-Medina A, Roldán A and Pascual JA 2011. Interaction between arbuscular mycorrhizal fungi and *Trichoderma harzianum* under conventional and low input fertilization field condition in melon crops, Growth response and *Fusarium* wilt biocontrol. *Applied Soil Ecology* **47**(2): 98-105.

Neethu TM, Dubey PK and Kaswala AR 2018. Prospects and applications of hydrogel technology in agriculture. *International Journal of Current Microbiology and Applied Sciences* **7**: 3155-3162.

Orikiriza LJB, Agaba H, Eilu G, Kabasa JD, Worbes M and

Hüttermann A 2013. Effects of hydrogels on tree seedling performance in temperate soils before and after water stress. *Journal of Environmental Protection* **4**: 713-721.

Sureshrao KS, Pradeeprao KT, Dnyanobarao GS, Agrawal T and Kotasthane AS 2016. Root growth stimulation in rice (*Oryza sativa* L.) by seed biopriming with Trichoderma sp. *Applied Biological Research* **18:** 30-38.

Tian XY, He MR, Wang ZL, Zhang JW, Song YL, He ZL 2015. Application of nitric oxide and calcium nitrate enhances tolerance of wheat seedlings to salt stress. *Plant Growth Regulator* **77**: 343-356.

Witt C, Gaunt J, Galicia C, Ottow G and Neue U 2000. A rapid chloroform-fumigation extraction method for measuring soil microbial biomass carbon and nitrogen in flooded rice soils. *Biology and Fertility of Soils* **30:** 510-519.

Wu M, Li D, Wang LJ, Zhou YG, Brook MS, Chen XD and Mao ZH 2008. Extrusion detoxification technique on flaxseed by uniform design optimization. *Separation and Purification Technology* **61**: 51-59.

Yadav RL, Shukla SK, Suman A and Singh PN 2009. *Trichoderma* inoculation and trash management effects on soil microbial biomass, soil respiration, nutrient uptake and yield of ratoon sugarcane under subtropical conditions. *Biology and Fertility of Soils* **45**: 461-468.

Zhang F, Yunqian H, Adam B, Cobb L, Luo G, Zhou J, Yang G, Gail WT, Wilson and Zhang Y 2018. *Trichoderma* biofertilizer links to altered soil chemistry, altered microbial communities, and improved grassland biomass. *Frontier in Microbiology* **9**: 848-856.

Zhang ZS, Li D, Wang LJ, Ozkan N, Chen XD, Mao ZH and Yang HZ 2007. Optimizations of ethanol–water extraction of lignans from flaxseed. *Separation and Purification Technology* **57**: 17-24.

Received 11 July, 2021; Accepted 12 November, 2021

Indian Journal of Ecology (2021) 48(6): 1821-1828

Manuscript Number: 3455
NAAS Rating: 5.79

Ichthyofaunal Diversity and Conservation Status in the River Teesta, West Bengal, India

Tapan Sarkar and Joydeb Pal[1]

Department of Zoology, Raiganj University, Raiganj-733 134, India
[1]Department of Zoology, North Bengal University, Siliguri-734 014, India
E-mail: tapan.ruzoo@gmail.com

***Abstract*:** A study on ichthyofaunal diversity was conducted in the River Teesta from March 2014 to February 2016 at two sapling sites. Objectives of the study were assessing the fish diversity and their conservation status. Sampling was done monthly interval with the help of professional fisherman. A total 140 fish species belonged to 11 orders, 31 families and 78 genera found from the River Teesta. Cyprinidae was the most dominant family. CPUE, number of ichthyofauna genera, Shannon diversity index, Margalef's richness index, evenness index and dominance index varied from 41 to 158 individual/100m^2, 30 to 85, 3.34 to 4.32, 8.50 and 16.66, 0.901 to 0.992 and 0.014 to 0.057 respectively. 5% and 45.71 % fish species are under threatened category according to IUCN and CAMP and NBFGR conservation status respectively. Over and indiscriminate fishing, construction of damp and introduction of exotic fish species are major threat of ichthyofauna in the River Teesta.

***Keywords*:** Ichthyofaunal diversity, Teesta, Shannon diversity index, Margalef's, Conservation status

India is a mega bio-diversity country and ranks ninth in terms of freshwater bio-diversity. Species diversity of an ecosystem indicates a stable and good environmental condition. Among the vertebrates fishes are the most abundant group in world. Out of two thousands fifty fish species reported in India 930 are lives in fresh water. North Bengal is designated as 'Hot spot' of freshwater fish due to presence of many endemic fish species (Barman 2007) and is blessed with many rivers and all are rich in ichthyofauna diversity. Most of the rivers of North Bengal are originated from the Himalaya. Riverine fishes of North Bengal are important source of protein for local people. The river Teesta is a 309 Km long river and part of the Brahamaputra drainage system. The river originates from the Pahunri glacier near Khangehung Lake in North Sikkim (Meetei et al 2007). Many workers have been studied the fish diversity in the Dooars and Terai region of West Bengal, such as Shaw and Shebbeare (1937), Sarkar and Pal (2015) and Acherjee and Barat (2013). Aims of the study were assess the fish diversity and their conservation status in the River Teesta.

MATERIAL AND METHODS

Sampling sites-Two sampling sites were selected for study such as site 1 and 2. Sampling site 1 is located at village Gajoldoba **(**latitude-26^{0}44'55.4''N and longitude **-** 88^{0}35'37.0"E) and sampling site 2 is situated at Haldi Bari (latitude-26^{0}23'01.2"N and longitude **-** 88^{0}50'38.0"E) (Fig. 1).The survey was conducted from March 2014 to February 2016.

Methods: Survey was conducted at every month with the help of professional fishermen. Fishes were collected with the cast net (mesh size 0.5 mm). The numbers of individuals in each species were counted and immediately photographs were taken with digital camera (Canon X160). Then collected fishes were preserved in 8-9 % formalin solution for further study. Identification of ichthyfauna species were done by Shaw and Shebbeare (1937) and Sen (1992). Conservation status was assigned on the basis of Molur and Walker (1998), Lakra et al (2010)and IUCN category (2013).

Diversity indices: Shannon diversity index, evenness index, Margalef's richness index and dominance index were calculated by PAST 3.0 software (Hammer 2001). One-way ANOVA was done for show the differences between the months of two year with the help of PAST 3.0 software (Hammer 2001).

RESULTS AND DISCUSSION

A total of 140 species belonged to 11 order, 31 families and 78 genera were obtained during the study period in the River Teesta. Cyprinidae was the dominant family comprising 53 species then followed by Sisoridae, Bagridae, Nemacheilidae, Cobitidae etc. (Table 1). Order wise distribution of fish shown in fig.-2. Number of fish species recorded more than the previous work such as Shaw and Shebbeare (1937), Dey et al(2015) and Das(2015).

Catch per unit effort: CPUE was ranged from 41 to 158 individual/100m^{2}in the River Teesta. Highest catch per unit effort (CPUE) was in October at both sampling sites. Monthly

variation of CPUE between the two years did not show any significant differences at site 1 ad 2 (Table 2 and 3).

Ichthyofauna genera: Ichthyofauna genera were ranged from 30 to 85 in the River Teesta. The maximum number of ichthyofauna genera was in October at both sites. Monthly variation of number of ichthyofauna genera between the two years did not show any significant differences at site 1 and 2 (Table 2 and 3).

Shannon-Wiener diversity index (H'): Shannon-Wiener diversity index was ranged from 3.34 to 4.32 in the River Teesta.Maximum was recorded in October at both sites. Monthly variation of Shannon-Wiener diversity index between the two years did not show any significant differences at site 1 and 2 (Table 2 and 3). The greater fish diversity in rainy season was due to increased water depth with huge nutrient (Shahnawaz et al 2011). According to Shannon-Weiner legislation, the river is classified as good to very good (Shannon-Weiner diversity value 3-4 is goodor 4> is very good) (Shannon and Weaver 1949).

Ichthyofaunal evenness index (J'): Evenness index was ranged from 0.901 to 0.992 in the River Teesta. Monthly variation of evenness index between the two years did not show any significant differences at site 1 and 2 (Table 2 and 3).Acherjee and Barat (2013) reported that the evenness index (J') varied from 0.882 to 0.988 in the hill stream Relli. Sengupta and Homechaudhuri (2015) observed maximum evenness index in rainy season (0.94) and the least in summer (0.84).

Margalef's richness index (R): Margalef's richness index was ranged between 8.50 and 16.66 in the River Teesta. Maximum was observed in October at both sites. Monthly variation of Margalef's richness index between the two years did not show any significant differences at site 1 and 2 (Table 2 and 3).The average value of Margalef's richness index was 6.64 reported by Rahaman et al (2015) in the river Talma, Bangladesh. Highest average seasonal value of Margalef's richness index was found in rainy seasons at all the two sites. Sengupta and Homechaudhuri (2015) observed maximum species richness during the rainy season, similar finding was suggested by Hanif et al (2016) and Rahaman et al (2015).

Index of dominance (λ): Dominance index was ranged from 0.014 to 0.057 in the River Teesta. Low dominance index indicates species were evenly distributed. Monthly variation of dominance index between the two years did not show any significant differences at site 1 and 2 (Table 2 and 3). Acherjee and Barat (2013) reported the dominance index range from 0.055 to 0.281 in the hill stream Relli and river Teesta.

Two sapling sites (courtesy-Google Map) | Sampling site 1 | Sampling site 2

Fig. 1. Sampling sites 1 and 2

Five exotic fishes were found in the River Teesta. Many migratory and cold water fishes also recorded. Fish diversity decreased in winter season due to diversion of river water in to the Teesta feeder canal. Most dominant fish species were *Barilus* spp., *Puntius* spp., *Garra* spp. etc. during the study. *Labeo* spp. were more dominant in winter season because most of the species are migratory and migrated from upstream to downstream in winter.

Conservation status: According to IUCN conservation status two fish species are Endangered (EN), 5 species Vulnerable (VU), seven species near threatened (NT) and 119 fish species are least concern (LC). On the basis of CAMP-NBFGR (Molur and Walker 1998, Lakra et al 2010) conservation and threat status, one species is Critically endangered (CR), 20 fish species are Endangered (EN), 43 species Vulnerable (VU), 32 species are Low risk near threatened (LRnt) and 17 fish species are Low risk least concern. Five exotic fish species were reported during the study from this river.

One Endangered (EN), 2 Vulnerable (VU) and 10 near Threatened fish species globally were reported from the river Torsa and its tributaries (Das 2015). Patra et al (2011) found 20% fish species under threatened category in the river Karola. Dey et al(2015) recorded 1 CR (1%), 12 EN (8%), 33 VU (23%) and 66 (47 %) LRnt fishes from the different rivers of the Dooars region. Highest CPUE, number of ichthyofauna genera, species diversity index (H'), Margalef's species richness index (R) and species dominance index were reported in rainy season and lowest in summer season. Present investigation corroborates with the findings of Acherjee and Barat (2013). Rakshit and Roy (2021) reported maximum number of ichthyofauna genera and species diversity index (H') in rainy season.Species evenness index (J') was reported highest in summer and lowest in rainy season (Table 4).

Threat of Ichthyofauna

Over and indiscriminate fishing: Over and illegal fishing are major threat of the fish diversity in the River Teesta. Mosquito net is also used for fishing at site 1 which even not excluded the fingerlings and brooders. Similar findings suggested by Patra et al (2011).

Construction of dam: Dam on Gajoldoba prevents the migration of fishes from upstream to downstream and vice

Table 1. Checklist of ichthyofauna with conservation status in the River Teesta

Family	Fish species found	Conservation status		2014-15		2015-16	
		IUCN	NBFGR	Site-1	Site-2	Site-1	Site-2
Amblycipitidae	*Amblyceps mangios* (Hamilton)	LC	LRnt	+	+	+	+
Aplocheilidae	*Aplocheilus panchax* (Hamilton)	LC	DD	-	-	+	+
Anabantidae	*Anabas testudineus* (Bloch)	DD	VU	+	+	+	+
Osphronemidae	*Trichogaster chuna* (Bloch & Schneider)	LC	NK	+	-	+	+
	T. fasciata (Schneider)	LC	LRnt	+	-	+	-
	T. labiosa (Das)	LC	NK	-	+	+	-
	Ctenops mobiles (McClelland)	LC	VU	+	-	+	+
Anguillidae	*Anguilla bengalensis* (Gray)	NT	EN	+	+	-	+
Bagridae	*Batasio batasio* (Hamilton)	LC	NK	+	+	+	+
	B. tengana (Hamilton)	LC	LRlc	+	-	+	-
	B. fasciolatus (Ng)	NE	LRlc	+	+	-	+
	Hemibarus menoda (Hamilton)	LC	EN	+	-	+	+
	Mystus vittatus (Bloch)	LC	VU	+	+	+	+
	M. bleekeri (Day)	LC	VU	+	+	+	+
	M. tengra (Hamilton)	LC	LRlc	+	+	+	-
	Sperata seenghala (Sykes)	LC	VU	+	+	+	+
	S. aor (Hamilton)	LC	VU	+	+	-	-
	Rita rita (Hamilton)	LC	LRnt	-	-	+	-
Nemacheilidae	*Aborichthys elongatus* (Hora)	LC	EN	+	+	+	+
	Balitora bruccei (Gray)	NT	LRnt	+	+	+	+
	Acanthocobitis botia (Hamilton)	LC		+	+	+	+
	Schistura devdevi (Hora)	NT	EN	+	-	+	-
	S. corica (Hamilton)	LC	LRnt	+	+	+	+
	S. rupecula (McClelland)	LC	LRnt	+	+	+	-
	S. savona (Hamilton)	LC	LRlc	+	+	+	+
	S. bevani (Gunther)	LC	EN	+	+	+	+
Belonidae	*Xenentodon cancila* (Hamilton)	LC	VU	+	+	+	+
Channidae	*Channa punctata* (Bloch)	LC	LRnt	+	+	+	+
	C. striata (Bloch)	LC	LRlc	-	+	+	+
	C. marulius (Hamilton)	LC	LRnt	+	-	+	+
	C. gachua (Hamilton)	LC	EN	+	+	+	-
Clupeidae	*Gudusia chapra* (Hamilton)	LC	LRlc	+	+	+	+
Cobitadae	*Botia dayi* (Hora)	NE	VU	+	+	+	+
	Pangio pangio (Hamilton)	LC	VU	+	+	-	-
	Botia dario (Hamilton)	LC	VU	+	-	+	+
	B. lohachata (Chaudhuri)	LC	EN	+	+	+	+
	Lepidocephalicthys guntea (Hamilton)	LC	VU	+	+	+	+
	Lepidocephalicthys annandalei (Chaudhuri)	DD	LRnt	-	-	+	-
	Somileptes gongota (Hamilton)	LC	VU	+	+	+	+
Clariidae	*Clarias batrachus* (Linnaeus)	EN	VU	+	+	+	+
	*Clarias gariepinus (*Burchill)	EX	EX	+	+	-	-

Cont...

Table 1. Checklist of ichthyofauna with conservation status in the River Teesta

Family	Fish species found	Conservation status		2014-15		2015-16	
		IUCN	NBFGR	Site-1	Site-2	Site-1	Site-2
Cyprinidae	*Amblypharyngodon mola* (Hamilton)	LC	LRlc	+	+	+	+
	A. microlepis (Bleeker)	LC		-	+	+	+
	Aspidoparia morar (Hamilton)	LC	LRnt	+	+	+	+
	A. jaya (Hamilton)	LC	VU	+	+	+	+
	Barilius barila (Hamilton)	LC	VU	+	+	+	+
	B. barna (Hamilton)	LC	LRnt	+	+	+	+
	B.bola (Hamilton)	LC	VU	+	+	+	+
	B. shacra(Hamilton)	LC	LRnt	+	-	+	-
	B. vagra (Hamilton)	LC	VU	-	+	+	+
	B. bendelisis (Hamilton)	LC	LRnt	+	+	+	-
	B. tileo (Hamilton)	LC	LRnt	+	+	+	+
	Bengala elanga (Hamilton)	LC		-	+	+	+
	Catla catla (Hamilton)	LC	VU	+	-	-	-
	Chagunius chagunio (Hamilton)	LC	EN	+	+	+	+
	Chela laubuca (Hamilton)	LC	LRlc	+	+	+	+
	Cirrhinus mrigala (Hamilton)	LC	VU	-	+	+	+
	C. reba (Hamilton)	LC	VU	+	+	+	+
	Crossocheilus latia (Hamilton)	LC	VU	-	+	+	+
	Devario devario (Hamilton)	LC	LRnt	+	+	+	+
	D. aequipinnatus (McClelland)	LC		-	+	+	-
	Danio rerio(Hamilton)	LC	VU	+	+	+	+
	D. dangila (Hamilton)	LC	VU	+	+	+	+
	Esomus danricus(Hamilton)	LC	LRlc	+	+	+	+
	Rasbora daniconius (Hamilton)	LC	LRlc	-	+	+	+
	Garra gotyla (Gray)	LC	VU	+	+	+	+
	G. kempi (Hora)	LC	LRlc	+	+	+	+
	G. lamta (Hamilton)	LC	VU	+	-	+	-
	G. mcclellanei (Jerdon)	LC	LRlc	+	+	+	+
	G. naganensis (Hora)	LC	VU	+	-	-	-
	Labeo bata (Hamilton)	LC	LRnt	+	+	+	-
	L. boga (Hamilton)	LC	LRnt	+	+	+	+
	L. dero (Hamilton)	LC	VU	+	+	+	+
	L. dyocheilus (McClelland)	LC	VU	+	+	+	+
	L. gonius (Hamilton)	LC	LRnt	+	+	+	+
	L. pangusia (Hamilton)	LC	LRnt	+	+	+	-
	L. rohita (Hamilton)	LC	LRnt	+	+	+	+
	Neolissocheilus hexagonolepis (McClelland)	LC	VU	+	-	+	-
	Osteobrama cotio (Hamilton)	LC	LRnt	+	+	+	+
	Puntius conchonius (Hamilton)	LC	VU	+	+	+	+
	P. gelius (Hamilton)	LC	LRlc	+	+	+	-
	P. phutunio (Hamilton)	LC	LRlc	+	-	+	+
	P. stigma (Val.)	LC		+	+	-	-
	P. sophore (Hamilton)	LC	LRnt	+	+	+	+
	P. sarna (Hamilton)	LC	VU	+	-	+	-

Cont...

Table 1. Checklist of ichthyofauna with conservation status in the River Teesta

Family	Fish species found	Conservation status		2014-15		2015-16	
		IUCN	NBFGR	Site-1	Site-2	Site-1	Site-2
	P. ticto (Hamilton)	LC	LRnt	+	+	+	+
	Oreichthys cosuatis (Hamilton)	LC		+	+	+	+
	Schizothoraichthys progastus (McClelland)	LC	LRnt	+	+	+	+
	S. richardsonii (Gray)	LC	VU	+	-	+	-
	Semiplotus semiplotus (McClelland)	LC	VU	+	+	+	+
	Tor putitora (Hamilton)	EN	EN	+	+	+	-
	T. tor (Hamilton)	DD	EN	+	+	+	+
	Cyprinus carpio (Linnaeus)	EX	EX	-	+	+	+
	Hypophthalmichthys molitrix (Valenciennes)	EX	EX	+	+	+	-
Centropomidae	*Parambassis baculis* (Hamilton)	DD	LRlc	+	-	+	+
	P. ranga (Hamilton)	LC	LRlc	+	+	+	+
	Chanda nama (Hamilton)	LC	LRlc	+	+	+	+
Cichlidae	*Oreochromis mossambica* (Peter)	EX	EX	+	-	+	-
	O. nilotica (Linnaeus)	EX	EX	+	+	-	-
Chacidae	*Chaca chaca* (Hamilton)	LC	EN	+	+	+	+
Gobiidae	*Glossogobius giuris* (Hamilton)	LC	LRnt	+	+	+	+
Heteropneustidae	*Heteropneustes fossilis* (Bloach)	LC	VU	+	-	-	+
Mastacembelidae	*Mastacembelus armatus* (Lacepede)	LC	VU	+	+	+	+
	Macrognathus pancalus (Hamilton)	LC	NT	+	+	+	+
Mugilidae	*Rhinomugil corsula* (Hamilton)	LC	VU	+	+	+	+
Nandidae	*Badis badis* (Hamilton)	LC	VU	+	+	+	+
	B. kanabos Kullander & Britz	DD	NK	+	+	+	-
	Nandus nandus (Hamilton)	LC	LRnt	+	+	-	+
Ophichthidae	*Pisodonophis boro* (Hamilton)	LC	NE	+	+	-	+
Olyridae	*Olyra kempi* (Chaudhuri)	LC		+	+	+	+
	O. longicaudata (McClelland)	LC		-	-	+	+
Notopteridae	*Notopterus notopterous* (Pallas)	LC	EN	+	+	+	-
	Chitala chitala (Hamilton)	LC	EN	+	-	-	-
Pangasiidae	*Pangasius pangasius (Hamilton)*	LC	CR	-	-	+	-
Psilorhynchidae	*Psilorhynchus balitora* (Hamilton)	LC	VU	+	+	+	+
	P. sucatio (Hamilton)	LC	EN	+	+	+	+
Schilbeidae	*Ailia coila* (Hamilton)	NT	VU	+	-	+	+
	Clupisoma garua(Hamilton)	LC	VU	+	+	+	+
	Eutropiichthys murius(Hamilton)	LC	LRnt	+	+	-	+
	E. vacha (Hamilton)	LC	VU	+	+	+	+
Siluridae	*Ompok bimaculatus* (Bloch)	NT	EN	-	+	+	+
	O. pabda (Hamilton)	NT	EN	+	+	+	+
	Wallago attu (Schenider)	VU	LRnt	+	+	+	+
Sisoridae	*Bagarius bagarius* (Hamilton)	NT	VU	+	+	+	+
	Conta conta (Hamilton)	DD	NK	+	+	+	+
	Glyptothorax cavia (Hamilton)	LC	EN	+	-	-	-

Cont...

Table 1. Checklist of ichthyofauna with conservation status in the River Teesta

Family	Fish species found	Conservation status		2014-15		2015-16	
		IUCN	NBFGR	Site-1	Site-2	Site-1	Site-2
	Nangra punctata (Day)	LC		+	-	+	+
	Pseudolaguvia ribeiroi (Hora)	LC	LRnt	+	-	+	+
	P. shawi (Hora)	LC	EN	+	+	+	+
	Pseudecheneis sulcatus (McClelland)	LC	VU	+	+	-	+
	Sisor rhabdophorus (Hamilton)	LC	EN	-	+	-	+
Synbranchidae	*Monopterus cuchia* (Hamilton)	LC	LRnt	+	+	+	-
Tetraodontidae	*Tetraodon cutcutia* (Hamilton)	LC	LRnt	+	+	+	+

Table 2. Ichthyofaunal CPUE and diversity indices at site 1 (Gajoldoba) of the River Teesta during first and second year

Study period		March 2014- February 2016												ANOVA
Diversity Indices		March	April	May	June	July	August	September	October	November	December	January	February	
Catch Per Unit Effort	1st yr	135	56	92	63	112	129	139	154	66	43	70	63	F=1.91 P=0.18
	2nd yr	71	43	51	49	65	82	113	155	60	50	68	76	
Number of Genera (S)	1st yr	67	41	55	47	61	61	78	84	45	33	40	44	F=0.321 P=0.576
	2nd yr	51	34	41	37	46	55	79	85	48	38	48	50	
Species Diversity Index(H')	1st yr	4.06	3.64	3.82	3.78	3.73	3.78	4.29	4.32	3.70	3.43	3.40	3.65	F=0.012 P=0.91
	2nd yr	3.85	3.47	3.66	3.52	3.76	3.94	4.28	3.98	3.81	3.57	3.81	3.81	
Species Evenness Index (J')	1st yr	0.967	0.984	0.954	0.982	0.908	0.920	0.976	0.976	0.972	0.992	0.991	0.965	F=0.743 P=0.398
	2nd yr	0.981	0.986	0.985	0.976	0.984	0.984	0.980	0.901	0.986	0.985	0.984	0.962	
Margalef's Species Richness Index (R)	1st yr	13.45	9.93	11.94	11.1	12.72	12.35	15.6	16.48	10.5	8.50	9.18	10.38	F=0. 046 P=0.83
	2nd yr	11.73	8.77	10.17	9.25	10.78	12.25	16.5	16.66	11.48	9.45	11.14	11.31	
Species Dominance Index (λ)	1st yr	0.019	0.027	0.030	0.024	0.050	0.044	0.0157	0.014	0.028	0.034	0.051	0.030	F=0. 002 P=0.96
	2nd yr	0.022	0.032	0.027	0.083	0.024	0.020	0.015	0.048	0.023	0.029	0.023	0.024	

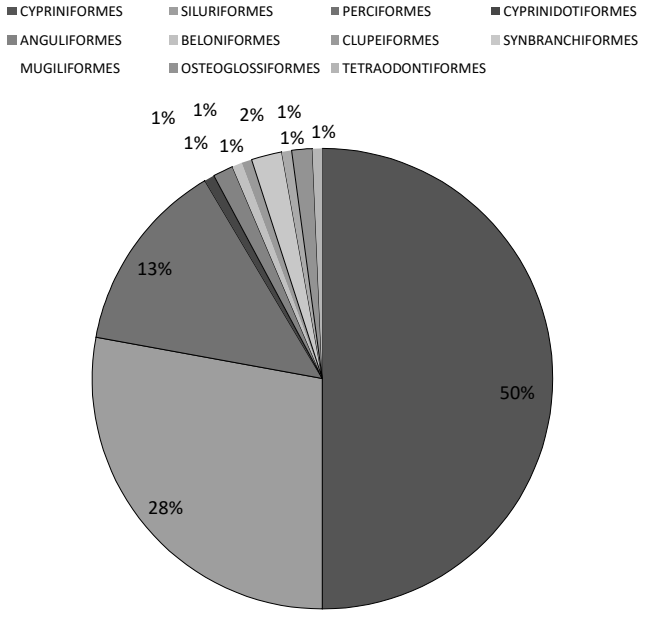

Fig.1. Percent composition of ichthyofaunal order in the river Teesta

versa. The construction of dams and barrages along the river courses results in decreased water flow (Hassan et al 1998). Dams or barrages cause physical alteration in downstream areas, changes in channel morphology and loss of rearing and spawning habitat due to upstream flooding, thus reduction of indigenous fish species.

Exotic fish species: Introduction of exotic fishes from the neighboring ponds during rainy season may be created problem in future.

River bed used as agriculture field: Water melon and in few places arum are cultivated in the river bed which may affected the fish diversity.

Flood: River Teesta often faced devastating flood and also flash flood which reduced the fish diversity particularly fry and fingerlings.

Pollution: Anthropogenic activities at sampling site 1 polluted the river water badly. Sampling site 1 is now become reputed tourist place in the Dooars region.

Table 3. Ichthyofaunal CPUE and diversity indices at site 2 (Haldi Bari) of the River Teesta during first and second year

Study period		March 2014- February 2016												ANOVA
Diversity Indices		March	April	May	June	July	August	September	October	November	December	January	February	
Catch Per Unit Effort	1st yr	49	41	51	56	44	85	122	158	41	57	56	55	F=0. 176 P=0.678
	2nd yr	59	41	63	46	63	99	155	143	65	45	70	43	
Number of Genera (S)	1st yr	42	31	43	42	35	58	77	85	35	45	47	42	F=0.135 P=0.716
	2nd yr	41	30	42	38	43	59	68	70	47	34	48	35	
Species Diversity Index(H')	1st yr	3.69	3.37	3.71	3.66	3.48	3.97	4.27	4.32	3.51	3.75	3.80	3.68	F=0.438 P=0.514
	2nd yr	3.65	3.34	3.67	3.58	3.70	4.01	3.71	4.16	3.79	3.46	3.80	3.49	
Species Evenness Index (J')	1st yr	0.988	0.983	0.987	0.979	0.981	0.978	0.983	0.978	0.987	0.985	0.987	0.984	F=0. 994 P=0.33
	2nd yr	0.984	0.982	0.982	0.988	0.984	0.984	0.879	0.98	0.984	0.985	0.982	0.981	
Margalef's Species Richness Index (R)	1st yr	10.53	8.07	10.68	10.19	8.98	12.83	15.82	16.59	9.15	10.88	11.43	10.23	F=0.583 P=0.431
	2nd yr	9.81	7.80	9.89	9.66	10.14	12.62	13.28	13.9	11.02	8.66	11.06	9.04	
Species Dominance Index (λ)	1st yr	0.026	0.036	0.025	0.028	0.033	0.020	0.014	0.014	0.031	0.024	0.023	0.026	F=01.16 P=0.293
	2nd yr	0.027	0.037	0.026	0.029	0.025	0.019	0.057	0.016	0.023	0.033	0.023	0.032	

Fig. 2. Photographs of few fishes

Table 4. Seasonal ichthyofaunal density and diversity indices in the river Teesta from March 2014 – February 2016

Study period	March 2014 – February 2016		
Diversity indices	Summer	Rainy	Winter
Catch per unit effort	54.5	107.75	57.11
Number of genera (S)	64.5	100.5	91
Species diversity Index (H')	4.21	4.35	4.29
Species Evenness Index (J')	0.955	0.944	0.952
Margalef's species richness Index (R)	15.5	16.405	15.63
Species dominance Index (λ)	0.0195	0.02115	0.02

CONCLUSION

Moderate number of ichthyofauna genera was reported from the River Teesta and cyprinidae was the most dominant family with 53 genera. Maximum number of fish genera, Shannon diversity index, and Margalef's species richness index was reported in rainy season when water level of the river is high. Out of 140 fish species 7 % (according to IUCN category) and 50 % (according to CAMP and NBFGR category) are under threatened category. Major threats of ichthyofauna in the River Teesta are over fishing, construction of damp, introduction of exotic fish species etc. This study will be helpful in future planning of conservation strategy.

REFERENCES

Acherjee MLand Barat S2013. Ichthyofaunal diversity of Teesta River in Darjeeling Himalaya of West Bengal, India. *Asian Journal of Experimental Biological Sciences* **4**(1): 112-122.

Barman RP 2007. *Records of the Zoological Survey of India, Occasional Paper*263, 1.

CAMP 1998. *Conservation Assessment and Management Plan Workshops,* (Ed) Sanjay Molur and Sally Walker. Published by Zoo Outreach organization. National Bureau of Fish Genetics Resources. Lucknow, India.

Das D 2015. Ichthyofaunal diversity of river Torsa and it's tributaries at Terai region of west Bengal, *International Journal of Science and Nature* **6**(2): 256-263.

Dey A, Sarkar K and Barat S 2015. Evaluation of fish biodiversity in rivers of three districts of eastern Himalayan region for conservation and sustainability. *International Journal of Applied Research* **1**(9): 424-435.

Hammer Ø, DAT Harper and PD Ryan PAST 2001.Paleontological statistics software package for education and data analysis. *Palaeontologia Electronica* **4**(1): 9.

Hanif MA, Siddik MAB, Nahar A, Chaklader MR and Rumpa RJ 2016. The current status of Small Indigenous Fish Species (SIS) of River Goral, a Distributary of the River Ganges, Bangladesh. *Journal Biodiversity Endanger Species* **4**: 162.

Hassan SS, Sinha RK, Ahsan SN and Hassan N 1998. Impact of Fishing Operations and HydrobiologicalFactors on Recent Fish Catch in Ganga near Patna, India. *In: Inland Fish Society* **30**(1): 1- 12.

IUCN, 2013. Red List of Threatened Species. Version 2013.1. <www.iucnredlist.org>.

Lakra WS, Sarkar UK, Gopalkrishnan A and Kathirvelpandian A 2010. Threatened Freshwater Fishes of India. *National Bureau of Fish Genetic Resources*, Lucknow, 1-20.

Meetei LI, Pattyanayak SK, Bhaskar A, Pandit MK and Tendon SK 2007. Climate imprints in quaternary valley fill deposits of the middle Teeesta valley, Sikkim Himalaya. *Quaternary International* **159**(1): 32-46.

Molur S and Walker S (eds.) 1998. Report of the Workshop "Conservation Assessment and Management Plan (CAMP) for Fresh water Fishes of India". Report # 18. Zoo Outreach Organisation /Conservation Breeding Specialist Group, India, Coimbatore, India and NBFGR, Lucknow, India.

Patra AK, Sengupta S and Datta T 2011. Physico-Chemical properties and Ichthyofauna Diversity in Karala river, A tributary of Teesta river at Jalpaiguri district of West Bengal, India. *International Journal of Applied Biology and Pharmaceutical Technology* **2**(3): 47-58.

Rahman A 2015. Present status of fish biodiversity in Talma River at Northern Part of Bangladesh. *International Journal of Fisheries and Aquatic Studies* **3**(1): 341-348.

Rashit A and Roy R 2021. Ichthyofaunal migration causes realized niche amplification leading to habitat adaptation and speciation in rivers of Bengal delta. *Indian Journal of Ecology* **48**(4): 1155-1164.

Sarkar T and Pal J 2015. Ichthyofaunal diversity of Rivers Mechi and its conservation status. *Global Journal of Environmental Science and Research* **2**(3): 55-59.

Sen TK 1992. *Freshwater Fish. State Fauna Series 3: Fauna of West Bengal, Part 2*, Zoological Survey of India: 101-242

Sengupta S and Homechaudhuri S 2015. Taxonomic and functional diversity of Fish assemblage in three interconnected river in India in accordance with limiting similarity hypothesis. *Journal of Global Bioscience* **4**(27): 2842-2858.

Shahnawaz A, Venkateshwarlu M, Somashekar DS and Santosh K 2011. Fish diversity with relation to water quality of Bhadra River of Western Ghats (India). *Environmental Monitoring Assessment* **161**: 83-91.

Shaw GE and Shebbeare EO 1937. The fishes of Northern Bengal. *Journal of Royal Asiatic Society of Bengal. Science Article* **III**(1): 137.

Shannon CE and WeaverW 1949.The mathematical theory of communication. Urban. University of Illinois Press, Urbana.

Received 24 June, 2021; Accepted 12 November, 2021

Indian Journal of Ecology (2021) 48(6): 1829-1836

Manuscript Number: 3456
NAAS Rating: 5.79

Production of Polyhydroxtbutyratye from Marine Source: A Review

A. Ranganadhareddy and Ch. Chandrasekhar[1]

Department of Biotechnology, VFSTR, Guntur-522 213, India
[1]Department of Biotechnology, KL Deemed to be University, Guntur-522 502, India
E-mail: rangaaluri@gmail.com

***Abstract*:** The increasing importance of the non-degradable plastics has emerged as one of the major concerns. For this, research is being ventured from the existing reserve to produce bioplastics on the basis of biodegradability properties. The experts are now searching for cost effective alternative sources such as microalgae, bacteria, cyanobacteria, actinomycetes and plants. A thermoplastic that is both biodegradable and environmental friendly, as well as biocompatible is PHB. Depending on their formulation, they vary in toughness and flexibility. Due to this variation they are used in many different ways that are analogous to the many non-biodegradable petrochemical plastics. Genetic engineering of micro organisms for the introduction of production pathways which have been examined for the last two decades are promising strategies. Making up the most commercially attractive field are the research that focus on using eccentric substrates, innovative methods for extraction and also species that are genetically modified with appraisal to create PHB from other micro-organisms. Hence, one of the survival mechanisms for microbes that exist in highly competitive and stressful marine micro-environment may be seen as the synthesis of biopolymer. These micro-environments may include bacteria associated with sponge, endosymbiotic, or macroalgae. The increasing awareness as well as the promising nature of utilizing marine microbes as a source of PHB is highlighted in this review, along with the applications in various fields such as medicine, aquaculture and antifouling.

Keywords: Polyhydroxtbutyratye (PHB), Marine microbes, Biopolymer, Thermoplastics

Feasibility, concerns related to environment as well as the design of chemical products and processes that reduce the use or generation of hazardous substances in the coming years have played a vital role in developing a newer generation of processes, products as well as materials. There has been a steady decline in the petroleum assets and landfill space due to the tenacity of different plastics in the environment. A need arises to develop polymers that are biodegradable from the renewable resources due to the damage the toxic gases cause during the ignition process (Ubani and Atagana 2021). To replace petroleum feedstock a renewable resource i.e., agricultural and biomass feedstock have been found to have potential to be used in eco-efficient packaging (Vasile 2009). Biopolymers that are acquired from marine prokaryotes both Bacteria and Archaea have showed promising material possessions and commercial aspects. Many products that range from adhesives to emulsifiers are made by exploiting the features like exopolysaccharides, Polyhydroxtbutyratye and melanins that are the reason for the survival of marine organisms. From various studies it has been understood that during severe stress conditions many marine microbes pile upon poly-β-hydroxybutyrate particles that are intracellular because these particles are the reserves for carbon and energy inside the cells (Ranganadha et al 2018). One of the potent materials for biodegradable plastics is polyhydroxyalkanoates even though they play an entirely different role in prokaryotes they are an effective base material for the production of biodegradable plastics. The PHB can be synthesized under stressful conditions like limited nitrogen source and excess of carbon hence can be used for industrial exploitation. But under incredibly stressful conditions like sodium chloride stress, stress of heat and chilling as well as under insufficient conditions of calcium, magnesium and potassium negative effects are seen for the collection of PHB. The accumulation of PHB up to 29% dry cell weight was seen by studies with *Synechocytis* sp. PCC 6803, when in phosphate and gas exchange limitation as well as with a presence of 0.4% acetate and glucose (Indira et al 2016). The accumulation of PHB has been boosted to 43% dry cell weight in *Nostoc muscorum* by the supplementation of 0.4% acetate, under chemoheterotrophy 65% dry weight of PHAs in bacterial strain *Haloferax mediterranei*in phosphate limiting conditions and glucose or sucrose as best carbon source (Garcia Lillo and Rodriguez-Valera 1990, Vishal 2021).

Poly-β- hydroxybutyrate: Chemical composition and physical properties: PHAs are one of the best contenders in biodegradable plastics due to their ample biodegradability and similarity to the commercially produced plastics. PHA is Polyhydroxtbutyratye (PHB) it's one of the most commonly used polymers and its metabolic pathway gas be explained in a brief (Khanna and Srivastava 2005). A relation between PHB properties to various synthetic plastics including polypropylene was shown. Polyesters like

polyhydroxyalkanoates (PHAs) are accumulated by bacteria under unhinged growth conditions of carbon substrate as well as other nutrients like sulphur, nitrogen, phosphorus or oxygen (Ranganadha et al 2019).

Elastomeric polyesters (polyoxo esters) of R-hydroxyalkanoic acid (HA) monomers are PHAs. Based on the structure polymers can be classified. The number of carbon atoms range from 4-14. Another way to classify polymers is based on the type of monomer, either producing homopolymers or heteropolymers. PHAs with 3-5 carbons are short chain length PHAs (scl- PHAs). Examples of this class include Poly (3- hydroxybutyrate), P (3HB) and poly (4-hydroxybutyrate), P (4HB) (Ranganadha et al 2014). Medium chain length PHAs (mcl- PHAs) are the PHAs with 4-14 carbon atoms. Examples are Poly (3- hydroxyhexanoate), P(3Hx), poly (3- hydroxyoctanoate), P(3HO) and heteropolymers like P(3HHx-co-3HO). The PHAs that have more than 15 carbon atoms are called long chain length (lcl-PHAs). The medium chain length PHAs and short chain length PHAs differ in the physical properties including poly (3-hydroxybutyrate) (PHB) which is crystalline and stiff material due to their structural differences. However, medium chain length PHAs show elastomeric properties. The long chain saturated and unsaturated monomers have different properties where the double bonds clinch the opportunity for more chemical alterations due to inherent biocompatible and biodegradable nature of the PHAs they contain. One of the best studies polymers belonging to the PHA biopolymer family is the polymer Polyhydroxtbutyratye. PHB has a linear structure as shown in Figure 1 that displays 60-70% crystallinity, as a homopolymer. Due to robust intermolecular interaction, the high melting temperature results in the variation between the two temperatures. When compared with commercial polymers, polymerization with co monomers can eradicate these problems with pure PHBs (Ranganadha et al 2017).Under antagonistic environmental conditions; the survival of microbes can be augmented by the accumulation of PHA (Teja et al 2020). Due to the high assorting and perplexing environments microbial strains can be used as a source for isolating the novel PHA. Only a little information was found on the on the microorganisms that produce PHA

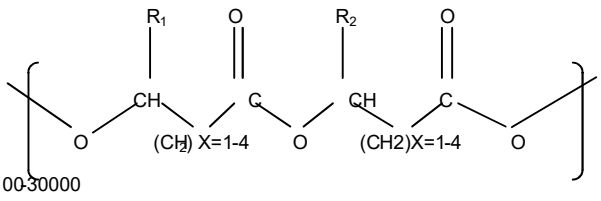

Fig. 1. Structure of Polyhydroxyalkanoates with R_1 and R_2 are alkyl groups (C-C)

until recently (Wei et al 2011). Among the commensally heterotrophic bacteria, vibrios were said to be assertive. Improvement of several PHA accumulating strains can be aided by the marine ethnic environment. The PHA accumulating strains may contain species other than vibrio. Intensive studies have been conducted by both researchers and industrialists on petrochemical polyesters due to their similarity of PHAs. PHAs are therefore, considered to be good candidates for elastomers as well as biodegradable plastics (Ranganadha et al 2020).

Biosynthetic pathway of polyhydroxtbutyratye production: Lemoigne discovered homopolymer PHB in the year 1920s in the bacteria *Bacillus megaterium*. In prokaryotic cells the Polyhydroxyalkanoates (PHA) act as carbon and energy reserves (Reddy et al 2021). When excess of carbon is provided during the inadequate growth nutrient availability a variety of bacteria accumulate them. PHA synthase (PhaC) is a requirement for synthesizing PHA. B-hydroxyacyl-coenzyme A substrates is used by the enzyme PhaC for the polymerization process. Such substrates are produced in various pathways using the enzymes b-ketothiolase (encoded by phaA) and acetoacetyl-CoA reductase (encoded by phaB) b-oxidation, and de novo synthesis of fatty acid pathway (Xu et al 2016). Using a diverse number of bacteria more than 20 different varieties of PHA synthesis operons have been cloned and analysed. A divergence has been noticed when the proteins were analyzed which play a vital role in the biosynthetic pathways. The synthesis of PHA takes place in three steps with the reaction initiated by two acetyl-CoA from tricarboxylic acid cycle (TCA). b-thiolase (PhaA) enzyme, then condensed to acetyl-CoA acetoacetyl-CoA. NADH-dependent enzyme acetoacetyl-CoA reductase (phaB) reduces it at position 3. Polymerase (PhaC) esterifies the monomers to the PHB polymer in the step. The only place this step takes place is in the granular surface. The intracellular mediation of acetyl-CoA controls the formation of PhaB. Without restricting any nutrients the pool of CoASH is enhanced in growth conditions during the exponential growth phase. However, PHB synthesis is favored when the growth is restricted for nutrients e. g. CoASH level condensed by phosphate or ammonium. Under oxygen limitation, a high PHB content was found and implicated as a substitute electron sink for tumbling equivalents.

Detection and analysis of Polyhydroxtbutyratye in microbes: The occupancy of PHA is not only limited to intracellular assortment in bacteria and granules. Marine bacteria such as *Bacillus subtilis* and *Streptomyces lividans* which are closely related to calcium and polyphosphate ions have been found to have PHB with less molecular weight

(14,000 Da) (Hassan et al 2019). Studies show that cPHB is not only present in eubacteria but also present in eukaryotic cells like yeast, spinach, sheep (intestine), cat muscles and many more. Hence, it can be understood that PHB is biocompatible with the animals (Tomasz et al 2015). By using easy staining methods the PHB were detected in the marine microbes. Sudan Black staining methods other than Nile blue can be used for phenotypic detection of intracellular PHA. These staining methods are sensitive but it takes time and is very strenuous to screen a lot of environmental isolates (Juengert et al 2018). By using Nile blue A or Nile red staining the colonies or bacteria growing in plates can be fluorescently viewed by using UV illumination. Large number of bacterial strains can be stained by using the above mentioned colony staining method. Still it is mandatory that for accumulation of PHA granules suitable carbon sources are required which is followed by lengthy incubation period.The double bonds present in monomers of monounsaturated 3-hydroxyalkenoic acids can be localized and detected by using a new gas chromatography-mass spectrometry technique (Simon-Colin et al 2012).

Poly-β-hydroxybutyrate and marine microbes: Significant and incipient biological resources are exploited to marine biopolymers. Made from petroleum, Polyhydroxtbutyratye is a biomedical material that is eco friendly and also has the potential to replace plastics. It can be used in surgical pins, stapes, blood vessel replacements, bone replacements and plates, medical implant and drug delivery devices due to its biodegradable and biocompatible nature. Numerous marine microorganisms including marine actinomycetes, algae and halophilic bacteria synthesize polyesters called polyhydroxyalkanoates (PHAs).

Actinomycets: Actinomycetes are gram positive bacteria. They consist of assorted group of unicellular microbes. They are appraised to be a profound resource due to their ability to yield antibiotics. But actinomycetes can also produce PHB which could be an efficacious replacement to synthetic plastics, serving several commercial purposes. Only a few reports are available pertaining to actinomycetes for PHB production due to poor understanding (Vikineswary et al 1997). *Streptomyces* are another group of adaptable bacteria that are capable of synthesizing metabolites, both primary and secondary, but mainly antibiotics (Sivakumar et al 2017). With regard to the synthesis and production of PHB by *streptomyces*, only preliminary data is available. 12 different strains of *streptomyces* produce poly-3-hydroxybutyric aid (PHB), which was explored. It was indicated by gas chromatographic estimation that PHB was produced in all the halophilic strains with a maximum accumulation between 1.5 and 11.8% dry cell weight. Isolation of PHB from *S.coelicolor* A3 (2) M145and characterization were done using FT-IR. The interrelationship between utilizing PHB and producing antibiotics in *Streptomyces coelicolor* A3 (2) M145 was inspected. It was noticed in the results that PHB has a role in

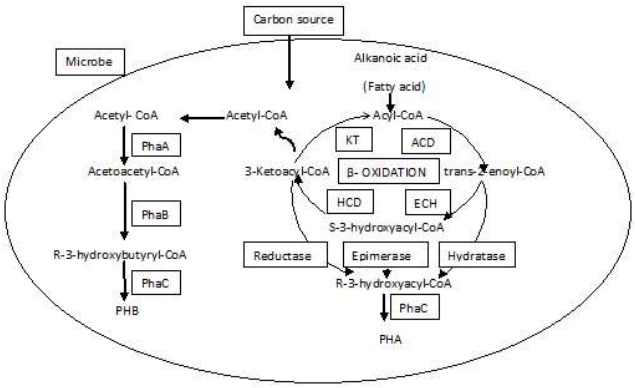

Fig. 2. Biosynthetic pathway of Polyhydroxtbutyratye in microbes

Table 1. PHB production by various marine bacteria

Microorganism	Carbon source	PHA	PHA content (%w/v)	References
Acinetobacter nosocomialis RR20	Molasses	PHB	7.8	Reddy et al 2019
Vibrio proteolyticus	Fructose	PHA	54.7	Hong et al 2019
Pseudodonghicola xiamenensis	Date syrup	PHBV	38.8	Mostafa et al 2020
Bacillus subtilis	Cane molasses	PHB	30.4	Hassan et al 2019
Micrococcus luteus	Glucose	PHB	56.5	Mohanrasu et al 2021
Bacillus cereus NDRMN001	Cane molasses	PHB	91.4	Mathiyazhagan et al 2020
Halomonas pacifica ASL10	*Corallina mediterranea* hydrolysates	PHB	67.0	Fady et al 2021
Salinivibrio sp. TGB10	Glucose	PHB	80	Guan-Bao et al 2021
Cobetia strain	Mannitol	PHB	61	Rima et al 2021
Halomonas sp. YLGW01	Fructose	PHB	94.6	Ye-Lim et 2020

reducing the antibiotics as a reserve material for carbon (Manna et al 1999).

Algae: The micro algae based scaffolds obtained from Spirulina were used for the production of biopolymers it was seen that there was a boost in growth of cell for preventing the rejection of tissue or organs after transplant. By adding the spirulina LEB 18 to nanofibers there was an escalation in properties such as conductivity, elasticity, tensile strength, breaking and elongation. They are comparatively much more refined when compared to the commercial PHB trials. From the studies it was found that, the mechanical properties of nanofibers have been improved when they were made from spirulina PHB (Morais et al 2015). By implanting the bacteria *Ralstonia eutropha* U16 into the PHB pathway into the *Phaeodactylum tricornutum* diatom is able to produce PHB upto a 10.6% dry weight of their biomass. As blending material along with PHB, commonly used were polysaccharides from macroalgae. Inspite of having high content of siliceous material the algal fiber when blended with PCL and PHB shows much more compatibility. In *Ulva ammoricana* upon the adding the macroalgae polysaccharides showed that when it is PHB is combined in optimum concentrations it can be used as good filter. Further it has been understood that by thermal labeling the processing of blends at high temperatures can be done with little to noticeable problems (Hempel et al 2011).

Halophilic bacteria: Halophiles are the microbes that are able to grow optimally in 5% (w/v) but are unable to grow in salt medium less than 10%.Several of these halophilic micro organisms like *Haloferax mediterranei*, Vibrio spp., *V. nereis, V. natriegens* and *V. harveyi* have been seen to yield PHB (Oren 2008). The *V. cholera* and *V. parahemolyticus* have been used to identify the gene polyhydroxyalkanoic acid synthase, which is involved in PHA synthesis. The benefit of using microorganisms that are halophilic in the producing PHA is that this microbe yields PHA with high molecular weight, such as P (3HB-co-3HV). For this reason, these halophilic microbes have imminent applications in industries and there is also cost reduction by using certain fermentation approaches like the confinement of NaCl upon the bioreactor walls (Chen et al 2006). The main disadvantage of using the halophilic micro organisms in manufacturing of PHA is low efficacy. Several reports have been published on marine micro organisms that produce PHA. So far, the best studied PHA producer is *Haloferax mediterranei* which is from the Halobacteriaceae family (Tao et al 2010). From earlier studies it has been understood that Halobacteriaceae species with the help of either glucose or starch as carbon source under limited phosphorous conditions were able to accumulate the 65 wt% PHA (Lillo and Rodriguez-Valera, 1990). It was also reported that some moderate halophiles produced PHA. For accumulation of PHB in *Halomonas boliviensis* by using various carbon sources such as glucose, xylose, sucrose, malt oligosaccharides, sodium acetate and butyric acid with optimum salt concentration has shown growth of cell between 4% and 5% (Quillaguaman et al 2006). When 36 hours of fed batch cultivation passes by it is observed that the content of PHB and the Cell dry weight (CDW) reaches 81% and 44g/L respectively (Quillaguaman et al 2008).

Mechanism of PHB production by marine microbes: For coping with the depleted nutrient conditions different marine archae and bacteria which includes various Halomonas species accrue poly-b-hydroxyalkanoates (carbon and energy storage materials). To avoid molecular impairment caused due to cellular freezing and dehydration definitive osmotic adaptations are developed in many of the marine strains. The approaches comprises of (i) Osmotic pressure balance over certain transmembrane exchange of salts and transport proteins and (ii) Aggregation of protective compatible solutes like betaine or ectaine. The appropriate solutes of Halomonas species are accumulated by uptake or by synthesis. Before in *Haloarculamaris mortui*, a holoarchaea the PHA granules were seen whereas many halophiles were used for the accumulation of PHB. Recently the use of few halophiles for the production of PHA and characterization of copolymers was studied (Cui et al 2016). The use of marine micro organisms for producing PHB has been gaining lot of attention due to their lowering fermentation and cost effectiveness (Mohanrasu et al 2018). Due to less contamination possibility by other microbes due to the increased salt concentrations the cost for the sterilization process also has decreased. In salt deficient water by using the osmotic shock treatment causes lysis of the haloarchae cells due to which there is reduction in costs for the recovery of polymers. After the fermentation process the concentrated residual salt present in the broth can be recycled thereby reducing the cost of p-production. This avoids the ecological snags that cause the waste product depletion. In Halomonas elongate the gene clusters like pha (responsible for PHA synthesis), ect (responsible for ectoine synthesis), phaC (coding for PHA synthase) and phaP (coding for phasing) were well preserved according to the comparative genomic investigations. From the preservation it was understood that the adaptable success and colonization competency of the Halomonas species maybe due to the selective stress wielded on these genes (Tao et al 2017).

The biocompatible nature of PHA in invitro conditions has been demonstrated at various cell cultures like fibroblasts, mesenchymal stem cells, osteoblasts, bone marrow cells,

articular cartilage chondrocytes, endothelial cells, smooth muscle cells, etc. The cell cultures isolated from kidneys of monkeys, AGMK and FRLK4 which were grown on PHB films in the form of scaffolds for 360 days also proved to be biocompatible of PHB. During the whole time of incubation of cell culture it was found that the growth and cell viability was not improved by PHB. The cells did not display any polymeric dependent factors such as toxic substance deliverance (polymer destruction production), incompatible surface of polymer etc,. The growth, enlargement and migration of cells are not influenced by the cytotoxic nature of PHB films at the cell culture. Hence, PHB was found to be biocompatible and biologically inert for the isolated cell cultures in invitro conditions (Chen 2009). PHA is considered to be a substitute for synthetic plastics derived from petroleum and also has been found to have a wide array of use in aquaculture, agriculture, medicine, tissue engineering, antifouling, pharmacy, food industry, raw material for enantiomerically pure chemicals, and the paint industry as well (Nath et al 2008). One of its major limiting factors is the cost production of PHB, which constrains its commercial applications. Hence, it has been inevitable to use an economical process for the hyper producing strains for the development of PHB as ecofriendly plastics for commercial use (Castillo et al 2009).

PHB nanocomposites: In this era, the development of more advanced and effective processes and modernisation have led to great enhancements in the quality of one's life. One, thus, needs to exploit these renewable and sustainable resources to meet this growing trend. One of the environment friendly methods that is easy and also economical is the microbial biosynthesis of Nanoparticles of metal like gold, silver and platinum (Wifaq and Alaa Abd 2021). There was also a need to improve the toughness of PHB, and thus nanocomposites of the same were produced. One can see, from studies, that these nanocomposites with different compositions improved their substantial properties with the increase in the elongation rate of about 5-80% in comparison to 2% for PHB (Ohashi et al 2009). A vital role in a wide range of areas from electronics to photonics, steering materials to sensors, medicine to biotechnology, pollution control to environmental technology is played by the polymer Nanoparticles (PNP) which has been gaining popularity (Ching-Hung et al 2017). PNPs have been found to be in use as carriers of drugs and also imaging agents (Ojha et al 2021). One of the modest and most appropriate methods for mass production of Nanoparticles that has gathered a lot of attention is oil in water emulsion method (Castro-Mayorga et al 2018). The key properties like viscosity, surface area, and packing density are regulated by the particle size and its distribution. The cancer cells that are malignant can be killed by polymeric Nanoparticles due to their biocompatible and hyperthermal activity (Köksal et al 2020).

Applications of polyhydroxtbutyratye: Poly-3-hydroxybutyrate has a wide range of applications, some of which include its employment in agriculture and construction materials, automotive interior materials, electrical devices, containers, sanitary goods, packaging materials, etc. Poly-3-hydroxybutyrate (PHB) is an example of one commercially accessible product. Nevertheless, PHBV, short for poly (3-hydroxybutyrate-co-hydroxyvalerate) proved to be better in terms of its thermo chemical properties, for its use-in materials like sutures and bone nails, disposable items like pens and tableware, film products mostly used in the covering of little things, like bags and covers. For that matter, it can be used in food packaging as well (Olejnik et al, 2021). PHB can be thrusted, moulded and spun into fibres and then drawn into pruned films. In addition to its ability to fuse with synthetic polymers, it is found to amplify the physical properties of bio plastics. PHB is also found to be compliant with body tissues, which facilitates usage in medical areas like surgical sutures, wound dressings and ocular devices (Olejnik et al, 2021).

Aquaculture: The application of the anti adhesive characteristics of PHB to the field of aquaculture is still not completely explored at the moment however,there are a few studies that have been carried out through experiments on model organism in aquaculture field i.e., *Artemia franciscana* (Duan et al 2017). The characteristic of cell adhesion of many aliphatic polyesters was assessed by Lee et al. He concluded that due to accumulation of methyl groups on the cell surface, PHB has minimal cell adhesion (Lee et al 2013). The studies conducted by Laranja et.al. Stated that PHB, which is a short chain of fatty acids, displayed a strong inhibition against a pathogen *V.campbellii* (Laranja et al 2018). To understand the epidemics of PHB, vibrio pathogens in shrimp agriculture can be studied by using a new nontoxic antibiofilm or anti-adhesive process. The pathogens of shrimp such as *Vibrioal ginolyticus*, *V. harveyi, V. fischeri, V. vulnificus* and *V. parahaemolyticus* can be affected by using PHB as an anti adhesive agent. By using a bacterium *Brevibacter iumcasei* MSI04, which is a marine species, the infection was controlled by biofilm disruption or the biomass formation was prevented by intercepting its development. This served as the precondition phase for virulence expression. Hence, by inhibiting the formation of biofilm instead of growth, it can be used as a substitute process for conventional procedures (Anna et al 2017). Not many reports have been found on PHB for its anti adhesive activity in shrimp aquaculture. The trials conducted on Nile tilapia larvae for the pathogen Edward

siellaictaluri revealed that feed enriched with PHB-*Artemia nauplii* challenged the larvae, which led to a 20% rise in the rate of survival for the tested control larvae. Therefore it was ratified that PHB can be used as an effective antimicrobial agent in Nile tilapia larvae culture from the above conducted study, as it has shown improved body weight due to proper digestion, absorption and deposition of intestinal lipids (Situmorang et al 2014). Another atypical approach of an anti-infective in aquaculture rearing is the use of Poly-β Hydroxybutyrate. When the feed was replaced by PHB, it was observed to act as a source of energy as well. The use of PHB as a feed supplement is not only beneficial to aquaculture animals but also cost effective. Additionally, PHB is also believed to have a beneficial effect on the growth of fish (Giri et al 2020).

Antifouling agents: Bio fouling has been known to bring about several hurdles in operations such as economic losses at the shipping industries, industrial equipment, offshore platforms, underwater pipelines and desalination plants (Abhishek et al 2020). Antifouling technologies are a global industry that has progressed with a net field of US$ 4 billion annually; the cause for this success is the economical costs of hull fouling (Hu et al 2020). The increase in the marine transport of cargo and people is said to be analogous to the establishment of antifouling technology. PHB has found purpose as a great antifoulant here. To prevent the disposition of marine organisms, PHB nano composite coatings can be used on vessel. Toxicants like copper and tributyltin are traditionally integrated into these as a paint matrix that gradually lets the biocide out from the surface layer of PHB. There are other harmless approaches like incorporation of natural antifouling compounds from marine sources like actinomycetes, bacteria, algae and sponges into coatings. The marine organisms can be used to synthesize the PHB nanocomposites the varied effects of marine biofouling systems by using metal coupons. Therefore, for the effective development of harmless ecofriendly antifoulants, marine sources can be used.

Medicine: Several industries and academia have been able to appreciate its biocompatibility and biodegradability, with considerable potential applications in drug delivery, biomedical applications as medical implants and drug delivery carriers. Therefore it is in high demand. PHA also, has found a wide variety of applications in medical field as a tissue engineering material that can be used for drug delivery and for the management of wound (Mohammed Nadeem et al 2021). When PHB and its copolymers related to hydroxyvalerate [P(HBHV)] are used as replacements and entrapped drugs can be released using soil erosion strategy. From the early 1990s, PHA's were found to possess extraordinary use as carriers of drugs due to their biodegradable and biocompatible nature (Kavitha et al 2018).

CONCLUSION

For the exploration of various PHB accumulating strains, the marine environment can be excavated. Polyhydroxtbutyratye play an important part in building a feasible environment by supplanting non-biodegradable synthetic plastics. To overtake the thermoplastics dominated market, it is important to produce cost effective biodegradable polymers. By reducing the production cost of polymers that are biodegradable their application range can be broadened. The imperative properties of biopolymers like biodegradability and biocompatibility have made them compatible for usage in biomedical field, aquaculture field and antifouling. Limited information is available on the commercial exploitation of PHB produced from actinomycetes and halophiles. Therefore with the help of this report, it can be said that PHB is a resilient class of biopolymers that can be used for better designing of new applications in various fields.

Conflict of interest: The author that they do not have any conflicts of interest to declare.

REFERENCES

Abhishek Kumar A, Quanyin T and Jinhui L 2020. Biotechnological potential for microplastic waste. *Trends in Biotechnology* **38**(11): 1196-1199.

Anna VT, Andrei VS, Yulia AD, Yulia AF and Alexander AK 2017. FTIR spectroscopic study of biofilms formed by the rhizobacterium *Azospirillum brasilense* Sp245 and its mutant *Azospirillum brasilense* Sp245.1610. *Journal of Molecular Structure* **1140**: 142-147.

Castillo LR, Mitchell DA and Freire DMG 2009.Production of Polyhydroxyalkanoates (PHAs) from waste materials and by products by submerged and solid-state fermentation. *Bioresource Technology* **100**(23): 5996-6009.

Castro-Mayorga JL, Freitas F, Reis MAM, Prieto MA and Lagaron JM 2018. Biosynthesis of silver nanoparticles and polyhydroxybutyrate nanocomposites of interest in antimicrobial applications. *International Journal of Biological Macromolecules* **108**: 426-435.

Chen CW, Don TM and Yen, HF 2006. Enzymatic extruded starch as a carbon source for the production of poly (3-hydroxybutyrate-co-3-hydroxyvalerate) by *Haloferax mediterranei*. *Process Biochemistry* **41**(11): 2289-2296.

Chen GQ 2009. A microbial polyhydroxyalkanoates (PHA) based bio and materials industry. *Chemical Society Reviews* **38**(8): 2434-2446.

Ching-Hung L and Yi-Ming S 2017. Influence of the surface properties of nano-silica on the dispersion and isothermal crystallization kinetics of PHB/silica nanocomposites. *Materials Chemistry and Physics* **199**: 88-97.

Cui YW, Zhang HY, Lu PF and Yong-Zhen P 2016. Effects of carbon sources on the enrichment of halophilic polyhydroxyalkanoate-storing mixed microbial culture in an aerobic dynamic feeding process. *Scientific Reports* **6:** 30766.

De Schryver P, Sinha AK, Kunwar PS, Baruah K, Verstraete W, Boon

N, De Boeck G and Bossier, P 2010. Poly-β-hydroxybutyrate (PHB) increases growth performance and intestinal bacterial range-weighted richness in juvenile European sea bass, *Dicentrarchus labrax*. *Applied Microbiology and Biotechnology* **86**: 1535-1541.

Duan Y, Zhang Y, Dong H, Yun Wang and Jiasong Z 2017. Effects of dietary poly-β-hydroxybutyrate (PHB) on microbiota composition and the mTOR signaling pathway in the intestines of *litopenaeus vannamei*. *Journal of Microbiology* **55**: 946-954.

Fady AE, Marian R, Aida F, Sanaa O and Heba K 2021. Polyhydroxyalkanoate nanoparticles produced by marine bacteria cultivated on cost effective Mediterranean algal hydrolysate media. *Journal of Biotechnology* **328**: 95-105.

Garcia Lillo J and Rodriguez-Valera F 1990. Effects of culture conditions on poly(*β*-hydroxybutyrate acid) production by *Haloferax mediterranei*. *Applied and Environmental Microbiology* **56** (8): 2517-2521.

Giri SS, Hyoun JK, Sang GK, Sang WK, Jun K, Sung BL and Se CP 2020. Immunomodulatory role of microbial surfactants, with special emphasis on fish. *International Journal of Molecular Sciences* **21**: 19.

Guan-Bao T, Bi-Wei T and Zheng-Jun L 2021. Production of polyhydroxyalkanoates by a moderately halophilic bacterium of *Salinivibrio* sp. TGB10. *International Journal of Biological Macromolecules* **186**: 574-579.

Hassan MA, Bakhiet EK, Hussein HR and Ali SG 2019. Statistical optimization studies for polyhydroxybutyrate (PHB) production by novel *Bacillus subtilis* using agricultural and industrial wastes. *International Journal of Environmental Science Technology* **16**: 3497-3512.

Hempel F, Bozarth AS, Lindenkamp N, Klingl A, Zauner S, Linne U, Steinbuchel A and Maier UG 2011. Microalgae as bioreactors for bioplastic production. *Microbial Cell Factories* **10**: 81.

Hong JW, Song HS, Moon YM, Yoon-Gi H, Shashi KB, Hye-Rim J, Tae-Rim C, Soo-yeon Y, Hyung-Yeon P, Yong-Keun C and Yung-Hun Yang 2019. Polyhydroxybutyrate production in halophilic marine bacteria Vibrio proteolyticus isolated from the Korean peninsula. *Bioprocess Biosystem Engineering* **42**: 603-610.

Hu J, Yi C, Jiawei L, Xiaokun F, Jie L, Zhihan L, Guangsheng Z and Wenyong LA 2020. Self-supported gel filter membrane for dye removal with high anti-fouling and water flux performance. *Polymer* **201**:122531.

Inbakandan D, Kumar C, Stanley Abraham L, Kirubagaran R, Venkatesan R and Ajmal Khan S 2013. Silver nanoparticles with anti microfouling effect: a study against marine biofilm forming bacteria. *Colloids and Surfaces B* **111**(1): 636-643.

Indira M, Venkateswarulu TC, Chakravarthy K, Ranganadha Reddy A, John Babu D and Vidya PK 2016. Morphological and biochemical characterization of exopolysaccharide producing bacteria isolated from dairy effluent. *Journal of Pharmaceutical Sciences and Research* **8**(2): 88-91.

Juengert JR, Bresan S and Jendrossek D 2018. Determination of polyhydroxybutyrate (PHB) content in *Ralstonia eutropha* using gas chromatography and nile red staining. *Bio-protocol* **8**(5): 2748.

Kavitha G, Ramasamy R and Dhinakarasamy I 2018. Polyhydroxtbutyratye production from marine source and its application. *International Journal of Biological Macromolecules* **111**: 102-108.

Khanna S and Srivastava AK 2005. Recent advances in microbial polyhydroxyalkanoates. *Process Biochemistry* **40**(2): 607-619.

Köksal R and Yalcin S 2020. The cytotoxic effect of *Annona muricata*-loaded PHB-Coated magnetic nanoparticles on cancer cell lines and molecular docking analyses. *Current Pharmacology Reports* **6**: 121-130.

Koning GD 1995. Physical properties of bacterial poly ((R)-3-hydroxyalkanoates). *Canadian Journal of Microbiology* **41**: 303-309.

Laranja JLQ, Peter DS, Gladys L, Ludevese-Pascual EC, Amar MA, Peter V and Peter B 2018. High amorphous poly-beta-hydroxybutyrate (PHB) content in a probiotic Bacillus strain displays better protective effects in Vibrio-challenged gnotobiotic Artemia. *Aquaculture* **487**: 15-21.

Lee C, Song B, Jegal J and Kimura Y 2013. Cell adhesion and surface chemistry of biodegradable aliphatic polyesters: Discovery of particularly low cell adhesion behavior on poly (3-[RS]-hydroxybutyrate). Macromolecular Research **21**(2): 305-313.

Lillo JG and Rodriguez-Valera F 1990. Effects of culture conditions on poly (3-hydroxybutyric acid) production by *Haloferax mediterranei*. *Applied and Environmental Microbiology* **56**(8): 2517-2521.

Manna A, Banerjee R and Paul AK 1999. Accumulation of poly (3-hydroxybutyric acid) by *some soil Streptomyces*. *Current Microbiology* **39**(3): 153-158.

Mathiyazhagan N, Sabariswaran K, Suresh K, Keerthana G, Muthusamy R and Gajendiran K 2020. Screening of polyhydroxybutyrate producing indigenous bacteria from polluted lake soil. *Heliyon* **6**(10): 05381.

Mohammed Nadeem KH, Hussein Ali S, Emad Adnan M and Kareem AH 2021. Antifungal activity of and alcoholic extracts *Saccharomyces cerevisiae S. boulardii* and alcoholic extracts of *Populus euphratica* and Myrtus *communis* against *Macrophomina phaseolina* in Vitro. *Indian Journal of Ecology* **48**(13): 222-226.

Mohanrasu K, Premnath N, Siva Prakash G, Muniyasamy S, Boobalan T and Arun A 2018. Exploring multi potential uses of marine bacteria; an integrated approach for PHB production, PAHs and polyethylene biodegradation. *Journal of Photochemistry and Photobiology B: Biology* **185**: 55-65.

Mohanrasu K, Guru Raj Rao R, Dinesh GH, Kunyu Z, Muniyasamy S, Pugazhendhi A, Jeyakanthan J, Kumar P, Govarthanan M and Arun A 2021. Production and characterization of biodegradable polyhydroxybutyrate by *Micrococcus luteus* isolated from marine environment. *International Journal of Biological Macromolecules* **186**: 125-134.

Morais MGD, Stillings C, Dersch R, Rudisile M, Pranke P, Costa JAV and Wendorff J 2015. Biofunctionalized nanofibers using *Arthrospira* (Spirulina) biomass and biopolymer. *Biomed Research International* **1**: 1-8.

Mostafa YS, Alrumman SA, Alamri SA, Kholod A, Otaif MSM and Abdulkhaleg M 2020. Alfaify Bioplastic (poly-3-hydroxybutyrate) production by the marine bacterium *Pseudodonghicola xiamenensis* through date syrup valorization and structural assessment of the biopolymer. *Scientific Reports* **10:** 8815.

Nath A, Dixit M, Bandiya A, Chavda S and Desai AJ 2008. Enhanced production and scale up studies using chess whey in fed batch culture of Methylobacterium sp. ZP24. *Bioresource Technology* **99**(13): 5749-5755.

Ohashi E, Drumond WS, Zane NP, de Faria Barros PW, Lachtermacher MG, Wiebeck H and Wang SH 2009. Biodegradable poly (3-hydroxybutyrate) nanocomposite. *Macromolecular Symposia* **279**: 138-144.

Ojha N and Das N 2021. Green formulation of microbial biopolyesteric nanocarriers toward In vitro drug delivery and its characterization. *Current Microbiology* **78:** 2061-2070.

Olejnik Olga, Anna Masek, and Jakub Zawadziłło. 2021. Processability and mechanical properties of thermoplastic polylactide/polyhydroxybutyrate (PLA/PHB) bioblends. *Materials* **14**(4): 898.

Oren A 2008. Microbial life at high salt concentrations: phylogenetic and metabolic diversity. *Saline Systems* **4**(2): 1-13.

Quillaguaman J, Doan-Van T, Guzman H, Guzman D, Martin J,

Everest A and HattiKaul R 2008. Poly (3-hydroxybutyrate) production by Halomonas *boliviensis* in fed- *batch culture. Applied Microbiology and Biotechnology* **78**: 227-232.

Quillaguaman JO, Delgado B, Mattiasson R and Kaul H 2006. Poly (betahydroxybutyrate) production by a moderate halophile, *Halomonas boliviensis* LC1. *Enzyme and Microbial Technology* **38**(1-2): 148-154.

Ranganadha RA, Bharath KR and Vidyaprabhakar K 2017. Isolation and identification of polyhydroxtbutyratye (PHB) producing bacteria from sewage sample. *Research Journal of Pharmacy and Technology* **10**(4): 01-05.

Ranganadha RA, Krupanidhi S, Venkateswarulu TC, Bharath KR, Sudhakar P and Vidyaprabhakar K 2019. Molecular characterization of a biopolymer producing bacterium isolated from sewage sample. *Current Trends in Biotechnology and Pharmacy* **13**(3): 325-335.

Ranganadha RA, Venkateswarulu TC, John BD and Shyamala DN 2014. Homology modeling, simulation and docking studies of Tau-Protein Kinase. *Research Journal of Pharmacy and Technology* **7**(3): 376-388.

Ranganadha RA, Venkateswarulu TC, Sudhakar P, Krupanidhi S and Vidyaprabhakar K 2018. Optimization of process parameters for Polyhydroxtbutyratye production from isolated *Acinetobacter nosocomialis* RR20 through submerged fermentation. *Current Trends in Biotechnology and Pharmacy* **12**(2): 16-25.

Ranganadha RA, Vidyaprabhakar K,Venkateswarulu TC, Krupanidhi S, Nazneen Bobby Md, Abraham PK, Sudhakar P and Vijetha P 2020. Statistical optimization of Polyhydroxtbutyratye (PHB) production by novel *Acinetobacter nosocomialis* RR20 strain using Response Surface Methodology. *Current Trends in Biotechnology and Pharmacy* **14**(1): 62-69.

Ranganadhareddy A, SravaniK, Sanjana N and Chandrasekhar Ch 2021. Production of biopolymer from bacteria: A review. *Environmental and Earth Sciences Research Journal* **8**(2): 91-96.

Rasmussen TB, Skindersoe ME, Bjarnsholt T, Phipps RK, Christensen KB, Jensen PO, Andersen JB, Koch B, Larsen TO, Hentzer M, Eberl L, Hoiby N and Givskov M 2005. Identity and effects of quorum-sensing inhibitors produced by *Penicillium* species. *Microbiology* **151**(5): 1325-1340.

Ravi Teja KS, Abraham Peele K, Venkateswarulu TC, Vijetha P, Krupanidhi S and Ranganadha R A 2020. Computational Modeling of Chitinase (Cs CHIO) Protein from *Chitiniphilus shinanonensis*. *Indian Journal of Ecology* **47**(1): 151-153.

Reddy AR, Peele KA, Krupanidhi S, Prabhakar KV and Venkateswarulu TC 2019. Production of Polyhydroxtbutyratye from *Acinetobacter nosocomialis* RR20 strain using modified mineral salt medium: a statistical approach. *International Journal of Environment Science and Technology* **16:** 6447-6452.

Rima G, Mark P, Razan U, Julia S, Michael G and Alexander G 2021. Marine bacteria associated with the green seaweed Ulva sp. for the production of polyhydroxyalkanoates. *Bioresource Technology* **328**: 124815.

Sapkota A, Sapkota AR, Kucharski M, Burke J, McKenzie S, Walker P and Lawrence R 2008. Aquaculture practices and potential human health risks: current knowledge and future priorities. *Environment International* **34**(8): 1215-1226.

Simon-Colin C, Gouin C, Lemechko P, Kervarec N and Guezennec J 2012. Development of a three-step derivatization assay for the localization of double bond in monounsaturated monomers of poly-beta-hydroxyalkanoates by GC-MS. *Journal of Chromatography* B **900**: 64-70.

Situmorang ML, Dierckens K, Mlingi FT, Van Delsen B and Bossier P 2014. Development of a bacterial challenge test for gnotobiotic Nile tilapia *Oreochromis niloticus* larvae. *Diseases of Aquatic Organisms* **109**: 23-34.

Sivakumar K, Gandhi Shree C and Palani P 2017. Polyhydroxtbutyratye by *Streptomyces* sp. production and characterization. *International Journal of Biological Macromolecules* **104**:1165-1171.

Tao W, Lv L and Chen, GQ 2017. Engineering *Halomonas* species TD01 for enhanced polyhydroxyalkanoates synthesis via CRISPRi. *Microbial Cell Factories* **16:** 48.

Tomasz G, Tomasz G, Claudia H, Michael G, Christiane KK 2015. Histological and molecular-biological analyses of poly(3-hydroxybutyrate) (PHB) patches for enhancement of bone regeneration. *Annals of Anatomy - Anatomischer Anzeiger* **199**: 36-42

Ubani O and Atagana HI 2021. Biological Degradation of complex crude oil refinery waste sludge by consortia of bacteria during tailored composting. *Indian Journal of Ecology* **48**(1): 166-176.

Vasile C 2009. Environmentally degradable polymeric materials: definition and back- ground. In: C. Vasile, G. Zaikov (Eds.), *Environmentally Degradable Materials Based on Multicomponent Polymeric Systems*, Koninklijke Brill NV, Leiden, Netherlands.

Vikineswary S, Nadaraj P, Wong WH and Balabaskaran S 1997. *Actinomycetes* from a tropical mangrove ecosystem - antifungal activity of selected strains. *Asia Pacific Journal of Molecular Biology and Biotechnology* **5**(2): 81-86.

Vishal R D 2021. Comparative Analysis and Characterization of Lipase Producing Alkaliphilic Bacteria Isolated from Lonar Soda Lake, India. *Indian Journal of Ecology* **48**(1): 123-127.

Wei YH, Chen WC, Wu HS and Janarthanan OM 2011. Biodegradable and biocompatible biomaterial, Polyhydroxtbutyratye, produced by an indigenous *Vibrio sp*. BM-1 isolated from marine environment. *Marine Drugs* **9**(4): 615-624.

Wifaq A M and Alaa Abd A A 2021. Efficacy of biosynthesized silver nanoparticles by *Pleurotus ostreatus* on growth of *Staphyllococcus aureus* and Pseudomonas *aeruginosa*. *Indian Journal of Ecology* **48**(1): 292-295.

Xu M, Qin J, Rao Z, Hengyi Y, Xian Z, Taowei Y, Xiaoyuan W and Zhenghong X 2016 . Effect of Polyhydroxybutyrate (PHB) storage on l-arginine production in recombinant *Corynebacterium crenatum* using coenzyme regulation. *Microbial Cell Factories* **15:** 15.

Ye-Lim P, Shashi KB, Ranjit G, Tae-Rim C, Hyun JK, Hun-Suk S, Jun-Young P, Yeong-Hoon H, Sun Mi L, Sol Lee P, Hye Soo L, Yun-Gon K and Yung-Hun Y 2020. Fructose based hyper production of poly-3-hydroxybutyrate from Halomonas sp. YLGW01 and impact of carbon sources on bacteria morphologies. *International Journal of Biological Macromolecules* **154**: 929-936.

Received 06 July, 2021; Accepted 22 November, 2021

Indian Journal of Ecology (2021) 48(6): 1837-1845

Manuscript Number: 3457
NAAS Rating: 5.79

Seasonal Investigation of Rainbow Trout Waterbodies in Western Ghats, South India

J.C. Walter Devaa and U. Ramesh*

Department of Molecular Biology, School of Biological Sciences
Madurai Kamaraj University, Madurai-625 021, India
**E-mail: ramesh.biological@mkuniversity.org*

***Abstract*:** Rainbow Trout (*Oncorhynchus mykiss*) was introduced in Munnar, Ooty and Kodaikanal in the Western Ghats regions of South India in the 19th century. After successful introductions, the trout stocks have vanished from many waterbodies and is currently limited to one waterbody in each of three geographical locations. Therefore, this study was done to know the habitat suitability by assessing the water quality (Physiochemical and Heavy metal analysis) on a seasonal basis in three waterbodies (where rainbow trout inhabits) namely, Rajamallay Stream of Munnar, Upper Bhavani Reservoir of Ooty, Gundar Stream of Kodaikanal because of constant size diminishment of the rainbow trout. Results showed the presence of ammonia to be above range for all the waterbodies in all seasons and significant difference was observed with Total Dissolved solids, while there was absence of all heavy metals. The presence of ammonia is a possible factor for size diminishment of the fish along with other human activities. However, the water quality for all the waterbodies was fair, good, excellent and marginal category according to the Canadian Council of Ministers of the Environment - Water Quality Index. But other water quality parameters were below limits and the three waterbodies studied were found suitable for the rainbow trout.

***Keywords*:** Water quality, Rainbow trout, Temperature, Dissolved oxygen

Rainbow Trout (*Oncorhynchus mykiss*) have been introduced in all continents except Antarctica. This fish species survives at higher elevations and are preferred for sport and recreational fishery. As time progressed, the increase for aquaculture production became sufficiently greater when compared to other manufactured foods of animal origin (Amirkolaie 2011) and production depends on environmental conditions. The survival and growth of the fish species not only depend on the acceptable amount of water, but also high-water quality and ambient temperature which are conducive (Bhatnagar and Devi 2013, Yapo et al 2017). Rainbow trout currently inhabit the water bodies of Ooty, Munnar and Kodaikanal regions of the Western Ghats, South India. Though after introduction and establishment, this salmonid species has vanished from a majority of the waterbodies in the above-mentioned locations in the Western Ghats. Rainbow trout are currently limited to one water body in each of the three locations. Trout stocks have been declining in these waterbodies in size and number and a fish of trophy potential size (trout measuring a foot) has been rarely caught for decades, therefore as a preliminary step towards habitat conservation, the water quality profile was investigated. Water quality guidelines provide information about water quality parameters and ecologically relevant information about water and toxicological threshold values to protect the water's quality standards (Chitmanat and Traichaiyaporn 2010). Freshwater fish are one of the most threatened taxonomic groups (Dudgeon et al 2006) because they are highly sensitive to the quantitative and qualitative alteration of aquatic habits (Laffaille et al 2005). The present study aimed at monitoring the seasonal variations of the physicochemical water quality parameters of the Rajamallay Stream of Munnar, Gundar Stream of Kodaikanal and Upper Bhavani Reservoir of Ooty where rainbow trout inhabits and to find out whether they are within the desirable limits for sustainable living for the rainbow trout in the long run.

MATERIAL AND METHODS

Study areas: Water samples (one litre) were collected in sterile polypropylene bottles from two different sampling points and site IDs were given accordingly (Spawning Sites in each waterbody were mainly chosen for the study) for the three waterbodies namely, Rajamallay Stream of Munnar, Upper Bhavani Reservoir of Ooty, Gundar Stream of Kodaikanal (Table 1) which were chosen for analysis in this study during 2019.

Analysis of physio-chemical parameters and water quality index: Physical parameters (pH, temperature, total dissolved solids) were analysed using Eutech PC Testr 35. Chemical parameters such as iron, magnesium, calcium, phosphate and dissolved oxygen were analysed by

argentometric, gravimetric, ultraviolet, spectrophotometric screening methods, respectively. Water Quality Index (WQI) was calculated for water samples from each sampling site of all locations. In this study, the Canadian Council of Ministers of the Environment (CCME) water quality index was done based on the following formula, The CCME Water Quality Index (CCME WQI):

$$CCME\ -WQI\ = 100 - \left(\frac{\sqrt{F1^2 + F2^2 + F3^2}}{1.732} \right)$$

To enable the CCME-WQI calculation, seventeen parameters were used, following their limits which helped in determination of the water quality (Table 2, 3) for Salmonid species with accordance with the Council Directive 78/659/EEC on the quality index of fresh waters requiring protection and support of fish life (Directive Council 1978) stipulated in the Regulation of the Minister of the Environment.

Analysis of heavy metal parameters and metal index: The water samples for heavy metal analysis were stored in polypropylene containers at 4ºC until further analysis was performed. Heavy metals such as arsenic (As), cadmium (Cd), chromium (Cr), lead (Pb), copper (Cu), nickel (Ni) and zinc (Zn) were analysed by Inductively Coupled Plasma-Mass Spectrometry (Nex ION 300X-Perkin Elmer). Metal Index was calculated based on the total trend evaluation of the present status. If the metal concentration is higher when compared to its MAC value, the water quality is worse. If the MI value is >1, it is a threshold of warning (Bakan et al 2010). The MI is calculated by using the following formula according to (Tamasi and Cini 2004):

$$MI\ = \sum_{i=1}^{n} \frac{C_i}{(MAC)_i}$$

Ci: The concentration of each element, MAC: maximumallowable concentration.

Agglomerative hierarchical clustering: Agglomerative Hierarchical Clustering (AHC) was done based on Ward's method and Euclidean distance. The statistical significance was done using Graph Pad Prism 6 software for Physiochemical and Heavy Metal Parameters.

RESULTS AND DISCUSSION

Water Quality Analysis (Physiochemical Parameters)

Pre-monsoon season: The CCME-WQI of the sampling points of the three waterbodies (RS1 = 76.24, RS2 = 82.5; UBS1 = 95.17, UBS2 = 83.8; GS1 = 83.62, GS2 = 89.87) was Fair, Excellent and Good. The two sites of the three waterbodies had surface temperature above range. Further ammonia, nitrate and nitrite were also above range in the Rajamallay and Gundar streams (Table 4).

Monsoon season: The CCME - WQI of the sampling points (RS1 = 83.62, RS2 = 65.71; UBS1 = 81.19, UBS2 = 83.39; GS1 = 88.24, GS2 = 91.19) was Fair and Good. The two sites of the two waterbodies (Rajamallay Stream and Upper Bhavani reservoir) had water temperatures above range followed by elevated levels of ammonia, nitrate and nitrite in the three water bodies (Table 5).

Post-monsoon season: The CCME - WQI of the sampling points (RS1 = 72.95, RS2 = 60.91; UBS1 = 75.15, UBS2 = 87.12; GS1 = 88.52, GS2 = 92.97) was Fair, Marginal and Good. Toxic parameters such as ammonia were above acceptable levels in all three waterbodies and rise in phosphate levels were also observed (Table 6). Amongst the water quality parameters, the important parameters that serve as controls for a trout habitat are dissolved oxygen and temperature (Elliot 1981). The surface temperature in the sites of the waterbodies during the pre-monsoon and monsoon times were beyond range due to varying climatic conditions. Rainbow trout require well oxygenated waters and are poikilothermic, where they can adapt to high summer temperature (Narum and Campbell 2015) with swimming performances at temperatures up to 24°C (Rodnick et al 2004). Toxic parameters such as ammonia exceeded limits in all seasons and can be attributed to the excretion of protein

Table 1. Geographical locations of the sampling sites

Site ID	Location	Latitude	Longitude
Rajamallay Stream, Munnar			
RS1	Rajamallay Stream Site 1	10º15'43"96 N	77º00'38"71E
RS1	Rajamallay Stream Site 2	10º15'28"709 N	77º00'32"278E
Upper Bhavani Reservoir, Ooty			
UBS1	Upper Bhavani Reservoir Site 1	11º26'71"013N	76º56'45"327E
UBS2	Upper Bhavani Reservoir Site 2	11º26'99"699N	76º56'51"902E
Gundar Stream, Kodaikanal			
GS1	Gundar Stream Site 1	10º21'55"852N	77º42'73"394E
GS2	Gundar Stream Site 2	10º21'42"129N	77º42'66"581E

metabolism by fish, bacterial decomposition of organic matter like food waste, faecal matter and dead planktonic matter (Bhatnagarand Devi 2013). Other reasons include organic decay from forest fires and other nitrogen fixation processes (Environment Canada 1997), these could also be the contributing factors for ammonia rise in the three aquatic locations of the Western Ghats. Lower ammonia concentrations affect fish growth and cause bacterial infections, while higher concentrations cause loss of trout production (Ruth Francis-Floyd 2009), the issue of ammonia is the possible reason for size diminishment of rainbow trout but did not cause mortalities. Ammonia conversion is essential because of its toxicity (Smil 2000), it is converted into nitrites and further by oxidation into nitrates. Similarly

Table 2. Reference range for water quality of trout waters (Physiochemical and heavy metals)

Physio – chemical parameters	Reference range	References
Temperature	6ºC - 13ºC	MacIntyre et al 2008
Turbidity NT units	2 - 12 NTU	Klein 2003
TDS	<200 mg l^{-1}	Wedemeyer 1996
pH	6.5 - 8.5	MacIntyre et al 2008
Total Alkalinity as $CaCO_3$	20 mg l^{-1}	MacIntyre et al 2008
Total Hardness as $CaCO_3$	75 – 150 mg l^{-1}	MacIntyre et al 2008
Calcium	4 – 160 mg l^{-1}	Heinen 1996
Magnesium	<15 mg l^{-1}	Heinen 1996
Iron	<0.5 mg l^{-1}	Industry Standard 1988
Ammonia	<0.02 mg l^{-1}	MacIntyre et al 2008
Nitrite	<0.1 mg l^{-1}	MacIntyre et al 2008
Nitrate	<1 mg l^{-1}	MacIntyre et al 2008
Fluoride	<1 mg l^{-1}	Camargo 2003
Sulphate	<50 mg l^{-1}	Heinen 1996
Phosphate	<0.3 mg l^{-1}	Industry Standard 1988
Dissolved Oxygen	≥9.0 mg l^{-1}	Industry Standard 1988
BOD (Biological Oxygen Demand)	5 ppm	Svobodova et al 1993
Heavy metal parameters	Reference range	References
Aluminium	0.01	Heinen 1996
Cadmium	0.006	Heinen 1996
Copper	0.006	Heinen 1996
Lead	0.02	Heinen 1996
Mercury	0.000012	Heinen 1996
Selenium	0.01	Heinen 1996
Arsenic	0.05	Heinen 1996
Chromium	0.011	Heinen 1996
Zinc	0.005	Heinen 1996

Table 3. Water quality rating (Chen et al 1997)

WQI value	Water quality	Description
95 - 100	Excellent	Water quality is protected with a virtual absence of threat or impairment, conditions very close to natural or pristine levels
80 - 94	Good	Water quality is protected with only a minor degree of threat or impairment, conditions rarely depart from natural or desirable levels
65 - 79	Fair	Water quality is usually protected but occasionally threatened or impaired, conditions sometimes depart from natural or desirable levels
45 - 64	Marginal	Water quality is frequently threatened or impaired, conditions often depart from natural or desirable levels
0 - 44	Poor	Water quality is almost always threatened or impaired, conditions usually depart from natural or desirable levels

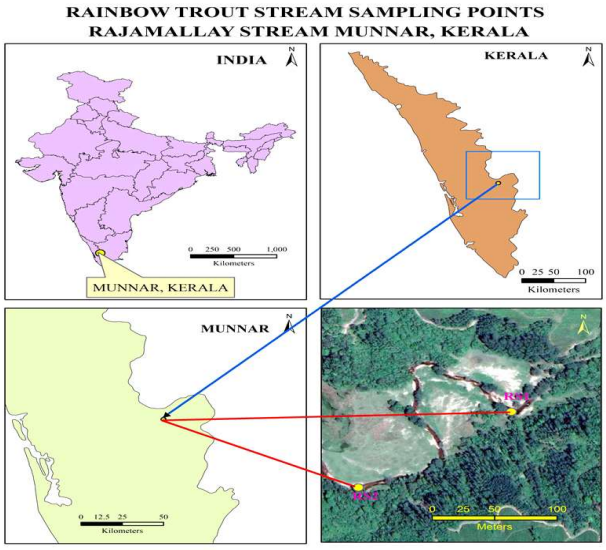

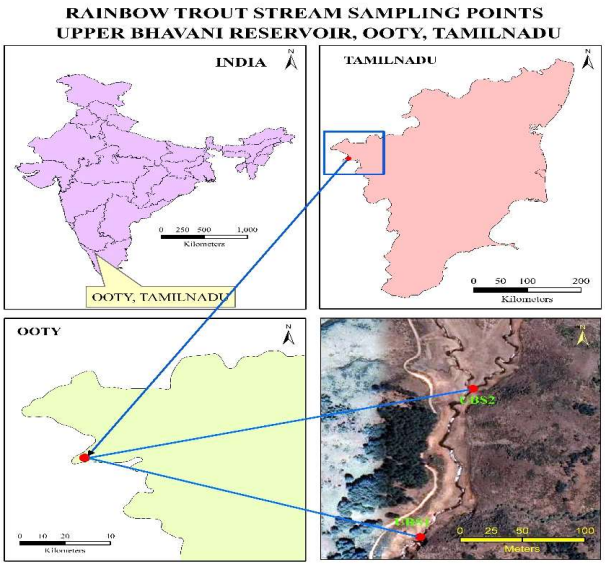

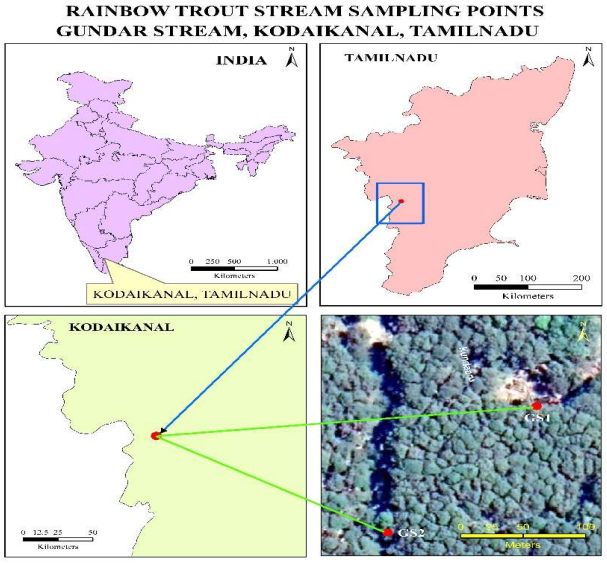

higher concentrations of nitrates affect the trout and were above range in the RS2 and GS2 sites, but minor concentrations can still be lethal for the fish, but concentrations keep varying according to the prevailing climatic conditions. Rise in phosphate levels can lead to limits in growth rate of plants, but can cause eutrophication by promoting algal growth in the aquatic environments (Kim et al 2013). Phosphate levels rose only during the post-monsoon season but posed no serious threats to rainbow trout. Water quality affects species composition and abundance and the physical and chemical parameters are directly related to the trout and the productivity of water bodies (Thomaz et al 1992). Trout species have tolerable limits to water quality and changes in limits have adverse effects on their body functions (Kiran 2010).

Total Dissolved Solids showed significant difference in all sites and seasons of the waterbodies and difference was also observed with total hardness as $CaCO_3$ in RS2, UBS1, GS2 sites of the three locations during the pre-monsoon season. While other parameters showed absence of any significant difference in all seasons of the locations (Table 4, 5, 6). Changes occurring in TDS concentrations in natural waters can occur due to changes in water balance which happens by limiting inflow and by increased water use and precipitation. The most commonly occurring anion is sulphate which is found at very minor quantities in all waterbodies while the cation that is most commonly occurring is calcium (Table 4, 5, 6) (Weber-Scannell and Lawrence Duffy 2007) and it changes on a seasonal basis. This was mainly attributed to low water levels in all waterbodies because of less water flow in the pre-monsoon season and water levels rise with strong water currents during the south-west monsoon. The water levels were maintained with medium currents with frequent usage of the spawning sites by the fish during the post-monsoon season. But the level of total dissolved solids observed was below range, thereby proving safe for trout life throughout all seasons. TDS can affect rainbow trout based on the concentrations and an upperlimit is 80 mg/L, thereby safe for trout. Differences with Total Hardness as $CaCO_3$ levels in certain sites (RS2, UBS1, GS2) of the three locations can be mainly attributed to seasonal changes and water flow modification. Other water quality parameters were found below range throughout the study and did not disturb the trout stocks and no significant difference was observed in all the three waterbodies of the locations, thereby proving conditions to be ambient for trout sustenance. Therefore, not much of seasonal variations were observed with the physicochemical water quality parameters of the Rajamallay Stream of Munnar, Gundar Stream of Kodaikanal and Upper

Table 4. Physicochemical parameters of the Rajamallay Stream of Munnar, Upper Bhavani Reservoir of Ooty, Gundar Stream of Kodaikanal during the Pre-monsoon season

Physico – chemical parameters	Reference range	Rajamallay Stream, Munnar		Upper Bhavani Reservoir, Ooty		Gundar Stream, Kodaikanal	
		RS1	RS2	UBS1	UBS2	GS1	GS2
Temperature (ºC)	6ºC - 13ºC	15.37±1.79	15.75±1.5	13.77±1.03	15.62±0.75	15±2.16	7.27±0.48
Turbidity NT units	5	ND	0.25±0.5	1.75±0.5	1.75±0.95	0.75±0.95	ND
TDS (mg L^{-1})	<200 mg L^{-1}	24.75±8.81^{abc}	23.25±5.2^{abcd}	15.5±10.51^{a}	21.62±14.32^{abcd}	22.25±13.01^{abcd}	12.12±0.75^{ab}
pH	6.5 -8.5	6.62±0.41	7.15±0.51	6.47±0.68	7.1±0.24	7.2±0.27	7.47±0.25
Total alkalinity as $CaCO_3$ (mg L^{-1})	20 mg L^{-1}	5±2.58	5.5±1.29	4.5±0.57	4.5±1.29	12.5±2.38	12.75±2.21
Total Hardness as CaCO3 (mg L^{-1})	75-150 mg L^{-1}	14.12±5.07	8.25±3.5^{abc}	6.87±6.2^{abc}	9.5±3.5ab	6.87±2.59	14.37±8.07^{ab}
Calcium (mg L^{-1})	4-160 mg L^{-1}	4.12±1.75	5.62±3.9	3.25±1.5	3.87±2.49	2.75±0.95	5.7±4.99
Magnesium (mg L^{-1})	<15 mg L^{-1}	2.75±2.53	1.87±1.31	0.75±0.5	1±0.81	0.62±0.75	2.12±1.93
Iron (mg L^{-1})	<0.5 mg L^{-1}	0.05±0.05	0.06±0.04	0.06±0.04	0.1±0	0.02±0.05	0.3±0.46
Ammonia (mg L^{-1})	<0.02 mg L^{-1}	0.15±0.17	0.32±0.21	0.12±0.05	0.31±0.07	0.19±0.23	0.47±0.05
Nitrite (mg L^{-1})	<0.1 mg L^{-1}	0.12±0.12	0.2±0.14	0.06±0.04	0.10±0.11	0.20±0.22	0.45±0.05
Nitrate (mg L^{-1})	<1 mg L^{-1}	1.02±0.85	1.25±0.95	0.50±0.57	1±0.81	1±1.41	1.75±0.95
Fluoride (mg L^{-1})	<1 mg L^{-1}	0.1±0	0.17±0.35	0.1±0	0.32±0.22	0.8±0	0.35±0.3
Sulphate (mg L^{-1})	<50 mg L^{-1}	1±0	0.24±0.13	0.5±0.08	0.54±0.38	0.15±0.12	0.91±0.11
Phosphate (mg L^{-1})	<0.3 mg L^{-1}	0.17±0.05	0.18±0.06	0.1±0.08	0.32±0.15	0.11±0.12	0.23±0.07
Dissolved oxygen (mg L^{-1})	≥9.0 mg L^{-1}	7.1±0.11	7.7±0.67	7.3±0.72	7.91±0.27	8.15±0.72	8.6±0.45
BOD (ppm)	<5 ppm	0.75±0.5	0.5±0.57	0.75±0.5	1.12±0.75	0.25±0.5	0.5±0.57
CCME-WQI value and quality		76.24 (Fair)	82.5 (Good)	95.17 (Excellent)	83.8 (Good)	83.62 (Good)	89.87 (Good)

^{abcd}Different superscript letters indicate significant difference between the three water bodies and parameters ($p<0.0001$) (Mean ± SD); **ND -**not detected

Table 5. Physicochemical parameters of the Rajamallay Stream of Munnar, Upper Bhavani Reservoir of Ooty, Gundar Stream of Kodaikanal during the monsoon season

Physico – chemical parameters	Reference range	Rajamallay Stream, Munnar		Upper Bhavani Reservoir, Ooty		Gundar Stream, Kodaikanal	
		RS1	RS2	UBS1	UBS2	GS1	GS2
Temperature (ºC)	6ºC - 13ºC	14.87±0.85	20.12±2.7	13.87±2.17	10.37±1.79	7.75±2.21	10±2.16
Turbidity NT units	5	ND	ND	2.75±0.5	1.25±0.5	ND	ND
TDS (mg L^{-1})	<200 mg L^{-1}	30.5±1.29^{abcd}	21.25±0.95^{abcd}	22.25±1.65^{abcd}	22.62±2.13^{abcd}	34.62±2.28^{abcd}	21.25±0.95^{ab}
pH	6.5 -8.5	6±0.81	6.47±0.36	7.07±0.09	7.17±0.23	6.7±0.46	6.52±0.45
Total alkalinity as $CaCO_3$ (mg L^{-1})	20 mg L^{-1}	7.5±2.88	8.75±2.5	4.5±1	5±0	4.25±1.5	3.75±1.5
Total Hardness as CaCO3 (mg L^{-1})	75-150 mg L^{-1}	23.25±10.9	6.87±0.26	8.25±0.95	4.5±2.38	8.75±1.5	6.87±0.26
Calcium (mg L^{-1})	4-160 mg L^{-1}	1.87±0.62	2.87±0.62	1.5±0.57	1.25±0.5	2.25±0.95	2.75±1.7
Magnesium (mg L^{-1})	<15 mg L^{-1}	1±0	2.25±0.95	0.25±0.5	ND	0.25±0.5	1.5±1
Iron (mg L^{-1})	<0.5 mg L^{-1}	0.07±0.04	0.55±0.51	0.01±0	0.1±0	0.01±0	0.3±0
Ammonia (mg L^{-1})	<0.02 mg L^{-1}	0.25±0.49	0.01±0	0.12±0.05	0.15±0.05	0.23±0.18	0.05±0.04
Nitrite (mg L^{-1})	<0.1 mg L^{-1}	0.03±0.04	0.4±0.18	0.15±0.1	0.1±0	0.15±0.05	0.13±0.07
Nitrate (mg L^{-1})	<1 mg L^{-1}	0.55±0.51	0.4±0.4	0.87±0.25	0.2±0	0.5±0.57	0.42±0.38
Fluoride (mg L^{-1})	<1 mg L^{-1}	0.42±0.17	0.27±0.05	0.10±0.06	0.17±0.05	0.5±0.34	0.1±0
Sulphate (mg L^{-1})	<50 mg L^{-1}	0.62±0.47	0.52±0.05	0.4±0.08	0.42±0.09	0.75±0.95	0.52±0.32
Phosphate (mg L^{-1})	<0.3 mg L^{-1}	0.15±0.12	0.15±0.05	0.11±0.1	0.1±0.08	0.2±0.08	0.2±0
Dissolved oxygen (mg L^{-1})	≥9.0 mg L^{-1}	7±0.81	8.25±1.25	7±0	7.12±0.25	8.8±0.54	8.75±0.64
BOD (ppm)	<5 ppm	1.12±0.25	1±0	1±0	1±0	1±0	0.75±0.5
CCME-WQI value and quality		83.62 (Good)	65.71 (Fair)	81.19 (Good)	83.39 (Good)	88.24 (Good)	91.19 (Good)

See Table 4 for details

Bhavani Reservoir of Ooty. The water quality of any waterbody changes with regards to seasons, geographical areas, even during the absence of pollution or contamination. The health status and mortality rate of the rainbow trout depend on the elements connected with water quality (Brown and Day 2002). Waterbodies inhabited by rainbow trout show them to be a good water quality indicator (Randak and Pokorny 2001) and they play a vital role in ecological significance. Altogether all the three waterbodies were suitable for the rainbow trout.

Water quality analysis (Heavy metal parameters): The MI (Metal Index) Values of the sampling points of the three waterbodies (RS1, RS2, UBS1, UBS2, GS1, GS2) showed that the metal indices were very below limits and did not pose any threats to rainbow trout or any aquatic life in all three seasons. The MI value was not >1 and was <1 (Bakan et al 2010). Significant difference was observed with Lead and Chromium which be due to environmental and climatic conditions seasonally (Table 7,8,9). Heavy metals in streams are emitted by forest fires, rock weathering, biogenic sources and wind-borne soil particles (Herawati et al 2000). Trace amounts in natural waters are toxic even at very low concentrations and can impose serious problems to ecosystems (Lee et al 2002).

Agglomerative Hierarchical Clustering

Physiochemical Parameters

Pre-monsoon: Agglomerative Hierarchical Clustering (AHC) of the WQIs of all the waterbodies observed during the pre-monsoon season was classified into 4 different clusters (Fig. 1). In Sites RS2, UBS2, GS1 and GS2 the water quality has a minor degree of impairment with conditions rarely departed from natural levels. In RS1, the water quality is usually protected but occasional threats make conditions sometimes to depart from natural levels. In UBS1, the water quality is protected with virtual absence of threat with conditions very close to natural levels.

Monsoon: Agglomerative Hierarchical Clustering (AHC) of the WQIs of all the waterbodies observed during the monsoon season was classified into 4 different clusters (Fig. 2). In RS1, UBS1, UBS2, GS1 and GS2, the water quality had a minor degree of threat with conditions rarely departing from natural levels. In RS2, the water quality is usually protected with occasional threats making conditions sometimes departing from natural levels.

Post-monsoon: Agglomerative Hierarchical Clustering (AHC) of the WQIs of all the waterbodies observed during the post-monsoon season was classified into 4 different clusters (Fig. 3). In RS1 and UBS1, the water quality is protected with

Table 6. Physicochemical parameters of the Rajamallay Stream of Munnar, Upper Bhavani Reservoir of Ooty, Gundar Stream of Kodaikanal during the Post-monsoon season

Physico – chemical parameters	Reference range	Rajamallay Stream, Munnar		Upper Bhavani Reservoir, Ooty		Gundar Stream, Kodaikanal	
		RS1	RS2	UBS1	UBS2	GS1	GS2
Temperature (ºC)	6ºC - 13ºC	15.5±2.61	18.12±2.78	11.65±0.72	14.5±4.2	9.4±0.45	12.5±1.73
Turbidity NT units	5	0.25±0.5	ND	6±0.81	1±0	ND	0.25±0.5
TDS (mg L^{-1})	<200 mg L^{-1}	41.5±9.32^{a}	28±2.94^{abcd}	50.75±2.87^{ab}	31.37±3.03^{abcd}	40.12±1.65^{abcd}	52±3.34^{abcd}
pH	6.5 -8.5	7.17±0.23	6.02±0.28	7.22±0.32	6.55±0.52	6.75±0.64	7.12±0.26
Total alkalinity as $CaCO_3$ (mg L^{-1})	20 mg L^{-1}	8±2.94	13.25±2.36	14.5±4.2	13.75±4.78	11.25±2.5	11.25±1.5
Total Hardness as CaCO3 (mg L^{-1})	75-150 mg L^{-1}	14.87±1.93	10.87±2.32	17.62±2.05	13.75±1.5	11±3.36	17±3.55
Calcium (mg L^{-1})	4-160 mg L^{-1}	3.5±1.29	4±1.22	4.5±1.08	3.12±0.85	4±1.63	3.25±2.06
Magnesium (mg L^{-1})	<15 mg L^{-1}	2±0.4	1.75±0.95	2.37±0.75	1.5±0.57	1.87±0.25	1.75±0.5
Iron (mg L^{-1})	<0.5 mg L^{-1}	0.12±0.05	0.05±0.04	0.08±0.01	0.06±0.01	0.04±0.01	0.02±0.01
Ammonia (mg L^{-1})	<0.02 mg L^{-1}	0.07±0.005	0.03±0.003	0.06±0.003	0.02±0.003	0.04±0.003	0.01±0.003
Nitrite (mg L^{-1})	<0.1 mg L^{-1}	0.02±0.004	0.01±0.001	0.02±0.001	0.008±0.001	0.01±0.001	0.004±0.001
Nitrate (mg L^{-1})	<1 mg L^{-1}	0.47±0.37	0.43±0.28	0.55±0.51	0.65±0.43	0.52±0.35	0.37±0.42
Fluoride (mg L^{-1})	<1 mg L^{-1}	0.47±0.12	0.45±0.12	0.27±0.17	0.35±0.23	0.12±0.05	0.37±0.09
Sulphate (mg L^{-1})	<50 mg L^{-1}	2±0.81	0.37±0.25	0.95±0.75	0.82±0.88	0.47±0.38	0.45±0.4
Phosphate (mg L^{-1})	<0.3 mg L^{-1}	0.5±0.25	0.2±0.08	0.52±0.25	0.55±0.33	0.62±0.28	0.27±0.17
Dissolved oxygen (mg L^{-1})	≥9.0 mg L^{-1}	7.75±0.5	7.47±0.55	7±1.35	8.22±0.6	8.4±0.45	9±0
BOD (ppm)	<5 ppm	0.75±0.5	0.25±0.5	1.25±0.5	1.5±0.57	1±0	1±0
CCME-WQI value and quality		72.95 (Fair)	60.91 (Marginal)	75.15 (Fair)	87.12 (Good)	88.52 (Good)	92.97 (Good)

See Table 4 for details

occasional threats with conditions sometimes departing from natural levels. In UBS2, GS1 and GS2, the water quality is protected with a minor degree of threat with conditions rarely to depart from natural levels. In RS2, the water quality is frequently threatened and water conditions often departed from natural levels.

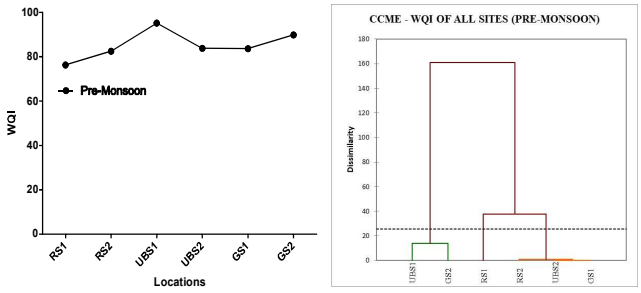

Fig. 1. CCME-water quality index and agglomerative hierarchical clustering based on Ward's method and Euclidean distance for all sites monsoon season

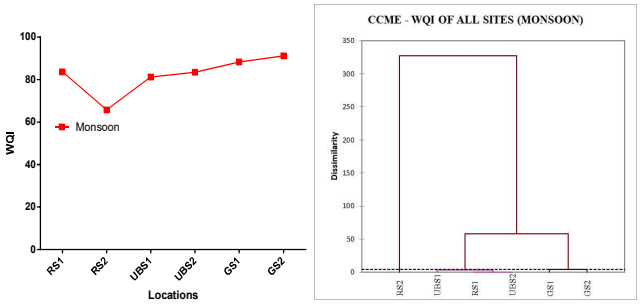

Fig. 2. CCME-water quality index and agglomerative hierarchical clustering based on Ward's method and Euclidean distance for all sites during monsoon season

Table 7. Heavy metal parameters of the Rajamallay Stream of Munnar, Upper Bhavani Reservoir of Ooty, Gundar Stream of Kodaikanal during the Pre-monsoon season

Heavy metal parameters	Reference range (ppm)	Rajamallay Stream, Munnar		Upper Bhavani Reservoir, Ooty		Gundar Stream, Kodaikanal	
		RS1	RS2	UBS1	UBS2	GS1	GS2
Aluminium	0.01	-0.001	-0.001	-0.0002	-0.0001	-0.002	-0.001
Cadmium	0.006	-0.0092	-0.0039	-0.0013	-0.0005	-0.0011	-0.0004
Copper	0.006	-0.0007	-0.0001	0.0022	0.0003	0.0018	0.0008
Lead	0.02	-0.049[ab]	-0.0019[abc]	-0.0496[ab]	-0.0013[abc]	-0.21[abc]	-0.004[abc]
Mercury	0.000012	-0.0007	-0.0109	-0.0001	-0.0011	-0.0021	-0.0293
Selenium	0.01	-0.01	-0.01	0.0013	0.0079	0.0013	0.01
Arsenic	0.05	0.0017	0.0132	0.0028	0.0219	0.0029	0.0295
Chromium	0.011	0.0034	0.0005	-0.0746	-0.0023	-0.03	-0.0009
Zinc	0.005	-0.0004	-0.0002	-0.0029	-0.0016	0.0021	0.0011
MI value		-0.55	-0.12	-1.03	0.19	-2.00	0.04

See Table 4 for details

Table 8. Heavy metal parameters of the Rajamallay Stream of Munnar, Upper Bhavani Reservoir of Ooty, Gundar Stream of Kodaikanal during the Monsoon season

Heavy metal parameters	Reference range (ppm)	Rajamallay Stream, Munnar		Upper Bhavani Reservoir, Ooty		Gundar Stream, Kodaikanal	
		RS1	RS2	UBS1	UBS2	GS1	GS2
Aluminium	0.01	-0.0002	-0.0001	0.0001	0.0001	-0.0001	-0.001
Cadmium	0.006	-0.0062	-0.0026	-0.0019	-0.0007	-0.0009	-0.0004
Copper	0.006	-0.0016	-0.0002	0.0025	0.0004	0.0092	-0.0011
Lead	0.02	-0.063	-0.0025	-0.0537	-0.0014	0.0009	-0.0032
Mercury	0.000012	0.0003	0.0049	0.0000	-0.0004	0.0004	-0.0021
Selenium	0.01	-0.0001	-0.00012	0.0011	0.0066	0.0009	-0.0059
Arsenic	0.05	0.0019	0.0146	0.0028	0.0216	0.0025	-0.0268
Chromium	0.011	0.0008[ab]	0.0001[ab]	-0.0884[ab]	-0.0027[ab]	-0.0394	-0.0032[ab]
Zinc	0.005	0.0025	0.0013	-0.0029	-0.0016	0.0046	-0.0023
MI value		-0.55	0.13	-1.18	0.18	-0.18	-0.38

See Table 4 for details

Table 9. Heavy metal parameters of the Rajamallay Stream of Munnar, Upper Bhavani Reservoir of Ooty, Gundar Stream of Kodaikanal during the Post-Monsoon season

Heavy metal parameters	Reference range (ppm)	Rajamallay Stream, Munnar		Upper Bhavani Reservoir, Ooty		Gundar Stream, Kodaikanal	
		RS1	RS2	UBS1	UBS2	GS1	GS2
Aluminium	0.01	-0.0001	-0.0001	-0.0006	-0.0066	-0.002	-0.0001
Cadmium	0.006	-0.0081	-0.0034	-0.0006	-0.0006	-0.0011	-0.0009
Copper	0.006	-0.0003	0.0000	0.0001	-0.0027	-0.0018	-0.0092
Lead	0.02	-0.0551[a]	-0.0022[abc]	-0.0019[abc]	-0.0016[abc]	-0.21[abc]	-0.0001[abc]
Mercury	0.000012	-0.0008	-0.0111	-0.0025	-0.0066	-0.002	-0.0059
Selenium	0.01	-0.00001	-0.00002	-0.0001	-0.0028	-0.0009	-0.0268
Arsenic	0.05	0.0018	0.0135	-0.0001	-0.0884	-0.0092	-0.0032
Chromium	0.011	0.0043	0.0007	-0.0005	-0.0029	-0.0009	-0.0023
Zinc	0.005	0.002	0.001	-0.0003	-0.0003	-0.00001	-0.0059
MI value		-0.47	-0.01	-0.05	-0.95	-1.93	-0.46

See Table 4 for details

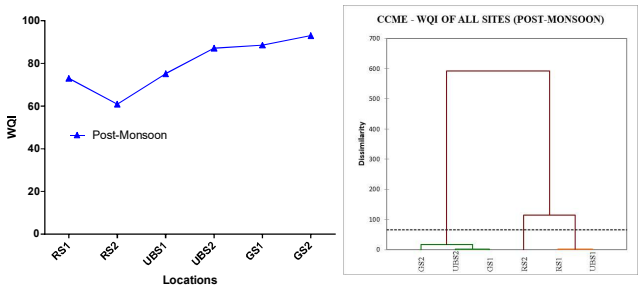

Fig. 3. CCME-water quality index and agglomerative hierarchical clustering based on Ward's method and Euclidean distance for all sites during post-monsoon season

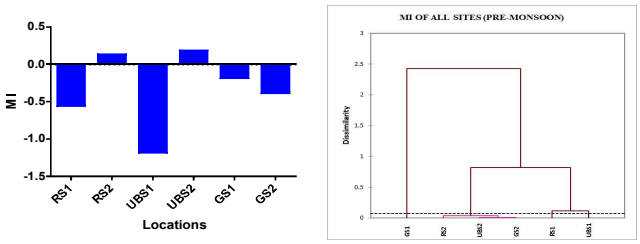

Fig. 4. MI values and agglomerative hierarchical clustering based on Ward's method and Euclidean distance for all sites during pre-monsoon season

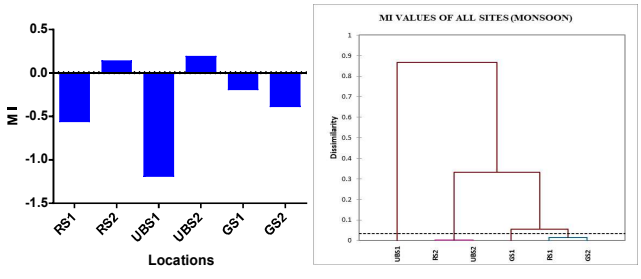

Fig. 5. MI values and agglomerative hierarchical clustering based on Ward's method and Euclidean distance for all sites during monsoon season

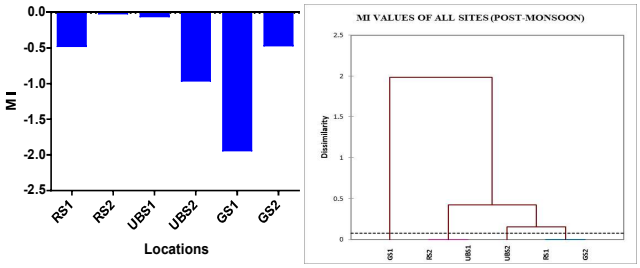

Fig. 6. MI values and agglomerative hierarchical clustering based on Ward's method and Euclidean distance for all sites during post-monsoon season

Heavy metal parameters: Agglomerative Hierarchical Clustering (AHC) of the MIs of all the waterbodies observed during the pre-monsoon, monsoon and post-monsoon seasons were classified into 4 different clusters (Fig. 4, 5, 6). All sites (RS1, RS2, UBS1, UBS2, GS1, GS2) showed that the water quality is protected and showed very low or absence of concentrations of the presence of heavy metals analysed (Table 7, 8, 9).

CONCLUSION

All the waterbodies in Munnar, Ooty and Kodaikanal showed fluctuations in water temperature. The ammonia's presence was above limits and is a causative factor for decline in fish growth and size but did not cause mortalities. The CCME – Water Quality Index and Metal Index of all the three waterbodies during the three seasons showed that water quality is protected at times with a virtual absence and

minor degree of threat, but at times occasionally or frequently threatened, but are always close to natural or desirable levels. The three waterbodies studied have sustained rainbow trout for more than 75 years and have adapted to the cold-water conditions of South India. Diminishment of size and number of the trout was also linked with poaching and animal intrusion. However, continual monitoring needs to done as an act of habitat conservation. But the water quality profile for all three locations have proved favourable for the long-term sustainability for the rainbow trout stocks. Trout farming can be a boon in these habitats because of the suitable water quality, ecology and environment.

REFERENCES

Amirkolaie AK 2011. Reduction in the environmental impact of waste discharged by fish farms through feed and feeding. *Reviews in Aquaculture* **3**(1): 19-26.

Bakan G, Özkoç HB, Tülek S and Cüce TH 2010. Integrated environmental quality assessment of the Kızılırmak River and its coastal environment. Turkish Journal of *Fisheries and Aquatic Sciences* **10**(4): 453-462.

Bhatnagar A and Devi P 2013. Water quality guidelines for the management of pond fish culture. *International Journal of Environmental Scie*nces **3**(6): 1980-2009.

Brown C and Day RL 2002. The future of stock enhancements: lessons for hatchery practice from conservation biology. *Fish and Fisheries* **3**(2): 79-94.

Camargo JA 2003. Fluoride toxicity to aquatic organisms: A review. *Chemosphere* **50**(3): 251-264.

Chen S, Coffin DE and Malone RF 1997. Sludge production and management for recirculating aquacultural systems. *Journal of the World Aquaculture Society* **28**(4): 303-315.

Chitmanat C and Traichaiyaporn S 2010. Spatial and temporal variations of physical-chemical water quality and some heavy metals in water, sediments and fish of the Mae Kuang River, Northern Thailand. *International Journal of Agriculture and Biology* **12**(6): 816-820.

Directive Council 78/659/EEC of 18 July 1978. On the quality of fresh waters needing protection or improvement in order to support fish life. *European Communication* 222, pp. 1–10.

Dudgeon D, Arthington AH, Gessner MO, Kawabata ZI, Knowler DJ, Lévêque C, Naiman RJ, Prieur-Richard AH, Soto D, Stiassny ML and Sullivan CA 2006. Freshwater biodiversity: Importance, threats, status and conservation challenges. *Biological Reviews* **81**(2): 163-182.

Elliot JM 1981. *Some aspects of thermal stress on freshwater teleosts*, In Pickering AD ed., Stress in fish: London, Academic Press, p 209-245.

Environment Canada 1997. *Problem formulation for Ammonia in the aquatic environment.* Canadian Environmental Protection Act Priority Substances List 2. Version 5.0, November 4.

Heinen JM 1996. *Water quality criteria, uptake, bioaccumulation, and public health considerations for chemicals of possible concern in West Virginia mine waters used for the culture of rainbow trout: Shepherdstown, W.Va.* The Conservation Fund's Freshwater Institute, prepared for U.S. Department of Agriculture, Agricultural Research Service, under grant agreement 59-1931-1-108, p 55.

Herawati N, Suzuki S, Hayashi K, Rivai IF and Koyama H 2000. Cadmium, copper, and zinc levels in rice and soil of Japan, Indonesia, and China by soil type. *Bulletin of Environmental Contamination and Toxicology* **64**(1): 33-39.

Industry Standard 1988. *The Nature Conservancy. Hydrosphere. Water for fish farms. General requirements and standards.* Moscow. Handout.

Kim E, Yoo S, Ro HY, Han HJ, Baek YW, Eom IC, Kim HM, Kim P and Choi K 2013. Aquatic toxicity assessment of phosphate compounds. *Environmental Health and Toxicology* **28**: 1-7.

Kiran BR 2010. Physico-chemical characteristics of fish ponds of Bhadra project at Karnataka. *RASĀYAN Journal of Chemistry* **3**(4): 671-676.

Klein LA 2003. *Investigation of the trout fishery in the Chattahoochee River below Buford Dam.* Georgia Department of Natural Resources, Wildlife Resources Division, January, pp 1-55.

Laffaille P, Acou A, Guillouët J and Legault A 2005. Temporal changes in European eel, Anguilla anguilla, stocks in a small catchment after installation of fish passes. *Fisheries Management and Ecology* **12**(2):123-129.

Lee G, Bigham JM and Faure G 2002. Removal of trace metals by coprecipitation with Fe, Al and Mn from natural waters contaminated with acid mine drainage in the Ducktown Mining District, Tennessee. *Applied Geochemistry* **17**(5): 569-581.

MacIntyre CM, Ellis T, North BP and Turnbull JF 2008. The influences of water quality on the welfare of farmed rainbow trout: a review. Fish welfare, pp. 150-184. In: Edward J Branson (eds). *Fish Welfare*. Blackwell Publishing Ltd, Oxford, United Kingdom.

Narum SR and Campbell NR 2015. Transcriptomic response to heat stress among ecologically divergent populations of redband trout. *BMC Genomics* **16**(1): 1-12.

Randak T and Pokorny J 2001. Use of rainbow trout for checking water inflowing to the drinking water purification plants. In *Toxicity and biodegradability of matters important in water management*, Ceske Budejovice (Czech Republic), Jihoceska Univerzita. 20-22 August, 2001.

Rodnick KJ, Gamperl AK, Lizars KR Bennett MT, Rausch RN and Keeley ER 2004. Thermal tolerance and metabolic physiology among redband trout populations in south-eastern Oregon. *Journal of Fish Biology* **64**(2): 310-335.

Ruth FF, Craig W, Denise PD and Pouder B 2009. *Ammonia in aquatic systems.* University of Florida/Institute of Food and Agricultural Services (UF/IFAS), Florida FA-16.

Smil V. 2000. *Cycles of life*. Scientific American Library, New York, 360.

Svobodová Z, Lloyd R, Máchová J and Vykusová B 1993. *Water Quality and Fish Health*. EIFAC Technical Paper, FAO: Rome, Italy. pp 54.

Tamasi G and Cini R 2004. Heavy metals in drinking waters from Mount Amiata (Tuscany, Italy). Possible risks from arsenic for public health in the Province of Siena. *Science of the Total Environment* **327**(1-3): 41-51.

Thomaz SM, Lansac Tôha FA, Roberto MD, Esteves FA and Lima AF 1992. Seasonal variation of some limnological factors of lagoa do Guarana: A varzea lake of the High Rio Parana, state of Mato Grosso do Sul, Brazil. *Revue d'Hydrobiologie Tropicale* **25**(4): 269-276.

Weber-Scannell PK and Duffy LK 2007. Effects of total dissolved solids on aquatic organism: A review of literature and recommendation for salmonid species. *American Journal of Environmental Sciences* **3**(1): 1-6.

Wedemeyer 1996. *Interactions with Water Quality Conditions in Physiology of Fish* in Intensive Culture Systems. Chapman and Hall publisher, New York.

Yapo M L, Yalamoussa T U O, Mouhamadou K O N E, Atsé B C and Kouassi P 2017. Can use the Biotic Index as an indication of fish farm pond water quality. *Journal of Advanced Botany and Zoology* **4**(4): 23-38.

Received 12 July, 2021; Accepted 12 November, 2021

Indian Journal of Ecology (2021) 48(6): 1846-1851

Manuscript Number: 3458
NAAS Rating: 5.79

Analysis of Financial Performances and Environmental Sustainability of Coldwater Inland Fisheries in Sikkim Himalaya

Kul Bahadur Chettri and Ruma Kundu[1]

Department of Economics, Nar Bahadur Bhandari Government College, Tadong, Gangtok-737 102, India
[1]Department of Economics, Sikkim University, Tadong, Gangtok-737102, India
E-mail: kulchettri33@gmail.com

***Abstract*:** This paper analyses the financial performances in terms of productivity and profitability indices and environmental sustainability with regards to maximum sustainable yield (MSY) through the application of the Gordon-Schaefer Model for the coldwater Primary Fishermen Cooperative Society (PFCS). The data was collected from secondary sources for the periods 2013-14 to 2018-19. The PFCS of Upper Sribadam, Maneybong-Sopakha and Mangshilla have performed better in financial management but there is a probability of threat of sustainability in the future because in some of the periods their actual yield surpasses the MSY. The PFCS like Upper Rimbik, Chujachen and Dalep have not been able to bring their financial performances up to the mark because they were more concerned for sustainability. Excessive extraction of fish from the water bodies for higher profit motive may lead to less availability for the coming generations. The estimated mean yield per unit of effort of the trout and carp fish was 116.84 kg/51m^3 and 87 kg/51m^3 water areas respectively. The MSY is equal to 202.814 kg/51m^3 water areas for trout and 114.069 kg/51m^3 water areas for carp. The study suggests that in aquaculture or fish farming, there should maintain equilibrium between financial benefits and environmental sustainability and the resource should be utilised on a sustainable basis.

Keywords: Coldwater fisheries, PFCS, Productivity, Profitability, Environmental sustainability

The Himalayan regions have the largest biological diversity in the world characterized by the presence of coldwater many of which harbor fish and largely support subsistence, ornamental and commercial fisheries (Singh 2015). In the Himalayas, the fish diversity comprises a large population of indigenous and exotic, cultivable and non-cultivable fish species having the potential for aquaculture practices, capture fisheries and sport fishing (Munilkumar and Nandeesha 2007, Mahanta et al 2010). The different fish species such as trout (rainbow and brown trout) and carp (grass carp, common carp, Chinese carp, and some species of Indian carp) are the major cultivable fishes of the coldwater (Singh 2015). Sikkim is a mountainous state endowed with numerous coldwater resources in the forms of lakes, streams, perennial springs, rivers, reservoirs, etc. which support both capture and culture fisheries in the upland and lowland regions. To utilise the available water resources fruitfully and to develop a capture and culture fishery, people have taken an initiative to make fish farming their subsidiary occupation and feel the urge to develop local water resources on sustainable basis fish farming through the formation of cooperatives (Dahlf 2017). At present state has Primary Fishermen Cooperatives Societies (PFCS) at the village level. The water bodies are gradually being brought under aquaculture with the formation of PFCS. The Department of Fisheries, Sikkim initiated the creation of fish farmers cooperatives based on the available number of farmers in clusters. The effectively functioning six PFCS are Upper Sribadam, Maneybong-Sopakha, Upper Rimbik, 20th Chujachen, Mangshilla and Dalep. The main motives behind the formation of fishermen cooperative societies in Sikkim were to increase the level of fish production, generate employment opportunities and ensure a sustainable source of livelihood, raise adequate revenue for reinvestment and to manage and conserve the fishery resources on a sustainable basis.

Fishery resources are renewable natural resources but natural stocks of fish have been decreasing day by day because of the rapid explosion of the human population and the resultant persistent and indiscriminate fish harvest (Petr and Swar 2002, Narayankumar 2017). Besides these, excessive extraction of fish from water bodies for speedy and higher returns has resulted in imbalances in ecology and sustainability (Datta et al 2006). Samuel et al (2018) investigated the estimation of MSY and the corresponding efforts of artisanal fisheries resources of River Niger (RN) and River Benu (BN) in the Kogi state of Nigeria with the help of Schaefer's surplus production model. The empirical results indicate that the MSY of 47.8 kg was achieved E_{MSY} level of 10.3 hours/day in RN while in the case of RB, MSY of about 34.7 kg was obtained at the E_{MSY}level of 11.4 hours/day. Datta et al (2006) analyse the trade-off between financial and

environmental management of two fish production units in Burdwan district of West Bengal. For Khatpukur PFCS, the percentage average catch to MSY is estimated to be 77.27 leaving a relatively smaller portion for a stock generation. No study has been undertaken in the context of financial performances and environmental sustainability in the coldwater fisheries in the Himalayas and Sikkim lacks study on this area. Therefore, this paper attempts to evaluate the financial performances of PFCS in terms of productivity and profitability, assess environmental sustainability and examine the trade-off between the financial performances and environmental management of the PFCS.

MATERIAL AND METHODS

The study was based on secondary data collected for six years i.e., from the periods 2013-14 to 2018-19 for six PFCS located in four districts of Sikkim. The data were collected from different sources such as cooperative societies, Department of Fisheries and the Department of Cooperation, Government of Sikkim. Three cooperatives from the West district and one each from East, South and North districts have been selected based on the existence of the number of cooperatives in each district. Of these 6 PFCS, 4 belong to trout farming and 2 carp farming.

Evaluation of financial performances of PFCS: To evaluate the financial performances of PFCS, the productivity and profitability ratios have been calculated as follows:

$$\text{Productivity} = \frac{\text{Total output of fish in monetary terms}}{\text{Total inputs in monetary terms}}$$

$$\text{Profitability} = \frac{\text{Profit}}{\text{Cost}}$$

If the profitability ratio is greater than 1, investment in fish farming is profitable.

Profit (Π) = Total revenue – Total cost

Total Revenue (TR) = Total fish output X unit price of fish in ₹.

Total Cost (TC) = sum of labor cost, input cost and other costs (maintenance cost, fishing cost etc.) in ₹

Environmental sustainability and fisheries management: The study analyses whether the PFCS's annual fish catch lies below the MSY or falls in the borderline case, or surpasses. The environmental sustainability of the different cooperative societies is examined by using the concept of MSY through the application of the Gordon-Schaefer Model (Ajay 1982, Datta et al 2006, Gupta and Bhattacharya 2007). According to Schaefer's model, catch per unit of effort (Y/E) is assumed to be proportional to the density of fish. The density of fish is supposed to be proportional to stock whereby the harvest level is written as Y = qEX, where q represents the catchability coefficient. The equation Y = qEX is known as the Gordon-Schaefer production function.

Effort index is calculated as follows:

$$\text{Effort index} = \frac{\text{Labour cost per fishermen}}{\text{Other input costs}} \times 100$$

The effort index is defined as the fishing labour cost (rearing and harvesting) per fishermen as a percentage of other input cost. The other input costs include the cost of seeds and feeds, maintaining and repairing costs and miscellaneous costs. The growth of fish population X can be expressed mathematically by the well-known logistic equation

$$\frac{dx}{dt} = rX\,(1 - \frac{X}{K})$$

Subject to harvest at rate Y, we rewrite the net rate of growth as

$$X = \frac{dx}{dt} = rX\,(1 - \frac{X}{K}) - Y$$

However, using the production function we can rewrite the equation as

$$X = rX\,(1 - \frac{X}{K}) - qEX$$

Here r = intrinsic growth rate of fish stock (1/year) and qE=Y/E implies catch standardized for fish stock or catch per unit of biomass.

The criterion of sustainability requires the equality dx/dt = Y which implies

$$rX\,(1 - \frac{X}{K}) - qEX \text{ where by we get }, X = K\,(1 - \frac{qE}{r})$$

After some mathematical manipulation, we get

$$Y = aE - bE^2$$

$$Y = E\,(a - bE)$$

It implies that

$$\left(\frac{Y}{E}\right) = a - bE \text{ ....}(1)$$

$$Y = aE - bE^2 \text{ …….. } (2)$$

The optimum effort level and MSY corresponding to this equation can be found by using the first-order condition as

$$\frac{dy}{dE} = 1 - 2bE = 0$$

$$\hat{E} = \frac{\hat{a}}{2\hat{b}} \text{ .....}(3)$$

Substituting equation 3 into equation 2, we get

$$Y = a\left(\frac{a}{2b}\right) - b\left(\frac{a}{2b}\right)^2$$

$$or \ \frac{a^2}{2b} - \frac{a^2}{4b}$$

$$or \ \frac{2a^2 - a^2}{4b}$$

$$\hat{Y}_{MSY} = \frac{\hat{a}^2}{4\hat{b}} \ldots\ldots\ldots\ldots\ldots (4)$$

$$Hence \ , \hat{E} = \frac{\hat{a}}{2\hat{b}} \ and \ MSY = \frac{\hat{a}^2}{4\hat{b}}$$

For incorporating species-specific effect, we carried out regression analysis with a categorical dummy by using the Least Square Dummy Variable (LSDV) model. For this purpose, the following modified Gordon-Schaefer model has been used.

$$\left(\frac{Y}{E}\right)_{it} = a_1 - bE_{it} + a_2 D_i + \mu_{it} \qquad (5)$$

where the subscript i = 1,….,N indicates the PFCS and subscript t =1,…,T indicates the time (year). In the regression model, a and b are the constants, the dependent variable (Y/E) is the yield per unit of effort, E represents effort index, D_i (dummy variable)= 1 if the fish species belong to the carp family, 0 otherwise, u_{it} represents the error term. The coefficients a_1, a_2 and b are estimated by applying equation (3) using the least-squares technique.

RESULTS AND DISCUSSION

In Sribadam, productivity and profitability were showing a more or less growing trend except for a slight decline in 2015-16, because in this period the cooperative had to bear extra costs for maintenance. During the period 2016-17, profit was declined due to a decrease in fish and an increase in input costs. However, the overall performances of the cooperative indicate an improvement in all indicators along with positive returns from the investment. In Maneybong-Sopakha, production had increased over the periods but slightly declined in 2015-16 and 2018-19 which was because of the less availability of the fish feeds from the government. But there were improvements in productivity and profitability because the members managed their ponds effectively. Conversely, in the period 2017-18, productivity and profitability had declined as a consequence of the rise in labour wages and input costs.

Productivity and profitability had declined significantly in Upper Rimbik during the periods 2014-15 and 2015-16 due to landslides. Profitability became negative and the rate of productivity was also less than 1 during those periods. The government refinanced and provided economic and technical support for its quick resuscitation. In 20th Chujachen, production was lowest in the year 2016-17 and declined for the periods 2015-16 and 2016-17 due to some biological causes. However, there was less variability in productivity and profitability of the society over the periods due to the hike in fish price. In Mangshilla, production was recorded lowest during the year 2016-17 and 2017-18 due to the non-availability of required fish seeds on time. This cooperative had the highest level of productivity and profitability among all others because the cost of inputs like the price of seeds and feeds was less for carp farming compared to trout farming. Similarly, for Dalep, there was less variation in profitability and productivity ratios. This cooperative had the lowest level of fish production compared to others because it had fewer fish farmers and ponds with water scarcity.

Table 1. Evaluation of financial performances of trout growers' PFCS

Year	Production (Kg 51m^{-3} water area)	Productivity (in ₹)	Profit (in ₹)	Profitability (in ₹)
Upper Sribadam				
2013-14	175	4.883	69583.33	3.883
2014-15	250	3.546	89758.33	2.546
2015-16	195	3.052	91775.69	2.052
2016-17	175	3.288	85245.88	2.288
2017-18	206	4.189	125660.21	3.189
2018-19	254	4.063	153199	3.063
Maneybong-Sopakha				
2013-14	140	4.560	54651.99	3.560
2014-15	219	3.408	77394.37	2.408
2015-16	165	3.684	72130.84	2.684
2016-17	200	4.462	108625.35	3.462
2017-18	220	4.009	132104.61	3.009
2018-19	192	4.235	117524.38	3.235
Upper Rimbik				
2013-14	145	3.128	49325	2.128
2014-15	47.5	0.772	-7000	-0.227
2015-16	83.333	0.942	-2520.83	-0.057
2016-17	150	2.769	47916.66	1.769
2017-18	146.666	2.476	52466.67	1.476
2018-19	100	2.258	54500	1.258
20th Chujachen				
2013-14	125	2.463	42000	1.463
2014-15	132	2.587	44242	1.587
2015-16	120.5	2.689	56369.75	1.689
2016-17	84.2	2.567	39885	1.567
2017-18	126	2.682	67725	1.682
2018-19	158.88	2.970	104540	1.970

Source: Author's estimation based on secondary data

The effort is significant at 5 percent level implying an increase in effort decreases yield per unit of effort. The dummy variable is also significant at 1 percent level which indicates that the species-specific effect exists on the level of effort as well as on the harvest level. The estimated mean yield per unit of effort of the trout fish is 116.84 kg while that of the carp fish is lower by 29.86 kg, i.e. 87 kg (Table 3). The value of R^2 and F indicates that the model is rather a good fit. Based on the result obtained from the LSDV model (Table 3), MSY for trout and carp growers' PFSC has been calculated separately (Table 4). The value of MSY is equal to 202.814 kg for trout and 114.069 kg for carp. The average yield of trout and carp are 158 kg and 91 kg per pond respectively.

Table 2. Evaluation of the financial performance of carp growers' PFCS

Year	(Production (Kg/ 51m^3 water area)	Productivity (in ₹)	Profit (in ₹)	Profitability (in ₹)
Mangshilla				
2013-14	120	5.419	19571.428	4.419
2014-15	128	7.314	22100	6.314
2015-16	110.33	6.572	23386.071	5.572
2016-17	93.2	4.807	18453.333	3.807
2017-18	102.6	5.463	25146.666	4.463
2018-19	120.024	5.374	29307.2	4.374
Dalep				
2013-14	90	5.688	11126.66	4.688
2014-15	63	3.705	9200	2.705
2015-16	79.5	3.816	11733.333	2.816
2016-17	93	3.838	13754	2.838
2017-18	63.2	3.019	10566.666	2.019
2018-19	76.8	3.217	13233.333	2.217

Source: Author's estimation based on secondary data

Table 3. Least square dummy variable model

Variables	Coefficient	t-value
Effort	-16.587**	-2.14
D_i	-29.863***	-2.91
constant	116.839***	5.42
F -statistic	7.31***	
R^2	0.307	

Source: Author's estimation based on secondary data
Note: ***, ** and * indicates the significance levels at 1%, 5 % and 10 % respectively

In Sribadam, the actual yield is higher than the MSY and the ratio of actual yield to MSY exceeds 1 for the periods 2014-15, 2017-18 and 2018-19 and the remaining years it is close to 1 indicating that there is a greater threat of actual yield surpassing the MSY. A harvest level greater than or close to MSY indicates that there is less concern for environmental sustainability, future growth of the fish resource and stock generation. The mean actual yield is 209.22 and the mean absolute deviation of the ratio from 1 is 0.1358 indicating that on average 86.42% of MSY is harvested keeping only 13.58 % for a stock generation. Similarly, for Maneybong- Sopakha, the actual yield is higher than the MSY and the ratio of actual yield to MSY exceeds 1 for the years 2014-15 and 2017-18 and is very close to 1 for the remaining years. Harvest levels exceeding the MSY indicate a disregard for environmental sustainability and complete unconcern regarding the future stock of resources. The mean actual yield is 189.39 with the mean absolute deviation of the ratio from 1 being 0.1211, indicating that on average 87.89 % is harvested leaving relatively smaller stocks for future generations of about 12.11 %. Considering the case of Upper Rimbik, their actual yield is lower than the MSY in all the years and the ratio of actual yield to MSY is also less as compared to the previous two societies. The mean actual yield is rather low at 112.08 and the mean absolute deviation of the ratio from 1 is 0.4474 indicating that on average 55.26% is harvested leaving 44.74% for a future stock generation. In 20th Chujachen, their actual yield is lower than MSY and the ratio of actual yield to MSY is moderate for all the years. The mean actual yield is 124.5052 and the mean absolute deviation of the ratio from 1 is 0.3308, indicating that on average 66.92% of MSY is realized keeping 33.08% for a stock generation.

Considering Mangshilla, their actual yield is higher than the MSY for the years 2013-14 and 2014-15 and also exceeds the value 1 in the ratio of actual yield to MSY while for the remaining years, it is close to 1. The mean actual yield is rather high at a value of 106.325 and the mean absolute deviation of the ratio from 1 is 0.1285 signifying on the average 87.15% of MSY is harvested keeping a relatively smaller portion of about 12.85% for a further stock generation. Lastly, for Dalep, their average yield of fish is less than the MSY level in all the years while the ratio of actual

Table 4. Estimation of the yield–effort equation for PFCS

PFCS	Constant (a_1, a_2)	Coefficient (b)	R^2	F	MSY	Average yield
Trout	116*** (5.42)	-16.587** (-2.41)	0.30	7.31***	202.814	158.80
Carp	87*** (-2.91)	-16.587** (-2.41)	0.30	7.31***	114.069	91.95

See Table 3 for details

Table 5. Comparative results for actual yield and MSY for trout growers' PFCS

Year	Actual yield	MSY (Y_m)	Ratio of Y_a to Y_m	$\|Y_a/Y_m-1\|$
Upper Sribadam				
2013-14	175	202.814	0.862	0.137
2014-15	250	202.814	1.232	0.232
2015-16	195	202.814	0.961	0.038
2016-17	175	202.814	0.862	0.137
2017-18	206.315	202.814	1.017	0.017
2018-19	254	202.814	1.252	0.252
Maneybong- Sopakha				
2013-14	140	202.814	0.690	0.309
2014-15	219.047	202.814	1.080	0.080
2015-16	165	202.814	0.813	0.186
2016-17	200	202.814	0.986	0.013
2017-18	220	202.814	1.084	0.084
2018-19	192.307	202.814	0.948	0.051
Upper Rimbik				
2013-14	145	202.814	0.714	0.285
2014-15	47.5	202.814	0.234	0.765
2015-16	83.333	202.814	0.410	0.589
2016-17	150	202.814	0.739	0.260
2017-18	146.666	202.814	0.723	0.276
2018-19	100	202.814	0.493	0.506
20th Chujachen				
2013-14	125	202.814	0.616	0.383
2014-15	132.142	202.814	0.651	0.348
2015-16	120.714	202.814	0.595	0.404
2016-17	84.285	202.814	0.415	0.584
2017-18	126	202.814	0.621	0.378
2018-19	158.888	202.814	0.783	0.216

Source: Author's estimation based on secondary data

Table 6. Comparative results for actual yield and MSY for carp growers' PFCS

Year	Actual yield	MSY (Y_m)	Ratio of Y_a to Y_m	$\|Y_a/Y_m-1\|$
Mangshilla				
2013-14	120	114.069	1.051	0.051
2014-15	128.88	114.069	1.129	0.129
2015-16	110.33	114.069	0.967	0.032
2016-17	93.22	114.069	0.817	0.182
2017-18	85.5	114.069	0.749	0.250
2018-19	100.02	114.069	0.876	0.123
Dalep				
2013-14	90	114.069	0.788	0.211
2014-15	63	114.069	0.552	0.447
2015-16	79.5	114.069	0.696	0.303
2016-17	93	114.069	0.815	0.184
2017-18	63.2	114.069	0.554	0.445
2018-19	76.8	114.069	0.673	0.326

Source: Author's estimation based on secondary data

yield to MSY is higher for the years 2013-14 and 2016-17; it is moderate in the remaining years. The mean actual yield is 77.58 and the mean absolute deviation of the ratio from 1 is 0.3198 revealing that on average 68.11% of MSY is being reaped leaving 31.98 % for a future stock generation. From the above discussion, it is clear that the PFCS like Rimbik, 20th Chujachen and Dalep are much more concerned with the stock generation and maintaining sustainability as compared to the other three cooperatives.

CONCLUSION

PFCS such as Upper Sribadam, Manebong -Sopakha and Mangshilla achieved higher financial achievements in fish farming; at the same time, there is a threat of sustainability because in some of the years the actual yield surpasses the MSY. These cooperatives had paid more attention to profit generations and relatively less to environmental sustainability. On the other hand, PFCS like Upper Rimbik, Chujachen and Dalep had not been able to keep their financial management up to the mark but then they had given more concern to the sustainability and maintained a relatively substantial amount for the future generations as compared to the former three cooperatives. Their actual yield is less than the MSY in all the periods. More financial gains like more productivity and profitability mean more extraction of existing resources implying less scope of regeneration for the future which indicates a trade-off between the financial management and environmental sustainability of resources. Although sustainability is maintained by the cooperatives, there is a lack of stability in the sustainability factor as is evident from the observed fluctuations in the considered ratio of actual yield to MSY. A positive return from investment in fisheries is very essential for proper functioning and reinvestment for the succeeding periods but coldwater fish species in the Himalayas have been greatly shrunk due to manmade activities and natural factors resulting in the degradation of ecology. Hence, it has become very crucial to conserve, manage and utilize resources on a sustainable basis.

REFERENCES

Ajayi TO 1982. The maximum sustainable yields of the inshore fish and shrimp resources of the Nigerian continental shelf. *Journal of Fish Biology* **20**(5): 571-577.

Gupta AC and Bhattacharya RN 2007. *Fish biodiversity of Digha fishery in eastern India: An empirical analysis. Ecology and Human Well-being,* Sage Publications, New Delhi: pp 69-92

Datta SK, Ghosh AR and Kundu R 2006. The tradeoff between economic and environmental management of two fish production units in Burdwan district of West Bengal. *Environment and Ecol*ogy **24**(1): 237-241.

Department of Animal Husbandry, Livestock, Fisheries and Veterinary Services, Government of Sikkim, Annual Report

2017-2018. http://www.sikkimahvs.gov.in/fisheries_development.html

Mahanta PC, Singh SD and Sarma D 2010. *Coldwater Fisheries Development in India with Special Reference to North-East India.*

Munilkumar S and Nandeesha MC 2007. Aquaculture practices in Northeast India: Current status and future directions. *Fish Physiology and Biochemistry* **33**(4): 399-412.

Narayanakumar R 2017. Maximum economic yield and its importance in fisheries management: 252-257.

Received 12 August, 2021; Accepted 28 November, 2021

Petr T and Swar DB 2002. *Coldwater fisheries in the trans-Himalayan countries* (No. 431), Food and Agriculture Organisation

Samuel A, Eniola AY and Tosan FB 2018. Estimates of maximum sustainable yield of artisanal fisheries resources of Rivers Niger and Benue in Kogi state, Nigeria. *International Journal of Fisheries and Aquatic Studies* **6**(3): 272-275.

Singh AK 2015. Advances in Indian coldwater fisheries and aquaculture. *Journal of Fisheries Sciences* **9**(3): 48-54.

Indian Journal of Ecology (2021) 48(6): 1852-1857

Manuscript Number: 3459
NAAS Rating: 5.79

Protective Effect of Phitofert on Testicular Function and Fertility in Rats Exposure to Lead Acetate

Osama Jabbar Hussein and Jawad Kadhim Arrak

Department of Physiology, Biochemistry and Pharmacology
College of Veterinary Medicine, University of Baghdad, Iraq
E-mail: firasrashad@gmail.com

***Abstract*:** The present study was carried out to investigate the protective role of phitofert as an antioxidant in ameliorating the deleterious effects of lead acetate on testes function and fertility in adult male rats. Thirty-two adult male and twenty-four female rats were used. Male rats were randomly divided into four equal groups and were treated daily for 56 days as follow: Group 1 received distilled water and was considered as control, the second group (G1) was intubated lead acetate orally 10 mg kg^{-1} body weight the third group (G2) was intubated phitofert 43 mg kg^{-1} body weight and the fourth group (G3) gave lead acetate 10 mg/ body weight plus phitofert 43 mg kg^{-1}. Blood samples were collected for estimation of testosterone hormone, Luteinizing Hormone (LH), malondialdehyde (MDA) and glutathione (GSH) concentrations. The results revealed a significant decrease in testosterone hormone and significant increase in LH in the group G1 as compared with others groups. The phitofert caused a significant decrease in the MDA with increase of GSH levels in group G3 indicating that the antioxidant effect of phitofert. In conclusion, phitofert at dose 43 mg kg^{-1} body weight has shown a dominant effect to decrease the harmful side effects of lead acetate toxicity on reproductive performance in adult male rats.

***Keywords*:** Phitofert, Lead acetate, Testosterone, LH, MDA, GSH

Lead is a common persistent environmental pollutant and has no obvious physiological function, except its tendency to associate with the sulfa-hydroxyl group, or organic protein bonds and ability to mimic major biological metals, such as iron, zinc, and especially calcium that act as catalysts in many enzymatic reactions and prevent them from binding to the active enzymes. Therefore can disrupt the essential enzymes based on these ions, that might represent its toxic effects (Garza et al 2006 and Khodabandeh et al 2020). Lead is capable to bind with the enzymes of some minerals such as zinc, iron, and calcium, however, it does not properly work as a co-factor. Lead interferes with the activity of aminolaevulinic acid dehydratase (ALALD) which is important in the bio-processing of hem, in addition to inhibition of ferrocholinate which is essential in the formation of hem (Kosnett 2006, Gourlaouen and Parisel 2007, Lamidi et al 2020). In domestic animals, clinical signs of lead toxicity are variable and depend on the species and age of the animal, in severe cases, rapid signs of depression and circular walking are shown by blindness, teeth grinding, convulsive seizures, anemia, and diarrhea (Linda 2006). Lead is produced oxidative stress (OS) through the overproduction of reactive oxygen species (ROS) and promotes lipid peroxidation (Verstraeten et al 2008, Martinez-Haro et al 2011 and Lopes et al 2016). The mechanism of lead-induced oxidative stress involves an imbalance between generation and removal of ROS (reactive oxygen species) in tissues and cellular components causing damage to membranes, DNA and proteins (Patra et al 2011, Bihaqi 2019, Murad and AL-okaily 2020).

Phitofertis one of food supplement contain Maca extract and considered as synthetic drug used for the adaptogenic and tonic action due to its content of components of Maca root extract. Phitofert used for man with selenium and for woman with folic acid and useful for improvement the function of reproductive system and fertility (Gonzales, et al 2001, Taher and Al-Shahery 2020), but there is few researches about its role in animals. Maca is one of its component was utilized to remedy the infertility in both sex via increased fertility (Cui et al 2003). The phitofert is also characterized by possessing of antioxidant role (Hermann and Bernet 2009). Furthermore, Maca contains several secondary metabolites, such as macamides, macaridine, alkaloids, and glucosinolates (Gonzales 2012). The most abundant glucosinolates detected in Maca are aromatic Mglucosinolates, namely benzyl glucosinolate (glucotropaeolin) and m-methoxybenzyl glucosinolate (glucolimnanthin). The use of herbal supplements to enhance sexual functions is increasing worldwide. Uncontrolled availability of these products could be of public

health concern (Corazza et al 2014). Maca has been described as a plant with effects as a sexual behavior enhancer in animals and humans (Balick and Lee 2002, D'Anza et al 2021). In male rats, maca produced a small effect on sexual behavior during acute and short-term administration (Lentz et al 2007). Therefore, current study was carried out to investigate the protective role of phitofert against the effect of lead acetate on testicular functions, fertility and pregnancy indices in rats model.

MATERIAL AND METHODS

Thirty-two healthy adult male rats and 24 adult female rats, weighed 250-350 g and were held in plastic cages and placed in a room for two weeks for acclimation. Room temperature was maintained at 22 ± 25°C, air of the room was altered continuously using ventilation with light/dark cycle of 12:12 hours per day. Animals were allowed freely reached to water and pellets along the experimental period. The study was carried out in animal house College of Veterinary Medicine/University of Baghdad. Rats were randomly divided into four equal groups control group (C) received only distilled water, the second group (G1) intubated lead acetate at dose 10 mg kg^{-1} B.W by oral daily (Elgawish and Abdelrazek 2014), third group (G2) were administered orally 43 mg kg^{-1} B.W of Phitofert® once daily (Yousif et al 2018) while group G3 were administered orally 43 mg kg^{-1} B.W of Phitofert® once plus lead acetate at dose 10 mg kg^{-1} B.W. by oral daily. After 56 days of treatment 4 male rats from each group were mating with 24 adult female rats (4 male/ 6 female) for calculate the fertility and pregnancy indexes. Blood samples were collected at day zero, 28 and 56 of the experiment via cardiac puncture technique from each anesthetized animal, then centrifuged at 2500 rpm for 15 minutes and sera samples were isolated and stored in freezer at -18°C till their use. Serum testosterone, LH was estimated by using enzymatic kit (Monobind Inc. (USA)) while MDA and GSH were estimated by using enzymatic kits (Cohesion bioscience). At the end of the experiment four male rats from each group were mating with 24 adult female rats (4 male/ 6 female) for calculate the fertility and pregnancy index. The statical data were presented as mean ±SE one, and two-way analysis of variance and least of significant deference (LSD) were performed between means. Statistical analysis of data was performed using statistical analysis system- version 9.1 (SAS 2012).

RESULTS AND DISCUSSION

Lead acetate caused significant decrease of serum testosterone concentration G1 group at 28 and 56 days as compare with other groups (Fig. 1A). However, results showed non-significant differences in LH hormone concentration between all groups at zero time, but lead acetate caused significant increase in hormone concentration in (1)group at 28 and 56 days of experiment as compared with control group. There were significant increase of LH hormone concentration at 28 and 56 days as compared with zero time ,with no significant differences in G2 and G3 at all periods (Fig. 1: A and B).

The decrement of testosterone concentration in rats treated with lead acetate at 28 and 56 days (G1) group reflect the toxic effect of lead on testicular tissue (Lopes et al 2016, Khodabandeh et al 2020, Olaniyan et al 2021). Lead acetate caused ROS elevation, LPO, oxidative damage, depletion in antioxidative enzymes and inhibition of steroid biosynthesis (Baty et al 2020, Oluranti et al 2021), as well as reduction in the expression of enzymes cytochromes P450scc, P450c17 and the 3β- hydroxy steroid dehydrogenase implied in the biosynthesis of testosterone hormone. Oxidative stress by lead acetate caused decrease in testosterone hormone may be due to reduction of utilization of cholesterol by Leydig's cells (Zakaria and AL-Busadah 2015, Algefare et al 2021) or it may be due reduction in reduction in number of LH receptors on Leydig cells that cause fall in the secretion of testosterone (Sehemby et al 2020). The lead acetate has a strong toxic effect on hypothalamic-pituitary axis and caused a disruption of the feed-back mechanism control exerted by testosterone on the synthesis of gonadotropins in pituitary or on the secretion of GnRH in hypothalamus which depend especially on the testosterone (Sechemby et al 2020, Mohsin 2021). Lad acetate also caused increase level of LH may be due to its negative effect on testes and caused reducing tubular diameters, reduction of testicular size and weight causing decrease in testosterone concentration that caused elevation in pituitary gland secretion luteinizing hormone (Elgawish and Abdelrazek 2014). Treatment of animals with phitofert caused an increase of serum testosterone concentration this may be due to antioxidant role of phitofert which contain antioxidant components (He et al 2010, Dulce et al 2021).The phytoestrogen have antioxidant properties though hydrogen electron donation via hydroxyl groups ,there for lead acts as free radical scavengers and inhibit toxicity of lead acetate (Li et al 2017, Inoue et al 2016). Phitofert improved the levels of testosterone and the sperm parameters function as demonstrated in many researchers (Gonzales et al 2003, Zhao et al 2005, Ohta et al 2015).

There was significant increase of MDA concentration in group G1 as compared with control groups (Fig. 2 A). Lead acetate with phitofert G3 group showed significant decreased in MDA activity as compared with G1 and G2. G2 group showed significant decrease as compared with control

group especially at 28 days of experiment. The significant decrease in GSH concentration in group G1 as compared with control and other treated groups at two treated periods was observed (Fig. 2 B). There was significant increase in group G3 at 28 and 56 days as compared with G1 and G2 treated groups.

The significant decrease in serum MDA and elevation in GSH in lead acetate treated groupcould be attributed to oxidative stress (Abdulmajeed et al 2016, Kucukler et al 2020, 2021) induced by lead acetate, where MDA is the degradation product of lipid peroxidation, SOD, CAT and GPx are oxidation enzymes that provide antioxidant defense in the body (Zheng et al 2000). Lead acetate caused disruption of the balance between the antioxidant system and formation of ROS causing oxidative damage to different tissues result in loose membrane function and increase MDA or lipid peroxidation causes decrease of GSH (Tarasub et al 2011, Dorostghoal et al 2014, Koksal et al 2017, Taslimi et al 2019). Lead acetate linking to SH groups of antioxidant enzymes, decreased the activities of these enzyme caused depletion of antioxidant defense system (Alcaraz-Contreras et al 2016).

Rats received lead acetate G1 group show a decrease in fertility index (33%) as compared with all other experimental

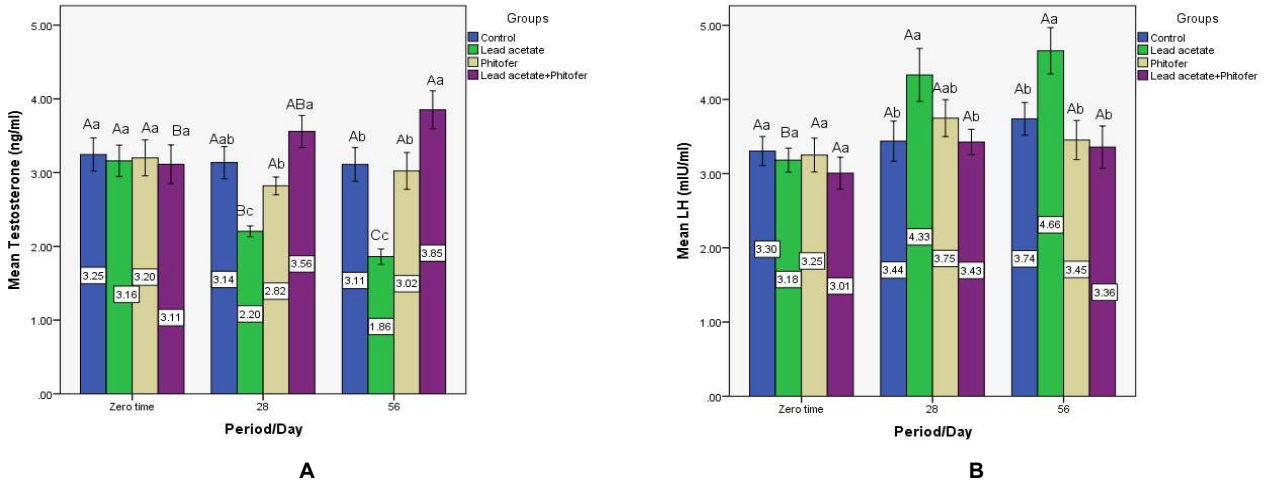

Values represent as mean ±SE (n= 8 rats/group)
Means with a different small letter denote significantly difference (P<0.05) between groups
Means with a different capital letter denote significantly difference (P<0.05) within the time

Fig. 1. Effect of phitofert, lead acetate and phitofert plus lead acetate on serum testosterone(A) and LH concentrations in male rats

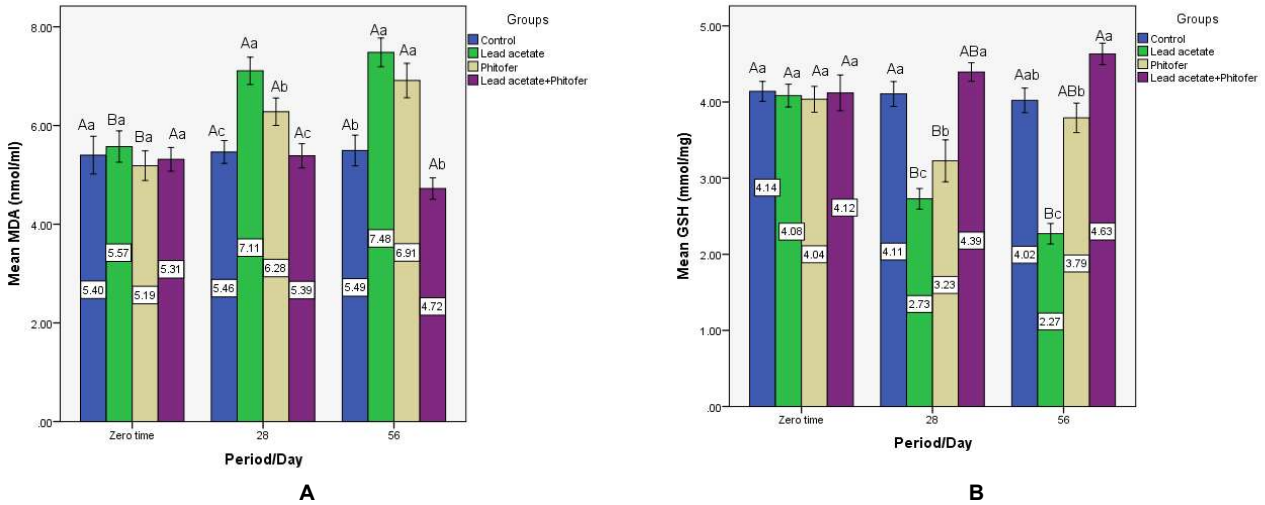

See Figure 1 for details

Fig. 2. Effect of phitofert, lead acetate and phitofert plus lead acetate on MDA and GSH activity in male rats

groups (Table 1), G2 and G3 group animals treated with phitofert showed increase of this index (83% and 83%) as compared with G1 group and less than control group. The pregnancy index was same in all groups and no changes occurred among all animals groups and the pregnancy index was 100% (Table 2).

The female rats treated with lead acetate have a lower fertility index, indicated reprotoxic effect of lead acetate (Ilerituerk et al 2021, Olaniyan et al 2021, Taher and Al-Shahery 2020). Testicular dysfunction caused by lead acetate (El-Khadragy et al 2020, Murad and Al-Okaily 2020) could be a mechanism for suppression of spermatogenesis, defect in semen quality and quantity (Hasanein et al 2018, Flora et al 2012, Ahmed et al 2021) causing decrease in fertility index.

Treatment the male rats with phitofert caused increase of fertility and pregnancy .The antioxidant components of phitofert and its role as supplement in improvement of fertility causing elevation of these indices (Sanchez et al 2017, Yu et al 2020). Maca has been documented to be used as sexual enhancement products (Ohta et al 2017), improved sexual behavior, libido and rate of fertilization (Lvavana et al 2013, Owolabi et al 2012, Mohsin et al 2021). Increase fertility index could be via improvement of semen quality (Yousif et al 2018, D'Anza et al 2021) and quantity (Inoue et al 2016, Tafuri et al 2019) by Phitofert. Furthermore, maca was beneficial as a helpful to improvement fertility and have sexual tonic in male because of its components especially selenium, phitofert include 300mg of maca and 54 mg of selenium (Gonzales 2012). Selenium was a mineral with high cabability in attenuated the oxidative stress and improve sperm function. Hamza and Al-Harbi (2014) reported that selenium could a meliorate the amino sodium glutamate induced testicular toxicity and reduce oxidative stress in testicular tissues. Also Taghizadeh et al (2017) refer to selenium caused prevent of oxidative stress and elevate of antioxidant status in rats.

Phitofert treated animals showed depletion MDA and elevation in GSH concentration indicated its antioxidants activity, caused attenuation of LPO and act as a powerful free radical scavenger can decrease MDA level (Soliman et al 2015), where antioxidants of different plant have been reported to inhibit free radical formation and minimizing lipid peroxidation in several different biological system (Zheng et al 2003, Aksu et al 2018).

Table 1. Effect of phitofert, lead acetate and phitofert plus lead acetate on fertility index in male rats

Group/Animal	Control	G1	G2	G3
Female mated successfully	6	6	6	6
Pregnant animal	6	2	5	5
None pregnant animal	0	4	1	1
Fertility index	100%	33%	83%	83%

Table 2. Effect of phitofert, lead acetate and phitofert plus lead acetate on pregnancy index in female rats

Group/Animal	Control	G1	G2	G3
Pregnant animals	6	2	5	5
Pregnant animal give life babies	6	2	5	5
Pregnancy index	100%	100%	100%	100%

CONCLUSION

Phitofert as supplement improved of passive toxicological effect of lead acetate on testes function and improved fertility and pregnancy of female mated with lead acetate exposed male rats.

REFERENCES

Abdulmajeed WI, Sulieman HB, Zubayr MO, Imam A, Amin A, Biliaminu SA and Owoyele BV 2016. Honey prevents neurobehavioural deficit and oxidative stress induced by lead acetate exposure in male wistar rats: A preliminary study. *Metabolic Brain Disease* **31**(1): 37-44.

Ahmed HA, Ali HA and Mutar TF 2021. Protective effects of olive leaf extract against reproductive toxicity of the lead acetate in rats. *Environmental Science and Pollution Research* 1-9. https://doi.org/10.1007/s11356-021-15240-3

Aksu EH, Kandemir FM, Kucukler S and Mahamadu A 2018. Improvement in colistin-induced reproductive damage, apoptosis, and autophagy in testes via reducing oxidative stress by chrysin. *Journal of Biochemical and Molecular Toxicology* **32**(11): e22201.

Alcaraz-Contreras Y, Mendoza-Lozano RP, Martinez-Alcaraz ER, Martinez-Alfaro M, Gallegos-Corona MA, Ramirez-Morales MA, Vazquez-Guevara M 2016. Silymarin and dimercaptosuccinic acid ameliorate lead-induced nephrotoxicity and genotoxicity in rats. *Human & Experimental Toxicology* **35**(4): 398-403.

Algefare A, Sedky AM and Alfwuaires M 2021. Apigenin Ameliorates lead Acetate induced Hyperlipidemia, Hypothyroidism and Hypogonadism in male rats. *Research Square* DOI: 10.21203/rs.3.rs-600247/v1

Balick MJ and Lee R 2002. Maca: from traditional food crop to energy and libido stimulant. *Alternative Therapies in Health and Medicine* **8**(2): 96-98.

Baty RS, Hassan KE, Alsharif KF, El-Hennamy RE, Elmahallawy EK, Hafez MM and Kassab RB 2020. Neuroprotective role of luteolin against lead acetate-induced cortical damage in rats. *Human & Experimental Toxicology* **39**(9): 1200-1212.

Bihaqi SW 2019. Early life exposure to lead (Pb) and changes in DNA methylation: Relevance to Alzheimer's disease. *Reviews on Environmental Health* **34**(2): 187-195.

Corazza O, Martinotti G, Santacroce R, Chillemi E, Di Giannantonio M, Schifano F and Cellek S 2014. Sexual enhancement products for sale online: Raising awareness of the psychoactive effects of yohimbine, maca, horny goat weed, and *Ginkgo biloba*. *BioMed Research International* 2014: 841798. doi: 10.1155/2014/841798.

Cui B, Zheng BL, He K and Zheng QY 2000. Imidazole alkaloids from *Lepidium meyenii*. Journal of Natural Products **66**(8): 1101-1103.

D'Anza E, Albarella S, Galdiero G, Tafur, S, Del Prete C and Peretti V 2021. DNA fragmentation and morphometric studies in sperm of

stallions supplemented with maca (*Lepidium meyenii*). *Zygote* **29**(4): 325-330.

Dorostghoal M, Seyyednejad SM and Jabari A 2014. Protective effects of *Fumaria parviflora L.* on leadinduced testicular toxicity in male rats. *Andrologia* **46**(6): 437-446.

Dulce EAY, Valeria MPA and Gustavo FG 2021. The antioxidant effect of Peruvian maca (*Lepidium meyenii*). High Altitude Research Institute, Universidad Peruana Cayetano Heredia, Lima, Peru. DOI: 10.1016/B978-0-12-819092-0.00050-9

Elgawish RAR and Abdelrazek HMA 2014. Effects of lead acetate on testicular function and caspase-3 expression with respect to the protective effect of cinnamon in albino rats. *Journal of Toxicology Reports* **1**: 795-801.

El-Khadragy M, Al-Megrin WA, AlSadhan NA, Metwally DM, El-Hennamy RE et al 2020. Impact of coenzyme Q10 administration on lead acetate-induced testicular damage in rats. *Oxidative Medicine and Cellular Longevity*, https://doi.org/10.1155/2020/4981386.

Flora G, Gupta D and Tiwari A 2020. Toxicity of lead: A review with recent updates. *Interdisciplinary Toxicology* **5**(2): 47-58.

Garza A, Vega R and Soto E 2006. Cellular mechanism of lead neurotoxicity. *Medical Science Monitor* **12**(3): RAS57-65.

Gonzales GF 2012. Ethnobiology and ethnopharmacology of lepidiummeyenii (Maca), a plant from the peruvian highlands. *Evidence-Based Complementary and Alternative Medicine* 193496.

Gonzales GF, Rubio J, Chung A, Gasco M and Villegas L. 2003. Effect of alcoholic extract of *Lepidium meyenii* (Maca) on testicular function in male rats. *Asian Journal of Andrology* **5**(4): 349-352.

Gonzales GF, Cordova A, Gonzales C, Chung A, Vega K and Villena A 2001. *Lepidium meyenii* (Maca) improved semen parameters in adult men. *Asian Journal of Andrology* **3**(4): 301-303.

Gourlaouen C and Parisel O 2007. Is an electronic shield at the molecular origin of lead poisoning? A computational modeling experiment. *Angewandte Chemie International Edition* **46**(4): 553-556.

Hamza RZ and Al-Harbi MS 2014. Monosodium glutamate induced testicular toxicity and the possible ameliorative role of vitamin E or selenium in male rats. *Toxicology Reports* **1:** 1037-1045.

Hasanein P, Fazeli F, Parviz M and Roghani M 2018. Ferulic acid prevents lead induced testicular oxidative stress and suppressed spermatogenesis in rats. *Andrologia* **50**(1): e12798.

He Z, Feng Y and Xu LF 2010. In vitro antioxidant activity of ethanol extract of maca (*Lepidium meyenii walpers*) cultivated in Yunnan. *Food Science* **31**(15): 39-43.

Hermann M and Bernet T 2009. The transition of maca from neglect to market prominence: Lessons for improving use strategies and market chains of minor crops. 62 Agricultural Biodiversity and Livelihoods Discussion Papers 1. Bioversity International, Rome, Italy: 101.

Ileriturk M, Benzer F, Aksu EH, Yildirim S, Kandemir FM, Dogan T and Genc A 2021. Chrysin protects against testicular toxicity caused by lead acetate in rats with its antioxidant, anti-inflammatory, and antiapoptotic properties. *Journal of Food Biochemistry* **45**(2): e13593.

Inoue N, Farfan C and Gonzales GF 2016. Effect of butanolic fraction of yellow and black maca (*Lepidium meyenii)* on the sperm count of adult mice. *Andrology* **48**: 915-921.

Khodabandeh Z, Dolati P, Zamiri MJ, Mehrabani D, Bordbar H, Alaee S and Azarpira N 2020. Protective effect of quercetin on testis structure and apoptosis against lead acetate toxicity: A Stereological Study. *Biological Trace Element Research* **199:** 3371-3381.

Köksal E, Bursal E, Gülçin İ, Korkmaz M, Çağlayan C, Gören AC and Alwasel SH 2017. Antioxidant activity and polyphenol content of Turkish thyme (*Thymus vulgaris*) monitored by liquid chromatography and tandem mass spectrometry. *International Journal of Food Properties* **20**(3): 514-525.

Kosnett MJ 2006. Lead. In: Olson KR *Poisoning and Drug Overdose* (5th ed). McGraw-Hill Professional.

Kucukler S, Benzer F, Yildirim S, Gur C, Kandemir FM, Bengu AS and Dortbudak MB 2021. Protective effects of chrysin against oxidative stress and inflammation induced by lead acetate in rat kidneys: a biochemical and histopathological approach. *Biological Trace Element Research* **199**(4): 1501-1514.

Lamidi IY, Hudu MG, Akefe IO, Adamu S and Salihu SI 2020. Subchronic administration of flavonoid fraction Daflon improves lead-induced alterations in delta-aminolevulinic acid dehydratase activity, erythrocytic parameters, and erythrocyte osmotic fragility in Wistar rats. *Comparative Clinical Pathology* **29**(5): 955-963.

Lavana A, Vazquez R, Palma-Irizarry M and Orihuela A 2013. Effect of supplementation with maca (*Lepidium meyenii*) in libido and semen characteristics in hair sheep rams (Ovisaries). Boletín Latinoamericano y del Caribe de Plantas Medicinales y Aromáticas **12**(3): 238-242.

Lentz A, Gravitt K, Carson CC and Marson L 2007. Acute and chronic dosing of *Lepidium meyenii* (Maca) on male rat sexual behavior. *The Journal of Sexual Medicine* **4**(2): 332-339.

Li J, Sun Q, Meng Q, Wang L, Xiong W and Zhang L 2017. Anti-fatigue activity of polysaccharide fractions from *Lepidium meyenii* Walp. (maca), *International Journal of Biological Macromolecules* **95**: 1305-1311.

Lopes AC, Peixe TS, Mesas AE and Paoliello MM 2016. Lead exposure and oxidative stress: A systematic review. *Reviews of Environmental Contamination and Toxicology* **236**: 193-238.

Martinez-Haro M, Green AJ and Mateo R 2011. Effects of lead exposure on oxidative stress biomarkers and plasma biochemistry in water birds in the field. *Environmental Research* **111**(4): 530-538.

Mohsin AR 2021. *Fertilization and embryonic development after oral administration of Lepidium meyenii (Maca) and Glycyrrhiza glabra crude aqueous extract in mice*. Doctoral dissertation, University of Baghdad, Iraq.

Murad HF and Al-Okaily BN 2020. Protective effect of alfa lipolic acid against lead induced oxidative stress and DNA fragmentation to testicular function in rat. *Iraqi Journal of Veterinary Sciences*, **35**(2): 305-312.

Ohta Y, Kawate N, Inaba T, Morii H and Takahashi K 2017. Feeding hydroalcoholic extract powder of Lepidium meyenii (maca) enhances testicular gene expression of 3β-hydroxysteroid dehydrogenase in rats. *Andrologia* **49**(10): E 12792.

Ohta Y, Yoshida K, Kamiya S, Kawate N, Takahashi M, Inaba T, Hatoya S, Morii H, Takahashi K, Ito M, Ogawa H and Tamada H 2015. Feeding hydroalcoholic extract powder of *Lepidium meyenii* (maca) increases serum testosterone concentration and enhances steroidogenic ability of Leydig cells in male rats. *Andrologia* **48**(3): 347-354.

Olaniyan OT, Ojewale OA, Dare A, Adebayo O, Enyojo JE, Okotie GE and Eweoya OO 2021. *Cocos nucifera* L. oil alleviates lead acetate-induced reproductive toxicity in sexually-matured male Wistar rats. *Journal of Basic and Clinical Physiology and Pharmacology* **32**(3): 145-153.

Oluranti OI, Adeyemo VA, Achile EO, Fatokun BP and Ojo AO 2021. Rutin improves cardiac and erythrocyte membrane–bound ATPase activities in male rats exposed to cadmium chloride and lead acetate. *Biological Trace Element Research* DOI: 10.1007/s12011-021-02711-4. PMID: 33844168.

Owolabi JO, Ghazal OK, Williams FE and Ayodele EO 2012. Effect of Moringa oleifera (Drumstick) leaf extracts on lead induced testicular toxicity in adult Wistar rat (*Rattus novergicus). Biomedical and Biotechnology Research Journal* **2**(12): 4003-4009.

Patra RC, Rautray AK and Swarup D 2011. Oxidative stress in lead and cadmium toxicity and its amelioration. *Veterinary Medicine*

International **20**: 457327. doi: 10.4061/2011/457327.

Sanchez JM, Serrano ZA, Durán JA, Morales HS and Álvarez PB 2017. Peruvian maca and possible impact on fertility. *Journal of Nutritional Health & Food Engineering* **6**(5): 00217.

SAS (Statistical analysis system) 2012. *User guide for personal computers*. SAS Institute Inc. Cam, N.C., USA.

Sehemby M, Lila AR, Sarathi V, Shah R, Sankhe S, Jaiswal SK, and Bandgar T 2020. Predictors of chronic LH-testosterone axis suppression in male macroprolactinomas with normoprolactinemia on cabergoline. *The Journal of Clinical Endocrinology & Metabolism* **105**(12): e4551-e4557.

Soliman MM, Baiomy AA and Yassin MH 2015. Molecular and histopathological study on the ameliorative effects of curcumin against lead acetate-induced hepatoxicity and nephrototoxicity in Wistar rats. *Biological Trace Element Research* **167**(1): 91-102.

Tafuri S, Cocchia N, Vassetti A, Carotenuto D, Esposito L, Maruccio L and Ciani F 2019. *Lepidium meyenii* (Maca) in male reproduction. *Natural Product Research* 1-10.doi.org/10.1080/14786419.2019.1698572

Taghizadeh L, Eidi A, Mortazavi P and Rohani AH 2017. Effect of selenium on testicular damage induced by varicocele in adult male Wistar rats. *Journal of Trace Elements in Medicine and Biology* **44**: 177-185.

Taher HH and Al-Shahery NJ 2020. The protective role of phitofert aginst naprooxen-induced toxicity in prostate gland of rats. *Annals of Tropical Medicine and Public Health* **23**: 239-259.

Tarasub N, Tarasub C and Ayutthaya WD 2011. Protective role of curcumin on cadmium-induced nephrotoxicity in rats. *Journal of. Environmental Chemistry and Ecotoxicology* **3**(2): 17-24.

Received 12 June, 2021; Accepted 10 November, 2021

Taslimi P, Kandemir FM, Demir Y, Ileriturk M, Temel Y, Caglayan, C and Gulcin I 2019. The antidiabetic and anticholinergic effects of chrysin on cyclophosphamide-induced multiple organ toxicity in rats: pharmacological evaluation of some metabolic enzyme activities. *Journal of Biochemical and Molecular Toxicology* e22313. doi:https://doi.org/10.1002/ jbt.22313.

Verstraeten SV, Aimo L and Oteiza PI 2008. Aluminium and lead: molecular mechanisms of brain toxicity. *Archives of Toxicology* **82**(11): 782- 789.

Yousif MH and Al-Arrak JK 2018. *Effect of maca aqueous extract on the epididmal sperms quality and DNA normality of vasectomized mature mice.* A thesis, Department of Physiology and Pharmacology/College of Vet. Medicine/Iraq

Yu Z, Liu H, Li D, Chen X, Ao M, Jin W and Yu L 2020. N-(3-Methozybenzyl)-(9 Z, 12 Z, 15 Z)-octadecatrienamide from maca (*Lepidium meyenii Walp.*) ameliorates corticosterone-induced testicular toxicity in rats. *Food & Function* **11**(9): 7762-7774.

Zakaria A and Al-Busadah K 2015. Pentoxifyllin efficiency in protecting testes against cadmium toxicity. *Journal of Animal and Veterinary Advances* **14**(1): 18-29.

Zhao J, Muhammad I, Dunbar D. Ch, Mustafa J and Khan I 2005. New Alkamides from Maca (*Lepidium meyenii*). *Journal of the Agricultural and Food Chemistry* **53**(3): 690-693.

Zheng B, He K, Kim CH, Rogers L, Shao Y and Hunag ZY 2000. Effect of lipidic extract from Lepidium meyenii on sexual behavior in mice and rats. *Urology* **55**(4): 598-602.

Zheng X, Meng WD, Xu YY, Cao JG and Qing FL 2003. Synthesis and anticancer effect of chrysin derivatives. *Bioorganic & Medicinal Chemistry Letters* **13**(5): 881–884.

Indian Journal of Ecology (2021) 48(6): 1858-1862

Manuscript Number: 3460
NAAS Rating: 5.79

Effect of Purified Bioactive Compounds for *Streptomyces griseus* on Proliferation Lymphocyte *in Vitro*

Eslah Shaker Rajeb, Mohsen Hashim Risan and Zainab Yaseen Mohmmed Hasan[1]

College of Biotechnology, [1] Biotechnology Research Center, University Al-Nahrain, Iraq
E-mail: eslah_bio@yahoo.com

***Abstract*:** This study employed local *Streptomyces griseus*isolatescapable of producing novel bioactive compounds (Fredericamycin), as well as investigating their biological activity on normal human blood lymphocytes cultured. The characteristics *Streptomyces griseus*strain *has been recorded* based on culture morphology of Arial mycelium colors which was Pale yellowon ISP2 media at 28°Cfor 7-14 days and the biochemical tests. The extraction method to obtain the bioactive compounds from the isolated *S. griseus*was employed by run about 500ml ISP2medium broth of *Streptomyces griseus* to get the extra and intra cellular production. The pH of the broth was adjusted to 2.0 with dilute sulfuric acid and left at 4°C for 96 hours. The lysate was filtered and the filtrate was transferred to reparatory fennel for extract the secondary metabolites yields with ethyl acetate. The acetate layers were collected and evaporated to dryness then to be subjected for purification of bioactive compounds by preparative TLC. The solvent system was ethyl acetate: methanol: water (10:1.5:1) on silica gel plates. Two major compounds were obtained named as (E1 and E2) which represented the purified components from the isolated local strain**.**The proliferative cultured lymphocytes by MTT assay after treated with purified active substance (E1 and E2) provided same results for both compounds. However; the E2 give low proliferation when cultured lymphocytes with higher concentration of 500 µg/ml.

Keywords: *Streptomyces griseus,* Fredericamycin, Lymphocyte

The genus *Streptomyces* belongs to order Actinomycetes. These bacteria are filamentous, aerobic, gram positive and spread mainly in soil and considered as a good source for more than half of all antibiotic, also, it is known to produce many other products like extra cellular enzymes and inhibitors (Vaurnakis and Blander 2014). *Streptomyces griseus* is specie of bacteria which commonly found in soil. Very few strains have also been reportedly sourced from deep-sea sediments. It is a Gram-positive bacterium with high GC nucleic acid content (Vaurnakis and Blander 2014). These strains are known producers of 32 different structural types of bioactive compounds, (Amin et al 2016, Risan et al 2006, Qasim and Risan 2017, Risan et al 2017, Risan et al 2018, Al-Rubaye et al 2018a, b, Risan et al 2019, Al-Rubaye et al 2020) and produced more than 70% of the known natural antibiotics produced such as streptomycin (Labeda 2010). Fredericamycin is a novel antibiotic produced by a soil isolate of *Streptomyces griseus* with strain named as FCRC-48. *In vitro*, fredericamycin exhibits antibacterial, antifungal, and cytotoxic activities. *In vivo*, fredericamycin exhibits very good antitumor activity (Rajeb et al 2021). Lymphocytes are central to the progression of autoimmune disease, transplant rejection, leukemia, lymphoma and lymphocyte-resident viral diseases such as HIV/AIDs. The three major types of lymphocyte are T cells, B cells and natural killer (NK) cells. Lymphocytes can be identified by their large nucleus. Strategies to target drug treatments to lymphocytes, therefore, represent an opportunity to enhance therapeutic outcomes in disease states where many current treatment regimens are incompletely effective and promote significant toxicities (Kelleher and Zaunders 2006). The present study was aimed to estimate the ability of the soil *Streptomyces griseus* grown at different Baghdad regionson proliferation of lymphocytes by methyl thiazolyl tetrazolium (MTT) assay after treatingwith purified active substance (E1 and E2).

MATERIAL AND METHODS

Samples collection of soil: Samples collected from different region of Baghdad city. One hundred samples were collected from November 2019 up to February 2020. The soil samples were exposed to the air for a week, also pretreated with $CaCO_3$(10:1 soil: $CaCO_3$) and kept at ambient temperature for a week (Abdulhameed 2013).

Isolation of *Streptomyces griseus*from soil: One gram of dried and treated soil samples were suspended in distilled water to get a concentration 1%W/V. The samples were shacking in a shaker incubator at 120 rpm for 30 minutes at room temperature. put on supplemented malt extract yeast extract agar (ISP2), using dextrose as source of Carbone, with addition of Nystatin and Streptomycin 50 µg ml^{-1} each, then the inoculum was spread by a sterile swab to make a

uniform distribution of the suspension on the surface of the media. The inoculated plates were incubated at 28°C for 7 to 14 days (Oskay et al 2004).

Identification of *Streptomyces griseus* isolated from soil: Suspected bacterial isolates of *S. griseus* were primarily identified by microscopic and cultural examinations, then by the biochemical tests for Czapeck Medium, Citrate Utilization, Cellulase, Urease, Catalase And Melanin, final identification.

Fermentation condition: Secondary screening for the production of antimicrobial metabolites was done by the inoculation of 1.5ml of prepared stock suspension cultures into 150 ml of ISP_2 medium using glucose as carbon source with $CaCO_3$ and incubated at 28±1°C, 150 rpm for 7days in a shaking incubator (Khan and Patel 2011, Pallavi et al 2013).

Extraction of the bioactive compound from isolated *S. griseus:* The extraction method to obtain the bioactive compounds from the isolated *S. griseus*was employed according to Pandey et al (1981) method with some modification, Briefly the whole broth from different fermentation media run with about 500 ml ISP2 medium was used to get *Streptomyces griseus* extra and intra cellular production. The pH of the broth was adjusted to 2.0 with dilute sulfuric acid and left at $4^{\circ}C$ for 96 hours. The lysate was filtered through whattman filter paper and the filtrate was transferred to reparatory fennel for extract the secondary metabolites yields with ethyl acetate. The process was repeated many times. All acetate layers were collected and washed with distilled water to get rid of any access acid residues. The aqueous phase was discarded and the combined ethyl acetate layers were evaporated to dryness using rotary evaporator apparatus at 45°C. The residue that yielded was as a dark red powder (Rajeb et al 2021(.

Purification of bioactive compounds: Purification technique for the yielded bioactive compounds by Preparative TLC was involved. The best solvent system gave separated clear spot was the solvent ethyl acetate: methanol: water (10:1.5:1). Application 2ml of crude extract in concentration of 100mg\1ml methanol on the reparative TLC glass plate was done then scrapping for each separated band to be subjected to further analysis. Two major compounds were obtained named as (E1 and E2) which represented the purified components get from the isolated local strain**.**

Lymphocyte proliferation (*in vitro)*: To determine *in vitro,* the immune activity of two active substances (E1 and E2) on lymphocytes; culturing and viable counting was employed

Lymphocytes Culturing and Viable Counting (Rafael and Vaclav, 2000)

- About five milliliters of venous blood were taken from 6 healthy volunteers, their ages in the range of (25-35) year's old, never taken medication at least 10 days ago and each blood sample was transferred into vacuumed tubes containing 0.2% EDTA as anticoagulant with continuous gentle shaking.
- The human peripheral blood was diluted PBS (pH=7.2) in 1:1 ratio.
- About 5 milliliters of the diluted cell suspension was layered onto three milliners of Ficoll-isopaque separation fluid (lymph prep; specific gravity=1.077g/l, placed into vacuumed tubes (10 ml capacity).
- The tubes were centrifuged at 2000 rpm for 30 minutes.
- The mononuclear cells were collected with sterile pasture pipette, transferred into 10ml vacuumed tubes, suspended with 5ml RPMI 1640, and centrifuged for 10minutes at 2000 rpm. The step was repeated twice.
- The isolated lymphocyte cells were collected again and suspended in RPMI-1640 medium supplemented with 10% fetal calf serum, 100 units/ml penicillin, and 100µg/ml streptomycin, then transferred into appropriate tissue culture falcons and incubated for 24 hours at $37^{0}C$ in 5% CO_2 incubator.

Measurement the Proliferative Cultured Lymphocytes by MTT Assay (Freshney 2012)

- About 100µl of the suspended cells was seeded in each of the 96 well microtiter plates, about (10^{5}-10^{6} cell ml^{-1}). The plate was incubated at least for 2 hours in a Co_2incubator.
- Serial concentrations from each purified extract (E1and E2) were prepared from each stock solution (1000 µg ml^{-1}) to get (500, 250, 125, 62.5, 31.25, 15.625, and 7.8125) µg/ml, then sterilized with 0.22 µm Millipore filter.
- About 100 µl from each concentration of the extract was added in triplicate to the lymphocytes seeding plate. Negative control represented by untreated lymphocytes suspended in RPMI medium.
- The plate was incubated in a CO_2 incubator for 24 hours at $37C^{0}$.
- About 50 µl of MTT dye(2mg/ml) was added to all wells, then incubate for further 4 hours.
- The MTT-formazan crystals which formed only by live cells were dissolved with100µl DMSO added to all wells.
- Absorbance at 620 nm was recorded immediately by ELISA reader.
- Viable cell Lymphocytes as a percentage was calculated as follow:
- [Absorbance of the test /Absorbance of negative control]X 100.
- A comparison between the results of both extracts (E1

and E2) at different concentrations was statically calculated to choose the most effective dosages of each extract that may cause lymphocytes proliferation that to be used in further experiment as immune-stimulants.

RESULTS AND DISCUSSION

Samples collection from soil: From 100 samples, only 85 samples gave bacterial growth, these isolate were further purified and subjected to a full identification according to their morphological and cultural characteristics and biochemical tests. From 85 soil sources, have 45 (52%) samples are a species of *Streptomyces*. It showed that from the local *Streptomyces* spp.; only 15 soil isolates (17.6%) were suspected to contain *Streptomyces.griseus*.

Isolation of *Streptomyces griseus* from soils: As shown in Figure 1 and 3, only 15 soil sources which represented 15% of total collected samples were suspected to be the *Streptomycesgriseus* strain with a different morph types and the color of colonies characterized by color ranged from pale yellow to grey yellow, grown on a malt extract yeast extract agar (ISP2), as recommended by Oskay et al 2004) and Kämpfer (2006), and this was in agreement with that described by Saadoun et al (2015).

Identification of *Streptomyces griseus* Isolated from Soils

Cultural characteristics: *Streptomyces griseus* isolates produced diffusible pigment in the surrounding media in accordance with the aerial mycelium color. Soluble pigment was also observed in some isolates. Distinctive color established, in the Bergey's manual of systemic bacteriology (Buchanan and Gibbons 1974) (Table 2).

The biochemical results of *Streptomyces griseus:* The resulting in Table 3 showed the biochemical tests of the isolates from Iraqi's soil.

Extraction of the bioactive antimicrobial metabolites from *Streptomyces griseus*isolate: Each 500ml broth yielded 1.8 grams crude complex as a dark red powder which

Table 3. Biochemical tests results of Streptomyces griseus isolates

Test	Reaction	Result
Czapeck medium	Growth	Positive
Citrate utilization	Deep blue color	Positive
Cellulase	Clear zone	Positive
Urease	No change	Negative
Catalase	No bubbles	Negative

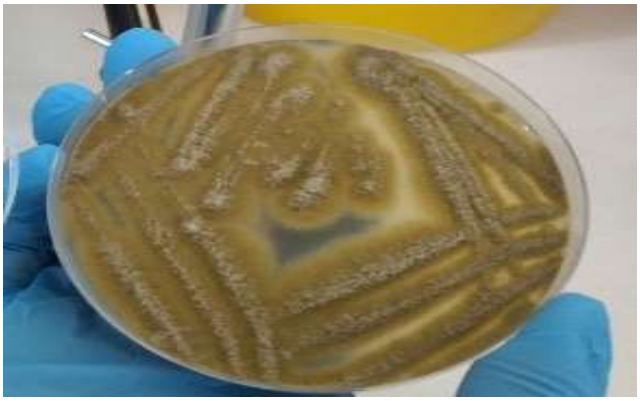

Fig. 1. Local isolate *Streptomyces griseus* distinguished by color on ISP2 at 28c after 7-14 days

Fig. 2. Mycelium surface of four isolate of *Streptomyces griseus* distinguished by color on ISP2 at 28c after 7-14 days

Table 1. *Streptomyces griseus* isolated from soil of local regions at Baghdad city

Locally region	Number of samples collected	Number of isolate give growth	Percentage of growing isolate	Suspected Streptomyces griseus	Suspected Streptomyces sp.
Harthyia (HA)	15	10	11.7	4	7
Jadreia (JA)	25	23	27.2	2	10
ALQadesia (QA)	30	27	31.7	2	13
Karada (KA)	30	25	29.4	7	15
Total	100	85	100	15 (33.3%)	45 (52%)

Table 2. Cultural cha

Colony morphology	Arial mycelium	Mycelium surface	Soluble pigment	Spore surface
Irregular edge	Pale yellow	Yellowish	Yellow	Hairy

represented the bioactive compounds produced by *Streptomyces griseus* isolate extra and intracellularly. The extraction method for obtain the bioactive compounds preform on *Streptomyces griseus* isolate could be intracellular compounds that might be degraded the cell well of the bacteria to achieve high amount the bioactive compounds present inside it (Bekatorou et al 2006). It was suggested that the secondary metabolite production began at 4th day after seed build-up and also at the production level. The pH rose to a maximum of 7.2 and gradually decreased to pH 6.2 as the secondary metabolite production peaked. At 36 hours the dissolved oxygen dropped to zero and the rate of glucose consumption became 0.1% per hour. As in shake flasks, production closely followed glucose utilization. The rate of a production increased. (Khan and Patel 2011, Rajeb et al 2021.

Figure (3) showed the band of resulting compound by using the solvent composed of ethyl acetate: methanol: water(10:1.5:1).

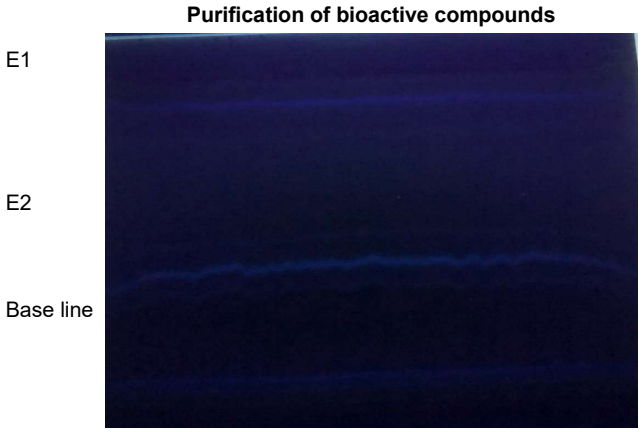

Fig. 3. Preparative TLC Chromatography from Streptomyces griseus crude extract show two layers represented as two compounds obtained

Lymphocyte proliferation (*in vitro)* of purified active substance (E1 and E2): This work was held at Al-Nahrain Biotechnology Center Laboratories. So, the Lymphocyte proliferation was determined using MTT method. Results of the effect of different concentrations of purified active substance (E1 and E2) on normal human lymphocyte proliferation was shown in Figure 4. In this experiment show the different results between E1and E2, so the last one give high proliferation when cultured lymphocytes and determined by MTT assay.

The high concentration 500mg\ml give cell viability (101%) of E1and E2 give 60.9%.

Measurement of proliferative responses of human lymphocytes is a fundamental technique for the assessment of their biological responses to various stimuli. Most simply, this involves measurement of the number of cells present in a culture before and after the addition of a stimulating agent. This unit contains several different prototype protocols to induce proliferation in lymphocytes following exposure to antigens, allogeneic or soluble factors. (Muul et al 2011). The isolation and purification techniques that followed with properties of Fredericamycins that done by Pandey et al (1981) open the way to discovered the physicochemical properties and applications to this material.

The pure material Fredericamycin A which were the major components., slow-moving material (Rf 0.68), that behaves as an indicator which is red in acidic solution and green to blue in basic solution. It is soluble in acetic acid, dimethylsulfoxide, N,N-dimethylformamide and pyridine; partially soluble in acidic methanol, acidic chloroform and acidic ethyl acetate; and insoluble in water, petroleumether and ether. It showed a single spot in various TLC solvent

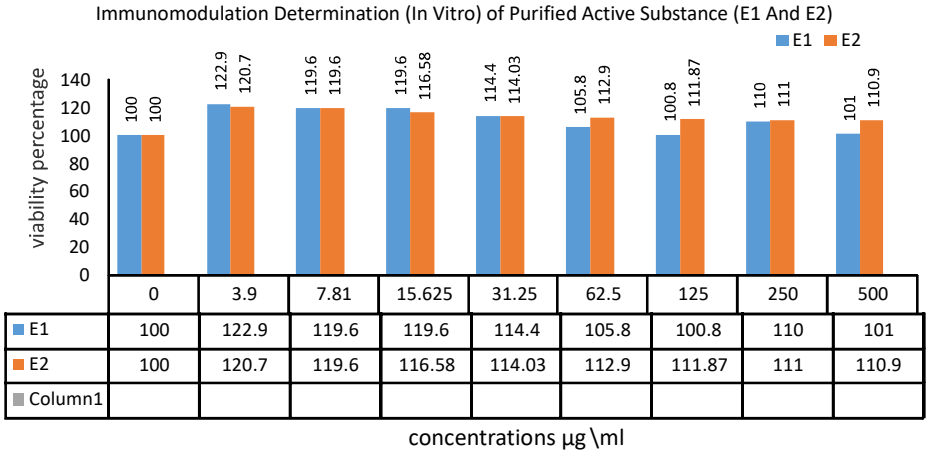

Fig. 4. Measurement the proliferative cultured lymphocytes by MTT assay after treated with purified active substance (E1 and E2)

systems and plates and was homogeneous in HPLC under normal-phase and reverse-phase conditions. Its melting point is > 350°C (dec.). The color change (red->green ->blue) and spectral shift in base indicate the presence of phenolic hydroxyl groups. (Pandey et al 1981). The two minor components, fredericamycin B, a fast moving material with Rf from 0.94 to 0.89 in some researches and fredericamycin C, were thus isolated fredericamycin Cwere not isolated in this study (Pandey et al 1981). The fast moving material with Rf 0.86 was fredericamycin B that named in this study with E1 while the slow-moving material (Rf 0.63) was Fredericamycin A that named E2 Rajeb et al (2021).

REFERENCES

Abdulhameed ZT 2013. The Isolation and Study of Morphological Characterization of *Streptomyces* Isolated from the Soil as a Source of Active Antibiotic. *Colle Bas Educ Rese J.* **12**(3): 77-89.

Al-Rubaye T, Risan MH, Al-Rubaye D and Radi OR 2018b. Identification and In vitro antimicrobial activities of Marine Streptomyces spp. Bacteria from Tigris River Sediments in Baghdad City. *World Journal of Pharmaceutical and Life Sciences* **4**(10): 120-134.

Al-Rubaye TS, Risan MH, Al-Rubaye D and Radi OR 2018a. Characterization of marine *Streptomyces* spp. bacterial isolates from Tigris river sediments in Baghdad city with Lc-ms and 1 HNMR. *Journal of Pharmacognosy and Phytochemistry* **7**(5): 2053-2060.

Al-Rubaye Talib Saleh, Mohsen Hashim Risan and Dalal Al-Rubaye 2020. Gas chromatography-mass- spectroscopy analysis of bioactive compounds from *Streptomyces* spp. isolated from Tigris river sediments in Baghdad city. *Journal of Biotechnology Research Center* 14(1): 63-71.

Amin SM, Risan MH and Abdulmohimin N 2016. Antimicrobial and antioxidant activities of biologically active extract from locally isolated actinomycetes in garmian area. *Journal of Garmian University* **1**(10): 625-639.

Buchanan RE and Gibbons NE 1974. *Bergey's manual of determinative bacteriology*, 7th edn, London. Bergey Taxon; **24**: 377-378.

Kelleher AD and Zaunders JJ 2006. Decimated or missing in action: CD4+ T cells as targets and effectors in the pathogenesis of primary HIV infection. *Current HIV/AIDS Reports* **3**(1): 5-12.

Khan JA and Patel AS 2011. Extraction and purification of antibacterial metabolites from actinomycetes spp. isolated from soil sample. *International Journal of Pharmaceutical Sciences and Research* **3**(10): 63-71.

Krainsky A 1914. Die Aktinomyceten und ihren Bedeutung in der Natur. Zentralbl Bakteriol Parasitenkd Infektionskr *Hyg Abt II (in German)* **41**: 649-688.

Received 12 July, 2021; Accepted 10 November, 2021

Labeda DP 2010. Multilocus sequence analysis of phytopathogenic species of the genus *Streptomyces*. *International Journal of Systematic and Evolutionary Microbiology* **61**(10): 2525.

Muul LM, Heine G, Silvin C, James SP, Candotti F, Radbruch A and Worm M 2011. Measurement of proliferative responses of cultured lymphocytes. *Current Protocols in Immunology*. doi: 10.1002/0471142735.im0710s82.

Oskay M, Tamer UA and Azeri C 2004. Antibacterial activity of some actinomycetes isolated from farming soils of Turkey. *African Journal of Biotechnology* **3**: 441-446.

Pallavi S, Manasa M, Kambar Y, Asha M, Chaithra M, Vivek M and Mallikarjun N 2013. Anti-Staphylococcus aureus and Anti-yeast activity of *Streptomyces* species isolated from rhizosphere soil of Sahyadri Science College, Shivamogga, Karnataka. *Asian Journal of Biomedical and Pharmaceutical Sciences* **3**(24): 7-11.

Pandey RC, Toussaint MW, Stroshane RM, Kalita CC, Aszalos AA, Garretson AL, Wei TT, Byrne KM, Geoghegan RF Jr and White RJ 1981. Fredericamycin A, a new antitumor antibiotic. I. Production, isolation and physicochemical properties. *Journal of Antibiotics* **34**: 1389-1401.

Qasim B and Risan MH 2017. Anti-tumor and Antimicrobial Activity of Antibiotic Produced by *Streptomyces* spp. *World Journal of Pharmaceutical Research* **6**(4): 116-128.

Rafael F and Vaclav V 2000. *Advanced Methods in Cellular Immunology*. CRC-Press LLC.U.S.A. , vol. 3

Rajeb E, Hashim Z and Risan M 2021. Extraction and purification of Fredericamycin A, B from *Streptomyces griseus. Annals of the Romanian Society for Cell Biology* **25**(4): 16971-16978

Risan MH, Amin SM and Abdulmohimin N 2016. Production, partial purification and antitumor properties of bioactive compounds from locally isolated actinomycetes (KH14). *Iraqi Journal of Biotechnology* **15**(3): 51- 64.

Risan MH, Rusul J and Subhi SA 2019. Isolation, characterization and antibacterial activity of a Rare Actinomycete: *Saccharopolyspora* sp. In Iraq. *East African Scholars Journal of Biotechnology and Genetics* **1**(4): 60-49.

Risan MH, Taemor SH, Muhsin AH, Saja M Hafied, Sarah H Ghayyib and Zahraa H Neama 2018. Activity of *Lactobacillus acidophilus, L. Planetarium*, *Streptomyces* and *Saccharomyces cerevisiae* with extracts of date palm and dried shell of pomegranate to reduce aflatoxin M1 in Iraq, *World Journal of Pharmaceutical and Life Sciences* **4**(6): 119-113.

Risan MH, Qasim B, Abdel-jabbar B and Muhsin AH 2017. Identification active compounds of bacteria *Streptomyces* using high-performance liquid chromatography. *World Journal of Pharmaceutical and Life Sciences* **3**(6): 91-97.

Saadoun I, AL-Joubori B and Al-Khoury R 2015. Testing of Production of Inhibitory Bioactive Compounds by Soil *Streptomycetes* as Preliminary Screening Programs in UAE for Anti-Cancer and Anti-Bacterial Drugs. *International Journal of Current Microbiology and Applied Sciences* **4**(3): 446-459.

Vaurnakis JN and Blander RP 2014. Genetic Manipulation on of Antibiotic Producing.2-8 (Complete this reference).

Indian Journal of Ecology (2021) 48(6): 1863-1865

Manuscript Number: 3461
NAAS Rating: 5.79

Effect of Sex, Age and Location on Prevalence of *Brucellosis* among Goats in Baghdad, Iraq

Akram Sattar Gabbar and Sahar Mahdi Hayyawi*

Department of Microbiology,College of Veterinary Medicine, University of Baghdad, Iraq
** E-mail: sahar_1900@yahoo.com*

***Abstract*:** The present study aimed to estimate the prevalence of brucellosis in goat in Alrusafa and Alkarkh by using ELISA and serological test (Rose Bengal plate test) along with estimation of the IgG antibodies titer and interleukin-10 to evaluate these two markers for detection of disease by using the receiver operation characteristics curve. A total of 96 local goats (11 males and 85 females) were chosen randomly. Blood samples were collected from jugular veins of these goats in order to diagnose brucellosis. Prevalence of Brucellosis was significantly high by using ELISA (39.6%) as compared with RBT 33.3%. Highest sensitivity rate was to IL-10 (84.21%) followed by IgG (78.95) and RBT (71.05). The highest specificity rate was detected for IgG (82.76%) followed by RBT (81.03) and IL-10 (74.14). The infection rate of goat was significantly higher in Al-Resafa (48%) as compared with Al-Karhk (35%). The Odds Ratio (OR) was 2.98. Goats in the age of about 25 months recorded the highest infection rate (50%) while goats in age of 12 and 12-24 month recorded 28% and 20% respectively. The effect of sex on the infection rate showed significant difference between females and males.

***Keywords*:** *Brucellosis*, Goats, ELISA, IgG, IL-10

Brucellosis is a highly contagious zoonosis worldwide with economic and public health impacts (Khan et al 2019). Infection with *Brucella* spp. is one of the most important causes of abortion in goats and sheep and also causes severe systemic disease in exposed humans (Tekle et al 2019). Brucellosis in livestock is mainly caused by *B. abortus, B. melitensis, B. suis, B. canis* and *B. ovis*. Among these species, *B. melitensis* and *B. ovis* are the common infections disease in sheep and goats (Rossetti et al 2017). *B. melitensis* of goats is the most pathogenic agent for humans (Primatika et al 2016). The key for the control of the disease in humans is the control infected animals because the mammary gland is a very important source for transmission of *Brucella* (Primatika et al 2016). The goats become persistently infected and can shed the bacteria in their milk throughout their lifetime, healthy asymptomatic carriers are a source of infection, other signs include death of weak offspring, low weaning weight, decreased milk production, orchitis, epididymitis, and reduced fertility (more common in sheep) (Facciola et al 2018). The present study aimed to find out the prevalence of brucellosis in goat in of Baghdad and to study the effect of location, age, and sex.

MATERIAL AND METHODS

Ninety-six goats of different sexes (11 males and 85 females) from two locations in Baghdad were chosen randomly. Ten ml of peripheral blood samples were drawn from the jugular vein of goats and immediately transformed five ml of the blood sample into disposable tubes with clot activator and another five ml of blood sample transformed into disposable tubes without clot activator (contain EDTA) and kept cool. Goat IgG (immunoglobulin G), and Goat (IL-10) CUSABIO (China) were used to determine Immunoglobulin G (IgG) level and IL-10 level according to the protocol and instructions of a manufacturing company.

Statistical analysis: Statistical analysis of data was performed using SAS (Statistical Analysis System - version 9.1) (SAS, 2010). The receiver operating characteristic curve was used to identify the validity of markers as an indicator of infection. The markers were compared according to the area under the curve. The analysis was done by using MedCalc Software. The Kappa statistic was estimated to identify the degree of agreement between Elisa and RB.

RESULTS AND DISCUSSION

The prevalence of Brucellosis in goats in Baghdad city was 39.60 % in goats by ELISA test and 33.3 % by Rose Bengal test. The higher seroprevalence rate of goat brucellosis was in Al-Resafa district (48.0%), while the lower was in Al-Karhk district (35.0%) (Table 1 and 2). The risk of animals infected by brucellosis in the Al-Resafa represented by odds ratio of 2.39 which indicated that the animals in this region are approximately at double risk as compared with animals in the Al-Karhk. The highest sensitivity rate was for IL-10 (84.21%) followed by IgG (78.95%) and RBT (71.05%), while the highest specificity rate was detected for IgG (82.76)

followed by RBT (81.03%) and IL-10 (74.14%). The sensitivity (71.05%) and specificity (81.03) of the RBT was acceptable (Table 3). Al- Naqshabendy et al (2014) recorded the seroprevalence of brucellosis a 39.1% in non-vaccinated ewes in Dohuk and slightly higher than reported in Baghdad city by Salman et al (2014) in goats (34.31%). The reasons for this variation could be due to the variation in breeds, environment, management practices and frequent introduction of new animals without proper serological testing and detection and removal of animals with high incidence of abortions (Hamidullah et al 2009). There are number of factors influencing the susceptibility of animals to brucellosis, including natural resistance, age, level of immunity, nutrition, and environmental stress (Tesfaye et al 2011). Therefore, the prevalence of brucellosis was appeared too high in current study. The Kappa was 0.52 between ELISA and RBT and this value indicate a moderate agreement between the two tests.

The cut-off for IgG was >21.5 mg ml^{-1} which means that any animal have more than this value this could indicate that the animal was infected with sensitivity 78.95% and specificity 82.76% (Table 3). The cut-off for the IL-10 was >2.4 ng ml^{-1}. To identify the best marker (IgG or IL-10) a pairwise comparison of their AUC was done and the resulted showed that the difference between them was not significant. The two markers are useful for detection the brucellosis in goats. Goats in the age of ≥ 25 months recorded the highest infection rate (50%) (Odds ratio= 4.14 P<0.01), while goats in age of 12-24 month recorded (28%) (odds Ratio 1.60 P=0.54) and age of >12 recorded 20% (Table 4.8). Rahman et al (2011a, b) recorded that infection in age >24 months was 18.18% and was higher than younger animals. Junaidu et al (2010) stated that a higher infection was detected at age of 13-24 months (9.42%) and Negash et al (2012) reported that the higher infection (10.19%) at age of (1-2) year month. These differences may be due to the difference in the number of animals, age groups, breed, method of detection, and different countries.

The percent of infected female and male goats were 56.5 and 36.4 6 respectively with significant higher infected female compared to infected male. The total of 85 female goats sera were tested, 48 (56.5%) were positive**,** while on male goat, 11 sera were tested and 36.4% were positive with higher significant differences in females compared to males (Table 5). The odds ratio was 1.27 which means that females have a risk about one and quarter compared with male. Mohammed et al (2010) recorded that the infection in female and male kids was 55 and 0.0%, respectively and Hawari (2012) found that the infection in the female goat was higher

Table 1. Prevalence of *Brucella* in the goats using ELISA and Rose Bengal test

Prevalence	Total No	No. positive	Percent
ELISA	96	38	39.6
Rose Bengal Test (RBT)	96	32	33.3
Value	---	---	4.23
P-value			<0.01

Table 3. Sensitivity and specificity of RBT as compared with ELISA (IgG, and IL-10)

Test	Sensitivity	Specificity	Cutoff point
RBT	71.05	81.03	-
IgG	78.95	82.76	>21.5 mg ml^{-1}
IL-10	84.21	74.14	>2.4 ng ml^{-1}

Table 2. Comparison of the infection rate between two regions

Region	No. infected goats	No. non-infected goats	Odds ratio	95 per cent CI	P-value
Karhk	14 (28.6%)	35 (71.4%)	---	---	<0.05
Resafa	23 (48.9%)	24 (51.1%)	2.39	5.56-1.03	
X^2	4.20				
P-value		<0.05			

95% CI= 95% confidence interval

Table 4. Comparison the infection rate according to the age

Age/Month	Infected	Non-infected	Odds ratio	95% CI	P-value
12-24	5 (20.0%)	20 (80.0%)	-		
<12	4 (28.6%)	10 (71.4%)	1.60	0.35-7.30	0.54
≥25	29 (50.9%)	28 (49.1%)	4.14	1.36-12.55	<0.01
Chi square	7.75				
P-value	<0.01				

Table 5. Comparison the infection rate according to the sex

Sex	No. infected	Non-infected	Odds ratio	95% CI	P-value
Male	4 (36.4%)	7 (63.6%)	--		
Female	48 (56.5%)	37 (43.5%)	1.27	0.42-3.80	0.01
Chi-square	6.80				
P-value	0.01				

than that of male goat 19.7 and 17.4% respectively. Rahman et al (2012a) observed that the seroprevalence rates of female goat was higher than male goat (3.84% and 2.00%, respectively). The reason for this higher in females than males could be attributed to that the male infection resulting in clinical disease present with observation signs of epididymitis and scrotal hardening to the farmer and the clinicians leading to the culling of more infected male than females, in which the only noticeable signs of the disease may be obtain. In conclusion: *Brucella* infection in goat is relatively high in Baghdad City. ELISA (IgG and IL-10) is much better than Rose Bengal Test for diagnosis of disease.

REFERENCES

Al-Izzi SA and Barhoom SS 1988. Prevalence of brucellosis among sheep and goat in Baghdad, Iraq. *Iraqi Journal of Veterinary Sciences* **1**(1-2): 108-115.

Al-Naqshabendy AA, Ibrahiem AA and Azeez OH 2014. Effect of Brucella melitensis on the serum lipids profiles in ewes. *Assiut Veterinary Medical Journal* **60**(142):156-159.

Brisibe F, Nawathe DR and Bot CJ 1996. Sheep and goat brucellosis in Borno and Yobe States of arid northeastern Nigeria. *Small Ruminant Research* **20**(1): 83-88.

Facciolà A, Palamara MA, D'Andrea G, Marano F, Magliarditi D, Puglisi G and Visalli G 2018. Brucellosis is a public health problem in southern Italy: Burden and epidemiological trend of human and animal disease. *Journal of Infection and Public Health* **11**(6): 861-866.

Hamidullah M, Khan R and Khan I 2009. Seroprevalence of brucellosis in animals in district Kohat NWFP and comparison of two serological tests. *Pakistan Veterinary Journal* **61**(4): 242-243.

Hawari A 2012. Epidemiological studies seroprevalance and some risk factors of brucellosis in sheep and goats in the south province of (West Bank). *Jordan Asian Journal of Animal and Veterinary Advances* **7**(2): 535-539.

Junaidu AU, Daneji AI, Salihu MD, Magaji AA, Tambuwal FM, Abubakar MB and Nawawi H 2010. Sero Prevalence of brucellosis in goat in Sokoto, Nigeria. *Research Journal of Biological Sciences* **2**(4): 275-277.

Khan AU, Shell WS, Melzer F, Sayour AE, Ramadan ES, Elschner MC, Moawad AA, Roesler U, Neubauer H and El-Adawy H 2019. Identification, genotyping and antimicrobial susceptibility testing of *Brucella* spp. isolated from livestock in Egypt. *Microorganisms* **2**(*7*):1-19.

Mohmmed BA, Hassan SD, Hussain KJ and Esmaeel SA 2010. Detection of anti *Brucella* antibodies in lambs and goat kids using rose bengal test and indirect ELISA in Gugjeli-Ninavah province, Iraq. Iraqi Journal of Identification, Genotyping and Antimicrobial Susceptibility Testing of *Brucella* spp. Isolated from Livestock in Egypt. *Veterinary Sciences* **24**(1): 23-26.

Negash E, Shimelis S and Beyene D 2012. Seroprevalence of small ruminant brucellosis and its public health awareness in selected sites of Dire Dawa region, Eastern Ethiopia. *Journal of Veterinary Medicine and Animal Health* **4**(4): 61-66.

Primatika RA, Nugroho WS and Septana AI 2016. Survey of brucellosis in goats using Rose Bengal Test (RBT) and Complement Fixation Test (CFT) methods in Gunungkidul district, special region of Yogyakarta, Indonesia. In *AIP Conference Proceedings* (Vol. 1755, No. 1, p. 040006). AIP Publishing LLC.

Rahman MS, Her M, Kim J, Kang S, Lee K, Uddin MJ, Chakrabartty A and Jung SC 2012a. Brucellosis among ruminants in some districts of Bangladesh using four conventional serological assays. *African Journal of Microbiology Research* **6**(22): 4775-4781.

Rahman MS, Mithu S, Islam MT, Uddin MJ, Sarker RR, Sarker MAS and Akhter L 2012b. Prevalence of *brucellosis* in Black Bengal goats in Bangladesh. *Bangladesh Journal of Veterinary Medicine* **10**(1&2): 51-56.

Rossetti AO, Tovar QDF, Juan E, Novy J, White RD, Ben-Hamouda N and Rabinstein AA 2017. Electroencephalography predicts poor and good outcomes after cardiac arrest: A two-center study. *Critical Care Medicine* **45**(7): e674-e682.

Salman SS, Al-Samarrae IA and Mahmood AK 2014. Serological survey of Brucellosis in some areas of Baghdad city. *Al-Anbar Journal of Veterinary Sciences* **7**(1): 6-10.

SAS 2010. SAS/STAT Users Guide for Personal Computer. Release 9.13.SAS Institute, Inc., Cary, N.C., USA.

Shuterland SS and Mackenzie RM 1983. Applied serology in the latter stages of the eradication of bovine brucellosis. *Australian Veterinary Journal* **60**: 240–242.

Tekle BF, Kebebe KK, Etana B, Woldie M and Feyissa TR 2019. Disrespect and abuse during childbirth in Western Ethiopia: Should women continue to tolerate? *PloS One* **14**(6): e0217126.

Tesfaye G, Tsegaye W, Chanie M and Abinet F 2011. Seroprevalence and associated risk factors of bovine brucellosis in Addis Ababa dairy farms. *Tropical Animal Health and Production* **43**: 1001-1005.

Received 12 July, 2021; Accepted 12 November, 2021

Indian Journal of Ecology (2021) 48(6): 1866-1870

Manuscript Number: 3470
NAAS Rating: 5.79

Evaluation of Power Tiller Operated Vertical Rotary Plough for Tillage

Chandrashekar, H.K. Venkata Reddy and Jayant Singh[1]

Department of Farm Machinery and Power Engineering, Kelappaji College of Agricultural Engineering & Technology, Tavanur-679 573, India
[1]Department of Farm Machinery and Power Engineering GBPUAT Pantnagar-2631 45 India
E-mail: chandrurc001@gmail.com

***Abstract*:** The small size fields with uneven topography, lack of skilled labour, poor repair and maintenance facilities, low purchasing capacity of farming community and non-availability of improved farm implements and machines are some of the main reasons for low level of mechanization in the hilly region of the state. In hilly areas to promote farm mechanization a new type of rotary plough is designed. Power from main engine shaft is transmitted to the rotary blades by using bevel and spur gear transmission system. The maximum actual field capacity of vertical rotary plough (0.097 ha h^{-1}) was obtained when the rotor speed was 350 rpm, with the forward speed 2 km h^{-1} and the soil moisture content of at 14 %. The highest field efficiency of vertical rotary plough was 88.09 % when the soil moisture content was 14 % with a rotor speed 350 rpm and 2 km h^{-1} forward speed. The minimum fuel consumption of vertical rotary plough was 0.84 l h^{-1} when the rotary plough operated at 350 rpm of rotor speed with 1.5 km h^{-1} forward speed of operation and soil moisture content was 14 %. The maximum energy per unit area of vertical rotary plough 1298.71 MJ ha^{-1} was obtained when the machine is operated at 2 km h^{-1} forward speed, 12 % soil moisture content with 550 rpm of rotor speed.

Keywords: Rotor speed, Forward speed, Rotary plough, Depth of operation

In Uttarakhand state, about 70 % population is living in rural areas and depends directly or indirectly on agriculture. However, the degree of farm mechanization, mainly in hills is very poor with respect to mechanical power, efficient tools and implements used by the farmers. The undulating and sloppy geography, small size fields with uneven topography, lack of skilled labour, poor repair and maintenance facilities, low purchasing capacity of farming community and unavailability of enhanced farm tools and machines are some of the main reasons for low level of mechanization in the hilly region of the state. There is a need to fulfil the small and marginal farmer's requirement by developing the required size of power tiller with matching implements. About 78 % of the farmers possess an area less than 2 ha with poor resources at their command, especially in the dry-land regions. Tillage is the most significant operation for crop production. The purpose of tillage is to create favourable environment for seed placement and plant development (Jakasania et al 2017). It has always been one of the larger power consuming operations on a farm. This operation includes breaking the soil surface up to a certain depth and to loosen the soil mass using equipment's like mould board plough, disc plough, disc harrow, cultivators and it requires multiple operations. These multiple operations consist of primary and secondary tillage. Primary tillage results in preparing suitable seed bed and destroy weeds grown on the surface and improves the soil physical condition followed by secondary tillage, which improves soil pulverization, conserves the moisture, cuts the crop residue and mixes vegetative matter with top soil. In case of the sliding action tillage implements, frictional resistance is high, whereas, in rotary tillage implements it is low enough (Jakasania et al 2017). Vertical rotary plough gives a better quality of soil tilth than horizontal axis rotary plough. Soil resistance in vertical axis rotary plough is less than horizontal axis rotary plough and soil disturbed in vertical axis rotary plough is much more than horizontal. Rotary plough saves 30-35 % of time and 20-25% operation cost as compared to tillage by cultivator. It gives a better quality of tilth by 25-30 % than the tillage by cultivator (Kadu et al 2015).

Some pull type light weight power tillers also exist in the country to pull plough, harrows and cultivators (Narang et al 2005). In Tarai, foot hills and valley region, some farmers have hand tractors/power tillers to field operation. There is a necessity to develop gender friendly small tools and implements for tillage, sowing, intercultural, harvesting and threshing operations, so that the requirement of about 71% marginal farmers could be met. Farmers can execute tillage operation in their personal fields as well as on custom hiring basis (Singh, 2014).In case of terraces having high vertical interval, lightweight power tiller (80-100 kg) with appropriate corresponding equipment can be used widely for doing

various agricultural operations and can be lifted with the assistance of 2-3 men from one terrace to another terrace (Mandal et al 2016). So it is felt necessary to develop a lightweight power tiller fitted with 5-10 hp engines with a gearbox having minimum two forward speeds.

MATERIAL AND METHODS

The development work was carried at Department of Farm Machinery and Power Engineering, College of Technology, Pantnagar, Uttarkand. The field trials were carried at research farm.

Construction details of vertical rotary plough: The frame was made of (50 × 50 × 5 mm) mild steel angle iron section of 600 mm length and 200 mm width to accommodate the gearbox and cutting unit and flats of mild steel was also used for the supporting the main frame. Plates of mild steel have dimensions of 500 × 190 mm were used for fitting the gearbox. In this experiment the straight knife blades were used for ploughing operation. The high carbon steel was used for making the blades. The blades are attached to the rotary shaft by means of nuts and bolts. The length, width and thickness of blade were 200, 30 and 5 mm respectively. The blade is having 10 mm diameter of holes for attachment to the rotor shaft with the nut, bolts and washer. In this experiment the single cylinder, four stroke diesel engine, recoil start of 325 cc (3.73 kW) with side valve and the air-cooled engine was used as a prime mover for the rotary plough. The hand operated throttle lever was provided for regulatory the speed of the machine during tillage operation and was attached to right-hand side of the handle. A gauge wheel which is connected to the back side of the frame for the adjustment of depth of operation which is having diameter of 152.4 mm was utilized for the ploughing operation. The gauge wheel was connected to the frame with the support of nuts and bolts. The depth of operation can be adjusted by raising and lowering gauge wheel on the frame. The gear-box connected horizontally to the engine through the help of flat frame. The power, which is produced in the engine, was transmitted to the rotor with the help of the bevel gear arrangement. The rotary wheels were rotated through the help of power transmission from the engine.

Bulk density of soil: The bulk density of soil was determined by using core cutter method. For determining the bulk density of the soil, the soil samples were taken randomly from the experimental plot with the help of core sampler having 12.7 and 9.7 cm height and diameter respectively. The bulk density was determined previously and afterward operation of rotary plough according to procedure mentioned in IS: 2720 (P: 29): 1975.

Moisture content of soil: The soil moisture content was determined by hot air oven method. Soil samples were collected randomly from experimental plot and the known weight of soil sample was kept in the hot air oven at a temperature of 105^{0}C for 24 hours. The water content of soil sample was calculated according to procedure mention in IS: 2720 (P 2) 1973.

Cone index: Cone index is an indication of soil strength and is expressed as force per square centimetre required for

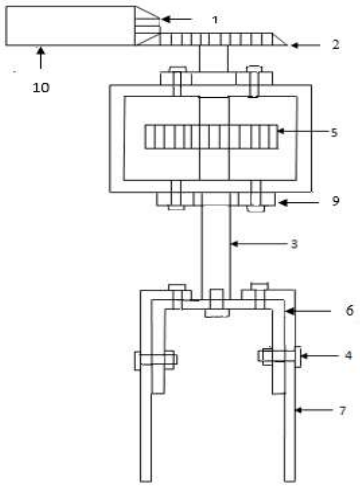

Description		
S. N0	Parts Name	Specification
1	Bevel pinion	Teeth = 10
2	Bevel crown	Teeth = 40
3	Shaft	Dia = 25 mm
4	Bolt	Dia = 10 mm
5	Spur gear	Teeth = 39
6	Flange	Dia = 260mm
7	Blade	200*30*5mm
8	Gearbox	180*100 mm
9	Bearing block	10 mm
10	Main shaft	Dia = 40

Fig. 1. Side view of transmission system of rotary plough

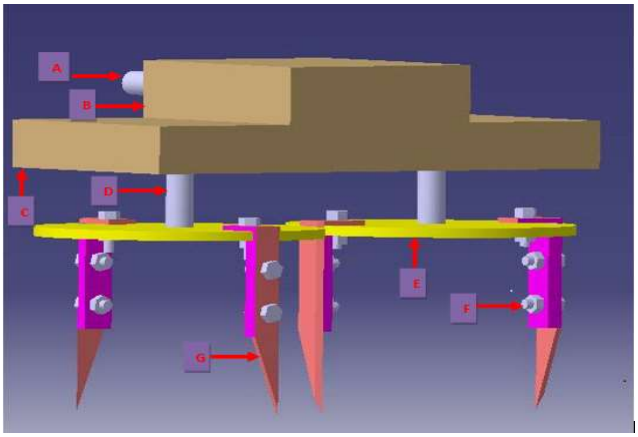

Fig. 2. Isometric view of vertical rotary plough

Table 1. Specification of vertical rotary plough

Specification	Value
Working width	550 mm
No. of blades	2 per rotor
Depth of ploughing	9 cm
Rotor speed	300-900 rpm
Power transmission	Sliding mesh gearbox
Material of blade	High carbon steel
Total weight	120 kg
No. of rotor	2

penetrating into the soil. Cone index was measured with the assistance of cone penetrometer for a different depth of 3 to 10 cm range. The cone index was determined by following equation (Bist 2017).

Theoretical field capacity: It is the amount of field coverage that would be obtained if the machine were performing its function 100 % of the time at the rated forward speed and always covered 100 % of its rated width. The theoretical field capacity was determined by following equation (Bainer et al 1978).

RESULTS AND DISCUSSION

Performance evaluation of vertical rotary plough was done at moisture content,12 and 14 %, at 3 forward speed1.5, 1.75 and 2 km h^{-1} and 3 rotor speeds350, 450 and 550 rpm respectively. Bulk density, cone index, actual field capacity, field efficiency, fuel consumption, clod mean weight diameter and energy requirement were estimated.

Bulk Density: The average the bulk density of soil before operation was 1.38 g cc^{-1}. It was observed that, the bulk density of soil after the operation varied from 1.13 to 1.31 g cc^{-1} with different forward speed, rotor speed and moisture content. The maximum bulk density of soil after operation 1.31 g cc^{-1} was at a forwarded speed 1.5 km h^{-1} with rotor speed 350 rpm at 12 % moisture content while minimum bulk density of soil after operation 1.13 g cc^{-1} was at a forward speed of 2 km h^{-1} with rotor speed 550 rpm and 14 % moisture content respectively.

Cone index: The average cone index of soil before the operation was 1.53 kg cm^{-2}after operation varied from 1.22 to 1.42 kg cm^{-2} was recorded with different forward speed, rotor speed and moisture content.

Actual field capacity: The actual field capacity of the rotary plough was varied from 0.053 to 0.096 ha h^{-1} with different forward speeds, rotor speeds and moisture contents. The maximum actual field capacity 0.096 ha h^{-1} was recorded at a forward speed 2 km h^{-1} with rotor speed 350 rpm at 14 % moisture content while minimum actual field capacity 0.053 ha h^{-1} was at a forward speed 1.5 km h^{-1} with rotor speed 550 rpm and 12 % moisture content respectively.

Field efficiency: The field efficiency of rotary plough was varied from 64.72 to 88.09 % with different forward speed, rotor speed and moisture content. The maximum field efficiency of rotary plough 88.09 % was at forward speed 2 km h^{-1} with 350 rpm of rotor speed and 14 % moisture content while minimum field efficiency 64.72 % was at forward speed 1.5 km h^{-1} with 550 rpm of rotor speed and 12 % of moisture content respectively. It was observed that, the actual field capacity decreased from 88.09 to 64.72 % as the rotor speed increases from 350 to 550 rpm due to increases in depth of operation from 5.1 to 9.5 cm with 12 and 14 % respectively.

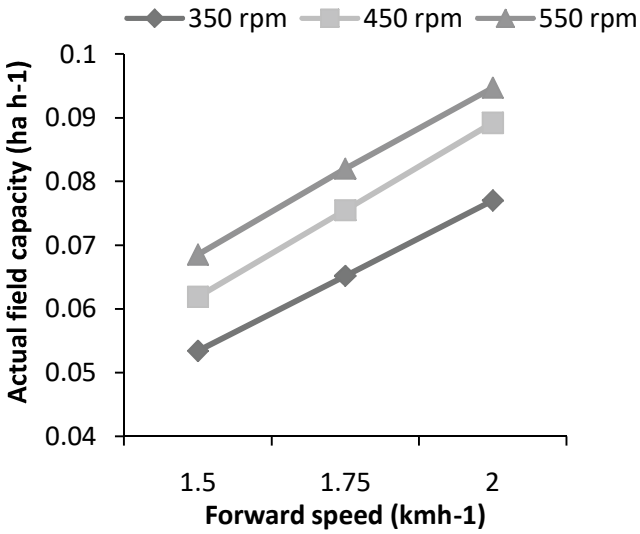

Fig. 3. Effect of forward and rotor speed on actual field capacity at 12% moisture content

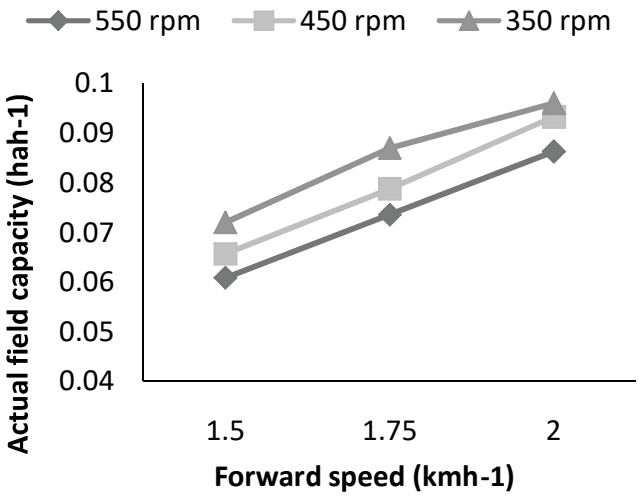

Fig. 4. Effect of forward and rotor speed on actual field capacity at 14% moisture content

Fuel consumption: The average fuel consumption of rotary plough varied from 0.84 to 1.4 l h^{-1} with different forward speed, rotor speed and moisture content. The maximum fuel consumption of rotary plough 1.4 l h^{-1} was observed at 2 km h^{-1} forward speed with 550 rpm of rotor speed and 12 % of moisture content while minimum fuel consumption of rotary plough 0.84 l h^{-1} was recorded at 1.5 km h^{-1} forward speed with 350 rpm of rotor speed and 14 % of moisture content respectively.

Wheel slip: The average wheel slip of rotary plough was varied from 7.25 to 11.50 % with different forward speed, rotor speed and moisture content. The maximum wheel slip of

rotary plough (11.50 %) was recorded at a forward speed 2 km h^{-1} with rotor speed 550 rpm at 14 % moisture while minimum wheel slip of rotary plough was 7.25 % at a forward speed 1.5 km h^{-1} with rotor speed 350 rpm at 12 % moisture content respectively.

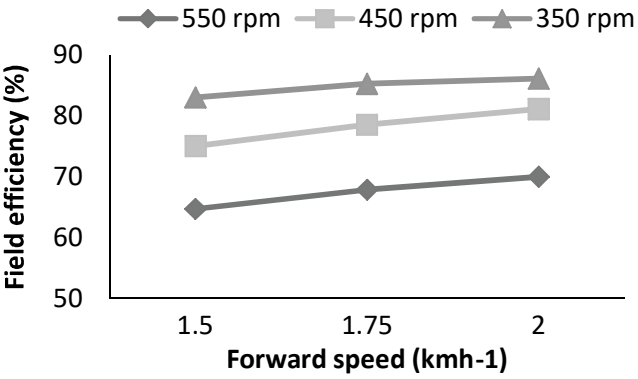

Fig. 5. Effect of forward speed and rotor speed on field efficiency at 12% of moisture content

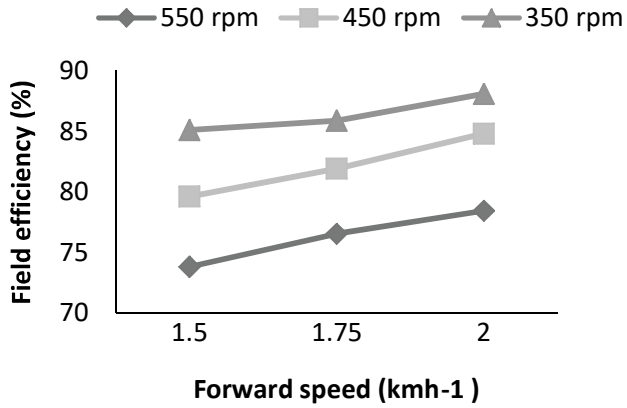

Fig. 6. Effect of forward speed and rotor speed on field efficiency at 14% of moisture content

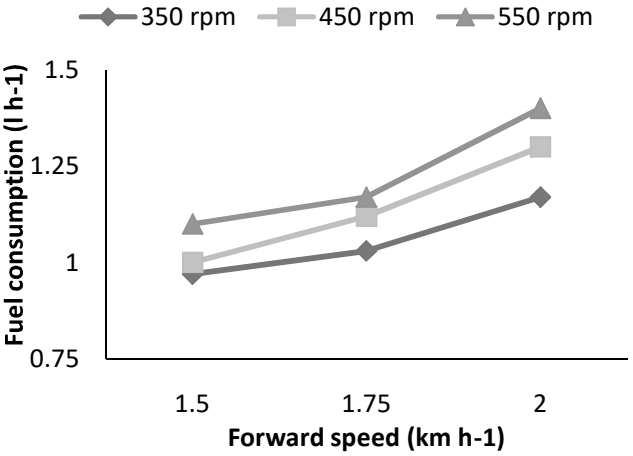

Fig. 7. Effect of forward and rotor speed on fuel consumption at 12 % of moisture content

Clod mean weight diameter: The clod mean weight diameter of soil was varied from 4.1 to 5.6 mm with different forward speed, rotor speed and moisture content. The maximum clod mean weight diameter of soil 5.6 mm was at a forward speed 1.5 km h^{-1} with rotor speed 350 rpm at 12 % moisture content while minimum clod mean weight diameter of soil 4.1 mm was at a forward speed 2 km h^{-1} with rotor speed 550 rpm at 14 % moisture respectively.

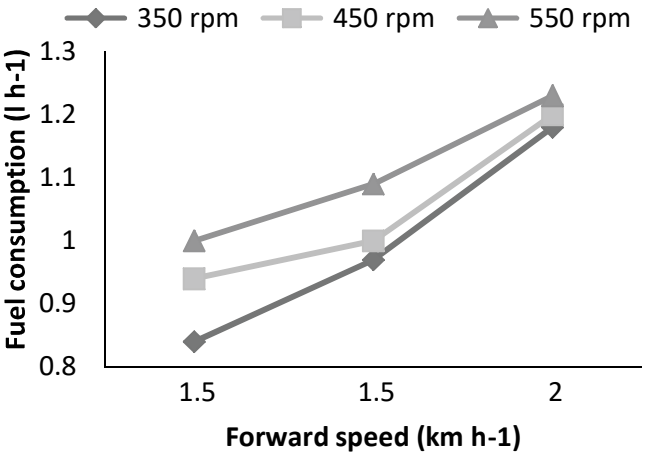

Fig. 8. Effect of forward and rotor speed on fuel consumption at 14% of moisture content

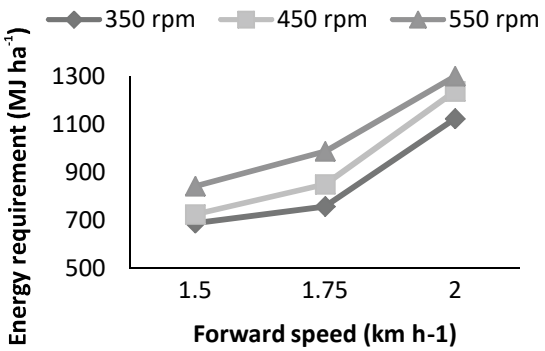

Fig. 9. Effect of forward and rotor speed on energy requirement of operation at 12% moisture content

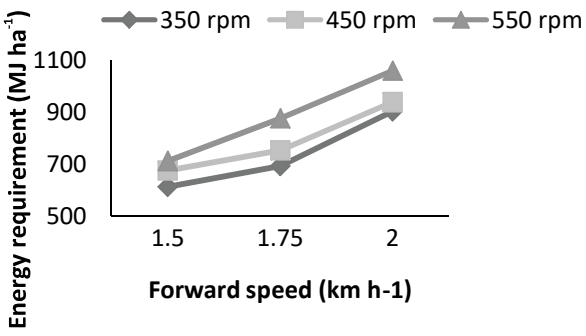

Fig. 10. Effect of forward and rotor speed on energy requirement of operation at 14% moisture content

Energy requirement: The total energy requirement of rotary plough was varied from 612.5 to 1298.71 MJ ha^{-1} at different forward speed, rotor speed and moisture content. A maximum energy requirement of rotary plough 1298.71 MJ ha^{-1} was observed at 2 km h^{-1} forward speed with 550 rpm of rotor speed and 12 % of moisture content while minimum energy requirement of rotary plough 612.5 MJ ha^{-1} was observed at 1.5 km h^{-1} forward speed with 350 rpm of rotor speed and 14 % of moisture content respectively.

CONCLUSION

In all field trials as the moisture content increases, the bulk density, cone index, clod mean weight diameter, fuel consumption, energy requirement per unit area and total cost of operation reduces and the actual field capacity, field efficiency, wheel slip, increases with respect to moisture content. The maximum field capacity, field efficiency and energy requirement was obtained at high rpm and forward speed. The minimum fuel consumption was obtained at low rpm at low forward speed.

REFERENCES

Bist VS 2017. *Design and Development of Rotary Plough for Hills*. Master Dissertation, Govind Ballabha Pant University of Agriculture and Technology Pantnagar, India.

Dange AR, Thakare SK and Rao IB 2011. Cutting energy and force as required for Pigeon pea stems. *Journal of Agricultural Technology* **7**(6): 1485-1493.

Kepner RA, Bainer R and Barger EL 1978. *Principles of Farm Machinery*. CBS Publishers & Distributors, New Delhi,p155.

Kumar S, Mishra BP, Patel SK and Dave AK 2014. Design and development of a power tiller operated seed cum-fertilizer-drill machine. *African Journal of Agricultural Research* **9**(51): 3776-3781.

IS: 2720 [P: 2]: 1973. Methods of test for soil. Determination of water content, Bureau of Indian Standards, New Delhi.

IS: 2720 [P: 29]: 1975. *Methods of test for soil. Determination of dry density of soils in-place by the core – cutter,* Bureau of Indian Standards, New Delhi.

Jakasania RG, Vadher AL and Kathiria RK 2017. Performance Evaluation of Vertical Rotary Plough. *Journal of Scientific Research and Reports* **13**(6): 1-7.

Kadu LS, Kadam GB, Jadhav KP, Gawade VS, Garje A and Gosavi A 2015. Design, development and operation of 3.5 HP power tiller. *International Journal of Recent Research in Civil and Mechanical Engineering* **2**(1): 149-154.

Kamboj P 2012. Study of farm machinery services provided by selected cooperative societies. *Agricultural Engineering International: CIGR Journal* **14**(4): 123-133.

Makange N R and Tiwari V K 2015. Effect of horizontal and vertical axis rotavators on soil physical properties and energy requirement. *Trends in Biosciences* **8**(12): 3225-3234.

Mandal S K, Bhattacharyya B and Mukherjee S 2015. Design of rotary tiller's blade using Specific Work Method (SWM). *Journal of Applied Mechanical Engineering* **4**(3): 01-06.

Mandal SK, Maity A and Prasad AK 2016. Performance evaluation of a lightweight power tiller. *Agriculture for Sustainable Development* **3**(4): 126-139.

Narang S and Tiwari PS 2005. Performance studies on selected light weight power tillers. *Journal of Agricultural Engineering* **42**(3): 50-56.

Niyamapa T and Chertkiattipol S 2010. Development of blades for rotary tiller for use in Thai soils. *Journal of Food, Agriculture & Environment* **8**(3&4): 1336-1344.

Potekar JM and Tekale DD 2010. Comparative performance of tractor drawn implements tillage system with rotavator tillage system. *Karnataka Journal of Agricultural Sciences* **17**(1): 76-80.

Singh S 2014. Farm mechanization in hills of Uttarakhand, India: A review. *Agriculture for Sustainable Development* **2**(1): 65-70.

Received 18 June, 2021; Accepted 22 November, 2021

Indian Journal of Ecology (2021) 48(6): 1871-1875

Manuscript Number: 3463
NAAS Rating: 5.79

Development of Prototype Air Water Generator to Condense Water from Atmospheric Moisture

M. Subash Sundar, Aminul Islam[1]* and Yellamanda Reddy[2]

Department of Applied Engineering, Vignan's Foundation for Science, Technology and Research (Deemed to be University), Vadlamudi-522 213, India
[1]School of Agriculture and Allied Sciences, The Neotia University, Sarisha-743 368, India
[2]Accion Fraterna Ecology Centre, Anantapur-515 002, India
**E-mail: aminul.ubkv@gmail.com*

Abstract: To solve the issue of water scarcity, other than ground water and surface water resources alternative is the use of atmospheric water which is equivalent to 6 times of water present in all rivers on earth. This manuscript deals with design and testing of atmospheric water harvesting device i.e. Air Water Generator (AWG) used to condense water from the abundant atmospheric moisture. This system is based on Thermo Electric Cooler (TEC) or Peltier principle with the help of 12 volts Peltier modules, 110 cubic feet per minute DC brushless fan, heat sinks. This design creates an environment which is capable of condensing atmospheric moisture, but the water productivity from the device is not satisfactory due to very less humidity. Although the design is able to decrease the ambient temperature up to 20°C and able to condense water if the inlet ambient temperature is 25°C and the relative humidity is above 50%. The proposed system is a small step towards the water scarcity in the Anantapur district but the prototype should be run test once in the high humid conditions.

Keywords: Atmospheric water harvesting, Air Water Generator (AWG), Thermo Electric Cooler (TEC), Peltier's, Humidity

To prevent the looming water crisis, certain measures like improving freshwater generation technologies should be adopted, but it should not only limit to water conservation and reducing pollutants entering the water system. Due to lack of abundant traditional water resources like river water and even fog in the Anantapur district, other possibility to solve this issue is dew (water vapour) which is captured from atmosphere. Nandal et al (2020) reported that the water quality of freshwater bodies is rapidly declining. The atmosphere nearly consists of 12.900 km^3 of freshwater which is having 98% in the form of water vapour and 2% in the form of clouds which is equivalent to 6 times of water in all rivers on earth. Sharan et al (2011) reported that world's largest dew collector in Gujarat yielded about 6545 L in 2007 on an average of 7.7 mm $night^{-1}$ which is 42% lower yield than 1 m^2 dew condensers due to folds in the plastic foil decreasing radiative cooling (Xi et al 2007) before construction of it preliminary studies conducted by using four dew condensers having surface area of 1 m^2 collected 12.6 mm/night. In 2016, conducted studies on different desiccants like silica gel, activated alumina, molecular sieve 13x in Solar Glass Desiccant Box Type System (SGDBS) (Kumar and Yadav 2016) and was 60, 20 and 35 ml/kg/day, respectively. Renyuan Li et al (2018) reported that each gram of copper chloride ($CuCl_2$) able to harvest 0.21g water even at lower RH of 20%. Rahbar and Esfahan (2012) explored the new type of water extraction device using peltiers. Jradi et al (2012) reported that using five peltiers length of 1.2 m integrated with photovoltaic system for fresh water production able to condense 10 L day^{-1}. Muñoz-García et al (2013) developed a prototype for water harvesting younger plants by using peltier modules powered by photovoltaic cell and came to conclusions that best period to collect atmospheric water is between 5 – 8 AM and water condensation is not practical for if relative humidity is less than 20 %. Shanshan Liu et al (2017) designed a potable water generator reported that amount of generated water and condensation rate increased with the RH rose. Joshi et al (2016) investigated experiments on moisture condensing parameters like air flow rate, electric current and humidity on prototype based on thermo electric cooler consisting 10 peltiers. Runze et al (2020) reported that started an experimental prototype to meet the minimum requirement of drinking water by WHO i.e., 2.5 L day^{-1} by using 4 peltier modules, 5.38 (m^3/min) brushless DC fan able to collect water of 14.6 L day^{-1} this is very satisfactory. Farshid Bagheri (2018) reported that water yield increases by simultaneous increase of water content or dew point temperature. Anbarasu and Pavithra (2011) reported that vapour compression refrigeration system is more effective than the peltier system but the system is very costlier, creates a lot of sound and it is not portable. The above literature on peltier based atmospheric water harvesting reveals the fact that system is very effective in water production and it is portable. The objective of the current study was done to design and test

peltier based Atmospheric water harvesting device to harvest the water during high humid conditions and also with less cost than available air water generators available in the market.

MATERIAL AND METHODS

Study area: The present experiment is design and development of an air water generator based on peltiers and tested at Accion Fraterna Ecology Centre, Anantapur (Andhra Pradesh) which is located at 14º41'N and 77º35'E. It has an average elevation of 351 meters above mean sea level (MSL). The long period average (LPA) rainfall of Anantapur district is 570 mm and during the year 2014 and 2017 received only 375.2 mm and 284.5 mm, respectively. The average annual humidity is 75%. Anantapur district is dry farming region and being a rain shadow region and does not receive needed rainfall for irrigation in both North West and South East monsoons.

Design and development of peltier based atmospheric water harvesting device: The atmospheric water harvesting device was developed using 3 units of peltier module TEC1-12706 12 V, 2 units of brushless DC cooling fan, 3 units of fan cooled heat sinks and 12 V DC power suppliers. The components of Air Water Generator and their specifications are mentioned in Table 1.

Development of AWG prototype: During the past decades, thermoelectric (TE) technology has drawn attention around the world. TECs take use of Peltier effect to produce temperature difference when direct current (DC) is applied. Without moving parts, refrigerant and emission gases, TECs are quiet, reliable and environmental-friendly. The DC supplier of 12 V, 30 A and it converts the alternate current into direct current. It converts AC input 110/220 V into DC output 12 V - 30 A. It consists of total 9 terminals i.e. three positive terminals, three negative terminals, one ground, one live and one neutral terminal. Brushless cooling fan also run with 12 V DC supply and used for sucking maximum air flow into the system over the condensing aluminum plate and is able to suck max air flow rate up to 110 cubic feet per minute. Here three units of basic thermoelectric (Peltier) plate TEC – 12706 4 x 4 cm were used. The description 12706 represents it is operated using 12 V and 6 A. The fan cooled heat sinks have four pins i.e., black (negative), yellow, blue and green in which other than black was acts as speed regulators. These were placed over the other side of the peltier i.e. hot side to dissipate maximum heat from the peltier to the outside. The housing of the prototype with size of 50 x 35 x 50 cm is made up of Mild steel MS -216 with thickness of 1 mm and prototype was fully covered with Styrofoam sheets to avoid heat transfer from outside to inside of the system. The experimental setup of the prototype is fully completed by supplying electrical connection to the prototype. The two DC brushless cooling fans were given parallel connection i.e., connecting two positive wires (red) and two negative wires (black) and directly connected to the DC supplier. Similarly, three peltiers were given parallel connection and directly connected to the DC supplier. At last AC supply is given to the DC supplier. Then the temperature sensor is placed at the condensing plate to record the condensing surface temperature. Then thermo-hygrometer is placed over the prototype to record relative humidity and temperature.

Table 1. Components and specifications of developed atmospheric water harvesting device

Device name	Quantity	Specifications
DC supplier	1	Input – 110/220 V; Output -12 V, 30 A
DC brushless cooling fan	2	Size - 120 X 120 X 38 mm; 12 V, 0.40 A Air flow rate – 58.86 m^3/min
Aluminum plate	1	Thickness – 2 mm Size – 30 x 30 cm
Peltier's TEC – 12706	3	Size – 4 x 4 cm 12 V DC, 6 A
Thermal compound paste	2	150 g
Fan cooled heat sink	3	12 V DC, 0.60 A
Digital thermometer	1	Temperature probe length-30 cm
Digital thermo-hygrometer	1	Temperature ranges-(-10 – 50^{o}c) Humidity ranges – (10 – 99 %)

Energy consumption of atmospheric water harvesting device: Energy consumption was calculated

Power, W = Volts, V Amperes, A

The energy consumption of 2 units of DC Brushless fans, 3 units of peltiers, 3 units of fan cooled heat sinks were calculated and found to be 247 w/ hr.

The experimental setup of the prototype is fully completed by supplying electrical connection to the prototype. The two DC brushless cooling fans were given parallel connection i.e., connecting two positive wires (red) and two negative wires (black) and directly connected to the DC supplier. In the similar way three peltiers were given parallel connection and directly connected to the DC supplier. The fan cooled heat sinks were given the parallel connection and directly connected to the DC supplier. At last AC supply is given to the DC supplier. Then the temperature sensor is placed at the condensing plate to record the condensing surface temperature. Then thermo-hygrometer is placed over the prototype to record relative humidity and temperature. The housing of the prototype with size of 50 × 35× 50 cm is made up of MS -216 with thickness of 1 mm, and at last prototype was fully covered with Styrofoam sheets to avoid heat transfer from outside to inside of the system (Fig. 1).

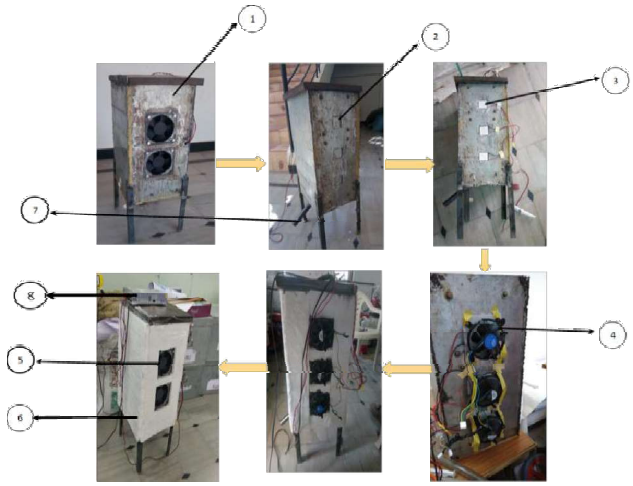

1. Housing MS– 216
2. Aluminium plate
3. Peltier TEC-12706
4. Fan cooled heat sink
5. DC brushless cooling fan
6. Styrofoam sheet
7. Water collecting outlet
8. DC supplier

Fig. 1. Components of AWG

Operation of peltier based atmospheric water harvesting device: DC moves across Peltier TEC- 12706, it causes temperature differential between TEC sides. As a result, one thermoelectric cooler face, which is called cold, will be cooled while its opposite face, which is called hot, simultaneously is heated. The heat generated on the TEC hot side is effectively dissipated into heat sink through fans and further into the surrounding environment, then the temperature on the thermoelectric cooler cold side will be much lower than that of the ambient by dozens of degrees. The cold side of TEC is attached with aluminum plate which acts as condensing plate and helps in condensation of air into water droplets when maximum air will flow into the system through DC brushless fan. The water droplets over the aluminum plate slowly falls due to gravitational force and collected below at the funnel. The thermoelectric coolers cooling capacity is proportional to the current passing through it, air flow rate and heat dissipated through heat sinks.

Dew formation and problem of latent heat release: For condensing pure air (homogenous nucleation), air can be chilled down than dew point temperature hence experience daily dew formation on leaves, over chilled cans). The latent heat or heat of vaporization releases during the phase change of gas to liquid. For condensing 1 ml of water, releases latent heat of 2450 J at 200c and this heat must be dissipated before the condensed water to re evaporating before storage. Water vapour molecules possess the kinetic energy and rotational energy. By cooling volume of moist air decreases the kinetic energy because in gas phase molecules movement decreases as the temperature decreases and promotes hydrogen bonding. When hydrogen bonding occurs between water vapour molecules forms cage like structure known as calathrate and does not permit internal rotations. The internal rotational energy of water vapour molecule which is rejected accounts for the energy equal to the latent heat of vaporization (Wahlgren 2001).

Dew point temperature: Magnus formula is used to calculate the dew point temperature (T_{dp}) for different atmospheric conditions (Tripathi et al 2016)

$$\gamma(T, RH) = In\left(\frac{RH}{100}\right) + \frac{b \times T}{C + T} \quad (1)$$

$$T_{dp} = \frac{c\gamma(T, RH)}{b - \gamma(T, RH)} \quad (2)$$

(Where, b = 17.67 & c = 243^{0}C and T is in ^{0}C)

Where,

T is actual ("dry bulb") air temperature and RH relative humidity (in percent)

Testing of the developed device: The device is designed and conducted at research laboratory of Action Fraterna Ecology Centre, Anantapur, as there is very less humidity recording during the summer of March where the ambient humidity is even less than the air-conditioned humidity. Then the device tested under ambient conditions for two days and the readings like ambient temperature, peltier temperature were taken by digital thermometer. By using digital hygrometer Ambient humidity readings were taken for every half an hour for one day and every one hour for one day. Dew point temperature is calculated by using magnus equation condensed water is collected through syringe.

RESULTS AND DISCUSSION

This section reveals the results of the experiment which has been conducted at research laboratory of Accion Fraterna Ecology Centre, Anantapur District. There is a constant humidity recording in the air-conditioned room when compared to the ambient conditions (Table 2) but air conditioner main principle is cooling and dehumidification so

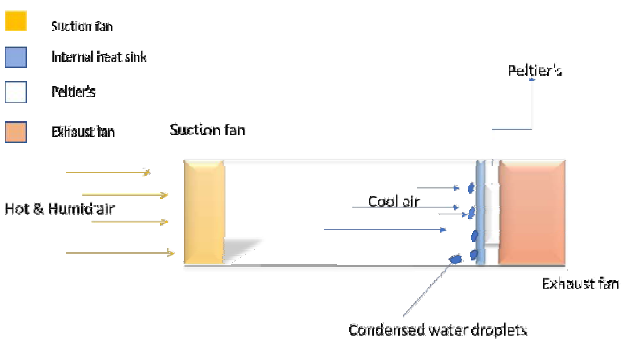

Fig. 2. Principle of operation of AWG

that it cools the air and removes the humidity present in the air. Then the developed device was tested in ambient conditions and readings were taken hourly basis. The peltier temperature or condensing surface temperature recorded is always higher than the required dew point temperature and this indicates that device not able to condense water (Table 3). The reasons for device not able condense water is analyzed by dismantling the fan cooled heat sink over the peltiers and observed there is air gap between the Peltier and aluminum plate, due to frame having undulations which resulted in unable to cool the aluminum plate and thickness of the plate was high.

Table 2. Comparison of ambient conditions to the air-conditioned atmospheric conditions

Time 24hr	Ambient temperature (°C)	Ambient humidity (%)	Dew point temperature (°C)	Room temperature (A.C) °C	Room humidity (A.C) (%)	Dew point temperature (°C)
9.00	30.00	37.00	13.70	31.60	31.00	12.40
10.00	32.00	31.00	12.70	31.50	30.00	11.80
11.00	34.00	26.00	11.80	30.70	28.00	10.10
12.00	36.00	25.00	12.80	30.80	29.00	10.70
13.00	37.00	23.00	12.40	31.30	27.00	10.00
14.00	37.00	21.00	11.00	31.70	26.00	9.86
15.00	37.00	22.00	11.70	31.00	27.00	9.83
16.00	36.00	23.00	11.60	31.00	27.00	9.83
17.00	33.00	23.00	9.10	32.30	27.00	10.94
18.00	31.00	25.00	8.60	31.50	27.00	10.25

Table 3. Temperature difference between the dew point temperature and peltier on March 12, 2019

Time (24Hr)	Ambient temperature (°C)	Ambient humidity (%)	Dew point temperature (°C)	Peltier temperature (°C)	Temperature difference td (°C)
9.00	30.00	37.00	13.70	31.60	-19.20
10.00	32.00	31.00	12.70	31.40	-19.60
11.00	34.00	26.00	11.80	31.60	-21.50
12.00	36.00	25.00	12.80	31.90	-21.20
13.00	37.00	23.00	12.40	32.20	-22.20
14.00	37.00	21.00	11.00	31.80	-21.90
15.00	37.00	22.00	11.70	29.70	-16.80
16.00	36.00	23.00	11.60	29.60	-19.70
17.00	33.00	23.00	9.10	29.90	-20.80
18.00	31.00	25.00	8.60	29.90	-21.30

Table 4. Temperature difference between the dew point temperature and peltier on February 26, 2019

Time (24 Hr)	Ambient temperature (°C)	Ambient humidity (%)	Dew point temperature (°C)	Peltier temperature (°C)	Temperature difference (t_d) °C	Water collected from each peltier having 16 cm2 (ml hr^{-1})
10.15	32.1	30.00	12.36	12.60	- 0.24	-
10.45	32.6	31.00	13.29	12.60	0.69	-
11.15	33.0	30.00	13.12	13.40	- 0.28	5
11.45	33.2	30.00	13.31	13.60	-0.29	-
12.15	33.4	29.00	12.96	12.40	0.56	4
12.45	33.6	29.00	13.12	11.10	2.02	-
13.00	33.6	29.00	13.12	12.10	1.02	-
13.30	33.6	29.00	13.12	7.40	5.72	-
14.00	34.00	27.00	12.38	14.70	-2.32	2
14.30	35.00	27.00	13.23	13.20	0.03	I

Table 5. Ambient humidity calculations at 14°C Dew point temperature and different dry bub temperature (ambient) conditions from psychometric chart

Dew point temperature (°C)	Ambient humidity (%)	Ambient temperature (°C)
14	68.4	20
14	64.3	21
14	60.5	22
14	56.9	23
14	53.6	24
14	50.5	25
14	47.6	26
14	44.8	27
14	42.3	28
14	39.9	29
14	37.7	30

The water collected through syringe from each peltier is very less due to less ambient humidity. It was observed during the experiment that the device able to decrease the ambient temperature i.e. temperature difference between ambient and peltier temperature up to 20^{0}C. It also shows that the temperature difference is mostly positive values i.e., peltier temperature is less than dew point temperature so that it is able to condense water from the air though it is having less humidity. The average peltier temperature is 13.78^{0}C i.e., nearly 14^{0}C (Table 4).

The required humidity conditions at different ambient temperature conditions, at which the device able to condense water using psychometric chart, if the inlet ambient temperature is 25^{0}C and the relative humidity is above 50.5 %. If the inlet ambient temperature is 30^{0}C and the relative humidity is above 37 % the device is able to condense water. The device condenses water if the temperature is 35 ^{0}C and if the relative humidity is above 28 %.

CONCLUSIONS

Water collected from the device is very low due to low humidity in the experimented area. The device will condense more water in places like coastal areas having high humidity or during the spring season in the Anantapur district. The device is able to condense water if the inlet ambient temperature is 25^{0}c and if the relative humidity is above 50 % and if the inlet ambient temperature is 30^{0}c and the relative humidity is above 37 % the device is able to condense water. In future prototype, to condense more water by incorporating more no of peltiers (TEC) instead of three peltiers. The peltiers efficiency can be increased by integrating the components like heat sink, peltier and aluminum plate tightly and cooling the hot side of Peltier effectively by using large heat sinks or water-cooled heat sinks. To be eco-friendly, it may include solar power source instead of using AC power.

Received 27 July, 2021; Accepted 12 November, 2021

REFERENCES

Anbarasu T and Pavithra KS 2011. Vapour compression refrigeration system generating fresh water from humidity in the air. *Sustainable Energy and Intelligent System* **2**(1): 75 -79.

Farshid B 2018. Performance investigation of atmospheric water harvesting systems. *Water Resources and Industry* **20**(1): 23-28.

Joshi VP, Joshi VS, Kothari HA, Mahajan MD, Chaudhari MB and Sant KD 2017. Experimental investigations on a portable fresh water generator using a thermoelectric cooler. *Energy Proced*ia **109**(1): 161-166.

Jradi M, Ghaddar N and Ghali K 2012. Optimized operation of a solar-driven thermoelectric dehumidification system for fresh water production. *Journal of Energy and Power Engineering* **6**(1): 878-891.

Kumar M and Yadav A 2016. Comparative study of solar powered water production from atmospheric air using different desiccant materials. *International Journal of Sustainable Engineering* **9**(6): 1-11.

Muñoz-García MA, Moreda GP, Raga-Arroyo MP and Marín-González O 2013. Water harvesting for young trees using Peltier modules powered by photovoltaic solar energy. *Computers and Electronics in Agriculture* **93**(1): 60-67.

Nandal K, Kaushik N, Yadav S.S, Rao AS, Singh N and Gulia SS 2020. Water quality assessment of pond water of Kalanaur Block, Rohtak, Haryana. *Indian Journal of Ecology* **47**(1): 1-6.

Rahbar N and Esfahani JA 2012. Experimental study of a novel portable solar still by utilizing the heat pipe and thermoelectric module. *Desalination* **284**(2): 55-61.

Renyuan L, Yusuf S, Le Shi, Mossab Alsaedi, Peng Wang 2018. Harvesting water from air: Using anhydrous salt with sunlight. *Environmental Science and Technology* **52**(9): 5398 -5406.

Runze D, Qingfen M, Hui L, Wang G, Wei Y, Guangfu C, Yifan C 2020. Experimental investigations on a portable atmospheric water generator for maritime rescue. *Journal of Water Reuse and Desalination* **10** (1): 30-44.

Sharan G, Clus O, Singh S, Muselli M and Beysens D 2011. Avery large dew and rain ridge collector in Kutch area (Gujarat, India). *Journal of Hydrology* **405**(1): 171-181.

Xi H, Luo L and Fraisse G 2007. Development and applications of solar-based thermoelectric technologies. *Renewable and Sustainable Energy Reviews, Elsevier* **11**(5): 923-936.

Wahlgren RV 2001. Atmospheric water vapour processor designs for potable water production: A review. *Water Research* **35**(7): 1860-1860.

Indian Journal of Ecology (2021) 48(6): 1876-1879

Manuscript Number: 3464
NAAS Rating: 5.79

Accumulation of Heavy Metals in *Fejervarya limnocharis* Tadpoles Inhabiting Two different Wetlands in Cachar District, Assam

T.H. Sharma and M. Dey

Department of Ecology and Environmental Science, Assam University, Silchar-788 011, India
E-mail: henashrees@gmail.com

***Abstract*:** The study was conducted to estimate the level of heavy metals chromium (Cr), copper (Cu), lead (Pb), nickel (Ni) and zinc (Zn) in tadpoles (*Fejervarya limnocharis*) in two different wetlands of Cachar district, Assam during winter and rainy season. Tadpole, water and sediment samples were collected from both Chatla haor and Ramnagar anua to determine the accumulation of metals. Difference of metal content was seen in all the five metals analysed in both the sites and the seasons. The present study indicates that tadpoles can be considered good bio indicators of heavy metal contamination in the aquatic water bodies like ponds, marshes, floodplain wetlands etc.

***Keywords*:** Accumulation, Bioaccumulation factor, Heavy metals, Tadpoles, Wetlands

Anura is an order of class Amphibia which includes frogs and toads. Ecologically, the anurans are significant due to their biphasic life style, sensitivity to environmental changes, position within the food web as both prey and predator and their widespread distribution. Aquatic pollution has become an issue of worry as a result of the health hazard it possess to aquatic lives and human population (Singh et al 2016). Heavy metals are non-degradable along the line so, they tend to be deposited, assimilated or incorporated in water, sediment and aquatic animals causing pollution in the water bodies (Malik et al 2010). Accumulation of metals are higher in larval amphibians than adults due to differences in ratio of surface area to volume and their semi permeable skin which points to cutaneous respiration and high accumulation of environmental pollutants in the tissue from water and soil directly. Considerable numbers of studies have reported the capability of aquatic organisms to concentrate heavy metals but only few studies have linked heavy metals in tadpoles to metals in the immediate environment like water and sediment (Hofer et al 2005).The objective of the present study was to evaluate the levels of heavy metals; chromium, copper, lead, nickel and zinc in tadpoles of *Fejervarya limnocharis* (Gravenhorst 1829) in two different wetlands in Cachar district, Assam during winter and rainy season.

MATERIAL AND METHODS

Study sites: The study area has several wetlands of which Chatla haor and Ramnagar anua were selected for the present study. Chatla haor is a floodplain located 20 km away from Silchar at 92˚46'26"E longitude and 24˚42'69"N latitude. It is the biggest wetland in Cachar district occupying 4014 ha area. The topography of the area is fenland type with small hillocks strewn among large stretches of lowland (Purkayastha et al 2012).Ramnagar anua is situated close to Silchar town, and is an oxbow lake at 92˚75'96"E longitude and 24˚83'32"N latitude. It occupies 139.899 ha area and is fully covered by hydrophytes and surrounded by some wild plants, banana trees, bamboos, etc. Seasonal vegetation is planted along the bank.

Collection of samples: Water samples were collected from both the sites in sampling bottles which were preconditioned with dilute nitric acid and later rinsed thoroughly with double distilled water. Pre cleaned polyethylene sampling bottles were immersed about 10cm below the water surface and 1 litre of the water sample was taken. For estimation of heavy metals in water, 500 ml of the sample was filtered with Whatman filter paper number 1 and subjected to nitric acid digestion. For digestion, 5 ml of 6NHNO_3 was added to 50 ml water sample followed by heating to slow boil till the digestion completed which is indicated by a clear solution. The digested samples were used for metal estimation using atomic absorption spectrophotometer as per (APHA 2005). Sediment samples were dried at 40˚C in the oven, ground and passed through mesh sieves (2 mm pore size). Ten gram of dried sample was digested with 40 ml of acid mixture (HNO_3:H_2SO_4: 3:1) for half an hour, and then cooled, decanted and filtered at room temperature. Distilled water was added to make up the volume of the solution to 50 ml, which was further used for estimating heavy metals by atomic absorption spectrophotometer (APHA 2005).Tadpoles of *Fejervarya limnocharis* were collected from both the sites with the help of dip net and were washed properly with double

distilled water in the laboratory and dried until it reaches a constant weight and then subjected to acid digestion. To every sample (0.1 g), 10 ml of perchloric acid, conc. HNO_3 (3:2 v/v) was added and heated at 60˚C until a clear solution was obtained (FAOSIDA 1983). The resulting solutions were cooled and the volumes made up to 50 ml using double distilled water. The samples were then stored in plastic bottles until analysis by AAS.

Bioaccumulation assay: Bioaccumulation factor (BAF) was determined as ratio of heavy metals in tadpoles to that in water and sediment samples (Barron 1995).

RESULTS AND DISCUSSION

The current study investigates accumulation of Cr, Cu, Pb, Ni and Zn in two different wetlands in Cachar district during winter and rainy season. The metal accumulation in the water samples during winter season (Fig. 1) in Chatla haor indicated higher accumulation in the sequence Ni>Cu>Pb>Zn>Cr than that of Ramnagar anua (Ni>Pb>Cu>Cr>Zn) except in Cr. However, during rainy season the water samples from Ramnagar anua showed higher metal accumulation in the sequence Ni>Pb>Cr>Cu>Zn (Fig. 2). This might be brought about by the consequent dilution of water ensuring precipitation and runoff during the rainy season (Bhatt et al 1999).Samples from Chatla haor indicated high accumulation in Cu, Pb and Ni. Whereas during rainy season Ramnagar showed higher value of accumulation than that of Chatla except in Ni (Fig. 3, 4). Thus in sediment Ni was found to have low accumulation in both the sites. The difference in accumulation of heavy metal may be due to difference in solubility and bioavailability as also reported by Duman et al (2008).

Higher accumulation in Tadpole was observed in Chatla during winter season in the sequence Ni>Cu>Zn>Pb>Cr (Fig. 5). Same result was seen in a study by Omer et al (2021). Ramnagar showed higher metal accumulation in tadpoles during rainy season compared to Chatla (Fig. 6) except in that of zinc. Current estimates indicates that over one third of the world's amphibians are facing extinction, one factor that has been generally implicating the population decline is the contamination of freshwater systems with heavy metals derived from industrial and agricultural sources (Greig et al 2010, Hopkins et al 2010).

The overall result indicated that samples from Chatla haor recorded higher metal accumulation during winter season. In rainy season samples from Ramnagar anua showed higher value of accumulation than that of Chatla. This may be due to entry of water originating from surrounding regions which conveys pesticides, agricultural fertilizers, etc which mixes with the waters in the wetland and increases the toxicity levels. Few issues, including delayed development, morphological deformities, limitations in the type of food they consume and decrease in growth and metamorphosis of the tadpoles can also be identified to heavy metal pollution (Snodgrass et al 2005, Sparling et al

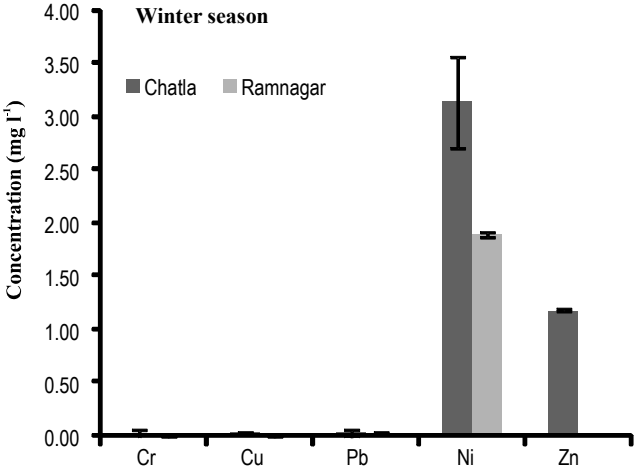

Fig. 1. Bioaccumulation of heavy metal in water (ppm)

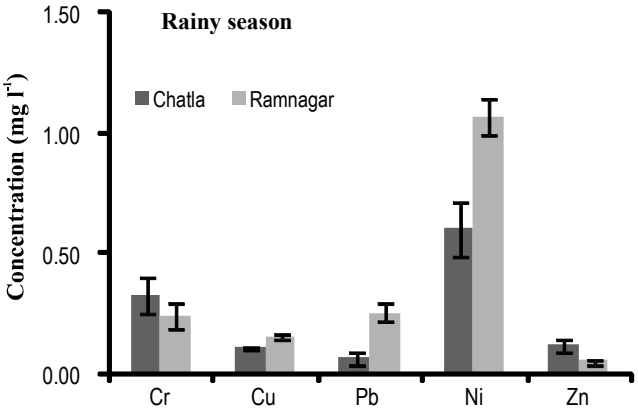

Fig. 2. Bioaccumulation of heavy metal in water (ppm)

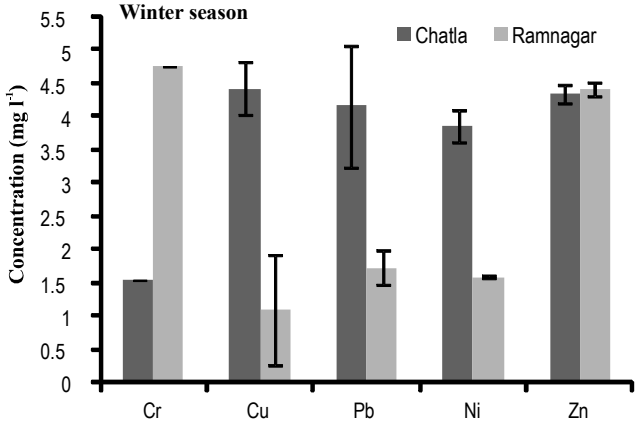

Fig. 3. Bioaccumulation of heavy metal in sediment (ppm)

Table 1. Bioaccumulation factor (BAF) ratio of heavy metals in tadpoles to that in water and sediment samples

Heavy metals	Sites	Tadpole/ Water		Tadpole/Sediment	
		Winter season	Rainy season	Winter season	Rainy season
Cr	Chatla	92.2	1.07	0.53	0.56
	Ramnagar	66.8	1.59	0.06	0.60
Cu	Chatla	42.7	1.60	0.38	0.45
	Ramnagar	126	1.75	1.15	0.63
Pb	Chatla	36.8	3.73	0.27	0.68
	Ramnagar	95	1.29	1.09	0.62
Ni	Chatla	0.8	1.08	0.8	0.71
	Ramnagar	1.11	0.89	1.32	0.47
Zn	Chatla	42.1	2.29	0.27	0.53
	Ramnagar	13.26	2.42	0.05	0.33

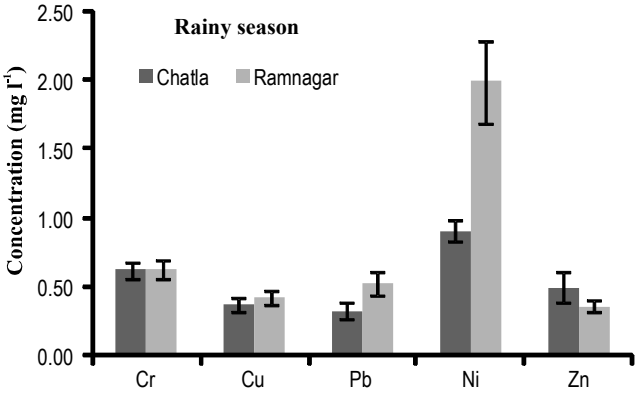

Fig. 4. Bioaccumulation of heavy metal in sediment (ppm)

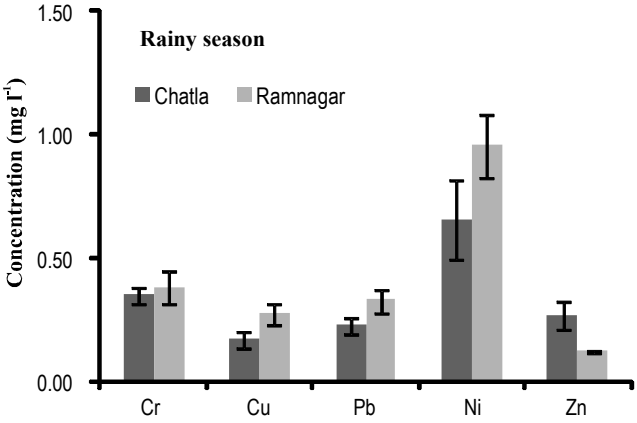

Fig. 6. Bioaccumualtion of heavy metal in tadpole (ppm)

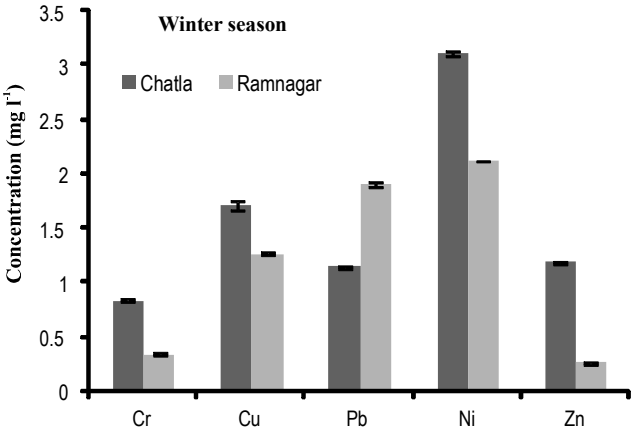

Fig. 5. Bioaccumulation of heavy metal in tadpole (ppm)

2006). In any case, the specific impacts of heavy metal on their growth, physiology and behavior need further investigation. The bioaccumulation factor from both the sites showed greater value in tadpole/water than that of tadpole/sediment ratio for most samples. This demonstrates that the tadpoles gather heavy metals from the water in which they were found. The water soluble form of metal is viewed to be the most bioavailable and toxic to aquatic organisms, leading to an accelerated uptake of metal ions that are in the solution (Gerhardt 1993). Amphibian larvae have been reported to be sensitive to increased aqueous concentrations of several metals.

CONCLUSION

The tadpoles can be a good bio indicator for heavy metal contamination in water bodies. They are said to be the health indicators of temporary ponds and shows the health of the ecosystem by balancing the energy transfer from lower to upper trophic levels which also structures the biotic composition of the entire system. However, subsequent accumulation along the food chain is a potential threat to human wellbeing (Swain et al 2014). The sources of heavy metals in water bodies are disposal of domestic waste, agricultural drainage water, domestic sewage, fitting of pipes for water supply purposes and dissolution of metals from rocks. Measures should be taken and awareness should be

spread to stop disposal in the water bodies and keep it clean. Regular monitoring is also recommended.

REFERENCES

APHA 2005. *Standard methods for the examination of water and waste water analysis*, 21st edition, Washington DC, USA.

ASTM 2002. Standard guide for conducting acute toxicity tests on aqueous effluents with fishes, micro-invertebrates and amphibians. *American Society for Testing and Materials,* pp 729- 96.

Barron M G and Woodburn K B 1995. Ecotoxicology of *chlorpyrifos*. *Reviews of Environmental Contamination and Toxicology* **144**: 1-93.

Bhatt LR, Laconl P, Lakhak HD and Jha PK 1999. Physiochemical characteristics and phytoplankton of Taudaha lake, Kathmandu. *Pollution Research* **18**(14): 353-358.

Duman F and Obali O 2008. Seasonal variation of metal accumulation and translocation in yellow pond lily (*Nuphar lutea). Chemical Speciation and Bioavailability* **20**(3): 181-190.

FAO/SIDA 1987. *Manual of methods in aquatic environmental research part 9, Analysis of metals and organochlorines in fish*, FAO fisheries/technical paper, 212.

Frost DR 2011. *Amphibian species of the world: An online reference*, Version 5.5 (31 January, 2011), New York, USA.

Gerhardt A 1993. Review of impact of heavy metals on stream invertebrates with special emphasis on acid conditions. *Water Air Soil Pollution* **66**: 289-314.

Gosner K L 1960. A simplified table for staging anuran embryos and larvae with notes on identification. *Herpetelogica* **16**: 183-190.

Gravenhorst JLC 1829. *Deliciae Muusei Zoologici Vratislaviensis, Facciculuus Primus continens Chelonios et Batrachia,* Leopold Voss, Lipsiae.

Greig HS, Niyogi DK, Hogsden KL, Jellyman PG and Harding JS 2010. Heavy metals: Confounding factors in the response of New Zealand Freshwater fish assemblages to natural and anthropogenic acidity. *Science of the Total Environment* **408**: 3240-3250.

Hayes TB, Falso P, Gallipeau S and Stice M 2010. The cause of global amphibian declines: A developmental endocrinologist's perspective. *Journal of Experimental Biology* **213**: 921-933.

Hofer R, Lackner R and Lorbeer G 2005. Accumulation of toxicants in tadpoles of the common frog (*Rana temporaria*) in high mountains. *Archieves of Environmental Contamination and Toxicol*ogy **49**: 192-199.

Hopkins W and Rowe C 2010. *Interdisciplinary and hierarchical approaches for studying the effects of metals and metalloids on amphibians*. *Ecotoxicology of Amphibians and Reptiles*, Second Edition, CRC Press.

Received 12 June, 2021; Accepted 10 November, 2021

Kar D 2016. Wetlands, Rivers, Fish, Plankton Resources and Fish disease and aquaculture in North East India: An Overview. Lake 2016: *Conference on Conservation and sustainable management of ecologically sensitive regions in Western ghats.*

Kelepertzis K, Argyraki A, Valakos E and Daftsis E 2012. Distribution and Accumulation of metals in tadpoles inhabiting the Metalliferous streams of Eastern Chalkidiki, Northeast Greece. *Geoderma* **8**: 82-90.

Luoma SN and Rainbow PS 2008. *Metal contamination in aquatic environment: Science and lateral management*, New York: Cambridge.

Malik N, Biswas AK, Qureshi TA and Boranak VR 2010. Bioaccumulation of Heavy metals in fish tissues of the Freshwater lake of Bhopal. *Environmental Monitoring and Assessment* **160**: 267-267.

Omer AE, Elfadil AG and Abdelelah ME 2021. Analysis of Heavy metals concentrations in water samples nearby Wadaflea Dumpsite of solid waste in the Khartoum North, Sudan. *Indian Journal of Ecology* **48**(3): 784-788.

Purkayastha P and Gupta S 2012. Insect diversity and water quality parameters of two ponds of Chatla wetland, Barak Valley, Assam. *Current World Environment* **7**(2): 243-250.

Sakshi J Kaur, Bhatia H and Aruna 2011. *Evaluation of heavy metal accumulation in some tissues of the Edible fish from the river Satluj in Punjab*. Shodhganga.inflibnet 10603/3635.

Singh P, Dey M and Ramanujam SN 2016. Bioaccumulation of heavy metals in anuran tadpoles: A study in Barak Valley, Assam. *International Journal of Aquatic Biology* **4**(3): 171-178.

Singh P, Dey M and Ramanujam SN 2016. A Study on Bioaccumulation of Heavy Metals in two Anuran Tadpoles: *Clinotarsus alticola* and *Leptobrachium smithi* from Rosekandy Tea Estate, Cachar, Assam. *Current World Environment* **11**(1). http://dx.doi.org/10.12944/CWE.11.1.39

Snodgrass JW, Hopkins WA, Jackson BP, Baionno JA and Broughton J 2005. Influence of larval period on responses of overwintering green frog (*Rana clamitans*) larvae exposed to contaminated sediments. *Environmental Toxicology and Chemistry* **24**: 1508-1514.

Sparling DW, Krest S and Ortiz-Santaliestra, M 2006. Effects of lead contaminated sediment on *Rena sphenocephata* tadpoles. *Archieves of Environmental Contamination and Toxicology* **51**: 458-466.

Swain G, Adhikari S and Mohanty P 2014. Phytoremediation of Copper and Cadmium from water using Water hyacinth, *Eichhornia crassipes. International Journal of Agricultural Science and technology* **2**(1): 1-6.

Zhang M H 2009. The toxic effect analysis of heavy metal ions on tadpoles of *Pelophylax nigromaculatus*. *Journal of Guiyang College (Natural Science Edit)* **4**(1): 19-23.

Indian Journal of Ecology (2021) 48(6): 1880-1886

Manuscript Number: 3465
NAAS Rating: 5.79

Bio Concentration Factor of Aquatic Plants and Heavy Metals as Exchangeable and Residual in Sediment at Marshes, Southern Iraq

Maha K. Al-Mishrey, Rehab S.K. Al-Atbee[1], Salah M. Saleh[1] and Abbas A. Hantoush[1]

Department of Biology, College of Science, University of Basrah, Baseah, Iraq
[1]Marine Science Centre, University of Basrah, Iraq
E-mail: htalsaad@yahoo.com

***Abstract*:** Concentration and accumulation of six heavy metals (Cd, Cr, Pb, Cu, Zn and Ni) were measured in the sediment as (exchangeable and residual phase) and in two species of merged aquatic plants (*Typha domingensis* and *Phragmits australis*) during summer 2019 to spring 2020 at Al-Hammar marsh. Geoaccumulation index (I-geo) and Bio-concentration factor (BCF) were calculated as indicators of heavy metals pollution in sediment and aquatic plant, respectively. Higher concentration of metals were observed in residual phase more than their concentration in exchangeable phase, while the mean contents of metals were in decreasing order Ni > Cr > Zn > Cu > Pb > Cd. According to I-geo index, the sediment of Al-Hammar marsh can categorized as strongly polluted with Cd, while considered as unpolluted to moderately with Cr and Cu, but unpolluted with Pb and Zn. The BCF show different capacity of both studied plants to accumulate heavy metals from the surrounding media and are useful for management of pollutants.

Keywords: BCF, Sediment, Heavy metals, Southern marshes, Iraq

The Tigris and Euphrates rivers have formed about 15,000 km^2 of marshes called as the Mesopotamian marshes and are considered the most extensive wetland ecosystem in the Middle East, which encompass a complex of interconnected shallow freshwater lakes and marshlands (Al-Hussieny and Thijar 2016). Southern wetlands of Iraq form a triangular region limited by main cities of Iraq: Nasiriyah to the west, Amarah to the northeast, and Basrah to the south. Three geographic zones of the Mesopotamian Al-Hammar, the Central, and the Al-Hawizeh Marshes form the core of the wetland Iraqi southern are with vast area of 20,000 km^2 of open water and comprises permanent and seasonal marshes.

The urban areas have been affected by pollution from hazardous waste, transport activities, vehicles emissions and industrial waste (Al-Khafaji and Jalal, 2020). Pollution of aquatic environment with different contaminants such as heavy elements is a major ecological crisis in our natural ecosystem because they are not readily degraded environmental pollutants and many of them are poisonous (Branković1 et al 2011). Metals such as copper and zinc are released into the aquatic ecosystem by anthropogenic activities such as agricultural, industrial and mining (Al-Yasari et al 2020). These metals enter to a body of water can remain there for some time and usually found in trace concentrations, but high concentration of them in sediments can indicate anthropogenic rather than biogenic sources (Tylmann et al 2011).In recent years, the concentration of heavy elements has expanded because of different human activities such us use of pesticides and fertilizers, burning of petroleum derivatives, waste release and so forth (Mehmood et al 2019). Aquatic ecosystems usually fail to eliminate heavy metals from waste discharge using their own natural processes (Goswami et al 2020). The Mesopotamian marshlands are known to accumulate many types of chemicals that introduced the aquatic environment through natural and anthropogenic activities, in natural system, sediment of marshes can act as a sink of various pollutants through sedimentation processes (Singh et al 2017, Al-Atbee 2018).

Heavy elements accumulate in sediments, in which they may not cause significant ecological risk in the water system but may be remobilized through biogeochemical processes, during exchange reactions like redox reactions, re-suspension and desorption reactions into the water column, so enhancing the elevation of the dissolved elements concentration to a poisonous level for aquatic biota (Vukosa et al 2014, Yan et al 2017). But sometimes when the sediment surfaces are saturated with heavy elements, it can act as non-point source of water pollution, particularly when the elements concentrations in freshwater are reduced. This effect is most distinct at high temperatures, velocity of water

and fine sediment particles (Hassan et al 2010, Tytla and Kostecki 2019). In sediments, many types of geochemical elements associated with sediments, one of them is known as exchangeable elements in which elements are linked with the sediment in the most labile mode. Another type called the residual phase, that fraction of elements strongly join the lithogenic minerals of the sediments (Al-Hejuje 2014). Elements accumulation in the sediment that result of long term exposure, while in the water as dissolved form concentration of element is mainly result of recent pollution (Varol and Sen 2012). Therefore, measuring of heavy elements concentration in the sediments gives a clear perception of the level of pollution in the aquatic environment.

Aquatic plants accumulate these pollutants through roots and shoots structures because of their high biomass and fast growth (Singh et al 2017). The macrophytes take up metals by variety of the process, phyto-extraction, phyto-stabilization, phyto-filtration, rhizo-remediation and phyto-stimulation. The metals accumulation ability of some plant species is an interesting evolutionary problem, whereas it could have a practical application in phytoremediation of metal contaminated soils (Alobaidi et al 2020). Though, the heavy metals cannot be metabolized but accumulate in the plant biomass (Bdewi et al 2019). The wetland plants such as a genus of Typha, Phragmites, Eichhornia, Lemna and Azolla can possibly remove the heavy metal due to their morphological change (Dipu et al 2012). The main objective of this study is to determine the spatial distributions and concentration of Cd, Cr, Ni, Pb, Cu and Zn in surface sediments in Al-Hammar marsh, using geo accumulation index (I-geo) to assess the heavy metal pollution of sediments and assessment the ability of two aquatic plant spices in management of heavy metal pollution by calculating the bio-concentration factor.

MATERIAL AND METHODS

Description of area: The research site Hor Al-Hammar extends from Souq Al-Shuyukh in Al Nasiriyah city in the west to Qarmat Ali in Al-Basrah in the east. The marsh area is about 2800 Km^2, expanding during the flood season to over 4500 Km^2, while during the dry period to 600 Km^2. Al-Hammar marsh receive water from Euphrates River and also from Tigris River (UNEP 2006).

Collection and analysis of samples: Sediment and plants samples were collected seasonally during summer 2019 to spring 2020 from six stations (Fig. 1). The sediment samples were collected by a Van veen grab sampler. Aquatic plants (*Typha domingensis* and *Phragmites australis*) were collected by hand and washed by marsh water to remove periphyton and adherence particulate, then using plastic

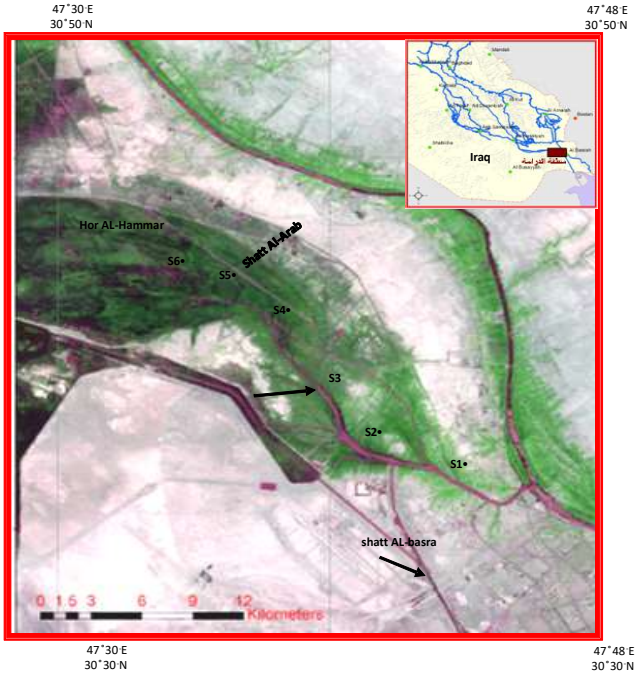

Fig. 1. Samples locations

bags for preserved the samples, and placed in an ice box. In laboratory the samples were dried in an air, grind finely using an electrical mortar and sieved through a 63 µm mesh sieve. One gm of sample from sediment was put it in 50 ml polyethylene tube. The exchangeable heavy metals were extracted according to the method of Chester and Voutsinou (1981). The residual heavy metals were extracted according to Sturgeon et al (1982). Samples were stored in tight stopper polyethylene vials for analysis. 0.5 g dry weight of plant samples were digested according to procedure of Barman et al (2000). All the samples were analyzed using flam atomic absorption spectrophotometer (FAAS). The geo accumulation index I-geo (Table 1) was calculated using the following equation adopted by Müller (1969) to assess the sediment pollution in the current study:

Where:

C_n: The concentration of element (n) which measured in the sediments.

Table 1. Geo accumulation index to classification sediments pollution

I-geo	Pollution sediments case
< 0	Unpolluted.
0 < Igeo < 1	Unpolluted to moderately.
1 < Igeo < 2	Moderately polluted.
2 < Igeo < 3	Moderately polluted to strongly polluted.
3 < Igeo < 4	Strongly polluted.
4 < Igeo < 5	Strongly to very strongly polluted.
> 5	Strongly polluted.

Bn: The geochemical background value to the element (n).
1.5: The constant factor used because of possible variation in reference values due to lithological variability.

The bio-concentration factors (BCF) were used as a measurement of quantitative to the efficiency of aquatic plants to accumulate heavy metals inside their tissue comparison with the surrounding environment. It was calculated according the equation explain by Wilson and Pyatt (2007).

$$BCF\ (\%) = \frac{C\ plant\ tissue}{C\ (sediment)} \times 100$$

Where:

$C_{plant\ tissue}$ the heavy metals concentration in the plant tissue.

$C_{(sediment)}$ the heavy metals concentration in sediment.

RESULTS AND DISCUSSION

In the present study heavy metals were measured as exchangeable and residual phases in the sediments samples. Concentrations of metals in the exchangeable fraction were 9.01-22.27 µg g^{-1} for Cd and (30.25-58.48 µg g^{-1}) for Cr and (16.24-35.28 µg g^{-1}) for Pb and (18.03-35.91 µg g^{-1}) for Cu and 26.24-48.98 µg g^{-1} for Zn and 40.01-64.63 µg g^{-1} for Ni (Table 2). Sequences of metal concentrations were as follows: Ni > Cr > Zn > Cu > Pb > Cd. The average mean of all stations of Cd, Cr, Pb, Cu, Zn and Ni were 15.22, 45.32, 23.48, 26.98, 37.58, 49.33 µg g^{-1}, respectively. Statistical analysis showed significant differences ($P<0.05$) between seasons and stations for all studied metals. Sediments act as the most important reservoir of pollutants such us heavy metals from natural and anthropogenic sources in the aquatic

Table 2. Concentrations of heavy metals (µg g^{-1}) in the sediments as exchangeable phase from summer 2019 to spring 2020 (Mean ± SD)

Stations	Seasons	Heavy metals (µg g^{-1})					
		Cd	Cr	Pb	Cu	Zn	Ni
St.1	Summer	9.01±0.74	44.14±0.04	24.51±0.03	22.50±0.01	40.26±0.06	58.39±0.02
	Autumn	10.01±0.40	45.58±0.04	28.52±0.07	24.63±0.05	42.87±0.02	60.29±0.04
	Winter	12.42±0.40	50.56±0.04	35.28±0.06	30.51±0.03	48.98±0.03	64.63±0.02
	Spring	10.25±0.40	46.13±0.28	31.81±0.06	24.99±0.28	45.29±0.05	60.08±0.11
St.2	Summer	10.61±0.58	46.12±0.12	22.40±0.80	26.32±0.03	39.28±0.02	50.25±0.03
	Autumn	12.19±0.09	48.06±0.09	24.52±0.06	28.96±0.05	40.20±0.02	49.99±0.05
	Winter	18.03±0.46	54.28±0.30	30.95±0.05	35.91±0.08	45.01±0.04	54.29±0.06
	Spring	17.03±0.43	50.84±0.03	28.25±0.04	28.33±0.02	41.26±0.02	52.02±0.06
St.3	Summer	18.55±0.56	50.23±0.02	20.56±0.08	28.65±0.03	32.52±0.04	46.26±0.04
	Autumn	20.94±0.60	53.11±0.04	23.62±0.05	30.60±0.02	34.28±0.05	48.21±0.04
	Winter	22.27±0.42	58.48±0.03	28.92±0.02	34.84±0.05	42.69±0.07	53.41±0.03
	Spring	20.49±0.64	53.88±0.21	25.25±0.07	30.25±0.03	40.27±0.06	50.12±0.11
St.4	Summer	16.41±0.58	40.66±0.39	20.18±0.19	24.36±0.05	30.24±0.03	43.34±0.04
	Autumn	18.19±0.13	41.73±0.87	22.61±0.16	28.41±0.03	38.29±0.02	41.21±0.03
	Winter	20.56±0.10	48.76±0.05	25.30±0.08	32.24±0.02	43.29±0.04	50.46±0.02
	Spring	18.83±0.04	44.24±0.03	23.39±0.04	30.40±0.02	42.69±0.05	50.11±0.03
St.5	Summer	14.23±0.33	38.39±0.02	18.96±0.07	20.43±0.03	28.29±0.01	40.25±0.02
	Autumn	16.14±0.06	40.26±0.05	18.05±0.06	22.40±0.02	30.25±0.04	42.24±0.02
	Winter	18.22±0.07	42.32±0.38	20.51±0.02	34.28±0.02	40.39±0.03	48.28±0.04
	Spring	16.68±0.38	41.33±0.32	18.99±0.03	25.85±0.04	32.65±0.02	44.21±0.02
St.6	Summer	10.31±0.10	30.25±0.03	18.06±0.05	18.34±0.04	26.24±0.02	40.01±0.04
	Autumn	11.11±0.22	36.28±0.27	16.24±0.03	18.03±0.06	28.24±0.05	40.55±0.03
	Winter	11.56±0.53	40.81±0.03	18.70±0.06	25.68±0.03	38.26±0.02	48.09±0.09
	Spring	11.31±0.40	41.21±0.04	18.01±0.06	20.64±0.02	30.25±0.04	48.21±0.03
Mean		15.22	45.32	23.48	26.98	37.58	49.33

systems (Brankovic et al 2011). These also act as bio-indicator for pollution of water (Habeeb et al 2015).

The concentration of these metals as residual phase were 15.27-30.25 ,44.64-65.95 , 21.58-40.26 ,20.94-47.27, 32.43-64.62 and 44.09-79.72 µg g^{-1} for Cd , Cr , Pb , Cu , Zn and Ni (Table 3). Metal contents of residual phase was in order Ni > Cr > Zn > Cu > Pb > Cd. Significant differences were observed between seasons for Cd, Pb, Cu and Zn and also between stations for all metals under study. These fluctuations are s because of difference levels of pollution between stations, also the influence of different chemical and physical factors between the seasons (Al-Khafaji 2015). Additionally, most of the metals in the sediments had higher concentrations than the background according to CBSQG (2003) values, except Zn because of it's ability to accumulate in biota more than in sediment (Aydin-Onen et al 2015). These results may be due to the high drainage of wastes directly into the drain, as a result of plant residues and decomposition. This is in agreement to the finding of Habeeb et al (2015). The spatial distribution of selected trace metals in all sites of the present study indicates to the occurrence of non-point origin like agricultural run-off and aquaculture.

Their concentrations in the exchangeable phase lower than their concentrations in the residual phase. These may be due to the fraction of exchangeable, which includes the weakly absorbent forms of metals that held on the sediment grins surface by weak electrostatic reactions and ion-exchange processes. The metals as residual phases includes are those associated minerals that are bounded by their structure of crystalline (Al-Mur 2020). To determining the extent of heavy metals pollution in sediments, can use the Geo-accumulation Index (I_{geo}) which introduced by Muller (1969).

Table 3. Concentrations of heavy metals (µg g^{-1}) in the sediments as residual phase at the studied stations during summer 2019 to spring 2020 (Mean ± SD)

Stations	Seasons	Heavy metals (µg g^{-1})					
		Cd	Cr	Pb	Cu	Zn	Ni
St.1	Summer	15.27±0.04	59.17±0.83	36.51±0.07	25.32±0.02	54.68±0.02	71.25±0.03
	Autumn	18.43±0.04	60.09±0.19	38.97±0.04	28.45±0.03	58.25±0.03	73.45±0.02
	Winter	20.82±0.03	65.45±0.05	40.26±0.04	35.63±0.06	64.62±0.04	79.72±0.04
	Spring	20.11±0.23	63.65±0.03	38.99±0.03	28.67±0.05	58.29±0.07	74.26±0.02
St.2	Summer	18.14±0.54	60.03±0.30	30.82±0.03	30.42±0.04	52.72±0.03	63.48±0.02
	Autumn	18.97±0.08	63.61±0.35	28.53±0.01	34.59±0.46	56.28±0.03	65.29±0.06
	Winter	21.35±0.38	65.94±0.06	38.95±0.05	40.44±0.03	60.94±0.07	72.45±0.04
	Spring	20.34±0.04	64.05±0.08	33.22±0.03	36.44±0.06	58.98±0.04	70.11±0.04
St.3	Summer	22.25±0.33	64.18±0.34	30.02±0.05	40.10±0.03	50.54±0.05	60.50±0.01
	Autumn	24.25±0.05	64.92±0.03	31.01±0.03	44.27±0.18	53.69±0.03	63.20±0.03
	Winter	30.25±0.05	65.95±0.03	36.58±0.03	47.27±2.37	60.84±0.02	70.28±0.03
	Spring	25.28±0.27	64.43±0.04	31.25±0.03	45.02±0.05	55.44±0.04	68.41±0.03
St.4	Summer	20.98±0.76	50.61±0.05	28.95±0.06	28.54±0.03	44.64±0.03	52.12±0.03
	Autumn	21.13±0.09	60.12±0.15	29.54±0.01	25.41±0.03	48.43±0.03	55.40±0.01
	Winter	21.54±0.53	63.28±0.25	38.29±0.04	32.25±0.03	58.98±0.04	60.68±0.03
	Spring	21.25±0.04	62.10±0.05	32.63±0.04	30.45±0.05	50.25±0.03	55.49±0.06
St.5	Summer	20.06±0.04	48.98±0.89	22.52±0.03	23.43±0.04	40.33±0.05	48.21±0.01
	Autumn	21.33±0.36	48.97±0.07	24.64±0.04	25.26±0.06	42.45±0.02	48.25±0.02
	Winter	22.67±0.39	50.47±0.04	28.97±0.05	32.13±0.06	50.01±0.06	55.21±0.04
	Spring	21.28±0.34	50.21±0.03	25.26±0.03	28.93±0.07	45.25±0.02	50.10±0.1
St.6	Summer	16.64±0.40	44.64±0.06	21.58±0.05	20.94±0.07	32.43±0.05	44.09±0.11
	Autumn	16.42±0.05	45.20±0.05	22.67±0.02	22.41±0.07	36.25±0.01	46.19±0.04
	Winter	20.52±0.07	46.04±0.10	30.52±0.01	28.54±0.03	45.44±0.04	50.20±0.02
	Spring	18.56±0.04	45.31±0.04	26.94±0.06	25.26±0.06	40.07±0.07	50.02±0.07
Mean		20.74	57.39	31.15	31.67	50.82	60.35

In the present study the mean values of I_{geo} in sediments were 4.58, 0.66 ,- 0.01 , 0.26 , -1.01 and 1.65 for Cd, Pb Cr, Cu, Zn and Ni (Table 4).

According to the (I_{geo}) mean values at all studied stations had no significant pollution and were considered as unpolluted with Pb and Zn (as Igeo<0), but unpolluted to moderately with Cr and Cu (0< I_{geo} < 1). Moderately polluted with Ni (1< I_{geo}< 2). Cd, was categorized as strongly to extremely strongly polluted (4< I_{geo}<5). This results could be due to the elements concentrations in surface sediments was higher than average of world surface rock according to CBSQG (2003). These results was in agreement with Al-Taie (2013).

Two plant species samples were selected from the marshes which are *Typha domingensis*, *Phragmites australis* to determine the heavy metals concentration in order to calculated the bio-concentration factor (BCF) and determine the role of these tow plant species to accumulation these heavy metals. Their mean concentration in *T. domingensis* were 0.38, 3.94, 4.46, 7.37, 2.48 and 1.90 µg/g dry weight for Cd, Cr, Ni, Pb, Cu and Zn, respectivily. Their sequences concentration of metals as follows: Pb > Ni > Cr > Cu > Zn > Cd, while their mean concentration in *P.australis* were 0.42, 3.96, 4.89, 6.49, 2.20 and 2.55 µg/g dry weight for Cd, Cr, Ni, Pb, Cu and Zn, respectivly. Their concentration squences were as follows: Pb > Ni > Cr > Zn > Cu > Cd (Table 5).

Bio-cncentration factor of different metals for tow studied species of aquatic plants is shown in Table 6 and order of BCF was followed an order:

Cd: *P. australis* > *T. domingensis*
Cr: *P. australis* > *T. domingensis*
Ni: *P. australis* > *T. domingensis*
Pb: *T. domingensis* > *P. australis*
Cu: *T. domingensis* > *P. australis*
Zn: *P. australis* > *T. domingensis*

Table 4. I-geo values and the descriptions status of sediments pollution at the studied stations during the studied periods

Stations	Season	I-geo Cd value	Description	I-geo Cr value	Description	I-geo Pb value	Description	I-geo Cu value	Description	I-geo Zn value	Description	I-geo Ni value	Description
St. 1	Summer	4.03	S-E polluted	0.68	U-M polluted	0.18	U-M polluted	-0.01	Unpolluted	-0.92	Unpolluted	1.91	Moderately
	Autumn	4.26	S-E polluted	0.71	U-M polluted	0.32	U-M polluted	0.15	U-M polluted	-0.90	Unpolluted	1.95	Moderately
	Winter	4.48	S-E polluted	0.85	U-M polluted	0.48	U-M polluted	0.46	U-M polluted	-0.82	Unpolluted	2.06	M-S polluted
	Spring	4.35	S-E polluted	0.77	U-M polluted	0.39	U-M polluted	0.16	U-M polluted	-0.75	Unpolluted	1.96	Moderately
St. 2	Summer	4.27	S-E polluted	0.72	U-M polluted	-0.02	Unpolluted	0.24	U-M polluted	-0.97	Unpolluted	1.72	Moderately
	Autumn	4.39	S-E polluted	0.79	U-M polluted	-0.03	Unpolluted	0.40	U-M polluted	-1.03	Unpolluted	1.74	Moderately
	Winter	4.73	S-E polluted	0.90	U-M polluted	0.37	U-M polluted	0.67	U-M polluted	-0.83	Unpolluted	1.88	Moderately
	Spring	4.65	S-E polluted	0.83	U-M polluted	0.19	U-M polluted	0.43	U-M polluted	-0.79	Unpolluted	1.82	Moderately
St. 3	Summer	4.81	S-E polluted	0.83	U-M polluted	-0.09	Unpolluted	0.52	U-M polluted	-1.12	Unpolluted	1.63	Moderately
	Autumn	4.93	S-E polluted	0.87	U-M polluted	0.02	U-M polluted	0.64	U-M polluted	-1.05	Unpolluted	1.69	Moderately
	Winter	5.14	E- polluted	0.95	U-M polluted	0.28	U-M polluted	0.77	U-M polluted	-0.82	Unpolluted	1.84	Moderately
	Spring	4.95	S-E polluted	0.88	U-M polluted	0.07	U-M polluted	0.65	U-M polluted	-0.88	Unpolluted	1.78	Moderately
St. 4	Summer	4.65	S-E polluted	0.50	U-M polluted	-0.14	Unpolluted	0.14	U-M polluted	-1.27	Unpolluted	1.45	Moderately
	Autumn	4.73	S-E polluted	0.66	U-M polluted	-0.05	Unpolluted	0.17	U-M polluted	-1.31	Unpolluted	1.49	Moderately
	Winter	4.83	S-E polluted	0.80	U-M polluted	0.24	U-M polluted	0.43	U-M polluted	-1.12	Unpolluted	1.69	Moderately
	Spring	4.75	S-E polluted	0.72	U-M polluted	0.05	U-M polluted	0.34	U-M polluted	-0.94	Unpolluted	1.61	Moderately
St. 5	Summer	4.54	S-E polluted	0.44	U-M polluted	-0.38	Unpolluted	-0.13	Unpolluted	-1.39	Unpolluted	1.36	Moderately
	Autumn	4.66	S-E polluted	0.47	U-M polluted	-0.34	Unpolluted	-0.01	Unpolluted	-1.48	Unpolluted	1.39	Moderately
	Winter	4.78	S-E polluted	0.52	U-M polluted	-0.13	Unpolluted	0.47	U-M polluted	-1.25	Unpolluted	1.58	Moderately
	Spring	4.68	S-E polluted	0.51	U-M polluted	-0.29	Unpolluted	0.19	U-M polluted	-1.07	Unpolluted	1.45	Moderately
St. 6	Summer	4.21	S-E polluted	0.22	U-M polluted	-0.45	Unpolluted	-0.29	Unpolluted	-0.83	Unpolluted	1.29	Moderately
	Autumn	4.21	S-E polluted	0.34	U-M polluted	-0.47	Unpolluted	-0.25	Unpolluted	-0.71	Unpolluted	1.33	Moderately
	Winter	4.43	S-E polluted	0.43	U-M polluted	-0.13	Unpolluted	0.18	U-M polluted	-0.75	Unpolluted	1.51	Moderately
	Spring	4.33	S-E polluted	0.42	U-M polluted	-0.26	Unpolluted	-0.06	Unpolluted	-1.20	Unpolluted	1.51	Moderately
Mean		4.58		0.66		-0.01		0.26		-1.01		1.65	

M-S Polluted: Moderate-Strongly Polluted, U-M Polluted: Unpolluted-Moderately Polluted, S-E Polluted: Strongly-Extremely Polluted, E-polluted: Extremely Polluted

Table 5. Mean concentrations (µg g^{-1}) and stander division in tow studied species in the period from summer 2019 to spring 2020 (Mean ± SD)

Metals	Aquatic plants	Seasons					
		Summer	Autumn	Winter	Spring	Mean Conc. (µg g^{-1})	± SD
Cd	*T. domingensis*	0.31	0.36	0.45	0.40	0.38	0.06
	P. australis	0.35	0.38	0.54	0.42	0.42	0.08
Cr	*T. domingensis*	3.66	3.87	4.13	4.1	3.94	0.22
	P. australis	3.26	3.84	4.54	4.2	3.96	0.55
Ni	*T. domingensis*	3.58	4.12	5.2	4.93	4.46	0.74
	P. australis	4.52	4.44	5.68	4.92	4.89	0.57
Pb	*T. domingensis*	9.35	6.13	7.12	6.87	7.37	1.39
	P. australis	5.49	6.31	7.25	6.89	6.49	0.77
Cu	*T. domingensis*	2.11	2.15	3.01	2.65	2.48	0.43
	P. australis	1.76	2.01	2.98	2.03	2.20	0.54
Zn	*T. domingensis*	1.43	1.98	2.16	2.01	1.90	0.32
	P. australis	1.98	2.32	3.01	2.87	2.55	0.48

Table 6. Bioconcentration factor (BCF) of heavy metals in two studied aquatic plants

Plant species	Metals	Metals Conc. (µg g^{-1})		BCF (%)
		Plant	Sediment	
T. domingensis	Cd	0.38	35.97	1.06
	Cr	3.94	102.71	3.84
	Ni	4.46	109.68	4.06
	Pb	7.37	54.63	13.49
	Cu	2.48	58.65	4.23
	Zn	1.90	78.25	2.42
P. australis	Cd	0.42	35.97	1.17
	Cr	3.96	102.71	3.86
	Ni	4.89	109.68	4.46
	Pb	6.49	54.63	11.87
	Cu	2.20	58.65	3.74
	Zn	2.55	78.25	3.25

Two species vary in abilities of heavy metals accumulation in their tissue, that is due to many factors as the quality of water, growth form of plant and pollution origin (Habeeb et al 2015). Wetland sediments are a basin for receiving and storing heavy metals, so must be observed continuously (Das and Maiti 2008). The high values of heavy metals in sediments as compared with plants, is due to the tendency of these metals to accumulate in the phytoplankton, plants and aquatic organisms (Sasaki et al 2003), and the reduse flow rate of water in marsh allows sufficient time to precipitate of suspended matter which have concentration to the sediments, this is confirmed by a study of Mashkhool (2012).

CONCLUSIONS

This study concluded that studied emergent aquatic macrophytes have ability to concentration some of heavy metal. In sediments the concentrations of heavy metals in the residual phase were higher than that exchangeable. According to I-geo values, the sediment of Al-Hammar marsh was considered as unpolluted with Pb and Zn, and to moderately unpolluted with Cr and Cu. But, moderately polluted with Ni to strongly pollute with Cd.

REFERENCES

Al-Atbee RSK 2018. *Assessment of Some Heavy Elements and Hydrocarbons in the Water, Sediments and Dominant Aquatic Plants at Al-Chibayish marshes.* M.Sc. Thesis, College of Science, University of Basrah pp. 208.

Al-Hejuje MM 2014. *Application of water quality and pollution indices to evaluate the water and sediments status in the middle part of Shatt Al-Arab River.* Ph.D. Thesis, Biology Department, College of Science, University of Basrah p. 239.

Al-Hussieny A and Thijar L 2016. Thirty-eight new records for Algal Species of Iraq's Marshes. *Open Access Library Journal* **3**: 1-16.

Al-Khafaji BY 2015. Comparison in accumulations of heavy metals in two species of aquatic plants in Al-Chibayish marsh south of Iraq. *Marsh Bulletin* **10**(2): 112-122.

Al-Khafaji SJ and Jalal GK 2020. Spatial characteristics and heavy metals pollution in urban soils of Basrah, Iraq. *Indian Journal of Ecology* **47**(4): 969-978.

Al-Mur BA 2020. Geochemical fractionation of heavy metals in sediments of the Red Sea, Saudi Arabia. *Oceanologia* **62**(1): 31-44.

Alobaidi KH, Oraibi AG, Yahya HN and Al-Obaidi JR 2020. Phytoremediation of zinc ion using faba bean plant *Vicia faba* in vitro. *Indian Journal of Ecology* **47**(4): 965-968.

Al-Shamsi ZSR 2017. *Heavy metals in sediments core along the Shatt Al-Arab Estuary.* M.Sc. thesis, College of Science, University of Basrah p. 130.

Al-Taie EOA 2013. *Evaluation of Pollution in the Hor Al-Azim Sediments by hydrocarbons and Heavy Metals, Missan*

Government, South of Iraq. M.Sc. thesis, College of Sciences, University of Basrah p. 125.

Al-Yasari WAK, Al-Nafie RI and Al-Yaseen BM 2020. Effect of copper concentrations on some biochemical properties of the *Cladophora*. *Indian Journal of Ecology* **46**(8): 31-35.

Aydin-Onen S, Kucuksezgin F, Kocak F and Açik S 2015. Assessment of heavy metal contamination in *Hediste diversicolor* (O.F. Müller 1776), *Mugil cephalus* (Linnaeus 1758), and surface sediments of Bafa Lake (Eastern Aegean). *Environmental Science and Pollution Research* **22**: 8702-8718.

Barman SC, Sahu RK, Bhargava SK and Chatterjee C 2000. Distribution of heavy metals in wheat, mustard and weed grains irrigated with industrial effluents. *Bulletin of Environmental Contamination and Toxicology* **64**: 489-496.

Bdewi SY, Al-Mahdawi MM and Shrtooh SM 2019. A comparative study among three species of aquatic plants in the ability of absorption and bio-accumulation of some heavy metals on Euphrates river in Al-Ramadi city. *Plant Archives* **19**: 86-93.

Brankovic S, Muratspahic D, Topuzovic M, Glisic R, Milivojevic J and Dekic V 2011. Metals concentration and accumulation in several aquatic macrophytes. *Biotechnology & Biotechnological Equipment* **26**(1): 2731-2736.

CBSQG Consensus-Based Sediment Quality Guidelines of Wisconsin 2003. *Consensus-Based Sediment Quality Guidelines; Recommendations for Use and Application Interim Guidance*. Department of Natural Resources, Wisconsin, *December* p. 35.

Chester R and Voutsinou FG 1981. The initial assessment of trace metal pollution in coastal sediments. *Marine Pollution Bulletin* **12**(3): 84-91.

DalCorso G, Fasani E, Manara A, Visioli G and Furini A 2019. Heavy metal pollutions: State of the art and innovation in phytoremediation. *International Journal of Molecular Sciences* **20**(14): 3142.

Das M and Maiti SK 2008. Comparison between availability of heavy metals in dry and wetland tailing of an abandoned tailing bond. *Environmental Monitoring and Assessment* **137**(3): 343-350.

Dipu S, Kumar AA and Thanga SG 2012. Effect of chelating agents in phytoremediation of heavy metals. *Remediation Journal* **22**(2): 133-146.

Goswami M, Goswami K, Chalapathy CV, Shivasharanappa K, Kalva PK and Patil SJ (2020). Physicochemical properties and heavy metal analysis of Avalahalli Lake, Bengaluru, Karnataka, India. *Indian Journal of Ecology* **47**(4): 917-923.

Habeeb MA, Al-Bermani AK and Salman JM 2015. Environmental study of water quality and some heavy metals in water, sediment and aquatic macrophytas in lotic ecosystem, Iraq. *Mesopotamia Environmental Journal* **1**(2): 66-84.

Hassan FM, Saleh MM and Salman JM 2010. A study of physicochemical parameters and nine heavy metals in the Euphrates River, Iraq. *Journal of Chemistry* **7**(3): 685-692.

Lu Q, He ZL, Graetz DA, Stoffella PJ and Yang X 2011. Uptake and distribution of metals by water lettuce (*Pistia stratiotes* L.). *Environmental Science and Pollution Research* **18**(6): 978-986.

Mashkhool MA 2012. *Concentrations of some heavy metals in water, sediments and two types of plants in Al-Chibayish Marsh in Thi-Qar province in southern Iraq*. M.Sc. Thesis, School of Geography, University of Queensland, Australia, p. 79.

Mehmood MA, Qadri H, Bhat RA, Rashid A, Ganie SA, Dar GH and Shafiq R 2019. Heavy metal contamination in two commercial fish species of a trans-Himalayan freshwater ecosystem. *Environmental Monitoring and Assessment* **191**: 104.

Müller G 1969. Index of geoaccumulation in sediments of the Rhine River. *Geological Journal* **2**(3): 108-118.

Farkas A, Erratico C and Viganò L 2007. Assessment of the environmental significance of heavy metal pollution in surficial sediments of the River Po. *Chemosphere* **68**: 761-768.

Sasaki K, Ogino T, Hori O, Endo Y, Kurosawa K and Tsunekawa M 2003. Chemical transportation of heavy metals in the constructed wetland impacted by acid drainage. *Materials Transactions* **44**(2): 305-312.

Singh N, Kaur M and Katnoria JK 2017. Analysis on bioaccumulation of metals in aquatic environment of Beas River Basin: A case study from Kanjli wetland. *Geo. Health* **1**: 93-105.

Sturgeon RE, Desaulniers JAH, Berman SS and Russell DS 1982. Determination of trace metals in estuarine sediments by graphite furnace atomic absorption spectrometry. *Analytica Chimica Acta* **134**: 288-291.

Tylmann W, Lysek K, Kinder M and Pempkowiak J 2011. Regional pattern of heavy metal content in Lake sediments in Northern Poland. *Water, Air, & Soil Pollution* **216**: 217-228.

Tytla M and Kostecki M 2019. Ecological risk assessment of metals and metalloid in bottom sediments of water reservoir located in the key anthropogenic “hot spot” area (Poland). *Environmental Earth Sciences* **78**(5): 179.

UNEP (United Nations Environmental Program) 2006. *UNEP project on support for environmental management of the Iraqi marshlands. International Environmental Technology Centre* p. 21.

Varol M and Şen B 2012. Assessment of nutrient and heavy metal contamination in surface water and sediments of the upper Tigris River, Turkey. *CATENA*.

Vukosav P, Mlakar M, Cukrov N, Kwokal Z, Pizeta I and Pavlus N 2014. Heavy metal contents in water, sediment and fish in a karst aquatic ecosystem of the Plitvice Lakes National Park (Croatia). *Environmental Scientific Pollution Research International* **21**(5): 3826-3839.

Wilson B and Pyatt FB 2007. Heavy metal bioaccumulation by the important food plant, *Olea europaea* L., in an ancient metalliferous polluted area of Cyprus. *Bulletin of Environmental Contamination and Toxicology* **78**(5): 390-394.

Yan W, Yihui Z, Yanling Q, Da C, Zhiliang Z, Jianfu Z and Åke B 2017. Occurrence and risk assessment of trace metals and metalloids in sediments and benthic invertebrates from Dianshan Lake, China. *Environmental Science Pollution Research* **24**: 14847-14856.

Received 20 August, 2021; Accepted 20 November, 2021

Indian Journal of Ecology (2021) 48(6): 1887-1890

Manuscript Number: 3466
NAAS Rating: 5.79

Combined Effect of Antibiotics and Copper on Catalase of Haplic Chernozem

D. Trufanov, S. Kolesnikov, Yu. Akimenko, T. Minnikova* and K. Kazeev

Southern Federal University, Academy of Biology and Biotechnology, Rostov-on-Don, Russia
**E-mail: loko261008@yandex.ru*

Abstract: The purpose of this study is to assess the influence combined effect antibiotics (oxytetracycline, tylosin) and copper (Cu) on catalase activity of Haplic Chernozem. A model experiment on the pollution of Haplic Chernozem with antibiotics and Cu was carried out in laboratory conditions. Bactericidal antibiotic oxytetracycline (OTC), bacteriostatic antibiotic tylosyn (TyL) and Cu were chosen to study the combined effect of antibiotics and heavy metals on catalase activity of Haplic Chernozem. In present study, the combined effect antibiotics and heavy metal on catalase activity of Haplic Chernozem was studied after the 30-days exposure. Two treatments of single OTC and TyL (1, 10, 100 mg kg^{-1}), two treatments of single Cu (100 mg kg^{-1}), two treatments of combined OTC and Cu (1, 10, 100 mg kg^{-1} and 100 mg kg^{-1}), two treatments o combined TyL and Cu (1, 10, 100 mg kg^{-1} and 100 mg kg^{-1}) and a control treatment with equal deionized water were performed in laboratory experiments. It is defined, that the combined effects antibiotics and Cu has a more negative influence on catalase activity of Haplic Chernozem than the individual effect of antibiotic or heavy metal. Copper makes a more contribution to the inhibition on activity of catalase than antibiotics in the combined effect.

Keywords: Oxytetracyline, Tylosin, Copper, Haplic chernozem, Enzymes

In past few years, concern increased to combined effect of antibiotics and heavy metals on soils. Despite the great interest to this problem, however, the consequences of this exposure are poorly studied. Nowadays, a lots of research of the combined effect antibiotics and heavy metals is carrying on. Some of this studies are showed the toxic influence of combined effect on soil environment, in particular on soil microorganisms and their genetic structure (Gao et al 2016, Kong et al 2006, Wang et al 2018, Xu et al 2016). In most cases, antibiotics are released into agricultural soils due to continued land application of manure for fertilizing and when using wastewater for irrigation agricultural fields (Wang et al 2014, Hou et al 2015). Residual antibiotics in agricultural soils are usually detected at high levels reaching up to the order of mg kg^{-1} (Xu et al 2016). Some heavy metals and metalloids (Cu, Zn, Co, Fe, Mn and Se) are widely applied into animal husbandry and poultry feed to maintain various physiological processes and prevent animal diseases. Since not all these elements added in the diet are assimilated by the animals, increasing concentrations of these elements have been observed in livestock manure (Sager 2007). The antibiotics and heavy metals both individual and combined effect could cause changes in the properties of soil microbial community structure such as biomass, population, metabolism, size, composition and activity (Sandaa et al 2001, Joynt et al 2006, Gomes et al 2010, Wang et al 2007). Soil microorganisms play important roles in many ecosystem processes such as biogeochemical cycling of nutrients, soil structural and hydrological properties and energy flow (Wang et al 2018) and are also sensitive to antibiotics and heavy metals and are often used as indicators of soil quality, health and fertility (Valclavik et al 2004). In studying the effect of the combined effect of OTC and Cu on the functional structure of microbial soil communities, earlier, it was observed that combined effect OTC and Cu in high concentrations was negative influenced on the studied indicator (Kong et al 2006). Due to this fact, important functions of microbial communities, such as decomposition of residues, etc., can be reduced in soils that have been contaminated by antibiotics and heavy metals (Kong et al 2006). The combined and individual effects of enrofloxacin and cadmium on soil microbial biomass and the ammonia-oxidizing functional gene observed (Xu et al 2016). The investigated concentrations of the antibiotic were 10 and 100 mg kg^{-1}, and the concentration of the heavy metal was 20 and 200 mg kg^{-1}. Both individual and combined pollution by enrofloxacin and cadmium were demonstrated different levels of inhibitory action on bacteria, fungi and actinomycetes, also, the inhibitory effect increased with increasing concentration. The toxicity of combined effects of enrofloxacin and cadmium was detected, and toxicity was more than that of pollutants, acting individually.

Catalase is an intracellular enzyme found both in aerobic and anaerobic bacteria (Trasar-Cepeda et al 2000, Shiyin et al 2004). Catalase has a protection function connected with the decomposition of hydrogen peroxide to prevent accumulation of toxic peroxides in the cell (Zhang et al 2008). The individual effect both heavy metals and antibiotics has a negative influence on catalase (Gao et al 2008, Stepniewska et al 2009). It is necessary to study comprehensive the combined effect of antibiotics and heavy metals on the biological properties of the soils, using not only microbiological indicators, but also with other sensitive and informative biological indicators of the state and function of soils, e.g. biochemical indicators. The presentstudy is to assess the influence combined effect antibiotics (oxytetracycline, tylosin) and Cu on catalase activity of Haplic Chernozem. The objective of investigation is to determine the regularities of the influence combined effect of antibiotics and Cu on activity of catalase of Haplic Chernozem and to define the contribution of each of the pollutants to the change in this indicator.

MATERIAL AND METHODS

Soil samples: The soil for the study was classified as Haplic Chernozemand with no history of manure application was collected from the Botanical Garden of the Southern Federal University, Rostov on Don, Russia (47◦14017.54" N, 39◦38033.22" E). This soil type was characterized as a heavy loam granulometric composition, an average organic matter content of 3.7% and pH_{H2O} = 7.8 (nearly neutral). The upper soil layer (0–20 cm.) was studied to assess the combined effect of antibiotics and Cu on the activity of catalase. A model experiment on the pollution of Haplic Chernozem with antibiotics and Cu was carried out in laboratory conditions.

Features of the used antibiotics and heavy metal: Bactericidal antibiotic oxytetracycline (OTC), bacteriostatic antibiotic tylosyn (TyL) and heavy metal copper (Cu) were chosen to study the combined effect of antibiotics and heavy metals on catalase activity of Haplic Chernozem. These antibiotics are widely used for the control of intestinal and respiratory infections of animal in intensive farming systems (Boxall et al 2003, Li et al 2011, Xu et al 2015). Cu was in water soluble form ($CuSO_4 \cdot 5H_2O$) and is also widely used in agriculture. Copper concentrations are high in soils because of the input of agricultural chemicals containing Cu and the use of Cu in animal feed as growth promoter (Sager 2007).

Soil treatment with antibiotics and Cu: In present study, the combined effect antibiotics and heavy metal on catalase activity of Haplic Chernozem was studied after the 30-days exposure. Two treatments of single OTC and TyL (1, 10, 100 mg kg^{-1}), two treatments of single Cu (100 mg kg^{-1}), two treatments of combined OTC and Cu (1, 10, 100 mg kg^{-1} and 100 mg kg^{-1}), two treatments o combined TyL and Cu (1, 10, 100 mg kg^{-1} and 100 mg kg^{-1}) and a control treatment with equal deionized water were performed in laboratory experiments. These concentrations were selected based on the previously obtained results (Akimenko et al 2015). This Cu concentration was chosen, because initial negative effect was noted beginning with that amount (Kolesnikov et al 2000). Water-soluble forms of antibiotics and Cu were used and were introduced in the form of solutions. The soil was placed in vegetative pots. Haplic Chernozem with contaminants was incubated under temperature of air (22–25°C) and soil moisture (60%).

Measurement procedures: The enzyme activity was measured by the gasometric method by the rate of decomposition of 5% hydrogen peroxide after contact with the soil (temperature of air - 20–22 °C). This biological indicator was chosen due to the fact that activity of catalase reflects the intensity of the processes of mineralization of organic substances in the soil and serves to assess the potential biological activity of soils. Analytical measurements were carried out in triplicate.

Statistical analyses: An analysis of the rate of variation (standard deviation) at $p \leq 0.05$ to determine the reliability of the results. Statistical data processing was carried out using Statistica 12.0. The data from interaction between antibiotics and Cu were compared by two-way analysis of variance with the Statistica 12.0.

The contribution of each factors was calculated using Equation:

$$E_x = \frac{SS_x \times 100}{SS_{total}}$$

where, E_x – the factor contribution; SS_x – sums of squares of factor A or B; SS_{total} – total sum of squares.

RESULTS AND DISCUSSION

A reliable dose-response relationship between the concentration of the antibiotic and the degree of decrease catalase activity is established only in OTC effect, catalase activity decreases from 7% to 20% relative to the control (Fig. 1). Cu causes the inhibition of catalase activity by 44% relative to the control. It is defined, that combined effects antibiotics and Cu has a more negative influence on catalase activity of Haplic Chernozem than individual effect of antibiotic, but less than that of heavy metal. The Dose-response relationship between the concentration of the antibiotic and the degree of decrease catalase activity is not observed both individual and combined effects of antibiotic. The individual effect of TyL cases indicated the decrease of catalase activity by 19-22% relative to the control. The

combined effect of TyL and Cu inhibits enzymatic activity by 33-34% relative to the control (Fig. 2). Previous studies shown the negative influence of the combined effects of antibiotic and heavy metals on soil microorganisms The combined effect of OTC and Cu had negative impacts on the total number of bacteria, actinomycetes and functional diversity of soil microbial communities (Kong et al 2006, Gao et al 2016, Xu et al 2016, Wang et al 2018). It is established, that the combined effect of antibiotic and heavy metal on catalase activity is more than individual effect of OTC or TyL.

The individual and combined exposure of sulfadiazine and Cu also had a significant influence on soil microbial activity, biomass, and community structure (Xu et al 2016). *Eisenia fetida* was used as test organism to define behavior in OTC and heavy metal-contaminated soils and tried to avoid combined exposure more than individual heavy metal or antibiotic contamination It was also documented that the combined exposure of antibiotics and heavy metals had a more negative effect on the functions of the soil microbial community and enzymatic activities (Kong et al 2013 and Gao et al 2016). There was the interaction between heavy metal and both antibiotics. The higher the concentration of the antibiotic, the more pronounced interaction with the heavy metal and accordingly the most effect of inhibition of catalase activity is observed. The contribution of Cu to the interaction with OTC and TyL was 72 and 68% respectively. The contribution of OTC and TyL was 10 and is 4%. The contribution of the interaction of factors in combined effect of Cu with OTC or TYL was 17 and 26% respectively.

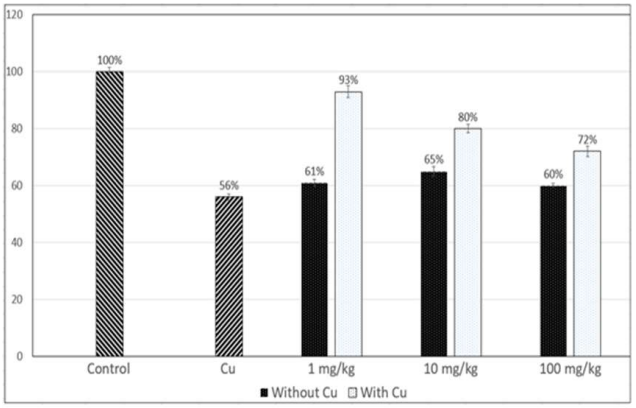

Data are means of three replicate biological samples. Error bars show least significant difference (LSD) at $p \leq 0.05$ level

Fig. 1. Combined effect of OTC and Cu on activity of catalase of Haplic Chernozem, % of the control

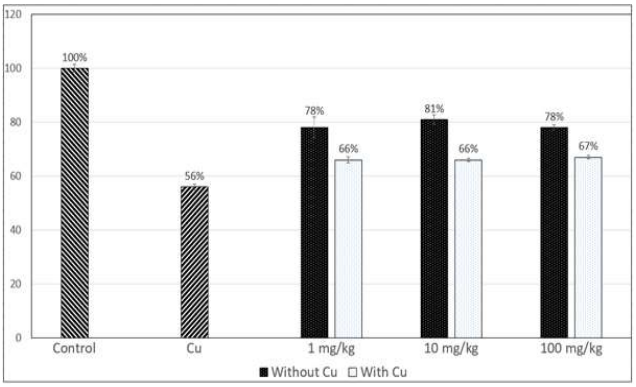

See Figure 1 for details

Fig. 2. Combined effect of TyL and Cu on activity of catalase of Haplic Chernozem, % of the control

CONCLUSIONS

The combined effects antibiotics and Cu has a more negative influence on catalase activity of Haplic Chernozem than individual effect of antibiotic, but less than that of heavy metal. Cu makes a more contribution to the inhibition of catalase activity than antibiotics in combined effect. The contribution is 72%, when Cu interacts with OTC and 68% with TyL. A reliable dose-response relationship between the concentration of the antibiotic and the degree of decrease catalase activity is established only in OTC effect, unlike in TyL effect and complexes of these antibiotics with Cu.

ACKNOWLEDGEMENTS

The study was carried out with the support of the Ministry of Science and Higher Education of the Russian Federation within the framework of a state assignment (Southern Federal University, project No. 0852-2020-0029) and state support of the leading scientific schools of the Russian Federation (grant of the President of the Russian Federation No. SSh-2511.2020.11).

REFERENCES

Akimenko Yu V, Kolesnikov SI and Kazeev K Sh 2015. Environmental impact assessment of tylosin and nystatin on biological properties of chernozem. *International Multidisciplinary Scientific GeoConference Surveying Geology and Mining Ecology Management* (Book 3, vol. 2) ed. Alexander Malinov (NY: Curran Associates) 131-138.

Boxall ABA, Kolpin DW and Tolls J 2003. Are veterinary medicines causing environmental risks? *Environmental Science and Technology* **37**(15): 287A-294A.

Galstyan AS 1978 Unification of methods for studying the activity of soil enzymes. *Eurasian Soil Science* **2**: 107-113.

Gao Y, Sun X, Sun Z, Zhao N and Li Y 2008. Toxic effects of enrofloxacin on growth rate and catalase activity in *Eisenia fetida*. *Environmental Toxicology and Pharmacology* **26**(2): 177-180.

Gao M, Song W, Zhou Q, Ma X and Chen X 2013. Interactive effect of oxytetracycline and lead on soil enzymatic activity and microbial biomass. *Environmental Toxicology and Pharmacology* **36**(2): 667-674.

Gao M, Lva M, Hanc M, Songa W and Wang D 2016. Avoidance behavior of *Eisenia fetida* in oxytetracycline and heavy metal-contaminated soils. *Environmental Toxicology and Pharmacology* **47**: 119-123.

Gomes NCM, Landi L, Smalla K, Nannipieri P, Brookes PC and Renella G 2010. Effects of Cd- and Zn-enriched sewage sludge on soil bacterial and fungal communities. *Ecotoxicology and Environmental Safety* **73**(6): 1255-1263.

Hou J, Wan WM, Mao DQ, Wang C, Mu QH, Qin SY and Luo Y 2015. Occurrence and distribution of sulfonamides, tetracyclines, quinolones, macrolides, and nitrofurans in livestock manure and amended soils of Northern China. *Environmental Science and Pollution Research* **22**(6): 4545-4554.

Joynt J, Bschoff M, Turco R, Konopka A and Nakatsu CH 2006. Microbial Community Analysis of Soils Contaminated with Lead, Chromium and Petroleum Hydrocarbons. *Microbial Ecology* **51**(2): 209-219.

Kolesnikov SI, Kazeev KS and Val'kov VF 2000. Effects of heavy metal pollution on the ecological and biological characteristics of common chernozem. *Russian Journal of Ecology***31**(3): 174-181.

Kolesnikov SI, Yaroslavtsev MV, Spivakova NA and Kazeev K Sh 2013. Comparative assessment of the biological tolerance of chernozems in the south of Russia towards contamination with Cr, Cu, Ni, and Pb in a model experiment enzymes. *Eurasian Soil Science* **46**(2): 176-181.

Kong WD, Zhu YG, Fu B, Marschner P and He J 2006. The veterinary antibiotic oxytetracycline and Cu influence functional diversity of the soil microbial community. *Environmental Pollution* **143**(1): 129-137.

Li YW, Wu XL, Mo CH, Tai YP, Huang XP and Xiang L 2011. Investigation of Sulfonamide, Tetracycline, and Quinolone Antibiotics in Vegetable Farmland Soil in the Pearl River Delta Area, Southern China. *Journal of Agricultural and Food Chemistry* **59**(13): 7268-7276.

Sager M 2007. Trace and nutrient elements in manure, dung and compost samples in Austria. *Soil Biology and Biochemistry* **39**(6): 1383-1390.

Sandaa RA, Torsvik V and Enger 2001. Influence of long-term heavy-metal contamination on microbial communities in soil. *Soil Biology and Biochemistry* **33**: 287–295.

Received 12 September, 2021; Accepted 30 November, 2021

Shiyin L, Lixiao N, Panying P, Cheng S and Liansheng W 2004. Effects of pesticides and their hydrolysates on catalase activity in soil. *Bulletin of Environmental Contamination Toxicology* **72**(3): 600-606.

Stepniewska Z, Wolinska A and Ziomek J 2009. Response of soil catalase activity to chromium contamination. *Journal of Environmental Sciences* **21**(8): 1142-1147.

Trasar-Cepeda C, Leiros MC, Seoane S and Gil-Sotres F 2000. Limitations of soil enzymes as indicators of soil pollution. *Soil Biology & Biochemistry* **32**(13): 1876-1875.

Vaclavik E, Halling-Sørensen B and Ingerslev F 2004. Evaluation of manometric respiration tests to assess the effects of veterinary antibiotics in soil. *Chemosphere* **56**(7): 667-676.

Wang YP, Shi JY, Wang H, Lin Q, Chen XC and Chen YX 2007. The influence of soil heavy metals pollution on soil microbial biomass, enzyme activity, and community composition near a copper smelter. *Ecotoxicology and Environmental Safety* **67**(1): 75-81.

Wang FH, Qiao M, Su JQ, Chen Z, Zhou X and Zhu YG 2014. High throughput profiling of antibiotic resistance genes in urban park soils with reclaimed water irrigation. *Environmental Science & Technology* **48**(16): 9079-9085.

Wang L, Wang J, Zhu L and Wang J 2018. Toxic effects of oxytetracycline and copper, separately or combined, on soil microbial biomasses. *Ecotoxicology and Environmental Safety* **40**(2): 763-776.

Xu Y, Yu W, Ma Q and Zhou H 2015. Occurrence of (fluoro) quinolones and (fluoro) quinolone resistance in soil receiving swine manure for 11 years. *Science of The Total Environment* **530**: 191-197.

Xu Y, Yu W, Ma Q, Wang J, Zhou H and Jiang C 2016. The combined effect of sulfadiazine and copper on soil microbial activity and community structure. *Ecotoxicology and Environmental Safety* **134**: 43-52.

Zhang X and Jin J 2008. Binding analysis of pazufloxacin mesilate to catalase using spectroscopic methods. *Journal of Molecular Structure* **882**: 96-100.

Indian Journal of Ecology (2021) 48(6): 1891-1895

Manuscript Number: 3467
NAAS Rating: 5.79

Evaluating the Potential of Vetiver Grass [*Chrysopogon zizanioides* (L.)] and Organic Amendments for Restoration of Tannery Effluent Contaminated Soil

R. Rizam, K. Suganya*, V. Davamani, R. Anandham[1] and M. Maheswari

Department of Environmental Sciences, [1]Department of Agricultural Microbiology
Tamil Nadu Agricultural University, Coimbatore-641 003, India
**E-mail: suganya.k@tnau.ac.in*

Abstract: Vetiver grass [*Chrysopogon zizanioides* (L.)], a perennial C_4 grass is prized for its aromatic essential oil found in the roots. Vetiver has gained international recognition as a natural remedy for various environmental issues, including the detoxification of deteriorated soil. Coupling of organic amendments such as vermicomposting, farmyard manure and biocompost with vetiver were assessed. The effectiveness of vetiver soil amended with vermicompost (5 t ha^{-1}) + 100% STCR (T_3) exhibited vast growth and reduced salinity. The ratio of K/Na (>1) of vetiver shoot was 11.21 for T_3 while a least ratio was observed for root (K/Na = 1.22). Vetiver exhibited a high K^+ and low Na^+ levels under salt stress and a higher $S_{K/Na}$ ratio (9.99) in T_3 was obtained favouring K accumulation than Na in shoot. Based on the study, it was evident that vetiver grass is a potential candidate for restoring tannery sites that have been contaminated with high amounts of salts and other pollutants.

Keywords: Vetiver grass (*Chrysopogon zizanioides)*, Tanneries, Vermicompost, Salinity

Soil pollution has become a serious environmental concern on a global scale, and human beings are the primary cause of ongoing soil contamination via industrial and domestic activities. The contaminated soils contain large quantity of heavy metals and recalcitrant compounds that has serious health-related repercussions. The conventional methods utilized for the removal of heavy metals and salts are expensive, time consuming and environmentally devastating. Thus, a cost effective and environment friendly is needed to clean up the pollutants from the contaminated sites. Most of the industries are located in the vicinity of rural, agricultural, and natural areas. The tannery sector is one of the major contributors among various industries and it has been observed that persistent use of Cr-containing wastewater from leather tanning companies in agricultural fields has resulted in high Cr levels in soils and crops grown there (Gravand et al 2021). Tanneries are the oldest and fastest-growing industry in India and categorised as 'Red-most polluting industries'. Around 2161 tanneries process, 500,000 tonnes of hides and 314 tonnes of skins are released per year. Over 1120 tanneries are situated in Vellore, Ranipet, Trichy, Dindugal, Erode, and Chennai districts of Tamil Nadu (Noorjahan 2014). Phytoremediation is an alternative technology that utilizes plants for the removal of pollutants from the contaminated soils and promoted as a cost-effective, aesthetically appealing, and economically advantageous remedial method (Ramos-Arcos et al 2021). Several plants have been studied over the years, with reports indicating that Vetiver grass *Vetiveria zizanioides* (Linn) is one of the most promising and fast growing with the ability to adapt and tolerate to a wide range of environmental conditions and stress in soils. It is a graminaceous perennial plant native to the tropics and subtropics. Vetiver is distinguished by its robust and extensive root system, which could reach a depth of 5 metres in tropical conditions (Sinha et al 2013). The plant's broad, thick, and deep root system, with tensile strength of 1/6 that of mild steel gives it an edge in adapting to a variety of environmental stressors including drought, flood, high temperatures, heavy metals, acidity and alkalinity, and salt stress (Mickovski et al 2005). Vetiver grass is currently being used to remediate saline soil. In rain-fed agriculture, deep-rooted perennial grasses in rotation with annual crops may help maintain the balance between water use and rainfall, preventing salts from reaching the surface (Liu et al 2016a). The present study investigated the potential application of Vetiver in phytoremediation of soils contaminated with tannery effluent. The salt uptake in shoots and roots of Vetiver plant has been investigated. In addition, the efficacy of different amendments such as vermicompost, Biocompost and farm yard manure on vetiver growth was evaluated in this study.

MATERIAL AND METHODS

Experiment details: The field experiment was carried out at

tannery effluent contaminated site at Brahma Peria Agraharam, Erode district (11°22'14.897" N, 77°42'27.443" E) using Vetiver (*Chrysopogon zizanioides*) of variety Samridhi. The field trial was subjected to eight different treatments with randomized block design. The treatments includes, T_1 (Control), T_2 (Soil Test Crop Response (STCR) based application), T_3 (vermicompost @ 5 t ha^{-1} + 100% STCR), T_4 (vermicompost @ 5 t ha^{-1} + 50% STCR), T_5 (Biocompost @ 5 t ha^{-1} + 100% STCR), T_6 (Biocompost @ 5 t ha^{-1} + 50% STCR), T_7 (FYM@ 12.5 t ha^{-1} + 100% STCR), and T_8 (FYM@ 12.5 t ha^{-1} + 50% STCR).

Sample collection: The soil samples were collected from the tannery effluent contaminated site at B.P. Agraharam, Erode district. The collected soil samples were shade dried, sieved (0.2 mm) and stored in air tight containers. The physical and chemical properties of the soil and effluent were carried out using standard analytical procedure. The vetiver samples (shoot and root) were collected at 60th and 180th day for the analysis. The collected plant samples were oven dried at the temperature between 60° and 70° C. The dried samples were stored in airtight containers for further analysis.

Determination of physico-chemical characteristics of tannery contaminated soil and the vetiver plant: The pH and Electrical Conductivity (EC) of the soil were determined by a glass electrode using water suspension ratios of 1:2.5 (w/v) (Jackson 1973). The initial physicochemical parameters of soil, including available nitrogen (N), available phosphorus (P), and available potassium (K) were estimated. The alkaline permanganate method was used to determine available N (Prasad 1965). Available P was estimated using the sodium hydrogen carbonate ($NaHCO_3$) extract colorimetric method (Braun et al 2019) and available K through mixing neutral normal ammonium acetate with soil and measuring the filtrate using flame photometer (Ma et al 2020). Total (N, P, K, and Na) were assessed in plant samples collected from the tannery contaminated site. Total N was determined using the diacid extract (5:2 – H_2SO_4:$HClO_4$) method using a semi-automatic kjeldahl distillation unit (U.S. Environmental Protection Agency, 1993). Total P was determined from Triacid extract (9:2:1 -HNO_3:H_2SO_4:$HClO_4$) by following the Vanadomoybdate colorimetric method using UV-Visible Spectrophotometer (Shimadzu UV-1800) while the total K and sodium (Na) was measured from the Triacid extract using flame photometer (Bhatti et al 2016).

Assay of Na^+ and K^+: The Vetiver roots and shoot were rinsed with tap water and then distilled water. The separated roots and shoot were oven dried for 48 hours at 75°C, later crushed and sieved for the estimation. The concentrations of Na^+ and K^+ were determined using 0.2 g of dried plant material. The material was kept in a muffle furnace at 200°C for 30 minutes and subsequently at 550°C for 24 hours, followed by dissolving the obtained ash in 0.2 ml concentrated nitric acid. Later, the extraction volume was raised to 100 ml using double distilled water, and the quantities of Na^+ and K^+ were quantified using the flame photometer (Song et al 2009). The following formula was used to calculate the ability of ion selective transportation ($S_{k/Na}$) (Zhou and Yu 2009):

$$S_{k/Na} = (K^+/ Na^+ \text{ in leaf}) / (K^+/ Na^+ \text{ in root})$$

Statistical analysis: All data in response to the treatments were subjected to one-way analysis of variance. Treatment differences were determined by Duncan's multiple range test at $p < 0.05$ level. The statistical analyses were conducted using SPSS18.0 for windows (SPSS Inc., Chicago, IL, USA).

RESULTS AND DISCUSSION

Initial characteristics of the tannery effluent contaminated soil: The pH was of the soil was alkaline (8.30) with an EC of 3.30 dS m^{-1}. The EC of the soil was moderately high indicating that the soil had considerable amount of soluble salts. The available nitrogen (305 kg ha^{-1}) was in the medium range whereas the available phosphorus (23.9 kg ha^{-1}) and potassium (426 kg ha^{-1}) were high in the range of soil fertility rating. The organic carbon status of the soil was medium (0.42 %).

Changes in physico - chemical characteristics of soil: The pH varied from 8.10 to 8.20 during 60th day and 7.40 to 7.68 on 180th day (Table 1). The EC varied from 2.90 to 2.99 dS m^{-1} in 60th day and 0.87 to 1.79 dS m^{-1} in 180th day. During both 60th and 180th day, no significant variation among the treatments were observed. However, pH and EC significantly decreased from 60th to 180th day in treatments. The, pH and EC showed a decreasing trend in all the treatments indicated the acidifying effect of organic acids produced during microbial metabolism and mineralization of free ions present in the compost and soil, respectively. The pH varied from neutral (180th day) to slightly alkaline (60th day) in all the treatments. The pH of the vermicompost treated vetiver soil on 180th day was neutral to slightly alkaline (7.40), whereas it was alkaline (8.10) during 60th day. The change in pH from alkaline to near neutral is attributed to the production of vetiver root exudates containing significant amount of phenolic acids (Mudhiriza et al 2015). Application of vermicompost in the soil had changed the soil pH favourably compared to the 60th day soil pH (8.30). The production of NH_4^+, CO_2 and the organic acids during higher organic decomposition rate by the microorganisms and their interaction with soil nutrients has decreased the soil pH (T_3). The observations were similar to the effect of vermicompost

on the vetiver growth in presence of gold mine tailings (Laxman et al, 2014). The vermicompost has the potential for treating the tannery contaminated soils. Soil EC in the experimental field soil planted with vetiver grass drastically decreased from 60th to 180th day, indicating that the crop has promising tolerance capacity under salt stress conditions.

Total nitrogen (N), phosphorus (P) and potassium (K) content of the shoot: There was significant difference in N, P and K between the 60th and 180th day in all treatments (Table 2). In T_3, there was a drastic increase in the nutrients (N, P, K) of the plant shoot during the 180th day with values of 4.40 mg kg^{-1}, 1.35 mg kg^{-1}, and 15.50 mg kg^{-1}, respectively. Furthermore, in comparison to other treatments, these parameters are least in the control from 60th to 180th day.

Among the treatments, the N content of the vetiver was 2.80 mg kg^{-1} on 60th day and on 180th day it has been increased to 3.20 mg kg^{-1} in the control whereas, T_3 recorded highest N content of 2.80 mg kg^{-1} and 4.40 mg kg^{-1} at 60th and 180th day respectively. In general, compared to control, all other treatments recorded the highest N content on 180th day. This may due to the fact that the amendments (vermicompost, biocompost, and farmyard manure) applied to the experimental soil has improved the nutrient availability in the soil and thereby increase N content in the vetiver. The impact of changing salinity content on the nitrogen metabolism of vetiver was observed by Liu et al (2016b). The plant's nitrate-nitrogen concentration was higher in vetiver. The dose–effect connection of salt levels on osmotic regulators, nutrient intake, growth, and the viability of transplanting vetivers, however, is little understood. Similar observation was recorded in shoot having increased N concentration with increasing N application rate, reaching a concentration of 2.5% when 10,000 kg ha^{-1} year^{-1} of N was supplied (Anas et al 2020).

The phosphorus content of the plant was 1.30 mg kg^{-1} on the 60th and 180th day in the control, whereas T_3 had the highest P content of 1.30 mg kg^{-1}and 1.35 mg kg^{-1} at the 60th and 180th day, respectively. In general, all other treatments had the greatest P content on the 180th day compared to the control. This may be attributed due to the amendments (Vermicompost, Biocompost, and farmyard manure) which were added to the experimental soil thereby improving the crop's development and nutritional status, as seen by the crop's increased phosphorus content (Gopinath et al 2010). Similarly results of vetiver showed 0.1% of P in the shoot compared to the mature vetiver with 0.15% (Wagner et al 2003). The potassium content of the plant in the control was 9.80 mg kg^{-1} at the beginning and 12.00 mg kg^{-1} at the end,

Table 1. Influence of vetiver grass on pH and EC of the tannery contaminated soil

Treatments	pH		Conductivity (dS m^{-1})	
	60th day	180thday (Final)	60th day	180thday (Final)
T_1	8.20	7.68	2.99	1.70
T_2	8.19	7.59	2.99	1.59
T_3	8.10	7.40	2.90	0.87
T_4	8.12	7.43	2.92	0.95
T_5	8.15	7.47	2.95	1.05
T_6	8.17	7.49	2.96	1.18
T_7	8.17	7.50	2.97	1.27
T_8	8.18	7.54	2.97	1.35
Mean	8.16	7.51	2.95	1.24
CD (p=0.05)	0.25	0.30	1.06	0.09

Table 2. Influence of various amendments in total N, P and K content of the shoot of the vetiver

Treatments	Total nutrients (mg kg^{-1})					
	N		P		K	
	Initial	Final	Initial	Final	Initial	Final
T_1	2.80	3.20	1.30	1.30	9.80	12.00
T_2	2.70	3.40	1.25	1.25	9.85	13.50
T_3	2.80	4.40	1.30	1.35	9.75	15.50
T_4	2.75	4.00	1.35	1.35	9.75	15.00
T_5	2.60	3.80	1.20	1.25	9.80	14.75
T_6	2.80	4.00	1.30	1.30	9.70	14.50
T_7	2.70	3.80	1.30	1.35	9.60	14.50
T_8	2.50	3.70	1.25	1.30	9.75	14.40
Mean	2.70	3.78	15.6	1.30	9.75	265.0
CD (p=0.05)	0.13	0.1772	0.5492	0.0844	0.5450	0.3450

whereas the K content of the T_3 was 9.75 mg kg^{-1} on 60th day and 15.50 mg kg^{-1} on 180th day. In general, when compared to the control, all other treatments had the highest K content on the 180th day. This could be due to the amendments such as vermicompost, biocompost, and farmyard manure applied to the experimental soil, thereby boosting the crop's development and nutritional quality, as seen by the higher potassium content of the crops. The plant maintains a low Na^+ concentration and a concurrent high K^+ concentration in the cytosol, where enzymes for metabolism are located, to avoid an ion homeostasis disorder under saline conditions (Gao et al 2016).

Soil nutrient status: Vetiver grown in the tannery contaminated soil amended with different treatments showed growth potential regardless of pH or salinity (Table 3). Vetiver grew well in the treatments T_2 - T_8. The N (280 kg ha^{-1}), P (20.3 kg ha^{-1}) and K (418 kg ha^{-1}) levels in soil when amended with vermicompost (T_3) were increased than those of control soil due to the higher nutrients absorption potential of vetiver. In addition, the farmyard manure (T_7) registered higher available N (305 kg ha^{-1}), K (505 kg ha^{-1}) and P (17.9 kg ha^{-1}) in the soil compared to other soil amendments. The vermicompost treated tannery effluent contaminated soil, greatly enhanced the growth of *C. zizanioides*. The results were similar to the study carried out using vetiver in the textile contaminated soil (Jayashree et al 2011). It demonstrated that vermicompost and farmyard application had a pronounced influence on vetiver growth in terms of root length, shoot length and chlorophyll content. Vermicompost loosens the contaminated soil and makes the soil texture suitable for root growth.

Na^+ & K^+ assay of the vetiver: The potassium (K) transfer coefficients from roots to shoots were all >1, ranging from 2.40 to 3.54 (Table 4). Similarly, the sodium (Na) transfer coefficient from roots to shoots ranged from 0.24 to 0.88. Just as Na was concentrated in the roots of the vetiver, K was concentrated in the shoots. In vetiver shoots, the ratios of K/Na (>1) tends to increase to a peak at $T_3$with 11.21 and was lower in control (4.65). The K/Na ratios of roots ranged from 1.22 to 1.60, with the control having the highest value (1.60) and T_3having the least (1.22).

The vetiver plants thrived in T_3, suggesting that their shoots and roots contains the most biomass. Salt-tolerant plants have been revealed to have unique systems that helps the cells to regulate osmotic stress. Tolerant plants restrict Na accumulation in the shoots by decreased absorption, reduced root to shoot movement, sodium compartmentalization into vacuoles, and/or salt ejection from the surface. Plants defend themselves from the negative consequences of ionic Na stress by compartmentalising Na in their roots and keeping it out of their leaf tissues. Plants maintain high K^+ and low Na^+ levels under salt stress to reduce the impacts of NaCl (Liu et al 2016b). A higher $S_{K/Na}$

Table 3. Effect of different soil amendments on the soil nutrient status

Treatments	Available nutrients (Kg ha^{-1})		
	N	P	K
T_1	251	12.3	423
T_2	261	14.8	325
T_3	280	20.3	418
T_4	253	12.5	368
T_5	258	23.9	426
T_6	243	16.2	368
T_7	305	17.9	505
T_8	269	17.1	475
Mean	265	16.875	413.5
CD (p=0.05)	12.2476	0.5492	19.6421

Table 4. Na^+ & K^+ assay of the vetiver

Treatments	Transfer coefficients (TC's)		R_{shoot} (K Na^{-1})	R_{root} (K Na^{-1})	S (K Na^{-1})
	Na^+	K^+			
T_1	0.88	2.40	4.65	1.60	2.91
T_2	0.67	2.43	5.03	1.47	3.42
T_3	0.24	3.54	11.21	1.22	9.19
T_4	0.29	3.10	8.97	1.25	7.18
T_5	0.32	2.71	7.99	1.26	6.34
T_6	0.37	2.65	6.83	1.31	5.21
T_7	0.44	2.53	6.41	1.33	4.82
T_8	0.54	2.47	5.78	1.37	4.22
Mean	2.0	1.1	7.10	1.35	5.41
CD (p=0.05)	0.0906	0.0557	1.2353	0.0896	0.2726

ratio indicates that the K/Na ratio in leaves is more important, favouring K accumulation than Na. $S_{K/Na}$ ratio was greater in all treatments compared to control, indicating that vetiver's NaCl tolerance is attributable to Na^+ sequestration in roots and Na^+ exclusion in leaves. Similarly, the $R_{K/Na}$ ratios were lower than the $S_{K/Na}$ ratios, indicating that the vetiver's root system accumulates more Na than the shoot system. Although the K uptake reduced due to high salt stress, the high biomass of roots contributed for the accumulation of K in the roots. Consequently, they highly reduced the ratio of $R_{K/Na}$ in T_3. Liu et al (2016) hypothesised that the high ability of K^+/Na^+ for selective transportation could be the key strategy for salt tolerance of vetiver grass.

CONCLUSION

The vetiver grass grown in tannery-contaminated soil treated with vermicompost has grown well compared to farmyard manure and biocompost. The ratios of K/Na (>1) was higher in all treatments in vetiver shoot whereas lower in roots. Due to their exclusive morphological and physiological characteristics, vetiver grass acquires large amount of nutrients and salts for its shoot and root biomass indicating its potential for tolerating and remediating soil with higher salt load and to restore tannery-contaminated soil.

ACKNOWLEDGEMENT

Authors are highly thankful to Tamil Nadu State Land Use Research Board (TNSLURB), State Planning Commission, (SPC), Chennai for their financial support and the Department of Environmental Science, Tamil Nadu Agricultural University, Coimbatore for conducting the experiment successfully.

REFERENCES

A. Ramos-Arcos, Edith G. González-Mondragón, Eduardo S. López-Hernández, Ana R. Rodríguez-Luna, Carlos M. Morales-Bautista, Selene Lagunas-Rivera and Sugey López-Martínez 2021. Phytoremediation Potential of Chrysopogon zizanioides for Toxic Elements in Contaminated Matrices, In: *Biodegradation* [Working Title]. Intech Open. https://doi.org/10.5772/intechopen.98235

Anas M, Liao F, Verma KK, Sarwar MA, Mahmood A, Chen ZL, Li Q, Zeng XP, Liu Y and Li YR 2020. Fate of nitrogen in agriculture and environment: Agronomic, eco-physiological and molecular approaches to improve nitrogen use efficiency. Biological Research https://doi.org/10.1186/s40659-020-00312-4

Bhatti SS, Kumar V, Singh N, Sambyal V, Singh J, Katnoria JK and Nagpal AK 2016. Physico-chemical properties and heavy metal contents of soils and *Kharif* crops of Punjab, India. Procedia *Environmental Science* **35**: 801-808.

Received 12 September, 2021; Accepted 12 November, 2021

Braun S, Warrinnier R, Börjesson G, Ulén B, Smolders E and Gustafsson JP 2019. Assessing the ability of soil tests to estimate labile phosphorus in agricultural soils: Evidence from isotopic exchange. *Geoderma* **337**: 350-358.

Gao Y, Lu Y, Wu M, Liang E, Li Y, Zhang D, Yin Z, Ren X, Dai Y, Deng D and Chen J 2016. Ability to remove Na+ and retain K+ correlates with salt tolerance in two maize inbred lines seedlings. *Frontiers in Plant Science* **7**: 1716.

Gopinath KA, Bandi V, Banshi LM, Nataraja KC and Konda DG 2010. Dynamic Soil, Dynamic Plant Utilization of Vermicompost as a Soil Amendment in Organic Crop Production.

Gravand F, Rahnavard A and Pour GM 2021. Investigation of vetiver grass capability in phytoremediation of contaminated Soils with heavy metals (Pb, Cd, Mn, and Ni). *Soil Sediment Contam* **30**: 163-186.

Jayashree S, Rathinamala J and Lakshmanaperumalsamy P 2011. Determination of heavy metal removal efficiency of Chrysopogon zizanioides (Vetiver) using textile wastewater contaminated soil. *Journal of Environmental Science and Technology* **4**: 543-551.

Laxman et al 2014. International journal of advances in pharmacy, biology and chemistry Research Article.

Liu WG, Liu JX, Yao ML and Ma QF 2016a. Salt tolerance of a wild ecotype of vetiver grass (*Vetiveria zizanioides* L.) in southern China. *Botanical Studies* **57**: 1–8.

Ma L, Duan T and Hu J 2020. Application of a universal soil extractant for determining the available NPK: A case study of crop planting zones in central China. *Science of the Total Environment* **704**: 135253. https://doi.org/10.1016/j.scitotenv.2019.135253

Mickovski SB, Van Beek LPH and Salin F 2005. Uprooting of vetiver uprooting resistance of vetiver grass (*Vetiveria zizanioides*). In: *Plant and Soil.* Springer, pp. 33–41. https://doi.org/10.1007/s11104-005-2379-0

Mudhiriza T, Mapanda F, Mvumi BM and Wuta M 2015. Removal of nutrient and heavy metal loads from sewage effluent using vetiver grass, *Chrysopogon zizanioides* (L.) Roberty. *Water SA* **41**: 457–463.

Noorjahan CM 2014. Physicochemical characteristics, identification of bacteria and biodegradation of industrial effluent. *Indian Journal of Applied Research* **4**: 678-682.

Prasad R 1965. Determination of potentially available nitrogen in soils: A rapid procedure. *Plant Soil* **23**: 261-264.

Sinha S, Mishra RK, Sinam G, Mallick S and Gupta AK 2013. Comparative evaluation of metal phytoremediation potential of trees, grasses, and flowering plants from tannery-wastewater-contaminated soil in relation with physicochemical properties. *Soil and Sediment Contamination* **22**: 958-983.

Song J, Chen M, Feng G, Jia Y, Wang B and Zhang F 2009. Effect of salinity on growth, ion accumulation and the roles of ions in osmotic adjustment of two populations of Suaeda salsa. *Plant Soil* **314**: 133-141.

U.S. Environmental Protection Agency, 1993. Method 351.2, revision 2.0: determination of total kjeldahl nitrogen by semi-automated colorimetry 15.

Wagner S, Truong P, Vieritz A and Smeal C 2003. Response of vetiver grass to extreme nitrogen and phosphorus supply. *Proceedings of the Third International Conference on Vetiver and Exhibition,* Guangzhou, China 100-108.

Zhou Q and Yu BJ 2009. Accumulation of inorganic and organic osmolytes and their role in osmotic adjustment in NaCl-stressed vetiver grass seedlings. *Russian Journal of Plant Physiology* **56**: 678-685.

Indian Journal of Ecology (2021) 48(6): 1896-1901

Manuscript Number: 3468
NAAS Rating: 5.79

Evaluation of Global DNA Methylation Levels in Medical Workers Exposed to Low-Dose of Ionizing Radiation

Zahraa M. Mohammed, Fadhel M. Lafta[1*] and Haider Y. Lafta

Department of Biology, College of Science, University of Baghdad, Baghdad, Iraq
[1]Ministry of Science and Technology, Central Laboratories Directorate, Baghdad, Iraq
**E-mail: fadhellafta@sc.uobaghdad.edu.iq*

Abstract: Occupational exposure to low dose ionizing radiation (LDIR) has the potential to adversely affect genomic integrity. The normal epigenetic marks, including DNA methylation, havea key role in maintaining genomic stability. Accordingly, this study was conducted to investigate the potential influence of occupationally exposure to LDIR on the global DNA methylation levels in a set of blood samples collected from medical imaging workers. Blood samples were collected from 40 subjects (mean of age 47.07 years ranging from 25 to 60 years) occupationally-exposed to LDIR and 20 age-matched radiation-not-exposed individuals. Global DNA methylation (5mC %) levels were estimated using MethylFlash™-Methylated DNA Quantification Kit. The occupational exposure to LDIR resulted in significant increase in the level of global DNA methylation in medical imaging workers when compared to radiation-not-exposed controls (0.502 vs. 0.221, P= 0.0181) and this change in the level of 5mC% was directly affected by the exposure period. Overall, study showed that medical imaging workers who are occupationally-exposed to LDIR have increased levels of global DNA methylation and this increase could be due to increase in the expression of epigenetic modifiers genes in the LDIR occupationally-exposed subjects.

Keywords: LDIR, Occupational exposure, Global DNA methylation, Medical workers

Radiation is a natural energy resource that continuously emits ionizing radiations (IR) to the environment. IR emits different forms by radioactive elements including electromagnetic waves (such as γ or X-ray) and particles (β, ɣ and protons). In addition to several man-made activities that increase the emission of radiations around us such as tobacco smoking (Shyti et al 2019), the use of certain building materials (Madrugaet al 2019), nuclear reactors and medical imaging as well as radiation therapy (Al-Abdulsalam et al 2014). The potential health effects of exposure to high doses radiation are now well-understood and thus radiation protection regulations were put in place accordingly. Additionally, occupational and environmental exposure to mutagenes, including IR has been attracting considerable interest due to the potential harm of such exposure that could increase the risk of genomic instability which may contribute to the raise of serious health problems including malignancies development. Consequently, it is thought that monitoring of genomic integrity would be a very useful addition to the medical surveillance for those occupationally exposed to ionizing radiation products and/or waste (Guleriaet al2019).DNA methylation, that involves the addition of methyl group to the cytosine nucleotide in the CpG site, along with other epigenetic modifications, including micro RNA expression and histone modification, are heritable modifications that regulate gene transcription. Furthermore, it is believed that normal epigenetic marks have an important role in maintaining genomic stability and thus act as the guardian of our genome integrity (Fioriniello et al 2020). Although these modifications are required for normal health and development, aberrant epigenetic marks can also contribute to the development of various diseases including cancers. Aberrant epigenetic marks, including global hypomethyation, are believed to contribute to the lack of genomic stability (Sheaffer et al 2016). This is evident since the genome mobile elements (transposable) and repetitive regions are inactived and silenced by DNA hypermethylation in healthy tissues (Misiak et al 2019). The loss of normal DNA methylation signature could reactivate such regions/ elements and eventually disrupts the maintaining of genomic integrity. Such epigenetic ″aberrations″ could be a missing link among radiation exposure, radiation-induced genomic instability, and radiation-induced carcinogenesis. While recent studies have shown that IR can induce epigenetic changes in animals (Tang et al 2017, Kamstra et al 2018) and cell lines (Bae et al 2015), there is a lack of information in respect to the epigenetic alterations following occupational exposure to LDIR. The rationale behind setting the present study is the growing health concern over the risk of LDIR exposure from medical procedures including diagnostic imaging tests (Nguyen et al 2011, Linet et al 2020). Accordingly, this study was conducted to investigate the

potential influence of occupational exposure to LDIR on the global DNA methylation levels in diagnostic radiology workers.

MATERIAL AND METHODS

DNA extraction: Genomic DNA was extracted from 40 peripheral blood (pbl) samples collected from subjects (mean of age 47.07years ranging from 25 to 60 years)whom occupationally exposed to LDIR due to their routine work in medical diagnostic imaging and 20 not-exposed to radiation age-matched controls matched (tobacco smokers and/or alcoholic were exclude from the present study). For genomic DNA extraction, Quick-g DNA™ Blood MiniPrep, ZYMO RESEARCH CORP kit was used. Following the manufacturer's instructions, 400µl of genomic lysis buffer were added to 100 µl of each of the analyzed peripheral blood samples; then mixed well by vortexing for 5 mints and let to stand for 10 mints. This was proceeded by transforming mixture into aZymo-Spin IIC™ Column2 in a collection tube that spun at 10,000 x g for one minute; the collection tube with the flow through was discarded post this centrifugation. The Zymo-Spin™ IIC column then transferred to a new collection tube. This is followed by adding 200 µl of DNA pre-wash buffer to the spin column and centrifuged at 10,000 x g for one minute. Thereafter, the spin column was washed by adding 500 µl of g-DNA wash buffer and centrifuge at 10,000 x g for one minute. The genomic DNA was collected by transferring the spin column to a clean micro centrifuge tube, adding 50 µl of elution buffer to the spin column, incubating it for 2-5 minutes at room temperature and then centrifuged at top speed for 30 seconds. Following the extraction, the DNA samples were namedropped to estimate their concentration and purity. The extracted DNA samples the stored at -20°C for the subsequent molecular analysis.

Global DNA methylation estimation: The levels of global DNA methylation in the studied occupationally exposed to LDIR medical diagnostic imaging workers and their LDIR not-exposed age-matched healthy controls were estimated using MethylFlash™ Methylated DNA Quantification Kit (Colorimetric) Base Catalog # P-1034, Epigentek, USA. Following the manufacturer protocol, 100ng of the extracted genomic DNA diluted in the provided binding solution and loaded into 48 or 96 well-assay strips. Monoclonal antibody, provided within the kit was used as respective capture to detect the methylation fraction in the tested samples. In addition to the wash solution, detection antibody, enhancer solution, developer and stoop reaction solution, are also supplied by the ELISA-based technique -MethylFlash™ Methylated DNA Quantification Kit, that were used as it specified by the instruction provided. A micro plate reader (Thermo Fisher Scientific Inc) was set at optical density(OD) of 450nm and the DNA methylation levels were evaluated as proportional to the OD intensity read. For each sample, the relative percentage of global DNA methylation was estimated by subtracting the OD of the positive controls, provided in this kit, from the OD of each tested sample. All of the analyzed samples were run in duplicate and the obtained values were averaged to ensure that the signals generated are validated. The results were presented and analyzed using Excel data analysis software. The mean of the investigated parameters were compared between the studied groups using t-Test. In addition to of the linear correlation regression using http://vassarstats.net/ web site.

RESULTS AND DISCUSSION

Global DNA methylation analysis using MethylFlash™ Methylated DNA Quantification Kit (Colorimetric) showed that diagnostic radiology workers occupationally-exposed to LDIR have higher mean level of 5mC% than their age-matched not exposed controls (Fig. 1). The mean of the estimated 5 m C% for radiation occupationally-exposed medical workers was 0.502 in comparison to 0.221 in control with significant differences (P= 0.0181) when the global DNA methylation levels of the two studied groups were statistically compared.

The correlation analysis explores the strength and directionality of the linear relationship between two investigated variables. Thus linear correlation and regression provide useful information about whether the two examined variables increased or decreased in respect to tested situation. In the present study, http://vassarstats.net/ web site utilized as statistical analysis of the correlation between age of the studied subjects and the measured global DNA methylation levels. This analysis showed that medical workers who occupationally-exposed to LDIR have lower correlation (R^2= 0.0051) between age and the global methylation level estimated as 5mC% (Fig. 2).

While in LDIR not-exposed healthy controls examined group the correlation between age and the global methylation levels seemed much higher (R^2= 0.1449) than that of in their age matched occupationally-exposed to radiation subjects (Fig. 3). This may suggest stronger positive correlation between age and global 5mC in the LDIR not exposed individuals (controls) in comparison to the LDIR occupationally exposed subjects. In respect to periods of occupational exposure to LDIR, the global DNA methylation levels (5mC %) showed to be positively correlated with the years occupationally exposure. This was evident when the correlation value (R^2) was relatively high (0.439) in relation to the period of LDIR exposure and the levels of global DNA

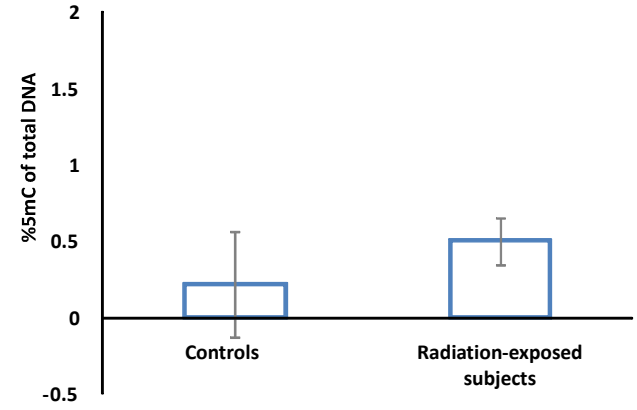

Fig.1. Global DNA methylation levels as estimated by 5mC% using Methyl Flash™ Methylated DNA Quantification Kit (Colorimetric) in LDIR occupationally-exposed medical workers and their age-matched healthy LDIR not exposed controls. Higher mean level of 5mC% in the radiation occupationally-exposed subjects than controls

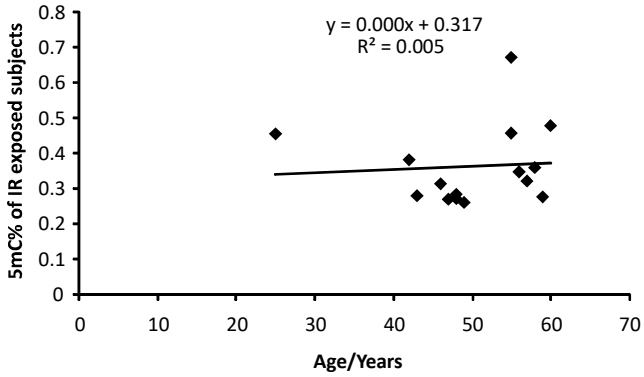

Fig. 2. Correlation analysis between the estimated global DNA levels and age in the LDIR occupationally exposed individuals

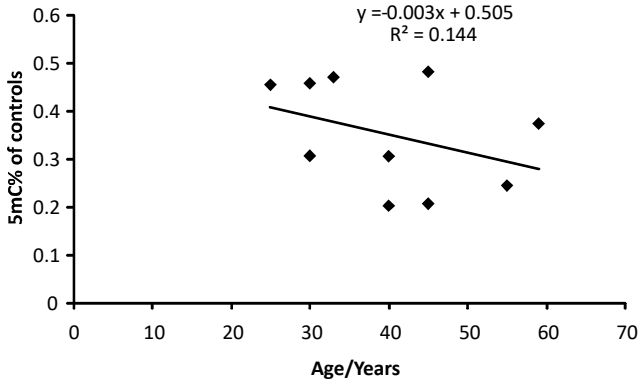

Fig. 3. Correlation analysis between the estimated global DNA levels and age in the LDIR not exposed individuals (controls)

methylation (Fig. 4). These results also suggest that the longer period of radiation occupationally exposure may correlate the more changes the global DNA levels.

However, this was not the case when as the correlation between the years of work (other jobs donot involve exposure to LDIR) and the levels of global DNA methylation (5mC) in the radiation not-exposed controls. The correlation value (R^2) was 0.0174 (Fig. 5) which is 25 folds lower than that recorded in occupationally exposure to LDIR medical workers and may provide a useful in indicator for the how strong the relation between the global DNA methylation changes and their directionality in relation to the period of occupationally exposure to LDIR.

The global methylation levels estimation in the studied subjects affected by the period of work environment that involve the exposure to very LDIR. The investigated workers serving in the medical imaging (dealing with X-ray, computed tomography “CT”, magnetic resonance imaging “MRI”, 3D mammography) have shown increased levels of global DNA methylation levels (5mC) that seems to be LDIR exposure-time dependent. In this respect, medical imaging workers who served for 31-35 years have higher global methylation levels than that estimated for those served 21-30 years and 10-20 years (0.388, 0.340 and 0.272 respectively (Table 1, Fig. 6).

Therewere significant differences in the mean level of global DNA methylation (5mC) upon different occupational exposure periods to LDIR (Table 1, Fig. 6) in the comparisons between the group of medical workers who served 10-20years and those worked for 21-30years, P= 0.006, t-Test). Similar trend of global DNA methylation significant changes (P= 0.005, t-Test) was observed when the medical imaging workers in shorter exposure period group (10-20years) was compared with those in the longer exposure period group (31-35Years). All the three categorized different exposure period's groups seemed to have higher methylation levels

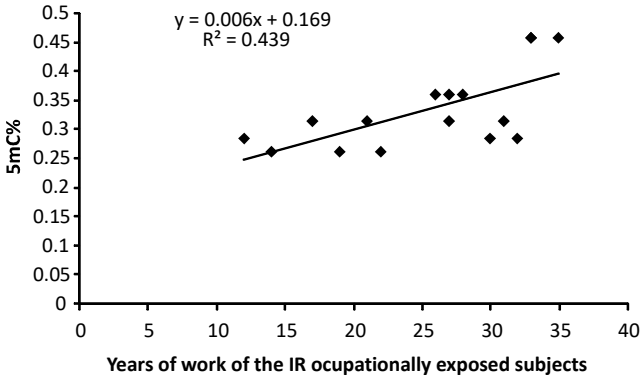

Fig. 4. Correlation between the global DNA methylation levels and the period of occupational exposure to radiation in the studied medical workers

than the LDIR not exposed controls.

The epigenetic modifications (including histone modifications and DNA methylation) have an integrating role in regulating the transcription activity of the genome. DNA methylation represents the most studied epigenetic modification that is linked to several important biological processes including embryonic development, differentiation, and tissue specific gene expression. In addition to the aforementioned, these epigenetic marks are also considered as the guardian of the genome since they contribute to the genomic stability. Furthermore, it is believed that these epigenetic marks are susceptible to be affected by the chemical and physical environmental pollutants including ionizing radiation (Cao 2015, Vaiserman 2015, Ladd-Acostaet al 2019). The effects of ionizing radiation exposure on the genome are well-established and have been covered by a large number of studies (Prihoda 2008, Verschaeve 2009, Ali et al 2015). However, a little known about the potential effect of LDIR on the epigenome, especially in line with the current scientific debate in relation to the radiation occupational exposure associated effects (Vaisermanet al 2018). The results showed that subjects whom occupationally exposed to LDIR have higher levels of global methylation (5mC) in comparison to their age-matched not exposed controls. The medical imaging workers-occupationally exposed to LDIR individuals in our study showed two folds increase in the global DNA methylation levels than the controls (0.502 vs. 0.221, Fig. 1). This two folds increase in the mean of global 5mC may reflect the enrichment of differentially hypermethylated sites upon occupational exposure to LDIR. Additionally, medical imaging workers investigated in our study who worked for longer periods in such LDIR- exposure environment showed to the grater changes in the global DNA methylation levels than those worked for relatively shorter periods. This increased in the global DNA methylation levels (5mC) could be due to the increase in the expression of DNMT3A which is known to be responsible for de novo DNA methylation. In this regard, a recent study has reported the over expression of DNMT3A following the exposure to fractionated LDIR in mouse model (Koturbashet al 2016). Consistence with the finding of our study, sperm cells global DNA hypermethylation was reported in medical occupationally exposed to LDIR (Kumar et al 2013). Similarly, the sperms' quantity, morphology, mortality and their DNA integrity seemed to be highly affected by chronic long-term exposure to LDIR in males from Jilin Province, China (Zhou et al 2016). However, other studies have reported, using different global methylation estimation methods, reduced global DNA methylation, based on *LINE1*pyrosesquencing assay, among industrial radiographers in comparison to the controls (Cho 2014). Similar effects of global DNA methylation reduction were observed in workers of nuclear power plant workers in South Korea (Lee et al 2015). Miousse et al (2014) revealed the exposure low-dose Fe-Ion radiation induces long-term epigenetic alterations in mouse bone marrow

Table 1. Global DNA methylation levels (5mC %) in respect to the period of occupational exposure to LDIR in the studied medical workers

Period of occupational exposure to LDIR	5m C% mean ± SD	P value t-Test
10-20 years (n=7)	0.272 ± 0.020	0.006
21-30 years (n=24)	0.340 ± 0.057	
31-35 years (n=9)	0.388 ± 0.088	0.005

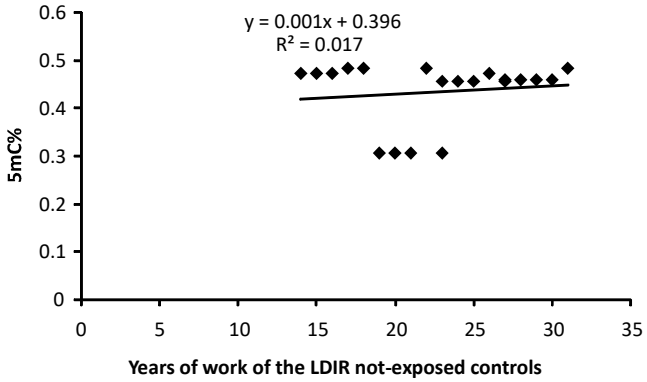

Fig. 5. Correlation between the global DNA methylation levels and years of work of the not-exposure to radiation controls

Fig. 6. The global DNA methylation levels (5mC %) in respect to the period of occupational exposure to LDIR in the studied medical workers. The investigated subjects were sub grouped into three groups based on the occupational periods of exposure to LDIR (10-20, 21-30 and 31-35Years). Longer periods of LDIR exposure seem to have high impact on the global DNA methylation levels in the studied subjects

hematopoietic progenitor and stem cells. These were represented by four folds hepermethylation of *LINE1* and *SINE B1* repetitive elements. To clearly understand the potential effects of ionizing radiation on the epigenome, mouse model experiments have revealed that low dose X-ray induce profound DNA methylation changes represent by reduced global methylation and promoter hypermethylation (Wang et al 2014). However, recent study showed no global methylation changes when medaka fish (*Oryzias latipes*) chronically exposed to LDIR, but the expression profile of the hepatic tissue significantly altered (Bertucciet al 2020). In respect to the correlation between the estimated global DNA methylation levels and age of the investigated subjects, our study results showed a very lower positive correlation in the LDIR exposed medical imaging workers than the not exposed controls (R^2= 0.0051 vs. 0.1449). The methylation levels are affected and correlated with age (Jansen et al 2019, Sturm et al 2019, Jiang et al 2020), the very weak correlation of global DNA methylation with age observed in our study may suggest a disruption of global DNA methylation dynamic changes in the LDIR exposed investigated subjects in comparison to the controls. Similarly, relatively higher positive correlation value (R^2= 0.439) of the global DNA methylation levels and the period of occupational exposure to LDIR. This may reflex the causality and directionality of the changes in the global DNA methylation levels(5mC %) following the occupational exposure to LDIR. However, this is not the case in the LDIR- non exposed controls when the global DNA methylation levels (5mC %) exhibited a weak positive correlation with the years of work (R^2= 0.0174). Moreover, our study results also suggested that longer periods of LDIR exposure seems to have more impact on the global DNA methylation levels in the studied subjects, that is to say that the longer occupational exposure to radiation the bigger global methylation 5mC change. This finding is consistence with the large body of evidence that linked the global DNA methylation changes in response to the environmental pollutants, especially ionizing radiations (Bollatiet al 2010, Budak2020,Sabiet al 2020). The studies have highlighted that DNA methylation may affected by the different type of the exposed ionizing radiation. For example, the galactic cosmic 56Fe ions radiation, differ from X-ray, found to induce mostly hypermethylation, and the primarily affected regions were open chromatin including enhancers, promoters and the edges (“shores”) of CpG islands (Kennedy et al 2018). The occupational exposure to LDIR can affect the epigenetic modifiers such as the expression dysreguation of genes encode to enzymes related to the process of DNA methylation catalyzing and inducing oxidative damages (Bernal 2012, Tharmalingam et al 2017). However, Chen et al.'s study has not reported DNA methylation changed in the medical worker due to dose burden of occupational exposure to ionizing radiation (Chen et al 2019). The high variation in the results on the potential effect of LDIR occupational exposure could be due to the different methods utilized for estimating the global DNA methylation levels. In this regard, a study conducted by Silva and colleagues has revealed that exposed workers to LDIR have associated with higher promoter DNA methylation levels of key tumor suppressor genes (CDKN2A, APC and MLH1) and decreased LINE-1 methylation in comparison to not exposed workers (Silva et al 2019).

CONCLUSIONS

The study has highlighted the potential effect of LDIR occupational exposure on global DNA methylation levels in increasing the levels of 5mC in comparison to the radiation not-exposed controls. Changing of global DNA methylation levels could be used use as potential biomarker for monitoring the epigenetics dynamic in response to LDIR occupational exposure.

REFERENCES

Al-Abdulsalam A and Brindhaban A 2014. Occupational radiation exposure among the staff of departments of nuclear medicine and diagnostic radiology in Kuwait. *Medical Principles and Practice* **23**(2): 129-133.

Ali A, Muttar A, Khayon S, Haider Y, Ali H and Abdullah A 2015. Assessment of DNA Damage in Peripheral Blood Lymphocytes of Radiation Workers at Al-Tuwaitha Site by Using the Sister Chromatid Exchange and the Comet Assay.

Bae J-H, Kim J-G, Heo K, Yang K, Kim T-O and Yi JM 2015. Identification of radiation-induced aberrant hypomethylation in colon cancer. *BMC Genomics* **16**(1): 56.

Bernal AJ Epigenetic Response to Low-Dose Ionizing Radiation, Duke University, 2012.

Bertucci EM, Mason MW, Camus AC, Rhodes OE and Parrott BB 2020. Chronic low dose irradiation alters hepatic transcriptional profiles, but not global DNA methylation in medaka (Oryzias latipes). *Science of The Total Environment* 138680.

Bollati V and Baccarelli A 2010. Environmental epigenetics. *Heredity* **105**(1)**:** 105-112.

Budak M 2020. Radiation and DNA Methylation Mechanisms. In. *DNA Methylation Mechanism*, edn: IntechOpen. p^pp.

Cao Y 2015. Environmental pollution and DNA methylation: carcinogenesis, clinical significance, and practical applications. *Frontiers of Medicine* **9**(3)**:** 261-274.

Chen B, Dai Q, Zhang Q, Yan P, Wang A and Qu L 2019. The relationship among occupational irradiation, DNA methylation status, and oxidative damage in interventional physicians. *Medicine* **98**(39).

Cho YH 2014. Radiation-induced genomic instability and LINE-1 hypomethylation in radiographers.

Fioriniello S, Marano D, Fiorillo F, D'Esposito M and Della Ragione F 2020. Epigenetic Factors That Control Pericentric Heterochromatin Organization in Mammals. *Genes* **11**(6)**:** 595.

Guleria R, Bhushan B, Guleria A, Bhushan A and Dulari P 2019. Harmful effects of ionizing radiation. *International Journal for Research in Applied Science and Engineering Technology*

(IJRASET) **7:** 12.

Jansen RJ, Tong L, Argos M, Jasmine F, Rakibuz-Zaman M, Sarwar G 2019. The effect of age on DNA methylation in whole blood among Bangladeshi men and women. *BMC Genomics* **20**(1): 704.

Jiang S, Guo Y 2020. Epigenetic Clock: DNA Methylation in Aging. *Stem Cells International* 2020.

Kamstra JH, Hurem S, Martin LM, Lindeman LC, Legler J and Oughton D 2018. Ionizing radiation induces transgenerational effects of DNA methylation in zebrafish. *Scientific Reports* **8**(1)**:** 1-13.

Kennedy E, Powell D, Li Z, Bell J, Barwick B and Feng H 2018. Galactic cosmic radiation induces persistent epigenome alterations relevant to human lung cancer. *Scientific Reports* **8**(1): 1-14.

Koturbash I, Jadavji NM, Kutanzi K, Rodriguez-Juarez R, Kogosov D and Metz GA 2016. Fractionated low-dose exposure to ionizing radiation leads to DNA damage, epigenetic dysregulation, and behavioral impairment. *Environmental Epigenetics* **2**(4): 025.

Kumar D, Salian SR, Kalthur G, Uppangala S, Kumari S and Challapalli S 2013. Semen abnormalities, sperm DNA damage and global hypermethylation in health workers occupationally exposed to ionizing radiation. *PLoS One* **8**(7): e69927.

Ladd-Acosta C, Feinberg JI, Brown SC, Lurmann FW, Croen LA and Hertz-Picciotto I 2019. Epigenetic marks of prenatal air pollution exposure found in multiple tissues relevant for child health. *Environment International* **126:** 363-376.

Lee Y, Kim YJ, Choi YJ, Lee JW, Lee S and Cho YH 2015. Radiation-induced changes in DNA methylation and their relationship to chromosome aberrations in nuclear power plant workers. *International Journal of Radiation Biology* **91**(2)**:** 142-149.

Linet MS, Schubauer-Berigan MK and Berrington de González A 2020. Outcome Assessment in Epidemiological Studies of Low-Dose Radiation Exposure and Cancer Risks: Sources, Level of Ascertainment, and Misclassification. *JNCI Monographs* **2020**(56)**:** 154-175.

Madruga M, Miró C, Reis M and Silva L 2019. Radiation exposure from natural radionuclides in building materials. *Radiation Protection Dosimetry* **185**(1)**:** 49-57.

Miousse IR, Shao L, Chang J, Feng W, Wang Y, Allen AR2014. Exposure to low-dose 56Fe-ion radiation induces long-term epigenetic alterations in mouse bone marrow hematopoietic progenitor and stem cells. *Radiation Research* **182**(1)**:** 92-101.

Misiak B, Ricceri L and Sąsiadek MM 2019. Transposable elements and their epigenetic regulation in mental disorders: Current evidence in the field. *Frontiers in Genetics***10:** 580.

Received 24 June, 2021; Accepted 12 November, 2021

Nguyen PK and Wu JC 2011. Radiation exposure from imaging tests: is there an increased cancer risk? *Expert Review of Cardiovascular Therapy* **9**(2): 177-183.

Prihoda TJ 2008. Genetic damage in mammalian somatic cells exposed to radiofrequency radiation: A meta-analysis of data from 63 publications (1990–2005). *Radiation Research* **169**(5)**:** 561-574.

Sabi SH, Khabour OF, Alzoubi KH, Cobb CO and Eissenberg T 2020. Changes at global and site-specific DNA methylation of MLH1 gene promoter induced by waterpipe smoking in blood lymphocytes and oral epithelial cells. *Inhalation Toxicology* **32**(3): 124-130.

Sheaffer KL, Elliott EN and Kaestner KH 2016. DNA hypomethylation contributes to genomic instability and intestinal cancer initiation. *Cancer Prevention Research* **9**(7): 534-546.

Silva IR, Ramos MC, Arantes LM, Lengert AV, Oliveira MA and Cury FP 2019. Evaluation of DNA methylation changes and micronuclei in workers exposed to a construction environment. *International Journal of Environment Research Public Health* **16**(6): 902.

Sturm G, Cardenas A, Bind M-A, Horvath S, Wang S and Wang Y 2019. Human aging DNA methylation signatures are conserved but accelerated in cultured fibroblasts. *Epigenetics* **14**(10): 961-976.

Tang FR, Loke WK and Khoo BC 2017. Low-dose or low-dose-rate ionizing radiation-induced bioeffects in animal models. *Journal of Radiation Research* **58**(2): 165-182.

Tharmalingam S, Sreetharan S, Kulesza AV, Boreham DR and Tai T 2017. Low-dose ionizing radiation exposure, oxidative stress and epigenetic programing of health and disease. *Radiation Research* **188**(4.2): 525-538.

Vaiserman A 2015. Epidemiologic evidence for association between adverse environmental exposures in early life and epigenetic variation: A potential link to disease susceptibility? *Clinical epigenetics* **7**(1)**:** 96.

Vaiserman A, Koliada A, Zabuga O and Socol Y 2018. Health impacts of low-dose ionizing radiation: Current scientific debates and regulatory issues. *Dose-Response* **16**(3)**:** 1559325818796331.

Verschaeve L 2009. Genetic damage in subjects exposed to radiofrequency radiation. *Mutation Research/Reviews in Mutation Research* **681**(2-3): 259-270.

Wang J, Zhang Y, Xu K, Mao X, Xue L and Liu X2014. Genome-wide screen of DNA methylation changes induced by low dose X-ray radiation in mice. *PLoS One* **9**(3): e90804.

Zhou D, Hao J, Guo K, Lu C and Liu X 2016. Sperm quality and DNA damage in men from Jilin Province, China, who are occupationally exposed to ionizing radiation. *Genetics Molecular Research* **15**(1): 1-7.

CONTENTS

3461	Effect of Sex, Age and Location on Prevalence of *Brucellosis* among Goats in Baghdad, Iraq *Akram Sattar Gabbar and Sahar Mahdi Hayyawi*	1863
3462	Evaluation of Power Tiller Operated Vertical Rotary Plough for Tillage *Chandrashekar, H.K. Venkata Reddy and Jayant Singh*	1866
3463	Development of Prototype Air Water Generator to Condense Water from Atmospheric Moisture *M. Subash Sundar, Aminul Islam and Yellamanda Reddy*	1871
3464	Accumulation of Heavy Metals in *Fejervarya limnocharis* Tadpoles Inhabiting Two different Wetlands in Cachar District, Assam *T.H. Sharma and M. Dey*	1876
3465	Bio Concentration Factor of Aquatic Plants and Heavy Metals as Exchangeable and Residual in Sediment at Marshes, Southern Iraq *Maha K. Al-Mishrey, Rehab S.K. Al-Atbee, Salah M. Saleh and Abbas A. Hantoush*	1880
3466	Combined Effect of Antibiotics and Copper on Catalase of Haplic Chernozem *D. Trufanov, S. Kolesnikov, Yu. Akimenko, T. Minnikova and K. Kazeev*	1887
3467	Evaluating the Potential of Vetiver Grass [*Chrysopogon zizanioides* (L.)] and Organic Amendments for Restoration of Tannery Effluent Contaminated Soil R. *Rizam, K. Suganya, V. Davamani, R. Anandham and M. Maheswari*	1891
3468	Evaluation of Global DNA Methylation Levels in Medical Workers Exposed to Low-Dose of Ionizing Radiation *Zahraa M Murtada, Fadhel M. Lafta and Haider Y. Lafta*	1896

CONTENTS

3440	Effect of Spacing and Fertility Levels on Growth, Yield and Economics of Green Gram (*Vigna radiata* L) under Rainfed Conditions *S.K. Sharma, Kuldeep Singh, Kautilya Chaudhary and S.K. Thakral*	1732
3441	Assessment of Variation for Pterostilbene in Heartwood of *Pterocarpus marsupium* Roxb., a Vulnerable Medicinal Tree from Central India *Naseer Mohammad, Hari Om Saxena, Raj Singh Yadav and Ganesh Pawar*	1736
3442	Cytogenetic Investigations and Karyological Relationships of Eight *Medicago* species (Fabaceae) *Z.A. Turki and M.M. Hegazy*	1740
3443	Ecological Studies on Southern Secondary Moist Deciduous Forest of Shendurney Wildlife Sanctuary, Kollam, Kerala, India *Halliru Bilyaminu, K. Vidyasagaran, S. Gopakumar and Nadan Vijaykumar*	1747
3444	Conjoint Effect of Organic Formulations and Inorganic Fertilizers on Growth, Yield and Quality in Strawberry (*Fragaria* × *ananassa* Duch.) *Praveen Verma, Jitender K. Chauhan, D.P. Sharma, N.C. Sharma and Uday Sharma*	1755
3445	Seed Traits and Germination in *Syzygium caryophyllatum* (L.) Alston: An Endangered Species of the Western Ghats *A. Joglekar, M. Tadwalkar, P. Ghate, R.P. Gunaga and A. Patwardhan*	1760
3446	Characterization of Few Fabaceous Plants towards their Medicinal Application *Neena Bagchi, Amit Sharma and Santosh K. Sar*	1766
3447	Generation of Paddy Straw Composts in Rice Based Integrated Farming System and Evaluating in Organic Production of Fodder Maize *K.V. Athira, B. Sudha, Jacob John, Shalini Pillai P and R.V. Manju*	1772
3448	Antimicrobial Activity of Endophytic Microorganisms Isolated from *Allium Sativum* *U. Dutta, D. Khajuria and J.D. Bandral*	1780
3449	Improvement of Xylanase Activity of *Aspergillus* sp. by Physical and Chemical Mutagenesis *T. Venkatram Reddy, M. Rajashekhar, N. Kishore and D. Madhusudan Reddy*	1789
3450	Protective Role of Allicin Compared with Kcl administration on some Cardiac Markers, Electrolyte, Oxidative Status and Gene Expression of NOS in Ovariectomized Rabbits *Hayder S. Rwayyih and Luma Waleed Khaleel*	1793
3451	Natural Occurrence of *Euphorbia leaf curl virus* (EuLCV) Infecting Zinnia in India *Shikha Sharma, Vineet K. Sharma and Tapish Pawar*	1798
3452	Screening the Virulence of *Metarhizium anisopliae* MT193505 against Spider Mite, *Tetranychus urticae* Koch *Dalia A. Waked and M. Eleawa*	1802
3453	Assessment of the Diversity of Thrips species (Thysanoptera) in Solanaceous Vegetable Crops *Amit Kumar, Tamoghna Saha, R. Rachana, Nithya Chandran and K. Santosh*	1809
3454	Evaluation of Hydrogel and *Trichoderma* based Formulations on Root Characteristics and Water Use Efficiency in Linseed under Rainfed Ecology *K. Dujeshwer, R.K. Singh and N.R. Sandhya*	1815
3455	Ichthyofaunal Diversity and Conservation Status in the River Teesta, West Bengal, India *Tapan Sarkar and Joydeb Pal*	1821
3456	Production of Polyhydroxtbutyratye from Marine Source: A Review *A. Ranganadhareddy and Ch. Chandrasekhar*	1829
3457	Seasonal Investigation of Rainbow Trout Waterbodies in Western Ghats, South India *J.C. Walter Devaa and U. Ramesh*	1837
3458	Analysis of Financial Performances and Environmental Sustainability of Coldwater Inland Fisheries in Sikkim Himalaya *Kul Bahadur Chettri and Ruma Kundu*	1846
3459	Protective Effect of Phitofert on Testicular Function and Fertility in Rats Exposure to Lead Acetate *Osama Jabbar Hussein and Jawad Kadhim Arrak*	1852
3460	Effect of Purified Bioactive Compounds for *Streptomyces griseus* on Proliferation Lymphocyte *in Vitro* *Eslah Shaker Rajeb, Mohsen Hashim Risan and Zainab Yaseen Mohmmed Hasan*	1858

Indian Journal of Ecology (2021) 48(6)

Indian Journal of Ecology

CONTENTS

3421	Using Spectral Indices in Detecting the Degradation of Soil Physiographic Units in Al-Wahda Project South of Baghdad *Jinan Abdul Ameer Abbas*	1595
3422	GIS-Based Projected Best Land Use: A Case Study of Dhanbad District, Jharkhand, India *S.E. Saranaathan and S. Vaishaly*	1611
3423	Impact of Pre-Monsoonal Rainfall Trend on Vegetation for Ranchi Plateau, Jharkhand, India *Amit Kumar Jha, Ajai Singh and Pratibha Warwade*	1621
3424	Determination of Geomorphological Characteristics of Jakham River Basin using GIS Technique *Vinay Kumar Gautam, Mahesh Kothari, P.K. Singh and K.K. Yadav*	1627
3425	Runoff Estimation by Integration of GIS and SCS-CN Method for Kanari River Watershed *Ayushi Trivedi and Manoj Kumar Awasthi*	1635
3426	Seasonal Rainfall Prediction for Tamil Nadu Using Climate Predictability Tool *G. Senbagavalli, N.K. Sathyamoorthy, S. Kokilavani, G.A. Dheebakaran and Patil Santosh Ganapati*	1641
3427	Efficient Internet of Things Smart Agricultural Crops Growth using Machine Learning with Mobile Applications *V. Arulkumar, G. Kalpana, Sweta Gupta, A. Devipriya and Saroj Kumar*	1647
3428	Exploration of SCATSAT-1 Ku Band Data to Develop MPDI and Assessment of Rice Crop Ecosystem using Brightness and Temperature *Mahesh Palakuru and Sirisha Adamala*	1655
3429	Consul Multiphasic 3.5a Package for Modeling of Groundwater Protection from Amoxicillin using Modified Bentonite *Zahra Abdel Sahib and Said Tab Ali*	1658
3430	Water Quality Assessment of Kela and Ejersa Rivers Using Benthic Macroinvertebrates, Ethiopia *Mekonnin Dula, Girum Tamire and Gezahegn Degefe*	1670
3431	Repercussions of Urbanization on Surface Water Quality in Northern Hilly State of India *Diksha Rana and S.K. Bhardwaj*	1679
3432	Delineation of Groundwater Potential Zone in Foothill of Western Himalayan State *Pravidhi Sharma, R.K. Aggarwal and S.K. Bhardwaj*	1685
3433	Bioindication Assessment of Drinking Water Toxicity in Large Cities of Ukraine *Svitlana Skok and Denys Breus*	1692
3434	Impact Assessment of Invasive Alien Plants on Soil Organic Carbon (SOC) Status in Disturbed and Moderately Disturbed Patches of Hailakandi District in an Indo Burma Hotspot Region *Zingthoi Khuppi Sakachep and Prabhat Kumar Rai*	1698
3435	Effect of Micronutrients Application on Growth, Yield and Quality of Guava (*Psidium guajava* L.) *Shahroon Khan, Ashwani Kumar and Jeet Ram Sharma*	1705
3436	Species Diversity and Composition of Spiders (Arachnida: Araneae) of Different Micro-habitats in Nilgiri Foothills, Western Ghats, Tamil Nadu, India *Vijay Kumar Yadav, John T.D. Caleb and R. Revathi*	1709
3437	Diversity of Weed Flora in Citrus of the Oranian Phytogeographical Sector *Karima Hanitet, Nadia Bemmansour and Zoheir Mehdadi*	1715
3438	Clonal Variation in Gas Exchange Traits Linked to Water Use Efficiency in Eucalyptus M. *Karthikeyan, K.T. Parthiban, P. Boominathan, S. Umesh Kanna and C. Cinthia Fernandaz*	1721
3439	Impacts of Seasonal Variation on Habitat Selection by Sichuan Golden Snub-nosed Monkey: A Case Study of Tangjiahe National Nature Reserve *Majda Aouititen, Aravinda Ravibhanu, Wancai Xia, Dayong Li and Xiaofeng Luan*	1726

Date of Publication 15.12.2021